DECLARATION OF JUNE ANN MUNFORD

HANWHA 1004
Part 1 of 2

TABLE OF CONTENTS

Page

I. INTRODUCTION 1
II. QUALIFICATIONS AND EXPERIENCE 1
III. BACKGROUND INFORMATION 3
IV. SUMMARY OF OPINIONS 7
V. Istratov 9
A. Public Accessibility of Istratov at Pennsylvania State University Library as of June 2005 10
VI. Marvin 12
A. Public Accessibility of Marvin on the NTIS Database as of August 1990 12
B. Public Accessibility of Marvin on Online Searchable Databases as of February 24, 2013 and July 7, 2013 15
VII. Granek 19
A. Public Accessibility of Granek on University Library Websites as of April 7, 2010 19
B. Public Accessibility of Granek on Beacon Website as of April 12, 2013 and July 23, 2013 23
VIII. CONCLUSION 26

I, June Ann Munford, declare as follows:

I. INTRODUCTION

1. My name is June Ann Munford. I am over the age of 18 and am competent to testify to the same.

2. I have been retained on behalf of Hanwha Solutions Corporation ("Hanwha" or "Petitioner") to provide assistance in evaluating the authenticity and public accessibility of documents discussed in this Declaration for proceedings before the United States Patent and Trademark Office. I understand that my Declaration will be submitted in the following *Inter Partes* Review proceedings:

Challenged Patent	Patent Owner	Case No.
11,251,315	Maxeon Solar Pte. Ltd.	IPR2024-0118

3. I am being compensated for my services in this matter at the rate of $200.00 per hour plus reasonable expenses. My compensation does not depend on the outcome of this matter. My testimony in this Declaration is based on the information cited in this Declaration and my experience in library science for nearly twenty years.

II. QUALIFICATIONS AND EXPERIENCE

4. I earned a Master of Library and Information Science (MLIS) from the University of Wisconsin-Milwaukee in 2009. I have nearly twenty years of experience in the library/information science field. Beginning in 2004, I have served

in various positions in the public library sector including Assistant Librarian, Youth Services Librarian, and Library Director. I have attached my Curriculum Vitae as **Appendix CV**.

5. During my career in the library profession, I have been responsible for materials acquisition for multiple libraries, including the Dowagiac District Library in Dowagiac, Michigan; the Anchorage Public Library in Anchorage, Alaska; and the Hart Area Public Library in Hart, Michigan. These libraries relied on me and my expertise in the library sciences to catalogue, purchase and process incoming library works correctly and efficiently. These responsibilities included purchasing materials directly from vendors, recording publishing data from the material in question, creating detailed material records for library catalogs, and physically preparing that material for circulation.

6. In addition to my experience in acquisitions, during my time as a Library Director for the Dowagiac District Library, I was also responsible for analyzing large collections of library materials, tailoring library records for optimal catalog search performance, and creating lending agreements between libraries. As a part of my analysis of large collections, I audited library collections, including Machine Readable Cataloging (herein referred to as "MARC") records, gathered usage statistics for various works, and evaluated MARC record fields to ensure completeness and accuracy. Similarly, in my work as a researcher, I have examined

thousands of MARC records authored by others. I am therefore familiar with and experienced in interpreting these records to make determinations based on the data contained within these records.

III. BACKGROUND INFORMATION

7. I have extensive experience with the catalog record creation process in the library sector. In preparing material for public accessibility, a library catalog record describing that material would be created. These records are typically written in MARC code and contain information such as a physical description of the material, metadata from the material's publisher, and date of library acquisition. MARC records are vital to the function of a library's services, as they facilitate the library staffs' and patrons' ability to search, explore, and secure materials within that library's collection. Libraries or similar institutions that rely upon MARC records dedicate significant resources to ensure that the records are accurate and sufficiently descriptive. Librarians and patrons alike therefore routinely rely on their accuracy and completeness.

8. Typically, in creating a MARC record, a librarian gathers various pieces of metadata, such as the publication's title, publisher and subject headings, among others, and assigns each datum to a relevant numerical field. For example, a book's physical description is tracked in field 300 while title/attribution is tracked in field 245. The 008 field of the MARC record is reserved for denoting the creation

of the library record itself. The 008 field accurately indicates the date of an item's public accessibility, as it is the only date reflecting the inclusion of said materials within the library's collection.

9. During the relevant time period, which I understand to be 1990-2014, MARC records and other digital library cataloging systems were typically indexed to facilitate searches. This indexing is necessary for both providing patron services and maintaining library records. Indexing is generally done using cataloging software, which creates searchable fields for data like the title and author of a work. Using searchable fields allows a librarian, for example, to ensure that the library does not duplicate works, which is an essential function for libraries.

10. Cataloging practices for librarians depend on the format of the material being catalogued. For instance, a one-time publication such as a textbook is cataloged as a "monograph," and only that specific edition of the book is described in the MARC record. Time-sensitive materials such as magazines, academic journals, and newspapers are cataloged as periodicals, with the MARC record describing the publication as a whole, rather than each individual issue. New issues of these periodicals do not receive their own MARC records, and are instead added to the inventory of the publication's existing MARC record. This ensures timely access to new issues as soon as possible after publication by minimizing the effort required to catalogue the material.

11. For periodicals, the 008 field of the MARC record indicates date of first record creation at that particular library for the periodical. All subsequent issues are added to that same record and are often indicated in an individual holdings field that lists all issues held by the library. For example, a MARC record for an academic journal listing January 2000 in the 008 field indicates that the library first began housing the journal in January 2000. A separate item record for the same record might indicate that the library holds issues of the periodical, for example from the January 2000 issue through to the January 2022 issue. This would indicate that the library began subscribing to the periodical beginning with the January 2000 issue, and that the library continued to receive and hold subsequent issues until January 2022. Even if the subscription ceased, the presence of the record would indicate continuous accessibility to the public for all held issues indicated in the item record. This can be confirmed by, for example, obtaining the copy of the periodical associated with one of the holdings in the record.

12. Based on my experience, a library should make issues of periodicals available to the public within at least six months of the issue's date. This allows more than enough time to receive, catalogue, and shelve the issue. It would only be under exceptional circumstances that a periodical issue is not shelved within six months.

13. I am also familiar with various digital and online practices relating to publications of periodicals, such as academic journals. For example, many academic journals have posted issues or individual articles online for public access as early as the late 1990s.

14. Services like PubMed—an online database maintained by the United States National Library of Medicine (NLM) at the National Institutes of Health (NIH)—also maintain online records of certain academic journals. *See* https://pubmed.ncbi.nlm.nih.gov/about/. That database, which has been accessible to the public since 1996, includes searchable abstracts and bibliographic information for biomedical literature. *Id.* PubMed also provides links to the articles, when accessible. *Id.*

15. The Internet Archive "Wayback Machine" is a website that has been maintaining an archival record of the internet since the mid-1990s, catalogued by URL and date. *See* https://archive.org/about/. The Internet Archive's public facing website—which is searchable by URL—has been accessible to the public since the year 2000. My colleagues in the profession regard the Internet Archive and the associated metadata as reliable records of online resources, including records of when websites were publicly accessible.

IV. SUMMARY OF OPINIONS

16. Based on my review of the documents cited in this Declaration and those included in Exhibits 1012, 1008, 1010, it is my opinion that the following journal articles are authentic and were publicly accessible on the dates identified below:

Journal Article	Date Publicly Accessible	Addressed In	Exhibit
"Gettering in Silicon-on-Insulator Wafers: Experimental Studies and Modelling" by Andrei A. Istratov as published in *Semiconductor Science and Technology*, June 2005	June 2005	Section V	1012
"Interdigitated Back Contact Solar Cell Analysis and Design Recommendations for Space Use," by D.C. Marvin, S.L. Froedege, Space Systems Division Air Force Systems Command, Report 88D-TR-90-04	August 1990; or alternatively February 24, 2013; or alternatively July 7, 2013	Section VI	1008
"High-Efficiency Back Contact Back-Junction Silicon Solar Cells" by F. Granek (Ph.D. Dissertation, Fraunhofer Institute for Solar Energy Systems ISE) (2009)	April 7, 2010; or alternatively April 12, 2013; or alternatively July 23, 2013	Section VII	1010

17. In addition to my experience in the field of library sciences, my opinions are supported by the appendices to my Declaration, which are included in the following exhibits:

Appendices	Associated Journal Article
ISTRATOV01	"Gettering in Silicon-on-Insulator Wafers: Experimental Studies and Modelling" by Andrei A. Istratov as published in *Semiconductor Science and Technology*, June 2005
ISTRATOV02	"Gettering in Silicon-on-Insulator Wafers: Experimental Studies and Modelling" by Andrei A. Istratov as published in *Semiconductor Science and Technology*, June 2005
ISTRATOV03	*Semiconductor Science and Technology* publication website for "Gettering in Silicon-on-Insulator Wafers: Experimental Studies and Modelling" by Andrei A. Istratov (July 25, 2024) (available at https://iopscience.iop.org/article/10.1088/0268-1242/20/6/016).
MARVIN01	National Technical Reports Library, "Interdigitated Back Contact Silicon Solar Cell Analysis and Design Recommendations for Space Use" (available at: https://ntrl.ntis.gov/NTRL/dashboard/searchResults/titleDetail/ADA220414)
MARVIN02	D.C. Marvin, S.L. Froedege, Interdigitated Back Contact Solar Cell Analysis and Design Recommendations for Space Use," Space Systems Division Air Force Systems Command, Report 88D-TR-90-04 ("Marvin") (available at https://ntrl.ntis.gov/NTRL/dashboard/searchResults/titleDetail/ADA220414.xhtml#)
MARVIN03	National Technical Reports Library, "National Technical Reports Library Search Tips" (available at https://ntrl.ntis.gov/NTRL/help.xhtml)
MARVIN04	June 12, 2024 Letter from Wayne Strickland
MARVIN05	National Technical Reports Library, "About Us" (available at https://www.ntis.gov/about/about-us.xhtml)
MARVIN06	February 24, 2013 Internet Archive record of https://www.ntis.gov/pdf/dbguid-2013.pdf (available at https://web.archive.org/web/20130715000000*/https://www.ntis.gov/pdf/dbguid-2013.pdf)
MARVIN07	July 7, 2013 Internet Archive record of http://www.ntis.gov/products/ntisdb.aspx (available at https://web.archive.org/web/20130707063952/http:/www.ntis.gov/products/ntisdb.aspx)

GRANEK01	FreiDok Plus: Universitätsbibliothek Freiburg, "High-Efficiency Back-Contact Back-Junction Silicon Solar Cell" (available at https://freidok.uni-freiburg.de/data/7372)
GRANEK02	F. Granek, High-Efficiency Back Contact Back-Junction Silicon Solar Cells (2009) (Ph.D. Dissertation, Fraunhofer Institute for Solar Energy Systems ISE) (available at https://freidok.uni-freiburg.de/jsonApi/v1/download?publicationId=7372&grouping=1)
GRANEK03	Universität Hamburg MARC record for "High-Efficiency Back-Contact Back-Junction Silicon Solar Cell" (available at https://url.us.m.mimecastprotect.com/s/84y2C820jmiExEpKc1fZi1?domain=katalogplus.sub.uni-hamburg.de)
GRANEK04	Leuphana Universität Lüneburg MARC record for "High-Efficiency Back Contact Back Junction Silicon Solar Cell"" (available at https://url.us.m.mimecastprotect.com/s/UXYCC9rPknUDPDEpi39IYr?domain=lux.leuphana.de)
GRANEK05	Beacon, "Index of /resources" (available at www.beacon.no/resources/)
GRANEK06	FreiDok Plus: Universitätsbibliothek Freiburg, "High-Efficiency Back-Contact Back-Junction Silicon Solar Cell" (available at https://beacon.no/resources//PhD_Granek_Filip.pdf)
GRANEK07	June 9, 2016 Internet Archive record of http://beacon.no/resources/PhD_Granek_Filip.pdf (available at https://web.archive.org/web/20160609110833/http://beacon.no/resources/PhD_Granek_Filip.pdf)
GRANEK08	July 23, 2013 Internet Archive record of http://beacon.no/resources.html (available at https://web.archive.org/web/20130723163345/https:/www.beacon.no/resources.html)

V. Istratov

18. I have reviewed Exhibit 12, which is "Gettering in Silicon-on-Insulator Wafers: Experimental Studies and Modelling" by Andrei A. Istratov as published in

Semiconductor Science and Technology, June 2005 (hereinafter "Istratov"). It is my opinion that Istratov was publicly accessible at least within six months of its publication in June 2005.

19. Attached hereto as Appendix ISTRATOV03 is a screen capture of a website entitled "Gettering in silicon on insulator wafers: experimental studies and modelling" as hosted on the IOPscience website. I secured these screen captures myself from https://iopscience.iop.org/article/10.1088/0268-1242/20/6/016. This web page, hosted by the publisher of *Semiconductor Science and Technology*, indicates "Gettering in Silicon-on-Insulator Wafers: Experimental Studies and Modelling" was first published as of April 15, 2005.

A. Public Accessibility of Istratov at Pennsylvania State University Library as of June 2005

20. Attached hereto as Appendix ISTRATOV01 is a true and correct copy of the MARC record for *Semiconductor Science and Technology* as held by the Pennsylvania State University library. I secured this record myself from the library's public catalog. The MARC record contained within Appendix ISTRATOV01 accurately describes the title, author, publisher, and ISSN number of *Semiconductor Science and Technology*. The "Availability" field of this record visible on page 5 indicates this collection includes the June 2005 edition of *Semiconductor Science*

and Technology containing "Gettering in Silicon-on-Insulator Wafers: Experimental Studies and Modelling."

21. Attached hereto as Appendix ISTRATOV02 is a true and correct copy of "Gettering in Silicon-on-Insulator Wafers: Experimental Studies and Modelling" as published in *Semiconductor Science and Technology* as held by the Penn State University library. I secured these scans myself from the library's collection. In comparing Exhibit 12 to Appendix ISTRATOV02, I determined that Exhibit 12 is a true and correct copy of "Gettering in Silicon-on-Insulator Wafers: Experimental Studies and Modelling" by Andrei A. Istratov as published in *Semiconductor Science and Technology*, June 2005.

22. The 008 field of the MARC record in Appendix ISTRATOV01 indicates the date of record creation. The 008 field of Appendix ISTRATOV01 indicates the Penn State University library first acquired this journal as of July 9, 1986 and held the journal in perpetuity until 2012. Considering this information, I determined that *Semiconductor Science and Technology* June 2005 and therefore "Gettering in Silicon-on-Insulator Wafers: Experimental Studies and Modelling" was made available to the public shortly after its initial release in June 2005.

* * *

23. Considering this information, I determined that "Gettering in Silicon-on-Insulator Wafers: Experimental Studies and Modelling" by Andrei A. Istratov as

published in *Semiconductor Science and Technology*, June 2005 was first accessible to the public within six months of June 2005, if not earlier, by virtue of being accessible at the Pennsylvania State University library.

VI. Marvin

A. Public Accessibility of Marvin on the NTIS Database as of August 1990

24. Attached hereto as Appendix MARVIN01 is a screen capture of a website entitled "Interdigitated Back Contact Silicon Solar Cell Analysis and Design Recommendations for Space Use" as hosted on the National Technical Reports Library website. I secured these screen captures myself from https://ntrl.ntis.gov/NTRL/dashboard/searchResults/titleDetail/ADA220414.xhtml. Appendix MARVIN01 is a National Technical Information Service (hereby referred to as NTIS) records describing "Interdigitated Back Contact Silicon Solar Cell Analysis and Design Recommendations for Space Use" by D.C. Marvin, S.L. Froedege (hereinafter, the "Marvin paper"). This record indicates that the Marvin paper was published in NTIS Issue Number 16 (1990) and published under the following subject categories: Solar Energy, Unmanned Spacecraft and Manned Spacecraft.

25. Attached hereto as Appendix MARVIN02 is a PDF file entitled Interdigitated Back Contact Silicon Solar Cell Analysis and Design

Recommendations for Space Use" as hosted on the National Technical Reports Library website. I secured this file myself from https://ntrl.ntis.gov/NTRL/dashboard/searchResults/titleDetail/ADA220414.xhtml # by clicking the "Download" option under "Actions." In comparing Appendix MARVIN02 to Exhibit 8, I determined that Exhibit 8 is a true and correct copy of "Interdigitated Back Contact Silicon Solar Cell Analysis and Design Recommendations for Space Use."

26. Page 1 of both Appendix MARVIN02 and Exhibit 8 indicate that this paper is "approved for public release; distribution unlimited" and that this paper was selected for DTIC inclusion as of April 11, 1990. Page 2 of both Appendix MARVIN02 and Exhibit 8 indicates: "This report has been reviewed by the Public Affairs Office (PAS) and is releasable to the National Technical Information Service (NTIS). At NTIS, it will be available to the general public, including foreign nationals." Accordingly, both Appendix MARVIN02 and Exhibit 8 indicate that the Marvin paper was made publicly available at NTIS "for the exchange and stimulation of ideas."

27. Attached hereto as Appendix MARVIN03 is a screen capture of a website entitled "National Technical Reports Library Search Tips" as hosted on the National Technical Reports Library website. I secured these screen captures myself from https://ntrl.ntis.gov/NTRL/help.xhtml. This page contains the following

passage describing the public availability of NTIS holdings: "The first two digits of the Issue Number represent the year of the announcement; while the second two digits represent the NTIS issue in which the title was made publicly available." Appendix MARVIN01 lists the issue number associated with Interdigitated Back Contact Silicon Solar Cell Analysis and Design Recommendations for Space Use" as '199016,' indicating that the Marvin paper was made publicly available by the NTIS as of 1990.

28. Attached hereto as Appendix MARVIN04 is a document from the National Technical Information Service authored by the Associate Director of the National Technical Information Service's Office of Program Management, Wayne Strickland. I was provided this document upon requesting the NTIS to describe the public availability of "Interdigitated Back Contact Silicon Solar Cell Analysis and Design Recommendations for Space Use." This document contains the following passage outlining the availability of the Marvin reference: "The bibliographic reference/abstract was added to the NTIS Bibliographic Database as part of issue 199016 available 'on or about' July 1990. 'On or about' refers to the document being available in the NTIS Database within a month of the date provided above."

29. Attached hereto as Appendix MARVIN05 is a screen capture of a website entitled "About Us" as hosted on the National Technical Reports Library website. I secured these screen captures myself from

https://www.ntis.gov/about/about-us.xhtml. Appendix MARVIN05 is a page describing the mission of the NTIS as follows: "As a bureau within DOC, NTIS has been instrumental for over 70 years in making Federal information and data available to American businesses and the Public." This statement indicates that the stated goal and common practice of the NTIS is to distribute and make publicly available documents such as "Interdigitated Back Contact Silicon Solar Cell Analysis and Design Recommendations for Space Use."

30. Appendix MARVIN01, Appendix MARVIN02, Exhibit 8, Appendix MARVIN03, Appendix MARVIN04, and Appendix MARVIN05 indicate that the Marvin reference was included in, made publicly accessible on, and searchable using the NTIS database within a month of the July 1990 publication of NTIS Issue Number 16 (1990), i.e., by the end of August 1990. As I explain in the following section, the NTIS database was searchable using a number of online tools at least as of February 24, 2013 and July 7, 2013.

B. Public Accessibility of Marvin on Online Searchable Databases as of February 24, 2013 and July 7, 2013

31. Attached hereto as Appendix MARVIN06 is a screen capture of the Internet Archive Wayback Machine entry for https://www.ntis.gov/pdf/dbguid-2013.pdf. I secured these screen captures myself from https://web.archive.org/web/20130224205317/https://www.ntis.gov/pdf/dbguid-

2013.pdf. This record was captured by the Internet Archive as of February 24, 2013. Appendix MARVIN06 is a document describing the services of the NTIS. Page 2 of this Appendix indicates that organizations can subscribe to the National Technical Reports Library featuring "more than 2,000,000 NTIS Database metadata records with links to more than 600,000 corresponding digitized full-text reports." Pages 15-35 of this document indicates that at least the following vendors were offering access to the NTIS database as of February 24, 2013: the National Technical Reports Library, DataStar, Dialog LLC, EBSCO Publishing, Elsevier Engineering Information, Ovid Technologies, ProQuest, SilverPlatter Information, Inc. and STN International.

32. The document found in Appendix MARVIN06 describes the nature of the NTIS database as presented by the National Technical Reports Library—one of the vendors listed above. This document indicates that the National Technical Reports Library is a searchable version of the NTIS database, accessible to members of the general public via subscription access. This National Technical Reports Library version of the NTIS database includes both quick and advanced search features. Given that "Interdigitated Back Contact Silicon Solar Cell Analysis and Design Recommendations for Space Use" had been selected for inclusion in the NTIS database by the time Appendix MARVIN06 was available online, Appendix MARVIN06 indicates the Marvin paper was included in the searchable National

Technical Reports Library online database capable of complex search queries at least as of February 24, 2013. The Marvin reference remains available online on the National Technical Reports Library as shown by Appendix MARVIN01 and Appendix MARVIN02.

33. Attached hereto as Appendix MARVIN07 is a screen capture of the Internet Archive Wayback Machine entry for http://www.ntis.gov/products/ntisdb.aspx. I secured these screen captures myself from https://web.archive.org/web/20130707063952/http:/www.ntis.gov/products/ntisdb.aspx. This record was captured by the Internet Archive as of July 7, 2013.

34. Appendix MARVIN07 is an Internet Archive capture of a web page entitled "NTIS Bibliographic Database" as hosted on the National Technical Information Service. This page describes the various methods that an interested member of the public could use to access the NTIS Bibliographic Database, including via "subscription access" to the National Technical Reports Library as described in Appendix MARVIN06. According to Appendix MARVIN07, the NTIS "[s]ubject coverage includes" various subjects, including "Energy," "Manufacturing Technology," "Materials Sciences," "Physics," "Space Technology," "and Much More." This page further confirms the public accessibility of the NTIS database via the National Technical Reports Library online and therefore "Interdigitated Back

Contact Silicon Solar Cell Analysis and Design Recommendations for Space Use" as of July 7, 2013. The Marvin reference remains available online on the National Technical Reports Library as shown by Appendix MARVIN01 and Appendix MARVIN02.

35. Accordingly, the NTIS database, which included the Marvin reference, would have been searchable by members of the public using the National Technical Reports Library website at least as of February 24, 2013 and July 7, 2013.

* * *

36. Considering this information, I determined that that "Interdigitated Back Contact Silicon Solar Cell Analysis and Design Recommendations for Space Use" by D.C. Marvin and S.L. Froedege was made accessible to the public from August 1990 by virtue of being accessible in the NTIS Database, and from February 24, 2013 and July 7, 2013 by virtue of being accessible online in the National Technical Reports Library, if not earlier.

37. These dates are consistent with my investigation into other locations where the Marvin reference is available. For example, I inquired about the presence of "Interdigitated Back Contact Silicon Solar Cell Analysis and Design Recommendations for Space Use" by D.C. Marvin and S.L. Froedege at the Library of Congress, and I understand that a microfiche copy of the Marvin reference is available on Microfiche at the AD-A number AD-A 220414. Likewise, I inquired

as to the availability of the Marvin reference on the U.S Department of Energy - Office of Scientific and Technical Information (OSTI) website, and I understand that a copy of Marvin was received by the OSTI from the NTRL with a record creation date of August 15, 1990. Both of these sources confirm that the Marvin reference was publicly available through a variety of sources as early as August 15, 1990, and certainly by February 24, 2013 and July 7, 2013.

VII. Granek

A. Public Accessibility of Granek on University Library Websites as of April 7, 2010

38. Attached hereto as Appendix GRANEK01 is a screen capture of a website entitled "High-Efficiency Back-Contact Back-Junction Silicon Solar Cell" as hosted on the FreiDok Plus: Universitätsbibliothek Freiburg website. I secured these screen captures myself from https://freidok.uni-freiburg.de/data/7372. The web page included in Appendix GRANEK01 is a document describing "High-Efficiency Back-Contact Back-Junction Silicon Solar Cell" by Filip Granek (hereinafter, the "Granek dissertation") from the Universitätsbibliothek Freiburg's dissertation and thesis repository. The 'Year of publication' field found on page 1 of this appendix indicates "High-Efficiency Back-Contact Back-Junction Silicon Solar Cell" was first published as of 2009. The "Date of Exam" field present on page 1 of this appendix indicates that this dissertation was presented as of July 30,

2009. This Universitätsbibliothek Freiburg page offers a download of the Granek dissertation via a file link entitled 'Diss_Granek_Filip_2009.pdf'.

39. Attached hereto as Appendix GRANEK02 is a PDF copy of "High-Efficiency Back-Contact Back-Junction Silicon Solar Cell" as presented when following the link entitled 'Diss_Granek_Filip_2009.pdf' on the Universitätsbibliothek Freiburg's record for the Granek dissertation. I secured this PDF copy myself from https://freidok.uni-freiburg.de/jsonApi/v1/download?publicationId=7372&grouping=1. In comparing Appendix GRANEK02 to Exhibit 10, I determined that Exhibit 10 is a true and correct copy of "High-Efficiency Back-Contact Back-Junction Silicon Solar Cell" by Filip Granek.

40. Attached hereto as Appendix GRANEK03 is a true and correct copy of the MARC record for "High-Efficiency Back-Contact Back-Junction Silicon Solar Cell" as held by the Universität Hamburg library. I secured this record myself from the library's public catalog. The MARC record contained within Appendix GRANEK03 accurately describes the title, author and publisher of "High-Efficiency Back-Contact Back-Junction Silicon Solar Cell."

41. The 008 field of the MARC record in Appendix GRANEK03 indicates the date of record creation. The 008 field of Appendix GRANEK03 indicates the

Universität Hamburg library first indexed "High-Efficiency Back-Contact Back-Junction Silicon Solar Cell" as of April 7, 2010.

42. The "Full Text Access" link found on page 1 of Appendix GRANEK03 presents the user with the URL https://freidok.uni-freiburg.de/data/7372, the same Universitätsbibliothek Freiburg's dissertation and thesis repository page describing "High-Efficiency Back-Contact Back-Junction Silicon Solar Cell" included in this declaration as Appendix GRANEK01. The indexing of the Universitätsbibliothek Freiburg's dissertation and thesis repository present in the Universität Hamburg library's MARC record in Appendix GRANEK03 indicates that the Universitätsbibliothek Freiburg was distributing the Granek dissertation as of April 7, 2010 in a form that was publicly accessible when the MARC record at the Universität Hamburg was created.

43. Attached hereto as Appendix GRANEK04 is a true and correct copy of the MARC record for "High-Efficiency Back-Contact Back-Junction Silicon Solar Cell" as held by the Leuphana Universität Lüneburg library. I secured this record myself from the library's public catalog. The MARC record contained within Appendix GRANEK04 accurately describes the title, author and publisher of "High-Efficiency Back-Contact Back-Junction Silicon Solar Cell."

44. The 008 field of the MARC record in Appendix GRANEK04 indicates the date of record creation. The 008 field of Appendix GRANEK04 indicates the

Leuphana Universität Lüneburg library first indexed "High-Efficiency Back-Contact Back-Junction Silicon Solar Cell" as of April 7, 2010.

45. The "Free Full Text Access" link found on page 1 of Appendix GRANEK04 presents the user with the URL https://freidok.uni-freiburg.de/data/7372, the same Universitätsbibliothek Freiburg's dissertation and thesis repository page describing "High-Efficiency Back-Contact Back-Junction Silicon Solar Cell" included in this declaration as Appendix GRANEK01. The indexing of the Universitätsbibliothek Freiburg's dissertation and thesis repository present in the Leuphana Universität Lüneburg library's MARC record in Appendix GRANEK04 indicates that the Universitätsbibliothek Freiburg was distributing the Granek dissertation as of April 7, 2010 in a form that was publicly accessible when the MARC record at the Leuphana Universität Lüneburg library was created.

46. The Universität Hamburg and Leuphana Universität Lüneburg MARC records have a variety of subject fields (689 in total) that would have helped locate the Granek dissertation. Example subject fields include "Solarzelle," "Silicium," and "Fotovoltaik."

47. It is therefore my opinion that the Granek dissertation was publicly accessible online at the Universitätsbibliothek Freiburg, the Universität Hamburg, and the Leuphana Universität Lüneburg libraries' websites at least as of April 7, 2010.

B. Public Accessibility of Granek on Beacon Website as of April 12, 2013 and July 23, 2013

48. Attached hereto as Appendix GRANEK05 is a screen capture of a website entitled "Index of /resources" as hosted on the Beacon website. I secured these screen captures myself from https://beacon.no/resources/. Appendix GRANEK05 is a true and correct copy of the Apache directory page for www.beacon.no/resources/ as of July 5, 2024. This Apache page indicates that the file titled "PhD_Granek_Filip.pdf" was last modified on April 12, 2013.

49. By using Google to search "site: www.beacon.no/resources//," I have confirmed that the webpage www.beacon.no/resources// has been indexed by Google. This page therefore would have been available to the public and a skilled artisan through internet search engines using text searches.

50. Attached hereto as Appendix GRANEK06 is a PDF copy of "High-Efficiency Back-Contact Back-Junction Silicon Solar Cell" as presented when following the link entitled 'PhD_Granek_Filip.pdf' on the Beacon website's Apache directory page. I secured this PDF file from https://beacon.no/resources//PhD_Granek_Filip.pdf. In comparing Appendix GRANEK06 to Exhibit 10, it is my determination that Exhibit 10 is a true and correct copy of "High-Efficiency Back-Contact Back-Junction Silicon Solar Cell" by Filip Granek.

51. Attached hereto as Appendix GRANEK07 is a screen capture of the Internet Archive Wayback Machine entry for http://beacon.no/resources/PhD_Granek_Filip.pdf. I secured these screen captures myself from https://web.archive.org/web/20160609110833/http://beacon.no/resources/PhD_Granek_Filip.pdf. This record was captured as of June 9, 2016.

52. Appendix GRANEK07 is an Internet Archive capture of a web page entitled "PhD_Granek_Filip.pdf" as hosted on the Beacon. In comparing Appendix GRANEK02 to Exhibit 10, I determined that Exhibit 10 is a true and correct copy of "High-Efficiency Back-Contact Back-Junction Silicon Solar Cell" by Filip Granek.

53. Attached hereto as Appendix GRANEK08 is a screen capture of the Internet Archive Wayback Machine entry for http://beacon.no/resources.html. I secured these screen captures myself from https://web.archive.org/web/20130723163345/https:/www.beacon.no/resources.html. This record was captured as of July 23, 2013.

54. Appendix GRANEK08 is an Internet Archive capture of a web page entitled "Resources" as hosted on the Beacon. This page shows a link to the file "PhD_Granel_Filip.pdf," which was last modified on April 12, 2013, as shown in Appendix GRANEK05. Accordingly, the version of "PhD_Granel_Filip.pdf" that

would have been available to a skilled artist visiting beacon.no/resources on July 23, 2013, is the same version attached hereto as Appendix GRANEK06.

55. The Internet Archive uses automated web crawlers to create its archive pages. This is the same technique that search engines, including Google, use to index webpages for search. Thus, because the Wayback Machine has an archive of www.beacon.no/resources from July 23, 2013, it is my opinion that www.beacon.no/resources was accessible through public internet searching or publicly available internet links at least as early as July 23, 2013. At minimum, this page would have been available to skilled artisans through public searching of the Internet Archive as of that date.

* * *

56. Considering this information, I determined that "High-Efficiency Back-Contact Back-Junction Silicon Solar Cell" by Filip Granek was available publicly from at least April 7, 2010 by virtue of being available online availability at the Universitätsbibliothek Freiburg, the Universität Hamburg, and the Leuphana Universität Lüneburg libraries' websites, from at least April 12, 2013 by virtue of being uploaded to the Beacon website Apache server, and from at least July 23, 2013 by virtue of the Beacon website as archived on the Internet Archive, if not earlier.

VIII. CONCLUSION

In signing this Declaration, I recognize that the Declaration will be filed as evidence in a contested case before the Patent Trial and Appeal Board of the United States Patent and Trademark Office. I also recognize that I may be subject to cross examination in the case and that cross examination will take place within the United States. If cross examination is required of me, I will appear for cross examination within the United States during the time allotted for cross examination.

I reserve the right to supplement my opinions in the future to respond to any arguments that Patentee raises and to take into account new information as it becomes accessible to me.

I declare under penalty of perjury that the foregoing is true and correct. I hereby declare that all statements made herein of my own knowledge are true and that all statements made on information and belief are believed to be true; and further that these statements were made the knowledge that willful false statements and the like so made are punishable by fine or imprisonment, or both, under Section 1001 of Title 18 of the United States Code.

Dated: 8/5/2024



June Ann Munford

ISTRATOV01

PennState University Libraries | Catalog

Bookmarks 0 Course Reserves My Account

Keyword Search... Search Advanced search Start Over

Share Bookmark Report an Issue

MARC View

LEADER 14816nas a22016571a 4500
001 320098
003 SIRSI
005 20151212114611.0
008 860709c19869999xx mu 0 0eng d
010 a| 92645812 z| sn87012053
019 a| MARS
022 0 a| 0268-1242
030 a| SSTEET
035 a| LIAS445271
035 a| (OCoLC)13719465
040 d| UtOrBLW
050 0 0 a| QC610.9 b| .S45
245 0 0 a| Semiconductor science and technology.
264 1 a| London, England : b| Institute of Physics, c| [1986-]
264 4 c| ©1986-
300 a| volumes : b| illustrations ; c| 30 cm
310 a| Monthly. b| 1988?-
336 a| text b| txt 2| rdacontent
337 a| unmediated b| n 2| rdamedia
338 a| volume b| nc 2| rdacarrier
362 0 a| Vol. 1, no. 1 (July 1986)-
500 a| Six no. a year, 1986-
500 a| Title from cover.
515 a| Vol. 11, no. 1 (Jan. 1996) misnumbered as v. 10.
550 a| Published in association with the American Institute of Physics.
650 0 a| Semiconductors v| Periodicals.
710 2 a| Institute of Physics (Great Britain)
710 2 a| American Institute of Physics.
936 a| Vol. 6, no. 1 (Jan. 1991) LIC.
949 a| Electronic journal w| ASIS c| 1 i| 320098-2001 d| 1/17/2001 l| ONLINE m| ONLINE r| Y s| Y t| ONLINE u| 4/12/2001
949 a| TK7871.85.S468 v.1 1986 w| LCPER c| 1 i| 000051834920 l| CATO-2 m| UP-ANNEX r| Y s| Y t| PERIODICAL u| 4/9/2003 z| 6340
949 a| TK7871.85.S468 v.2 Jan-June 1987 w| LCPER c| 1 i| 000051834937 l| CATO-2 m| UP-ANNEX r| Y s| Y t| PERIODICAL u| 4/9/2003 z| 6340
949 a| TK7871.85.S468 v.2 July-Dec 1987 w| LCPER c| 1 i| 000051834944 l| CATO-2 m| UP-ANNEX r| Y s| Y t| PERIODICAL u| 4/9/2003 z| 6340
949 a| TK7871.85.S468 v.3 Jan-June 1988 w| LCPER c| 1 i| 000051834951 l| CATO-2 m| UP-ANNEX r| Y s| Y t| PERIODICAL u| 4/9/2003 z| 6340
949 a| TK7871.85.S468 v.3 July-Dec 1988 w| LCPER c| 1 i| 000051834968 l| CATO-2 m| UP-ANNEX r| Y s| Y t| PERIODICAL u| 4/9/2003 z| 6340
949 a| TK7871.85.S468 v.4 Jan-June 1989 w| LCPER c| 1 i| 000051834975 l| CATO-2 m| UP-ANNEX r| Y s| Y t| PERIODICAL u| 4/9/2003 z| 6340
949 a| TK7871.85.S468 v.4 July-Sept 1989 w| LCPER c| 1 i| 000051834982 l| CATO-2 m| UP-ANNEX r| Y s| Y t| PERIODICAL u| 4/9/2003 z| 6340
949 a| TK7871.85.S468 v.4 Oct-Dec 1989 w| LCPER c| 1 i| 000051834999 l| CATO-2 m| UP-ANNEX r| Y s| Y t| PERIODICAL u| 4/9/2003 z| 6340
949 a| TK7871.85.S468 v.5 Jan-Apr 1990 w| LCPER c| 1 i| 000051835002 l| CATO-2 m| UP-ANNEX r| Y s| Y t| PERIODICAL u| 4/9/2003 z| 6340
949 a| TK7871.85.S468 v.5 May-June 1990 w| LCPER c| 1 i| 000051835019 l| CATO-2 m| UP-ANNEX r| Y s| Y t| PERIODICAL u| 4/9/2003 z| 6340
949 a| TK7871.85.S468 v.5 July-Sept 1990 w| LCPER c| 1 i| 000051835026 l| CATO-2 m| UP-ANNEX r| Y s| Y t| PERIODICAL u| 4/9/2003 z| 6340
949 a| TK7871.85.S468 v.5 Oct-Dec 1990 w| LCPER c| 1 i| 000051835033 l| CATO-2 m| UP-ANNEX r| Y s| Y t| PERIODICAL u| 4/9/2003 z| 6340
949 a| TK7871.85.S468 v.6 Jan-Mar 1991 w| LCPER c| 1 i| 000051835040 l| CATO-2 m| UP-ANNEX r| Y s| Y t| PERIODICAL u| 4/9/2003

ASK A LIBRARIAN

z| 6340

949 a| TK7871.85.S468 v.6 Apr-June 1991 w| LCPER c| 1 i| 000051835057 d| 4/28/2005 l| CATO-2 m| UP-ANNEX q| 1 r| Y s| Y t| PERIODICAL u| 4/9/2003 z| 6340

949 a| TK7871.85.S468 v.6 July-Aug 1991 w| LCPER c| 1 i| 000051835064 l| CATO-2 m| UP-ANNEX r| Y s| Y t| PERIODICAL u| 4/9/2003 z| 6340

949 a| TK7871.85.S468 v.6 Sept-Oct 1991 w| LCPER c| 1 i| 000051835071 l| CATO-2 m| UP-ANNEX r| Y s| Y t| PERIODICAL u| 4/9/2003 z| 6340

949 a| TK7871.85.S468 v.6 Nov-Dec 1991 w| LCPER c| 1 i| 000051835088 l| CATO-2 m| UP-ANNEX r| Y s| Y t| PERIODICAL u| 4/9/2003 z| 6340

949 a| TK7871.85.S468 v.7 Jan-Feb 1992 w| LCPER c| 1 i| 000051835095 l| CATO-2 m| UP-ANNEX r| Y s| Y t| PERIODICAL u| 4/9/2003 z| 6340

949 a| TK7871.85.S468 v.7 Mar 1992 w| LCPER c| 1 i| 000051835101 l| CATO-2 m| UP-ANNEX r| Y s| Y t| PERIODICAL u| 4/9/2003 z| 6340

949 a| TK7871.85.S468 v.7 Apr-June 1992 w| LCPER c| 1 i| 000051835118 l| CATO-2 m| UP-ANNEX r| Y s| Y t| PERIODICAL u| 4/9/2003 z| 6340

949 a| TK7871.85.S468 v.7 July-Sept 1992 w| LCPER c| 1 i| 000051835125 l| CATO-2 m| UP-ANNEX r| Y s| Y t| PERIODICAL u| 4/9/2003 z| 6340

949 a| TK7871.85.S468 v.7 Oct-Dec 1992 w| LCPER c| 1 i| 000051835132 l| CATO-2 m| UP-ANNEX r| Y s| Y t| PERIODICAL u| 4/9/2003 z| 6340

949 a| TK7871.85.S468 v.8 Jan 1993 w| LCPER c| 1 i| 000051835149 l| CATO-2 m| UP-ANNEX r| Y s| Y t| PERIODICAL u| 4/9/2003 z| 6340

949 a| TK7871.85.S468 v.8 Feb-Mar 1993 w| LCPER c| 1 i| 000051835156 l| CATO-2 m| UP-ANNEX r| Y s| Y t| PERIODICAL u| 4/9/2003 z| 6340

949 a| TK7871.85.S468 v.8 Apr-May 1993 w| LCPER c| 1 i| 000051835163 l| CATO-2 m| UP-ANNEX r| Y s| Y t| PERIODICAL u| 4/9/2003 z| 6340

949 a| TK7871.85.S468 v.8 June 1993 w| LCPER c| 1 i| 000051835170 l| CATO-2 m| UP-ANNEX r| Y s| Y t| PERIODICAL u| 4/9/2003 z| 6340

949 a| TK7871.85.S468 v.8 July-Sept 1993 w| LCPER c| 1 i| 000051835187 l| CATO-2 m| UP-ANNEX r| Y s| Y t| PERIODICAL u| 4/9/2003 z| 6340

949 a| TK7871.85.S468 v.8 Oct-Dec 1993 w| LCPER c| 1 i| 000051835194 l| CATO-2 m| UP-ANNEX r| Y s| Y t| PERIODICAL u| 4/9/2003 z| 6340

949 a| TK7871.85.S468 v.9 Jan-Mar 1994 w| LCPER c| 1 i| 000051835200 l| CATO-2 m| UP-ANNEX r| Y s| Y t| PERIODICAL u| 4/9/2003 z| 6340

949 a| TK7871.85.S468 v.9 Apr-May 1994 w| LCPER c| 1 i| 000051835217 l| CATO-2 m| UP-ANNEX r| Y s| Y t| PERIODICAL u| 4/9/2003 z| 6340

949 a| TK7871.85.S468 v.9 May suppl. 1994 w| LCPER c| 1 i| 000051835224 l| CATO-2 m| UP-ANNEX r| Y s| Y t| PERIODICAL u| 4/9/2003 z| 6340

949 a| TK7871.85.S468 v.9 June-Aug 1994 w| LCPER c| 1 i| 000051835231 l| CATO-2 m| UP-ANNEX r| Y s| Y t| PERIODICAL u| 4/9/2003 z| 6340

949 a| TK7871.85.S468 v.9 Sept-Oct 1994 w| LCPER c| 1 i| 000051835248 d| 10/22/2003 l| CATO-2 m| UP-ANNEX q| 1 r| Y s| Y t| PERIODICAL u| 4/9/2003 z| 6340

949 a| TK7871.85.S468 v.9 Nov-Dec 1994 w| LCPER c| 1 i| 000051835255 l| CATO-2 m| UP-ANNEX r| Y s| Y t| PERIODICAL u| 4/9/2003 z| 6340

949 a| TK7871.85.S468 v.10 Jan-Mar 1995 w| LCPER c| 1 i| 000051835262 l| CATO-2 m| UP-ANNEX r| Y s| Y t| PERIODICAL u| 4/9/2003 z| 6340

949 a| TK7871.85.S468 v.10 Apr-June 1995 w| LCPER c| 1 i| 000051835279 d| 10/22/2003 l| CATO-2 m| UP-ANNEX q| 1 r| Y s| Y t| PERIODICAL u| 4/9/2003 z| 6340

949 a| TK7871.85.S468 v.10 July-Sept 1995 w| LCPER c| 1 i| 000051835286 l| CATO-2 m| UP-ANNEX r| Y s| Y t| PERIODICAL u| 4/9/2003 z| 6340

949 a| TK7871.85.S468 v.10 Oct-Dec 1995 w| LCPER c| 1 i| 000051835293 l| CATO-2 m| UP-ANNEX r| Y s| Y t| PERIODICAL u| 4/9/2003 z| 6340

949 a| TK7871.85.S468 v.11 Jan-Mar 1996 w| LCPER c| 1 i| 000051835446 l| CATO-2 m| UP-ANNEX r| Y s| Y t| PERIODICAL u| 4/9/2003 z| 6340

949 a| TK7871.85.S468 v.11 Apr-June 1996 w| LCPER c| 1 i| 000051835309 l| CATO-2 m| UP-ANNEX r| Y s| Y t| PERIODICAL u| 4/9/2003 z| 6340

949 a| TK7871.85.S468 v.11 July-Sept 1996 w| LCPER c| 1 i| 000051835316 l| CATO-2 m| UP-ANNEX r| Y s| Y t| PERIODICAL u| 4/9/2003 z| 6340

949 a| TK7871.85.S468 v.11 Oct-Dec 1996 w| LCPER c| 1 i| 000051835323 l| CATO-2 m| UP-ANNEX r| Y s| Y t| PERIODICAL u| 4/9/2003 z| 6340

949 a| TK7871.85.S468 v.12 Jan-Mar 1997 w| LCPER c| 1 i| 000051835330 l| CATO-2 m| UP-ANNEX r| Y s| Y t| PERIODICAL u| 4/9/2003 z| 6340

949 a| TK7871.85.S468 v.12 Apr-June 1997 w| LCPER c| 1 i| 000051835347 l| CATO-2 m| UP-ANNEX r| Y s| Y t| PERIODICAL u| 4/9/2003 z| 6340

949 a| TK7871.85.S468 v.12 July-Sept 1997 w| LCPER c| 1 i| 000051835354 d| 4/28/2006 l| CATO-2 m| UP-ANNEX q| 1 r| Y s| Y t| PERIODICAL u| 4/9/2003 z| 6340

949 a| TK7871.85.S468 v.12 Oct-Dec 1997 w| LCPER c| 1 i| 000051835361 l| CATO-2 m| UP-ANNEX r| Y s| Y t| PERIODICAL u| 4/9/2003 z| 6340

949 a| TK7871.85.S468 v.13 Jan-Mar 1998 w| LCPER c| 1 i| 000051835378 l| CATO-2 m| UP-ANNEX r| Y s| Y t| PERIODICAL u| 4/9/2003

z| 6340

949 a| TK7871.85.S468 v.13 Apr-June 1998 w| LCPER c| 1 i| 000051835385 l| CATO-2 m| UP-ANNEX r| Y s| Y t| PERIODICAL u| 4/9/2003 z| 6340

949 a| TK7871.85.S468 v.13 July-Sept 1998 w| LCPER c| 1 i| 000051835392 l| CATO-2 m| UP-ANNEX r| Y s| Y t| PERIODICAL u| 4/9/2003 z| 6340

949 a| TK7871.85.S468 v.13 Oct-Dec 1998 w| LCPER c| 1 i| 000051835408 l| CATO-2 m| UP-ANNEX r| Y s| Y t| PERIODICAL u| 4/9/2003 z| 6340

949 a| TK7871.85.S468 v.14 Jan-Mar 1999 w| LCPER c| 1 i| 000051835415 l| CATO-2 m| UP-ANNEX r| Y s| Y t| PERIODICAL u| 4/9/2003 z| 6340

949 a| TK7871.85.S468 v.14 Apr-June 1999 w| LCPER c| 1 i| 000051835422 l| CATO-2 m| UP-ANNEX r| Y s| Y t| PERIODICAL u| 4/9/2003 z| 6340

949 a| TK7871.85.S468 v.14 July-Dec 1999 w| LCPER c| 1 i| 000051835439 l| CATO-2 m| UP-ANNEX r| Y s| Y t| PERIODICAL u| 4/9/2003 z| 6340

949 a| TK7871.85.S468 v.15 Jan-Mar 2000 w| LCPER c| 1 i| 000047189706 l| CATO-2 m| UP-ANNEX r| Y s| Y t| PERIODICAL u| 3/25/2012 z| 7772

949 a| TK7871.85.S468 v.15 Apr-June 2000 w| LCPER c| 1 i| 000047186880 l| CATO-2 m| UP-ANNEX r| Y s| Y t| PERIODICAL u| 3/25/2012 z| 7772

949 a| TK7871.85.S468 v.15 July-Sept 2000 w| LCPER c| 1 i| 000048260695 l| CATO-2 m| UP-ANNEX r| Y s| Y t| PERIODICAL u| 12/18/2001 z| 7772

949 a| TK7871.85.S468 v.15 Oct-Dec 2000 w| LCPER c| 1 i| 000048260671 d| 1/17/2001 l| CATO-2 m| UP-ANNEX r| Y s| Y t| PERIODICAL u| 4/12/2001 z| 7772

949 a| TK7871.85.S468 v.16 Jan-Mar 2001 w| LCPER c| 1 i| 000048260688 l| CATO-2 m| UP-ANNEX r| Y s| Y t| PERIODICAL u| 12/18/2001 z| 7772

949 a| TK7871.85.S468 v.16 Apr-June 2001 w| LCPER c| 1 i| 000048418218 l| CATO-2 m| UP-ANNEX r| Y s| Y t| PERIODICAL u| 10/25/2002 z| 7772

949 a| TK7871.85.S468 v.16 July-Sept 2001 w| LCPER c| 1 i| 000048418225 l| CATO-2 m| UP-ANNEX r| Y s| Y t| PERIODICAL u| 10/25/2002 z| 7772

949 a| TK7871.85.S468 v.16 Oct-Dec 2001 w| LCPER c| 1 i| 000048418201 l| CATO-2 m| UP-ANNEX r| Y s| Y t| PERIODICAL u| 10/25/2002 z| 7772

949 a| TK7871.85.S468 v.17 Jan-Mar 2002 w| LCPER c| 1 i| 000048418195 l| CATO-2 m| UP-ANNEX r| Y s| Y t| PERIODICAL u| 10/25/2002 z| 7772

949 a| TK7871.85.S468 v.17 Apr-June 2002 w| LCPER c| 1 i| 000052501982 l| CATO-2 m| UP-ANNEX r| Y s| Y t| PERIODICAL u| 6/18/2003 z| 7772

949 a| TK7871.85.S468 v.17July-Sept 2002 w| LCPER c| 1 i| 000052501999 l| CATO-2 m| UP-ANNEX r| Y s| Y t| PERIODICAL u| 6/18/2003 z| 7772

949 a| TK7871.85.S468 v.17 Oct-Dec 2002 w| LCPER c| 1 i| 000052502002 l| CATO-2 m| UP-ANNEX r| Y s| Y t| PERIODICAL u| 6/18/2003 z| 7772

949 a| TK7871.85.S468 v.18 Jan-Mar 2003 w| LCPER c| 1 i| 000052806247 l| CATO-2 m| UP-ANNEX r| Y s| Y t| PERIODICAL u| 3/2/2004 z| 7772

949 a| TK7871.85.S468 v.18 Apr-June 2003 w| LCPER c| 1 i| 000052806131 l| CATO-2 m| UP-ANNEX r| Y s| Y t| PERIODICAL u| 3/2/2004 z| 7772

949 a| TK7871.85.S468 v.18 July-Sept 2003 w| LCPER c| 1 i| 000052806117 l| CATO-2 m| UP-ANNEX r| Y s| Y t| PERIODICAL u| 3/2/2004 z| 7772

949 a| TK7871.85.S468 v.18 Oct-Dec 2003 w| LCPER c| 1 i| 000052806124 l| CATO-2 m| UP-ANNEX r| Y s| Y t| PERIODICAL u| 3/2/2004 z| 7772

949 a| TK7871.85.S468 v.19 Jan-Mar 2004 w| LCPER c| 1 i| 000054823914 l| CATO-2 m| UP-ANNEX r| Y s| Y t| PERIODICAL u| 2/18/2005 z| 7772

949 a| TK7871.85.S468 v.19 Apr 2004 w| LCPER c| 1 i| 000054823891 l| CATO-2 m| UP-ANNEX r| Y s| Y t| PERIODICAL u| 2/18/2005 z| 7772

949 a| TK7871.85.S468 v.19 May-June 2004 w| LCPER c| 1 i| 000054823907 l| CATO-2 m| UP-ANNEX r| Y s| Y t| PERIODICAL u| 2/18/2005 z| 7772

949 a| TK7871.85.S468 v.19 July Sept 2004 w| LCPER c| 1 i| 000054823877 l| CATO-2 m| UP-ANNEX r| Y s| Y t| PERIODICAL u| 2/18/2005 z| 7772

949 a| TK7871.85.S468 v.19 Oct-Dec 2004 w| LCPER c| 1 i| 000054823884 l| CATO-2 m| UP-ANNEX r| Y s| Y t| PERIODICAL u| 2/18/2005 z| 7772

949 a| TK7871.85.S468 v.20 Jan-Mar 2005 w| LCPER c| 1 i| 000054977747 l| CATO-2 m| UP-ANNEX r| Y s| Y t| PERIODICAL u| 4/18/2006 z| 7772

949 a| TK7871.85.S468 v.20 Apr-June 2005 w| LCPER c| 1 i| 000054977822 l| CATO-2 m| UP-ANNEX r| Y s| Y t| PERIODICAL u| 4/18/2006 z| 7772

949 a| TK7871.85.S468 v.20 July-Sept 2005 w| LCPER c| 1 i| 000054977662 l| CATO-2 m| UP-ANNEX r| Y s| Y t| PERIODICAL u| 4/18/2006 z| 7772

949 a| TK7871.85.S468 v.20 Oct-Dec 2005 w| LCPER c| 1 i| 000054977785 l| CATO-2 m| UP-ANNEX r| Y s| Y t| PERIODICAL u| 4/18/2006 z| 7772

949 a| TK7871.85.S468 v.21 Jan-Mar 2006 w| LCPER c| 1 i| 000055199155 l| CATO-2 m| UP-ANNEX r| Y s| Y t| PERIODICAL u| 3/8/2007 z| 7772

949 a| TK7871.85.S468 v.21 Apr-June 2006 w| LCPER c| 1 i| 000055199148 l| CATO-2 m| UP-ANNEX r| Y s| Y t| PERIODICAL u| 3/8/2007 z| 7772

949 a| TK7871.85.S468 v.21 July-Sept 2006 w| LCPER c| 1 i| 000055199162 l| CATO-2 m| UP-ANNEX r| Y s| Y t| PERIODICAL u| 3/8/2007 z| 7772

949 a| TK7871.85.S468 v.21 Oct-Dec 2006 w| LCPER c| 1 i| 000055199179 l| CATO-2 m| UP-ANNEX r| Y s| Y t| PERIODICAL u| 3/8/2007 z| 7772

949 a| TK7871.85.S468 v.22 Jan-Mar 2007 w| LCPER c| 1 i| 000059636434 l| CATO-2 m| UP-ANNEX r| Y s| Y t| PERIODICAL u| 5/9/2008 z| 7772

949 a| TK7871.85.S468 v.22 Apr-June 2007 w| LCPER c| 1 i| 000059636427 l| CATO-2 m| UP-ANNEX r| Y s| Y t| PERIODICAL u| 5/9/2008 z| 7772

949 a| TK7871.85.S468 v.22 July-Sept 2007 w| LCPER c| 1 i| 000059636410 l| CATO-2 m| UP-ANNEX r| Y s| Y t| PERIODICAL u| 5/9/2008 z| 7772

949 a| TK7871.85.S468 v.22 Oct-Dec 2007 w| LCPER c| 1 i| 000059636441 l| CATO-2 m| UP-ANNEX r| Y s| Y t| PERIODICAL u| 5/9/2008 z| 7772

949 a| TK7871.85.S468 v.23 Jan-Mar 2008 w| LCPER c| 1 i| 000059801313 l| CATO-2 m| UP-ANNEX r| Y s| Y t| PERIODICAL u| 2/27/2009 z| 7772

949 a| TK7871.85.S468 v.23 Apr-June 2008 w| LCPER c| 1 i| 000059801290 l| CATO-2 m| UP-ANNEX r| Y s| Y t| PERIODICAL u| 2/27/2009 z| 7772

949 a| TK7871.85.S468 v.23 July-Sept 2008 w| LCPER c| 1 i| 000059801320 l| CATO-2 m| UP-ANNEX r| Y s| Y t| PERIODICAL u| 4/6/2009 z| 7772

949 a| TK7871.85.S468 v.23 Oct-Dec 2008 w| LCPER c| 1 i| 000059801306 l| CATO-2 m| UP-ANNEX r| Y s| Y t| PERIODICAL u| 2/27/2009 z| 7772

949 a| TK7871.85.S468 v.24 Jan-Mar 2009 w| LCPER c| 1 i| 000061848788 l| CATO-2 m| UP-ANNEX r| Y s| Y t| PERIODICAL u| 2/9/2010 z| 7772

949 a| TK7871.85.S468 v.24 Apr-June 2009 w| LCPER c| 1 i| 000061848634 l| CATO-2 m| UP-ANNEX r| Y s| Y t| PERIODICAL u| 2/9/2010 z| 7772

949 a| TK7871.85.S468 v.24 July-Sept 2009 w| LCPER c| 1 i| 000061848641 l| CATO-2 m| UP-ANNEX r| Y s| Y t| PERIODICAL u| 2/9/2010 z| 7772

949 a| TK7871.85.S468 v.24 Oct-Dec 2009 w| LCPER c| 1 i| 000061848627 l| CATO-2 m| UP-ANNEX r| Y s| Y t| PERIODICAL u| 2/9/2010 z| 7772

949 a| TK7871.85.S468 v.25 no.1-3 2010 w| LCPER c| 1 i| 000061817098 l| CATO-2 m| UP-ANNEX r| Y s| Y t| PERIODICAL u| 2/17/2011 z| 7772

949 a| TK7871.85.S468 v.25 no.4-6 2010 w| LCPER c| 1 i| 000061817081 l| CATO-2 m| UP-ANNEX r| Y s| Y t| PERIODICAL u| 2/18/2011 z| 7772

949 a| TK7871.85.S468 v.25 no.7-9 2010 w| LCPER c| 1 i| 000061817104 l| CATO-2 m| UP-ANNEX r| Y s| Y t| PERIODICAL u| 2/18/2011 z| 7772

949 a| TK7871.85.S468 v.25 no.10-12 2010 w| LCPER c| 1 i| 000061817128 l| CATO-2 m| UP-ANNEX r| Y s| Y t| PERIODICAL u| 2/18/2011 z| 7772

949 a| TK7871.85.S468 v.26 no.1-3 2011 w| LCPER c| 1 i| 000059377269 d| 3/26/2012 e| 2/26/2012 l| CATO-2 m| UP-ANNEX r| Y s| Y t| PERIODICAL u| 2/26/2012 z| 7772

949 a| TK7871.85.S468 v.26 no.4-6 2011 w| LCPER c| 1 i| 000059377290 d| 3/26/2012 e| 2/26/2012 l| CATO-2 m| UP-ANNEX r| Y s| Y t| PERIODICAL u| 2/26/2012 z| 7772

949 a| TK7871.85.S468 v.26 no.7-9 2011 w| LCPER c| 1 i| 000059377283 d| 3/26/2012 e| 2/26/2012 l| CATO-2 m| UP-ANNEX r| Y s| Y t| PERIODICAL u| 2/26/2012 z| 7772

949 a| TK7871.85.S468 v.26 no.10-12 2011 w| LCPER c| 1 i| 000059377276 d| 3/26/2012 e| 2/26/2012 l| CATO-2 m| UP-ANNEX r| Y s| Y t| PERIODICAL u| 2/26/2012 z| 7772

949 a| TK7871.85.S468 v.27 no.1-3 2012 w| LCPER c| 1 i| 000059453949 d| 12/3/2012 e| 11/4/2012 l| CATO-2 m| UP-ANNEX r| Y s| Y t| PERIODICAL u| 11/4/2012 z| 7772

949 a| TK7871.85.S468 v.27 no.4-6 2012 w| LCPER c| 1 i| 000059453932 d| 12/3/2012 e| 11/4/2012 l| CATO-2 m| UP-ANNEX r| Y s| Y t| PERIODICAL u| 11/4/2012 z| 7772

949 a| TK7871.85.S468 v.27 no.7-9 2012 w| LCPER c| 1 i| 000059461180 d| 2/10/2013 e| 1/13/2013 l| CATO-2 m| UP-ANNEX r| Y s| Y t| PERIODICAL u| 1/13/2013 z| 7772

949 a| TK7871.85.S468 v.27 no.10-12 2012 w| LCPER c| 1 i| 000059461173 d| 2/10/2013 e| 1/13/2013 l| CATO-2 m| UP-ANNEX r| Y s| Y t| PERIODICAL u| 1/13/2013 z| 7772

852 0 1 a| PSt b| UP-ANNEX c| ANNEX h| TK7871.85 i| .S468

866 0 8| 0 a| v.1(1986)-v.27(2012)

PennState

Copyright @2019 The Pennsylvania State University. All rights reserved. Except where otherwise noted, this work is subject to a Creative Commons Attribution 4.0 license. Details and exceptions.

Legal Statements | PSU Hostlens

PENN STATE UNIVERSITY LIBRARIES

Libraries Home (814) 865-6368
Libraries Intranet (Staff Only)
Accessibility Help
Website Feedback
Policies and Guidelines
Staff Directory

CONNECT WITH PENN STATE UNIVERSITY LIBRARIES

Facebook
Twitter
Instagram

Semiconductor science and technology

Published	London, England : Institute of Physics, [1986-]
Copyright Date	©1986-
Physical Description	volumes : illustrations ; 30 cm
Additional Creators	Institute of Physics (Great Britain) and American Institute of Physics

ASK A LIBRARIAN

Availability

Browse Nearby on Shelf I Want It

Library Storage (106 items)

Call number	Material	Location
Annexed Material: Holdings Summary v.1(1986)-v.27(2012)		
TK7871.85.S468 v.1 1986	Bound Journal	Annexed Material
TK7871.85.S468 v.2 Jan-June 1987	Bound Journal	Annexed Material
TK7871.85.S468 v.2 July-Dec 1987	Bound Journal	Annexed Material
TK7871.85.S468 v.3 Jan-June 1988	Bound Journal	Annexed Material
TK7871.85.S468 v.3 July-Dec 1988	Bound Journal	Annexed Material
TK7871.85.S468 v.4 Jan-June 1989	Bound Journal	Annexed Material
TK7871.85.S468 v.4 July-Sept 1989	Bound Journal	Annexed Material
TK7871.85.S468 v.4 Oct-Dec 1989	Bound Journal	Annexed Material
TK7871.85.S468 v.5 Jan-Apr 1990	Bound Journal	Annexed Material
TK7871.85.S468 v.5 July-Sept 1990	Bound Journal	Annexed Material
TK7871.85.S468 v.5 May-June 1990	Bound Journal	Annexed Material
TK7871.85.S468 v.5 Oct-Dec 1990	Bound Journal	Annexed Material
TK7871.85.S468 v.6 Apr-June 1991	Bound Journal	Annexed Material
TK7871.85.S468 v.6 Jan-Mar 1991	Bound Journal	Annexed Material
TK7871.85.S468 v.6 July-Aug 1991	Bound Journal	Annexed Material
TK7871.85.S468 v.6 Nov-Dec 1991	Bound Journal	Annexed Material
TK7871.85.S468 v.6 Sept-Oct 1991	Bound Journal	Annexed Material
TK7871.85.S468 v.7 Mar 1992	Bound Journal	Annexed Material
TK7871.85.S468 v.7 Apr-June 1992	Bound Journal	Annexed Material
TK7871.85.S468 v.7 Jan-Feb 1992	Bound Journal	Annexed Material
TK7871.85.S468 v.7 July-Sept 1992	Bound Journal	Annexed Material
TK7871.85.S468 v.7 Oct-Dec 1992	Bound Journal	Annexed Material
TK7871.85.S468 v.8 Jan 1993	Bound Journal	Annexed Material
TK7871.85.S468 v.8 June 1993	Bound Journal	Annexed Material
TK7871.85.S468 v.8 Apr-May 1993	Bound Journal	Annexed Material
TK7871.85.S468 v.8 Feb-Mar 1993	Bound Journal	Annexed Material
TK7871.85.S468 v.8 July-Sept 1993	Bound Journal	Annexed Material
TK7871.85.S468 v.8 Oct-Dec 1993	Bound Journal	Annexed Material

TK7871.85.S468 v.9 May suppl. 1994	Bound Journal	Annexed Material
TK7871.85.S468 v.9 Apr-May 1994	Bound Journal	Annexed Material
TK7871.85.S468 v.9 Jan-Mar 1994	Bound Journal	Annexed Material
TK7871.85.S468 v.9 June-Aug 1994	Bound Journal	Annexed Material
TK7871.85.S468 v.9 Nov-Dec 1994	Bound Journal	Annexed Material
TK7871.85.S468 v.9 Sept-Oct 1994	Bound Journal	Annexed Material
TK7871.85.S468 v.10 Apr-June 1995	Bound Journal	Annexed Material
TK7871.85.S468 v.10 Jan-Mar 1995	Bound Journal	Annexed Material
TK7871.85.S468 v.10 July-Sept 1995	Bound Journal	Annexed Material
TK7871.85.S468 v.10 Oct-Dec 1995	Bound Journal	Annexed Material
TK7871.85.S468 v.11 Apr-June 1996	Bound Journal	Annexed Material
TK7871.85.S468 v.11 Jan-Mar 1996	Bound Journal	Annexed Material
TK7871.85.S468 v.11 July-Sept 1996	Bound Journal	Annexed Material
TK7871.85.S468 v.11 Oct-Dec 1996	Bound Journal	Annexed Material
TK7871.85.S468 v.12 Apr-June 1997	Bound Journal	Annexed Material
TK7871.85.S468 v.12 Jan-Mar 1997	Bound Journal	Annexed Material
TK7871.85.S468 v.12 July-Sept 1997	Bound Journal	Annexed Material
TK7871.85.S468 v.12 Oct-Dec 1997	Bound Journal	Annexed Material
TK7871.85.S468 v.13 Apr-June 1998	Bound Journal	Annexed Material
TK7871.85.S468 v.13 Jan-Mar 1998	Bound Journal	Annexed Material
TK7871.85.S468 v.13 July-Sept 1998	Bound Journal	Annexed Material
TK7871.85.S468 v.13 Oct-Dec 1998	Bound Journal	Annexed Material
TK7871.85.S468 v.14 Apr-June 1999	Bound Journal	Annexed Material
TK7871.85.S468 v.14 Jan-Mar 1999	Bound Journal	Annexed Material
TK7871.85.S468 v.14 July-Dec 1999	Bound Journal	Annexed Material
TK7871.85.S468 v.15 Apr-June 2000	Bound Journal	Annexed Material
TK7871.85.S468 v.15 Jan-Mar 2000	Bound Journal	Annexed Material
TK7871.85.S468 v.15 July-Sept 2000	Bound Journal	Annexed Material
TK7871.85.S468 v.15 Oct-Dec 2000	Bound Journal	Annexed Material
TK7871.85.S468 v.16 Apr-June 2001	Bound Journal	Annexed Material
TK7871.85.S468 v.16 Jan-Mar 2001	Bound Journal	Annexed Material
TK7871.85.S468 v.16 July-Sept 2001	Bound Journal	Annexed Material
TK7871.85.S468 v.16 Oct-Dec 2001	Bound Journal	Annexed Material
TK7871.85.S468 v.17 Apr-June 2002	Bound Journal	Annexed Material
TK7871.85.S468 v.17 Jan-Mar 2002	Bound Journal	Annexed Material
TK7871.85.S468 v.17 Oct-Dec 2002	Bound Journal	Annexed Material
TK7871.85.S468 v.17July-Sept 2002	Bound Journal	Annexed Material
TK7871.85.S468 v.18 Apr-June 2003	Bound Journal	Annexed Material
TK7871.85.S468 v.18 Jan-Mar 2003	Bound Journal	Annexed Material
TK7871.85.S468 v.18 July-Sept 2003	Bound Journal	Annexed Material
TK7871.85.S468 v.18 Oct-Dec 2003	Bound Journal	Annexed Material
TK7871.85.S468 v.19 July Sept 2004	Bound Journal	Annexed Material
TK7871.85.S468 v.19 Apr 2004	Bound Journal	Annexed Material
TK7871.85.S468 v.19 Jan-Mar 2004	Bound Journal	Annexed Material
TK7871.85.S468 v.19 May-June 2004	Bound Journal	Annexed Material
TK7871.85.S468 v.19 Oct-Dec 2004	Bound Journal	Annexed Material
TK7871.85.S468 v.20 Apr-June 2005	Bound Journal	Being transferred between libraries
TK7871.85.S468 v.20 Jan-Mar 2005	Bound Journal	Annexed Material
TK7871.85.S468 v.20 July-Sept 2005	Bound Journal	Annexed Material

TK7871.85.S468 v.20 Oct-Dec 2005	Bound Journal	Annexed Material
TK7871.85.S468 v.21 Apr-June 2006	Bound Journal	Annexed Material
TK7871.85.S468 v.21 Jan-Mar 2006	Bound Journal	Annexed Material
TK7871.85.S468 v.21 July-Sept 2006	Bound Journal	Annexed Material
TK7871.85.S468 v.21 Oct-Dec 2006	Bound Journal	Annexed Material
TK7871.85.S468 v.22 Apr-June 2007	Bound Journal	Annexed Material
TK7871.85.S468 v.22 Jan-Mar 2007	Bound Journal	Annexed Material
TK7871.85.S468 v.22 July-Sept 2007	Bound Journal	Annexed Material
TK7871.85.S468 v.22 Oct-Dec 2007	Bound Journal	Annexed Material
TK7871.85.S468 v.23 Apr-June 2008	Bound Journal	Annexed Material
TK7871.85.S468 v.23 Jan-Mar 2008	Bound Journal	Annexed Material
TK7871.85.S468 v.23 July-Sept 2008	Bound Journal	Annexed Material
TK7871.85.S468 v.23 Oct-Dec 2008	Bound Journal	Annexed Material
TK7871.85.S468 v.24 Apr-June 2009	Bound Journal	Annexed Material
TK7871.85.S468 v.24 Jan-Mar 2009	Bound Journal	Annexed Material
TK7871.85.S468 v.24 July-Sept 2009	Bound Journal	Annexed Material
TK7871.85.S468 v.24 Oct-Dec 2009	Bound Journal	Annexed Material
TK7871.85.S468 v.25 no.1-3 2010	Bound Journal	Annexed Material
TK7871.85.S468 v.25 no.4-6 2010	Bound Journal	Annexed Material
TK7871.85.S468 v.25 no.7-9 2010	Bound Journal	Annexed Material
TK7871.85.S468 v.25 no.10-12 2010	Bound Journal	Annexed Material
TK7871.85.S468 v.26 no.1-3 2011	Bound Journal	Annexed Material
TK7871.85.S468 v.26 no.4-6 2011	Bound Journal	Annexed Material
TK7871.85.S468 v.26 no.7-9 2011	Bound Journal	Annexed Material
TK7871.85.S468 v.26 no.10-12 2011	Bound Journal	Annexed Material
TK7871.85.S468 v.27 no.1-3 2012	Bound Journal	Annexed Material
TK7871.85.S468 v.27 no.4-6 2012	Bound Journal	Annexed Material
TK7871.85.S468 v.27 no.7-9 2012	Bound Journal	Annexed Material
TK7871.85.S468 v.27 no.10-12 2012	Bound Journal	Annexed Material

Dates of Publication and/or Sequential Designation
Vol. 1, no. 1 (July 1986)-

Subject(s)
Semiconductors—Periodicals

ISSN
0268-1242

Publication Frequency
Monthly. 1988?-

Note
Six no. a year, 1986-
Title from cover.

Special Numbering
Vol. 11, no. 1 (Jan. 1996) misnumbered as v. 10.

Issuing Body
Published in association with the American Institute of Physics.

View MARC record | catkey: 320098

PennState
Copyright @2019 The Pennsylvania State University. All rights reserved. Except where otherwise noted, this work is subject to a Creative Commons Attribution 4.0 license. Details and
PENN STATE UNIVERSITY LIBRARIES
Libraries Home (814) 865-6268
CONNECT WITH PENN STATE UNIVERSITY LIBRARIES


exceptions
Legal Statements
PSU Hotlines
Libraries Intranet (Sta
Only)
Accessibility Help
Website Feedback
Policies and Guideline
Staff Directory
Facebook
Twitter
Instagram

ISTRATOV02

ISTRATOV02 - 2

SEMICONDUCTOR SCIENCE AND TECHNOLOGY
20 APR-JUNE 2005
ENGIN TK7871 .85 .S468

SHELVED IN
BOUND
PERIODICAL
COLLECTION

ENGINEERING LIBRARY

ISSN 0268-1242

P

Semiconductor Science and Technology



Volume 20 Number 6 June 2005

Topical review: Trions in GaAs quantum wells
I Bar-Joseph

Online: www.iop.org/journals/sst

ISTRATOV02 - 5

Institute of Physics PUBLISHING

Semiconductor Science and Technology

Volume 20 Number 6 June 2005

TOPICAL REVIEW

R29 **Trions in GaAs quantum wells**
I Bar-Joseph

PAPERS

481 **Improvement of the radiation hardness of SIMOX buried layers using nitrogen implantation**
Z-S Zheng, Z-L Liu, G-Q Zhang, N Li, G-H Li, H-Z Ma, E-X Zhang, Z-X Zhang and X Wang

485 **High detectivity GaN metal–semiconductor–metal UV photodetectors with transparent tungsten electrodes**
C K Wang, S J Chang, Y K Su, Y Z Chiou, C S Chang, T K Lin, H L Liu and J J Tang

490 **Effect of well width on the electro-optical properties of a quantum well**
A Joshua and V Venkataraman

496 **Semiconducting $AgSbSe_2$ thin film and its application in a photovoltaic structure**
K Bindu, José Campos, M T S Nair, A Sánchez and P K Nair

505 **Theoretical analysis of multi-transverse-mode characteristics of vertical-cavity surface-emitting lasers**
X Li, W Pan, B Luo, D Ma and G Deng

514 **Effective generation lifetime depth profile in InAs quantum dots grown on InAlAs/InP(0 0 1)**
R Ajjel, M Baira, H Maaref, B Salem, G Brémond and M Gendry

519 **Electrical characteristics improvement of oxygen-annealed MOCVD-TiO_2 films**
M-K Lee, J-J Huang and T-S Wu

524 **A physical model for silicon anisotropic chemical etching**
Y Jiang and Q-a Huang

532 **A simple model for analysing the effects of band non-parabolicity in nanostructures**
J A López-Villanueva, J A Jiménez-Tejada, A Palma, S Rodríguez Bolívar and J E Carceller

540 **Study on GaN epilayer by infrared spectroscopic ellipsometry**
J Wang, X Y Li, J Liu and Z M Huang

544 **Monolithic integration of an InGaAsP–InP strained DFB laser and an electroabsorption modulator by ultra-low-pressure selective-area-growth MOCVD**
Q Zhao, J Q Pan, F Zhou, B J Wang, L F Wang and W Wang

548 **Comprehension and modelling of heterojunction phototransistors operated in the Gummel-plot and common-emitter modes**
H R Chen, W T Chen, M K Hsu, S W Tan and W S Lour

555 **CVD diamond devices for charged particle detection**
M Zhang, Y Xia, L Wang and B Gu

559 **SiGe δ-channel field-effect transistors on SIMOX substrates**
S L Wu

563 **Comparison of thermal characteristics of antimonide and phosphide MQW lasers**
C Zhu, Y G Zhang, A Z Li and Y L Zheng

568 **Gettering in silicon-on-insulator wafers: experimental studies and modelling**
A A Istratov, H Väinölä, W Huber and E R Weber

576 **Structural, optical and electrical properties of chemically deposited silver sulfide thin films**
A Núñez Rodríguez, M T S Nair and P K Nair

586 **A new method for determination of parasitic capacitances for PHEMTs**
J Gao, X Li, H Wang and G Boeck

(Continued on inside back cover)

Bibliographic codes CODEN: SSTEET 20 (6) R29–R40, 481–658 (2005) ISSN: 0268-1242

(Continued from outside back cover)

592 **Polar interface optical phonon modes and Fröhlich electron–phonon interaction Hamiltonians in wurtzite quantum well wires**
L Zhang and J-j Shi

601 **Improving high-temperature performance in continuous-wave mode InGaAsN/GaAsN ridge waveguide lasers**
Y-A Chang, H-C Kuo, C-Y Lu, Y-K Kuo and S-C Wang

606 **Back-to-back Schottky diode adopted for the measurement of GaN films and its Schottky contacts**
Q Luo, J Du, M Yang, L Wang, T Jin and Q Yu

611 **Ohmic contacts to moderately doped semiconductors—are they really Ohmic or low-barrier Schottky contacts?**
J Osvald

615 **Luminescent properties of annealed and directly wafer-bonded InAsP/InGaAsP multiple quantum wells**
Y-F Lao, H Wu and Z-c Huang

621 **High-power 808 nm lasers with a super-large optical cavity**
A Knauer, G Erbert, R Staske, B Sumpf, H Wenzel and M Weyers

625 **Temperature dependence of electrical parameters of the Au/n-InP Schottky barrier diodes**
H Cetin and E Ayyildiz

632 **Thermoelectric conversion in p–n structures based on separation of charge carriers by energy in space owing to electron–phonon drag**
Yu G Gurevich, G N Logvinov and O Yu Titov

638 **Photoluminescence signature of silicon interstitial cluster evolution from compact to extended structures in ion-implanted silicon**
P K Giri

645 **Structural defects near the film/substrate interface of a homo-epitaxial 4H–SiC film grown by the vapour–liquid–solid mechanism**
E K Polychroniadis

652 **Study of the extrinsic parasitics in nano-scale transistors**
S Xiong, T-J King and J Bokor

INSTITUTE OF PHYSICS PUBLISHING SEMICONDUCTOR SCIENCE AND TECHNOLOGY
Semicond. Sci. Technol. 20 (2005) 568–575 doi:10.1088/0268-1242/20/6/008

Gettering in silicon-on-insulator wafers: experimental studies and modelling

Andrei A Istratov[1], Hele Väinölä[2], Walter Huber[3] and Eicke R Weber[4]

[1] Electronics Research Laboratory, University of California, Berkeley, CA 94720, USA
[2] Helsinki University of Technology, Electron Physics Laboratory, FI-02015 TKK, Finland
[3] Sumitomo Mitsubishi Silicon Group, 49090 Milmont Drive, Fremont, CA 94538, USA
[4] Department of Materials Science and Engineering, University of California, Berkeley, CA 94720, USA

Received 14 January 2005, in final form 25 February 2005
Published 15 April 2005
Online at stacks.iop.org/SST/20/568

Abstract

Buried oxide, which separates the device area from the substrate in silicon-on-insulator (SOI) wafers, forms a diffusion barrier for transition metals in silicon. The impact of this barrier on the efficiency of traditional gettering techniques for iron and copper is evaluated using computer modelling. Several parameters essential for the modelling, such as the diffusivity of iron in SiO_2 and the segregation coefficient of iron and copper in SiO_2, are verified experimentally. It is found that all available data for the diffusivity of iron in SiO_2 (including data points from the literature and our own value of 1.4×10^{-13} cm s^{-2} at 1100 °C) could be fitted by the equation $D(\text{Fe in } SiO_2) = 2.2 \times 10^{-2} \times \exp(-3.05 \text{ eV}/k_BT)$ (cm^2 s^{-1}). The solubility of iron in silicon dioxide was found to be 4.5 times to 5.5 times less than that in silicon at temperatures from 1020 °C to 1100 °C, which indicates that iron does not segregate in SiO_2. The solubility of Cu in silicon dioxide was determined to be half of that in silicon at 1150 °C and 3.3 times higher than in silicon at 690 °C. Modelling of gettering using these parameters revealed that buried oxide prevents iron from diffusing to gettering sites in the substrate at typical processing temperatures, thus rendering the substrate gettering techniques inefficient. On the other hand, the diffusion barrier protects the device area from contamination from the backside of the wafer. Copper has sufficiently high diffusivity in SiO_2 to diffuse through the buried oxide within a short time at 1000 °C; however, it may be difficult to remove copper from the device area because heavily doped areas of the devices could provide competitive gettering sites for copper. Possible gettering strategies for the SOI wafers are discussed.

1. Introduction

The market share of silicon-on-insulator (SOI) wafers has been steadily increasing over the past few years, owing to a substantial performance gain of the SOI wafers over conventional substrates when used for microprocessor and automotive industry applications. A comprehensive review of the SOI technology can be found in [1]. An SOI wafer consists of a thin layer of silicon (typically, from 100 nm in oxygen-implanted (SIMOX) wafers up to several microns in bonded wafers), separated from the substrate by a thin (usually from 150 nm in SIMOX wafers up to a micron in bonded wafers) insulating layer of buried oxide (BOX).

The BOX layer not only provides electrical isolation between the top Si layer and the substrate, but also introduces a barrier for diffusion of metal impurities from the device layer to the gettering sites in the substrate. This barrier may render inefficient the traditional gettering techniques, which use intentionally introduced precipitation/segregation sites for metals in the bulk of the wafer or on its back surface. In this study, computer modelling was used to evaluate the feasibility of traditional (substrate) gettering techniques for iron and

0268-1242/05/060568+08$30.00 © 2005 IOP Publishing Ltd Printed in the UK

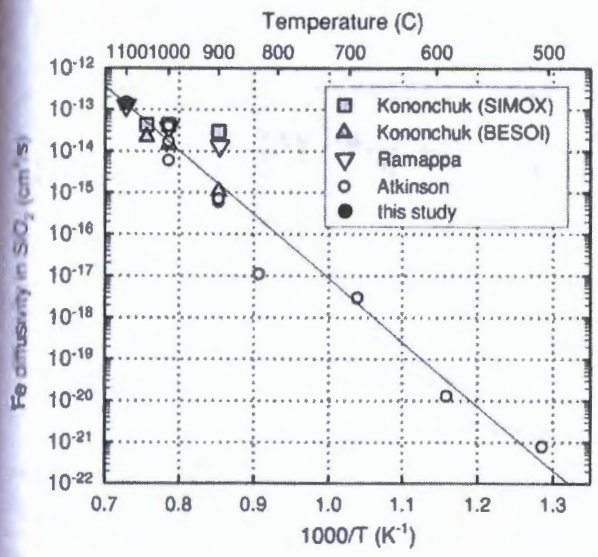


Figure 1. Diffusivity of iron in silicon dioxide, according to the data of Atkinson *et al* [2], Kononchuk *et al* [4] and Ramappa *et al* [3]. Black circle at 1100 °C denotes our data point obtained from the analysis of iron diffusion profile in figure 3.

copper in SOI wafers. To verify the parameters used for the modelling of gettering, the diffusion coefficient of iron in SiO_2 and segregation coefficients of iron and copper in SiO_2 were determined from secondary ion mass spectroscopy (SIMS) depth profiles.

2. Background: diffusivity and segregation coefficient of iron and copper in silicon dioxide

Several groups studied diffusion of iron and copper either through an oxide layer grown on top of a silicon wafer, or through the BOX layer in an SOI structure. The diffusivity of iron in silicon dioxide was studied by Atkinson and Gardner [2] (synthetic SiO_2 glass), Ramappa and Henley [3] (thermal oxide) and Kononchuk *et al* [4] (oxygen-implanted (SIMOX) and bonded (BESOI) silicon-on-insulator wafers). As follows from figure 1, their data agree reasonably well with the discrepancy less than two orders of magnitude at 1000 °C. The plot in figure 1 also includes our own data point at 1100 °C, which was obtained from the analysis of iron diffusion depth profile in a bonded wafer with thick BOX. The experiment from which this data point was extracted is described in the next section. A least-squares fit to all data in the plot in figure 1 gives the following equation:

$$D(\text{Fe in } SiO_2) = 2.2 \times 10^{-2} \times \exp\left(-\frac{3.05\ \text{eV}}{k_B T}\right)\ (\text{cm}^2\ \text{s}^{-1}). \quad (1)$$

In the following, we will use this equation as the most accurate to date.

The data on the diffusivity of copper in silicon dioxide are limited, to our knowledge, to only two reports, which disagree substantially. Gupta *et al* [5] studied diffusion of ^{67}Cu in 4% p-Si glass and found that Cu diffusivity in the temperature range from 227 °C to 550 °C was described by $D = 5.3 \times 10^{-11} \exp(-0.5\ \text{eV}/k_B T)\ (\text{cm}^2\ \text{s}^{-1})$. This dependence was obtained from a least-squares fit to seven data points. McBrayer *et al* [6] experimentally determined a diffusion coefficient of 1.2×10^{-11} cm^2 s^{-1} at a single temperature of 450 °C, and predicted from theoretical considerations that the expected diffusion barrier of Cu in SiO_2 should be 1.82 eV. This value is nearly three orders of magnitude higher than the diffusivity obtained for the same temperature by Gupta *et al* [5]. For the purpose of modelling of gettering, we have chosen to use the equation reported by Gupta *et al* [5] since the diffusion barrier in their equation was determined experimentally rather than predicted theoretically. Given the fact that McBrayer *et al* [6] reported a much higher diffusivity at 450 °C than Gupta *et al* [5], it is reasonable to assume that the equation of Gupta *et al* [5] gives a lower limit for the Cu diffusivity.

Several groups reported data on diffusion of Fe and Cu through SOI structures which are consistent with the very low diffusivity values for iron in silicon dioxide and a higher diffusivity for copper. The interested readers should refer to the papers by Shabani *et al* [7], Kamins and Chiang [8], Jablonski *et al* [9] and Zhang *et al* [10]. The data presented in these reports are insufficient to extract specific values of diffusion coefficients.

The kinetics of diffusion of metals from the device layer into the substrate through a buried oxide is determined by their flux, which is proportional to the product of metal diffusivity and solubility. If the metal solubility is higher in SiO_2 than in Si, the low diffusivity may be partly compensated by a high solubility, and the resulting flux of metals through the boundary with SiO_2 may turn out to be sufficiently high to achieve efficient gettering. Additionally, segregation of metals in SiO_2 would provide a proximity gettering mechanism for the metals dissolved in the top silicon layer. On the other hand, a lower solubility of metals in SiO_2 than in Si would decrease the flux of metal impurities through the BOX.

The available experimental reports on the solubility of iron in silicon dioxide fall in two groups: the reports that there is no segregation of iron in SiO_2, and reports which claim a strong segregation. Yoshimi *et al* [11] conducted a series of oxidations of iron-contaminated wafers with intermediate removal of the oxide layer. They did not observe any increase in the minority carrier lifetime after this procedure (which would be expected if iron were gettered by the oxide), and concluded that there was no significant segregation of iron in SiO_2. In contrast, Graff in section 6.2.3 of his book [12] stated just the opposite that several consecutive oxidations improve the lifetime through the process of gettering of iron by silicon dioxide. Likewise, Ramappa and Henley [3] found very high concentrations of iron in SiO_2, with the segregation coefficient given by $k = S(SiO_2)/S(Si) = 0.266 \exp(1.96\ \text{eV}/k_B T)$. On the other hand, Smith *et al* [13] found from their neutron activation analysis studies that the concentration of iron in silicon dioxide exceeds its concentration in the substrate only by a factor of 1.3. Hence, we have a significant conceptual and quantitative disagreement (by over seven orders of magnitude at 1000 °C) between the reported data.

To the best of our knowledge, no data have been reported for the solubility of copper in silicon dioxide.

To perform predictive modelling of gettering, we performed several experiments to determine or verify

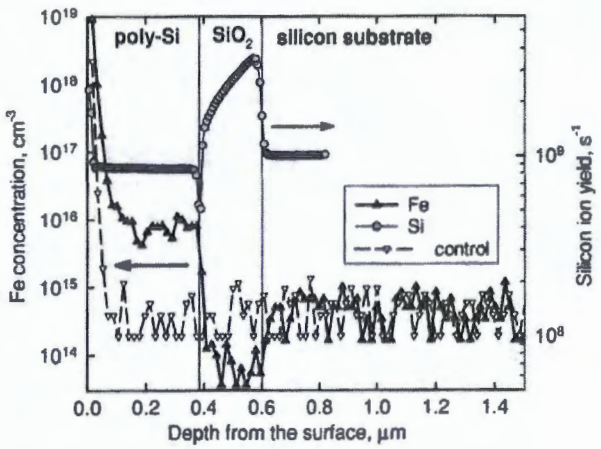


Figure 2. Iron depth profiles obtained on a 370 nm poly-Si—197 nm SiO_2—silicon substrate structure, contaminated with iron from the back and annealed at 1020 °C for 8 h. The sample was annealed in N_2 + 5% H_2 ambient and was quenched in silicon oil. A SIMS depth profile of a reference sample which does not contain an oxide or a top silicon layer, but was diffused and annealed at the same temperature, is shown for a comparison. The curve at the top of the graph represents the silicon ion yield which was used to calculate the absolute iron concentration and also serves as a marker for the silicon dioxide layer.

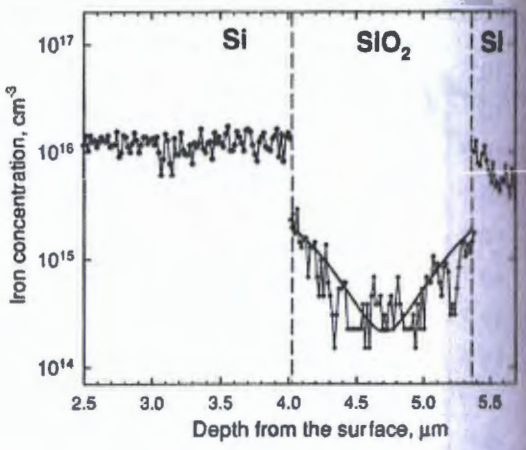


Figure 3. Iron depth profile obtained on a bonded SOI wafer after a 40 min anneal at 1100 °C.

the materials parameters essential for correct quantitative description of the processes involved in gettering of metals in SOI wafers.

3. Experimental: diffusivity and segregation coefficient of Fe in SiO_2 and segregation of Cu in SiO_2

Two types of samples were used, a bonded SOI wafer with the buried oxide thickness of 1 μm and the top silicon layer of 4 μm, obtained from a commercial supplier, and a poly-Si/SiO_2 structure, which consisted of 197 nm thick thermal oxide grown on a standard 4 in. 10 Ω cm substrate, covered by a 370 nm cap layer of CVD-grown poly-silicon. The oxide layer in our test structures was intentionally chosen thicker than that in typical production wafers in order to separate metal diffusion profiles and equilibrium metal concentration within the oxide from metals accumulated at Si/SiO_2 interfaces. Such accumulations were observed under certain conditions in copper- and iron-contaminated wafers in the past [14–19], and are also visible in our experimental data plotted in figure 4.

Iron contamination was performed by scratching the backside of the sample (i.e., the side opposite to the side on which poly-Si/SiO_2 was deposited) with a 99.999% pure iron wire. Annealing was performed in an N_2 + 5% H_2 ambient in a vertical furnace. All anneals were terminated by silicone oil quench (estimated cooling rate 100–250° s^{-1}) to freeze-in the iron distribution established during the high-temperature anneal. The iron depth profiles were measured by SIMS performed at Charles Evans and Associates and Qspec Technology.

The depth profiles obtained by SIMS after iron diffusion are presented in figures 2 and 3. Figure 2 presents a depth profile obtained on a poly-Si/SiO_2 sample after intentional contamination with iron and annealing for 8 h at 1020 °C. A depth profile obtained on a control sample is also shown. The control sample was a CZ wafer without the oxide and poly-silicon, contaminated with iron at the same temperature and for the same time as the poly-Si/SiO_2 sample.

The absolute values of iron concentration in the SIMS depth profiles were calibrated using iron-implanted standards. The concentration of iron in silicon dioxide was calculated using relative sensitivity factor (RSF) derived from measuring a standard. The RSF of Fe in SiO_2 is 0.67 of that in the Si matrix. The silicon ion yield plotted in the top part of figure 2 was used for calculation of the iron concentration in SiO_2, and also used as a marker for the position of the silicon dioxide layer.

The conclusion can be drawn from figure 2 that the equilibrium iron concentration established in SiO_2 after an 8 h anneal at 1020 °C (which according to our estimates is sufficient to equilibrate the iron through the SiO_2 layer) is 4.5 times lower than that in silicon. Additionally, it follows from figure 2 that the solubility of iron in poly-silicon at this temperature is more than an order of magnitude higher than in the silicon substrate. We interpret the latter observation as segregation gettering of iron by poly-silicon; further details of this effect are discussed elsewhere [20].

Figure 3 presents distribution of iron within a BOX in a bonded SOI wafer, annealed for 40 min at 1100 °C. The ratio between iron concentration in silicon and in SiO_2, both measured at the Si/SiO_2 interface, is 5.5. Additionally, a fit to the iron depth profile obtained using the simulator described in [21] within the silicon dioxide layer gives the diffusion coefficient of 1.4×10^{-13} cm s^{-2} at 1100 °C. This value is in a good agreement with the reports of the other groups, as can be seen from figure 1 where the Fe diffusivity extracted from figure 3 is plotted (filled circle) together with the other literature data.

Hence, our experimental data confirm that equation (1) provides an accurate description of the diffusivity of iron in silicon dioxide. Furthermore, we obtained evidence that in the temperature range from 1020 °C to 1100 °C the solubility of iron in silicon dioxide is 4.5–5.5 times lower than that in silicon.

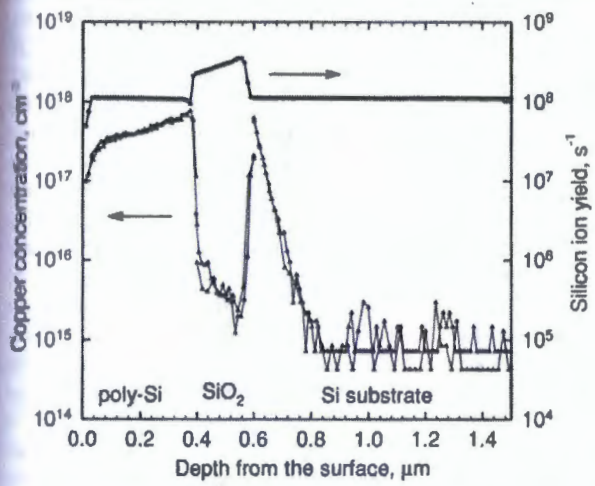


Figure 4. SIMS profile of poly-Si/SiO_2/Si structure intentionally contaminated with copper at 690 °C for 5 h and quenched to room temperature. The top curve is the silicon ion yield used as a marker for the oxide layer and for calibration purposes. The two bottom curves are SIMS depth profiles taken at two different locations of the same sample.

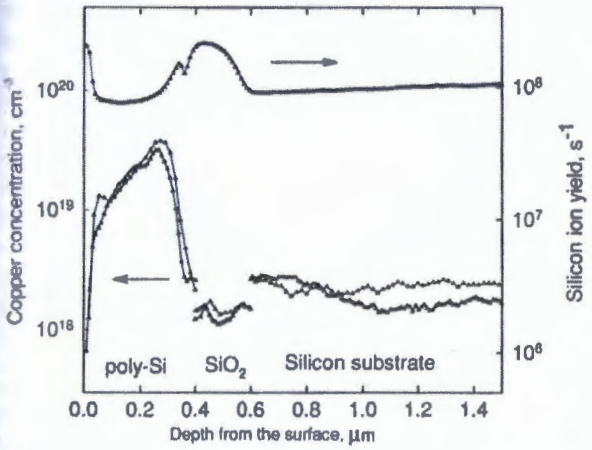


Figure 5. SIMS profile of poly-Si/SiO_2/Si structure intentionally contaminated with copper at 1150 °C for 2 h and quenched to room temperature. The top depth profile is the silicon ion yield used as a marker for the oxide layer and for calibration purposes. The two bottom curves are depth profiles taken at two different locations within the sample.

Segregation of copper in silicon dioxide was studied using the poly-Si/SiO_2 structure described in the previous section. Copper contamination was performed by scratching the backside of the wafer with a copper wire. Diffusions were performed at 690 °C for 5 h and at 1150 °C for 2 h, and were terminated by a silicone oil quench.

Figure 4 presents a SIMS depth profile obtained after Cu diffusion at 690 °C. Despite the strong agglomeration of Cu at the Si/SiO_2 interface, the difference between the equilibrium copper concentrations in the SiO_2 layer and in the substrate is clearly visible. The profile reveals a 3.3 times higher Cu concentration in SiO_2 than in Si.

SIMS profile obtained after Cu diffusion at 1150 °C is plotted in figure 5. The Cu concentration in the SiO_2 layer was found to be equal to half of that in the substrate. The enhancement factor of Cu solubility in poly-Si relatively to the Si substrate was only 7.

The higher concentration of Cu in the poly-silicon layer can be interpreted as segregation of Cu at structural defects in the poly-silicon layer. This is the same effect as the segregation of Cu to structural defects in silicon reported by Dorward and Kirkaldy in 1968 [22].

The conclusion important for our modelling is that, similar to iron, there is no significant segregation of copper in silicon dioxide deposited on silicon.

4. Modelling of substrate gettering of iron in SOI wafers

In this section, we will discuss the results of modelling of substrate gettering of iron in SOI wafers during cooling from 1000 °C to 200 °C. Modelling was performed using the one-dimensional gettering simulator described in [21]. Both internal gettering (precipitation of metals at oxide precipitates) and segregation gettering (gettering due to a higher metal solubility in heavily doped substrates) were modelled.

Gettering in SOI wafers was modelled using the assumption that the wafer consists of a 100 nm thick silicon layer on top of a 150 nm buried oxide on a 725 μm thick substrate. The substrate contains 10^{10} cm^{-3} of oxide precipitates with the average radius of 3.75×10^{-6} cm, formed by precipitating $\Delta O_i = 10^{17}$ cm^{-3} of interstitial oxygen. The doping level of the substrate was assumed to be equal to 2×10^{15} cm^{-3} (for the case of internal gettering only) and 10^{19} cm^{-3} (internal gettering combined with segregation gettering). For comparison, the case of substrate without any gettering sites was also modelled. The top silicon layer was assumed either weakly doped to the level of 2×10^{15} cm^{-3} (no devices), or heavily doped to the level of 10^{19} cm^{-3} to study competitive gettering to the heavily doped device area [23]. Three annealing modes were modelled: cooling with a constant cooling rate of 100 °C s^{-1} and 0.1 °C s^{-1}, and 30 min anneal at 1000 °C followed by a slow cool at a rate of 0.1 °C s^{-1}. Equation (1) was used to describe the diffusion coefficient of iron in silicon. The segregation coefficient of iron in silicon dioxide was assumed to be equal to the temperature-independent value of $S(SiO_2)/S(Si) = 0.2$.

Three initial iron distributions were used: (a) 10^{12} cm^{-3} of iron homogeneously dissolved through the wafer thickness (except the BOX layer, where the equilibrium iron concentration was assumed to be five times less, in agreement with its segregation coefficient), (b) 10^{12} cm^{-3} of iron in the substrate only and (c) 10^{12} cm^{-3} of iron in the device layer only. The results of modelling are presented in figure 6, where the residual iron concentration in the device area is plotted for six cases: weakly doped top silicon layer (no devices) and heavily doped top silicon layer (devices are present), in combination with the cases of weakly doped substrate without any gettering sites, weakly doped substrate with IG sites and heavily doped substrate with IG sites (combination of segregation and relaxation gettering). Figure 6 demonstrates that the presence of gettering sites in the substrate has only very weak impact on the residual iron concentration in the device layer, and the substrate gettering cannot efficiently

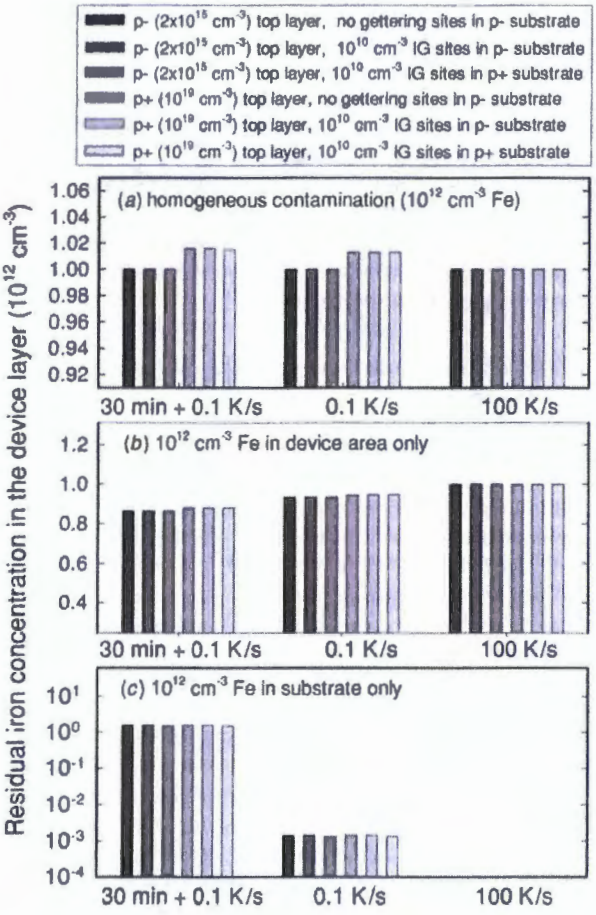


Figure 6. Results of computer modelling of residual iron concentration in the device area after a 30 min anneal at 1000 °C followed by a constant rate (0.1 K s^{-1}) cooling, and instant heating to 1000 °C and then cooling to room temperature with constant cooling rate of 0.1 K s^{-1} and 100 K s^{-1} for three initial iron distributions. The top 100 nm layer simulates the device area.

remove iron from the devices in SOI wafers. Internal gettering is inefficient because it requires that the iron dissolved in the substrate be supersaturated. Since we model low iron contamination levels (10^{12} cm^{-3}), iron gets supersaturated in the substrate at temperatures below 770 °C which corresponds to extremely slow diffusion of iron through the BOX. Likewise, segregation gettering by heavily doped substrates is known to lose its efficiency at temperatures above 800–1000 °C due to the temperature dependence of iron segregation coefficient in heavily doped silicon [24].

In the case (figure 6(*a*)) of a homogeneous contamination (10^{12} cm^{-3} in the device layer and in the substrate and 2×10^{11} cm^{-3} in SiO_2), the changes in iron concentration in the device layer after the gettering anneal are negligibly small. In the case of 30 min anneal followed by the slow cooling and in the case of slow cooling from 1000 °C, a small increase in iron concentration in the device area is observed in the case when the device area is heavily doped. This effect is due to gettering of metals by the device area. In the case of figure 6(*b*) (iron in the device area only), a minor reduction in the dissolved iron concentration is observed; however, this reduction is too insignificant to have a serious impact on the device yield. Finally, in the case of figure 6(*c*) (Fe in the substrate only), we see that iron can diffuse through the BOX layer from the substrate to the devices, but only if the slow cool is combined with a 30 min high-temperature anneal. Since the diffusion process takes place primarily at high temperatures when segregation and relaxation gettering mechanisms are inefficient, the iron concentration established in the device area is almost independent on the presence and type of gettering sites. On the other hand, no iron was found in the device area after a rapid cool, and the concentration of iron in the device area after a 0.1 K s^{-1} cool is substantially lower than after a 30 min anneal followed by a slow cool. In this case, we observe how the BOX protects the device area from metal contaminants in the substrate. Since typical short rapid thermal anneals used in integrated circuits device manufacturing are quite short, it can be expected that iron will not be able to diffuse through the BOX. Therefore, the buried oxide protects the device area from diffusion of metals from the substrate if the substrate gets contaminated.

5. Modelling of copper gettering in SOI wafers

Modelling of internal gettering of copper cannot be as accurate as that of iron since (a) the diffusion coefficient of Cu in SiO_2 is uncertain (see the discussion in section 2) and (b) no quantitative model of the efficiency of internal gettering of copper is available. It was observed in [25, 26] that copper can be efficiently gettered by oxide precipitates only if the dissolved Cu concentration exceeds approximately 10^{15} cm^{-3}. There are two factors which contribute to this effect. Since both copper-silicide precipitates and oxide precipitates are surrounded by compressive lattice strains, precipitation of copper at oxide precipitates is likely to be associated with a significant potential barrier because the growth of Cu_3Si precipitates would further increase the lattice strains [27]. Additionally, electrostatic effects have been pointed out as one of the mechanisms retarding precipitation of copper in p-Si [28]. A higher initial Cu concentration provides a higher Cu supersaturation levels and consequently a higher precipitation driving force.

For the purpose of this analysis and in lieu of a quantitative model for Cu gettering, we used a simplified model, which neglects the limited efficiency of internal gettering sites and utilizes Ham's law [29] to describe copper precipitation in the same way as it is done for iron [21]. Segregation of copper in heavily doped device layer was modelled using the equation discussed in detail by Hoelzl *et al* [30, 31]:

$$\langle Cu_{total} \rangle = 5.51 \times 10^{23} \exp\left(-\frac{1.51\ eV}{k_B T}\right) \times \left[1 + (B_S^-) \times 2.584 \times 10^{-20} \exp\left(\frac{4990}{T}\right)\right]. \quad (2)$$

To calculate the segregation coefficient of copper in silicon dioxide, we used the equation obtained by drawing a straight line through the two data points for the segregation coefficient of copper obtained in section 3,

$$K(SiO_2) = S(\text{Cu in } SiO_2)/S(\text{Cu in Si}) = 9.6 \times 10^{-3} \times \exp\left(\frac{0.48}{k_B T}\right). \quad (3)$$

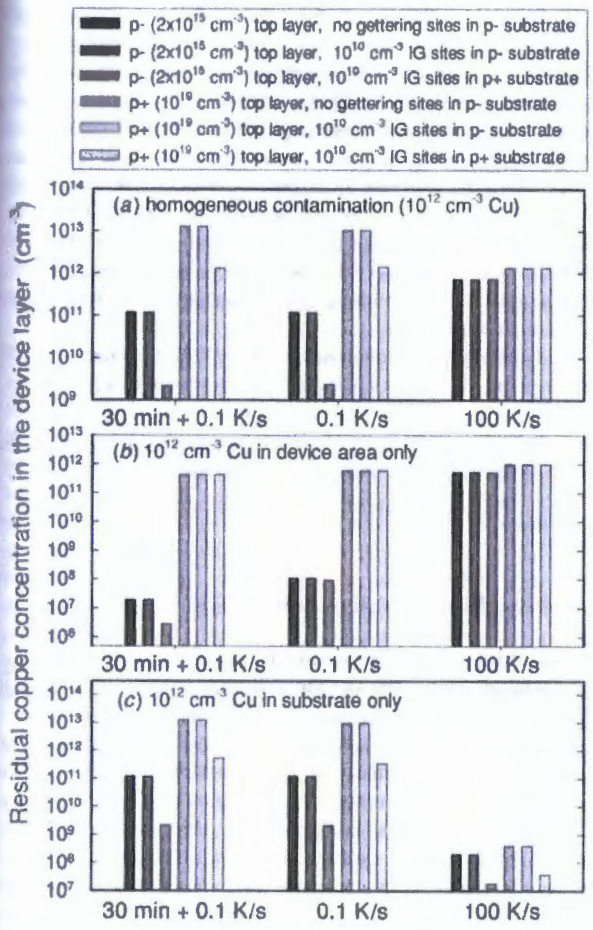


Figure 7. Results of computer modelling of residual copper concentration in the device area after a 30 min anneal at 1000 °C followed by a constant rate (0.1 K s^{-1}) cooling, and instant heating to 1000 °C and then cooling to room temperature with constant cooling rate of 0.1 K s^{-1} and 100 K s^{-1} for three initial iron distributions. The top 100 nm layer simulates the device area.

Since it is difficult to evaluate the error margins of the fit which uses only two data points, we suggest that equation (3) should be used only as a first-order approximation.

Cu gettering was modelled using the same wafer structure and the same cooling regimes as described in the previous section. The results of the modelling are presented in figure 7, which clearly demonstrates that copper can relatively easily diffuse through the BOX during the annealing/cooling used in our simulations. If no heavily doped regions are present in the device area of the wafer, Cu from the device area gets gettered by the substrate, and its residual concentration in the device area drops by one to six orders of magnitude. On the other hand, in the case when the device area is heavily doped, Cu is retained in the device area or even diffuses to the device area from the substrate. In the case when the substrate contains only internal gettering sites, the Cu content of the heavily doped device area may even increase over its initial concentration because the onset of segregation gettering by the devices is at higher temperature than the onset of relaxation gettering by the oxygen precipitates in the substrate; therefore, devices turn out to be more efficient sinks than the intentionally introduced gettering sites. A combination of relaxation and segregation gettering mechanisms in the substrate is more efficient in protecting the device area from copper than relaxation gettering alone. But even this combination can only provide gettering sufficiently efficient to prevent gettering of Cu by the devices and achieve the same concentration in the device area as in the substrate.

When only the substrate is contaminated (figure 7(*c*)), Cu can penetrate through the BOX during long anneals and during slow cooling. This makes Cu backside contamination more dangerous than iron backside contamination. However, short (several minutes at temperatures up to a 1000 °C) RTA treatments are insufficient for the copper to diffuse through the 100 nm thick buried oxide.

It is also interesting to note that the difference between the residual copper concentration in the device layer in the case of 30 min anneal and 0.1 K s^{-1} cooling and in the case of 0.1 K s^{-1} cooling is very small and visible only in figure 7(*b*). Hence, slow cooling at 0.1 K s^{-1} is sufficient for the copper to reach the condition close to its equilibrium distribution in the wafer. This is consistent with a higher diffusion coefficient of copper than of iron.

6. Summarizing discussion

A buried oxide layer provides an efficient diffusion barrier for nearly all transition metals, except copper (and possibly nickel, which is another very fast diffuser in silicon, although there is not enough data on diffusion and segregation of nickel in SiO_2 to make a quantitative assessment). Iron requires temperatures over 1100 °C to diffuse through a typical 150 nm buried oxide layer within a short time (under 30 min), whereas at lower temperatures (such as 1000 °C used in our modelling) the diffusion time becomes so long that the BOX forms almost impenetrable diffusion barrier. In contrast, as our modelling shows, copper can diffuse through the 150 nm BOX relatively easily at temperatures around 1000 °C. This conclusion is in agreement with the experimental observations reported in the literature. For instance, Shabani *et al* [7] found that BOX prevents diffusion of Fe from the device layer into the substrate after a 2 h anneal at 1000 °C, whereas Cu can diffuse through the BOX easily during the same anneal. Likewise, Jablonski *et al* [9] found that Cu can diffuse through the 90 nm thick BOX even at 600 °C.

Gettering of iron is complicated by the fact that the traditional substrate gettering techniques are inefficient at the temperatures around or above 1000 °C, i.e., in the temperature range where iron can penetrate the BOX after a sufficiently long annealing. For example, heavily doped p^+ substrates are known to lose their gettering ability at high temperatures [24]. Internal gettering requires metals be supersaturated and occurs only during cooling starting from the temperature where equilibrium metal solubility drops below the actual dissolved metal concentration. For the typical iron contamination levels around 10^{11}–10^{12} cm^{-3}, the onset of internal gettering falls below 770 °C. Additionally, the integrated circuit industry moves towards shorter processing times and lower temperatures.

Although BOX represents an almost impenetrable barrier for iron at normal processing temperatures, which makes substrate gettering of iron inefficient, one aspect of the

presence of a diffusion barrier is beneficial since it prevents degradation of the device yield in the event of contamination of the back surface of the wafer. As long as the front surface of the wafer is kept clean, the devices, which in a standard (non-SOI) wafer can collect metals from the whole substrate thickness [23], are protected from the contaminants residing in the substrate as long as short annealing times and fast cooling rates typical for rapid thermal processing are used.

On the other hand, contamination of the front (device) side of the SOI wafer becomes a serious problem. Due to the very small thickness of the device layer, even a small surface contamination level leads to a very high-volume metal concentrations. For example, 10^{10} cm^{-2} of metals on the surface translates into the bulk contamination level of 10^{15} cm^{-3} when dissolved in a 0.1 μm thin device layer. This level appears to be unreasonably high when compared to the typical critical bulk contamination level of the order of 10^{11} cm^{-3} or below. However, one should not forget that the contamination level of 10^{11} cm^{-3} is the metal contamination level averaged over the wafer thickness. The actual metal concentration in the device layer on top of a standard CZ wafer can often reach more than three orders of magnitude higher levels due to the effect of competitive gettering [23]. Briefly, the idea of the competitive gettering is as follows. Devices can be more efficient sinks for metals than the gettering sites in the substrate due to their extremely high-doping levels. If this is the case, the majority of metals will be collected by the devices rather than by the gettering sites. Since the thickness of the substrate is 10^3–10^4 times greater than the thickness of the device layer, the metal concentration in the device area could also increase by several orders of magnitude over its average concentration in the wafer.

Since metals typically go to the heaviest doped areas of the devices, which are nearly metallic, their electrical properties are not affected much by the metal contamination as long as no metal precipitates are formed at the interfaces between differently doped areas. This way, the devices can tolerate rather high *local* metal contamination levels, and the sensitivity of the device yield of SOI wafers to surface metal contamination can be expected to be comparable to that of traditional CZ wafers *without* intentionally introduced gettering sites.

In order to achieve efficient gettering in SOI wafers and increase the device yield tolerance to metal contamination, it was suggested to perform additional implantations of H, He or C [10, 32] to create gettering sites either on the device side of the BOX layer [33, 34], or beneath the BOX layer [10, 32, 35]. Horiuchi and Ohoyu [36] suggested to use a multilayer structure consisting of buried poly-Si, Si_3N_4 and SiO_2. A poly-Si interlayer just beneath the devices acted as a gettering layer, and a Si_3N_4 layer compensated the stress generated by the SiO_2 layer. This technology enabled to reduce the leakage current in p–n junction by ten times [36]. However, besides additional costs and processing steps, this technology is incompatible with fully depleted MOS technology which utilizes the entire overlying silicon film to fabricate devices.

Hence, it appears that the following gettering strategies can be proposed for SOI wafers. For high-temperature anneals ($T > 1150$ °C) which are no longer used for device processing, but find applications on the implanted SOI wafers (SIMOX) manufacturing stage to anneal the damage and homogenize the implanted oxygen distribution, iron and other metals can easily diffuse through the BOX. However, standard gettering techniques such as internal gettering or heavily doped substrate cannot be used because they work only at much lower temperatures. Additionally, internal gettering sites (oxygen precipitates) may dissolve at high temperatures. Poly-silicon backside layer appears to be the most suitable gettering technique for such applications as it is stable at high temperatures and combines relaxation and segregation components, thus providing effective gettering in a wide range of temperatures [20].

For low-temperature anneals ($T < 1000$ °C) used in device processing, it appears that the optimum gettering strategy would be to design the devices in such a way as to maximize the volume of the heavily doped areas which can provide proximity gettering areas. This can be achieved, e.g., by including special p^+ and n^+ wells into the chip layouts in order to getter metal contaminants within the device area itself. This strategy is based on the fact that the areas with the heaviest doping levels (which are nearly metallic) are the most attractive areas for Fe and Cu due to their segregation gettering effect, and at the same time their nearly metallic electrical properties are the least sensitive to the metal contamination level, as long as the metals do not form precipitates protruding through the boundaries with adjacent areas with a different doping level.

Gettering sites in the substrate can be efficient for quickly diffusing metals which can get through the BOX within a short time at temperatures below 1050 °C, such as Cu and possibly (although it was not verified in our study) Ni. Internal gettering and poly-Si backside gettering techniques (Hoelzl *et al* [37]) appear to work well for Ni, whereas Cu is efficiently gettered by polybackside or p^+ substrates. Heavily doped substrates are inefficient for gettering of nickel since there is no enhancement of Ni solubility in heavily doped silicon [38].

Acknowledgments

The authors would like to acknowledge the financial support from SiWEDS and Finnish National Technology Agency. The authors thank Okmetic Oyj for providing bonded SOI wafers for the experiments.

References

[1] Celler G K and Cristoloveanu S 2003 *J. Appl. Phys.* **93** 4955
[2] Atkinson A and Gardner J W 1981 *Corros. Sci.* **21** 49
[3] Ramappa D A and Henley W B 1999 *J. Electrochem. Soc.* **146** 3773
[4] Kononchuk O, Korablev K G, Yarykin N and Rozgonyi G A 1998 *Appl. Phys. Lett.* **73** 1206
[5] Gupta D, Vieregge K and Srikrishnan K V 1992 *Appl. Phys. Lett.* **61** 2178
[6] McBrayer J D, Swanson R M and Sigmon T W 1986 *J. Electrochem. Soc.* **133** 1242
[7] Shabani M B, Yoshimi T, Abe H, Nakai T and Cordts B 1996 *Silicon-On-Insulator, Technology and Devices* ed P L F Hemment, S Cristoloveanu, K Izumi, T Houston and S Wilson (Pennington: Materials Research Society) p 162
[8] Kamins T I and Chiang S Y 1985 *J. Appl. Phys.* **58** 2559
[9] Jablonski J, Miyamura Y, Imai M and Tsuya H 1995 *J. Electrochem. Soc.* **142** 2059

[10] Zhang M, Lin C, Duo X, Lin Z and Zhou Z 1999 *J. Appl. Phys.* **85** 94
[11] Yoshimi T, Shabani M B, Okuuchi S and Abe H 1997 *Diagnostic, Techniques for Semiconductor, Materials and Devices* ed P Rai-Choudhury, J L Benton, D K Schroder and T J Shaffner (Pennington: The Electrochemical Society) p 452
[12] Graff K 2001 *Metal Impurities in Silicon-Device Fabrication* 2nd edn (Berlin: Springer)
[13] Smith A R, McDonald R J, Manini H, Hurley D L, Norman E B, Vella M C and Odom R W 1996 *J. Electrochem. Soc.* **143** 339
[14] Kamiura Y, Hashimoto F and Iwami M 1988 *Appl. Phys. Lett.* **53** 1711
[15] Kamiura Y, Hashimoto F and Iwami M 1989 *Appl. Surf. Sci.* **41–42** 447
[16] Wendt H, Cerva H, Lehmann V and Pamler W 1989 *J. Appl. Phys.* **65** 2402
[17] Bai P, Yang G R and Lu T M 1990 *J. Appl. Phys.* **68** 3313
[18] Ohsawa A, Honda K and Toyokura N 1984 *J. Electrochem. Soc.* **131** 2964
[19] Hiramoto K, Sano M, Sadamitsu S and Fujino N 1989 *Japan. J. Appl. Phys.* **28** L2109
[20] Istratov A A, Huber W and Weber E R 2004 *Appl. Phys. Lett.* **85** 4472
[21] Hieslmair H, Balasubramanian S, Istratov A A and Weber E R 2001 *Semicond. Sci. Technol.* **15** 567
[22] Dorward R C and Kirkaldy J S 1968 *J. Mater. Sci.* **3** 502
[23] Istratov A A, Huber W and Weber E R 2003 *J. Electrochem. Soc.* **150** G244
[24] McHugo S A, McDonald R J, Smith A R, Hurley D L and Weber E R 1998 *Appl. Phys. Lett.* **73** 1424
[25] Istratov A A, Sachdeva R, Flink C, Balasubramanian S and Weber E R 2002 *Solid State Phenom.* **82–84** 323
[26] Isomae S, Ishida H, Itoga T and Hozawa K 2002 *Solid State Phenom.* **82–84** 349
[27] Istratov A A and Weber E R 2002 *J. Electrochem. Soc.* **149** G21
[28] Flink C, Feick H, McHugo S A, Seifert W, Hieslmair H, Heiser T, Istratov A A and Weber E R 2000 *Phys. Rev. Lett.* **85** 4900
[29] Ham F S 1958 *J. Phys. Chem. Solids* **6** 335
[30] Hoelzl R, Huber D, Range K J, Fabry L, Hage J and Wahlich R 2000 *J. Electrochem. Soc.* **147** 2704
[31] Hoelzl R, Range K J and Fabry L 2002 *Appl. Phys.* A **75** 525
[32] Yankov R A, Hatzopoulos N, Skorupa W and Danilin A B 1996 *Nucl. Instrum. Methods Phys. Res. B* **120** 60
[33] Hong S Q, Wetteroth T, Shin H, Wilson S R, Werho D, Lee T C and Schroder D K 1997 *Appl. Phys. Lett.* **71** 3397
[34] Papakonstantinou P, Somasundram K, Cao X and Nevin W A 2001 *J. Electrochem. Soc.* **148** G36
[35] Skorupa W, Hatzopoulos N, Yankov R A and Danilin A B 1995 *Appl. Phys. Lett.* **67** 2992
[36] Horiuchi M and Ohoyu K 1995 *IEEE Trans. Electron Devices* **42** 876
[37] Hoelzl R, Range K J, Fabry L, Hage J and Raineri V 2000 *Mater. Sci. Eng.* B **73** 95
[38] Istratov A A, Zhang P, McDonald R J, Smith A R, Seacrist M, Moreland J, Shen J, Wahlich R and Weber E R 2005 *J. Appl. Phys.* **97** 023505

ISTRATOV03

https://iopscience.iop.org/article/10.1088/0268-1242/20/6/016 July 25, 2024

IOPscience Journals Books Publishing Support Login

Semiconductor Science and Technology

PURPOSE-LED PUBLISHING™

Gettering in silicon-on-insulator wafers: experimental studies and modelling

Andrei A Istratov[1], Hele Väinölä[2], Walter Huber[3] and Eicke R Weber[4]

Published 15 April 2005 • 2005 IOP Publishing Ltd

Semiconductor Science and Technology, Volume 20, Number 6

Citation Andrei A Istratov *et al* 2005 *Semicond. Sci. Technol.* **20** 568

DOI 10.1088/0268-1242/20/6/016

References

Article and author information

Abstract

Buried oxide, which separates the device area from the substrate in silicon-on-insulator (SOI) wafers, forms a diffusion barrier for transition metals in silicon. The impact of this barrier on the efficiency of traditional gettering techniques for iron and copper is evaluated using computer modelling. Several parameters essential for the modelling, such as the diffusivity of iron in SiO_2 and the segregation coefficient of iron and copper in SiO_2, are verified experimentally. It is found that all available data for the diffusivity of iron in SiO_2 (including data points from the literature and our own value of 1.4×10^{-13} cm s^{-2} at 1100 °C) could be fitted by the equation $D(\text{Fe in } SiO_2) = 2.2 \times 10^{-2} \times \exp(-3.05\ \text{eV}/k_BT)(\text{cm}^2\ s^{-1})$. The solubility of iron in silicon dioxide was found to be 4.5 times to 5.5 times less than that in silicon at temperatures from 1020 °C to 1100 °C, which indicates that iron does not segregate in SiO_2. The solubility of Cu in silicon dioxide was determined to be half of that in silicon at 1150 °C and 3.3 times higher than in silicon at 690 °C. Modelling of gettering using these parameters revealed that buried oxide prevents iron from diffusing to gettering sites in the substrate at typical processing temperatures, thus rendering the substrate gettering techniques inefficient. On the other hand, the diffusion barrier protects the device area from contamination from the backside of the wafer. Copper has sufficiently high diffusivity in SiO_2 to diffuse through the buried oxide within a short time at 1000 °C; however, it may be difficult to remove copper from the device area because heavily doped areas of the devices could provide competitive gettering sites for copper. Possible gettering strategies for the SOI wafers are discussed.

Export citation and abstract BibTeX RIS

← Previous article in issue Next article in issue →

Access this article

The computer you are using is not registered by an institution with a subscription to this article. Please choose one of the options below.

Login

Access through your institution

IOPscience login

Find out more about journal subscriptions at your site.

Purchase from

Article Galaxy
CCC RightFind

Purchase this article from our trusted document delivery partners.

Rent from

Read this now at deepdyve

This article is available from DeepDyve.

Article metrics
704 Total downloads

18 3

Submit
Submit to this Journal

Permissions
Get permission to re-use this article

Share this article

Abstract
References

You may also like

JOURNAL ARTICLES

Modeling of Competitive Gettering of Iron in Silicon Integrated Circuit Technology

Proximity gettering of C_3H_5 carbon cluster ion-implanted silicon wafers for CMOS image sensors: Gettering effects of transition metal, oxygen, and hydrogen impurities

Thin and low light-induced degradation passivated emitter and rear cells based on boron-aluminum pre-gettering

Proposal of a Novel Gettering Technique for a Thin SOI Wafer

A Statistical Model Describing Temperature Dependent Gettering of Cu in p-Type Si

Proximity gettering technique using CH_3O multielement molecular ion implantation for the reduction of the white spot defect density in CMOS image sensor

physicsworld jobs

Technical Specialist - Senior Cleanroom Process Engineer
University of Bristol, School of Physics

Experimental Quantum Information Scientist (Experienced) - Onsite
Sandia National Laboratories

More jobs Post a job

Make a recommendation

To gain access to this content, please complete the Recommendation Form and we will follow up with your librarian or Institution on your behalf.

For corporate researchers we can also follow up directly with your R&D manager, or the information management contact at your company. Institutional subscribers have access to the current volume, plus a 10-year back file (where available).

▾ Show references

IOPSCIENCE

Journals
Books
IOP Conference Series
About IOPscience
Contact Us
Developing countries access
IOP Publishing open access policy
Accessibility

IOP PUBLISHING

Copyright 2024 IOP Publishing
Terms and Conditions
Disclaimer
Privacy and Cookie Policy

PUBLISHING SUPPORT

Authors
Reviewers
Conference Organisers

This site uses cookies. By continuing to use this site you agree to our use of cookies.

IOP Publishing

MARVIN01

NTRL

National Technical Reports Library

The National Technical Information Service acquires, indexes, abstracts, and archives the largest collection of U.S. government-sponsored technical reports in existence. The NTRL offers online, free and open access to these authenticated government technical reports. Technical reports and documents in its repository may be available online for free either from the issuing federal agency, the U.S. Government Publishing Office's Federal Digital System website, or through search engines.

Home Help

Details

Actions:

Download

Interdigitated Back Contact Silicon Solar Cell Analysis and Design Recommendations for Space Use.

ADA220414

Publication Date	1989
Personal Author	Marvin, D. C Froedge, S. L.
Page Count	30
Abstract	*The Interdigitated Back Contact (IBC) solar cell is a relatively new design which has shown unprecedentedly high efficiencies. Silicon Interdigitated Back Contact cells have been fabricated that show greater than 25% efficiency at 100 suns Air Mass 1.5. This is far superior to conventional silicon concentrator cells which are approximately 18% efficient. The purpose of this report is to describe briefly the differences between this technology and conventional cells, demonstrate a near optimum design achieved by two-dimensional numerical simulation, and assess the utility of these cells for space application. The end of life (EOL) performance of this cell design in the radiation environment of space is a critical issue since the high efficiency of the design is predicated on the use of very high quality, long-diffusion length silicon. The radiation-induced degradation of this material is expected to lead to severe efficiency losses. The optimization of cell design to minimize these losses was carried out using a modified version of the 2-dimensional PISCES semiconductor simulator. The final designs presented here show that the performance of IBC cells in space can significantly exceed that of conventional cells. PISCES Simulator, Electric power production, Power supplies, Solar cells, Semiconductors. (jg)*
Keywords	• Solar cells • Cells • Concentration(Composition) • Degradation • Efficiency • Electric power production • High rate • Intensity • Losses • Mathematical models • Numerical analysis • Optimization • Power supplies • Radiation • Radiation effects • Semiconductors • Silicon • Simulators • Space environments • Two dimensional • Silicon solar cells
Source Agency	• Air Force • Non Paid ADAS
NTIS Subject Category	• 97N - Solar Energy • 84G - Unmanned Spacecraft • 84C - Manned Spacecraft
Corporate Authors	Aerospace Corp., El Segundo, CA. Chemistry and Physics Lab.; Space Systems Div., Los Angeles AFS, CA.
Document Type	Technical Report
Title Note	Technical rept.
NTIS Issue Number	199016
Contract Number	• F04701-85-C-0086

MARVIN02

REPORT SSD-TR-90-04

DTIC FILE COPY

AD-A220 414

Interdigitated Back Contact Silicon Solar Cell Analysis and Design Recommendations for Space Use

Prepared by

D. C. MARVIN and S. L. FROEDGE
Chemistry and Physics Laboratory
Laboratory Operations
The Aerospace Corporation
El Segundo, CA 90245

30 September 1989

DTIC
ELECTE
APR 11 1990
S D
E

Prepared for

SPACE SYSTEMS DIVISION
AIR FORCE SYSTEMS COMMAND
Los Angeles Air Force Base
P.O. Box 92960
Los Angeles, CA 90009-2960

APPROVED FOR PUBLIC RELEASE;
DISTRIBUTION UNLIMITED

90 04 10 100 MARVIN02 - 2

This report was submitted by The Aerospace Corporation, El Segundo, CA 90245-4691, under Contract No. F04701-85-C-0086-P00019 with the Space Systems Division, P.O. Box 92960, Los Angeles, CA 90009-2960. It was reviewed and approved for The Aerospace Corporation by S. Feuerstein, Director, Chemistry and Physics Laboratory. Paul M. Propp was the project officer for the Mission-Oriented Investigation and Experimentation (MOIE) Program.

This report has been reviewed by the Public Affairs Office (PAS) and is releasable to the National Technical Information Service (NTIS). At NTIS, it will be available to the general public, including foreign nationals.

This technical report has been reviewed and is approved for publication. Publication of this report does not constitute Air Force approval of the report's findings or conclusions. It is published only for the exchange and stimulation of ideas.

PAUL M. PROPP, GM-14
MOIE Project Officer
SSD-WRDC-ML

RYMOND M. LEONG, MAJ, USAF
MOIE Program Manager
AFSTC/WCO OL-AB

UNCLASSIFIED

SECURITY CLASSIFICATION OF THIS PAGE

REPORT DOCUMENTATION PAGE

1a. REPORT SECURITY CLASSIFICATION Unclassified	1b. RESTRICTIVE MARKINGS
2a. SECURITY CLASSIFICATION AUTHORITY	3. DISTRIBUTION/AVAILABILITY OF REPORT Approved for public release; distribution unlimited.
2b. DECLASSIFICATION/DOWNGRADING SCHEDULE	
4. PERFORMING ORGANIZATION REPORT NUMBER(S) TR-0088(3945-01)-1	5. MONITORING ORGANIZATION REPORT NUMBER(S) SSD-TR-90-04
6a. NAME OF PERFORMING ORGANIZATION The Aerospace Corporation Laboratory Operations 6b. OFFICE SYMBOL (If applicable)	7a. NAME OF MONITORING ORGANIZATION Space Systems Division
6c. ADDRESS (City, State, and ZIP Code) El Segundo, CA 90245-4691	7b. ADDRESS (City, State, and ZIP Code) Los Angeles Air Force Base Los Angeles, CA 90009-2960
8a. NAME OF FUNDING/SPONSORING ORGANIZATION 8b. OFFICE SYMBOL (If applicable)	9. PROCUREMENT INSTRUMENT IDENTIFICATION NUMBER F04701-85-C-0086-P00019
8c. ADDRESS (City, State, and ZIP Code)	10. SOURCE OF FUNDING NUMBERS PROGRAM ELEMENT NO. / PROJECT NO. / TASK NO / WORK UNIT ACCESSION NO.
11. TITLE (Include Security Classification) Interdigitated Back Contact Silicon Solar Cell Analysis and Design Recommendations for Space Use	
12. PERSONAL AUTHOR(S) Marvin, Dean C. and Froedge, Sharon L.	
13a. TYPE OF REPORT 13b. TIME COVERED FROM _____ TO _____ 14. DATE OF REPORT (Year, Month, Day) 1989 September 1989 15. PAGE COUNT 30	
16. SUPPLEMENTARY NOTATION	

17. COSATI CODES		
FIELD	GROUP	SUB-GROUP

18. SUBJECT TERMS (Continue on reverse if necessary and identify by block number)
PISCES simulator, Electric Power Production, Power Supplies, Solar cells, Semiconductors (JG)

19. ABSTRACT (Continue on reverse if necessary and identify by block number)

The Interdigitated Back Contact (IBC) solar cell is a relatively new design which has shown unprecedentedly high efficiencies. Silicon IBC cells have been fabricated that show greater than 25% efficiency at 100 suns Air Mass 1.5. This is far superior to conventional silicon concentrator cells which are approximately 18% efficient. The purpose of this report is to describe briefly the differences between this technology and conventional cells, demonstrate a near optimum design achieved by two-dimensional numerical simulation, and assess the utility of these cells for space application. The end of life (EOL) performance of this cell design in the radiation environment of space is a critical issue since the high efficiency of the design is predicated on the use of very high quality, long-diffusion length silicon. The radiation-induced degradation of this material is expected to lead to severe efficiency losses. The optimization of cell design to minimize these losses was carried out using a modified version of the 2-dimensional PISCES semiconductor simulator. The final designs presented here show that the performance of IBC cells in space can significantly exceed that of conventional cells.

20. DISTRIBUTION/AVAILABILITY OF ABSTRACT ☒ UNCLASSIFIED/UNLIMITED ☐ SAME AS RPT. ☐ DTIC USERS	21. ABSTRACT SECURITY CLASSIFICATION Unclassified
22a. NAME OF RESPONSIBLE INDIVIDUAL	22b. TELEPHONE (Include Area Code) / 22c. OFFICE SYMBOL

DD FORM 1473, 84 MAR

83 APR edition may be used until exhausted.
All other editions are obsolete

SECURITY CLASSIFICATION OF THIS PAGE
UNCLASSIFIED

CONTENTS

I. BACKGROUND..... 3

II. THE PISCES SIMULATOR..... 7

III. RESULTS AND DISCUSSION..... 9

A. Scope Of Study..... 9

B. Cell Thickness..... 11

C. Carrier Collection Region Thickness..... 12

D. Carrier Collection Region Width..... 14

E. Abrupt Front Surface Field..... 15

F. Design Refinements..... 16

G. Concentrated Light Levels..... 23

IV. CONCLUSION..... 25

REFERENCES..... 27

FIGURES

1. Comparison of IBC Solar Cell with Conventional Point Contact Solar Cell..... 4

2. Carrier Flow in High Recombination Case..... 19

3. Carrier Flow in Low Recombination Case..... 20

4. Effect of Cell Thickness on EOL Efficiency..... 22

TABLES

1. Constant Cell Design Parameters..... 10

2. Baseline Cell Design..... 10

3. BOL Effects of Cell Thickness..... 12

4. EOL Effects of Cell Thickness..... 13

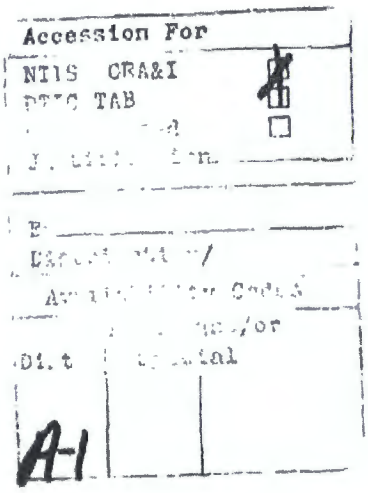
5. Effects of P^+ and N^+ Collection Region Thicknesses, BOL and EOL..... 13

6. Effects of P^+ and N^+ Collection Region Widths on 50 μm Thick Cell, BOL..... 15

7. Efficiency as a Function of FSF For 50 μm Cell at 1 Sun..... 18

8. EOL Efficiency as a Function of Cell Thickness and FSF at 100 Suns..... 23

9. High-Radiation Environment Cell Design Parameters..... 26

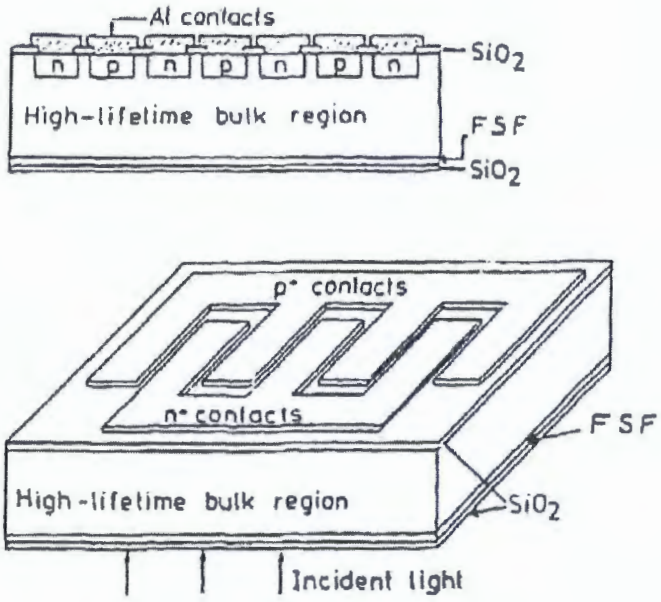


I. BACKGROUND

Silicon solar cells have served as the photovoltaic converters on virtually all DOD satellites. The state-of-the-art efficiency of these cells has risen from approximately 10% in the 1960s to nearly 15% Air Mass Zero (AM0) in the mid 1980s. The improvements in performance have been incremental during this period, resulting from the addition of such features as front and back surface field structures, back surface reflectors, and textured front surfaces. Each of these represents a modification of the solar cell; however, the basic structure of the solar cell has remained unchanged. It consists of a large area (several square centimeters) p-n junction, with a metal grid for the front face contact and complete metal coverage for the back contact. The features listed above are essentially modifications to the interfacial regions of the cell where much of the device physics occurs. In 1977 a group at Purdue University demonstrated 15% (AM1.3, 63 suns) efficiency and projected 20% (AM1.3, 300 suns) efficiency in radically redesigned solar cells,[1] named the Interdigitated Back Contact (IBC) solar cell. Further work at the University Louvain, Belgium, confirmed these findings. In 1987 researchers there fabricated IBC cells with demonstrated conversion efficiencies of 25.6% at 100 suns.[2]

The major difference between the IBC cell and a conventional cell is apparent in Fig. 1. In the IBC cell, the p-n junction is at the rear of the device (opposite the face where light enters) and consists of narrow strips under the contact metallization. This change carries with it a number of implications for device performance. The placement of the contact grid on the rear surface of the cell eliminates grid shadowing losses, which typically amount to 7-10%. Reduction of the junction area decreases the dark current, which in turn increases open circuit voltage (V_{oc}). Most light absorption occurs in a region doped much lower than a conventional cell emitter, resulting in much less recombination. Finally, the series resistance of this design is expected to be lower since the n^+ and p^+ contacts are close together, resulting in higher fill factors.

IBC Solar Cell



Conventional Solar Cell

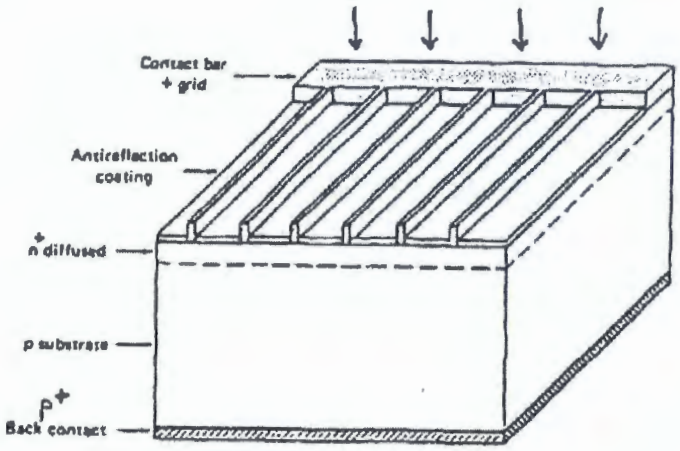


Fig. 1. Comparison of IBC Solar Cell with Conventional Poiint Contact Solar Cell

The Point Contact cell is similar in philosophy, but uses junction "islands" connected to contact grids rather than junction "lines" that are coincident with the metal grid. This further reduces the junction area but at the expense of added fabrication complexity. The predicted performances of the two designs are similar.

A primary concern about IBC cells in space applications is the expected sensitivity to radiation damage. The origin of the sensitivity is easily seen as follows. Light incident on the front surface of the cell is strongly absorbed in the first few micrometers of silicon, creating electron-hole pairs. These must diffuse through the entire thickness of the device without recombining in order to reach the doped contact regions which separate them at the rear of the cell. Thus, silicon with a minority carrier diffusion length of at least 100 um is typically required. This is no problem for present technology, except when the effects of electron irradiation are included. The damage caused by 1 MeV electron passage through the cell reduces the diffusion length substantially. For example, empirical results[3] on 10 ohm-cm silicon show an initial diffusion length of 700 um falls to 34 um after 1E15 1 MeV electron/cm^2 irradiation. A priori, one would therefore expect that cells of this design are unsuitable for high radiation environments.

The purpose of this study is to evaluate the IBC cell design for use in space missions. As described above the primary incentive for use of such cells is increased efficiency. This is especially true when the cells are operated under concentrated light. In order to properly simulate the operation of these cells, a two-dimensional solution of the carrier transport equations is necessary. This is in contrast to the situation with conventional cells where a one-dimensional treatment is often adequate. The distinction in treatments arises because of the localized nature of the p-n junction in the plane parallel to the front face in IBC cells. The study methodology is to vary the critical design parameters and simulate the cell current-voltage behavior at both the beginning and end of life under an assumed radiation environment. Basic IBC cell design parameters include base thickness and doping, contact region doping and dimensions, and front surface field (FSF) parameters. These are similar to the parameters in conventional

cells except for the additional degrees of freedom associated with the localized current collector regions, since in a conventional cell these cover the entire cell area on the front and rear faces.

II. THE PISCES SIMULATOR

The Poisson and Continuity Equation Solver (PISCES) computer code was developed at Stanford University. It is a true two-dimensional, two-carrier device modeling program. As supplied in Version 11b, the range of processes included is quite extensive. Fermi-Dirac carrier statistics, Auger and Shockley-Read-Hall (SRH) recombination, doping-induced band gap narrowing (BGN), and interface recombination are all treated. In addition, steady state and transient solutions are available. The program has been modified at Aerospace to include optical generation of carriers, thus allowing solar cell simulation. Optical generation functions for AM0 and AM1 light incident on silicon and gallium arsenide have been devised.

When used for absolute efficiency studies, as opposed to comparative studies, the accuracy of the generation function is important. In order to assess the accuracy of the AM0/silicon generation function, several simulations of IBC cells reported in the literature[4] were reproduced. These reports also used a two-dimensional simulator, along with all other processes included in PISCES, except for the use of Boltzmann instead of Fermi-Dirac statistics. The reported variation of IBC cell efficiency with cell thickness, illumination intensity, and interface recombination was investigated. It was necessary to normalize the PISCES results to the known intensity of AM0 light because the AM0/silicon generation function used in PISCES is not sufficiently accurate. This was done by computing the ratio of the known AM0 carrier generation in a given thickness of silicon[5] to the simulated short circuit current value obtained in the case of no recombination. All subsequent simulations of the same cell design were adjusted by this ratio, thus ensuring accurate absolute efficiencies. Having done this, the agreement in all cases tested was very good, not only with respect to relative variations, but also in the absolute sense.

III. RESULTS AND DISCUSSION

A. SCOPE OF THE STUDY

The purpose of this study is to evaluate the usefulness of Interdigitated Back Contact (IBC) solar cells in space applications. The scope of the study includes optimization of the IBC cell design under several different constraints and assessment of the effects of certain design parameters on cell performance. Since optimization is achieved by selecting parameters which produce the results desired to meet specific performance requirements, it is necessary to first understand how each parameter affects cell performance. Cell performance is assessed on the basis of overall cell efficiency η, maximum power P_{max}, short circuit current I_{sc}, open circuit voltage V_{oc}, fill factor FF, and collection efficiency. These are the parameters commonly used to judge solar cell performance, with perhaps the exception of collection efficiency. This quantity measures the fraction of photogenerated carriers which are ultimately delivered as current at the contacts. This is distinct from the cell efficiency which is defined as the fraction of incident optical power that is ultimately delivered as electrical power at the contacts. The collection efficiency is related to the overall cell efficiency through the open circuit voltage and fill factor.

A subset of all the possible design parameters was selected for study in order to have a manageable task. These include cell thickness, contact width, spacing and thickness, front surface field doping and thickness, and light intensity. The remaining parameters and constants were fixed at the values shown in Table 1. The baseline cell design is specified by the parameters in Table 2. These particular values were selected as representative of established silicon technology as applied to IBC structures. The carrier lifetime values for radiation scenario 1 are computed using a radiation degradation coefficient[6] obtained from a recent analysis of conventional silicon solar cell degradation. We regard these values as optimistic because they are extracted from experimental data by making certain unverified but reasonable assumptions. The assumed dose is 1E15 1 MeV electron/cm^2. Scenario 2 assumes

Table 1. Constant Cell Design Parameters

Electrode width	25 μm
p^+ doping concentration	5E18 cm^{-3}
n^+ doping concentration	5E18 cm^{-3}
p doping concentration	1.40E15 cm^{-3}
p Auger recombination	1.2E-31 cm^6s^{-1}
n Auger recombination	1.7E-31 cm^6s^{-1}
Hole mobility	475 $cm^2/V*s$
Electron mobility	1380 $cm^2/V*s$
Front surface recombination	1E3 cm/s
p^+/oxide recombination	1E4 cm/s
N^+/oxide recombination	1E6 cm/s
Metal contact resistance	0
Front surface reflectivity	0

Table 2. Basline Cell Design

p^+ width	35 μm
n^+ width	145 μm
p^+ thickness	1.0 μm
n^+ thickness	0.3 μm
p thickness	50 μm
τ_n in base	136 μs 1.10 μs[a] 0.32 μs[b]
τ_n in p^+ contact	0.128 μs 78 ns[a] 78 ns[b]
τ_p in n^+ contact	32.6 ns 12 ns[a] 12 ns[b]
FSF doping	5E18 p type
FSF thickness	0.5 μm

(a) After radiation scenario 1:
K_L = 2.5E-11 for p base
K_L = 1.10E-9 for p^+ region
K_L = 3.10E-8 for n^+ region

(b) After radiation scenario 2:
K_L = 8.40E-11 for p base
Other K_Ls same as scenario 1.

the same dose, but with an experimentally obtained radiation degradation coefficient[3] for the base region. As pointed out in reference 6, this degradation coefficient is probably pessimistic because of the overly simplistic method by which it was obtained from the data. The second line of Table 3 shows that this baseline cell has a 1 sun efficiency of 14.87% BOL.

A COMSAT "Violet" cell was simulated to provide a basis for comparison with conventional silicon technology. A 250 μm thick cell of this type at 1 sun gave approximately 14.67% BOL and 13.2 EOL (under scenario 1) efficiency.

Subsequent sections present the effect on cell performance of variations about this baseline design. Cell performance at illuminations of 1 and 100 suns was calculated to evaluate systems with and without light concentration. All simulations were performed at 25°C.

B. CELL THICKNESS

Cell thickness effects are relatively simple to interpret. Thicker cells absorb a larger fraction of the incident light, especially the near-bandgap infrared, making the cell more efficient. However, the increased distance to the contacts means that a longer diffusion length is required and, therefore, higher quality silicon. The increased distance also means that thicker cells will be more susceptible to radiation-induced degradation.

Cells of 25, 50, and 200 micrometer thicknesses were simulated. The beginning of life (BOL) results in Table 3 show trends of increasing performance at 1 sun and decreasing performance at 100 suns as cell thickness is increased.

At 1 sun, efficiency increases by 1.4% (absolute) as cell thickness is increased from 25 to 200 μm. This increase is due to the additional absorption efficiency, which overcomes the decrease in collection efficiency arising from the extra diffusion distance that a thicker cell requires. The increased terminal current gives rise to a slight increase in V_{oc}.

At 100 suns, the BOL efficiency drops by 4.28% (absolute) as the cell thickness increases. In this case the higher carrier density throughout the

Table 3. BOL Effects of Cell Thickness

Cell Thickness	% η		P_{max} $mWcm^{-2}$		I_{sc} $mAcm^{-2}$		V_{oc} mV		% FF		% Collection Efficiency	
(μm)	1x	100x	1x	100x	1x	100x	1x	100x	1x	100x	1x	100x
25	13.67	15.26	18.54	20.60	42.59	47.09	541	662	80.10	66.08	99.76	99.53
50	14.87	14.31	20.07	19.31	45.47	49.79	548	680	80.54	57.04	99.49	99.03
200	15.06	20.98	20.33	14.82	47.34	47.35	548	676	78.36	46.30	95.08	87.07

cell causes the collection efficiency to decrease much more rapidly than in the 1 sun case. At first, this result seems contrary to the expectation that IBC cells are highly efficient under concentrated light. As is shown below, this baseline cell does not exhibit this behavior strongly because the contact regions are far from optimum.

The end of life (EOL) behavior following the more optimistic radiation scenario is shown in the upper part of Table 4. Clearly the thinnest cell has the best EOL performance, as expected. Also, each cell thickness shows little variation in EOL efficiency between 1 sun and 100 suns. The 25 μm cell has a 2% advantage over the 50 μm cell EOL for the baseline design at 1 sun. Table 4 shows the behavior of the 50 μm cell under the more realistic scenario 2 radiation. The loss of almost a factor of 2 in efficiency between the two radiation scenarios demonstrates the need for accurate radiation modeling input data, which may be obtained from experiments on bulk material rather than completed cells.

C. CARRIER COLLECTION REGION THICKNESS

The 50 μm thick cell was selected to study the effects of carrier collection region thickness.*

*BOL and EOL data are presented in Table 5. Trends observed in this cell were verified in simulations of the 25 μm thick cell, which are not presented here.

Table 4. EOL Effects of Cell Thickness

Cell Thickness (μm)	% η		P_{max} mWcm^{-2}		I_{sc} mAcm^{-2}		V_{oc} mV		% FF		P^+/N^+ Thickness (μm)	
	1x	100x	1x	100x	1x	100x	1x	100x	1x	100x		
25[1]	11.49	11.83	15.51	15.97	38.15	38.80	510	560	79.72	63.31	1.0	0.3
50[1]	9.49	9.88	12.81	13.33	32.37	37.86	502	646	78.84	54.51		
50[2]	5.05	5.32	6.82	7.18	18.77	19.70	482	600	77.78	60.80		
200[1]	1.00	1.05	1.33	1.41	3.93	3.46	443	560	76.48	72.89		
25[1]	11.98		16.18		38.53		526		79.82		3.0	0.9
50[1]	10.09		13.63		33.84		506		79.58			

[1] Radiation scenario 1.
[2] Radiation scenario 2.

Table 5. Effects of P^+ and N^+ Collection Region Thicknesses, BOL and EOL

Cell Thickness (μm)	% η		P_{max} mWcm^{-2}		I_{sc} mAcm^{-2}		V_{oc} mV		% FF		P^+/N^+ Thickness (μm)	
	1x	100x	1x	100x	1x	100x	1x	100x	1x	100x		
50	14.87	14.31	20.07	19.31	45.47	49.79	548	680	80.54	57.04	1.0	0.3
50[1]	9.49	9.88	12.81	13.33	32.37	37.86	502	646	78.84	54.51		
50	15.62	16.22	21.08	21.90	45.47	49.85	572	696	81.09	63.13	3.0	0.9
50[1]	10.09		13.63		33.84		506		79.58			
50	15.64		21.12		45.47		572		81.19		3.0	3.0

[1] EOL, radiation scenario 1.

At light intensities of 1 sun and 100 suns, BOL cell performance improvements in efficiency, P_{max}, V_{oc}, and FF were observed when respective p^+ and n^+ regions were changed from 1.0/0.3 μm to 3.0/0.9 μm thick, as shown in Table 5. Collection efficiency and I_{sc} remained constant as expected. There was no change in performance when the n^+ collection region thickness was further increased to 3.0 μm. The results thus indicate that an approximate 0.8% increase in BOL efficiency can be obtained by increasing the thickness of the doped contact regions.

The EOL figures included in Table 5 show that most of this 0.8% BOL improvement is retained at EOL. Therefore, the conclusion of this portion of the study is that doped contact regions which are thicker than those in the baseline design will improve both BOL and EOL performance.

D. CARRIER COLLECTION REGION WIDTH

The 50 μm baseline cell described in Table 2 was again selected for study of the effects of minority (n^+) and majority (p^+) carrier collection region widths. Since the baseline cell was near optimum for 1 sun, the overall cell efficiency was expected to decrease as the region widths were changed. However, an incremental decrease in the n^+ region width from 145 μm to 90 μm resulted in higher cell efficiencies as shown in Table 6. This increase in cell efficiency at first seems contrary to intuition since the minority carrier diffusion length of 700 μm (BOL) is sufficient for these carriers to reach the contact effectively irrespective of its size. One possibility is that the increased efficiency is due to the reduced n^+/oxide interface area, which results in lower interface recombination losses. However, the table shows that while the contact width is reduced, the collection efficiency is also decreasing. In fact, the increase in efficiency is due to an increased V_{oc} and fill factor. This can be understood by remembering that the dark current of the cell I_0, which is caused by carrier injection from the contacts into the base region, is reduced when the area of the contact/base interface is reduced. Since V_{oc} varies as $\ln(I_{sc}/I_0)$, an increased V_{oc} is expected. Although the efficiency only increases by 0.25% at 1 sun BOL, it can be more significant at EOL. At 100 suns the improvement is 4.3%. For this study we have not performed a detailed EOL optimization of a concentrator cell.

Table 6. Effects of P^+ and N^+ Collection Region Widths on 50 μm Thick Cell, BOL

% η		P_{max} $mWcm^{-2}$		I_{sc} $mAcm^{-2}$		V_{oc} mV		% FF		% Collection	P^+/N^+ Thickness
1x	100x	1x	100x	1x	100x	1x	100x	1x	100x	100x	(μm)
14.87	14.31	20.07	19.31	45.47	49.79	548	680	80.5	57.0	98.98	35/145
14.79		19.96		45.41		548		80.2			35/135
14.84	15.25	20.04	20.59	45.43	49.75	548	681	80.5	60.8		35/125
14.93	16.47	20.16	22.24	45.18	49.59	552	686	80.8	65.4	98.58	35/90
	17.54		23.68		49.45		681		70.3	98.30	60/90
14.90	18.40	20.10	24.84	45.10	49.42	551	684	80.9	73.4	98.23	90/90
15.12	18.76	20.41	25.32	45.09	49.23	560	693	80.8	74.2	97.86	90/70
15.00	18.73	20.24	25.29	44.90	49.21	560	692	80.5	74.3	97.81	90/50

E. ABRUPT FRONT SURFACE FIELD

The front surface field (FSF) is a heavily doped region, p^+ in the present case, which covers the entire front face of the solar cell. Its purpose is to provide an electric field that repels one carrier type away from the front surface. This effectively reduces the surface recombination velocity by reducing the concentration of one type of carrier near the surface. The FSF is generally introduced by heavier doping in a thin layer near the interface. This doping may be a step function, in which case it is often referred to as a minority carrier mirror, or a graded region. The graded region, although more difficult to tailor experimentally, is somewhat more effective since the field is present over the entire region thickness.

The effects of FSF thickness and doping level were studied for the baseline cell geometry at BOL. For thicknesses of 0.25, 0.5, and 1.0 μm at 1E18 doping, no significant effect was observed at 1 sun. The FSF effectiveness is relatively constant over a rather broad range around 1E17 to 1E18 cm^{-3}, decreasing below this level due to the weakness of the electric field and decreasing above this level due to increased Auger recombination. As will be shown in the next section, the FSF doping level becomes very important for a graded FSF.

F. DESIGN REFINEMENTS

Using the baseline cell as a starting point, the IBC cell design has been investigated to show how the parameters should be varied to produce an optimum design for various applications. In cases where radiation exposure is not present as the result of shielding or terrestrial use, the 1 sun cell should be at least 50 μm thick, have contact doping widths approximately 90 μm for both minority and majority carriers with 20 μm spacing, and have doping thicknesses approximately 1 μm and 3 μm, respectively. The efficiency of this cell will be near 16% AMO. A 100 sun cell will be very similar but will have an efficiency near 20%.

For space use, where radiation is present, EOL performance must be considered. The baseline cell parameters are near optimum for EOL efficiency. One method of further optimizing for EOL performance is by reducing cell thickness to 25 μm and increasing the contact doping region thickness. The gain in EOL efficiency will be nearly 2% at both 1 sun and 100 suns as the cell is thinned from 50 μm to 25 μm. Thus, the improvement over the baseline cell at 1 sun and 100 suns under these conditions is a total of 2.5%, with 2% attributable to cell thinning and 0.5% to contact doping thicknesss.

Recognizing that silicon cells as thin as 25 μm represent a major challenge in fabrication, we have investigated whether this excellent EOL performance can be obtained in a more conventional 50 μm thick cell. The additional design variations which we consider are the collector region spacing, the use of a graded front doping, and the bulk silicon/oxide back surface passivation. The previous results considered recombination only at the collector/oxide interfaces, which has been shown to be less important than the bulk/oxide interface. The results presented below indicate that if the latter interface can be well passivated (S<1E3 cm/sec), high EOL efficiency can be maintained in a thicker cell.

The initial parameter variation aimed at re-optimizing the structure consisted of decreasing the collector spacing from 20 μm to 10 μm. This increased the EOL efficiency from 10.1% to 10.3%. This change does not increase the metal grid coverage on the cell--it only changes the arrangement

of the doping regions underlying the metal grid. Even if the interface between these doping regions and the oxide surface is poorly passivated (S = 1E4 cm/sec) this performance can be achieved. This result and that reported previously assume excellent passivation (S < 10 cm/sec) of the bulk/oxide interface between the doping regions. For comparison, the 25 μm cell with 20 μm spacing gave 11.98% EOL efficiency. Thus, changes in contact spacing alone are not sufficient to regain the EOL efficiency lost in going to a 50 μm thickness from 25 μm.

In order to regain more of the performance lost by doubling the cell thickness from 25 μm to 50 μm, the use of a graded front surface doping field was investigated. The previous design used a 0.5 μm thick front surface field (FSF) uniformly doped at 5E18. It was found that by replacing this with a Gaussian doping profile with a characteristic width of 15 μm and a peak concentration of 1E18, the EOL efficiency was 11.49% with a 10 μm collector region spacing. This feature restored most of the lost performance. Table 7 shows the effects of a graded FSF with characteristic length of 15 μm as a function of doping level (peak concentration ranges from 5E16 to 5E18).

However, the importance of the bulk/oxide passivation is greatly increased when graded FSF is used. In the ungraded FSF 50 μm cell reported previously, the EOL efficiencies are 10.1% and 9.77% for recombination velocities at this interface of 0 and 1E4 cm/sec, respectively. For the graded design studied here, the corresponding efficiencies are 11.49% and 7.2%. Thus the improved efficiency of the graded structure carries with it the requirement of good surface passivation. Figures 2 and 3 show how the carrier flow differs between the unpassivated (high recombination, Fig. 2) and passivated (low recombination, Fig. 3) cases. In each figure a portion of the simulated cell is shown. The large minority collector (n^+) is shown in the upper left corner and a fraction of the smaller majority collector (p^+) is in the upper right corner. The figures show a 20 μm thick portion of the cell. Thus the important bulk/oxide interface between the two collector regions is featured. The line segments in each figure are vectors whose length represents the minority carrier (electrons in this case, since the base region is p type) current at a particular point in the cell and whose orientation shows

Table 7. Efficiency as a Function of FSF for 50 μm Cell at 1 Sun

Graded FSF to 15 μm	Step FSF 0.5 μm	FSF Doping cm^{-2}	% Cell Efficiency BOL	EOL
X		5E16	15.09	12.12
X		1E17	15.07	12.30
X		5E17	14.56	12.09
X		1E18	13.98	11.49
X		3E18		9.29
X		5E18		7.66
	X	5E18		10.29

the current flow direction. In both figures the light is incident from below. Addressing the high recombination case first, observe the fate of electrons generated on the left side of the figure. In order to contribute to the cell output current, these electrons must reach the minority collector in the upper right corner of the figure. The current vectors show, however, that some current flows to the left around the majority collector, resulting in recombination at the bulk/oxide interface. A larger current flows around the right side of the majority contact and results in significant recombination at the interface between the two collectors. Electrons generated on the right side of the figure (near 60 and 70 μm) do succeed in reaching the minority collector. The interface losses shown in this figure explain the poor performance of the graded field cell when surface passivation is inadequate.

Now considering the low recombination figure, it is seen that even electrons generated on the left side of the figure are directed around the majority collector to the right so that they subsequently reach the minority collector. None of the vectors show currents directed toward the interfaces. Thus this cell has much higher efficiency. The added sensitivity of the graded doping cell to surface recombination probably arises from the doping-induced drift field which drives the minority carriers toward the rear of the

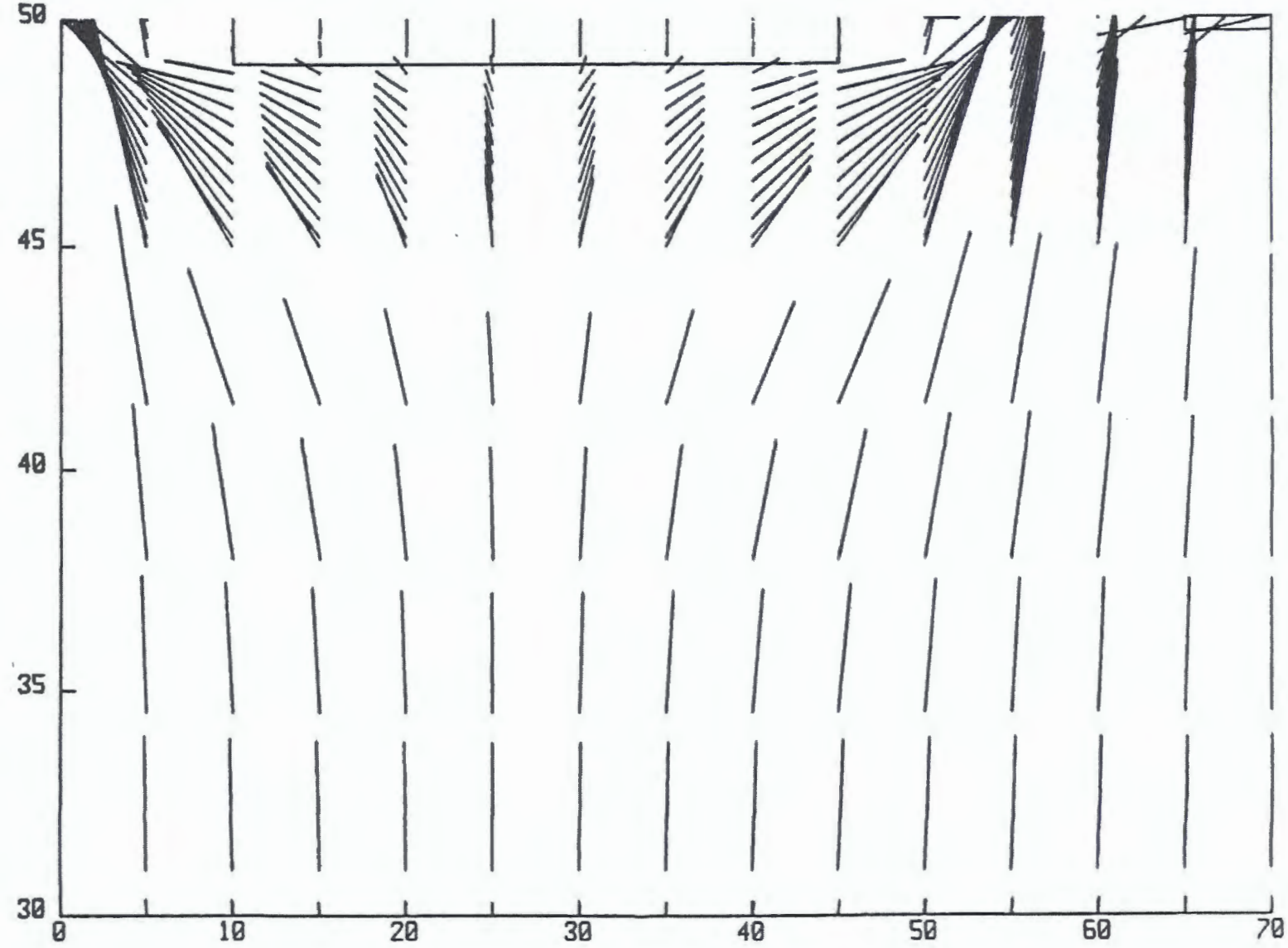


Fig. 2. Carrier Flow in High Recombination Case

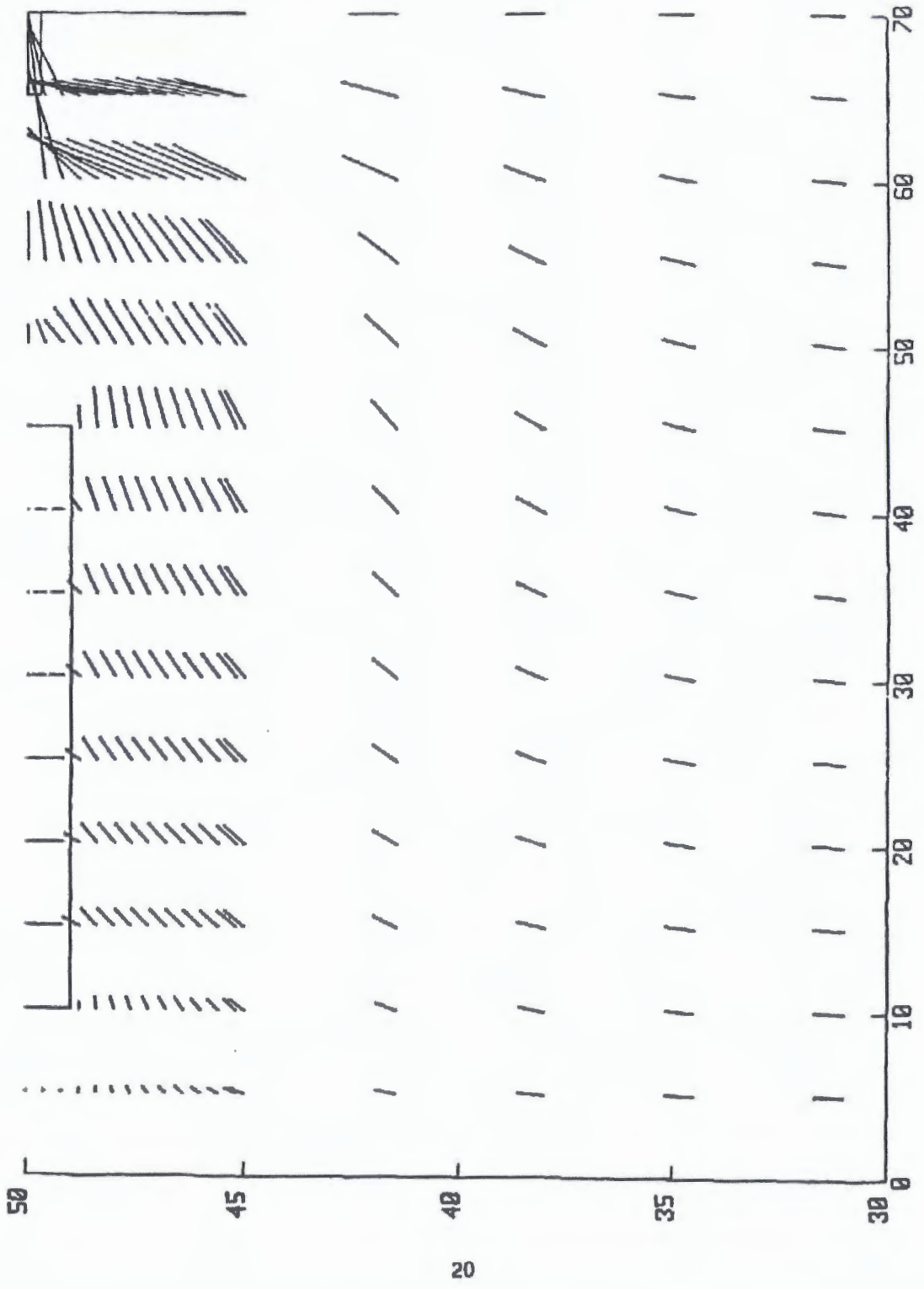


Fig. 3. Carrier Flow in Low Recombination Case

cell, rather than allowing them to diffuse toward the minority collector. Therefore, they are more likely to encounter the surface regions where recombination occurs.

Thus, the best 1 sun EOL performance is obtained with the 25 μm thick cell (11.98%), but a reasonable approximation of this can be obtained in a 50 μm cell (11.49%) with a graded front surface field with characteristic length approximately 15 μm and peak concentration roughly 1E18, combined with good interface control at the bulk/oxide interfaces.

Since breakage can be a significant problem for silicon cells 50 μm or less in thickness, we have made a study of 65 and 80 μm thicknesses which offer added mechanical strength at some expense of EOL efficiency. The attached graph (Fig. 4) shows the results.

The + signs represent cells with the 15 μm graded front surface field (FSF), 10 μm contact doping region spacing, 3 μm thick p^+ regions, and 0.9 μm thick n^+ regions. These parameters are identical to those for the optimized design reported previously. The loss in EOL efficiency in going from 50 to 80 μm is seen to be greater than 2%. The degradation assumed scenario 1 as described previously. The * signs represent cells with the same graded FSF but assuming the more pessimistic scenario 2 degradation. The change in efficiency is again near 2%, and is therefore roughly independent of the degradation scenario used.

For comparison, the effect of thickness on cell efficiency when a more conventional step front surface field is used is shown with the symbol X. The solid line portion of this graph is for cells of the same design as those just described except with a 0.5 μm thick FSF instead of the graded FSF. The two X symbols connected by the dashed line have the additional difference that the contact doping region spacing is 20 μm instead of 10 μm. These additional points are included simply to show how the trend extends to 25 μm.

The conclusion of this analysis on cell thickness is that both FSF cell designs suffer significant 1 sun EOL efficiency loss as the cell thickness increases from 50 to 80 μm, and that the amount of loss is roughly the same. Thus the graded FSF design retains its 2% efficiency advantage over the step FSF design under these conditions.

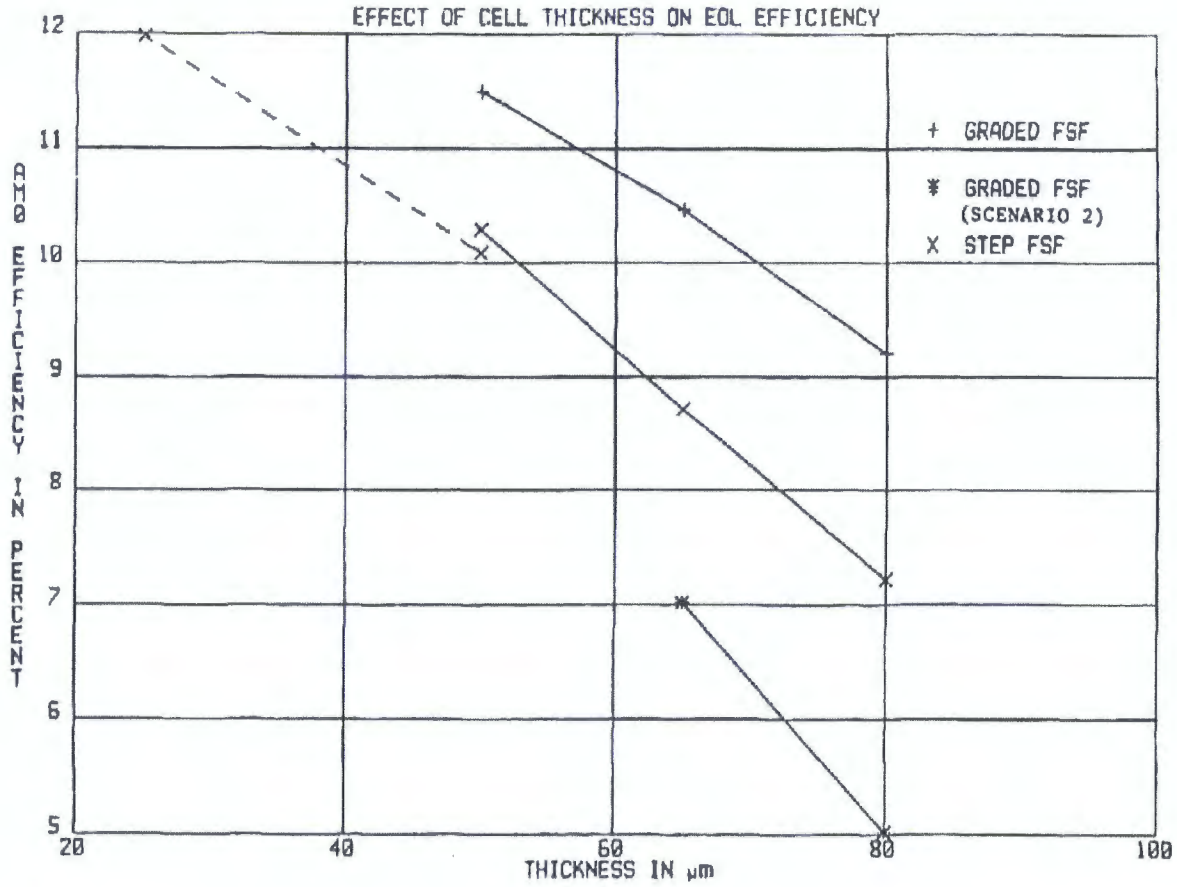


Fig. 4. Effect of Cell Thickness on EOL Efficiency

G. CONCENTRATED LIGHT LEVELS

IBC solar cells are designed to take advantage of concentrated light levels. Under concentration they are far superior to conventional cells in efficiency. Operation at 1 sun does not offer BOL efficiencies that significantly exceed those achievable with conventional designs. Therefore, simulations at 100 suns were performed to see whether or not the same optimum design rules applied at concentrated light levels. BOL efficiency for the 1 sun optimized design described above was approximately 18% at 100 suns. When the FSF was graded to 5 μm instead of 15 μm, BOL efficiency was about 16.6%.

Cell thicknesses of 50, 65, 80, and 200 micrometers were simulated at 100 suns using the near-optimal design parameters described above. We found that the 15.44% EOL efficiency for a 50 μm thick cell with this design is comparable to that of GaAs space cells. A 65 μm thick cell has an EOL efficiency of 11.57%. Table 8 summarizes the results of increased cell thickness at 100 suns for the optimum design. Included in Table 8 are results of increased cell thickness at 100 suns with the nonoptimum step FSF.

Table 8. EOL Efficiency as a Function of cell Thickness and FSF at 100 Suns

Cell Thickness (μm)	Graded FSF (μm)	Step FSF (μm)	FSF Doping cm^{-3}	*Spacing a/b/c	Cell Efficiency (%)
50	15	—	1E18	10/20/10	14.64
50	15	—	1E18	5/10/5	15.44
65	15	—	1E18	5/10/5	11.57
80	15	—	1E18	5/10/5	8.97
200	15	—	5E18	5/10/5	1.18
65	—	0.5	5E18	5/10/5	8.17
80	—	0.5	5E18	5/10/5	6.83

*a,c = spaces between right and left edges of collectors and unit cell boundaries, resp.; b = space between collectors. All dimensions are in micrometers.

The 18% BOL efficiency of the 1 sun optimized cell is significantly lower than the 25% efficiency quoted in Section I for two reasons. First, the present figure is for AMO illumination rather than AM1.3. For conventional cells this difference in spectrum leads to a 2-3% decrease (absolute) in efficiency. Second, the baseline design is intended for 1 sun operation whereas the cell referred to earlier is intended for and operated at several hundred suns. The BOL efficiencies of the cells described in Table 8 were not calculated for comparison with the 25% frame in Section I because these cells are optimized for EOL efficiency, while the 25% cell is optimized for BOL.

IV. CONCLUSION

The design of IBC solar cells for space use has been investigated using 2-dimensional computer simulations. Near-optimal designs have been presented for missions using either planar or 100 sun concentration for arrays, under high or negligible radiation fluences. In the low radiation environment, the minority and majority carrier collection regions should be of comparable width, with thicknesses of 0.9 μm and 3.0 μm, respectively. The FSF should be an approximately 0.5 μm step with doping concentration of 5E18 cm^{-3}. These parameters are much more critical for 100 sun operation. The 1 sun efficiency of IBC cells exceeds 15%, which makes them competitive with conventional design silicon cells. The 100 sun efficiency is nearly 19%, which greatly exceeds the conventional silicon cell capability. It is also in the expected efficiency range of GaAs concentrator cells, although the operating temperature of each is quite important in comparing efficiencies.

In a high radiation environment, a different design is used to maximize the EOL performance. At 1 sun after 1E15 1 MeV electron fluence, the design presented here shows over 12% efficiency. The carrier collection region widths in this design are in an approximately 4 to 1 ratio, unlike the low radiation case. The FSF is graded over 15 μm with a peak doping concentration of 1E17 to 1E18 cm^{-3}. At 100 suns the EOL efficiency approaches 16%, which is comparable to that expected for GaAs concentrator systems. The high radiation environment cell design is summarized in Table 9. The effect of proton irradiation has not been addressed here, but the very deep junction should lead to high resistance to low energy front side proton irradiation.

The overall conclusion of this study is that properly designed IBC cells can yield performance which is comparable with (or superior to) competing silicon and gallium arsenide technologies. Therefore, their use in space systems should be considered. It is especially important with IBC cells to optimize the design to the particular mission profile. The light intensity to be used and the radiation environment affect the design to a greater extent than in conventional cells.

Table 9. High-Radiation Environment Cell
Design Parameters

Electrode width	25 μm
p^+ doping concentration	5E18 cm^{-3}
n^+ doping concentration	5E18 cm^{-3}
p doping concentration	1.40E15 cm^{-3}
p Auger recombination	1.2E-31 cm^6s^{-1}
n Auger recombination	1.7E-31 cm^6s^{-1}
Hole mobility	475 $cm^2/V*s$
Electron mobility	1380 $cm^2/V*s$
Front surface recombination	1E3 cm/s
p^+/oxide recombination	1E4 cm/s
n^+/oxide recombination	1E6 cm/s
Metal contact resistance	0
Front surface reflectivity	0
p^+ width	35 μm
n^+ width	145 μm
p^+ thickness	1.0 μm
n^+ thickness	0.3 μm
p thickness	50 μm
τ_n in base	136 μs 1.10 μs[a] 0.32 μs[b]
τ_n in p^+ contact	0.128 μs 78 ns[a] 78 ns[b]
τ_n in n^+ contact	32.6 ns 12 ns[a] 12 ns[b]
FSF doping (peak concentration)	1E17 p type
Gaussian width	15 μm

(a) After radiation scenario 1:
K_L = 2.5E-11 for p base
K_L = 1.10E-9 for p^+ region
K_L = 3.10E-8 for n^+ region

(b) After radiation scenario 2:
K_L = 8.40E-11 for p base
Other K_L s same as scenario 1.

REFERENCES

1. M. D. Lammert and R. J. Schwartz, IEEE Electron Devices Transcripts, ED-24, 337 (1977).

2. P. Verlinden et al, 19th Photovoltaic Specialists Conference Proceedings, New Orleans, LA (1987), p. 405.

3. Jet Propulsion Laboratories, Solar Cell Radiation Handbook, pp. 3-27 (1982).

4. D. J. Chin and D. H. Navon, Solid State Electronics, 24, 109 (1981).

5. H. J. Hovel, "Solar Cells", Vol. 11 of Semiconductors and Semimetals, Eds. Willardson and Beer, Associated Press, New York (1975).

6. G. F. J. Garlick and J. A. Minahan, 18th Photovoltaic Specialists Conference Proceedings, Las Vegas, NV (1985), p. 669.

LABORATORY OPERATIONS

The Aerospace Corporation functions as an "architect-engineer" for national security projects, specializing in advanced military space systems. Providing research support, the corporation's Laboratory Operations conducts experimental and theoretical investigations that focus on the application of scientific and technical advances to such systems. Vital to the success of these investigations is the technical staff's wide-ranging expertise and its ability to stay current with new developments. This expertise is enhanced by a research program aimed at dealing with the many problems associated with rapidly evolving space systems. Contributing their capabilities to the research effort are these individual laboratories:

Aerophysics Laboratory: Launch vehicle and reentry fluid mechanics, heat transfer and flight dynamics; chemical and electric propulsion, propellant chemistry, chemical dynamics, environmental chemistry, trace detection; spacecraft structural mechanics, contamination, thermal and structural control; high temperature thermomechanics, gas kinetics and radiation; cw and pulsed chemical and excimer laser development including chemical kinetics, spectroscopy, optical resonators, beam control, atmospheric propagation, laser effects and countermeasures.

Chemistry and Physics Laboratory: Atmospheric chemical reactions, atmospheric optics, light scattering, state-specific chemical reactions and radiative signatures of missile plumes, sensor out-of-field-of-view rejection, applied laser spectroscopy, laser chemistry, laser optoelectronics, solar cell physics, battery electrochemistry, space vacuum and radiation effects on materials, lubrication and surface phenomena, thermionic emission, photosensitive materials and detectors, atomic frequency standards, and environmental chemistry.

Computer Science Laboratory: Program verification, program translation, performance-sensitive system design, distributed architectures for spaceborne computers, fault-tolerant computer systems, artificial intelligence, microelectronics applications, communication protocols, and computer security.

Electronics Research Laboratory: Microelectronics, solid-state device physics, compound semiconductors, radiation hardening; electro-optics, quantum electronics, solid-state lasers, optical propagation and communications; microwave semiconductor devices, microwave/millimeter wave measurements, diagnostics and radiometry, microwave/millimeter wave thermionic devices; atomic time and frequency standards; antennas, rf systems, electromagnetic propagation phenomena, space communication systems.

Materials Sciences Laboratory: Development of new materials: metals, alloys, ceramics, polymers and their composites, and new forms of carbon; nondestructive evaluation, component failure analysis and reliability; fracture mechanics and stress corrosion; analysis and evaluation of materials at cryogenic and elevated temperatures as well as in space and enemy-induced environments.

Space Sciences Laboratory: Magnetospheric, auroral and cosmic ray physics, wave-particle interactions, magnetospheric plasma waves; atmospheric and ionospheric physics, density and composition of the upper atmosphere, remote sensing using atmospheric radiation; solar physics, infrared astronomy, infrared signature analysis; effects of solar activity, magnetic storms and nuclear explosions on the earth's atmosphere, ionosphere and magnetosphere; effects of electromagnetic and particulate radiations on space systems; space instrumentation.

MARVIN03

National Technical Reports Library

The National Technical Information Service acquires, indexes, abstracts, and archives the largest collection of U.S. government-sponsored technical reports in existence. The NTRL offers online, free and open access to these authenticated government technical reports. Technical reports and documents in its repository may be available online for free either from the issuing federal agency, the U.S. Government Publishing Office's Federal Digital System website, or through search engines.

National Technical Reports Library Search Tips

Help Desk Contact

Our team of technical information specialists provide directional, technical, and informational help desk support of the NTRL. Telephone assistance is available Monday through Friday, 8:30 a.m. - 5 p.m. (ET) by calling (703) 605-6585. Email assistance is available from NTRLHelpDesk@ntis.gov

QUICK SEARCH: Use Quick Search for simple searches against the following fields: Accession Number, Title, Date, Report Number, Keywords, Abstract, Report Year and Full Text.

ADVANCED SEARCH: Use Advanced Search to search multiple criteria or to limit the search to a particular field. Any combination of fields can be used. Select the operator between fields from the *Choose Operator* drop down.

Example: To search for documents published in 2005 about air pollution and authored by Bechtel, enter *Keywords*: air pollution, *Corporate Author*: Bechtel, and *Published Date*: *Between January 1, 2005 and December 31, 2005* with the AND operator selected.

SEARCH TIPS FOR BOTH QUICK AND ADVANCED SEARCH

Strings are automatically stemmed. For example, searching for the term plant produces results for plant, plants and planting.

Multiple search terms are "ANDed" together automatically. This is not an exact phrase search.

Example: ionizing radiation

In Quick Search and in free text fields, such as title, keywords and authors, multiple terms can be combined together with Boolean operators **OR, AND, NOT** to form a more complex query. The operator must be entered in all uppercase.

Example: "nuclear power plants" AND radiation OR waste

Example: *Personal Author*: "Jones, P. N." AND "Smith, E. A"

Using Quick Search from the Advanced Search page searches the same fields as the Quick Search page: Accession Number, Title, Date, Report Number, Keywords, Abstract, Report Year and Full Text. The Quick Search can be combined with another field in Advanced Search to retrieve more precise results.

Phrase Search: Use quotes around the search terms to limit the search to results where the terms are adjacent. Stemming is applied to individual terms within the phrase.

Example: "ionizing radiation"

RESULTS DISPLAY

The *Default* display shows the Refine filters in the left column. Selecting *Citations Only* from the Display drop down, removes the refine options from the display and uses the full width of the page to display the citations.

REFINE: Refine filters appear on the left side of the Results page when the *Default* display is selected. To reduce results or filter the search, select from the Refine options.

Example: Select "ionizing radiation" under Keywords to limit the results to those records with "ionizing radiation" added as a keyword by the indexer. To refine by year, select the Published Year of interest, for example "2009".

Back to top

SELECTED ADVANCED SEARCH FIELD CONTENT EXAMPLES

Accession Number: Number assigned by NTIS to reflect the order of entry into the NTIS® database. May or may not contain punctuation. Here are few examples:

ACNP-64519(REV)
ACNP64519REV
AD-468 299
AD468299
N95-11834/5
N9511834
PB95-197604
PB95197604

Personal Author: Search by initials and/or last name.

P. N. Jones

Source Agency Code: The codes are limited to 6 characters. Here are a few examples:
DE
DODXA
DIBM
INIS
NASA
EPAOTS
DEE
EPAORD

Keywords: Keywords are identifiers or descriptors assigned by the NTIS indexers. They are assigned to enhance searching and focus on the key concepts in the document.

NTIS Subject Category Code: These codes appear on the results screen on the left side. They are assigned by the NTIS indexers to represent major topic groupings.

Report Number: This number can be an ISBN number, a monitoring agency number, or contractor assigned report number. The format may or may not include punctuation. Here are a few examples:

MAB-139-M(M3)
MAB139MM3
HUMRRO-TR-73
HUMRROTR73
TAOSTAN6961
USCGD2782

Contract Number: Search with punctuation. Here are a few examples:

AC06-76RL01830
NSF C260
AT(04-3)-167

Country of Publication: These are usually 2 letter codes. For example,

UR
FR
UK
NL
FI
SW
CA

Document Type: There are 22 document types. Some of the most common ones are: Technical Report, journal article, conference proceedings, thesis, and patent. The document types appear on the results screen under the Refine filters on the left side

Issue Number: New titles are announced within the NTRL on an ongoing basis. At the time they are announced, they are assigned a four digit "Issue Number" by NTIS. The first two digits of the Issue Number represent the year of the announcement, while the second two digits represent the NTIS issue in which the title was made publicly available. There are generally 26 issues in a year. For Example: 0907 = Issue number seven during Year 2009. Additional examples:

0509
0711
0920

Back to top

COPYRIGHT © 2014 - NTIS - NATIONAL TECHNICAL INFORMATION SERVICE

FOIA ABOUT NTIS PRIVACY POLICY INFORMATION QUALITY USA.GOV

MARVIN04

UNITED STATES DEPARTMENT OF COMMERCE
National Technical Information Service
5301 Shawnee Road
Alexandria, VA 22312

Office of Program Management

June 12, 2024

To Whom It May Concern,

This is in response to your inquiry in which you requested a confirmation of the availability of information from the National Technical Information Service (NTIS).

NTIS announced the document "Interdigitated Back Contact Silicon Solar Cell Analysis and Design Recommendations for Space Use." (ADA220414)
through the following means:

The bibliographic reference/abstract was added to the NTIS Bibliographic Database as part of issue 199016 available "on or about" July 1990.

"On or about" refers to the document being available in the NTIS Database within a month of the date provided above.

Best regards,

ARNETT STRICKLAND Digitally signed by ARNETT STRICKLAND
Date: 2024.06.12 14:28:16 -04'00'

Wayne Strickland, Associate Director
Office of Program Management
National Technical Information Service
email: wstrickland@ntis.gov
phone: (703)605-6543

MARVIN05

An official website of the United States government Here's how you know

U.S. National Technical Information Service
A bureau of the U.S. Department of Commerce

About Us

As a bureau within DOC, NTIS has been instrumental for over 70 years in making Federal information and data available to American businesses and the Public.

To continue this mission, NTIS is repositioning itself as a data service agency, building new solutions with our private-sector partners to grow capacity that extends traditional governmental data and analytic competency.

We help agencies leverage new and innovative capabilities, including artificial intelligence, machine learning, and robotics. Agencies can apply these capabilities across their information lifecycle: collect, store, analyze, use, and share.

For more information on NTIS, please visit www.ntis.gov to learn about the Agency and its evolving role in the data landscape.

By the numbers:

- **31** Federal agencies supported since 2018
- **27** Data analytics AI/MS projects
- **$34M** Largest single project
- **<99** Average number of days to project kick-off
- **3M+** Searchable publications in our National Technical Reports Library
- **138** Projects since 2018

Examples of Agencies Supported:

- United States Census
- HHS Inspector General
- JAIC
- USAID
- NTIA
- NIST
- Bureau of Industry and Security (Commerce)

National Technical Information Service
U.S. Department of Commerce

5301 Shawnee Rd,
Alexandria, VA 22312

Connect With NTIS

MARVIN06

Saved **3 times** between February 17, 2013 and July 21, 2013.



JAN

	1	2	3	4	5	
6	7	8	9	10	11	12
13	14	15	16	17	18	19
20	21	22	23	24	25	26
27	28	29	30	31		

FEB

					1	2
3	4	5	6	7	8	9
10	11	12	13	14	15	16
17	18	19	20	21	22	23
24	25	26	27	28		

MAR

					1	2
3	4	5	6	7	8	9
10	11	12	13	14	15	16
17	18	19	20	21	22	23
24	25	26	27	28	29	30
31						

APR

	1	2	3	4	5	6
7	8	9	10	11	12	13
14	15	16	17	18	19	20
21	22	23	24	25	26	27
28	29	30				

MAY

		1	2	3	4	
5	6	7	8	9	10	11
12	13	14	15	16	17	18
19	20	21	22	23	24	25
26	27	28	29	30	31	

JUN

						1
2	3	4	5	6	7	8
9	10	11	12	13	14	15
16	17	18	19	20	21	22
23	24	25	26	27	28	29
30						

JUL

	1	2	3	4	5	6
7	8	9	10	11	12	13
14	15	16	17	18	19	20
21	22	23	24	25	26	27
28	29	30	31			

AUG

				1	2	3
4	5	6	7	8	9	10
11	12	13	14	15	16	17
18	19	20	21	22	23	24
25	26	27	28	29	30	31

SEP

1	2	3	4	5	6	7
8	9	10	11	12	13	14
15	16	17	18	19	20	21
22	23	24	25	26	27	28
29	30					

OCT

		1	2	3	4	5
6	7	8	9	10	11	12
13	14	15	16	17	18	19
20	21	22	23	24	25	26
27	28	29	30	31		

NOV

					1	2
3	4	5	6	7	8	9
10	11	12	13	14	15	16
17	18	19	20	21	22	23
24	25	26	27	28	29	30

DEC

1	2	3	4	5	6	7
8	9	10	11	12	13	14
15	16	17	18	19	20	21
22	23	24	25	26	27	28
29	30	31				

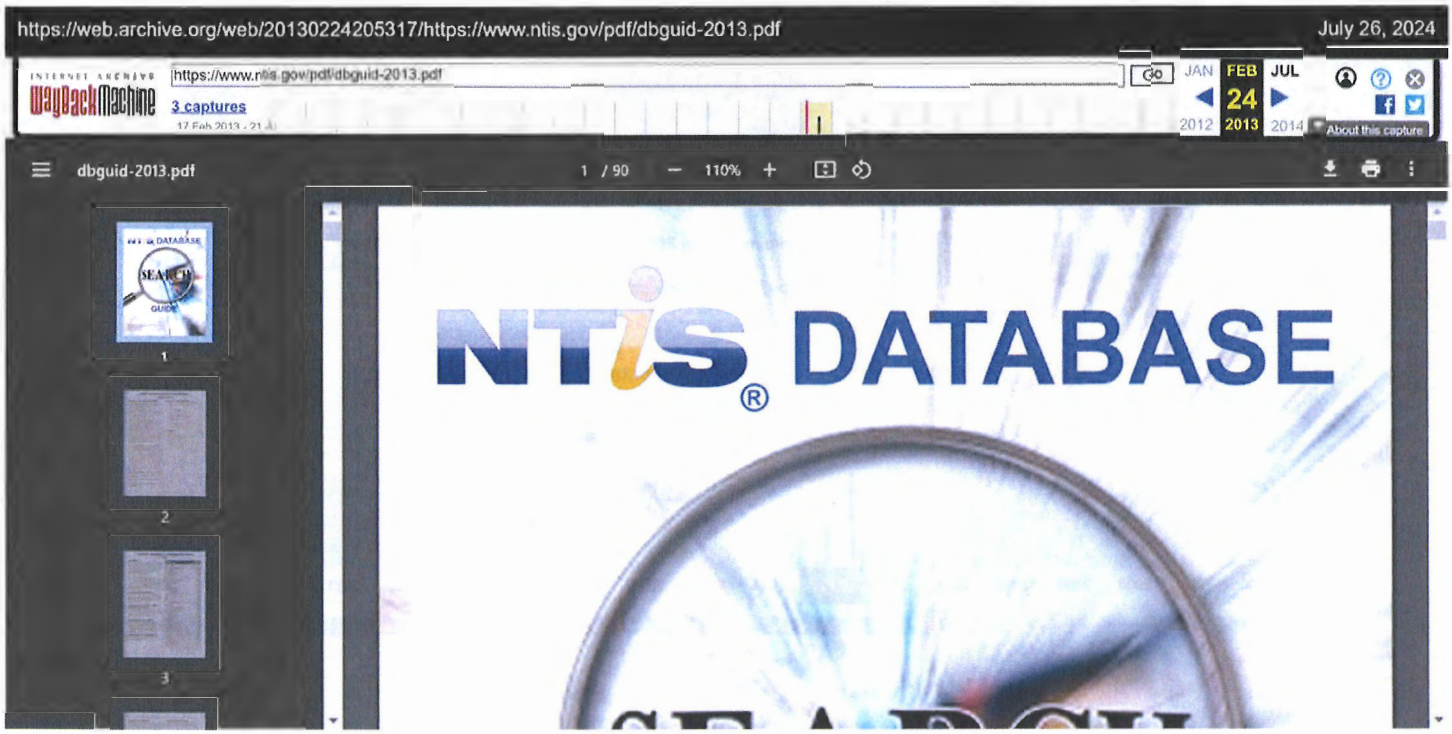
Note

This calendar view maps the number of times **https://www.ntis.gov/pdf/dbguid-2013.pdf** was crawled by the Wayback Machine, *not* how many times the site was actually updated. More info in the FAQ.

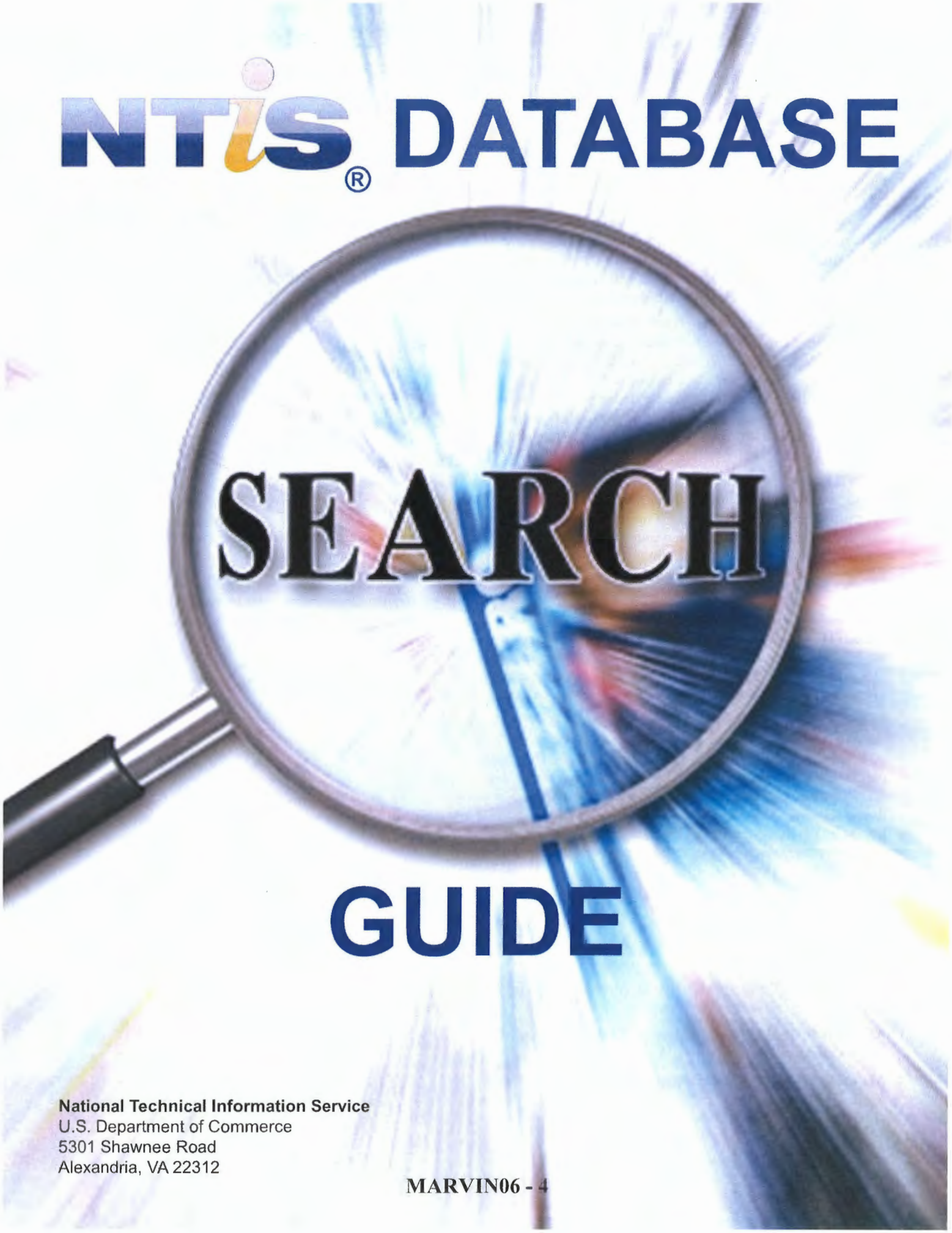
FAQ | Contact Us | Terms of Service (Dec 31, 2014)

The Wayback Machine is an initiative of the Internet Archive, a 501(c)(3) non-profit, building a digital library of Internet sites and other cultural artifacts in digital form. Other projects include Open Library & archive-it.org

Your use of the Wayback Machine is subject to the Internet Archive's Terms of Use


https://web.archive.org/web/20130224205317/https://www.ntis.gov/pdf/dbguid-2013.pdf
July 26, 2024
https://www.ntis.gov/pdf/dbguid-2013.pdf
3 captures
JAN
FEB
JUL
24
2012
2013
2014
About this capture
dbguid-2013.pdf
1 / 90
110%
NTIS DATABASE

NTIS® DATABASE



GUIDE

National Technical Information Service
U.S. Department of Commerce
5301 Shawnee Road
Alexandria, VA 22312

MARVIN06 - 4

Search Guide for the NTIS Database

Introduction

Organization of the Search Guide

Section I - Introduction: Provides a basic introduction to the features of the NTIS Database, how it differs from other government and/or scientific and technical databases and how it supplements other government databases.

Section II - NTIS Database Elements: Each component field of the bibliographic record is defined with examples. Presents the record structure and composition of the NTIS Database. Changes in the use of a field are discussed. NTIS' names and labels for the fields in the bibliographic citation are identified.

Section III – Online Searching Hints: Includes online searching hints arranged alphabetically by topic and field. Points covered are: searching accession numbers and specially assigned information product type numbers; abbreviations, acronyms; biological species; chemical studies; and verbalization of scientific and mathematical symbols. Distinctions between sponsoring agencies and performing agencies in the corporate author field are shown.

The NTIS Subject Category Codes are interpreted with emphasis on health care and medicine, environment, and business-related information. Geographic features and locations are demonstrated as well as discussions of developing country, foreign language documents and translations. Searching for reprints, maps, patents, and environmental impact statements are also covered. The placement and meaning of sponsoring agency acronym codes are also noted.

Section IV – Selected References for Assistance in Searching the NTIS Database: Contains a list of references to the authority files used by NTIS and its cooperating agencies at the Department of Energy, NASA and the Defense Technical Information Center.

Section V – Online Access: Presents contact information for the vendors that provide access to the database, including the company name, address, telephone number and fax number. Each online service's search and display commands are presented. An NTIS Database bibliographic record is furnished in each vendor's format showing the vendor Field Names and labels for the NTIS Database. Vendor system features are listed. For additional examples of the search process, request individual documentation from each online vendor.

Appendix A – NTIS Subject Categories: Alphabetical Listing by Major Categories

Appendix B – NTIS Subject Categories: Alphabetical Listing of All Categories

Appendix C – NTIS Subject Categories: Alphabetical Listing with Scope Descriptions

Appendix D – NTIS Subject Categories: Numerical Listing of Major Categories

Appendix E – NTIS Subject Categories: Numerical Listing with Scope Descriptions

Purpose of the Search Guide

This guide provides the information necessary for productive, efficient and cost-effective search and retrieval.

Use this manual to:

- Minimize "false hits," which are common to such large and varied databases;
- Clarify the NTIS Database information derived from multiple government sources;
- Gain an in-depth understanding of the database structure;
- Provide background references and historical perspective; and
- Serve as a reference manual for users, or a teaching tool at training seminars.

Audience

This publication targets:

- New online searchers;
- Users who are familiar with online search techniques but not familiar with the NTIS Database;
- Librarians or instructors who train users of library services; and
- Researchers using online systems.

The NTIS Database and Related Products

Section I

Introduction

The NTIS Database contains summaries of scientific, technical, engineering, and business information products acquired by NTIS from 1964 to the present. Printed or microform indexes provide access to the titles that predate the online database. The database is available to the public through a number of commercial vendors that are listed in Section V. The NTIS Database is updated on a weekly basis by NTIS. However, commercial vendor update schedules can vary.

The NTIS Database combines unclassified input from the Department of Defense, Department of Energy, and NASA, with that of numerous other government agencies, among which are the Environmental Protection Agency, National Institute of Standards and Technology, and Department of the Interior, to offer users a wide range of information resources. The full reports are available from NTIS for almost 90 percent of the titles announced on the database. There are more than 600,000 titles available in digital format.

Leasing the NTIS Database

Organizations making frequent use of the NTIS Database for research purposes, or wanting to develop and distribute value-added products, may wish to consider leasing the NTIS Database directly from NTIS. Requirements and pricing information may be obtained by contacting the Office of Product and Program Management 703-605-6515.

Subscription Access to the National Technical Reports Library

Organizations needing fixed-fee search and retrieval access to the more than 2,000,000 NTIS Database metadata records with links to more than 600,000 corresponding digitized full-text reports can subscribe to the National Technical Reports Library (NTRL). See page 15 for more information about the NTRL, or visit http://www.ntis.gov/products/ntrl.aspx.

Document Delivery via NTIS

Reports are available from NTIS for almost 90 percent of the titles found in the NTIS Database. Customers can order full-text reports from NTIS by calling 1-800-553-6847 or (703)-605-6000. Customers can e-mail their document requests to: orders@ntis.gov, or order from the NTIS Web site at http://www.ntis.gov/. NTIS Price Schedules are on the Web at http://www.ntis.gov/pdf/price200805.pdf.

NTIS Online Searching Help Desk

The Help Desk will answer your questions on searching the database and its subject content from 8:30 a.m. to 5 p.m., Eastern time. Call (703) 605-6585.

NTIS Database Distribution - Fiscal Year 2012

Subject Heading	*Percent*
Administration & Management	16.00
Aeronautics & Aerodynamics	3.00
Agriculture & Food	6.00
Astronomy & Astrophysics	3.00
Atmospheric Sciences	4.00
Behavior & Society	16.00
Biomedical Technology & Human Factors Eng.	1.50
Building Industry Technology	1.50
Business & Economics	12.00
Chemistry	3.50
Civil Engineering	4.00
Combustion, Engines, & Propellants	1.50
Communication	2.50
Computers, Control, & Information Theory	5.50
Detection & Countermeasures	2.00
Electrotechnology	1.50
Energy	7.00
Environmental Pollution & Control	11.00
Government Inventions for Licensing	0.10
Health Care	7.50
Industrial & Mechanical Engineering	2.50
Library & Information Sciences	3.50
Manufacturing Technology	1.50
Materials Science	4.00
Mathematical Sciences	2.00
Medicine & Biology	19.00
Military Sciences	12.00
Missile Technology	0.10
Natural Resources & Earth Sciences	11.00
Navigation, Guidance, & Control	0.50
Nuclear Science & Technology	4.00
Ocean Technology & Engineering	4.50
Ordnance	2.00
Photography & Recording Devices	0.50
Physics	8.00
Problem Solving Info for State & Local Gov.	10.00
Space Technology	4.00
Transportation	8.00
Urban & Regional Technology & Development	14.00

Note: Citations may have been coded with more than one category. The citations have been counted for each category used, on average 3-5 categories.

Scope of the Collection

On average, NTIS has added 30,000 new titles per year to the NTIS Database over the past ten years. These reports become a permanent part of the NTIS collection. As the U.S. Government's central technical and scientific information service, NTIS announces summaries of the research and studies sponsored by more than 600 Federal agencies as well as from state and local governments.

Subject Coverage

Because the U.S. Government funds more than half of the research and engineering activities in the United States, the NTIS Database contains information on most scientific and technical subjects. The chart on page 2 shows this coverage for FY 2012. The subject categories, which NTIS uses in coding its database entries, are explained in detail in the appendices.

Information Sources

The titles in the NTIS collection are submitted by hundreds of government agencies, numerous state and local governments, federal contractors, academic institutions, foreign governments, international organizations and private sector organizations.

Since the American Technology Preeminence Act (Public Law 102-245) passed in 1991, NTIS' wealth of information has increased dramatically. The ATPA requires all federal agencies to submit their federally-funded scientific, technical and engineering information to NTIS within 15 days of the date the product is made publicly available. Consequently, NTIS can provide its customers with timely access to a more diverse and comprehensive range of information.

International Sources

NTIS is the lead U.S. Government agency for cooperation in international technical information exchange. Overseas organizations that currently contribute to the NTIS collection include the Japan Aerospace Exploration Agency, Environment Canada, Swedish Defence Research Agency, and many more.

Top Ten Foreign Contributors Fiscal Year 2012

country of origin	*number of citations*
1. United Kingdom	61
2. International	50
3. Italy	36
4. Sweden	31
5. Finland	31
6. Hungary	6
7. Taiwan	5
8. Netherlands	2
9. Norway	1
10. Japan	1

Information Product Types

The NTIS information collection contains a wide variety of types of publications, as well as other media for distributing information. The following table provides a snapshot of some of the types of information products received by NTIS in 2012.

Types of Information Products

U.S. Government Produced	*Number*
Technical reports	26,523
Conference proceedings	1,323
Journal articles	1,717
Theses	1,123
Bibliographies	9
Computer Products	29
Audiovisuals	2
Patent application or Patents	5
Foreign Acquisitions	
Technical reports	224
Conference proceedings	0
Theses	0
Bibliographies	0

Data Elements of the NTIS Database

Section II

In the 1960's, under the aegis of the Committee on Scientific and Technical Information (COSATI), Federal Council on Science and Technology, the managers of scientific and technical information (STI) programs in the federal government adopted standard guidelines for cataloging technical reports. Four of these agencies, NTIS, the Department of Energy's Office of Scientific and Technical Information, the National Aeronautics and Space Administration's Scientific and Technical Information Program, and the Defense Technical Information Center, exchange bibliographic data and cooperate on information services-related projects. These agencies, along with the Department of Health and Human Services, sponsor more than 90 percent of federally funded research and development.

The fields of the NTIS Database are presented below in the order that they appear on the electronic media sent to online database vendors, and other organizations that lease the database from NTIS for internal use. Each vendor has a unique load of the NTIS Database and the placement of the fields and vendor Field Names may vary.

Field Name: NTIS Order No.

Examples:

Citations indexed and abstracted by NTIS
PB2000-123456/XAB

Citations provided by NASA
N2000-12345/6/XAB

Citations provided by the Department of Defense
AD-A123 456/7/XAB, AD-D123 456/XAB,
AD-M123456/XAB

Citations provided by the Department of Energy
DE2000123456/XAB

Definition: Each title has a unique NTIS order number (accession number/identification number/product number) assigned in this field. This number should be used when ordering the title from NTIS.

All NTIS order numbers have alphabetic prefixes. Some alphabetic prefixes indicate the originating agency of the report collections, as shown in the above examples. The alphabetic prefix is followed by a five- to eight-digit number and three alphabetic characters. When searching, it is a good practice to truncate after the first six digits to find an accession number; however, when placing an order, the entire alphanumeric number order must be used.

Note: *Not all of the government agencies that have individual accession number alphabetic prefixes are shown in the examples. The examples are limited to agencies with the largest volume of records in the database.*

Search and retrieval systems may require removal of select charactors (-, /, etc.) to retrieve the NTIS order number. Consequently, users are advised to refer to vendor documentation for search and retireval guidance and recommendations.

Field Name: Subject Category Codes

Examples: 70A, 48D

Definition: NTIS classifies citations into 39 subject categories. Each of these subject categories is divided into subcategories. This method provides sorting categories for both hard and soft sciences. All subject categories consist of three character codes: two numerics and one alpha character. The numeric codes represent entire categories, the alpha codes are used to designate subcategories within these broad categories.

Any one document may have up to five subject categories assigned to it, although some documents may have more. If a title covers three or more subcategories of a major subject category, it is assigned to the general section of the major category code. Each citation in the database contains the full number of subject category codes that reflect the subjects covered by 20 percent or more of the report.

The NTIS Subject Category Classification System has been used exclusively since July 1986. A list of the subject category codes is included in this guide as Appendix B. It is used to arrange the citations into subject areas. COSATI category codes used prior to 1986 were converted to the NTIS Subject Category Code(s), thus the NTIS Database no longer contains COSATI codes 1-22.

Field Name: NTIS Prices

Note: *This field is not searchable.*

Example: PC A02/MF A01

Definition: These are alphabetic codes for each medium in which the item is delivered:

Download (DL), Paper Copy (PC), Color dependent (AC), Microfiche (MF), CD-ROM (CD), Audiovisual (AV), magnetic tape (mag tape), and diskette. The numeric part of the code determines the price of an individual item. The current NTIS Price Schedules are accessible from the NTIS Customer Support Web Page at http://www.ntis.gov/pdf/price200805.pdf.

Field Name: Corporate Source(s)

Example: Army Information Systems Command, Chambersburg, Pennsylvania.

Definition: This is the name of the organization(s) and/or author affiliation(s) that performed the research and prepared the report(s). The corporate source is also known as the corporate author and performing organization.

Since 1980, NTIS has maintained an up-to-date machine-readable corporate source authority list with standardized names and a nine-digit organization code number. The nine-digit code appears in the database and is searchable.

Some online services asterisk the performing organization names to distinguish them from the sponsoring organization(s). The names of organizations have been entered in full and in abbreviated forms.

Examples: Massachusetts Inst. of Tech
Mass Inst. of Tech
Massachusetts Inst. of Technology

Field Name: Title

Example: Guide to Evaluating Thermal Effects in Concrete Pavements

Definition: The name of the document that appears on the title page or document cover. A colon is used when separating a subtitle from the main title.

Foreign language reports present the foreign language title first, followed by the English translated title in parenthesis. When English translations are made of foreign language documents, the English title is presented prior to the foreign language title.

Field Name: Journal and Database Issue

This field contains a title's original announcement journal volume and issue in the format "JVVII":

where J = a letter designating the journal
where VV = a two-digit volume number; and
where II = a two-digit issue number.

Example: u9412, GRAI9412, GRA&I9412.

This corresponds to reports that were announced in GRA&I Issue 9412. Following the GRA&I issue number are letter codes that designate other agencies' announcement journals. Some online vendors list the example shown and some translated the "u" into GRAI or GRA&I with the volume and issue. "n" was the designated prefix code for documents which were announced in the *Department of Energy Announcement Journals Nuclear Science Abstracts* from 1964–1976 and *Energy Research Abstracts* from January 1976 – August 1976. After August 1976, the "n" code in this field was discontinued. "s" is used in this field to identify NASA documents announced in the journal, Scientific and Technical Aerospace Reports (STAR). Some vendors use the "s" and some present the name of the STAR journal in this field. The GRA&I ceased publication in December 1996.

Definition: This field is used to identify the NTIS Announcement Journal volume and issue in GRA&I, and any source agency announcement journal volume and issue in which the citation first appeared.

Field Name: Title Note

Example: Datafile, Audiovisual, Thesis, Software, Final Report, Master's Thesis, Patent, Patent Application, Models-simulation, VHS video, CD-ROM.

Definition: Additional title information that clarifies the document or report type.

Field Name: Personal Author(s)

Example: Hyder, M. L., Smith, J. C.

Format: *Full last name comma [space] first initial period [space] middle initial [period].*

Definition: This field lists the personal author(s) name(s).

Format: Names are recorded in the same order and as they appear in the document, with first and middle initials. All titles, degrees, Jr., Sr., II, III and IV are omitted. Prior to 1984, some names appear with the last name followed by the first name and middle name or middle initial.

Note: *There is no authority list for personal author names. Searchers will need to develop search strategies to provide for variations, using truncation, adjacent, etc., to obtain all the reports by one author. Truncation in online searching means to cut a word short at any point in its order, for example, to retrieve all terms with a common root or both singular and plural forms.*

Field Name: Report Date

Example: Dec 2010
02 June 2010
c19 Mar 2001

Definition: This field contains the date the document was completed. However, on translations and journal articles this date may correspond to some other time, such as the date of the translation, the date of the journal issue, the date of a filing for a patent, or the date of publication in some other journal.

Note: *Beginning in mid-1978, a lower case "c" appears for the citations of copyrighted material, as seen in the third example.*

Field Name: Pagination or Number of Items

Example: 103 p*
1 mag tape
2 diskettes

Definition: This field contains the number of paper or microfiche pages in a document. Blank pages are not counted. The field also notes the number of magnetic tapes, diskettes, VHS tapes, cassettes, etc.

Note: *An asterisk appearing after the page count indicates that the report generated a great deal of interest when it was announced. This is not a searchable field.*

Field Name: Country of Publication

Example: France

Definition: The country in which the document originated or was published.

Note: *Each online vendor provides either the full country name or code in its specific search process. International agencies may supply the country in which they are located. In some cases, this field may be blank because the source agency did not provide the information.*

Field Name: Language of Document

Example: English, French

Definition: The language in which the full document was written.

Note: *If the abstract is in English, but the document is written in another language, then only the language of the full document is identified, and not the language of the abstract.*

Field Name: Report Number

Example: Department of Energy (DOE)
ORNL/TM-2009/149

National Science Foundation (NSF)
ISBN-0-309-11699-6

Definition: The number the sponsoring agency assigns to the title. Most report numbers have alpha prefixes followed by numerics. This field may be blank or may contain one or two report numbers assigned by the performing organization(s).

Note: *When the performing and sponsoring organization are the same, the sponsoring organization's report number will appear in this field, but not in the monitor agency number field. If the document doesn't have an agency report number, this field is blank.*

Field Name: Contract or Grant Number(s)

Example: USDA-88-COOP-2-3482
NSFNCCO-073158
DE-FC07-06ID14750
EAR-0625247

Definition: This field contains the contract or grant number assigned by a federal agency to the research project which resulted in the cited document.

Field Name: Project and Task Numbers

Note: *These have not been used since 1984.*

Example: UCAl-WRC-W-428 ARGUS Calibration

Field Name: Monitoring Agency Number

Example: AFGL-TR-85-0194
EPA/560/7-85/000-1

Definition: This field provides the report number(s) assigned by the sponsoring organization(s) unless the latter is also the performing organization(s). When the sponsoring and performing organization are the same, the monitoring agency numbers are placed in the report number field.

Field Name: Supplementary Notes

Example: See also...
Supersedes...
Other related reports
Pub. in Proceedings of the
American Control Conference...
Sponsored by Department of Energy,
Washington, D.C.
Sponsored in cooperation with...
Any additional information about the document

Definition: This field presents: the source of a translation; language of a report, if other than English; source of a periodical citation; supplemental performing or sponsoring organizations; additional contracts or grants; and conferences, etc.

Field Name: Availability Statement

Example: Also available as PBYYYY-1234
Also available as a set of reports

Definition: A statement of availability that appears when there are special ordering instructions, especially when a report is not available from NTIS or when the report is available from NTIS *and* another organization. Magnetic tapes and diskette products always carry a special descriptive statement in this field concerning their format.

Field Name: Descriptors

Example: *Corrosion prevention
Air pollution control
Mechanical properties

Definition: Descriptors are single or multiword subject terms assigned by NTIS or other contributing agencies. These descriptors use the controlled vocabulary thesauri or word lists which appear in the reference list Appendix A.

Descriptors preceded by an asterisk are those terms determined to be of greatest importance in describing the subject content of a report. Use these asterisked terms to limit an online search. Reports indexed by NTIS are assigned descriptors for the most specific concepts covered in the documents and for applications of the research.

Reports announced by NTIS but indexed by another agency contain that agency's descriptors from its own thesauri. The two major agencies currently providing their own descriptors are: the Department of Defense Technical Information Center (DTIC); and the National Aeronautics and Space Administration (NASA).

Field Name: Identifier

Example: Nanomaterials
National Study of Childcare Supply and
Demand (NSCCSD)
Aerodynamic braking
Nanoelectronics

Definition: Identifiers are single or multiword subject terms used to express concepts for which there are currently no adequate descriptors. As new concepts and technologies arise, new subject terms not found in existing thesauri are placed in the Identifier field.

Identifiers preceded by an asterisk have the same significance as Descriptors preceded by an asterisk. Identifiers include names of chemical compounds, cities, biological species, computer programs, research projects, scientific instruments, and more.

Field Name: Abstract

Example: Electron spectroscopy has become one of our most important tools for the study of electronic structure of solids and surfaces. Under this contract, we studied the passivation and inhibition of corrosion, utilizing the spectroscopic techniques of x-ray photoelectron absorption fine structure (NEXAFS).

Online Searching Hints
Section III

Definition: Abstracts in the NTIS Database may be either indicative or informative, based on the type of document. Informative abstracts identify the methods, results, applications, and conclusions. Indicative abstracts describe content or scope, i.e., a handbook of chemical formulas, chapter titles, or table of contents of a textbook.

Abstracts are usually limited to 200 words. The NTIS Database contains a mixture of author and NTIS-written abstracts. Many of the author abstracts are modified by NTIS.

Abbreviations

Abstracts and other fields often contain abbreviations. However, all subject terms are spelled out in the descriptor or identifier fields.

Accession Numbers (also known as NTIS Order Numbers)

NTIS order numbers consist of this pattern: alpha character-4 digit year-six digits-three letter code.

Example: PBYYYY-123456/XAB may be truncated as PBYYYY-123456 plus truncation symbol number, or PBYYYY123456.

When searching, truncate the number after the sixth digit. When searching for an NTIS order number there are two options: (1) to display a list of the neighboring order numbers to select the correct number and closing 3-letter code or; (2) to truncate the order number after the sixth digit following the year number.

NTIS produces PB numbers with a first digit or first two-digit number series designating a type of information product:

Example:

Subscription products	SUB
Standing order products	PB2010-9
Computer Products	PB2010-5
Computer Product Subscriptions	PB2010-59

(Each example should be followed by a truncation symbol, which varies by online vendor.)

Some agencies that maintain their own number series are noted in the accession number field description. The NTIS accession/order number is not always the same as the host vendor's. Searchers should review the record format and field qualifiers of the vendor(s) of their choice. Similarly, vendor Field Names may vary.

Searching for report numbers in the NTIS Database requires skill because of the punctuation used between letters and numbers. The above examples are specific to certain product types.

Hint: To limit a search to computer products, in addition to using descriptor or identifier terms such as "data file" and "software," combine the set with PBYYYY-5 plus truncation symbol.

Acronyms

NTIS spells out each acronym used in a citation if the author has supplied it, unless it is so common that it would be unnecessary to do so, e.g., DNA for Deoxyribonucleic Acid. Within the abstract, the phrase explaining the acronym is placed first, followed by the acronym in parenthesis. In the identifier field, both the complete phrase and acronym are provided for searching.

Biological Species

Plants, animals, and microorganisms are indexed with their genus and species names and/or the family name. The common name is also indexed if the author has used it and/or if it is known. If a biological subject term is in one of the recommended thesauri, it is posted in the descriptor field.

Examples:

Descriptors: Parasite diseases
Identifiers: Liriodendron tulipifera and also Tulip tree.
Descriptors: Mammals; Carnivora; Taxonomy; Laboratory animals
Identifiers: Hyaena; Hyaena Brisson; Striped Hyaena, Felidae; Panthera leo persica

Subject Category Codes/Classification

What they are

NTIS classifies citations into 39 subject categories. Each of these subject categories is divided into subcategories. This method provides sorting categories for both hard and soft sciences.

All subject categories consist of three character codes: two numerics and one alpha character. The numeric codes represent entire categories such as chemistry, environmental pollution and control, civil engineering, et al. The alpha codes are used to designate subcategories within these broad categories. The number of NTIS subcategories posted to an information product average from one to five, although there are some reports with more.

What they do

Although most online searching is conducted using subject index terms (keywords), subject categories are also very important. Subject categories can be combined with keywords to eliminate false retrievals ("hits").

Example: Combining "Lead" with the NTIS subject category 57Y (Toxicology), retrieves report citations about the toxicity of lead, rather than lead use as an additive in iron alloys.

Example: Citations for "Geothermal energy" reports can be retrieved by searching the NTIS category 97P because this category is specific to geothermal energy.

Note: Subject categories may be designated as Category Codes or Subject Headings by the online vendor. Always review field designations in the vendor(s) documentation.

NTIS Subject Categories

Listed in Appendix B are the subject categories NTIS uses to classify new documents. Each subject category is followed by a list of secondary subject categories. Searches can be conducted by using the actual text of a subject category (i.e., management information systems), or using the subject category code (i.e., 70C) that follows each subject. Because each abstract in the database is indexed on all words in the abstract, searching using the subject category code will reduce the number of stray hits and provide a list of more relevant documents.

Category Codes with Asterisks (Highlighted Subject Category Codes)

An asterisk displayed after the subject category code indicates that the report is highlighted for being particularly significant in its content, approach or presentation. To limit a search, use an asterisk with the subject code in the search statement.

Chemical Nomenclature

NTIS uses the chemical names, trade names, CAS registry numbers, and common names included in the document as descriptors or identifiers. For a comprehensive retrieval, search all known names and classes of a compound.

Chemical compounds are listed with their common name, chemical name, and class of compounds. NTIS lists compounds hierarchically with their chemical classes posted in the descriptor field as well as the individual chemical name. If numerous chemical compounds are the subjects of the research, the classes of compounds are generally listed, but not each individual chemical compound.

Standard chemical abbreviations for the elements may be used in the abstracts, but the name of the element is always posted in its entirety in the descriptor field. Chemical elements may also be posted in their element groups, such as alkali metals, alkaline earth metals, rare earth metals, etc.

Examples:
Descriptors: Hydrochloric acid
Chlorine
Anilines
Amines

Examples
1. Descriptors: Chlorobenzenes (general class)
Identifiers: Trichlorobenzenes
1,2,4-Trichlorobenzene
1,2,3-Trichlorobenzene

2. Descriptors: Metals
Platinum
Precious metals (general class)
Rhodium

3. Descriptor: Chlorobenzenes (general class)
Identifier: Pentachlorobenzene (specific compound not found in recognized thesauri)

4. Descriptors: Chlorine organic compounds (general class)
Chlorobenzenes
Chloroform
Carbon tetrachloride

5. Inorganic compounds not found in thesauri:
Lead acetate
Descriptor: Lead inorganic compounds
Identifier: Lead acetate

Since 1979, the Chemical Abstract Service's (CAS) Registry Number System cites unique numbers if they are mentioned in the item being indexed. Registry numbers are recorded in two formats: the standard format *with* dashes between numbers, or the abbreviated format *without* dashes. Thus the number may appear as "CAS Registry No: 10016-20-3" or as "CAS Registry No: 10016203" in the identifier field. It may also be known as "CAS No. 10016-20-3." Each online supplier has a field qualifier for these numbers.

Example:
Identifier: Chloramines, CAS 7782505.
Identifier: Formaldehyde, CAS 50-00-0.

For industrial chemicals, pesticides, and pharmaceuticals, NTIS uses the Chemical Abstracts Service nomenclature and the approved common name. NTIS uses the United States Adopted Names (USAN) (Reference No.) when classifying drugs.

Example:
Descriptor: Metal Complexes
Identifier: FDDC (Bis(trifluoroethyl)dithiocarbamate)

Example:
Descriptor: Chlorinated aromatic hydrocarbons
Identifier: PCBs(Polychlorinated biphenyls)
Polychlorinated biphenyls

Chemical Trade Names

Trade names such as Nylon are posted in addition to the generic plastic or polymer name.

Example: Descriptors: Nylon, Polyamide resins.

Computer Programs and Products

Computer products include data files and software available on magnetic tape, diskette, DVD, CD-ROM, videotapes, and optical disks.

Search for items that identify programs and products by adding the terms "software," "computer programs," "datafile," and/or "model-simulation" whenever applicable. When searching for computer programs in machine-readable form, combine the terms "software" or "computer program" and the terms "magnetic tape" or "diskette," (found in the Title Note field, see p. 5 of this manual) using the appropriate field qualifier.

Corporate Sources

Two types of corporate sources are found in the NTIS Database: performing organization(s) and sponsoring organization(s).

Performing Organization(s)

Most reports are cataloged with the name of the organization(s) that prepared the report. When searching for corporate sources for the years prior to 1980, users must be aware of the cataloging differences caused by multiple agency rules. These differences generally occurred in abbreviations and in punctuation. In 1980, NTIS created a corporate source authority database and a nine-digit code for each corporate source, eliminating these discrepancies. The nine-digit codes appear in each citation.

Sponsoring Organization(s)

The sponsoring organization is always a government agency. The sponsoring organization is listed if it is also the performing organization. Beginning with NTIS Database GRA&I issue 74-21, reports cataloged by NTIS have included the sponsoring organization as well as the performing organization. Beginning with NTIS Database GRA&I issue 76-21, DOE reports have been cataloged with the sponsoring organization.

Examples of performing organization(s) and sponsoring organization(s) in the same report(s):

Example:	PB2010-100486
P.O.	Federal Interagency Forum on Aging Related Statistics, Hyattsville, MD.
S.O.	Bureau of the Census, Washington, DC.
Example:	PB2010-100839
P.O.	Wichita State Univ., KS.
S.O.	Federal Aviation Administration, Washington, DC.
Example:	DE2010-963080
P.O.	Rutgers - The State Univ., New Brunswick, NJ.
S.O.	Department of Energy, Washington, DC

See also listing under "Sponsoring agency keyword acronyms" on page 19.

Data

Reports containing large amounts of tabular data are tagged by the keywords "Tables (Data)" or "Statistical data."

Delimited/Declassified Reports

Declassified materials and reports with limited distribution status are added to the NTIS Database with the date it was acquired by NTIS, rather than the date the report was prepared. Generally the phrase, "Distribution limitation now removed" will be included in the Supplemental Notes in any record for declassified/delimited materials.

Department of Defense (DoD) Declassified/Delimited Items

Declassified reports from the Department of Defense contain a special searchable code in the identifier field: NTISDODXA, NTISDODXB, NTISDODXD, etc. Using this code as a search term restricts a search to declassified reports, or, alternatively, to ensure that no such reports are included in the final search results. Between 1975 and 1977, more than 30,000 declassified items were added to the database. After 1977, NTIS receives documents from DOD as they are declassified. It is advisable to look for the phrase, "Distribution limitation now removed" on DOD reports in addition to the code.

Developing Countries

NTIS announces reports for and about developing countries. Since 1979, NTIS has used the descriptor "developing country application" for titles relevant to foreign governments. Reports about a developing country are usually indexed with one of the following descriptors: "developing countries" or "developing nations." See also subject category code 96G and 96H.

Environmental Impact Statements (EIS)

Environmental Impact Statements are the environmental reviews required for major federal projects that might adversely affect the environment. All previously released EIS were announced through the NTIS Database beginning with the June 1, 1971 update and ending with the April 15, 1974 update. Since then, NTIS has received irregular shipments of EIS.

Most of these environmental impact statements can be searched by entering the term, "environmental impact statements-Final" or "environmental impact statements-Draft" in the descriptor or identifier field. Some early EIS were not assigned either of these terms; however, they can be retrieved by searching for the prefix "EIS" as part of the NTIS accession/order number, truncating after the first three characters of the number, and using the appropriate field qualifier.

Another method of selecting EIS is to use the NTIS subject category code Environmental Impact Statements, 68H.

Note: This subcategory has been in use since March 15, 1973.

Foreign Language

In 1979, NTIS created a field to classify reports written in a language other than English. Prior to 1979, reports in foreign languages were mentioned in the notes field. English cannot be searched directly.

Reports of Non-U.S. Origin

Country names are assigned in the descriptor or identifier fields. Using a country name in the descriptor or identifier field searches for reports about that country.

Country names in citations prior to 1980 indicate that the document either originated in that country or that the document is about that country. In 1980, a field for country of publication was added to the bibliographic citation when the source country was other than United States. Since country codes are not assigned to documents originating in the United States, non-U.S. items can be eliminated using NOT logic.

Note: Each online supplier provides search instructions for documents originating in the United States.

Foreign Research and Technology

In 1979, NTIS began using the subject term "foreign technology" to identify documents about current foreign research, techniques, and technology. Many of these reports have been prepared outside of the U.S., and include documents published as a result of fellowships or research programs awarded to foreign nationals and sponsored by U.S. government agencies.

International Business Information

The NTIS Database contains a substantial amount of non-U.S. business-related information especially in the areas of science, engineering and technology. Reports include foreign market surveys, foreign sectoral analysis, industry subsector analysis, and other economic studies. Key sources of this type of information are: the U.S. Trade and Development Program, the International Trade Administration, and the Department of Commerce's Office of General Counsel. Titles are posted with "export trade information" and/or "foreign marketing" identifiers.

Note: The terms foreign marketing and foreign technology are different. For example, tourism doesn't have a technology component, but it does have a marketing component.

See also listing under "translations" on page 12.

Geographical Areas

Geographic location is included only when it is an important facet of an indexed item.

The following indexing guidelines apply:

1. Items referring to an area in a country covering two or more states or provinces are indexed to the region and not the individual states or provinces:

Example: Central Regions (United States)
Great Plains Region (United States)
New England (exception- region not included)

2. Reports referring to individual states, provinces, or parts of states within a country are indexed to the states, provinces, and its parent political unit:

Example: Northwest Region (Iowa)
Ozark Region (Missouri)
Northern Region (Virginia)

3. States and other political regions, including cities, are modified with the country name except for those of Great Britain, Canada and the United States. They may be posted in the descriptor or identifier field.

Example: Arkansas
Bavaria Region (Germany)
British Columbia

4. Coasts are modified with the country or land area and posted in the identifier field:

Example: Atlantic Coast (United States)
Atlantic Coast (Canada)
Gulf Coast (United States)
Pacific Coast (Mexico)

5. Natural features, other than coasts, do not receive a political modifier. The natural feature modifier appears last and is posted in the descriptor field.

Example: Mississippi Delta
Susquehanna River Basin
Mexico Gulf (for Gulf of Mexico)

6. Lakes and mountains appear as they are listed on standard maps. They are posted in the descriptor field.

Example: Alps Mountains (Europe)
Lake Erie
Great Salt Lake

Government-Owned Inventions for Licensing (See also Patents)

Effective with NTIS Database GRA&I Issue 72-23 (Dec. 1, 1972), NTIS began to announce all patents and patent applications issued to U.S. government agencies that are available for public licensing.

Hint: U.S. government-owned applications can be searched by combining the terms "patents" or "patent applications" with NTIS Subject Category 90. If NTIS subject category 90 is not combined with either of these terms, foreign patents will also be retrieved.

Health Care/Medicine Subjects

Since 1980, NTIS has used the National Library of Medicine's thesaurus, Medical Subject Headings-Annotated Alphabetic Listing, as its indexing authority for reports in the health care and medicine fields. The subject categories specific to this subject are:

- Medicine & Biology (57);
- Health Care (44); and
- Biomedical Technology and Human Factors Engineering (95).

Three subcategories specific to this subject are:

- Urban and Regional Technology and Development–Health Services (91F);
- Problem Solving for State and Local Governments–Human resources (43C); and Police, Fire and Emergency Services (43D).

Journal Reprints

NTIS receives and announces approximately 500 - 600 journal reprints each year. The majority of these articles are originated by the U.S. Department of Defense (others are from the Environmental Protection Agency, the USDA, the DOE, etc.).

Some journal articles are available from NTIS depending upon the funding agency. Beginning with NTIS Database GRA&I issue 75-03, February 1975, the descriptor "reprints" has been assigned to the majority of the reprints. The document type is also noted as a journal article.

Maps

The descriptor "maps" is used whenever maps are an integral part of a report. Reports describing the way maps are made are indexed with the descriptor "mapping."

Patents

All U.S. government patents and patent applications entered into the NTIS Database are assigned either "patents" or "patent applications" in the descriptor or title note field. Some online vendors display it as the document type field.

Sponsoring Agency Keyword Acronyms

Effective with NTIS Database issue 7309, May 1973, NTIS placed an acronym representing the report's sponsoring organization(s) in the identifier field. This information can also be found by entering the agency name as a search term in the corporate source/sponsoring agency field.

Beginning with NTIS Database issue 7419, October 1974, the agency acronyms are prefixed with the "NTIS" acronym.

Examples:

NTISDE	Department of Energy
NTISDOD	Department of Defense
NTISNASA	NASA
NTISCOMNBS	National Institute of Standards & Technology (NIST).

Note: This acronym combines the Department of Commerce and the former agency name of National Bureau of Standards (NBS).

These codes are helpful when searching for sponsoring organizations rather than performing organizations, or to find all reports submitted to NTIS by one specific agency.

Note: The meaning of an agency acronym often may be determined from the corporate source field.

Superfund

The U.S. Environmental Protection Agency (EPA) administers the Superfund program, which was established in 1980 with the passage of the Comprehensive Environmental Response, Compensation, and Liability Act (CERCLA). In 1986, Congress passed the Superfund Amendment and Reauthorization Act (SARA) which updated and improved CERCLA.

Publicly available documents from the Office of Emergency and Remedial Response (OERR) are available from NTIS.

Hint: Use the descriptor "Superfund" to locate relevant documents, such as Superfund Record of Decision reports.

Translations

Each year, NTIS announces approximately 1,000 translations received from and funded by government agencies. Prior to 1976, all translations, except those originating with DOE and NASA, were assigned the descriptor "translations." Since 1976, DOE and NASA translations also have been indexed with "translations."

See also listing under "foreign language."

Verbalization

All subscripts, superscripts, Greek letters, scientific and mathematical formulae are fully spelled out in the abstract of the record.

Example: alpha, beta, gamma, etc.
Peroxide appears as H2O2 or H sub 2 O sub 2.
Water appears as H2O or H sub 2 O

Selected References for Assistance in Searching the NTIS Database

Section IV

Items with an asterisk (*) are available from NTIS; U.S. Department of Commerce, NTIS, Alexandria, VA 22312. When ordering, you will need the NTIS order number as indicated. Your ordering options include: Online - insert order number as requested at http://www.ntis.gov/help/orderplacing.aspx, By phone (NTIS Sales Desk) - 1-800-553-6847 or 703-605-6000, Fax - 703-605-6900, via e-mail - orders@ntis.gov

The NTIS Sales Desk is available for assistance 8 a.m. - 6 p.m.; EST, Monday-Friday. The Sales representative will verify a title, order number or price for you. For further ordering information see the NTIS Web page at http://www.ntis.gov/help/orderplacing.aspx

Many of these references are made available online on the source agency's web site. Where available, these web addresses are listed at the end the entry.

***Countries, Dependencies, Areas of Special Sovereignty, and Their Principal Administrative Divisions.**
For diskette, NTIS Order No.: PB95-503504, $30

***Guidelines for Descriptive Cataloging of Reports: A Revision of COSATI Standard for Descriptive Cataloging of Government Scientific and Technical Reports.**
NTIS Order No.: PB86-112349

NTIS DIALOG Information Services, Inc. (File 6) Bluesheets.
DIALOG Information Services, Inc. Includes field-by-field description of DIALOG system search capabilities.
http://library.dialog.com/bluesheets/html/bl0006.html

List of Applicable Thesauri

***Defense Technical Information Center Thesaurus.**
Defense Technical Information Center, Alexandria, Va.
NTIS Order No.: AD-A 378 274
http://stinet.dtic.mil/str/index.html

http://www.dric.mil/dtic/stresources/techreports/DTICSearchTools/thesaurus_desc.html

International Energy Subject Thesaurus.
Joint Thesaurus: ETDE/INIS Joint Reference Series No. 1 (Rev. 1) June 2004
DOE report no.: IAEA-ETDE/INIS-1 (Rev.1). Contains over 21,000 terms and includes definitions, entry date, and broader and narrower terms.
http://www.etde.org/edb/reference.html

International Energy Subject Thesaurus Supplement.
ETDE/INIS Joint Thesaurus, IAEA-ETDE/INIS-1(Suppl.42) Updated monthly.
http://www.etde.org/edb/reference.html

***Medical Subject Headings Publications**
Alphabetical listing of all subject descriptors used by the indexers and catalogers at the National Library of Medicine (NLM). Update annually, for information about ordering from NTIS, go to http://www.ntis.gov/product/mesh.aspx
http://www.nlm.nih.gov/mesh/MBrowser.html

***NASA Thesaurus, Volume 1: Hierarchical Listing. January 1998.**
Contains over 25,000 subject terms that are used in the NASA Scientific and technical information system
NTIS Order No.: N1998-0010926
http://www.sti.nasa.gov/thesfrm1.htm

***NASA Thesaurus, Volume 2: Rotated Term Display. January 1998.**
NTIS Order No.: N1998-0010863
http://www.sti.nasa.gov/thesfrm1.htm

***NASA (National Aeronautics and Space Administration) Thesaurus Supplement: A Three-Part Cumulative Supplement to the 1998 Edition of the NASA Thesaurus.** Supplement 7.
The supplement to the 1998 edition of the *NASA Thesaurus* includes all new terms and associated heirarchies added since the cutoff for the 1998 edition (December 1997).
NTIS Order No.: N2001-0066734
http://www.sti.nasa.gov/thesfrm1.htm

TEST: Thesaurus of Engineering and Scientific Terms.
1967. Available from American Association of Engineering Societies, 1111 19th St, NW, Suite 403, Washington, D.C., 20036. 1-888-400-2237 or (202)296-2237.

Transportation Research Thesaurus (TRT).
July 1999. CD-ROM or paper copy available from CDB Enterprises, Inc.
Davidbatty@aol.com; Telephone: 301-593-8901.
http://trt.trb.org/trt.asp

***Thesaurus of Water Resources Terms: A Collection of Water Resources and Related Terms for Use in Indexing Technical Information**
1989. Bureau of Reclamation, Denver CO.
NTIS Order No.: PB95-146213

Online Services Access

Section V

The NTIS Database is available from several online vendors. Each online service has its own commands, prompts, menu screens, searchable fields, display and print formats, search software and special features. This section presents a summary of the basic features offered by the online vendors. For more detailed instructions, contact the individual online provider.

National Technical Reports Library (NTRL)

National Technical Information Service
5301 Shawnee Road
Alexandria, VA 22312

Telephone: 800-553-6847
Fax:703-605-6880
E-mail: subscriptions@ntis.gov

Coverage: 1964 to present
Update frequency: Each Government Business Day
Bibliographic Records: over 2 Million

System Features:

- Web-based Subscription Access
- Links to over 600,000 corresponding full-text reports
- Quick Search – intuitive interface supports access for novice researcher
- Advanced Search – more precise search and retrieval
- Easy access to Help and Search Tips
- E-mailing of results

For more information:

About NTRL: http://www.ntis.gov/pdf/ntrl-presentation.pdf

Where to get NTRL outside the U.S.: http://www.ntis.gov/help/cooperate.aspx

In Quick Search
Search fields include:
Accesion Number
Keyword
Title
Abstract
Author

In Quick Search
Search fields can be limited:
With All of the words
With the exact phrase
With at least one of the words
Exclude words
Refine your results by:
Subject Category
Year
Year Range
Source Agency

NTRL Search Tips:

You can make your search more precise and get more useful results by following these tips:

- Select the field to search from the drop down menu. Selecting All will search all fields.
- Enter search phrase/terms in the text box and click the search button.
- Do not use operators such as AND, OR in the search text box; use the appropriate text box instead.
- To search for all words (logical operator AND) enter your search in the With All of the words input text box.
- To force inclusion of certain search terms (logical operator OR), search in the With at least one of the words input box.
- To search for the exact phrase enter your search next to the With the exact phrase input text box.
- To limit results by category click on the Subject Category dropdown and select category from the dropdown list.
- To limit the results by year, select From Year and To Year from the dropdown list.
- You can sort the results by Relevancy or by Year using the Sort By dropdown list.

Sample NTRL Record	
Search Field Catagory	*Example Search Field Content/Response*
Accession Number:	PB2010-107926
Title:	Understanding Climate's Influence on Human Evolution.
Publication Year:	2010
Pages:	00127
Abstract:	The hominin fossil record documents a history of critical evolutionary events that have ultimately shaped and defined what it means to be human, including the origins of bipedalism; the emergence of our genus Homo; the first use of stone tools; increases in brain size; and the emergence of Homo sapiens, tools, and culture. The geological record suggests that some of these evolutionary events were coincident with substantial changes in African and Eurasian climate, raising the intriguing possibility that key junctures in human evolution and behavioral development may have been affected or controlled by the environmental characteristics of the areas where hominins evolved. However, with both a sparse hominin fossil record and an incomplete understanding of past climates, the particular effect of the environment on hominin evolution remains speculative. This presents an opportunity for exciting and fundamental scientific research to improve our understanding of how climate may have helped to shape our species, and thereby to shed light on the evolutionary forces that made us distinctively human.
Keyword:	Environmental effects, Homo sapiens, Culture, Geology, Fossil fuels, Earth sciences, Implementation, Research program, Climate change, Human impact, Hominin, Human revolution
Source Agency:	National Academy of Science National Research Council(NASNRC)
Category:	Natural Resources & Earth Sciences(48), Atmospheric Sciences(55), Environmental Pollution & Control(68)
Prime Corp Author Name:	National Research Council, Washington, DC. Division on Earth and Life Studies.
Document Type:	RPT
Document Type:	RPT
Contract Number:	EAR-0625247

DataStar

Dialog, LLC
2250 Perimeter Park Drive, Suite 300
Morrisville, North Carolina 27560
Telephone: 919-804-6400
Fax: 919-804-6410
E-mail: customer@dialog.com

Database Label: NTIS
Years Online: NTIS–October 1980–to date
NT80–1975 to September 1980
NT74–1970 to 1974
NTZZ–All of NTIS since 1970
Update frequency: Monthly

System Features:

- MAP–extracts and saves terms to use in another database
- RANK–statistical analysis of search results
- Left-hand truncation on Imsmarq trademark databases
- Telecommunications link to DIALOG
- Prompted offline print and alert requests
- Smart Alerts–you choose the day the Alerts run
- KWIC print format–see search terms in context
- Subaccount expanded to 16 characters

List of Selected DataStar Search Command

Label	*Description*	*Example*
AN	Accession number & update	ADA511653 ADJ XAB.AN.
AU	Author(s)	JAKOB-$.AU.
IN	Corporate source	MINERAL$ ADJ MANAGEMENT.IN.
TI	Title	AIR ADJ QUALITY WITH OZONE.TI.
TA	Annotated title	ANNUAL REPORT.TA.
NT	Notes	- Display only -
YR	Publication date	2010.YR.
JN	Journal announcement code	U200923.JN.
SN	Sponsoring agency	- Display only –
RN	Report number	JSC ADJ CN ADJ 18584.RN.
CN	Contract number	200 ADJ 205 ADJ 13434.CN.
PN	Task (project) number	NASA ADJ NCC8 ADJ 200.PN.
PR	Price	- Display only –
AV	Availability	- Display only –
CC	Classification codes	68D.CC.
MJ	Major descriptors	OFFSHORE-DRILLING.MJ.
MN	Minor descriptors	WATER-POLLUTION.MN.
ID	Keywords	OIL ADJ SPILL$.ID.
DE	Descriptors (superlabel)	OFFSHORE ADJ DRILLING.DE.
AB	Abstract	OIL WITH EXPLORATION.AB.

Limit Options

Label	*Description*	*Example*
YEAR	Accession number & update	ADA511653 ADJ XAB.AN.
UMONTH	Author(s)	JAKOB-$.AU.
JNYR	Corporate source	MINERAL$ ADJ MANAGEMENT.IN.
JNMO	Title	AIR ADJ QUALITY WITH OZONE.TI.

Print Formats		
Format name	*DataStar Label*	*Printing code*
SHORT	AN AU TI YR TA	-: ..P SHORT/1-5
MEDIUM	AN AU TI YR TA AB	-: ..P MEDIUM/1-10
LONG	AN AU TI YR TA AB DE	-: ..P LONG/2,6,9
By paragraph	(e.g., Title)	-: ..P TI/1-5
Full document	All paragraphs	-: ..P ALL/1-10

Speciall Printing Format notes
Note: There is no free format for this database.
RANK counts the occurrences of unique terms within a specific field from a search set you have created.
MAP automatically extracts and saves data from selected fields of a set of records, thereby eliminating time-consuming scanning and re-keying. The stored search may then be executed in another database, or saved for later use.

Sample Record - DataStar	
DataStar Label	*DataStar Contentl*
AN	ADA513500-XAB 201003.
AU	Kuo-S, Cheng-W, Snyder-A, Kossey-P, Battis-J.
AU	Performer(s): Air Force Research Lab., Hanscom AFB, MA. Space Vehicles Directorate. Performing author code(s): 114801001 434329.
TI	Contrasting O/X-mode Heater Effects on O-Mode Sounding echo and the Generation of Magnetic Pulsations.
TA	Contrasting O/X-mode Heater Effects on O-Mode Sounding echo and the Generation of Magnetic Pulsations.
NT	Journal article. Published in the Geophysical Research Letters v37 2010.
YR	6 Jan 2010, 6p
JN	u201012.
RN	AFRL-RV-HA-TR-2010-1001.
CN	Contract N00014-05-1-0109.
PN	Task HR, Proj. 1010.
PR	PC A02.
AV	Order this product from NTIS by: phone at 1-800-553-NTIS (U.S. customers); (703)605-6000 (other countries); fax at (703)605-6900; and email at orders@ntis.gov. NTIS is located at 5301 Shawnee Road, Alexandria, VA, 22312, USA.
CC	55A
MJ	Ionosphere, Heating, Micropulsations, Magnetic-fields.
MN	Sequences, Echoes, Magnetometers, Intensity, Excitation, Monitoring, Reprints, Facilities.
ID	X-mode, O-mode, HAARP-High-Frequency-Active-Auroral-Research-Program, Experimental-observations.
AB	The effects on the ionosphere of powerful O-mode and X-mode pump waves, modulated 3 minutes on and 1 minute off, were explored. The experiments were monitored using the digisonde and magnetometer located at the HAARP facility. The results show that the virtual heights of the O-mode sounding echoes shifted down/up as the O/X mode heater was turned on; the ionosphere *(Actual abstract abbreviated for this example.)*

DIALOG, LLC

http://www.dialog.com

2250 Perimeter Park Drive, Suite 300
Morrisville, North Carolina 27560
Telephone: +1 800 3-DIALOG (North America) or +1 919-804-6400

Fax: +1 919-804-6410
E-mail: customer@dialog.com

List of Selected DIALOG Search Commands

Command	*Explanation*	*Example*
Begin	To connect to NTIS file	B6
S term	Search term	SELECT (or S) MEDIA
E term	Expand term: displays online index in alpha order around search term	EXPAND (or E) MEDIA
T or D	To view online results using one of Dialog's eight formats	t5/3/1-4
PR	To print off-line search results	PR S5/3/1-4
PR-	To cancel off-line prints	pr-p002
AND, OR, NOT	Logical connectors	
(w)(1w)	Proximity connectors	
(n)(1n)	Proximity connectors	
(f)	Proximity connectors	field
(l)	Proximity connectors	descriptors
(s)	Proximity connectors	subfield
SAVE TEMP	To save search strategy for 7 days	SAVE TEMP
SAVE	To save search strategy permanently	save
EXS	To run a saved search	exs sa001
LOGOFF HOLD	To save a search for 30 minutes	
RECALL	To list search saves	recall save
RELEASE	To purge search saves	release save
HELP	To explain system commands	help file6;
	and file structure	help field6
	file price list	help rates6
	Limit by years	help limit6
DS	To display search history To display selected sets	DS3; DS 1-10
SORT	To sort search results by title, etc.	sort s1/all/ti
NTIS price code tables	Paper/Microfiche	HELP NTISCODE;
	Paper copy exception	HELP NTISECOD;
	Diskettes	HELP NTISECOD;
	Magnetic tape products	HELP NTISTCOD
Time & Charges	At logoff & end	COST
RANK<DE>	To analyze term frequency	
TARGET	Search using relevance ranking	

Print Options
User-defined formats: can be specified using the display codes indicated in the search options tables, e.g., TYPE S3/TI, JN, PY/1-5.

Predefined Format Options	
Number	***Record Content***
Format 1	DIALOG accession number
Format 2	Full record except abstract
Format 3	Bibliographic citation
Format 4	Full record with tagged fields
Format 5, 9	Full record
Format 6	Title
Format 7	Bibliographic citation and abstract
Format 8	Title and indexing

Note: Menu mode is also available

Predefined Format Options		
Label	***Content***	***Format Type***
AA	PB2001-104037/XAB	NTIS Accession No.
TI	Logic-Based, Performance Driven Electric Vehicle Software Design Tool (Final rept. Jul 98-Aug 00)	Title
AU	Blackketter, D. M. ; Alexander, D. G.	Personal Author
CS	Idaho Univ., Moscow. National Inst. for Advanced Transportation Technology.	Corporate Source
CS	Corp. Source Codes: 009858007	Corp. Source Codes
SP	Department of Transportation, Washington, D.C. Research and Special Programs Administration	Sponsoring Agency
RN	Report No.: NIATT-N01-10	Report No.
CN	DTRS98-G-0027	Contract Number
PY	Feb-01	Report date
PG	30p	pagination
NT	Sponsored by Department of Transportation, Washington, D.C., Research and Special ProgramsAdministration. Product reproduced from digital image. Order this product from NTIS by phone at 1-800-553-NTIS (U.S. customers); (703) 605-6000 (other countries); fax at (703) 605-6900; and email at orders@ntis.gov. NTIS is located at 5285 Port Royal Road, Springfield, VA 22161, USA.	Note
LA	English	Language
JA	Journal Announcement: USGRDR0113	Journal Announcement
PC	NTIS Prices: PC A03/MF A01.	–display only–
CP	United States	Country of Publication
AB	The goal of this research was to develop computer-based logic algorithms and build them into SmartHEV, a series hybrid electric vehicle software design program. *(Abstract abbreviated for this example.)*	Abstract
DE	Electric Vehicles; *Computer aided design; *Vehicle design; Vehicle Performance; Computer software; Algorithms; Hybrid vehicles;	Descriptors
ID	SmartHEV design program; NTISDOTOUR	Identifiers
SH	85H (Transportation – Road Transportation); 41A (Manufacturing Technology – Computer Aided Design (CAD))	Section Headings (Subject Categories)

EBSCO Publishing

EBSCO Publishing
10 Estes Street
Ipswich MA 01938
800-653-2726
http://www.epnet.com

The default fields included in unqualified (keyword) searches are: Personal Author, Corporate Source, Sponsoring Organization, Title, Number of Items, Note, Abstracts, Descriptors, Identifiers, Source, Subject Category Codes, and Subject Category.

The following list will help you locate detailed information referenced in this database as a field.

List of Searchable Field

Search tag	*Name/Description*	*Example*
AA	Abstract Available [Phrase Indexed] Searches the abstract available field	AA Y
AU	Author [Word Indexed] Searches author by Initials and last name	AU M. Beyermann
AB	Abstract [Word Indexed] Searches the Abstract summary for keywords	AB Phase Particles
AN	Accession number [Phrase Indexed] Searches the exact accession Number/unique identifier.	AN PB97-210801/XAB
CA	Corporate Source [Word Indexed] Searches corporate source by source name	CA Oak Ridge National Lab
CC	Subject Category Code [Word Indexed] Searches for words in the subject category code. This can be searched both by code and by spelled-out subject	CC 46C or CC Optics & Lasers
CR	Contract Number [Phrase Indexed] Searches for the exact contract number	CR AC05-96OR22464
CY	Country of Publication [Phrase Indexed] Searches for the exact country of publication	CY France
DE	Subject headings [Phrase Indexed] Searches for the exact descriptor	DE Sovereignty
DT	Publication Date [Numerically Indexed] Searches the Publication date in YYYY format	DT 1997

List of Searchable Field		
Search tag	***Name/Description***	***Example***
ID	Identifiers [Word Indexed] Searches for words within the identifiers field	ID International Affairs
LA	Language [Phrase Indexed] Searches the original language of the document	LA German
MC	Major Concepts [Phrase Indexed] Searches for the exact major concept	MC International Relations
NI	Number of Items [Word Indexed] Searches for words or numbers in the number of items field	NI 52
NO	Note [Word Indexed] Searches for keywords in the notes field	NO Report to Congress
PG	Pagination [Numerically Indexed] Searches the number of pages numerically	PG 10
RE	Report Number [Numerically Indexed] Searches the report number field	RE SUNY-TR-48
SO	Source [Word Indexed] Searches for words within a title listed in the source field of a review	SO Department of Energy
SP	Sponsoring Organization [Word Indexed] Searches for words in the sponsoring organization	SP Department of Energy
SU	Descriptors [Word Indexed] Searches for words in the Subject, Descriptors and Identifiers field	TI Preventive Action:Cases and Strategies
TI	Title [Word Indexed] Searches for words in the title of the article	TI Preventive Action:Cases and Strategies

For additional information, please refer to database specific help in EBSCOhost.

Elsevier Engineering Information

360 Park Avenue South
New York, NY 10010
T: +1-800-221-1044
F: +1-212-633-3680
E-mail: eicustomersupport@elsevier.com
Corporate site: http://www.ei.org

NTIS is available on Engineering Village on http://www.engineeringvillage2.org

- Years of coverage: 1964-present
- Total records: 2,250,000
- Updated Weekly

Engineering Village is the premier web-based discovery platform meeting the information needs of the engineering community. By coupling powerful search tools, an intuitive user interface and essential content sources, Engineering Village has become the globally accepted source of choice for engineers, engineering students, researchers and information professionals.

- Combined database searching of Compendex, Inspec with NTIS, including deduplication of Compendex and Inspec records.
- Referex Engineering e-book reference content
- Browsable Indexes to scan and retrieve variants of search terms
- The ability to save searches, set up e-mail alerts, and create personalized folders.
- Quick & Expert Search options, both of which allow you to save and combine searches.
- The ability to choose preferred output formats (citation, abstracts or detailed) for Selected Record sets, which can then be viewed, printed, saved, downloaded or e-mailed.
- OpenURL linking to the NTIS order form from abstract or detailed records
- Links to document delivery services
- OpenURL linking to Endeavor LinkFinder Plus, Ex Libris SFX, Serials Solutions Article Linker, Innovative Interfaces Web Bridge and others for local holdings checking and full text option presentation.
- Context sensitive help
- Reference Services: Ask a Librarian & Ask an Engineer

In Quick Search mode, fields that can be searched:
Search Field Options
Abstract
All fields
Author
Author Affiliation
Classification Code
Contract Number
Country of Origin
Monitoring Agency
NTIS Accession Number
NTIS Controlled Terms
Report Number
Subject/Title/Abstract
Title

In Expert Search, fields that can be searched:	
Field	***Field Code***
Abstract	AB
Accession number	AN
All fields	A11
Author	AU
Author affiliation	AF
Availability	AV
Classification code	CL
Contract number	CT
Controlled term	CV
Country of origin	CO
Document type	DT
Filing date	PA
Language	LA
Monitoring agency	AG
Notes	NT
Patent issue date	PI
Report number	RN
Subject/Title/Abstract	KY
Title	TI
Uncontrolled term	FL

NTIS can be viewed in 3 record formats: citation, abstract and detailed records. Each abstract and detailed record has a link named "Order From NTIS" which takes the user to the NTIS order system.

Hyperlinked Fields that can be searched from the record:

- Author
- NTIS Controlled Terms
- Uncontrolled Terms
- NTIS Classification Code
- Project Number
- Monitoring Agency
- Contract Number

Example of an NTIS Detailed Record	
Search Field Catagory	*Example Search Field Content/Response*
Accession number:	ADA410873
Title:	Energy Conversion in Laser Propulsion II
Authors:	Larson, C. W.; Mead, F. B.; Kalliomaa, W. M.
Author affiliation:	Air Force Research Lab., Edwards AFB, CA. Space and Missile Propulsion Div.
Author affiliation codes:	115210002 441421
Report number:	AFRL/PRS-ED-TP-2001-247
Publication date:	Dec-01
Pages:	22p
Language:	English
Country of origin:	United States
Document type:	Technical paper
Notes:	Paper presented at the AIAA Aerospace Sciences Meeting & Exhibit (40th) held in Reno, NV, on 14-17 Jan 2002.
Abstract:	This paper reports on an analysis of overall energy conversion in laser propulsion. Experimental studies of a laboratory-scale propulsion device that absorbs laser energy and converts that energy to propellant kinetic energy were carried out. The Myrabo Laser Lightcraft (MLL), propelled by laser-heated air, was studied.
Availability:	Product reproduced from digital image. Order this product from NTIS by: phone at 1-800-553-NTIS (U.S. customers); (703)605-6000 (other countries); fax at (703)605-6900; and email at orders@ntis.gov. NTIS is located at 5285 Port Royal Road, Springfield, VA, 22161, USA.
NTIS price code:	PC A03/MF A01
Project number:	1011
Task number:	Task 0046
Journal announcement:	u0314
NTIS controlled terms:	Laser applications | Energy conversion | Kinetic energy | Carbon dioxide lasers | Rocket propulsion | Solid propellants | Blowdown | Experimental data | Symposia | Spacecraft | Thermodynamics | Pulsed lasers | Thermal expansion | Heating | High energy lasers | Ionization | Chemical equilibrium | Reflectors | Equations of state | Delrin
Uncontrolled terms:	Laser heated propellant | Laser propulsion | Laser energy | Conversion efficiency | Laser heated air | Mll(Myrabo laser lightcraft) | Lightcraft | Equilibrium expansion | Frozen expansion | Air expansion | Equilibrium blowdown | Frozen blowdown
NTIS classification codes:	46C Optics and Lasers | 81B Combustion, Engines and Propellants Electric and Ion Propulsion | 81G Rocket Engines and Motors | 84A Astronautics
Database:	NTIS

Ovid Technologies

http://www.ovid.com

333 Seventh Avenue
New York, NY 10001
Telephone: 800-950-2035;
In New York City: 646- 674-6300
Fax: 646-674-6301
E-mail: sales@ovid.com

Coverage: 1964 to present

Document Delivery: Document availability from NTIS is indicated in each citation.

List of Selected Ovid Search Field

Record Structure

Label	*Field*	*Function*	*Example*
AN	Accession No.	Search	tib-b89-82561-xab.an
UP	Update Code	Search	9406.up
		Limit	..1/ 1 up = "9406"
AU	Author	Search	strueder, L.au
		Search	strueder, $.au
IN	Institution and Institution Code	Search	computer applications.in
		Search	ij535353.in
TI	Title	Search	eigenvalue problem.ti
TA	Title Annotation		–display only–
NT	Notes		–display only–
YR	Publication Year	Search	nov 1993.yr., 1993.yr
		Limit	..l/ 2 yr = 1993
JN	Journal Announcement	Search	u9006.jn
SA	Sponsoring Agency	Search	nasa-cr-194662.sa
		Search	nasa.sa
RN	Report Number	Search	mpi-pae-exp-el-208.rn
CN	Contract and/or Grant Numbers	Search	nasi-18605.cn
PN	Project and/or Task Numbers		–display only–
PR	Price		–display only–
AV	Availability		–display only–
CC	Subject Category Codes	Search	89d.cc. and 72b.cc
MJ	Major Descriptors	Search	problem solving.mj
MN	Major Descriptors	Search	energy resolution.mn
DE	Descriptors (MJ,MN)	Search	algorithms.de
		Search	reacting flow.de
ID	Identifiers	Search	ntisnasa.id
AB	Abstract	Search	supersonic
		Search	combustion.ab

Sample Record - Ovid Technologies	
Search Field Catagory	*Example Search Field Content/Response*
Accession number:	PB2001-107910-XAB
Author:	Bunte K; Abt SR.
Institution:	Rocky Mountain Research Station, Fort Collins, CO.; 114618000
Title:	Sampling Surface and Subsurface Particle-Size Distributions in Wadable Gravel- and Cobble-Bed Streams for Analyses in Sediment Transport, Hydraulics, and Streambed Monitoring.
Year of Publication:	May
Abstract:	This document provides guidance for sampling surface and subsurface sediment from wadable gravel- and cobble-bed streams. After a short introduction to streams types and classifications in gravel-bed rivers, the document explains the field and laboratory measurement of particle sizes and the statistical analysis of particle-size distributions. Analysis of particle parameters, including shape, density, and bulk density are also discussed. The document describes the spatial variability of bed-material particle sizes as well as the horizontal and vertical structure of particle deposits. The discussion of sampling procedures and equipment helps the user to make appropriate selections that support the sampling objective. Sample-size estimates may be obtained from empirical data or computed from statistical relationships between sample size and accuracy. The document explains a variety of methods, their usage and prerequisites. A detailed discussion of sampling schemes guides the ! user to select appropriate spatial sampling patterns necessary to produce representative samples.
Journal Announcement:	u0122
Report Number:	RMRS-GTR-74
Price:	NTIS Prices: PC A21/MF A04
Availability:	Product reproduced from digital image. Order this product from NTIS by: phone at 1-800-553-NTIS (U.S. customers); (703)605-6000 (other countries); fax at (703)605-6900; and email at orders@ntis.gov. NTIS is located at 5301 Shawnee Road, Alexandria, VA, 22312, USA.
Subject Category Codes:	48G. 48E
Major Subject Descriptors:	Hydraulics
	Streambeds
	Sediment transport
Minor Subject Descriptors:	Sampling procedures
	Sampling equipment
	Sample size
Identifiers:	*Particle-size analysis. Bed materials. Spatial sampling structures. Spatial variability
Notes:	Final rept. 454 PAGES
Update Code:	122

ProQuest

http://www.proquest.com/en-US/

789 E. Eisenhower Parkway

P.O. Box 1346
Ann Arbor, MI 48106-1346

Telephone: 734-761-4700
E-mail: customer_service@proquest.com

Dates of Coverage: 1964 - current

Update Frequency: Weekly

Size: Over 2,400,000 records as of March 2010

Field Codes	
Field Codes	*Field Codes Continued*
AB = Abstract	NU = Other Numbers
AG = Agency	PA = Patent Application Data
AN = Accession Number	PB = Publisher
AU = Author	PD = Publication Date
AV = Availability	PI = Patent Issue Date
CL = Classification	PY = Publication Year
CO = Country of Origin	RP = Report Number
DE = Descriptors	SF = Subfile
ID = Identifiers	SO = Source
LA = Language	TI = Title
NT = Notes	UD = Update

AN Accession Number: *Use this number to order the fulltext from NTIS.*

Sample Record - ProQuest		
Code	*Catagory Name*	*Catagory Content*
TI:	Title	Production, Prices, Employment, and Trade in Northwest Forest Industries, Fourth Quarter 1996
AU:	Author	Warren, DD
AV:	Availability	Order this product from NTIS by: phone at 1-800-553-NTIS (U.S. customers); (703) 605-6000 (other countries); fax at (703) 321-8547, and email: at orders@ntis.gov. NTIS is located at 5285 Port Royal Road, Springfield, VA 22161, USA. NTIS Prices: PC A08/MF A02
SO:	Source Performer:	Forest Service, Portland, OR. Pacific Northwest Research Station. July 1997. 143p. *Report: FSRB-PNW-226*
RP:	Report Number	FSRBPNW226; PB97199830
AB:	Abstract	Provides current information on lumber and plywood production and prices; employment in the forest industries; international trade in logs, lumber, and plywood; volume and average prices of stumpage sold by public agencies; and other related items.
LA:	Language	English
PY:	Publication Year	1997
PD:	Publication Date	19970700
CO:	Country of Origin	United States
PT:	Publication Type	Forest Service resource bulletin
DE:	Descriptors	Wood products; Forest industry; Sectoral analysis; Lumber; Plywood; Production; Prices; International Trade; Industries; Employment; Volume; Exports; Imports; Tables (Data); Agricultural economics
CL:	Classification	48D Natural Resources & Earth Sciences: Forestry; 96A Business & Economics: Domestic Commerce, Marketing, & Economics; 96C Business & Economics: International Commerce, Marketing & Economics
UD:	Update	199722
AN:	Accession Number	PB97199830

SilverPlatter Information, Inc.

http://www.silverplatter.com

100 River Ridge Drive
Norwood, MA 02062-5043
Telephone: 800- 343-0064 or 781-769-2599

Fax: 781-769-8763

E-mail: us_customerrelations@silverplatter.com

Below are the NTIS fields with their abbreviation. Fields listed in bold are limit fields.

List of Selected SilverPlatter Search Fields	
Label	***Field Name***
AB	Abstract
AG	Agency Source Code
AN	Accession Number
AU	Personal Author
AV	Availability Note*
CA	Corporate Author Code
CC	Subject Category Codes
CI	Country of Intellectual Origin
CN	Contract/Grant Number(s)
CS	Corporate Source
DE	Descriptors
DEM	Major Descriptors
DER	Minor Descriptors
ID	Identifiers
IDM	Major Identifiers
IDR	Minor Identifiers
LA	Language
NT	Descriptive Note*
PR	NTIS Price Codes*
PY	Publication Year
RD	Report Date/Pagination
RN	Report Number
SC	Subject Categories
TI	Title
UD	Update Date

** The AV, NT, PR, and RD fields are not searchable. The citation, a brief record, consists of the TI, AN, CS, RD, NT, AV, PR, RN, and CN fields. For more on NTIS fields, select Guide from the Help menu.*

Sample Record - ProQuest		
Code	*Catagory Content*	*Catagory Name*
TI	Preventing the Diseases of Aging: Special Focus: Healthy Aging. Chronic Disease Notes and Reports, Volume 12, Number 3, Fall 1999	Title
AN	PB2001102122XSP	Accession Number
AU	Ramsey-T.	Personal Authors
CS	Performer: National Center for Chronic Disease Prevention	Corporate Source
RD	1999. 20p.	Report Date/Pagination
PY	Jun-05	Publication Year
NT	Color illustrations reproduced in black and white	Descriptive Note
AV	Product reproduced from digital image. Order this product from NTIS by: phone at 1-800-533-NTIS (U.S. customers); (703) 605-6000 (other countries); fax at (703) 605-6900; and email at orders@ntis.fedworld.gov. NTIS is located at 5301 Shawnee Road, Alexandria, VA, 22312, USA	Availability Note
CI	UNITED-STATES	Country of Intellectual Origin
LA	ENGLISH	Language
PR	PC A03/MF A01	NTIS Price Codes
DE	Elderly-persons; Treatment-; Population-growth; Alzheimer's-	Descriptors
DE	*Aging-; *Chronic-diseases; *Prevention-;	Descriptors
ID	*CDC-Center-for-Disease-Control; *Center-for-Disease-Control	Identifiers
SC	Medicine-and-biology-Clinical-Medicine (57E); Medicine-and-biology-Public-health-and-industrial-medicine (57U); Health-planning-and-health-services-research-Community-and -population- characteristics (44C)	Subject Categories
CC	57E, 57U, 44C, 44, 57	Subject Category Codes
AB	The new millenium brings the nation many challenges, but none of Americans older than 65 years. Not only has the birthrate decreased since 1964, when the baby boom ended; at the same time, life expectancy has increased dramatically, from 47 years in 1900 to 76 years in 1990. Adults over than 85 years are the fastest-growing part of the population; by 2030, they are expected to number 8.5 million. 'If disease patterns stay the same, the health care system will have to spend an additional $400 to $500 billion to cover the costs of an older population', said James S. Marks, MD, MPH, Director, NCCDPHP. However lifesyle changes and increased emphasis on prevention could reverse the trends of increasing chronic disease, disability, and death.	Abstract
AG	HEWCDC	Agency Source Code
CA	104227000	Corporate Author Code
UD	200106	Update Date

STN International

In North America
CAS
STN North America
P.O. Box 3012
Columbus, Ohio 43210-0012 USA
Telephone: 800-753-4227 (North America)
614-447-3700 (worldwide)
Fax: 614-447-3751
E-mail: help@cas.org
Internet: http://www.cas.org

In Europe
FIZ Karlsruhe
STN Europe
P.O. Box 2465
76012 Karlsruhe
Germany
Phone: +49-7247-808-555
Fax: +49-7247-808-259
E-mail: helpdesk@fiz-karlsruhe.de
Internet: www.stn-international.com

In Japan
JAICI (Japan Association for
International Chemical Information)
STN Japan
Nakai Building
6-25-4 Honkomagome, Bunkyo-ku
Tokyo 113-0021, Japan
Phone: +81-3-5978-3601 (Technical Service)
+81-3-5978-3621 (Customer Service)
Fax: +81-3-5978-3600
E-mail: support@jaici.or.jp
customer@jaici.or.jp
Internet: www.jaici.or.jp

System Features:

- 1964 to the present
- More than 2,121,220 records (9/00)
- Updated weekly
- Automatic current-awareness searches (SDIs) are run weekly

STN Search and Display Field Codes

Search Field Name	*Search Code*	*Search Examples*	*Display Codes*
Basic Index* (contains single words from the title (TI), abstract (AB), controlled term (CT), uncontrolled term (UT) and CAS Registry Number (RN) fields)	None or /BI	S MOTORISTS S DRIVING HABIT# S DRIV?(2W)EXPER? S COAL(S)MINE# S PAT CL 110? S ANALYSIS/BI,CC S 50-23-7	TI, AB, CT, UT, RN
Accession Number	/AN	S "2001(17):03220"/AN	AN
Application Date (1)	/AD	S AD=JAN 1999	AI
Application Number	/AP	S US2001-983047/AP	AI
Application Year (1)	/AY	S AY=1999	AI
Author (patent inventor)	/AU (or /IN)	S MCCARTHY, P E/AU S AMES G/AU	AU
Availability	/AV	S CD ROM/AV	AV
Classification Codes, COSATI, NTIS etc. (code, main code (NTIS) and text) (2)	/CC	S 85/CC S 85A/CC S *57E/CC S TRANSPORTATION?/CC	CC
Controlled Term (main headings)	/CT	S ALCOHOL LAWS/CT S *HEAT RECOVERY/CT	CT
Controlled Word	/CW	S EARTH/CW	CT
Corporate Source (performing, sponsoring or cooperating performing organization, patent assignee)	/CS	S (DEPART?(2W)INTERIOR)/CS S COMBUSTION ENGINEERING?/CS	CS
Country (of Intellectual Origin) (code and text)	/CY	S GERMANY?/CY S GB/CY	CY
Document Type (code and text)	/DT (or /TC)	S PATENT/DT S P/DT	DT
Inventor	/IN	S MANDAVA N/IN	IN
Language (code and text)	/LA	S FRENCH/LA	LA

STN Search and Display Field Codes			
Search Field Name	***Search Code***	***Search Examples***	***Display Codes***
Note	/NTE	S SEAWIFS/NTE	NTE
Number of Contract (grant, project or task)	/NC	S AID-DSAN-C-0062/NC	NC
Number of Report, NTIS Order Number (number and prefix)	/NR	S PB85-138436/XAD/NR S PB85/NR	NR, AN
Other Source (journal and database issue)	/OS	S GRA&I8507/OS S GREENHOUSE# NOT INIS/OS	OS
Patent Assignee	/PA	S MARTIN MARIETTA/PA	PA
Patent Number	/PN	S US2804506/PN	PI
Publication Date (1)	/PD	S PD=FEB 2000	PD
Publication Year (1)	/PY	S 1983-1984/PY	PD
Source (contains number of contract, number of report)	/SO	S TRRLSR826/SO	SO
Title	/TI	S REAL-TIME/TI AND SOFTWARE/TI	TI
Update Date (1)	/UP (or /ED)	S UP=JUL 2002	UP
Word Count, Title (1)	/WC.T	S WC.T>=10	WC.T

(1) Numeric search field that may be searched with numeric operators or ranges.
(2) Search with implied (S) proximity is available.

STN DISPLAY and PRINT Formats		
Format	***Content***	***Examples***
AB	Abstract	D AB, TI
AI (AP)	Application Information	D AI
AN	Accession Number	D 1-5 AN
AU (IN)	Author (patent inventor)	D AU TI
AV	Availability	D AV
AY (1)	Application Year	D AY
CC	Classification Code	D CC
CS	Corporate Source	D CS
CT	Controlled Term	D CT
CY	Country (of Intellectual Origin)	D CY
DT (TC)	Document Type	D DT
IN	Patent Inventor	D IN
NC	Number of Contract (grant, project or task)	D NC
NR (SO)	Number of Report (patent number, application number)	D NR
NTE	Note	D NTE
OS	Other Source	D OS
PA	Patent Assignee	D PA
PD (1)	Publication Date	D PD
PI (PN)	Patent Information	D PI
PY (1)	Publication Year	D PY
RN	CAS Registry Number	D RN
TI	Title	D TI 1-10

STN DISPLAY and PRINT Formats

Format	*Content*	*Examples*
UP (1)	Update Date	D UP
UT	Uncontrolled Term	D CT UT 5-15
WC.T (1)	Word Count, Title	D WC.T
ALL	BIB, AB, CC, CT, UT, RN	D 1-3 ALL
DALL	ALL, delimited for post-processing	D DALL
IALL	ALL, indented with text labels	D IALL
BIB	AN, TI, AU, IN, CS, PA, NC, NR, PI, AI, CY, LA, NTE, AV, OS (BIB is default)	D 8 BIB
IBIB	BIB, indented with text labels	D IBIB
IND	AN, CC, CT, UT, RN	D IND
SCAN (2)	TI, CT	D SCAN
TRIAL (TRI, SAM, SAMPLE, FREE)	TI, CC, CT, UT, RN	D TRI
HIT	Hit term(s) and field(s)	D HIT
KWIC	Up to 50 words before and after hit term(s) (KeyWord-In-Context)	D KWIC
OCC	Number of occurrences of hit term(s) and field(s) in which they occur	D OCC

STN SELECT, ANALYZE and SORT Fields

The SELECT command is used to create E-numbers containing terms taken from the specified field in an answer set.
The ANALYZE command is used to create an L-number containing terms taken from the specified field in an answer set.
The SORT command is used to rearrange the search results in either alphabetic or numeric order of the specified field(s).

Field Name	*Field Code*	*ANALYZE / SELECT*	*SORT*
Abstract	AB	Y	N
Accession Number	AN	Y	N
Application Date	AD	Y	Y
Application Number	AP	Y	Y
Application Year	AY	Y	Y
Author (Patent Inventor)	AU	Y	Y
Availability	AV	Y	Y
CAS Registry Number	RN	Y	Y
Classification Code	CC	Y	Y
Controlled Term	CT	Y	N
Corporate Source	CS	Y	Y
Country (of Intellectual Origin)	CY	Y	Y
Document Type	DT	Y	Y
Language	LA	Y	Y
Note	NTE	Y	Y
Number of Contract	NC	Y	Y
Number of Report (NTIS Order Number)	NR	Y	Y
Other Source	OS	Y	Y
Patent Assignee	PA	Y	Y
Patent Information	PI	Y	Y
Patent Number	PN	Y	Y
Publication Date	PD	Y	Y
Publication Year	PY	Y	Y

STN SELECT, ANALYZE and SORT Fields			
Field Name	***Field Code***	***ANALYZE / SELECT***	***SORT***
Source	SO	Y	N
Title	TI	Y (default)	Y
Uncontrolled Term	UT	Y	N
Update Date	UP (ED)	Y	Y
Word Count, Title	WC.T	Y	Y

STN SELECT, ANALYZE and SORT Fields

DISPLAY ALL

AN 2010(12):01113 NTIS Order Number: PB2010-107165/XAB

TI Impacts of a 15-Percent Renewable Portfolio Standard.

CS Energy Information Administration, Washington, DC. Office of Integrated Analysis and Forecasting. (052896003)

NR PB2010-107165/XAB; SR/OIAF/2007-03
29p; Jun 2007

DT Report

CY United States

LA English

AV Order this product from NTIS by: phone at 1-800-553-NTIS (U.S.customers); (703)605-6000 (other countries); fax at (703)605-6900; and email at orders@ntis.gov. NTIS is located at 5301 Shawnee Road, Alexandria, VA, 22312, USA.
NTIS Prices: PC A03

OS GRA&I1012

AB This report responds to a request from Senator Jeff Bingaman asking EIA to analyze a renewable portfolio standard (RPS) requiring that 15 percent of U.S. electricity sales be derived from qualifying renewable energy resources. The proposal exempts smaller electricity providers - those with fewer than 4 billion kilowatt hours in annual sales - from meeting the requirement, and would not allow current generation from existing hydroelectric and municipal solid waste facilities to meet the requirement. However, retail sellers who generate from existing hydroelectric and municipal solid waste facilities are allowed to exclude this generation from their sales base when calculating their required renewable share. *(Actual abstract abbreviated for this example.)*

CC 97G Policies, regulations, and studies

CT *Energy market impacts; *Energy resources; Electric power generation; Impacts; Fuel use; Prices; Emissions; Expenditures; Tables (Data); Figures; Comparisons

*RENEWABLE PORTFOLIO STANDARD (RPS); *RENEWABLE ENERGY RESOURCES; ELECTRICITY SALES; RENEWABLE PORTFOLIO STANDARD PROPOSAL

DISPLAY BIB

ACCESSION NUMBER:	2010(13):01033
NTIS ORDER NUMBER:	ADD020436/XAB
TITLE:	Acceleration Strain Transducer with Increased Sensitivity. Patent Application.
INVENTOR:	Maguire, J. M.
PATENT ASSIGNEE:	Naval Undersea Warfare Center Div., Newport, RI. Office of Counsel. (103709005 602677)
NUMBER OF REPORT:	ADD020436/XAB; PAT-APPL-8-291048 17p; Filed 22 Sep 2009
APPLICATION INFORMATION:	US 2009-291048 20090922
CONTROLLED TERM:	Patent
COUNTRY:	United States
LANGUAGE:	English
AVAILABILITY:	This Government-owned invention available for U.S. licensing and, possibly, for foreign licensing. Copy of application available NTIS. Order this product from NTIS by: phone at 1-800-553-NTIS (U.S. customers); (703)605-6000 (other countries); fax at (703)605-6900; and email at orders@ntis.gov. NTIS is located at 5301 Shawnee Road, Alexandria, VA, 22312, USA.
NTIS Prices:	PC N03
OTHER SOURCE:	GRA&I1013

NTIS Subject Categories
Alphabetical Listing by Major Categories
Appendix A

70-Administration & Management
700-General
70A-Inventory Control
70B-Management Practice
70C-Management Information Systems
70D-Personnel Management, Labor Relations & Manpower Studies
70E-Research Program Administration & Technology Transfer
70F-Public Administration & Government
70G-Productivity

51-Aeronautics & Aerodynamics
510-General
51A-Aerodynamics
51B-Aeronautics
51C-Aircraft
51D-Parachutes & Decelerators
51E-Avionics
51F-Test Facilities & Equipment

98-Agriculture & Food
980-General
98A-Agricultural Chemistry
98B-Agricultural Economics
98C-Agricultural Equipment, Facilities, & Operations
98D-Agronomy, Horticulture, & Plant Pathology
98E-Animal Husbandry & Veterinary Medicine
98F-Fisheries & Aquaculture
98G-Agriculture Resource Surveys
98H-Food Technology

54-Astronomy & Astrophysics
540-General
54A-Astrogeology
54B-Astronomy & Celestial Mechanics
54C-Astrophysics
54D-Cosmic Ray Research

55-Atmospheric Sciences
550-General
55A-Aeronomy
55B-Dynamic Meteorology
55C-Meteorological Data Collection, Analysis, & Weather Forecasting
55D-Meteorological Instruments & Instrument Platforms
55E-Physical Meteorology
55F-Weather Modification

92-Behavior & Society
920-General
92A-Job Training & Career Development
92B-Psychology
92C-Social Concerns
92D-Education, Law, & Humanities
92E-International Relations

95-Biomedical Technology & Human Factors Engineering
950-General
95A-Prosthetics & Mechanical Organs
95B-Tissue Preservation & Storage
95C-Biomedical Instrumentation & Bioengineering
95D-Human Factors Engineering
95E-Life Support Systems
95F-Bionics & Artificial Intelligence
95G-Protective Equipment

89-Building Industry Technology
890-General
89B-Architectural Design & Environmental Engineering
89C-Construction Management & Techniques
89D-Structural Analyses
89E-Building Standards & Codes
89G-Construction Materials, Components, & Equipment
89H-Building Equipment, Furnishings, & Maintenance

96-Business & Economics
960-General
96A-Domestic Commerce, Marketing, & Economics
96C-International Commerce, Marketing, & Economics
96D-Consumer Affairs
96E-Minority Enterprises
96F-Banking & Finance
96G-Foreign Industry Economic Development
96H-Foreign Business & Economics

99-Chemistry

990-General
99A-Analytical Chemistry
99B-Industrial Chemistry & Chemical Process Engineering
99C-Polymer Chemistry
99D-Basic & Synthetic Chemistry
99E-Photochemistry & Radiation Chemistry
99F-Physical & Theoretical Chemistry

50-Civil Engineering

500-General
50A-Highway Engineering
50B-Civil Engineering
50C-Construction Equipment, Materials, & Supplies
50D-Soil & Rock Mechanics

81-Combustion, Engines, & Propellants

810-General
81A-Combustion & Ignition
81B-Electric & Ion Propulsion
81C-Fuel & Propellant Tanks
81D-Jet & Gas Turbine Engines
81G-Rocket Engines & Motors
81H-Rocket Propellants
81I-Nuclear Propulsion
81J-Reciprocation & Rotating Combustion Engines

45-Communication

450-General
45A-Policies, Regulations, & Studies
45B-Radio & Television Equipment
45C-Common Carrier & Satellite
45D-Sociopolitical
45E-Graphics
45F-Verbal
45G-Communication & Information Theory

62-Computers, Control & Information Theory

620-General
62A-Computer Hardware
62B-Computer Software
62C-Control Systems & Control Theory
62D-Information Processing Standards
62E-Information Theory
62F-Pattern Recognition & Image Processing
62R-Applications Software
62S-Data Files

63-Detection & Countermeasures

630-General
63A-Acoustic Detection
63B-Electromagnetic & Acoustic Countermeasures
63C-Infrared & Ultraviolet Detection
63D-Magnetic Detection
63E-Nuclear Explosion Detection
63F-Optical Detection
63G-Personnel Detection
63H-Radiofrequency Detection
63I-Seismic Detection

49-Electrotechnology

490-General
49A-Antennas
49B-Circuits
49C-Electromechanical Devices
49D-Electron Tubes
49E-Optoelectronic Devices & Systems
49F-Power & Signal Transmission Devices
49G-Resistive, Capacitive, & Inductive Components
49H-Semiconductor Devices

97-Energy

970-General
97A-Reserves
97B-Energy Use, Supply, & Demand
97E-Electric Power Transmission
97F-Fuel Conversion Processes
97G-Policies, Regulations & Studies
97I-Electric Power Production
97J-Heating & Cooling Systems
97K-Fuels
97L-Engine Studies (Energy Related)
97M-Batteries & Components
97N-Solar Energy
97O-Miscellaneous Energy Conversion & Storage
97P-Geothermal Energy
97Q-Selected Studies In Nuclear Technology
97R-Environmental Studies

68-Environmental Pollution & Control

680-General
68A-Air Pollution & Control
68B-Noise Pollution & Control
68C-Solid Wastes Pollution & Control
68D-Water Pollution & Control
68E-Pesticides Pollution & Control
68F-Radiation Pollution & Control
68G-Environmental Health & Safety
68H-Environmental Impact Statements

90-Government Inventions for Licensing

900-General
90A-Mechanical Devices & Equipment
90B-Chemistry
90C-Nuclear Technology
90D-Biology & Medicine
90E-Metallurgy
90F-Electrotechnology
90G-Instruments
90H-Optics & Lasers
90I-Ordnance
90J-Food Technology

44-Health Care

440-General
44A-Planning Methodology
44B-Agency Administrative & Financial Management
44C-Community & Population Characteristics
44D-Health Care Assessment & Quality Assurance
44E-Health Care Measurement Methodology
44F-Health Care Forecasting Methodology
44G-Environmental & Occupational Factors
44H-Health Care Technology
44J-Health Delivery Plans, Projects & Studies
44K-Health Services
44L-Health Care Needs & Demands
44M-Health Resources
44N-Health Care Utilization
44P-Health Education & Manpower Training
44Q-Health-Related Costs
44R-Economics & Sociology
44S-Legislation & Regulations
44T-Data & Information Systems
44U-Health Care Delivery Organization & Administration

94-Industrial & Mechanical Engineering

940-General
94A-Production Planning & Process Controls
94B-Quality Control & Reliability
94C-Plant Design & Maintenance
94D-Job Environment
94E-Environmental Engineering
94F-Tooling, Machinery, & Tools
94G-Manufacturing Processes & Materials Handling
94H-Industrial Safety Engineering
94I-Hydraulic & Pneumatic Equipment
94J-Nondestructive Testing
94K-Laboratory & Test Facility Design & Operation

88-Library & Information Sciences

880-General
88A-Operations & Planning
88B-Information Systems
88C-Marketing & User Services
88D-Personnel
88E-Reference Materials

41-Manufacturing Technology

410-General
41A-Computer Aided Design (CAD)
41B-Computer Aided Manufacturing (CAM)
41C-Robotics/Robots
41D-Productivity
41E-Manufacturing, Planning, Processing & Control
41F-Joining
41G-Quality Control & Reliability
41H-Plant Design & Maintenance
41I-Job Environment
41J-Tooling, Machinery, & Tools
41K-Engineering Materials
41L-Tribology
41M-Optics & Lasers
41N-Computer Software
41O-Domestic Commerce, Marketing, & Economics
41P-Research Program Administration & Technology Transfer

71-Materials Sciences

710-General
71A-Ablative Materials & Ablation
71B-Adhesives & Sealants
71C-Carbon & Graphite
71D-Ceramics, Refractories, & Glass
71E-Coatings, Colorants, & Finishes
71F-Composite Materials
71G-Corrosion & Corrosion Inhibition
71H-Elastomers
71I-Fibers & Textiles
71J-Iron & Iron Alloys
71K-Lubricants & Hydraulic Fluids
71L-Materials Degradation & Fouling
71M-Miscellaneous Materials
71N-Nonferrous Metals & Alloys
71O-Plastics
71P-Refractory Metals & Alloys
71Q-Solvents, Cleaners, & Abrasives
71R-Wood & Paper Products

72-Mathematical Sciences

720-General
72B-Algebra, Analysis, Geometry, & Mathematical Logic
72E-Operations Research
72F-Statistical Analysis

57-Medicine & Biology

570-General
57A-Anatomy
57B-Biochemistry
57C-Botany
57D-Clinical Chemistry
57E-Clinical Medicine
57F-Cytology, Genetics, & Molecular Biology
57G-Dentistry
57H-Ecology
57I-Electrophysiology
57J-Immunology
57K-Microbiology
57L-Nutrition
57M-Occupational Therapy, Physical Therapy, & Rehabilitation
57N-Parasitology
57O-Pathology
57P-Pest Control
57Q-Pharmacology & Pharmacological Chemistry
57S-Physiology
57T-Psychiatry
57U-Public Health & Industrial Medicine
57V-Radiobiology
57W-Stress Physiology
57X-Surgery
57Y-Toxicology
57Z-Zoology

74-Military Sciences

740-General
74A-Antiaircraft Defense Systems
74B-Antimissile Defense Systems
74C-Antisubmarine Warfare
74D-Chemical, Biological, & Radiological Warfare
74E-Logistics, Military Facilities, & Supplies
74F-Military Intelligence
74G-Military Operations, Strategy, & Tactics
74H-Nuclear Warfare
74I-Passive Defense Systems

75-Missile Technology

750-General
75A-Air & Space-Launched Missiles
75B-Missile Guidance & Control Systems
75C-Missile Launching & Support Systems
75D-Missile Tracking Systems
75E-Missile Trajectories & Reentry Dynamics
75F-Missile Warheads & Fuses
75G-Surface-Launched Missiles
75H-Underwater-Launched Missiles

48-Natural Resources & Earth Sciences

480-General
48A-Mineral Industries
48B-Natural Resource Management
48C-Natural Resource Surveys
48D-Forestry
48E-Soil Sciences
48F-Geology & Geophysics
48G-Hydrology & Limnology
48H-Snow, Ice, & Permafrost
48I-Cartography

76-Navigation, Guidance, & Control

760-General
76A-Control Devices & Equipment
76B-Guidance Systems
76C-Navigation & Guidance System Components
76D-Navigation Systems

77-Nuclear Science & Technology

770-General
77A-Fusion Devices (Thermonuclear)
77B-Isotopes
77C-Nuclear Auxiliary Power Systems
77D-Nuclear Explosions & Devices
77E-Nuclear Instrumentation
77F-Radiation Shielding, Protection, & Safety
77G-Radioactive Wastes & Radioactivity
77H-Reactor Engineering & Nuclear Power Plants
77I-Reactor Fuels & Fuel Processing
77J-Reactor Materials
77K-Reactor Physics

47-Ocean Sciences & Technology

470-General
47A-Marine Engineering
47B-Dynamic Oceanography
47C-Physical & Chemical Oceanography
47D-Biological Oceanography
47E-Marine Geophysics & Geology
47F-Oceanographic Vessels, Instruments, & Platforms
47G-Hydrography
47H-Underwater Construction & Habitats

79-Ordnance

790-General
79A-Ammunition, Explosives, & Pyrotechnics
79B-Armor
79C-Bombs
79D-Combat Vehicles
79E-Detonations, Explosion Effects, & Ballistics
79F-Fire Control & Bombing Systems
79G-Guns
79H-Rockets
79I-Underwater Ordnance

82-Photography & Recording Devices

820-General
82A-Holography
82B-Photographic Techniques & Equipment
82C-Recording Devices

46-Physics

460-General
46A-Acoustics
46B-Fluid Mechanics
46C-Optics & Lasers
46D-Solid State Physics
46E-Structural Mechanics
46G-Plasma Physics
46H-Radiofrequency Waves

43-Problem-Solving Information for State & Local Governments

430-General
43A-Finance
43B-Economic & Community Development
43C-Human Resources
43D-Police, Fire, & Emergency Services
43E-Energy
43F-Environment
43G-Transportation

84-Space Technology

840-General
84A-Astronautics
84B-Extraterrestrial Exploration
84C-Manned Spacecraft
84D-Spacecraft Trajectories & Flight Mechanics
84E-Space Launch Vehicles & Support Equipment
84F-Space Safety
84G-Unmanned Spacecraft

85-Transportation

850-General
85A-Air Transportation
85C-Metropolitan Rail Transportation
85D-Transportation Safety
85E-Pipeline Transportation
85F-Global Navigation Systems
85G-Marine & Waterway Transportation
85H-Road Transportation
85I-Railroad Transportation

91-Urban & Regional Technology & Development

910-General
91A-Environmental Management & Planning
91B-Transportation & Traffic Planning
91C-Fire Services, Law Enforcement, & Criminal Justice
91D-Communications
91E-Housing
91F-Health Services
91G-Urban Administration & Planning
91H-Regional Administration & Planning
91I-Emergency Services & Planning
91J-Economic Studies
91K-Social Services
91L-Recreation

NTIS Subject Categories
Alphabetical Listing by All Categories
Appendix B

Ablative Materials and Ablation ..... (71A)
Acoustic Detection ..... (63A)
Acoustics ..... (46A)
Adhesives and Sealants ..... (71B)
Administration and Management ..... (70)
Aerodynamics ..... (51A)
Aeronautics ..... (51B)
Aeronautics -Test Facilities and Equipment ..... (51F)
Aeronautics and Aerodynamics ..... (51)
Aeronomy ..... (55A)
Agricultural Chemistry ..... (98A)
Agricultural Economics ..... (98B)
Agricultural Equipment, Facilities, and Operations ..... (98C)
Agricultural Resource Surveys ..... (98G)
Agriculture and Food ..... (98)
Agronomy, Horticulture, and Plant Pathology ..... (98D)
Air and Space-Launched Missiles ..... (75A)
Air Pollution and Control ..... (68A)
Air Transportation ..... (85A)
Aircraft ..... (51C)
Algebra, Analysis, Geometry, and Mathematical Logic ..... (72B)
Ammunition, Explosives, and Pyrotechnics ..... (79A)
Analytical Chemistry ..... (99A)
Anatomy ..... (57A)
Animal Husbandry and Veterinary Medicine ..... (98E)
Antennas ..... (49A)
Antiaircraft Defense Systems ..... (74A)
Antimissile Defense Systems ..... (74B)
Antisubmarine Warfare ..... (74C)
Architectural Design and Environmental Engineering ..... (89B)
Armor ..... (79B)
Astrogeology ..... (54A)
Astronautics ..... (84A)
Astronomy and Astrophysics ..... (54)
Astronomy and Astrophysics Cosmic Ray Research ..... (54D)
Astronomy and Celestial Mechanics ..... (54B)
Astrophysics ..... (54C)
Atmospheric Sciences ..... (55)
Atmospheric Sciences Dynamic Meteorology ..... (55B)
Avionics ..... (51E)
Banking and Finance ..... (96F)
Basic and Synthetic Chemistry ..... (99D)
Batteries and Components ..... (97M)
Behavior and Society ..... (92)
Biochemistry ..... (57B)
Biological Oceanography ..... (47D)
Biomedical Instrumentation and Bioengineering ..... (95C)
Biomedical Technology and Human Factors Engineering ..... (95)
Bionics and Artificial Intelligence ..... (95F)
Bombs ..... (79C)
Botany ..... (57C)
Building Construction Management and Techniques ..... (89C)
Building Construction Materials, Components, and Equipment ..... (89G)
Building Equipment, Furnishings, and Maintenance ..... (89H)
Building Industry Technology ..... (89)
Building Standards and Codes ..... (89E)
Building Structural Analyses ..... (89D)
Business - Foreign Industry Development and Economics ..... (96G)
Business - International Commerce, Marketing, and Economics ..... (96C)
Business and Economics ..... (96)
Business Domestic Commerce, Marketing, and Economics ..... (96A)
Carbon and Graphite ..... (71C)
Cartography ..... (48I)
Ceramics, Refractories, and Glass ..... (71D)
Chemical, Biological, and Radiological Warfare ..... (74D)
Chemistry ..... (99)
Chemistry - Physical and Theoretical ..... (99F)
Chemistry - Photo and Radiation ..... (99E)
Circuits ..... (49B)
Civil Engineering ..... (50B)
Civil Engineering (Heading) ..... (50)

Civil Engineering Construction Equipment, Materials, and Supplies ..... (50C)
Clinical Chemistry ..... (57D)
Clinical Medicine ..... (57E)
Coatings, Colorants, and Finishes ..... (71E)
Combat Vehicles ..... (79D)
Combustion and Ignition ..... (81A)
Combustion, Engines and Propellants Electric and Ion Propulsion ..... (81B)
Combustion, Engines, and Propellants ..... (81)
Common Carrier and Satellite ..... (45C)
Communication ..... (45)
Communication Graphics ..... (45E)
Communication and Information Theory ..... (45G)
Communication Policies, Regulations, and Studies ..... (45A)
Communications - Sociopolitical ..... (45D)
Communications - Verbal ..... (45F)
Composite Materials ..... (71F)
Computer Aided design (CAD) ..... (41A)
Computer Aided Manufacturing (CAM) ..... (41B)
Computer Control Systems and Control Theory ..... (62C)
Computer Hardware ..... (62A)
Computer Information Processing Standards ..... (62D)
Computer Information Theory ..... (62E)
Computer Software ..... (62B)
Computers, Control, and Information Theory ..... (62)
Consumer Affairs ..... (96D)
Corrosion and Corrosion Inhibition ..... (71G)
Cytology, Genetics, and Molecular Biology ..... (57F)
Dentistry ..... (57G)
Detection and Countermeasures ..... (63)
Detonations, Explosion Effects, and Ballistics ..... (79E)
Dynamic Oceanography ..... (47B)
Ecology ..... (57H)
Education, Law, and Humanities ..... (92D)
Elastomers ..... (71H)
Electric Power Production ..... (97I)
Electric Power Transmission ..... (97E)
Electromagnetic and Acoustic Countermeasures ..... (63B)
Electromechanical Devices ..... (49C)
Electron Tubes ..... (49D)
Electronic Resistive, Capacitive, and Inductive Components ..... (49G)
Electrotechnology ..... (49)
Energy ..... (97)
Energy Environmental Studies ..... (97R)
Energy Policies, Regulations, and Studies ..... (97G)
Energy Reserves ..... (97A)
Energy Use, Supply, and Demand ..... (97B)
Engine Studies (Energy Related) ..... (97L)
Engineering Materials ..... (41K)
Environmental Engineering ..... (94E)
Environmental Health and Safety ..... (68G)
Environmental Impact Statements ..... (68H)
Environmental Pollution and Control ..... (68)
Fibers and Textiles ..... (71I)
Fisheries and Aquaculture ..... (98F)
Fluid Mechanics ..... (46B)
Food Technology ..... (98H)
Forestry ..... (48D)
Fuel and Propellant Tanks ..... (81C)
Fuel Conversion Processes ..... (97F)
Fuels ..... (97K)
Fusion Devices (Thermonuclear) ..... (77A)
Geology and Geophysics ..... (48F)
Geothermal Energy ..... (97P)
Global Navigation Systems ..... (85F)
Government Inventions - Biology and Medicine ..... (90D)
Government Inventions - Chemistry ..... (90B)
Government Inventions - Electrotechnology ..... (90F)
Government Inventions - Food Technology ..... (90J)
Government Inventions - Instruments ..... (90G)
Government Inventions - Mechanical Devices and Equipment ..... (90A)
Government Inventions - Metallurgy ..... (90E)
Government Inventions - Nuclear Technology ..... (90C)
Government Inventions - Optics and Lasers ..... (90H)
Government Inventions - Ordnance ..... (90I)
Government Inventions for Licensing ..... (90)
Guns ..... (79G)
Health Care ..... (44)
Health Care Agency Administrative and Financial Management ..... (44B)
Health Care Assessment and Quality Assurance ..... (44D)

Health Care Community and Population Characteristics ..... (44C)
Health Care Data and Information Systems ..... (44T)
Health Care Delivery Organization and Management ..... (44U)
Health Care Economics and Sociology ..... (44R)
Health Care Environmental and Occupational Factors ..... (44G)
Health Care forecasting Methodology ..... (44F)
Health Care Legislation and Regulations ..... (44S)
Health Care measurement Methodology ..... (44E)
Health Care Needs and Demands ..... (44L)
Health Care Technology ..... (44H)
Health Care Utilization ..... (44N)
Health Delivery Plans, Projects, and Studies ..... (44J)
Health Education and Manpower Training ..... (44P)
Health Planning Methodology ..... (44A)
Health Resources ..... (44M)
Health Services ..... (44K)
Health-Related Costs ..... (44Q)
Heating and Cooling Systems ..... (97J)
Highway Engineering ..... (50A)
Holography ..... (82A)
Human Factors Engineering ..... (95D)
Hydraulic and Pneumatic Equipment ..... (94I)
Hydrography ..... (47G)
Hydrology and Limnology ..... (48G)
Immunology ..... (57J)
Industrial and Mechanical Engineering ..... (94)
Industrial and Mechanical Engineering Plant Design and Maintenance ..... (94C)
Industrial and Mechanical Engineering Production Planning and Process Controls ..... (94A)
Industrial and Mechanical Engineering Quality Control and Reliability ..... (94B)
Industrial Chemistry and Chemical Process Engineering ..... (99B)
Industrial Job Environment ..... (94D)
Industrial Laboratory and Test Facility Design and Operation ..... (94K)
Industrial Safety Engineering ..... (94H)
Infrared and Ultraviolet Detection ..... (63C)
International Relations ..... (92E)
Inventory Control ..... (70A)
Iron and Iron Alloys ..... (71J)
Isotopes ..... (77B)
Jet and Gas Turbine Engines ..... (81D)
Joining ..... (41F)
Library and Information Science Marketing and User Services ..... (88C)
Library and Information Science Personnel ..... (88D)
Library and Information Sciences ..... (88)
Library and Information Sciences Operations and Planning ..... (88A)
Library Information Systems ..... (88B)
Life Support Systems ..... (95E)
Logistics, Military Facilities, and Supplies ..... (74E)
Lubricants and Hydraulic Fluids ..... (71K)
Magnetic Detection ..... (63D)
Management Information Systems ..... (70C)
Management Practice ..... (70B)
Manned Spacecraft ..... (84C)
Manufacturing Job Environment ..... (41I)
Manufacturing Computer Software ..... (41N)
Manufacturing Domestic Commerce, Marketing, and Economics ..... (41O)
Manufacturing Optics and Lasers ..... (41M)
Manufacturing Plant Design and Maintenance ..... (41H)
Manufacturing Processes and Materials Handling ..... (94G)
Manufacturing Productivity ..... (41D)
Manufacturing Quality Control and Reliability ..... (41G)
Manufacturing Research Program Administration and Technology Transfer ..... (41P)
Manufacturing Technology ..... (41)
Manufacturing Tooling, Machinery, and Tools ..... (41J)
Manufacturing, Planning, Processing, and Control ..... (41E)
Marine and Waterway Transportation ..... (85G)
Marine Engineering ..... (47A)
Marine Geophysics and Geology ..... (47E)
Materials Degradation and Fouling ..... (71L)
Materials Sciences ..... (71)
Mathematical Sciences ..... (72)
Medicine and Biology ..... (57)
Medicine and Biology Electrophysiology ..... (57I)
Meteorological Data Collection, Analysis, and Weather Forecasting ..... (55C)
Meteorological Instruments and Instrument Platforms ..... (55D)
Metropolitan Rail Transportation ..... (85C)

Microbiology ..... (57K)
Military Intelligence ..... (74F)
Military Operations, Strategy, and Tactics ..... (74G)
Military Sciences ..... (74)
Mineral Industries ..... (48A)
Minority Enterprises ..... (96E)
Miscellaneous Energy Conversion and Storage ..... (97O)
Miscellaneous Materials ..... (71M)
Missile Guidance and Control Systems ..... (75B)
Missile Launching and Support Systems ..... (75C)
Missile Technology ..... (75)
Missile Tracking Systems ..... (75D)
Missile Trajectories and Reentry Dynamics ..... (75E)
Missile Warheads and Fuses ..... (75F)
Natural Resource Management ..... (48B)
Natural Resource Surveys ..... (48C)
Natural Resources and Earth Sciences ..... (48)
Navigation and Guidance System Components ..... (76C)
Navigation Control Devices and Equipment ..... (76A)
Navigation Guidance Systems ..... (76B)
Navigation Systems ..... (76D)
Navigation, Guidance, and Control ..... (76)
Noise Pollution and Control ..... (68B)
Nondestructive Testing ..... (94J)
Nonferrous Metals and Alloys ..... (71N)
Nuclear Auxiliary Power Systems ..... (77C)
Nuclear Explosion Detection ..... (63E)
Nuclear Explosions and Devices ..... (77D)
Nuclear Instrumentation ..... (77E)
Nuclear Propulsion ..... (81I)
Nuclear Reactor Engineering and Nuclear Power Plants ..... (77H)
Nuclear Reactor Fuels and Fuel Processing ..... (77I)
Nuclear Reactor Materials ..... (77J)
Nuclear Reactor Physics ..... (77K)
Nuclear Science and Technology ..... (77)
Nuclear Technology Selected Studies ..... (97Q)
Nuclear Warfare ..... (74H)
Nutrition ..... (57L)
Occupational Therapy, Physical Therapy, and Rehabilitation ..... (57M)
Ocean Technology and Engineering ..... (47)
Oceanographic Vessels, Instruments, and Platforms ..... (47F)
Operations Research ..... (72E)
Optical Detection ..... (63F)
Optics and Lasers ..... (46C)
Optoelectronic Devices and Systems ..... (49E)
Ordnance ..... (79)
Ordnance - Fire Control and Bombing Systems ..... (79F)
Parachutes and Decelerators ..... (51D)
Parasitology ..... (57N)
Passive Defense Systems ..... (74I)
Pathology ..... (57O)
Pattern Recognition and Image Processing ..... (62F)
Personnel Detection ..... (63G)
Pest Control ..... (57P)
Pesticides Pollution and Control ..... (68E)
Pharmacology and Pharmacological Chemistry ..... (57Q)
Photographic Techniques and Equipment ..... (82B)
Photography and Recording Devices ..... (82)
Physical and Chemical Oceanography ..... (47C)
Physical Meteorology ..... (55E)
Physics ..... (46)
Physiology ..... (57S)
Pipeline Transportation ..... (85E)
Plasma Physics ..... (46G)
Plastics ..... (71O)
Polymer Chemistry ..... (99C)
Power and Signal Transmission Devices ..... (49F)
Problem Solving for State and Local Governments - Finance ..... (43A)
Problem Solving for State and Local Governments-Economic and Community Development ..... (43B)
Problem Solving for State and Local Governments Environment ..... (43F)
Problem Solving Information for State and Local Governments ..... (43)
Productivity ..... (70G)
Prosthetics and Mechanical Organs ..... (95A)
Protective Equipment ..... (95G)
Psychiatry ..... (57T)
Psychology ..... (92B)
Public Administration and Government ..... (70F)
Public Health and Industrial Medicine ..... (57U)
Radiation Pollution and Control ..... (68F)
Radiation Shielding, Protection, and Safety ..... (77F)

Radio and Television Equipment ..... (45B)
Radio Frequency Detection ..... (63H)
Radio Frequency Waves ..... (46H)
Radioactive Wastes and Radioactivity ..... (77G)
Radiobiology ..... (57V)
Railroad Transportation ..... (85I)
Reciprocating and Rotating Combustion Engines ..... (81J)
Recording Devices ..... (82C)
Reference Materials ..... (88E)
Refractory Metals and Alloys ..... (71P)
Research Program Administration and Technology Transfer ..... (70E)
Road Transportation ..... (85H)
Robotics/Robots ..... (41C)
Rocket Engines and Motors ..... (81G)
Rocket Propellants ..... (81H)
Rockets ..... (79H)
Seismic Detection ..... (63I)
Semiconductor Devices ..... (49H)
Snow, Ice, and Permafrost ..... (48H)
Social Concerns ..... (92C)
Soil and Rock Mechanics ..... (50D)
Soil Sciences ..... (48E)
Solar Energy ..... (97N)
Solid State Physics ..... (46D)
Solid Wastes Pollution and Control ..... (68C)
Solvents, Cleaners, and Abrasives ..... (71Q)
Space Extraterrestrial Exploration ..... (84B)
Space Launch Vehicles and Support Equipment ..... (84E)
Space Safety ..... (84F)
Space Technology ..... (84)
Spacecraft Trajectories and Flight Mechanics ..... (84D)
State and Local Governments - Transportation ..... (43G)
State and Local Government Energy ..... (43E)
State and Local Governments - Human Resources ..... (43C)
State and Local Governments Police, Fire, and Emergency Services ..... (43D)
Statistical Analysis ..... (72F)
Stress Physiology ..... (57W)
Structural Mechanics ..... (46E)
Surface-Launched Missiles ..... (75G)
Surgery ..... (57X)
Tissue Preservation and Storage ..... (95B)
Tooling, Machinery, and Tools ..... (94F)
Toxicology ..... (57Y)
Transportation ..... (85)
Transportation Safety ..... (85D)
Tribology ..... (41L)
Underwater Construction and Habitats ..... (47H)
Underwater Ordnance ..... (79I)
Underwater-Launched Missiles ..... (75H)
Unmanned Spacecraft ..... (84G)
Urban Administration and Planning ..... (91G)
Urban and Regional Technology and Development ..... (91)
Urban and Regional Technology Communications ..... (91D)
Urban Economic Studies ..... (91J)
Urban Emergency Services and Planning ..... (91I)
Urban Environmental Management and Planning ..... (91A)
Urban Fire Services, Law Enforcement, and Criminal Justice ..... (91C)
Urban Health Services ..... (91F)
Urban Housing ..... (91E)
Urban Recreation ..... (91L)
Urban Regional Administration and Planning ..... (91H)
Urban Social Services ..... (91K)
Urban Transportation and Traffic Planning ..... (91B)
Water Pollution and Control ..... (68D)
Weather Modification ..... (55F)
Wood and Paper Products ..... (71R)
Zoology ..... (57Z)

NTIS Subject Categories
Alphabetical Listing with Scope Descriptions

Appendix C

70-Administration & Management

700-General
Organizational structure and organization theory.

70A-Inventory Control
Inventory analysis; Inventory models; Obsolescence; Repair-replacement tradeoffs; Spare parts; Stock level control; Usage prediction; Warehouse automation; Stockpiling.

70B-Management Practice
Theory and concepts of management including record keeping, planning, scheduling, organization, coordination, decision making, policy making; Productivity management; Cost effectiveness; Systems management; Contact management; Management methods (PERT, PPB, etc.); Management games. Applied studies are classified in the application.

For research management, use 70E.

70C-Management Information Systems
Information systems which include data collection, data processing, and information delivery for use in decision making an evaluation by managers; Manual and automated systems.

See also 88B.

70D-Personnel Management, Labor Relations & Manpower Studies
Selection, recruitment, management, utilization, and evaluation of personnel; Job descriptions; Job analysis; Salary administration; Labor supply; Labor unions; Arbitration and bargaining; Industrial relations; Fringe benefits, and incentives; Manpower allocation requirements and utilization.

For library and information science personnel, use 88D.

For health personnel, use 44P.

70E-Research Program Administration & Technology Transfer
Research management, development, and forecasting; Research contract management; Research needs; Technology transfer and forecasting. Excludes research methods per se. Studies of specific programs are excluded unless they discuss a program at the national level, technology innovation, or trends and impacts of new technology.

70F-Public Administration & Government
National, state, and local government structure, operation, and administration. Operations of government agencies and their interactions; Intergovernmental relations.

See also 43, 91G, and 91H.

70G-Productivity
Productivity of businesses, government, employees, management, and services; Improving quality of work life; Measurement of productivity efficiency and effectiveness; Employee attitudes and motivation, manpower utilization and performance improvement, job satisfaction, job security; Labor-management cooperation, joint committees participative management, job redesign; Alternative work schedules; Incentive plans. Productivity barriers including regulations, obsolete practices, paperwork, and financing methods.

See also 70B, 70D, 70F, 96A, and 96G.

For specific applications of productivity to manufacturing, use 41D and 94.

51-Aeronautics & Aerodynamics

510-General
Includes landing mats.

51A-Aerodynamics
Aerodynamic characteristics and problems of bodies as they are affected by the dynamics of phenomena relating to boundary layer, lift, drag, laminar and turbulent flow, compressible flow, lift, aerodynamic heating, vortex flow, wake, etc. in aerodynamic regimes. Includes aircraft, ground vehicles, and structures.

See also 46B.

For missile reentry dynamics, use 75E.

For spacecraft reentry dynamics, use 84D.

51B-Aeronautics
Aircraft operations such as takeoff and landing, all-weather and night flight, taxiing, approach, letdown, in-flight refueling, etc. Includes aviation accidents.

51C-Aircraft
Design, production, and maintenance of aircraft, aircraft components and equipment. Structural studies of airframes, bodies, wings, fuselages; Military and commercial aircraft; Balloons (excludes meteorological balloons); Air cushion vehicles (excludes tracked vehicles).

See also 85A and 81D.

For meteorological balloons, use 55D.

For tracked air cushion vehicles, use 85C.

For electronic equipment, use 51E.

* Every primary subject category has a "General" subcategory which contains items whose subject matter falls either into several subcategories or none of the subcategories within a primary category.

In the generic example that follows, the Primary Subject Category is Administration & Management; the Subject Category Code is 70; the Subcategory and Code is 70A; and the descriptions follow. The descriptions are the concepts contained in a report; be careful to avoid "word matching."

70-Administration & Management

70A-Inventory control
Inventory analysis; Inventory models; Obsolescence; Repair-replacement tradeoffs; Spare parts; Stock level control; Usage prediction; Warehouse automation; Stock-piling.

51D-Parachutes & Decelerators
Deployable devices and structures to induce drag and deceleration of aircraft, spacecraft, and test vehicles such as rocket sleds.

51E-Avionics
Airborne electronic equipment. Includes electronic equipment used for communications; Navigation; Control systems; Onboard air traffic control; Detection.

See also 45, 49, 63, and 76.

51F-Test Facilities & Equipment
Wind tunnels; Simulators; Flight simulators.

For flight simulators used for training, use 92A.

98-Agriculture & Food

980-General

98A-Agricultural Chemistry
The application of chemistry and chemical analysis to agriculture; Fertilizer production; Soil chemistry; Chemistry of feeding stuffs; Crop chemistry; Biochemical studies.

For food chemistry, use 98H.

98B-Agricultural Economics
Economics conditions, markets, subsidies, and policies affecting agriculture; Farm management and finance; Land and labor economics; Prices and price control.

See also 96C.

98C-Agricultural Equipment, Facilities, & Operations
Agricultural engineering; Agricultural machinery and tools; Seed preservation; Planting, fertilizing, mulching, weeding, and harvesting; Pest and disease control techniques and equipment; Crop protection; Crop drying and storage; Farm water supplies; Irrigation systems; Farm safety; Farm construction and operation.

For pest control, see also 57P.

For food processing, use 98H.

98D-Agronomy, Horticulture, & Plant Pathology
Field crop production; Cultivation of orchards, gardens and nurseries; Plant biology; Plant breeding, propagation, and hybridizing; Hydroponics.

See also 57C.

98E-Animal Husbandry & Veterinary Medicine
Production and care of domestic and wild animals; Breeding, feeding, management, rearing, testing, and training; Pets; Animal pathology; Toxic effects on domestic animals; Animal quarantine; Disease resistance, control and treatment; Breeding, care, and utilization of laboratory animals.

See also 57Z.

98F-Fisheries & Aquaculture
Fishing, fishing equipment, and shipboard processing of fisheries products; Cultivation of fishes, shellfish, and algae in fresh or salt water for commercial or recreational use; Use of fish ladders and weirs; Sport fishing.

See also 47D, 48B, and 57Z.

For fish processing, use 98H.

98G-Agriculture Resource Surveys
Surveys to scan crop yields, soil moisture content, crop diseases, and forest diseases. Includes fishery surveys; Satellite and aerial surveys.

98H-Food Technology
Pasteurizing, curing, canning, dehydrating, freezing, irradiation, freeze drying, etc., of foods and other agricultural products; Sanitation and fumigation of products; Food additives and preservatives; Analysis and inspection of products; Storage, packaging, and display of products; Kitchen and cooking equipment.

For biochemical studies of foods, see also 57B.

54-Astronomy & Astrophysics

540-General

54A-Astrogeology
Studies of the structure and composition of planets and other bodies in the solar system.

For geology and geophysics, see also 48F.

54B-Astronomy & Celestial Mechanics
Positions and motions of the celestial bodies; Ephemerides, Eclipses.

54C-Astrophysics
Physical and chemical aspects of celestial bodies, their origin and evolution. Includes astronomical spectroscopy, radio astronomy, solar structure, and planetary atmospheres.

54D-Cosmic Ray Research
Detection and analysis of cosmic rays.

55-Atmospheric Sciences

550-General

55A-Aeronomy
Physics and chemistry of the upper atmosphere; Composition; Chemical reactions; Aurora; Airglow; Solar-terrestrial relationships.

For cosmic ray research, use 54D.

55B-Dynamic Meteorology
Studies of atmospheric motions; Atmospheric diffusion models; Atmospheric circulation.

For air pollution movement studies, use 68A.

55C-Meteorological Data Collection, Analysis, & Weather Forecasting
Climatology; Satellite meteorology; Weather prediction; Ice forecasting.

55D-Meteorological Instruments & Instrument Platforms
Instruments used to record meteorological parameters; Meteorological balloons; Weather stations; Sounding rockets; Remote sensors.

55E-Physical Meteorology
Acoustical, electrical, optical, and thermodynamic properties of the atmosphere; Cloud physics; Precipitation theory; Global warming.

See also 68A.

55F-Weather Modification
Change of weather conditions through artificial means; Fog dispersal; Artificial precipitation.

92-Behavior & Society

920-General

Includes general overall census studies; Political science.

92A-Job Training & Career Development

Vocational training; On-the-job training; Retraining; Vocational rehabilitation; Use and design of training simulators (including flight simulators) and equipment; Instructional aids; Professional development; Career development.

For curriculum development, use 92D.

92B-Psychology

Human behavior; Personality; Intelligence; Learning ability; Judgement; Motivation; Perception; Job satisfaction; Leadership characteristics; Psychometrics; Adaptability; Social, industrial, group, organizational, interpersonal, and experimental psychology; Clinical psychology; Physiological psychology.

For the measurement of hearing, vision, heart rate, respiration and other physiological responses as related to behavior, use 57T or 57W.

92C-Social Concerns

Sociology and sociometrics; Race relations; Age group and minority group studies; Social rehabilitation of drug abusers, alcoholics, physically, emotionally, and mentally handicapped, offenders, etc.; Cultural and economic deprivation; Social discrimination; Immigration; Demography; Social services, including child care, welfare, counseling, financial assistance, and employment and unemployment services; Attitude studies.

See also 43C, 44, and 91K.

92D-Education, Law, & Humanities

Formal education; School systems; Educational administration; Curricula; Instructional devices and materials, including audiovisual; Teaching methods; Computer-assisted instruction; Laws; Linguistics; Machine translation; Fine arts; Archaeology; History; Anthropology; Humanities; Religion.

92E-International Relations

Political and social indicators; Crises and crisis management; Conflict analysis; Foreign aid; Foreign policy and foreign affairs; International political science; Disarmament and arms control; Espionage; Includes international relationships concerning territorial seas, fishing, extradition, and natural resources.

See also 74H.

For international commerce, use 96C.

95-Biomedical Technology & Human Factors Engineering

950-General

95A-Prosthetics & Mechanical Organs

Includes materials and equipment going into human bodies, enabling them to function properly, either temporarily or permanently. Artificial limbs and limb braces; Facial prosthetics, including artificial eyes; Dental prosthetics; Mechanical organs and mechanical hearts; Circulatory assist devices; Artificial kidneys, etc.; Biocompatible materials including tissue adhesives, tissue compatible materials, and antithrombogenic materials.

For prosthodontics, use 57G.

95B-Tissue Preservation & Storage

Preservation of organs, tissue, and blood for transplantation or transfusion to living organs; Blood and tissue banks; Properties and evaluation of preserved and stored materials.

See also 57J, 57S, and 57X.

95C-Biomedical Instrumentation & Bioengineering

Includes materials and equipment used to monitor human body functions. Design, use, and performance of biomedical equipment; Biotelemetry including biotelemetry transducer and transmitter equipment; Hospital equipment and supplies; Dental materials and equipment; Equipment for physiological monitoring; Diagnostic equipment; Biomedical laboratory equipment.

See also 95A.

95D-Human Factors Engineering

Design of tools, instruments, equipment, and machinery with emphasis on optimum utilization by humans; Habitability of work and living space; Ergonomics; Interaction of man and equipment in terms of subsystem and system performance requirements and evaluation. Encompasses manual controls, tactical kinesthesis, and other human sensory modalities involved in operation of equipment and understanding of personnel subsystems; Man-machine systems. Includes anthropometric studies, protective equipment, protective clothing, and life support systems.

95E-Life Support Systems

Equipment and techniques for sustaining life in foreign environments, such as space, underground, and underwater; Closed ecological systems (includes pressure suits, diving gear, and breathing apparatus).

See also 95D.

95F-Bionics & Artificial Intelligence

Study of biological processes in order to develop engineering systems; Simulation of biological processes; Comparative studies of control systems formed by the brain and nervous system; Pattern recognition systems based on biological modes; Biological applications of information theory; Cybernetics.

95G-Protective Equipment

Equipment providing protection against such environmental elements as heat, cold, noise, machinery, and radiation.

For equipment and techniques for sustaining life in environments where normal respiration is not possible, use 95E.

89-Building Industry Technology

Includes fires in buildings.

890-General

Includes fires in buildings.

89B-Architectural Design & Environmental Engineering

Architecture; Human engineering; Site surveys; Interior design; Lighting; Heating, ventilating, and air conditioning; Heat loss studies. Includes environmental engineering equipment.

See also 97J and 94E.

89C-Construction Management & Techniques

Excavation; Fabrication (presite and onsite); Construction techniques; Reconstruction; Management including planning, manpower, and labor studies.

89D-Structural Analyses
Dynamics and statics of structures and structural members including kinetics, kinematics, vibration and stress analyses; Induced environmental stresses including earthquakes, wind, and flood; Foundation stresses; Soil-structure interactions.

89E-Building Standards & Codes
Standards and codes for buildings, equipment, components, and materials.

89G-Construction Materials, Components, & Equipment
Plumbing; Wiring; Insulation; Doors and windows; Walls; Joints; Beams; Construction equipment such as bulldozers and cranes. Includes flammability and fire studies. Cement and concrete.

See also 50C.

For cement properties, see also 71D.

89H-Building Equipment, Furnishings, & Maintenance
Equipment including security alarms (i.e. Burglar alarms), elevators, and fire safety devices; Furnishings, including major household appliances, rugs, and furniture; Maintenance, including repair, pest control, and cleaning.

For environmental engineering equipment, use 89B.

96-Business & Economics

960-General
Includes economic theory; Business and economic census studies; Insurance not covered by another subcategory; Small businesses.

96A-Domestic Commerce, Marketing, & Economics
National and state-level studies; Industrial costs and economics; Economic impact of industries; Economic impacts on industries; Industrial statistics; Agricultural economics; Productivity; Labor supply and demand; Labor costs and economics; Inflation; Economic aspects of unemployment; Employment and unemployment statistics; Wage surveys; United States commerce; Wholesale and retail trade; Domestic market surveys; Business, personal, and property taxes; Income tax data; Franchising.

See also 43B, 70D, 91J, and 98B.

For studies of individual plants or operations, see the field of application.

For economic impacts of individual plants or operations, see the field of application.

For regional development, use 43B and 91J.

96C-International Commerce, Marketing, & Economics
Foreign market surveys and research; International trade; Imports and exports; Customs and tariffs; Multinational businesses; Trends and forecasting.

For international finance, use 96F.

96D-Consumer Affairs
Consumer problems and protection; Truth in advertising; Commercial psychology; Product maintenance and reliability problems; Home appliances safety; Product comparison studies; Flammability studies; Motor vehicle recalls.

96E-Minority Enterprises
Minority owned and operated businesses; Business training of minority groups; Franchising; Equal opportunities in business.

96F-Banking & Finance
Investments; Credit; Banks and trust companies; Mortgage finance; Savings and loan associations; Security and commodity brokerage; Balance of payments; Gold and silver movement; Cash flow; Regulations; International finance.

For government financial operations, use 43A, 70F, 91G, and/or 91H.

96G-Foreign Industry Economic Development
Private and governmental industrial and economic development in foreign countries including industrialized and developing countries; International technology transfer.

For foreign market surveys and international trade, use 96C.

96H-Foreign Business & Economics
Foreign and developing countries; Businesses, economic conditions and socioeconomics.

For foreign market surveys and international trade, use 96C.

For social concerns related to economics, see also 92C.

99-Chemistry

990-General

99A-Analytical Chemistry
Techniques and instrumentation for the separation and analysis of individual compounds or specific groups or compounds, both inorganic and organic. Includes qualitative, quantitative, volumetric, gravimetric, optical, spectroscopic; electrochemical, ion exchange, chromatographic analysis; Test methods; Forensic chemistry; Data interpretation; Routine analysis or experimental results.

99B-Industrial Chemistry & Chemical Process Engineering
Techniques, processes, unit operations, and plant equipment that apply to chemical manufacturing, processing, transportation, and storage; Petroleum refining; Desalination technology; Pollution control equipment; Process control technology; Process engineering; Chemical reactors.

For coal gasification and liquefaction processes, see also 97F and 97K.

For specific environmental pollution control, see also 68.

For water purification, see also 50B and 68D.

99C-Polymer Chemistry
Synthesis, properties, reactions and theories of polymers and copolymers. Includes all types of polymerization, curing, crosslinking, reaction kinetics, etc.

For mechanical properties of polymers, use 71O and 71H.

99D-Basic & Synthetic Chemistry
Synthesis, properties, and reactions of inorganic and organic compounds; Studies of individual or specific groups of chemical elements; Molecular structure; Stereochemistry.

For chemical reaction mechanisms between atoms, ions, or molecules, see also 99F.

For spectrum analysis of compounds, use 99A and 99F.

99E-Photochemistry & Radiation Chemistry
Studies involving the interrelationships of electromagnetic or particle radiation and chemical reactions; Studies of radioactive elements and their reactions; Radiochemistry; Photochemical reactions.

See also 55A and 68A.

99F-Physical & Theoretical Chemistry

Physical chemistry; Thermodynamics; Thermochemistry; Colloids and gels; Surface chemistry; Catalysis and catalysts; Electrochemistry; Solutions; Chemical equilibria; Membranes; Reaction kinetics; Quantum mechanics; The mathematical determination of atomic or molecular orbitals, energy levels, or properties; The application of mathematics to chemical systems and electronic spectra, excluding routine analysis or experimental results; Molecular spectra interpretation; Chemical reaction mechanisms in the gas, liquid, or solid phase between atoms, ions, or molecules; Atomic and molecular energy studies; Phase studies of nonmetallic systems; Isotherms; Crystallography.

For advanced materials, use 71Gen or the field of application.

For solid state physics, use 46D.

For thermodynamics, see also 460 General.

50-Civil Engineering

500-General

50A-Highway Engineering

Construction of roads and highways; Highway and rights-of-way maintenance including weed control; Bridges and bridge systems; Highway paints and markings; Highway and road signs; Beautification; Slope stability and soil subbases.

50B-Civil Engineering

Dredging; Dams; Water purification; Reservoir engineering; Flood control; Sewers; Waterway engineering; Runway construction; Shore protection; Breakwaters; Harbor engineering; Tunneling.

See also 47.

For sewage treatment, use 68D.

For building construction, use 89.

For oil and gas reservoir engineering, use 97 or 48A.

50C-Construction Equipment, Materials, & Supplies

Excavation and earth moving equipment; Hoisting and conveying equipment; Concrete and cement.

See also 89G.

For properties of concrete and cement, see also 71D.

50D-Soil & Rock Mechanics

Physical properties of soil and rock for utilization in engineering; Landslides; Soil stabilization.

For soil sciences, use 48E.

For soil conservation, use 48B.

For geology and geophysics, use 48F.

81-Combustion, Engines, & Propellants

810-General

81A-Combustion & Ignition

Autoignition, ignition, and combustion. Includes flame studies; Combustion products studies; Ignition systems; Combustion chemistry; Flammability studies.

See also 89 and 94H.

81B-Electric & Ion Propulsion

All types of engines deriving power from free ions and electrons. Includes ion, plasma, and arc jet systems; Propulsion by means of solar wind; Laser propulsion.

For electrically propelled surface vehicles, use 85.

81C-Fuel & Propellant Tanks

Design, performance, and testing of fuel and propellant tanks including those for automobiles, petroleum products, and rocket propellants.

81D-Jet & Gas Turbine Engines

Design, performance, and testing of all types of jet and gas turbine engines, their components, engine nozzles. Includes Ramjet, Scramjet, and Turbofan engines, and hydroduct and turbomachinery as well as nonpropulsive turbines.

See also 97L and 51C.

81G-Rocket Engines & Motors

Design, performance, and testing of rocket engines and motors and their components.

81H-Rocket Propellants

Production, handling, stability, and performance of liquid, solid, thixotropic, and exotic propellants. Includes fuels, oxidizers, additives, and binders.

For combustion and ignition, use 81A.

81I-Nuclear Propulsion

Design, performance, and testing of nuclear engines for surface, air, and space propulsion.

See also 85.

81J-Reciprocation & Rotating Combustion Engines

Design, performance, and testing of reciprocating and rotating engines of various configurations for all types of propulsion. Includes internal and external combustion engines; Engine exhaust systems; Engine air systems components; Engine structures; Stirling and diesel engines.

See also 97L and 85H.

45-Communication

450-General

45A-Policies, Regulations, & Studies

Licensing; Legislation; National policies and Federal regulatory controls; Frequency management; Broadcasting standards; Time signals, etc.

45B-Radio & Television Equipment

Design and maintenance of radio and television transmitting and receiving equipment only.

See also 51E.

45C-Common Carrier & Satellite

All communication equipment except radio and television. Optical, radio, microwave, wire, and acoustic communication; Telephone, telemeter, telegraph, television, and radio communication systems; Computer network communications; Digital communication; Intercommunication systems; Optical scanning.

For information systems, see also 88B.

For design and construction of communication satellites, see also 84G.

45D-Sociopolitical

Propaganda; Social communication; Sign language, Effects of communication on society and behavior; Postal service; Mass media communication.

45E-Graphics

Publishing; Printing; Graphic arts; Reprography; Xerography; Facsimile; Desktop publishing.

45F-Verbal
Research and development in vocal communication; Speech intelligibility; Speech recognition.

45G-Communication & Information Theory
Theoretical studies relating to the measurement and transmission of information in a communication channel. Includes coding theory, information capacity, detection of signals in noise.

See also 62E.

62-Computers, Control & Information Theory

620-General
Includes computer security; Artificial intelligence; Signal processing (unapplied).

62A-Computer Hardware
Design and development of computers and peripheral equipment, including analog computers, digital computers, hybrid computers, special purpose computers, minicomputers, microcomputers; Computer accessories, supplies and installation; Logic circuits; Computer architecture; Computer network hardware.

For computer hardware applied to a specific application, see the field of application.

For Very Large Scale Integration (VLSI), use 49H.

62B-Computer Software
Computer programming; Programming languages; Compilers; Data base management systems; Software tools; Software reliability; Computer graphics.

For computer software and database development applied to a specific application, see the field of application.

For CAD/CAM, use 41A and 41B.

62C-Control Systems & Control Theory
Theoretical studies of open-loop and closed-loop control systems; Automatic control systems; Principles including adaptive, continuous, digital, distributed parameter, linear, multivariable, nonlinear, optional, predictive, and proportional; Process controllers.

See also 720 General.

For control systems applied to a specific application, see the field of application.

62D-Information Processing Standards
Standards for the use of automatic data processing equipment and systems. Includes standards for hardware, software, applications, and data; Federal Information Processing Standards (FIPS).

62E-Information Theory
Theoretical studies relating to the measurement and transmission of information in a communication channel, including coding theory, information capacity, and detection of signals in noise.

See also 45G.

62F-Pattern Recognition & Image Processing
Includes feature extraction; Image enhancement; Image restoration; Scene analysis; Character recognition; Barcoding; Computer vision.

62R-Applications Software

62S-Data Files

63-Detection & Countermeasures

630-General
Automated access control systems.

For industrial security, see also 940 General

63A-Acoustic Detection
Techniques and equipment used for the detection and tracking of objects by means of sound waves, including ultrasonic and infrasonic radiation; Sonar.

For acoustic testing, use 94.

For detection techniques applied to chemistry, meteorology, astronomy, oceanography, medicine, and manufacturing, use 99, 55, 54, 47, 57, 41, and 94, respectively.

63B-Electromagnetic & Acoustic Countermeasures
Interception, jamming, antijamming, and deception of acoustic and electromagnetic signals; Techniques to nullify the use of detection, surveillance, guidance, and communication systems; Radar jamming; Chaff; Counter-countermeasures.

See also 74.

63C-Infrared & Ultraviolet Detection
Techniques and equipment for the detection and tracking of objects by infrared and ultraviolet radiation; Infrared night vision devices; Infrared homing.

See also 76B.

For earth resource surveys, use 48C and 98G.

For mapping, use 48I.

For photography, use 82B.

For nondestructive testing, use 94J.

For detection techniques applied to chemistry, meteorology, astronomy, oceanography, medicine, and manufacturing, use 99, 55, 57, 41, and 94, respectively.

63D-Magnetic Detection
Techniques and equipment for the detection of objects by means of magnetic fields.

For geomagnetism, use 48.

63E-Nuclear Explosion Detection
Techniques and equipment for the detection of nuclear explosions at high altitude, underground, and in space. Includes the use of shock waves, earth movement, and measurement of nuclear radiation levels.

See also other applicable subcategories in 63, especially 63I.

63F-Optical Detection
Techniques and equipment for the detection by means of light. Includes the use of binoculars, periscopes, telescopes, and night vision devices for object detection, and smoke particle detectors.

See also 46C.

For detection using only infrared or ultraviolet radiation, use 63C.

For earth resources surveys, use 48C and 98G.

For photography, use 82B.

For detection techniques applied to chemistry, meteorology, astronomy, oceanography, medicine, and manufacturing, use 99, 55, 54, 47, 41, and 94, respectively.

63G-Personnel Detection
Techniques and equipment for the detection of personnel. Includes the use of acoustic, seismic, olfactory, chemical, and optical detectors; Antiintrusion devices; Motion detectors; Security devices.

For military passive defense systems, see also 74I.

63H-Radiofrequency Detection

Techniques and equipment for the detection and tracking by means of radiofrequency waves; Radar; Microwave detection.

See also 76.

For mapping, use 48I.

For detection techniques applied to meteorology, astronomy, oceanography, medicine, and manufacturing, use 55, 54, 57, 41, and 94 respectively.

63I-Seismic Detection

Techniques and equipment for the detection of objects by means of seismic waves.

For earthquake detection, use 48F.

For seismic prospecting, use 48A.

49-ELECTROTECHNOLOGY

490-General

Includes standards, measurements, and instrumentation not applied to any other subcategories.

49A-Antennas

Antennas; Antenna theory; Antenna radiation patterns; Radomes.

49B-Circuits

Circuit theory; Network analysis; Filters; Oscillators; Logic circuits; Printed circuits; Electronic modules; Commutators; Power supply circuits; Waveform generators; Analog to digital converters; Phase locked systems.

For integrated circuits, use 49H.

49C-Electromechanical Devices

Electric motors; Relays; Mechanical switches; Connectors; Circuit breakers; Electric fuses.

49D-Electron Tubes

All electron tubes except those in 49E.

49E-Optoelectronic Devices & Systems

Display systems; Phototubes; Image tubes; Cathode ray tubes; Electroluminescent panels; Light emitting diodes; Photodiodes; Phototransistors; Magnetooptics; Electrooptics; Optical detectors, including infrared and ultraviolet detectors.

See also 63C and 63F.

For solar cells, see also 97N.

For lasers, use 46C.

49F-Power & Signal Transmission Devices

Transmission lines; Electric wire and cable; Waveguides; Fiber optics transmission lines.

49G-Resistive, Capacitive, & Inductive Components

Resistors; Capacitors; Inductors; Transformers; Electromagnets; Potentiometers; Thermistors; Delay lines; Transducers; Crystal resonators. Includes miscellaneous and basic components.

49H-Semiconductor Devices

Transistors; Semiconductor diodes; Integrated circuits.

For photodiodes, phototransistors, light emitting diodes, and optical detectors, use 49E.

97-ENERGY

970-General

Includes energy source development.

97A-Reserves

Natural reserves; Fuel stockpiles; Mineral and fossil fuel deposits including coal, uranium, petroleum, natural gas, geothermal, peat, and oil shale; Water power potential; Site studies of wind power potential and solar radiation availability.

For individual mine studies, use 48A.

97B-Energy Use, Supply, & Demand

Electric power and fuel consumption and requirements; Supply and demand; Heat use, supply, and demand.

97E-Electric Power Transmission

Electric power distribution; Electric transmission lines and substations; Electric power pools; Wireless energy transmission.

97F-Fuel Conversion Processes

Methods to convert a fuel to a different chemical form including coal gasification and liquefaction; Upgrading fuels by chemical synthesis.

For petroleum refining, oil shale retorting and refining, use 97K and 99B.

For environmental studies, use 97R.

97G-Policies, Regulations & Studies

Energy conservation; Licensing; Legislation; Government policies and regulatory controls; Energy goals; Research needs; Energy management, economics, and financing; Depletion allowances and leasing policies; Rates and energy models; Energy shortages; International issues.

97I-Electric Power Production

Design and operation of electric power plants; Commercial, industrial, and residential electric power production; Site surveys; Large-scale nuclear, hydro, solar, geothermal, and fossil fuel electric power plants; Power plant boilers.

Note: usually restricted to large-scale electric power production.

For small-scale electric power production, use 97N, 97O, or 97P.

For pollution control and environmental impact, use 68 and 97R.

For some nuclear power plant studies, use 77 and 97Q. 97Q should be those that are most pertinent to the use of nuclear technology for energy production.

97J-Heating & Cooling Systems

Design and operation of space heating and cooling systems and equipment; Furnace and boiler studies when related to energy conservation and energy use; Cooling towers; MIUS technology; Total energy systems.

See also 97N.

97K-Fuels

Production, performance, properties, storage, prices, and transportation of all types of solid, liquid, and gaseous fuels; Chemical composition of fuels; Fuel compatibility; Hydrogen production; Refuse derived fuels; Fuel desulfurization; Oil shale retorting; Petroleum refining; Fuel additives; Growing plants for fuels; Bioconversion and biomass plantations.

See also 48D and 97N.

For fuel tanks, use 81C.

For nuclear fuels, use 77I.

For fuel conversion, use 97F.

For rocket fuels, use 81H.

For supply and demand, use 97B.

For oil and gas drilling and recovery, coal mining and other energy related mining studies, use 48A.

97L-Engine Studies (Energy Related)

Operation and design of engines when related to energy conservation and energy use. Covers turbine, rotary, and reciprocating engines.

See also 81.

97M-Batteries & Components

Electrochemical batteries of all types including alkaline cells, dry cells, metal-air batteries, primary cells, reserve batteries, storage batteries, thermal batteries, wet cells; Battery containers, depolarizers, electrodes, electrolytes, separators, and other components and materials; Battery chargers and testers; Battery electrochemistry.

For thermoelectric and thermionic batteries, use 97O.

97N-Solar Energy

Solar collectors, concentrators, and absorbers; Solar cells; Solar cookers, dryers, furnaces, generators; Solar heat engines; Solar heating and cooling systems; Solar power plants; Solar stills; Solar water heaters; Solar heat storage systems; Solar water pumps; Solar sea power plants; Orbital solar power plants; Optical coatings and filters for solar devices; Solar energy policies, use, supply, trends, and economics.

97O-Miscellaneous Energy Conversion & Storage

Fuel cells; Magnetohydrodynamics; Experimental electric generators; Turbogenerators; Heat storage; Compressed air energy storage; Mechanical conversion; Thermoelectric and thermionic conversion; Photovoltaic conversion (excludes solar cells); Wind power; Tidal power; Nuclear fusion power plants.

For commercial, industrial, and residential use of energy conversion and storage devices, use 97I or 97J.

97P-Geothermal Energy

Geothermal exploration and prospecting methods and equipment; Geothermal resources; Geothermal energy conversion; Geology applied to geothermal systems; Drilling; Reservoirs; Extraction; Site selection; Geothermal power plants; Corrosion studies; Materials used in geothermal systems.

97Q-Selected Studies In Nuclear Technology

Reports assigned to this subcategory are selected for their broad interest to users in the nuclear energy field.

For other nuclear energy subcategories, use 77.

97R-Environmental Studies

Air, noise, water, and solid waste pollution and pollution control from energy resource development, fuel production, energy production, and energy use; Environmental impacts of energy production and use.

See also 68.

68-Environmental Pollution & Control

680-General

Any study covering multiple types of pollution. Includes broad pollution studies, such as life-cycle analysis of wastes.

68A-Air Pollution & Control

Air pollution from flue gases, exhaust gases, odors, dust, smog, microorganisms, etc.; Control techniques and equipment; Sampling and analytical techniques, and equipment; Waste gas recovery; Biological and ecological effects; Air pollution chemistry; Acid precipitation; Atmospheric motion; Laws, legislation, and regulations; Public administration; Economics; Land use.

See also 43F, 91A, 57, 85, 81, 99A, 99B, and 97R.

For effects on human health, use 68G.

For pesticides and radioactive contaminants, use 68E and 68F respectively.

68B-Noise Pollution & Control

Pollution in the environment by noise from any source including engine noise, traffic and transportation noise, machinery noise, industrial noise, urban noise, sonic boom; Theory and devices for control; Biological and ecological effects; Noise detection; Building technology; Laws, legislation, and regulations; Public administration; Land use.

See also 41I, 43F, 91A, 46A, 57, 85, 89, 94D, and 97R.

For effects on human health, use 68G.

68C-Solid Wastes Pollution & Control

Pollution by solid wastes including garbage, scrap, junked automobiles, spoil, sludge, containers; Disposal methods such as composts or land application, injection wells, incineration, sanitary landfills; Mining wastes; Processing for separation and materials recovery; Solid waste utilization; Recycling; Biological and ecological effects; Superfund (Records of Decision, etc.); SITE technology; Laws, legislation, and regulations; Public administration; Economics; Land use. Includes disposal of concentrated or pure liquids such as brines, oils, chemicals, and hazardous materials.

See also 43F, 91A, 57, 99B, and 97R.

For effects on human health, use 68G.

For the disposal of pesticides and radioactive contaminants, use 68E and 68F.

For the controlled disposal of radioactive wastes from nuclear reactors, use 77G.

68D-Water Pollution & Control

Pollution by municipal wastes, agricultural wastes, industrial wastes, mine wastes, radioactive contaminants; Chemistry and analysis of pollutants; Thermal pollution; Oil pollution; Control techniques and equipment; Sewage treatment; Industrial waste water pretreatment; Hydrology and limnology; Biological and ecological effects; Waste water reuse; Laws, legislation, and regulations; Public administration; Economics; Land use.

See also 43F, 91A, 47, 48G, 57, 97R, 98, 99A, and 99B.

For effects on human health, use 68G.

For pollution by pesticides and radioactive contaminants, use 68E and 68F respectively.

For the design and construction of sewers, and drinking water treatment, use 50B.

68E-Pesticides Pollution & Control

Pollution by insecticides, herbicides, fungicides, rodenticides; Residues; Decomposition studies; Analysis and detection; Soil chemistry and biology; Adverse biological effects; Ecology; Laws, legislation, and regulations; Public administration; Economics.

See also 57, 68A, 68C, 68D, 43F, 91A, 98, and 99A.

For effects on human health, use 68G.

68F-Radiation Pollution & Control

Involves pollution of the environment by particle and electromagnetic radiation from natural and synthetic sources, including neutrons, X-rays, ultraviolet radiation, microwaves, alpha particles; Radon; Sampling and analytical techniques; Fallout; Biological and ecological effects; Laws, legislation, and regulations; Public administration; Economics.

See also 57, 68A, 68C, 68D, 91A, 97R.

For effects on human health, use 68G.

For the controlled disposal of radioactive wastes from nuclear reactors, use 77G.

68G-Environmental Health & Safety

Effects of pollution on public health and safety; Toxicology; Industrial health; Physiology; Psychology; Clinical medicine; Radiobiology; Animals used as research experimental models.

See also 41I, 57, 44G, 68A, 68B, 68C, 68D, 91A, 43F, 94D, and 97R.

68H-Environmental Impact Statements

Only actual draft and final statements are posted in this subcategory. Environmental impact statements describing national effects are posted here and to other appropriate subcategories.

For studies about environmental impact statements, use 680 General.

90-Government Inventions for Licensing

For patents and patent applications only (will be labeled as such in the report title); Not for bibliographies.

900-General

Computer software.

90A-Mechanical Devices & Equipment

Devices and equipment for fuel ignition; Heating, illumination, and refrigeration; Cleaning; Printing; Product handling and transportation; Sprinklers; Fire extinguishers; Safety; Motor and other land vehicles; Earthworking and excavating; Tools; Jacks; Hydraulic and pneumatic systems; Power transmissions; Couplings, fasteners, and joints; Piping; Drilling and mining; Separators; Locks; Sewing machines; Winding and reeling; etc.

For metal shaping and forming, use 90E.

For medical equipment, use 90D.

90B-Chemistry

Organic and inorganic compounds; Batteries; Electrochemistry; Hydrocarbons; Lubricating compositions; Propellents and rocket fuels; Acids; Polymers; Plastics; Inks; Bleaching; Dyeing; Fertilizers; Food fermentation; Sugar and starch; Paper making; Textiles; Paints; Coatings (except metal coatings); Chemical reactors; etc.

90C-Nuclear Technology

Reactors; Radioactive materials; Nuclear instrumentation; Nuclear radiation safety; Nuclear power plants and reactor engineering; Nuclear fusion; Particle accelerators; Plasma devices; etc.

90D-Biology & Medicine

Drugs; Cosmetics; Prosthetics; Medical equipment; Pesticide biology; Biological laboratory equipment; Life support equipment.

90E-Metallurgy

Metal stock; Metal coatings; Molding, shaping, and treating processes; Laminating; Glasses; Material shaping; Sheet metal and wire working; Bonding and joining; Cutlery; etc.

For use of mechanical equipment, use 90A.

90F-Electrotechnology

Antennas, circuits, and electromechanical devices; Electron tubes; Optoelectronic devices; Power and signal transmission devices; Resistive, capacitive and inductive components; Semiconductor devices; Information transmission, storage, and retrieval; Communications; etc.

90G-Instruments

Photographic equipment; Measuring and testing instruments and equipments; Acoustic devices; Etc.

For nuclear instruments, use 90C.

90H-Optics & Lasers

Optical materials, components, equipment, and systems; Infrared, visible, ultraviolet, and X-ray lasers; Masers.

90I-Ordnance

Production and performance of projectiles, fuzes, explosive materials, pyrotechnics, and weapon systems (not limited to military applications); Ordnance storage systems; Fire control systems; Weapons delivery systems; Missiles, rockets, and propellants directly related thereto; Weapons carriers (tanks, aircraft ships, etc); Guns; Laser weapons; Bombs.

90J-Food Technology

Pasteurizing, curing, canning, dehydrating, freezing, irradiation, freeze drying, etc., of foods and other agricultural products; Sanitation and fumigation of products; Food additives and preservatives; Analysis and inspection of products; Storage, packaging, and display of products; Cooking devices.

For food fermentation, use 90B.

44-Health Care

440-General

44A-Planning Methodology

Health planning theory including methods, tactics, techniques and policies; Evaluation of planning theories and processes.

44B-Agency Administrative & Financial Management

Management practices and policies regarding technical assistance, evaluation of health care agency activities, public relations; Financial management and accounting methods.

44C-Community & Population Characteristics

Data and numerical information including health status, quality of care, malpractice, health care needs/demands; Health care utilization, health care cost, vital statistics; Demographic information, economic, environmental, nutritional, and societal factors affecting health, and health resource distribution.

44D-Health Care Assessment & Quality Assurance

Financial feasibility review, economic impact review, and project review; Certificate of need theory; Health manpower education institutional accreditation; Judicatory procedures, review, and assessment; Quality assurance theory; Certificatory methodology; Health manpower proficiency testing, and public health education evaluation; Classification of health care facilities and health care personnel.

44E-Health Care Measurement Methodology

Measurement of health status, quality of care, health facility supply, health manpower supply, proficiency and productivity, and health care costs; Health care needs/demands and utilization measurement.

See also 44L, 44N, and 44Q.

44F-Health Care Forecasting Methodology

Projecting health care needs/demands and health care utilization; Health care facility supply; Health manpower supply; Health care costs; Home health care; Cross-impact projections.

44G-Environmental & Occupational Factors

Environmental factors affecting health including housing, sanitation, water pollution, solid waste pollution, noise pollution, disease vectors, safety hazards, and occupational and industrial hazards; Overpopulation; Health facility environmental considerations and environmental impact; Energy sources in the health field.

See also 57U and 68G.

44H-Health Care Technology

Descriptions and applications of new health care technology and equipment; Ailment prevention techniques, and technology regarding diagnosis, therapy, rehabilitation, and food and nutrition; Health care equipment and facility design and performance considerations.

See also 57 and 95.

44J-Health Delivery Plans, Projects & Studies

Plans, projects, and studies related to the institutional delivery of health services including state/local health plans, state/local medical facility plans, plans for specific health services, and health delivery feasibility studies.

44K-Health Services

Personal and public health services, patient care, and maintenance of an individual's health status including hospital services acute in-patient services, long-term inpatient services, nursing home services, emergency services, public health services, mental services, nursing services, dental services, and medically-related social services including institution discharge services.

44L-Health Care Needs & Demands

Measurement of health care needs/demands, hospital care, acute in-patient care, long-term in patient care, nursing home care, medical care, mental care, nursing care, dental care, and health insurance; Home health care; Measurements of health manpower requirements/demands.

See also 44E.

44M-Health Resources

Surveys, reports, and studies related to specific health care resources including manpower, facilities, sources of financing, and government and private health-related organizations, agencies and individuals.

44N-Health Care Utilization

Measurements regarding utilization of health resources including manpower, ambulatory care, emergency care, public health care, medical care, mental care, nursing care, dental care, health insurance, health care facilities, and home health care.

See also 44E and 44L.

44P-Health Education & Manpower Training

Health manpower education including curricula and costs; Health manpower education facility needs/demands; Institutional financing; Financing for health related educational institutions; Student recruiting and retention methods; Continuing education; Career guidance and career advancement; Consumer health education and public health education methods.

44Q-Health-Related Costs

Health care costs, indexes, projections, in-patient care costs, acute in-patient care costs, long-term care costs, nursing home care costs, ambulatory care costs, emergency care costs, public health care costs, medical care costs; Insurance costs; Manpower income; Equipment costs; Facility utilization and construction costs; Ailment costs including preventive medicine costs and injury costs; Transportation costs including emergency transportation costs.

44R-Economics & Sociology

Discussions of economic and sociological factors and theories relevant to health care.

44S-Legislation & Regulations

Laws, bills, regulations, and model legislation. Includes certificate of need, health insurance certification, health manpower licensing, health facility licensing, health manpower employment, and support regarding health manpower education.

44T-Data & Information Systems

Techniques regarding information systems including document sources, acquisition, surrogation, and storage; Information retrieval; Data systems, Data gathering; Data processing; Data processing hardware; Information system feasibility studies, and confidentiality of information.

44U-Health Care Delivery Organization & Administration

Hospital and medical practice administration and management; Organizational structure of health services; Management policies and practices regarding personnel, community participation and relations, and coordination with other agencies; Financial management and accounting methods; Financing of health delivery and facilities; Reporting methods and requirements.

94-Industrial & Mechanical Engineering

940-General

Includes bearings; Mechanical elements; Pipes; Tubes; Levers; Cams; Springs; Mechanical joints; Containers and packing materials; Refrigeration systems and equipment; Industrial furnaces and boilers; Heat exchangers; Heat pumps; Heat pipes; Industrial security; Metrology.

For rocket engine components, use 81G.

For fuel tanks, use 81C.

For cooling towers, use 97J.

For nuclear security, use 77Gen.

94A-Production Planning & Process Controls

Materials control; Numerical control and automation; Time and motion studies ; Scheduling; Production controls and programming; Modeling techniques and program controls; Inventory management.

See also 44A, 41A and 41B.

94B-Quality Control & Reliability

Tolerances allocations; Maintainability requirements; Probability of satisfactory performance of components and equipment; Inspection methods; Destructive industrial testing; Reliability theory; Quality assurance.

See also 41E and 41G.

94C-Plant Design & Maintenance

Site selection; Plant design; Layout; Maintenance management; Scheduled, routine, and corrective maintenance.

See also 41H.

94D-Job Environment

Industrial hygiene and occupational diseases and injuries in settings such as factories, and office and commercial buildings; Industrial psychology; Industrial sociology; Workplace layout and design; Worker interactions.

See also 44G, 57U, 41I, and 92B.

For industrial safety engineering and accident prevention, use 94H.

94E-Environmental Engineering

Lighting; Heating; Ventilating; Air conditioning. Includes environmental engineering equipment related to industrial use. Excludes pollution control.

See also 41I, 89B and 97J.

94F-Tooling, Machinery, & Tools

Machine subassemblies; Robots; Robotics; Tools; Machinery, including hoists, conveyors and pumps.

See also 41C and 41J.

94G-Manufacturing Processes & Materials Handling

Fabrication, assembling, cleaning, and finishing; Industrial and manufacturing processes (limited to in-depth studies that directly discuss specific processes); Bonding and joining, including gluing, welding, soldering, and brazing; Materials forming and machining; Heat treatment; Coating processes; Materials handling, including palletizing, conveying, warehousing, storing, containerization, and packaging.

See also 71, 41B, 41E, and 41F.

For processing and packaging of food, use 98H.

For production of materials, use 71.

For chemical engineering and processing, use 99B.

For the beneficiation and processing of minerals, use 48A.

94H-Industrial Safety Engineering

Accident prevention; Safety measures; Fire prevention; Warning systems; Safety equipment, structures, and clothing.

For industrial safety engineering applied to a specific application, use the field of application.

94I-Hydraulic & Pneumatic Equipment

Design, production, performance, and testing of hydraulic and pneumatic systems, accumulators, actuators, compressors, and distribution equipment; Fluidic and flueric devices.

See also 41J.

For hydraulic fluids, see 71K.

94J-Nondestructive Testing

Nondestructive testing having industrial application; Ultrasonic, radiographic, hydrostatic, magnetic, and optical nondestructive techniques and equipment; Nondestructive testing of flaws, thickness, opacity, strength.

For destructive industrial testing, use 94B.

94K-Laboratory & Test Facility Design & Operation

Measuring, testing, and simulation devices. Includes laboratories, test facilities, and test equipment measuring testing and simulation. If the test facility, equipment, etc. is applied to a specific application, use the field of application.

88-Library & Information Sciences

880-General

Includes general studies about microforms; Film readers; Copyrights; Privacy Act; Report writing.

88A-Operations & Planning

Acquisitions, classification, cataloging, abstracting, and indexing; Circulation and reference systems; Information services; Interlibrary loans; Distribution; Manual and computerized information retrieval; Individual libraries and information center.

For library or information networks, use 88B.

88B-Information Systems

Library and information networks; Operations and planning of these systems; File maintenance and management; Database management; Information superhighway, National Information Infrastructure; Applied information systems (Management, medical, transportation, etc.)

See also 44T, 62, and 70C.

For database management, use 62B.

For communications and computer networks, use 45C.

For geographic information systems, see 48I.

88C-Marketing & User Services

User needs, surveys; Promotions; Fees.

88D-Personnel

Training and education; Selection; Management; Performance; Schools and accreditation.

See also 70D.

88E-Reference Materials

Bibliographies; Directories; Glossaries; Catalogs; Thesauri; Indexes; Abstract and title periodicals.

41-Manufacturing Technology

410-General*

Includes mechanical elements; Pipes; Tubes; Levers; Cams; Springs; Clutches; Gears; Valves; Filters; Containers and packing materials; Refrigeration systems and equipment; Industrial furnaces and boilers; Heat exchangers; Heat pumps; Heat pipes; Energy management, economics, and financing; International issues.

See also 94O and 97G.

For engine components, use 81.

For fuel tanks, use 81C.

For cooling towers, use 97J.

41A-Computer Aided Design (CAD)

Application of computer hardware and software (programs) to enhance the design, computations, simulation, analysis and modeling, presentations, graphics, drafting, data base creation and human-machine interface, associated with the creation of engineering design specifications.

See also 94A.

41B-Computer Aided Manufacturing (CAM)

Application of computer hardware and software (programs) to enhance materials planning, processing and handling, tooling; Assembly; Quality and reliability control; Inspection; Tests; Scheduling and control; Facilities and equipment maintenance; Group technology applications; Inventory control (raw material, in process and finished); Numerical controls and automation; The creation of Direct Numerical Control (DNC) and Computer Numerical Control (CNC) manufacturing cells and systems.

See also 94A and 94G.

41C-Robotics/Robots

Application of computer hardware and software, controls, sensors, electromechanical and hydro-mechanical devices, to the creation of robots and the application of robots to all facets of manufacturing. Study of biological processes in order to develop engineering systems; Pattern recognition systems based on biological models. Includes feature extraction; Image enhancement; Image restoration; Scene analysis; Character recognition.

See also 95F and 62F.

41D-Productivity

Productivity of employees, management, and services; Improving quality of worklife; Measurement of productivity efficiency and effectiveness; Employee attitudes and motivation; Manpower utilization and performance improvement, job satisfaction, job security; Labor-management, job redesign; Alternative work schedules; Incentive plans; Productivity barriers including regulation, obsolete practices; Paperwork, and financing methods.

See also 70G and 70D.

41E-Manufacturing, Planning, Processing & Control

Fabrication, assembling, cleaning, and finishing; Industrial and manufacturing processes (limited to in-depth studies that directly discuss specific processes); Materials forming and machining; Heat treatment; Fabrication and manufacturing; Layout; Coating processes; Materials handling and control, including palletizing, conveying, warehousing, storing, containerization, and packaging; Time and motion studies; Scheduling; Production controls and programming; Modeling techniques and program controls; Inventory management.

See also 94A.

For the beneficiation and processing of minerals, use 48A.

For chemical engineering and processing, use 99B.

For computer-aided manufacturing, use 41B and 94G.

For lasers used in manufacturing, use 41M.

For processing and packaging of food, use 98H.

For production of materials, use 71.

41F-Joining

Bonding and joining including gluing, welding, soldering, brazing, and fastening; Joints and fasteners; Physical, mechanical, and structural properties of adhesives, sealants, glue, binders, seals, and gaskets.

See also 94G, 940 General, and 71B.

41G-Quality Control & Reliability

Tolerance allocation; Maintainability requirements; Probability of satisfactory performance of components and equipment; Inspection methods; Reliability theory; Quality assurance; Nondestructive testing having industrial application; Ultrasonic, radiographic, hydrostatic, magnetic, and optical nondestructive techniques and equipment; Nondestructive testing of flaws, thickness, opacity, strength; Destructive industrial testing; Metrology.

See also 94B, 94J, and 940 General.

41H-Plant Design & Maintenance

Site selection; Plant design; Maintenance Management; Scheduled, routine, and corrective maintenance; Security.

See also 94C.

41I-Job Environment

Industrial hygiene and occupational safety and health. See also 57U, 68G, and 44G. Workplace layout and design; Human factors engineering; Includes Industrial psychology and Industrial sociology; Worker interactions.

See also 94D and 95D.

Includes environmental engineering equipment related to industrial use. See also 97J, 89B, and 94E.

For mine safety, use 48A.

For ordnance safety, use 79A.

For nuclear radiation safety, use 77.

For transportation safety, use 85D.

41J-Tooling, Machinery, & Tools

Machine subassemblies; Tools; Machinery including hoists, conveyors, and pumps; Design, production performance, and testing of hydraulic and pneumatic systems, accumulators, actuators, compressors and distribution equipment; Fluidic and flueric devices; Ergonomics interaction of man and equipment in terms of subsystem and system performance requirements and evaluation; Man-machine systems and human factors engineering.

See also 94F, 94I, 94D, and 95D.

For hydraulic fluids, use 71K.

41K-Engineering Materials

Performance; Properties, fabrication and manufacturing methods of ceramics, coatings and composite materials including ceramic coatings, ceramic fibers, corrosion resistant coatings, reinforced plastics, graphite or carbon composites, laminates; Metal matrix composites, and fiber and particulate composites.

See also 71B, 71D, and 71F.

41L-Tribology

Friction, lubrication and wear, including bearings; Unwanted chemical reaction effects on metals, corrosion of metals and corrosion resistant coatings; Lubricants.

See also 71L, 71G, and 71K.

41M-Optics & Lasers

Design and performance of optical equipment for use in manufacturing applications. Includes laser applications such as laser annealing, cutting, drilling, and welding.

See also 46C.

41N-Computer Software

Computer programming; Programming languages; Compilers; Data base management systems; CAD/CAM robotics.

See also 62B.

41O-Domestic Commerce, Marketing, & Economics

Economic impacts on industries; Productivity; Wage surveys; Domestic market surveys.

See also 96A.

41P-Research Program Administration & Technology Transfer

Research needs; Technology transfer and forecasting.

See also 70E.

71-Materials Sciences

71O-General

Advanced materials.

See also 41K.

71A-Ablative Materials & Ablation

Physical, mechanical, and structural properties; Performance; Fabrication and manufacturing methods; Equipment directly related to processing; Ablation processes and chemistry; Reentry vehicle heat shields.

For production planning, use 41 and 94.

71B-Adhesives & Sealants

Adhesives; Glues; Binders; Sealants; Seals; Gaskets; Physical, mechanical, and structural properties; Performance; Fabrication and manufacturing; Equipment directly related to processing.

See also 71L and 94G.

For concrete cements, use 50C and 89G.

For propellant binders, use 79A and 81H.

For pollution studies, use 68.

For industry economics and marketing, use 96.

For production planning, use 41 and 94.

71C-Carbon & Graphite

Carbon and graphite fibers and textiles; Charcoal; Carbon black; Carbon and graphite coatings; Industrial diamonds; Physical, mechanical, and structural properties; Performance, fabrication and manufacturing methods; Equipment directly related to processing.

See also 71A, 71E, 71F, 71I, 71L, and 94G.

For carbon and graphite composites, use 71F.

For pollution studies, use 68.

For industry economics and marketing, use 96.

For production planning, use 41 and 94.

71D-Ceramics, Refractories, & Glass

Glasses; Brick; Porcelain; Ceramic coatings; Ceramic fibers; Physical, mechanical, and structural properties; Performance; Fabrication and manufacturing; Equipment directly related to processing; Studies of individual structural members; Cement properties.

See also 71E, 71I, 71L, and 94G.

For concrete and cement used as building materials, use 50C and 89G.

For pollution studies, use 68.

For industry economics and marketing, use 96.

For production planning, use 41 and 94.

71E-Coatings, Colorants, & Finishes

Paints and primers; Varnishes; Corrosion resistant coatings; Coating pigments; Carbon, ceramic, plastic, rubber and metal coatings; Physical, mechanical and structural properties; Performance; Fabrication and manufacturing methods; Equipment directly related to processing; Electroplating; Electrodeposition; Flame and plasma spraying; Vapor deposition.

See also 71G, 71L, and 94G.

For surface treatment not involved with coatings, use 94G.

For dielectric and semiconducting films, use 46 and 49.

For industry economics and marketing, use 96.

For production planning, use 41 and 94.

71F-Composite Materials

Materials composed of two or more physically distinct constituents; Reinforced plastics, graphite or carbon composites; Laminates; Metal matrix composites; Fiber and particulate composites; Physical, mechanical, and structural properties; Performance; Fabrication and manufacturing methods; Equipment directly related to processing; Studies of individual structural members.

See also 71L and 94G.

For wood composites, use 71R.

For concrete and reinforced concrete, use 50C and 89G.

For pollution studies, use 68.

For industry economics and marketing, use 96.

For production planning, use 41 and 94.

71G-Corrosion & Corrosion Inhibition

Unwanted chemical reaction effects on metals; Corrosion of metals; Rusting; Corrosion inhibitors; Corrosion resistant coatings; Corrosion electrochemistry.

See also 71E and 71L.

For concrete corrosion, use 50C and 89G.

71H-Elastomers

Rubbers; Additives; Curing agents; Elastomer polymerization; Physical, chemical, mechanical, and structural properties; Performance; Fabrication and manufacturing methods; Equipment directly related to processing; Studies of individual structural members.

See also 71E, 71I, 71L, 94G, and 99C.

For pollution studies, use 68.

For industry economics and marketing, use 96.

For production planning, use 41 and 94.

71I-Fibers & Textiles

Glass, carbon, ceramic, metal, and polymeric fibers; Threads, yarns, textile, and fiber finishing, including dyeing and sizing; Physical, chemical, mechanical, and structural properties; Performance; Fabrication and manufacturing methods; Equipment directly related to processing; Studies of individual structural members; Flame resistance.

See also 71L and 94G.

For fiber composites, use 71F.

For pollution studies, use 68.

For industry economics and marketing, use 96.

For production planning, use 41 and 94.

71J-Iron & Iron Alloys

Includes steels or alloys containing more than 50% iron. Coatings; Fibers; Extractive metallurgy; Refining; Embrittlement; Physical, mechanical, and structural properties; Microstructure; Phase studies; Performance; Fabrication and manufacturing methods; Equipment directly related to processing; Studies of individual structural members.

See also 71E, 71I, and 71L.

For corrosion, use 71G.

For beneficiation, use 48A.

For pollution studies, use 68.

For industry economics and marketing, use 96.

For production planning, use 41 and 94.

71K-Lubricants & Hydraulic Fluids

Solid and liquid lubricants; Additives; Greases; Drilling fluids; Brake fluids; Physical, chemical, mechanical and structural properties; Performance; Manufacturing; Equipment directly related to processing; Chemical synthesis.

See also 71L and 41L.

For pollution studies, use 68.

For industry economics and marketing, use 96.

For production planning, use 41 and 94.

71L-Materials Degradation & Fouling

Aging; Erosion and cavitation erosion; Wear; Weathering; Decay; Effects of radiation on materials; Biodeterioration, including fungus deterioration.

See also 71C, 71D, 71F, 71H, 71I, 71J, 71K, 71N, and 71R.

For nuclear reactor materials degradation, see also 77I or 77J. If concerned with nuclear propulsion, use 81I.

71M-Miscellaneous Materials

Materials not included in another group, including leather, fur, refrigerants, and waxes; Physical, mechanical, and structural properties; Performance; Fabrication and manufacturing methods; Equipment directly related to processing; Studies of individual structural members.

See also 94G.

For pollution studies, use 68.

For industry economics and marketing, use 96.

For production planning, use 41 and 94.

71N-Nonferrous Metals & Alloys

Includes studies not specifying the type of metal. Coatings; Fibers; Extractive metallurgy; Refining; Embrittlement; Physical, mechanical, and structural properties; Microstructure; Phase studies; Performance; Fabrication and manufacturing methods; Equipment directly related to processing; studies of individual structural members.

See also 71E, 71I, and 71L.

For metal fabrication, use 94G.

For corrosion, use 71G.

For beneficiation, use 48A.

For pollution studies, use 68.

For industry economics and marketing, use 96.

For production planning, use 41 and 94.

71O-Plastics

Additives; Curing agents; Plastic coatings; Plastic polymerization; Physical, chemical, mechanical, and structural properties; Performance; Fabrication and manufacturing methods; Equipment directly related to processing; Studies of individual structural members.

See also 71E, 71L, 94G, and 99C.

For plastic composites, use 71F.

For polymeric fibers, use 71I.

For pollution studies, use 68.

For industry economics and marketing, use 96.

For production planning, use 41 and 94.

71P-Refractory Metals & Alloys

Includes only the following metals and alloys having more than 50% of these metals: iridium, molybdenum, niobium (columbium), osmium, rhenium, tantalum, and tungsten. Coatings; Fibers; Extractive metallurgy; Refining; Embrittlement; Physical, mechanical, and structural properties; Microstructure; Phase studies; Performance; Fabrication and manufacturing methods; Equipment directly related to processing; Studies of individual structural members.

See also 71E, 71I, and 71L.

For metal fabrication, use 94G.

For corrosion, use 71G.

For beneficiation, use 48A.

For pollution studies, use 68.

For industry economics and marketing, use 96.

For production planning, use 41 and 94.

71Q-Solvents, Cleaners, & Abrasives

Cleaning compositions; Solvents; Detergents; Soaps and abrasives; Cleaning action of these materials; Physical and chemical properties; Performance; Manufacturing; Equipment directly related to processing.

For cleaning techniques, use 94G.

For pollution studies, use 68.

For industry economics and marketing, use 96.

For production planning, use 41 and 94.

71R-Wood & Paper Products

Sawing and milling; Lumbering; Plywood, particle and fiber board; Wood product fabrication; Pulping, papermaking, and conversion processes; Physical, chemical, mechanical, and structural properties; Performance; Fabrication and manufacturing methods; Equipment directly related to processing; Studies of individual structural members.

See also 94G.

For forestry and tree production, use 48D.

For pollution studies, use 68.

For industry economics and marketing, use 96.

For production planning, use 41 and 94.

72-Mathematical Sciences

720-General

72B-Algebra, Analysis, Geometry, & Mathematical Logic

Algebra and number theory, including field theory (algebra), group theory, ring theory; Analysis, including calculus of variations, complex variables, differential equations, Fourier analysis, functional analysis, functions (mathematics), measure, and integration; Geometry, tensor analysis, and topology; Mathematical logic, including foundations of mathematics, lattices (mathematics), metamathematics, and set theory.

For applications of mathematics, see the appropriate category of application.

72E-Operations Research

Game theory; Queueing theory; Management games; Mathematical models; Mathematical programming, Network flows; Search theory.

See also Managerial practice, 70B.

For operations research applied to a specific application, see the field of application.

72F-Statistical Analysis

Analysis of variance; Correlations techniques; Discriminate analysis; Distribution theory; Experimental design; Factor analysis; Nonparametric statistics; Probability theory; Regression analysis; Statistical decision theory; Statistical inference; Statistical tests; Stochastic processes.

For statistical analysis applied to a specific application, see the field of application.

57-Medicine & Biology

570-General

57A-Anatomy

Descriptive and comparative anatomy of humans; Anthropometry; Dissection; Neuroanatomy; Morphology.

For plant anatomy, use 57C.

For animal anatomy, use 57Z.

57B-Biochemistry

Studies of the chemical processes which take place in biological systems. Identification and measurement of biochemical substances and methods of analysis, including assaying.

See also 57F, 57L, 57Q, and 99A.

For measurement of biochemical substances for clinical diagnoses, use 57D.

57C-Botany

Study of macroscopic and microscopic plants; Plant anatomy, physiology, pathology, and taxonomy; Phytotoxicity; Includes algae and diatoms.

See also 57H, 57K, 57Y, and 98D.

57D-Clinical Chemistry

Techniques and instrumentation for chemical analysis of body fluids, including blood, and tissues for clinical diagnoses.

See also 99A.

57E-Clinical Medicine

Prevention, diagnosis, and therapy of diseases; Nuclear medicine; Experimental medicine; Clinical protocols.

See also 57J, 57O, and 57X.

For veterinary medicine, use 98E.

For health care services, use 44.

For epidemiology and disease control, use 57U.

57F-Cytology, Genetics, & Molecular Biology

Origin, structure, and functions of living cells and cell components; Hereditary diseases; Use of chemistry and physics to study biological phenomena on the molecular level; Structure and function of biological macromolecules, e.g. proteins and nucleic acids.

See also 57B.

57G-Dentistry

Prevention, diagnosis, and treatment of diseases of the teeth, oral cavity, and associated parts; Oral hygiene.

For dental materials and equipment, use 95C.

For dental prosthetics, use 95A.

For dental services, use 44.

57H-Ecology

Interrelationships of organisms and their environment; Animal, plant, and human ecology; Marine, fresh water, and terrestrial ecology; Ecosystems; Adaptation; Acclimatization; Natural selection; Species diversity; Food chains; Energy balance; Ecological succession; Effects of polluted environments on organisms; Biological productivity.

See also 47D, 48B, 48G, 57C, 57Y, 57Z, 68, 98D, and 98B.

For effects of extreme environments or stimuli on humans, use 57W.

For the interrelationships of humans and their social environments, use 92.

For the effects of industrial environments on humans, use 57U.

57I-Electrophysiology

Electrical activity associated with living organisms and life processes; Electrophysiologic recording including electrocardiography, electroencephalography, and electromyography; Neural transmission; Intracellular potential; Bioelectricity; Bioluminescence; Responses of organisms to electrical stimulation.

57J-Immunology

Mechanisms of immune responses; Antigens and antibodies; Vaccines; Immune serums; Immunization; Immunopathology; Immunohematology; Immunochemistry; Serology; Immunity; Allergy; Histocompatibility; Autoimmune diseases. HIV/AIDS.

See also 57E and 57K.

57K-Microbiology

Studies of microscopic plants and animals; Vaccine and interferon production; Microbial metabolism and biochemistry.

For diagnosis and therapy of infectious diseases, use 57E.

For disease control and epidemiology, use 57U.

For biotechnology applications, see also field of application.

57L-Nutrition

Processes by which humans assimilate and utilize food substances; Experimental nutrition; Nutritive value of foods; Malnutrition; Diet; Food habits; Nutrition surveys; Nutritional requirements; Clinical nutrition.

For food processing, use 98H.

For animal nutrition related to animal husbandry, veterinary medicine or zoology, use 98E or 57Z.

57M-Occupational Therapy, Physical Therapy, & Rehabilitation

Restoration of normal form and function after injury or physical illness; Occupational therapy; Physical therapy; Vocational rehabilitation.

See also 44K, 92A, 95A.

For mental rehabilitation, use 57T.

For social rehabilitation, use 92C and 91K.

For rehabilitation centers, use 44K.

57N-Parasitology

Parasites and parasitism; Host-parasite interactions; Vectors of parasites; Parasitic diseases; Life cycles of parasites.

See also 57H, 57K, and 57P.

57O-Pathology

Studies of the structural and functional changes in tissues and organs which cause or are caused by diseases, trauma or injuries; Gross pathology; Histopathology; Cytopathology; Pathophysiology; Comparative and experimental pathology; Histological techniques; Autopsy.

For plant diseases, use 98D.

For animal diseases, use 98E.

For diagnosis and treatment of diseases, use 57E.

For immunopathology, use 57J.

57P-Pest Control

Agents and methods for the control of plant and animal pests; Pesticides, algicides, herbicides, insecticides, molluscacides, fungicides, rodenticides, etc.; Repellants and attractants; Fumigation and extermination; Traps; Biological pest control.

See also 68E and 98C.

For ecological aspects of pest control, use 57H.

57Q-Pharmacology & Pharmacological Chemistry

Synthesis, composition, properties, and effects of drugs; Pharmacy, Pharmacodynamics.

See also 57Y.

For social effects of drugs, use 91C and 92C.

For radiopharmaceuticals, use 57V.

For business studies of the drug industry, use 96A.

57S-Physiology

Functions of the human organism and its parts and comparative physiology; Metabolism; Endocrinology; Neurophysiology; Respiration; Biological rhythms; Growth; Aging; Regeneration.

See also 57B, 57F, 57J, and 57L.

For plant physiology, use 57C.

For animal physiology, use 57Z and 98E.

For psychophysiology, use 57T and 92B.

For electrophysiology, use 57I.

For pathophysiology, use 57O.

For stress physiology, use 57W.

57T-Psychiatry

Prevention, diagnosis, and treatment of mental, emotional, and behavioral disorders; Psychopathology; Psychoanalysis; Neuropsychiatry; Orthopsychiatry; Psychotherapy; Psychophysiology; Psychophysics.

For psychological mechanisms and processes, use 92B.

57U-Public Health & Industrial Medicine

Protection and improvement of community health; Effects of environments on public health; School and public health programs, services, and education; Health screening; Health statistics; Epidemiology; Toxic and infectious disease control; Preventive medicine; Hygiene and sanitation; Drinking water quality; Industrial hygiene and medicine; Safety engineering; Occupational safety and health; Industrial safety and detection equipment; Site-specific investigations.

See also 94D, 94H, 41I and 68G.

For occupational and For occupational and environmental factors related to health planning, use 44G.

57V-Radiobiology

Biological effects of radiation; Dosimetry; Health physics; Radiation sickness and injury; Radiation hazards; Radiation protection; Radiopharmaceuticals. Includes electromagnetic, ultrasonic, and particle radiation.

See also 68F and 99E.

For radioecology, use 57H.

For nuclear medicine, radiology, and radiotherapy, use 57E.

57W-Stress Physiology

Effects of extreme environments or stimuli on human biological processes; Physiological effects of motion, gravity, sound, temperature, electromagnetic, fields, pressure, sensory deprivation, and fatigue; Acclimatization. Includes aerospace and underwater medicine.

See also 51B, 57H, and 84.

For plants, use 57C.

For animals, use 57Z.

For stress psychology, use 92B or 57T.

57X-Surgery

Treatment of diseases, injuries, and deformities by manual or operative methods; Organ and tissue transplantation; Pre-and post-management of surgical patients; Experimental surgery.

See also 95A and 95B.

For dental surgery, use 57G.

For histocompatibility, use 57J.

57Y-Toxicology

Study of the adverse effects of substances on biological systems and the diagnosis and treatment of toxic diseases; Toxicity studies; Risk assessment of chemicals; Antidotes.

See also 57C, 57Q, 57S and 57Z.

57Z-Zoology

Animal anatomy and physiology; Natural history; Animal behavior; Taxonomy.

See also 47D, 48B, 57Y, and 98F.

For animal models used in biomedical research, use the research discipline.

For laboratory and domesticated animal care, or animal diseases, use 98E.

74-Military Sciences

740-General

74A-Antiaircraft Defense Systems

Tactical and terminal countermeasures against attacking aircraft that includes tracking and computing equipment, antiaircraft guns, rockets, and missiles.

For specific missiles and rockets, use 75.

74B-Antimissile Defense Systems

Point and terminal defense and countermeasures against air-, surface-, or underwater-launched missiles, bombardment satellites. Includes land based and shipborne tracking and computing systems; Strategic Defense Initiatives (SDI), Star Wars; ballistic missile defense.

74C-Antisubmarine Warfare

Operations conducted against submarines, their supporting forces and operating bases. Include air, surface, and underwater operations.

See also 63.

74D-Chemical, Biological, & Radiological Warfare

Design, development, and utilization of chemical, biological, and radiological weapons; Production, generation, and stability of lethal and nonlethal agents; Biological agents including anticrop and defoliating agents.

For nuclear weapons, use 74H.

74E-Logistics, Military Facilities, & Supplies

Procurement, storage, distribution, issue, repair, replacement of military equipment; Deployment of troops and cargo; Industrial mobilization; stock level controls and inventory techniques; Defense conversion; Downsizing; Base closures; Force reduction; Dual Use Technology; Continuous Acquisition and Life-cycle Support (CALS), formerly Computer Aided Acquisition and Logistics Support.

For related civilian studies, use 70 and 94.

74F-Military Intelligence

Techniques for collecting, evaluating, and disseminating information concerning foreign nations. Includes damage assessment; Surveillance and reconnaissance systems.

74G-Military Operations, Strategy, & Tactics

Joint and combined operations, campaigns, battles, invasions, theater operations; Planning analysis, appraisal, and threat evaluation; Methods of attack and support; Armed Forces maneuvers; Limited and unconventional warfare; Sabotage, insurgency, and counterinsurgency; Guerrilla warfare; Psychological and cold warfare.

74H-Nuclear Warfare

Design, development, and applications of nuclear weapons and devices; Studies of the physical effects of nuclear weapons; Arms control.

For nuclear guided missile warheads, use 75F.

74I-Passive Defense Systems

Systems, structures, and devices to provide area monitoring security and denial. Includes camouflage, barbed wire, minefields, warning systems, barriers, and other anti-intrusion devices.

For civil defense, see also 91I.

For personnel detection, see also 63G.

75-Missile Technology

750-General

75A-Air & Space-Launched Missiles

Design, construction and performance of missiles launched from aircraft or spacecraft.

75B-Missile Guidance & Control Systems

Techniques for guidance and control of missiles from launching to impact. Includes optical guidance, television guidance, wire guidance, preset and terminal guidance, inertial guidance, command guidance, and homing guidance.

75C-Missile Launching & Support Systems

Missile handling and launching. Includes transportation, storage, and preparation for launching; Air, space, surface, and underwater launching and support equipment and techniques; Checkout equipment and procedures; Guided missile ranges.

75D-Missile Tracking Systems

Techniques and systems for tracking missiles as defensive measures. Can be from surface installations or air and spaceborne platforms.

For antimissile defense systems, use 74B.

75E-Missile Trajectories & Reentry Dynamics

Determination, analysis, and processing of missile trajectory data; Flight path analysis; Impact prediction; Atmospheric reentry. Includes aerodynamic studies.

For spacecraft reentry, use 84D.

75F-Missile Warheads & Fuses

Design and performance of all types of missile warheads and fuzes-chemical, biological, nuclear and explosive.

For rockets, use 79H.

75G-Surface-Launched Missiles

Design, construction, and performance of missiles launched from the ground, surface platforms, vehicles, silos, and surface ships.

75H-Underwater-Launched Missiles

Design, construction, and performance of missiles launched from underwater.

48-Natural Resources & Earth Sciences

480-General

48A-Mineral Industries

Industries and their processes that exploit metallic and nonmetallic, fuel and nonfuel resources. Includes coal mining, mining wastes, and acid mine drainage; Coal preparation; Petroleum exploration, drilling, and production; Metals exploration and mining; Exploration geophysics and seismology; Reserves; Mine safety; Mineral economics; Underwater and continental shelf mining; Natural resources studies (excluding Earth Resource Satellite Surveys).

If energy source production related, use 97.

For petroleum refining, use 97K and 99B.

48B-Natural Resource Management

Conservation and management of natural resources, including land and soil, water, forest, grassland, and other vegetation; Fish and wildlife management; Mineral management; Policies and legislation including game laws and licensing; Water resource management; Water supply; Deforestation; Forest fire prevention.

See also 98F, 48A, 48C, and 48D.

48C-Natural Resource Surveys

Use of scientific satellites, aerial photography, and other remote sensing techniques to scan the earth's surface in data gathering experiments on soils, mineral resources, hydrology, animals, forests, and other resources; Surveying techniques such as image processing, photointerpretation, and pattern recognition.

For agricultural resource surveys, use 98G.

For equipment studies, use 63.

48D-Forestry

Forest description and measurement; Forest influences; Forest protection and management; Harvesting, logging, sawmills, and transportation; Silviculture; Forest nurseries; Afforestation reforestation, and deforestation; Forest fires and prevention.

For wood utilization, use 71R.

48E-Soil Sciences

Soil biology, chemistry, moisture, mineralogy, classification, surveys; Soil erosion and its prevention; Land reclamation, terracing, contouring, polders, tillage, and fertility; Soil banks.

For irrigation, use 98C.

For mechanical and engineering properties, use 50D.

48F-Geology & Geophysics

Structure, properties, and classification of rocks; Paleontology; Stratigraphy; Geodesy; Structural geology; Engineering geology; Vulcanology; Petrology; Petrography; Tectonics.

For astrogeology, use 54A.

For geological studies relating to energy or mineral reserves, use 97A and 48A respectively.

For marine geology and geophysics, use 47E.

48G-Hydrology & Limnology

Properties, distribution, and circulation of fresh water, including its surface and underground occurrence; Physical and chemical conditions in fresh water bodies; Eutrophication; Chemical-biological interrelationships; Water runoff; Water losses; Ground water; Streams; Aquifers.

For studies of estuaries or sea water, use 47.

48H-Snow, Ice, & Permafrost

Physical characteristics including trafficability, stability, and mechanical properties; Glaciology.

For sea ice, use 47C, and for sea ice movement, use 47B.

48I-Cartography

Map making; Photogrammetry; Terrain models; Topography. Geographic information systems; Cartography; Actual physical processes, procedures, and methods of map making.

76-Navigation, Guidance, & Control

760-General

76A-Control Devices & Equipment

Navigation and guidance control equipment.

See also 76C.

76B-Guidance Systems

Design, development, and performance of complete guidance systems. Includes integration of specific components and subsystems necessary to assure course positioning.

76C-Navigation & Guidance System Components

Navigation computers; Gyros, radiators, sensors, indicators, etc., used in navigation of aircraft, ships, spacecraft, and ground vehicles.

76D-Navigation Systems

Design, development, and performance of complete navigation systems; Integration of specific components and subsystems necessary in direction finding (position, distance, and course of travel); Global navigation systems.

See also 85F.

77-Nuclear Science & Technology

770-General

Includes nuclear materials management, safeguards, accounting methods.

See also 77I.

77A-Fusion Devices (Thermonuclear)

Theory, design, construction, and operation of devices for producing controlled thermonuclear fusion reactions; Nuclear fusion reactor materials and fuels.

For plasma studies in thermonuclear devices, see also 46G.

77B-Isotopes

Identification, separation, and concentration of radioactive isotopes. Includes isotopic irradiation devices.

For radioactive isotopes polluting the environment, use 68F.

For the use of isotopes in labeling chemical reactions, use 99F.

For the use of isotopes in medical/biological applications, use 57.

77C-Nuclear Auxiliary Power Systems

SNAP technology, both isotopic and reactor; Isotopic power supplies; Small scale electricity generation by nuclear means.

For nuclear propulsion, see the field of application.

77D-Nuclear Explosions & Devices

Explosion effects, including shock waves, ground motion, electromagnetic pulses, primary radiation, injection of charged particles into radiation belts; Testing of nuclear devices (including nuclear simulation using chemical explosives); Peaceful applications (e.g., Plowshare).

For effects on communications and electronics systems, see the field of application.

For military applications, use 74H.

77E-Nuclear Instrumentation

Nuclear radiation detection and measurement devices and systems; Beta particle detectors.

For X-ray detectors, use 460 General.

For health physics instrumentation, use 57V.

77F-Radiation Shielding, Protection, & Safety

Shielding design, nuclear radiation transport properties of materials, decontamination; Container design and transportation requirements for radioactive materials; Fallout shelters.

See also 91I.

77G-Radioactive Wastes & Radioactivity

Separation, processing, handling, storage, disposal, and reuse of radioactive wastes; Radioactive fallout; Fission products; Man-made or natural radioactivity; Decommissioning.

For radiation pollution, use 68F.

77H-Reactor Engineering & Nuclear Power Plants

Engineering related directly to the design, safety, and operation of a reactor; Research and test reactors. Integrated assemblage, including reactor and turbogenerator equipment, plus control and regulatory devices of a nuclear power plant, either mobile or stationary; Includes site selection and feasibility studies; Engineering aspects of reactor accidents.

See also 77C.

For critical assemblies and reactor simulation, use 77K.

77I-Reactor Fuels & Fuel Processing

Production, testing, design, or reclamation of nuclear fuel materials, reactor fuel elements (includes cladding) and fuel assemblies. Includes nuclear fuelcycle studies for nuclear materials management; Nuclear fuel reprocessing.

For processing of nonrecoverable fuel materials and fuel contaminants, use 77G.

77J-Reactor Materials

Production, testing, design, or reclamation of coolants, control materials, moderators, structural materials such as pipe materials; Shielding materials, and steels. Includes fabricated elements or assemblies and specific configurations.

For the effects of radiation on materials, see also 71L or 71J.

For fuel materials, cladding, or fuel assemblies, use 77I. Excludes power generating equipment and nuclear fusion reactor materials.

77K-Reactor Physics

Reactor kinetics, reactor theory, neutron transport theory, and criticality. Includes critical assemblies and reactor simulators.

47-Ocean Sciences & Technology

470-General

Includes breakwaters; Onshore and offshore facilities; Ocean dredging operations; Beach erosion; Harbor engineering; Ocean mining; Anchors; Buoys; Seakeeping; Diving operations and equipment; Decompression equipment.

See also 50B, 47H, and 95E.

47A-Marine Engineering

Design, construction, and maintenance of ships, boats, and related equipment; Salvage operations; Naval architecture; Shipyards and shipbuilding; Submarines; Shipborne containerization.

See also 85G.

47B-Dynamic Oceanography

Ocean waves; Sea level changes; Ocean currents; Ocean tides; Littoral transport; Sea ice movement.

47C-Physical & Chemical Oceanography

Physical and chemical properties of sea water, the ocean bottom, and estuaries; Sea ice.

For glaciers and fresh water ice, use 48H.

47D-Biological Oceanography

Plant and animal life in the marine environment; Biological fouling; Marine ecology; Biological aspects of mariculture; Use of marine organisms as bioassay systems; Marine aspects of estuaries; Marine biology of anadromous fishes.

See also 57C, 57H, 57K, 57F, 57Z, and 98F.

47E-Marine Geophysics & Geology

Geophysical and geological studies and surveys as applied to a marine environment; Plate tectonics; Sea floor spreading; Continental drift.

See also 48F.

47F-Oceanographic Vessels, Instruments, & Platforms

Instrumentation and equipment to collect and process oceanographic data; Remote sensors.

47G-Hydrography

Hydrographic surveying; Ocean bottom topography; Bathymetry.

47H-Underwater Construction & Habitats

Closed environments; Underwater work and construction; Underwater construction equipment.

See also 470 General or 95E.

79-Ordnance

790-General

79A-Ammunition, Explosives, & Pyrotechnics

Projectiles, fuzes, demolition explosives, detonators, grenades, land mines, high explosives, primers, powder and liquid propellants, flame throwers, and equipment for handling these items; Production, performance, storage stability of incendiaries, pyrotechnics, screening agents (smokes), etc.

For nuclear weapons, use 74H.

For rocket propellants, use 81.

79B-Armor

Design, testing, and performance of armor and armor plate including bullet proof, flak proof, explosion proof, and fragment proof devices and related equipment.

For other types of protective devices, see the application.

79C-Bombs

High-explosive, fragmentation, antipersonnel, armor piercing, incendiary, napalm, general purpose, and similar types of bombs; Bomb handling equipment; Storage.

For bomb directors and bomb release mechanisms, use 79F.

For nuclear bombs, use 74H.

79D-Combat Vehicles

Military vehicles including armored wheeled and track-laying vehicles, tanks and reconnaissance vehicles, trucks, gun carriers; Components and accessories.

79E-Detonations, Explosion Effects, & Ballistics

Explosion effects (except nuclear) such as blast, shock waves, detonation waves, cratering, earth motion or movement, heat, etc.; Interior, exterior, and terminal ballistics; The study of motion, behavior, and aerodynamics of projectiles thrown or launched by ordnance projectors; Includes target vulnerability and damage assessment studies, weapons effects.

For nuclear explosion effects, use 77D.

79F-Fire Control & Bombing Systems

Fire control computers, sights, directors, range finders, gunlaying, bombing radar systems, boresighting, bomb releases, and other devices used specifically for directing the firing of weapons or the dropping of bombs.

79G-Guns

Small arms, automatic weapons, antipersonnel weapons, recoiless weapons, mortars, artillery and naval guns, their accessories and components; Gun carriages, gun mounts, remote control equipment, etc.

For ballistic studies, use 79E.

For gun control, social violence, use 92C or 43.

79H-Rockets

Unguided, self-propelled projectiles whose trajectory or course cannot be altered after launch; Ground launched, air launched, or ship launched rockets, launchers, and launch support equipment.

For sounding rockets, use 55D.

79I-Underwater Ordnance
Torpedoes, submarine mines, depth charges, hydrobombs, anti-submarine ammunition, etc.; Launching devices and support equipment.

82-Photography & Recording Devices

820-General

82A-Holography
Techniques, materials, and uses of holography and holograms; Acoustic holography.

See also 46C.

82B-Photographic Techniques & Equipment
Photographic techniques, including aerial photography, color photography, astronomical photography, cinematography, photomicrography, Schlieren photography; Cameras, lenses, shutters, projectors, photographic processes, and materials; Microphotography, Photographic copying; Direct recording and reproduction of visual images; Copying, reproduction and replication techniques; Thermography; Lithography, and related arts; Graphic arts, illustrating, visual design.

For photogrammetry, use 48I.

82C-Recording Devices
Techniques and devices for recording other than visual images. Includes disk, magnetic, thermoplastic, electrostatic recording systems, CD-ROM, and playback equipment such as record players, tape recorders, etc.

46-Physics

460-General
Includes electron and X-ray optics; Thermodynamics; Nuclear physics; elementary particles; Atomic and molecular physics.

46A-Acoustics
Generation and transmission of sound through various media or enclosures. Includes ultrasonic and infrasonic radiation.

See also 63A.

46B-Fluid Mechanics
Theoretical and experimental studies of the dynamics and statics of fluids and of relative motion between fluids and solid bodies; Aerodynamics and hydrodynamics; Water tunnel studies and equipment.

For wind tunnel equipment and facilities, use 51F.

For operational applications, use 51A, 75E, and 84D.

For plasma physics, use 46G.

46C-Optics & Lasers
Generation and propagation of electromagnetic waves in the infrared, visible, and ultraviolet region of the spectrum; Theory; Design and performance of optical equipment; Lasers and masers.

46D-Solid State Physics
Physical properties of solids as related to their structure. Fundamental research and theoretical studies on semiconductors, superconductors, structure of solids. Includes crystallography and superconductivity.

For semiconductor devices, use 49H.

For structural mechanics, use 46E.

For studies on ceramics, coatings, composite materials, metals, and alloys, use 71.

46E-Structural Mechanics
Dynamics and statics of solid bodies; Kinematics; Shock and vibration.

46G-Plasma Physics
Properties and actions of plasmas, including magnetohydrodynamics, pinch effect, plasma oscillations, plasma jets; Plasma diagnostics; Plasma dynamics. Plasmas in thermonuclear devices.

See also 77A.

For MHD generators, use 97O.

For astrophysics, use 54C.

For aeronomy, use 55A.

46H-Radiofrequency Waves
Generation and propagation of radiofrequency waves.

For communication systems, techniques, equipment, etc., use 45.

For radiofrequency detection, use 63H.

43-Problem-Solving Information for State & Local Governments

430-General
Includes internal government administration; State programs; Criminal justice, corrections planning, and administration.

43A-Finance
Taxation; Revenue; Budgeting; Revenue sharing; Financing; Allocation.

See also 91G and 91H.

For commercial banking and finance operations, use 96F.

43B-Economic & Community Development
Land use planning; Urban renewal; Economic effects; Economic planning and development; Recreation planning and development; Economic readjustment.

See also 91J and 96A.

43C-Human Resources
Education; Social services; Health care services; Manpower.

See also 9lK and 92C.

43D-Police, Fire, & Emergency Services
Police and fire services and administration; Disaster services; Civil defense; Emergency weather services, Pollution alerts; Civil disturbances; Ambulance services; Disaster relief.

See also 91C and 91I.

43E-Energy
Management and planning on energy resources, use and production; Government administration and forecasting.

See also 97.

43F-Environment
Air, water, noise, waste management and planning; Monitoring services.

See also 68.

43G-Transportation
Planning for modes of public, private, and cargo transportation; Highway planning, Parking; Traffic engineering.

See also 85 and 91B.

84-Space Technology

840-General
Extraterrestial biology, chemistry, and medicine.

84A-Astronautics
Space missions; Projects and logistics; Orbital rendezvous; Space exploration; Spacecraft operating problems; Extravehicular activity.

84B-Extraterrestrial Exploration
Space probe exploration; Space landings; Space construction and maintenance; Extravehicular activity on other planets.

84C-Manned Spacecraft
Design and construction of manned spacecraft, space stations, aerospace planes and their components.

84D-Spacecraft Trajectories & Flight Mechanics
Determination, analysis, processing of spacecraft trajectory data; Space mechanics; Orbital calculations; Flight path analysis; Atmosphere entry; Reentry dynamics.

84E-Space Launch Vehicles & Support Equipment
Handling and launching, including transportation, storage, preparation for launching, countdown, launching equipment, checkout equipment, ground support equipment, and information systems; Spacecraft tracking systems; Tracking networks; Recovery support.

84F-Space Safety
Safety measures and devices directed toward reducing the hazards of spaceflight.

84G-Unmanned Spacecraft
Design and construction of unmanned spacecraft, including space probes, scientific satellites, military satellites, communication satellites, reconnaissance satellites, and navigational satellites.

For satellites applied to a specific application, see the field of application.

85-Transportation

850-General

85A-Air Transportation
Operation of systems for transport by air; Civil aviation; Airports and airport access; Airline operations; Air routing; Air traffic control systems; Multimodal systems; Aviation safety and aviation accidents; Aircraft fires; Aircraft fuel fires.

See also 43G, 74E, 76, 85D, and 91B.

For design of aircraft and components, use 51 and 81.

For runway construction and design, use 50B.

85C-Metropolitan Rail Transportation
Urban rail transit; Underground and above-ground rapid transit railways, including subways; Automated guideway transit systems; Tracked air cushion vehicles.

See also 85I and 91B.

85D-Transportation Safety
Safety and accidents involving air, land, and water transportation; Accident studies and prevention; Alcohol related studies; Breakaway barriers and structures; Standards and testing of components and equipment; Crashworthiness; Traffic safety; Collision research; Safety equipment and devices.

See also 91B.

For pipeline accidents, use 85E.

85E-Pipeline Transportation
Transportation of liquids, gases, and slurries through long-distance pipelines; Accidents and safety.

85F-Global Navigation Systems
Worldwide navigational aids to transportation; Global positioning system (GPS).

See also 76D.

85G-Marine & Waterway Transportation
Shipping; Safety and accidents; Safety equipment; Cargo handling and equipment; Cargo movement; Passenger movement; Traffic control; Boating; Trade routes; Shipborne containerization.

See also 43G, 74E, 76, and 85D.

For marine engineering, use 47A.

For waterway engineering, use 50B.

85H-Road Transportation
Passenger and cargo movement; Design and standards for vehicles and components; Motor vehicle engine studies; Safety engineering; Safety devices; Traffic and road safety; Collision research; Accident studies; Highway traffic; Traffic engineering; Passenger and cargo vehicles; Trailers; Motorcycles; Bicycles and bikeways; Hiking trails.

See also 43G, 50A, 74E, 81J, 85D, and 91B.

85I-Railroad Transportation
Safety and accidents; Safety equipment; Cargo handling and equipment; Cargo movement; Passenger movement; Traffic control; Terminals; Amtrak; Track studies; Rolling stock; Scheduling; Railroad engineering and equipment.

See also 43G, 85D, and 91B.

91-Urban & Regional Technology & Development

910-General
Includes energy studies.

91A-Environmental Management & Planning
Air, water, noise, and waste management and control; Monitoring services; Solid wastes and recycling; Solid waste landfills; Water quality management; Environmental surveys; Design and operation of sewer systems (combined, etc.); Water supplies and services; Excludes natural resource management.

See also 68 and 43F.

91B-Transportation & Traffic Planning
Planning for modes of public and private, passenger and cargo transporation; Travel patterns and demand; Parking; Traffic engineering, traffic flow and control; Traffic surveys; Highway and street services; Rapid transit systems; Passenger transportation and planning; Pedestrian movement.

See also 43G and 85.

91C-Fire Services, Law Enforcement, & Criminal Justice
Fire, police, and court services and their administration; Law enforcement and criminal justice; Crime and fire prevention; Personnel recruitment, training, and utilization; Parole; Work release; Correctional institutions.

See also 43D.

For criminal justice and corrections, see also 430 General.

91D-Communications

Use and planning of communications; Mass media, emergency communications, public information.

See also 45.

91E-Housing

Surveys and assessments of existing housing; Planning and development; Building codes; Housing needs; Housing renovation; Public housing.

For design, architectural, or construction related studies, see also 89.

91F-Health Services

Urban health services; Emergency medical services; Mental health services; Nursing homes; Ambulatory health services; Hospital services; Public health access.

See also 43C, 43D, 44 and 91I.

91G-Urban Administration & Planning

General administration and planning; Feasibility studies; Appraisal of real property; Taxation; Land use and zoning; Urban revitalization; Financing.

See also 43 and 70F.

91H-Regional Administration & Planning

General administration and planning for county and regional areas that may also contain urban or urbanized areas; Intergovernmental relations and interactions (State, County, Local); Land use and zoning.

See also 43 and 70F.

For state government administration and planning, use 43.

91I-Emergency Services & Planning

Disaster services; Civil defense; Early warning systems and emergency preparedness for all types of disaster; Emergency weather services; Pollution alerts; Civil disturbances; Ambulance services; Flooding; Disaster relief.

See also 43D, 44, and 91F.

For military passive defense systems, see also 74I.

For personnel detection, see also 63G.

91J-Economic Studies

Economic analyses; Economic development; Industrial development; Economic impacts of development; Population-economy-income studies; Employment and earnings; Property values; Commercial area studies.

See also 43B and 96.

For government financial operations, use 43A, 70F, 91G, and 91H.

91K-Social Services

Child care; Family and youth counseling; Social rehabilitation; Foster homes and adoption; Welfare and public assistance; Financial assistance; Food stamp services; Employment services; Legal services.

See also 43C, 91F, and 92C.

NTIS Subject Categories
Numerical Listing of Major Categories
Appendix D

Primary category titles arranged by subject category code. This list will assist you in using the cross reference category codes provided in many of the descriptions.

41 Manufacturing Technology
43 Problem Solving Information for State & Local Governments
44 Health Care
45 Communications
46 Physics
47 Ocean Sciences & Technology
48 Natural Resources & Earth Sciences
49 Electrotechnology
50 Civil Engineering
51 Aeronautics & Aerodynamics
54 Astronomy & Astrophysics
55 Atmospheric Sciences
57 Medicine & Biology
62 Computers, Control & Information Theory
63 Detection & Countermeasures
68 Environmental Pollution & Control
70 Administration & Management
71 Materials Sciences
72 Mathematical Sciences
74 Military Sciences
75 Missile Technology
76 Navigation, Guidance &Control
77 Nuclear Science & Technology
79 Ordnance
81 Combustion, Engines, & Propellants
82 Photography & Recording Devices
84 Space Technology
85 Transportation
88 Library & Information Sciences
89 Building Industry Technology
90 Government Inventions for Licensing
91 Urban & Regional Technology & Development
92 Behavior & Society
94 Industrial & Mechanical Engineering
95 Biomedical Technology & Human Factors Engineering
96 Business & Economics
97 Energy
98 Agriculture & Food
99 Chemistry

NTIS Subject Categories
Numerical Listing with Scope Descriptions
Appendix E

41-Manufacturing Technology

410-General

Includes mechanical elements; Pipes; Tubes; Levers; Cams; Springs; Clutches; Gears; Valves; Filters; Containers and packing materials; Refrigeration systems and equipment; Industrial furnaces and boilers; Heat exchangers; Heat pumps; Heat pipes; Energy management, economics, and financing; International issues.

See also 94O and 97G.

For engine components, use 81.

For fuel tanks, use 81C.

For cooling towers, use 97J.

41A-Computer Aided Design (CAD)

Application of computer hardware and software (programs) to enhance the design, computations, simulation, analysis and modeling, presentations, graphics, drafting, data base creation and human-machine interface, associated with the creation of engineering design specifications.

See also 94A.

41B-Computer Aided Manufacturing (CAM)

Application of computer hardware and software (programs) to enhance materials planning, processing and handling, tooling; Assembly; Quality and reliability control; Inspection; Tests; Scheduling and control; Facilities and equipment maintenance; Group technology applications; Inventory control (raw material, in process and finished); Numerical controls and automation; The creation of Direct Numerical Control (DNC) and Computer Numerical Control (CNC) manufacturing cells and systems.

See also 94A and 94G.

41C-Robotics/Robots

Application of computer hardware and software, controls, sensors, electromechanical and hydro-mechanical devices, to the creation of robots and the application of robots to all facets of manufacturing. Study of biological processes in order to develop engineering systems; Pattern recognition systems based on biological models. Includes feature extraction; Image enhancement; Image restoration; Scene analysis; Character recognition.

See also 95F and 62F.

41D-Productivity

Productivity of employees, management, and services; Improving quality of worklife; Measurement of productivity efficiency and effectiveness; Employee attitudes and motivation; Manpower utilization and performance improvement, job satisfaction, job security; Labor-management, job redesign; Alternative work schedules; Incentive plans; Productivity barriers including regulation, obsolete practices; Paperwork, and financing methods.

See also 70G and 70D.

41E-Manufacturing, Planning, Processing & Control

Fabrication, assembling, cleaning, and finishing; Industrial and manufacturing processes (limited to in-depth studies that directly discuss specific processes); Materials forming and machining; Heat treatment; Fabrication and manufacturing; Layout; Coating processes; Materials handling and control, including palletizing, conveying, warehousing, storing, containerization, and packaging; Time and motion studies; Scheduling; Production controls and programming; Modeling techniques and program controls; Inventory management.

See also 94A.

For the beneficiation and processing of minerals, use 48A.

For chemical engineering and processing, use 99B.

For computer-aided manufacturing, use 41B and 94G.

For lasers used in manufacturing, use 41M.

For processing and packaging of food, use 98H.

For production of materials, use 71.

41F-Joining

Bonding and joining including gluing, welding, soldering, brazing, and fastening; Joints and fasteners; Physical, mechanical, and structural properties of adhesives, sealants, glue, binders, seals, and gaskets.

See also 94G, 940 General, and 71B.

41G-Quality Control & Reliability

Tolerance allocation; Maintainability requirements; Probability of satisfactory performance of components and equipment; Inspection methods; Reliability theory; Quality assurance; Nondestructive testing having industrial application; Ultrasonic, radiographic, hydrostatic, magnetic, and optical nondestructive techniques and equipment; Nondestructive testing of flaws, thickness, opacity, strength; Destructive industrial testing; Metrology.

See also 94B, 94J, and 940 General.

41H-Plant Design & Maintenance

Site selection; Plant design; Maintenance Management; Scheduled, routine, and corrective maintenance; Security.

See also 94C.

41I-Job Environment

Industrial hygiene and occupational safety and health. See also 57U, 68G, and 44G. Workplace layout and design; Human factors engineering; Includes Industrial psychology and Industrial sociology; Worker interactions.

See also 94D and 95D.

Includes environmental engineering equipment related to industrial use. See also 97J, 89B, and 94E.

For mine safety, use 48A.

For ordnance safety, use 79A.

For nuclear radiation safety, use 77.

For transportation safety, use 85D.

41J-Tooling, Machinery, & Tools

Machine subassemblies; Tools; Machinery including hoists, conveyors, and pumps; Design, production performance, and testing of hydraulic and pneumatic systems, accumulators, actuators, compressors and distribution equipment; Fluidic and flueric devices; Ergonomics interaction of man and equipment in terms of subsystem and system performance requirements and evaluation; Man-machine systems and human factors engineering.

See also 94F, 94I, 94D, and 95D.

For hydraulic fluids, use 71K.

41K-Engineering Materials
Performance; Properties, fabrication and manufacturing methods of ceramics, coatings and composite materials including ceramic coatings, ceramic fibers, corrosion resistant coatings, reinforced plastics, graphite or carbon composites, laminates; Metal matrix composites, and fiber and particulate composites.

See also 71B, 71D, and 71F.

41L-Tribology
Friction, lubrication and wear, including bearings; Unwanted chemical reaction effects on metals, corrosion of metals and corrosion resistant coatings; Lubricants.

See also 71L, 71G, and 71K.

41M-Optics & Lasers
Design and performance of optical equipment for use in manufacturing applications. Includes laser applications such as laser annealing, cutting, drilling, and welding.

See also 46C.

41N-Computer Software
Computer programming; Programming languages; Compilers; Data base management systems; CAD/CAM robotics.

See also 62B.

41O-Domestic Commerce, Marketing, & Economics
Economic impacts on industries; Productivity; Wage surveys; Domestic market surveys.

See also 96A.

41P-Research Program Administration & Technology Transfer
Research needs; Technology transfer and forecasting.

See also 70E.

43-Problem Solving Information for State & Local Governments

430-General
Includes internal government administration; State programs; Criminal justice, corrections planning, and administration.

43A-Finance
Taxation; Revenue; Budgeting; Revenue sharing; Financing; Allocation.

See also 91G and 91H.

For commercial banking and finance operations, use 96F.

43B-Economic & Community Development
Land use planning; Urban renewal; Economic effects; Economic planning and development; Recreation planning and development; Economic readjustment.

See also 91J and 96A.

43C-Human Resources
Education; Social services; Health care services; Manpower.

See also 91K and 92C.

43D-Police, Fire, & Emergency Services
Police and fire services and administration; Disaster services; Civil defense; Emergency weather services, Pollution alerts; Civil disturbances; Ambulance services; Disaster relief.

See also 91C and 91I.

43E-Energy
Management and planning on energy resources, use and production; Government administration and forecasting.

See also 97.

43F-Environment
Air, water, noise, waste management and planning; Monitoring services.

See also 68.

43G-Transportation
Planning for modes of public, private, and cargo transportation; Highway planning, Parking; Traffic engineering.

See also 85 and 91B.

44-Health Care

440-General

44A-Planning Methodology
Health planning theory including methods, tactics, techniques and policies; Evaluation of planning theories and processes.

44B-Agency Administrative & Financial Management
Management practices and policies regarding technical assistance, evaluation of health care agency activities, public relations; Financial management and accounting methods.

44C-Community & Population Characteristics
Data and numerical information including health status, quality of care, malpractice, health care needs/demands; Health care utilization, health care cost, vital statistics; Demographic information, economic, environmental, nutritional, and societal factors affecting health, and health resource distribution.

44D-Health Care Assessment & Quality Assurance
Financial feasibility review, economic impact review, and project review; Certificate of need theory; Health manpower education institutional accreditation; Judicatory procedures, review, and assessment; Quality assurance theory; Certificatory methodology; Health manpower proficiency testing, and public health education evaluation; Classification of health care facilities and health care personnel.

44E-Health Care Measurement Methodology
Measurement of health status, quality of care, health facility supply, health manpower supply, proficiency and productivity, and health care costs; Health care needs/demands and utilization measurement.

See also 44L, 44N, and 44Q.

44F-Health Care Forecasting Methodology
Projecting health care needs/demands and health care utilization; Health care facility supply; Health manpower supply; Health care costs; Home health care; Cross-impact projections.

44G-Environmental & Occupational Factors
Environmental factors affecting health including housing, sanitation, water pollution, solid waste pollution, noise pollution, disease vectors, safety hazards, and occupational and industrial hazards; Overpopulation; Health facility environmental considerations and environmental impact; Energy sources in the health field.

See also 57U and 68G.

44H-Health Care Technology

Descriptions and applications of new health care technology and equipment; Ailment prevention techniques, and technology regarding diagnosis, therapy, rehabilitation, and food and nutrition; Health care equipment and facility design and performance considerations.

See also 57 and 95.

44J-Health Delivery Plans, Projects & Studies

Plans, projects, and studies related to the institutional delivery of health services including state/local health plans, state/local medical facility plans, plans for specific health services, and health delivery feasibility studies.

44K-Health Services

Personal and public health services, patient care, and maintenance of an individual's health status including hospital services acute in-patient services, long-term inpatient services, nursing home services, emergency services, public health services, mental services, nursing services, dental services, and medically-related social services including institution discharge services.

44L-Health Care Needs & Demands

Measurement of health care needs/demands, hospital care, acute in-patient care, long-term in patient care, nursing home care, medical care, mental care, nursing care, dental care, and health insurance; Home health care; Measurements of health manpower requirements/demands.

See also 44E.

44M-Health Resources

Surveys, reports, and studies related to specific health care resources including manpower, facilities, sources of financing, and government and private health-related organizations, agencies and individuals.

44N-Health Care Utilization

Measurements regarding utilization of health resources including manpower, ambulatory care, emergency care, public health care, medical care, mental care, nursing care, dental care, health insurance, health care facilities, and home health care.

See also 44E and 44L.

44P-Health Education & Manpower Training

Health manpower education including curricula and costs; Health manpower education facility needs/demands; Institutional financing; Financing for health related educational institutions; Student recruiting and retention methods; Continuing education; Career guidance and career advancement; Consumer health education and public health education methods.

44Q-Health-Related Costs

Health care costs, indexes, projections, in-patient care costs, acute in-patient care costs, long-term care costs, nursing home care costs, ambulatory care costs, emergency care costs, public health care costs, medical care costs; Insurance costs; Manpower income; Equipment costs; Facility utilization and construction costs; Ailment costs including preventive medicine costs and injury costs; Transportation costs including emergency transportation costs.

44R-Economics & Sociology

Discussions of economic and sociological factors and theories relevant to health care.

44S-Legislation & Regulations

Laws, bills, regulations, and model legislation. Includes certificate of need, health insurance certification, health manpower licensing, health facility licensing, health manpower employment, and support regarding health manpower education.

44T-Data & Information Systems

Techniques regarding information systems including document sources, acquisition, surrogation, and storage; Information retrieval; Data systems, Data gathering; Data processing; Data processing hardware; Information system feasibility studies, and confidentiality of information.

44U-Health Care Delivery Organization & Administration

Hospital and medical practice administration and management; Organizational structure of health services; Management policies and practices regarding personnel, community participation and relations, and coordination with other agencies; Financial management and accounting methods; Financing of health delivery and facilities; Reporting methods and requirements.

45-COMMUNICATION

450-General

45A-Policies, Regulations, & Studies

Licensing; Legislation; National policies and Federal regulatory controls; Frequency management; Broadcasting standards; Time signals, etc.

45B-Radio & Television Equipment

Design and maintenance of radio and television transmitting and receiving equipment only.

See also 51E.

45C-Common Carrier & Satellite

All communication equipment except radio and television. Optical, radio, microwave, wire, and acoustic communication; Telephone, telemeter, telegraph, television, and radio communication systems; Computer network communications; Digital communication; Intercommunication systems; Optical scanning.

For information systems, see also 88B.

For design and construction of communication satellites, see also 84G.

45D-Sociopolitical

Propaganda; Social communication; Sign language, Effects of communication on society and behavior; Postal service; Mass media communication.

45E-Graphics

Publishing; Printing; Graphic arts; Reprography; Xerography; Facsimile; Desktop publishing.

45F-Verbal

Research and development in vocal communication; Speech intelligibility; Speech recognition.

45G-Communication & Information Theory

Theoretical studies relating to the measurement and transmission of information in a communication channel. Includes coding theory, information capacity, detection of signals in noise.

See also 62E.

46-Physics

460-General

Includes electron and X-ray optics; Thermodynamics; Nuclear physics; elementary particles; Atomic and molecular physics.

46A-Acoustics

Generation and transmission of sound through various media or enclosures. Includes ultrasonic and infrasonic radiation.

See also 63A.

46B-Fluid Mechanics

Theoretical and experimental studies of the dynamics and statics of fluids and of relative motion between fluids and solid bodies; Aerodynamics and hydrodynamics; Water tunnel studies and equipment.

For wind tunnel equipment and facilities, use 51F.

For operational applications, use 51A, 75E, and 84D.

For plasma physics, use 46G.

46C-Optics & Lasers

Generation and propagation of electromagnetic waves in the infrared, visible, and ultraviolet region of the spectrum; Theory; Design and performance of optical equipment; Lasers and masers.

46D-Solid State Physics

Physical properties of solids as related to their structure. Fundamental research and theoretical studies on semiconductors, superconductors, structure of solids. Includes crystallography and superconductivity.

For semiconductor devices, use 49H.

For structural mechanics, use 46E.

For studies on ceramics, coatings, composite materials, metals, and alloys, use 71.

46E-Structural Mechanics

Dynamics and statics of solid bodies; Kinematics; Shock and vibration.

46G-Plasma Physics

Properties and actions of plasmas, including magnetohydrodynamics, pinch effect, plasma oscillations, plasma jets; Plasma diagnostics; Plasma dynamics. Plasmas in thermonuclear devices.

See also 77A.

For MHD generators, use 97O.

For astrophysics, use 54C.

For aeronomy, use 55A.

46H-Radiofrequency Waves

Generation and propagation of radiofrequency waves.

For communication systems, techniques, equipment, etc., use 45.

For radiofrequency detection, use 63H.

47-Ocean Sciences & Technology

470-General

Includes breakwaters; Onshore and offshore facilities; Ocean dredging operations; Beach erosion; Harbor engineering; Ocean mining; Anchors; Buoys; Seakeeping; Diving operations and equipment; Decompression equipment.

See also 50B, 47H, and 95E.

47A-Marine Engineering

Design, construction, and maintenance of ships, boats, and related equipment; Salvage operations; Naval architecture; Shipyards and shipbuilding; Submarines; Shipborne containerization.

See also 85G.

47B-Dynamic Oceanography

Ocean waves; Sea level changes; Ocean currents; Ocean tides; Littoral transport; Sea ice movement.

47C-Physical & Chemical Oceanography

Physical and chemical properties of sea water, the ocean bottom, and estuaries; Sea ice.

For glaciers and fresh water ice, use 48H.

47D-Biological Oceanography

Plant and animal life in the marine environment; Biological fouling; Marine ecology; Biological aspects of mariculture; Use of marine organisms as bioassay systems; Marine aspects of estuaries; Marine biology of anadromous fishes.

See also 57C, 57H, 57K, 57F, 57Z, and 98F.

47E-Marine Geophysics & Geology

Geophysical and geological studies and surveys as applied to a marine environment; Plate tectonics; Sea floor spreading; Continental drift.

See also 48F.

47F-Oceanographic Vessels, Instruments, & Platforms

Instrumentation and equipment to collect and process oceanographic data; Remote sensors.

47G-Hydrography

Hydrographic surveying; Ocean bottom topography; Bathymetry.

47H-Underwater Construction & Habitats

Closed environments; Underwater work and construction; Underwater construction equipment.

See also 47Gen or 95E.

48-Natural Resources & Earth Sciences

480-General

48A-Mineral Industries

Industries and their processes that exploit metallic and nonmetallic, fuel and nonfuel resources. Includes coal mining, mining wastes, and acid mine drainage; Coal preparation; Petroleum exploration, drilling, and production; Metals exploration and mining; Exploration geophysics and seismology; Reserves; Mine safety; Mineral economics; Underwater and continental shelf mining; Natural resources studies (excluding Earth Resource Satellite Surveys).

If energy source production related, use 97.

For petroleum refining, use 97K and 99B.

48B-Natural Resource Management

Conservation and management of natural resources, including land and soil, water, forest, grassland, and other vegetation; Fish and wildlife management; Mineral management; Policies and legislation including game laws and licensing; Water resource management; Water supply; Deforestation; Forest fire prevention.

See also 98F, 48A, 48C, and 48D.

48C-Natural Resource Surveys

Use of scientific satellites, aerial photography, and other remote sensing techniques to scan the earth's surface in data gathering experiments on soils, mineral resources, hydrology, animals, forests, and other resources; Surveying techniques such as image processing, photointerpretation, and pattern recognition.

For agricultural resource surveys, use 98G.

For equipment studies, use 63.

48D-Forestry

Forest description and measurement; Forest influences; Forest protection and management; Harvesting, logging, sawmills, and transportation; Silviculture; Forest nurseries; Afforestation reforestation, and deforestation; Forest fires and prevention.

For wood utilization, use 71R.

48E-Soil Sciences

Soil biology, chemistry, moisture, mineralogy, classification, surveys; Soil erosion and its prevention; Land reclamation, terracing, contouring, polders, tillage, and fertility; Soil banks.

For irrigation, use 98C.

For mechanical and engineering properties, use 50D.

48F-Geology & Geophysics

Structure, properties, and classification of rocks; Paleontology; Stratigraphy; Geodesy; Structural geology; Engineering geology; Vulcanology; Petrology; Petrography; Tectonics.

For astrogeology, use 54A.

For geological studies relating to energy or mineral reserves, use 97A and 48A respectively.

For marine geology and geophysics, use 47E.

48G-Hydrology & Limnology

Properties, distribution, and circulation of fresh water, including its surface and underground occurrence; Physical and chemical conditions in fresh water bodies; Eutrophication; Chemical-biological interrelationships; Water runoff; Water losses; Ground water; Streams; Aquifers.

For studies of estuaries or sea water, use 47.

48H-Snow, Ice, & Permafrost

Physical characteristics including trafficability, stability, and mechanical properties; Glaciology.

For sea ice, use 47C, and for sea ice movement, use 47B.

48I-Cartography

Map making; Photogrammetry; Terrain models; Topography. Geographic information systems; Cartography; Actual physical processes, procedures, and methods of map making.

49-Electrotechnology

490-General

Includes standards, measurements, and instrumentation not applied to any other subcategories.

49A-Antennas

Antennas; Antenna theory; Antenna radiation patterns; Radomes.

49B-Circuits

Circuit theory; Network analysis; Filters; Oscillators; Logic circuits; Printed circuits; Electronic modules; Commutators; Power supply circuits; Waveform generators; Analog to digital converters; Phase locked systems.

For integrated circuits, use 49H.

49C-Electromechanical Devices

Electric motors; Relays; Mechanical switches; Connectors; Circuit breakers; Electric fuses.

49D-Electron Tubes

All electron tubes except those in 49E.

49E-Optoelectronic Devices & Systems

Display systems; Phototubes; Image tubes; Cathode ray tubes; Electroluminescent panels; Light emitting diodes; Photodiodes; Phototransistors; Magnetooptics; Electrooptics; Optical detectors, including infrared and ultraviolet detectors.

See also 63C and 63F.

For solar cells, see also 97N.

For lasers, use 46C.

49F-Power & Signal Transmission Devices

Transmission lines; Electric wire and cable; Waveguides; Fiber optics transmission lines.

49G-Resistive, Capacitive, & Inductive Components

Resistors; Capacitors; Inductors; Transformers; Electromagnets; Potentiometers; Thermistors; Delay lines; Transducers; Crystal resonators. Includes miscellaneous and basic components.

49H-Semiconductor Devices

Transistors; Semiconductor diodes; Integrated circuits.

For photodiodes, phototransistors, light emitting diodes, and optical detectors, use 49E.

50-Civil Engineering

500-General

50A-Highway Engineering

Construction of roads and highways; Highway and rights-of-way maintenance including weed control; Bridges and bridge systems; Highway paints and markings; Highway and road signs; Beautification; Slope stability and soil subbases.

50B-Civil Engineering

Dredging; Dams; Water purification; Reservoir engineering; Flood control; Sewers; Waterway engineering; Runway construction; Shore protection; Breakwaters; Harbor engineering; Tunneling.

See also 47.

For sewage treatment, use 68D.

For building construction, use 89.

For oil and gas reservoir engineering, use 97 or 48A.

50C-Construction Equipment, Materials, & Supplies

Excavation and earth moving equipment; Hoisting and conveying equipment; Concrete and cement.

See also 89G.

For properties of concrete and cement, see also 71D.

50D-Soil & Rock Mechanics

Physical properties of soil and rock for utilization in engineering; Landslides; Soil stabilization.

For soil sciences, use 48E.

For soil conservation, use 48B.

For geology and geophysics, use 48F.

51-Aeronautics & Aerodynamics

510-General

Includes landing mats.

51A-Aerodynamics

Aerodynamic characteristics and problems of bodies as they are affected by the dynamics of phenomena relating to boundary layer, lift, drag, laminar and turbulent flow, compressible flow, lift, aerodynamic heating, vortex flow, wake, etc. in aerodynamic regimes. Includes aircraft, ground vehicles, and structures.

See also 46B.

For missile reentry dynamics, use 75E.

For spacecraft reentry dynamics, use 84D.

51B-Aeronautics

Aircraft operations such as takeoff and landing, all-weather and night flight, taxiing, approach, letdown, in-flight refueling, etc. Includes aviation accidents.

51C-Aircraft

Design, production, and maintenance of aircraft, aircraft components and equipment. Structural studies of airframes, bodies, wings, fuselages; Military and commercial aircraft; Balloons (excludes meteorological balloons); Air cushion vehicles (excludes tracked vehicles).

See also 85A and 81D.

For meteorological balloons, use 55D.

For tracked air cushion vehicles, use 85C.

For electronic equipment, use 51E.

51D-Parachutes & Decelerators

Deployable devices and structures to induce drag and deceleration of aircraft, spacecraft, and test vehicles such as rocket sleds.

51E-Avionics

Airborne electronic equipment. Includes electronic equipment used for communications; Navigation; Control systems; Onboard air traffic control; Detection.

See also 45, 49, 63, and 76.

51F-Test Facilities & Equipment

Wind tunnels; Simulators; Flight simulators.

For flight simulators used for training, use 92A.

54-Astronomy & Astrophysics

540-General

54A-Astrogeology

Studies of the structure and composition of planets and other bodies in the solar system.

For geology and geophysics, see also 48F.

54B-Astronomy & Celestial Mechanics

Positions and motions of the celestial bodies; Ephemerides, Eclipses.

54C-Astrophysics

Physical and chemical aspects of celestial bodies, their origin and evolution. Includes astronomical spectroscopy, radio astronomy, solar structure, and planetary atmospheres.

54D-Cosmic Ray Research

Detection and analysis of cosmic rays.

55-Atmospheric Sciences

550-General

55A-Aeronomy

Physics and chemistry of the upper atmosphere; Composition; Chemical reactions; Aurora; Airglow; Solar-terrestrial relationships.

For cosmic ray research, use 54D.

55B-Dynamic Meteorology

Studies of atmospheric motions; Atmospheric diffusion models; Atmospheric circulation.

For air pollution movement studies, use 68A.

55C-Meteorological Data Collection, Analysis, & Weather Forecasting

Climatology; Satellite meteorology; Weather prediction; Ice forecasting.

55D-Meteorological Instruments & Instrument Platforms

Instruments used to record meteorological parameters; Meteorological balloons; Weather stations; Sounding rockets; Remote sensors.

55E-Physical Meteorology

Acoustical, electrical, optical, and thermodynamic properties of the atmosphere; Cloud physics; Precipitation theory; Global warming.

See also 68A.

55F-Weather Modification

Change of weather conditions through artificial means; Fog dispersal; Artificial precipitation.

57-Medicine & Biology

570-General

57A-Anatomy

Descriptive and comparative anatomy of humans; Anthropometry; Dissection; Neuroanatomy; Morphology.

For plant anatomy, use 57C.

For animal anatomy, use 57Z.

57B-Biochemistry

Studies of the chemical processes which take place in biological systems. Identification and measurement of biochemical substances and methods of analysis, including assaying.

See also 57F, 57L, 57Q, and 99A.

For measurement of biochemical substances for clinical diagnoses, use 57D.

57C-Botany

Study of macroscopic and microscopic plants; Plant anatomy, physiology, pathology, and taxonomy; Phytotoxicity; Includes algae and diatoms.

See also 57H, 57K, 57Y, and 98D.

57D-Clinical Chemistry

Techniques and instrumentation for chemical analysis of body fluids, including blood, and tissues for clinical diagnoses.

See also 99A.

57E-Clinical Medicine

Prevention, diagnosis, and therapy of diseases; Nuclear medicine; Experimental medicine; Clinical protocols.

See also 57J, 57O, and 57X.

For veterinary medicine, use 98E.

For health care services, use 44.

For epidemiology and disease control, use 57U.

57F-Cytology, Genetics, & Molecular Biology

Origin, structure, and functions of living cells and cell components; Hereditary diseases; Use of chemistry and physics to study biological phenomena on the molecular level; Structure and function of biological macromolecules, e.g. proteins and nucleic acids.

See also 57B.

57G-Dentistry

Prevention, diagnosis, and treatment of diseases of the teeth, oral cavity, and associated parts; Oral hygiene.

For dental materials and equipment, use 95C.

For dental prosthetics, use 95A.

For dental services, use 44.

57H-Ecology

Interrelationships of organisms and their environment; Animal, plant, and human ecology; Marine, fresh water, and terrestrial ecology; Ecosystems; Adaptation; Acclimatization; Natural selection; Species diversity; Food chains; Energy balance; Ecological succession; Effects of polluted environments on organisms; Biological productivity.

See also 47D, 48B, 48G, 57C, 57Y, 57Z, 68, 98D, and 98B.

For effects of extreme environments or stimuli on humans, use 57W.

For the interrelationships of humans and their social environments, use 92.

For the effects of industrial environments on humans, use 57U.

57I-Electrophysiology

Electrical activity associated with living organisms and life processes; Electrophysiologic recording including electrocardiography, electroencephalography, and electromyography; Neural transmission; Intracellular potential; Bioelectricity; Bioluminescence; Responses of organisms to electrical stimulation.

57J-Immunology

Mechanisms of immune responses; Antigens and antibodies; Vaccines; Immune serums; Immunization; Immunopathology; Immunohematology; Immunochemistry; Serology; Immunity; Allergy; Histocompatibility; Autoimmune diseases. HIV/AIDS.

See also 57E and 57K.

57K-Microbiology

Studies of microscopic plants and animals; Vaccine and interferon production; Microbial metabolism and biochemistry.

For diagnosis and therapy of infectious diseases, use 57E.

For disease control and epidemiology, use 57U.

For biotechnology applications, see also field of application.

57L-Nutrition

Processes by which humans assimilate and utilize food substances; Experimental nutrition; Nutritive value of foods; Malnutrition; Diet; Food habits; Nutrition surveys; Nutritional requirements; Clinical nutrition.

For food processing, use 98H.

For animal nutrition related to animal husbandry, veterinary medicine or zoology, use 98E or 57Z.

57M-Occupational Therapy, Physical Therapy, & Rehabilitation

Restoration of normal form and function after injury or physical illness; Occupational therapy; Physical therapy; Vocational rehabilitation.

See also 44K, 92A, 95A.

For mental rehabilitation, use 57T.

For social rehabilitation, use 92C and 91K.

For rehabilitation centers, use 44K.

57N-Parasitology

Parasites and parasitism; Host-parasite interactions; Vectors of parasites; Parasitic diseases; Life cycles of parasites.

See also 57H, 57K, and 57P.

57O-Pathology

Studies of the structural and functional changes in tissues and organs which cause or are caused by diseases, trauma or injuries; Gross pathology; Histopathology; Cytopathology; Pathophysiology; Comparative and experimental pathology; Histological techniques; Autopsy.

For plant diseases, use 98D.

For animal diseases, use 98E.

For diagnosis and treatment of diseases, use 57E.

For immunopathology, use 57J.

57P-Pest Control

Agents and methods for the control of plant and animal pests; Pesticides, algicides, herbicides, insecticides, molluscacides, fungicides, rodenticides, etc.; Repellants and attractants; Fumigation and extermination; Traps; Biological pest control.

See also 68E and 98C.

For ecological aspects of pest control, use 57H.

57Q-Pharmacology & Pharmacological Chemistry

Synthesis, composition, properties, and effects of drugs; Pharmacy, Pharmacodynamics.

See also 57Y.

For social effects of drugs, use 91C and 92C.

For radiopharmaceuticals, use 57V.

For business studies of the drug industry, use 96A.

57S-Physiology

Functions of the human organism and its parts and comparative physiology; Metabolism; Endocrinology; Neurophysiology; Respiration; Biological rhythms; Growth; Aging; Regeneration.

See also 57B, 57F, 57J, and 57L.

For plant physiology, use 57C.

For animal physiology, use 57Z and 98E.

For psychophysiology, use 57T and 92B.

For electrophysiology, use 57I.

For pathophysiology, use 57O.

For stress physiology, use 57W.

57T-Psychiatry

Prevention, diagnosis, and treatment of mental, emotional, and behavioral disorders; Psychopathology; Psychoanalysis; Neuropsychiatry; Orthopsychiatry; Psychotherapy; Psychophysiology; Psychophysics.

For psychological mechanisms and processes, use 92B.

57U-Public Health & Industrial Medicine

Protection and improvement of community health; Effects of environments on public health; School and public health programs, services, and education; Health screening; Health statistics; Epidemiology; Toxic and infectious disease control; Preventive medicine; Hygiene and sanitation; Drinking water quality; Industrial hygiene and medicine; Safety engineering; Occupational safety and health; Industrial safety and detection equipment; Site-specific investigations.

See also 94D, 94H, 41I and 68G.

For occupational and for occupational and environmental factors related to health planning, use 44G.

57V-Radiobiology

Biological effects of radiation; Dosimetry; Health physics; Radiation sickness and injury; Radiation hazards; Radiation protection; Radiopharmaceuticals. Includes electromagnetic, ultrasonic, and particle radiation.

See also 68F and 99E.

For radioecology, use 57H.

For nuclear medicine, radiology, and radiotherapy, use 57E.

57W-Stress Physiology

Effects of extreme environments or stimuli on human biological processes; Physiological effects of motion, gravity, sound, temperature, electromagnetic, fields, pressure, sensory deprivation, and fatigue; Acclimatization. Includes aerospace and underwater medicine.

See also 51B, 57H, and 84.

For plants, use 57C.

For animals, use 57Z.

For stress psychology, use 92B or 57T.

57X-Surgery

Treatment of diseases, injuries, and deformities by manual or operative methods; Organ and tissue transplantation; Pre-and post-management of surgical patients; Experimental surgery.

See also 95A and 95B.

For dental surgery, use 57G.

For histocompatibility, use 57J.

57Y-Toxicology

Study of the adverse effects of substances on biological systems and the diagnosis and treatment of toxic diseases; Toxicity studies; Risk assessment of chemicals; Antidotes.

See also 57C, 57Q, 57S and 57Z.

57Z-Zoology

Animal anatomy and physiology; Natural history; Animal behavior; Taxonomy.

See also 47D, 48B, 57Y, and 98F.

For animal models used in biomedical research, use the research discipline.

For laboratory and domesticated animal care, or animal diseases, use 98E.

62-Computers, Control & Information Theory

620-General

Includes computer security; Artificial intelligence; Signal processing (unapplied).

62A-Computer Hardware

Design and development of computers and peripheral equipment, including analog computers, digital computers, hybrid computers, special purpose computers, minicomputers, microcomputers; Computer accessories, supplies and installation; Logic circuits; Computer architecture; Computer network hardware.

For computer hardware applied to a specific application, see the field of application.

For Very Large Scale Integration (VLSI), use 49H.

62B-Computer Software

Computer programming; Programming languages; Compilers; Data base management systems; Software tools; Software reliability; Computer graphics.

For computer software and database development applied to a specific application, see the field of application.

For CAD/CAM, use 41A and 41B.

62C-Control Systems & Control Theory

Theoretical studies of open-loop and closed-loop control systems; Automatic control systems; Principles including adaptive, continuous, digital, distributed parameter, linear, multivariable, nonlinear, optional, predictive, and proportional; Process controllers.

See also 720 General.

For control systems applied to a specific application, see the field of application.

62D-Information Processing Standards

Standards for the use of automatic data processing equipment and systems. Includes standards for hardware, software, applications, and data; Federal Information Processing Standards (FIPS).

62E-Information Theory

Theoretical studies relating to the measurement and transmission of information in a communication channel, including coding theory, information capacity, and detection of signals in noise.

See also 45G.

62F-Pattern Recognition & Image Processing

Includes feature extraction; Image enhancement; Image restoration; Scene analysis; Character recognition; Barcoding; Computer vision.

62R-Applications Software

62S-Data Files

63-Detection & Countermeasures

630-General

Automated access control systems.

For industrial security, see also 940 General.

63A-Acoustic Detection

Techniques and equipment used for the detection and tracking of objects by means of sound waves, including ultrasonic and infrasonic radiation; Sonar.

For acoustic testing, use 94.

For detection techniques applied to chemistry, meteorology, astronomy, oceanography, medicine, and manufacturing, use 99, 55, 54, 47, 57, 41, and 94, respectively.

63B-Electromagnetic & Acoustic Countermeasures

Interception, jamming, antijamming, and deception of acoustic and electromagnetic signals; Techniques to nullify the use of detection, surveillance, guidance, and communication systems; Radar jamming; Chaff; Counter-countermeasures.

See also 74.

63C-Infrared & Ultraviolet Detection

Techniques and equipment for the detection and tracking of objects by infrared and ultraviolet radiation; Infrared night vision devices; Infrared homing.

See also 76B.

For earth resource surveys, use 48C and 98G.

For mapping, use 48I.

For photography, use 82B.

For nondestructive testing, use 94J.

For detection techniques applied to chemistry, meteorology, astronomy, oceanography, medicine, and manufacturing, use 99, 55, 57, 41, and 94, respectively.

63D-Magnetic Detection

Techniques and equipment for the detection of objects by means of magnetic fields.

For geomagnetism, use 48.

63E-Nuclear Explosion Detection

Techniques and equipment for the detection of nuclear explosions at high altitude, underground, and in space. Includes the use of shock waves, earth movement, and measurement of nuclear radiation levels.

See also other applicable subcategories in 63, especially 63I.

63F-Optical Detection

Techniques and equipment for the detection by means of light. Includes the use of binoculars, periscopes, telescopes, and night vision devices for object detection, and smoke particle detectors.

See also 46C.

For detection using only infrared or ultraviolet radiation, use 63C.

For earth resources surveys, use 48C and 98G.

For photography, use 82B.

For detection techniques applied to chemistry, meteorology, astronomy, oceanography, medicine, and manufacturing, use 99, 55, 54, 47, 41, and 94, respectively.

63G-Personnel Detection

Techniques and equipment for the detection of personnel. Includes the use of acoustic, seismic, olfactory, chemical, and optical detectors; Antiintrusion devices; Motion detectors; Security devices.

For military passive defense systems, see also 74I.

63H-Radiofrequency Detection

Techniques and equipment for the detection and tracking by means of radiofrequency waves; Radar; Microwave detection.

See also 76.

For mapping, use 48I.

For detection techniques applied to meteorology, astronomy, oceanography, medicine, and manufacturing, use 55, 54, 57, 41, and 94 respectively.

63I-Seismic Detection

Techniques and equipment for the detection of objects by means of seismic waves.

For earthquake detection, use 48F.

For seismic prospecting, use 48A.

68-Environmental Pollution & Control

680-General

Any study covering multiple types of pollution. Includes broad pollution studies, such as life-cycle analysis of wastes.

68A-Air Pollution & Control

Air pollution from flue gases, exhaust gases, odors, dust, smog, microorganisms, etc.; Control techniques and equipment; Sampling and analytical techniques, and equipment; Waste gas recovery; Biological and ecological effects; Air pollution chemistry; Acid precipitation; Atmospheric motion; Laws, legislation, and regulations; Public administration; Economics; Land use.

See also 43F, 91A, 57, 85, 81, 99A, 99B, and 97R.

For effects on human health, use 68G.

For pesticides and radioactive contaminants, use 68E and 68F respectively.

68B-Noise Pollution & Control

Pollution in the environment by noise from any source including engine noise, traffic and transportation noise, machinery noise, industrial noise, urban noise, sonic boom; Theory and devices for control; Biological and ecological effects; Noise detection; Building technology; Laws, legislation, and regulations; Public administration; Land use.

See also 41I, 43F, 91A, 46A, 57, 85, 89, 94D, and 97R.

For effects on human health, use 68G.

68C-Solid Wastes Pollution & Control

Pollution by solid wastes including garbage, scrap, junked automobiles, spoil, sludge, containers; Disposal methods such as composts or land application, injection wells, incineration, sanitary landfills; Mining wastes; Processing for separation and materials recovery; Solid waste utilization; Recycling; Biological and ecological effects; Superfund (Records of Decision, etc.); SITE technology; Laws, legislation, and regulations; Public administration; Economics; Land use. Includes disposal of concentrated or pure liquids such as brines, oils, chemicals, and hazardous materials.

See also 43F, 91A, 57, 99B, and 97R.

For effects on human health, use 68G.

For the disposal of pesticides and radioactive contaminants, use 68E and 68F.

For the controlled disposal of radioactive wastes from nuclear reactors, use 77G.

68D-Water Pollution & Control

Pollution by municipal wastes, agricultural wastes, industrial wastes, mine wastes, radioactive contaminants; Chemistry and analysis of pollutants; Thermal pollution; Oil pollution; Control techniques and equipment; Sewage treatment; Industrial waste water pretreatment; Hydrology and limnology; Biological and ecological effects; Waste water reuse; Laws, legislation, and regulations; Public administration; Economics; Land use.

See also 43F, 91A, 47, 48G, 57, 97R, 98, 99A, and 99B.

For effects on human health, use 68G.

For pollution by pesticides and radioactive contaminants, use 68E and 68F respectively.

For the design and construction of sewers, and drinking water treatment, use 50B.

68E-Pesticides Pollution & Control

Pollution by insecticides, herbicides, fungicides, rodenticides; Residues; Decomposition studies; Analysis and detection; Soil chemistry and biology; Adverse biological effects; Ecology; Laws, legislation, and regulations; Public administration; Economics.

See also 57, 68A, 68C, 68D, 43F, 91A, 98, and 99A.

For effects on human health, use 68G.

68F-Radiation Pollution & Control

Involves pollution of the environment by particle and electromagnetic radiation from natural and synthetic sources, including neutrons, X-rays, ultraviolet radiation, microwaves, alpha particles; Radon; Sampling and analytical techniques; Fallout; Biological and ecological effects; Laws, legislation, and regulations; Public administration; Economics.

See also 57, 68A, 68C, 68D, 91A, 97R.

For effects on human health, use 68G.

For the controlled disposal of radioactive wastes from nuclear reactors, use 77G.

68G-Environmental Health & Safety

Effects of pollution on public health and safety; Toxicology; Industrial health; Physiology; Psychology; Clinical medicine; Radiobiology; Animals used as research experimental models.

See also 41I, 57, 44G, 68A, 68B, 68C, 68D, 91A, 43F, 94D, and 97R.

68H-Environmental Impact Statements

Only actual draft and final statements are posted in this subcategory. Environmental impact statements describing national effects are posted here and to other appropriate subcategories.

For studies about environmental impact statements, use 680 General.

70-Administration & Management

700-General

Organizational structure and organization theory.

70A-Inventory Control

Inventory analysis; Inventory models; Obsolescence; Repair-replacement tradeoffs; Spare parts; Stock level control; Usage prediction; Warehouse automation; Stockpiling.

70B-Management Practice

Theory and concepts of management including record keeping, planning, scheduling, organization, coordination, decision making, policy making; Productivity management; Cost effectiveness; Systems management; Contact management; Management methods (PERT, PPB, etc.); Management games. Applied studies are classified in the application.

For research management, use 70E.

70C-Management Information Systems

Information systems which include data collection, data processing, and information delivery for use in decision making an evaluation by managers; Manual and automated systems.

See also 88B.

70D-Personnel Management, Labor Relations & Manpower Studies

Selection, recruitment, management, utilization, and evaluation of personnel; Job descriptions; Job analysis; Salary administration; Labor supply; Labor unions; Arbitration and bargaining; Industrial relations; Fringe benefits, and incentives; Manpower allocation requirements and utilization.

For library and information science personnel, use 88D.

For health personnel, use 44P.

70E-Research Program Administration & Technology Transfer

Research management, development, and forecasting; Research contract management; Research needs; Technology transfer and forecasting. Excludes research methods per se. Studies of specific programs are excluded unless they discuss a program at the national level, technology innovation, or trends and impacts of new technology.

70F-Public Administration & Government

National, state, and local government structure, operation, and administration. Operations of government agencies and their interactions; Intergovernmental relations.

See also 43, 91G, and 91H.

70G-Productivity

Productivity of businesses, government, employees, management, and services; Improving quality of work life; Measurement of productivity efficiency and effectiveness; Employee attitudes and motivation, manpower utilization and performance improvement, job satisfaction, job security; Labor-management cooperation, joint committees participative management, job redesign; Alternative work schedules; Incentive plans. Productivity barriers including regulations, obsolete practices, paperwork, and financing methods.

See also 70B, 70D, 70F, 96A, and 96G.

For specific applications of productivity to manufacturing, use 41D and 94.

71-Materials Sciences

710-General

Advanced materials.

See also 41K.

71A-Ablative Materials & Ablation

Physical, mechanical, and structural properties; Performance; Fabrication and manufacturing methods; Equipment directly related to processing; Ablation processes and chemistry; Reentry vehicle heat shields.

For production planning, use 41 and 94.

71B-Adhesives & Sealants

Adhesives; Glues; Binders; Sealants; Seals; Gaskets; Physical, mechanical, and structural properties; Performance; Fabrication and manufacturing; Equipment directly related to processing.

See also 71L and 94G.

For concrete cements, use 50C and 89G.

For propellant binders, use 79A and 81H.

For pollution studies, use 68.

For industry economics and marketing, use 96.

For production planning, use 41 and 94.

71C-Carbon & Graphite

Carbon and graphite fibers and textiles; Charcoal; Carbon black; Carbon and graphite coatings; Industrial diamonds; Physical, mechanical, and structural properties; Performance, fabrication and manufacturing methods; Equipment directly related to processing.

See also 71A, 71E, 71F, 71I, 71L, and 94G.

For carbon and graphite composites, use 71F.

For pollution studies, use 68.

For industry economics and marketing, use 96.

For production planning, use 41 and 94.

71D-Ceramics, Refractories, & Glass

Glasses; Brick; Porcelain; Ceramic coatings; Ceramic fibers; Physical, mechanical, and structural properties; Performance; Fabrication and manufacturing; Equipment directly related to processing; Studies of individual structural members; Cement properties.

See also 71E, 71I, 71L, and 94G.

For concrete and cement used as building materials, use 50C and 89G.

For pollution studies, use 68.

For industry economics and marketing, use 96.

For production planning, use 41 and 94.

71E-Coatings, Colorants, & Finishes

Paints and primers; Varnishes; Corrosion resistant coatings; Coating pigments; Carbon, ceramic, plastic, rubber and metal coatings; Physical, mechanical and structural properties; Performance; Fabrication and manufacturing methods; Equipment directly related to processing; Electroplating; Electrodeposition; Flame and plasma spraying; Vapor deposition.

See also 71G, 71L, and 94G.

For surface treatment not involved with coatings, use 94G.

For dielectric and semiconducting films, use 46 and 49.

For industry economics and marketing, use 96.

For production planning, use 41 and 94.

71F-Composite Materials

Materials composed of two or more physically distinct constituents; Reinforced plastics, graphite or carbon composites; Laminates; Metal matrix composites; Fiber and particulate composites; Physical, mechanical, and structural properties; Performance; Fabrication and manufacturing methods; Equipment directly related to processing; Studies of individual structural members.

See also 71L and 94G.

For wood composites, use 71R.

For concrete and reinforced concrete, use 50C and 89G.

For pollution studies, use 68.

For industry economics and marketing, use 96.

For production planning, use 41 and 94.

71G-Corrosion & Corrosion Inhibition

Unwanted chemical reaction effects on metals; Corrosion of metals; Rusting; Corrosion inhibitors; Corrosion resistant coatings; Corrosion electrochemistry.

See also 71E and 71L.

For concrete corrosion, use 50C and 89G.

71H-Elastomers

Rubbers; Additives; Curing agents; Elastomer polymerization; Physical, chemical, mechanical, and structural properties; Performance; Fabrication and manufacturing methods; Equipment directly related to processing; Studies of individual structural members.

See also 71E, 71I, 71L, 94G, and 99C.

For pollution studies, use 68.

For industry economics and marketing, use 96.

For production planning, use 41 and 94.

71I-Fibers & Textiles

Glass, carbon, ceramic, metal, and polymeric fibers; Threads, yarns, textile, and fiber finishing, including dyeing and sizing; Physical, chemical, mechanical, and structural properties; Performance; Fabrication and manufacturing methods; Equipment directly related to processing; Studies of individual structural members; Flame resistance.

See also 71L and 94G.

For fiber composites, use 71F.

For pollution studies, use 68.

For industry economics and marketing, use 96.

For production planning, use 41 and 94.

71J-Iron & Iron Alloys

Includes steels or alloys containing more than 50% iron. Coatings; Fibers; Extractive metallurgy; Refining; Embrittlement; Physical, mechanical, and structural properties; Microstructure; Phase studies; Performance; Fabrication and manufacturing methods; Equipment directly related to processing; Studies of individual structural members.

See also 71E, 71I, and 71L.

For corrosion, use 71G.

For beneficiation, use 48A.

For pollution studies, use 68.

For industry economics and marketing, use 96.

For production planning, use 41 and 94.

71K-Lubricants & Hydraulic Fluids

Solid and liquid lubricants; Additives; Greases; Drilling fluids; Brake fluids; Physical, chemical, mechanical and structural properties; Performance; Manufacturing; Equipment directly related to processing; Chemical synthesis.

See also 71L and 41L.

For pollution studies, use 68.

For industry economics and marketing, use 96.

For production planning, use 41 and 94.

71L-Materials Degradation & Fouling

Aging; Erosion and cavitation erosion; Wear; Weathering; Decay; Effects of radiation on materials; Biodeterioration, including fungus deterioration.

See also 71C, 71D, 71F, 71H, 71I, 71J, 71K, 71N, and 71R.

For nuclear reactor materials degradation, see also 77I or 77J. If concerned with nuclear propulsion, use 81I.

71M-Miscellaneous Materials

Materials not included in another group, including leather, fur, refrigerants, and waxes; Physical, mechanical, and structural properties; Performance; Fabrication and manufacturing methods; Equipment directly related to processing; Studies of individual structural members.

See also 94G.

For pollution studies, use 68.

For industry economics and marketing, use 96.

For production planning, use 41 and 94.

71N-Nonferrous Metals & Alloys

Includes studies not specifying the type of metal. Coatings; Fibers; Extractive metallurgy; Refining; Embrittlement; Physical, mechanical, and structural properties; Microstructure; Phase studies; Performance; Fabrication and manufacturing methods; Equipment directly related to processing; studies of individual structural members.

See also 71E, 71I, and 71L.

For metal fabrication, use 94G.

For corrosion, use 71G.

For beneficiation, use 48A.

For pollution studies, use 68.

For industry economics and marketing, use 96.

For production planning, use 41 and 94.

71O-Plastics

Additives; Curing agents; Plastic coatings; Plastic polymerization; Physical, chemical, mechanical, and structural properties; Performance; Fabrication and manufacturing methods; Equipment directly related to processing; Studies of individual structural members.

See also 71E, 71L, 94G, and 99C.

For plastic composites, use 71F.

For polymeric fibers, use 71I.

For pollution studies, use 68.

For industry economics and marketing, use 96.

For production planning, use 41 and 94.

71P-Refractory Metals & Alloys

Includes only the following metals and alloys having more than 50% of these metals: iridium, molybdenum, niobium (columbium), osmium, rhenium, tantalum, and tungsten. Coatings; Fibers; Extractive metallurgy; Refining; Embrittlement; Physical, mechanical, and structural properties; Microstructure; Phase studies; Performance; Fabrication and manufacturing methods; Equipment directly related to processing; Studies of individual structural members.

See also 71E, 71I, and 71L.

For metal fabrication, use 94G.

For corrosion, use 71G.

For beneficiation, use 48A.

For pollution studies, use 68.

For industry economics and marketing, use 96.

For production planning, use 41 and 94.

71Q-Solvents, Cleaners, & Abrasives

Cleaning compositions; Solvents; Detergents; Soaps and abrasives; Cleaning action of these materials; Physical and chemical properties; Performance; Manufacturing; Equipment directly related to processing.

For cleaning techniques, use 94G.

For pollution studies, use 68.

For industry economics and marketing, use 96.

For production planning, use 41 and 94.

71R-Wood & Paper Products

Sawing and milling; Lumbering; Plywood, particle and fiber board; Wood product fabrication; Pulping, papermaking, and conversion processes; Physical, chemical, mechanical, and structural properties; Performance; Fabrication and manufacturing methods; Equipment directly related to processing; Studies of individual structural members.

See also 94G.

For forestry and tree production, use 48D.

For pollution studies, use 68.

For industry economics and marketing, use 96.

For production planning, use 41 and 94.

72-Mathematical Sciences

720-General

72B-Algebra, Analysis, Geometry, & Mathematical Logic

Algebra and number theory, including field theory (algebra), group theory, ring theory; Analysis, including calculus of variations, complex variables, differential equations, Fourier analysis, functional analysis, functions (mathematics), measure, and integration; Geometry, tensor analysis, and topology; Mathematical logic, including foundations of mathematics, lattices (mathematics), metamathematics, and set theory.

For applications of mathematics, see the appropriate category of application.

72E-Operations Research

Game theory; Queueing theory; Management games; Mathematical models; Mathematical programming, Network flows; Search theory.

See also Managerial practice, 70B.

For operations research applied to a specific application, see the field of application.

72F-Statistical Analysis

Analysis of variance; Correlations techniques; Discriminate analysis; Distribution theory; Experimental design; Factor analysis; Nonparametric statistics; Probability theory; Regression analysis; Statistical decision theory; Statistical inference; Statistical tests; Stochastic processes.

For statistical analysis applied to a specific application, see the field of application.

74-Military Sciences

740-General

74A-Antiaircraft Defense Systems

Tactical and terminal countermeasures against attacking aircraft that includes tracking and computing equipment, antiaircraft guns, rockets, and missiles.

For specific missiles and rockets, use 75.

74B-Antimissile Defense Systems

Point and terminal defense and countermeasures against air-, surface-, or underwater-launched missiles, bombardment satellites. Includes land based and shipborne tracking and computing systems; Strategic Defense Initiatives (SDI), Star Wars; ballistic missile defense.

74C-Antisubmarine Warfare

Operations conducted against submarines, their supporting forces and operating bases. Include air, surface, and underwater operations.

See also 63.

74D-Chemical, Biological, & Radiological Warfare

Design, development, and utilization of chemical, biological, and radiological weapons; Production, generation, and stability of lethal and nonlethal agents; Biological agents including anticrop and defoliating agents.

For nuclear weapons, use 74H.

74E-Logistics, Military Facilities, & Supplies

Procurement, storage, distribution, issue, repair, replacement of military equipment; Deployment of troops and cargo; Industrial mobilization; stock level controls and inventory techniques; Defense conversion; Downsizing; Base closures; Force reduction; Dual Use Technology; Continuous Acquisition and Life-cycle Support (CALS), formerly Computer Aided Acquisition and Logistics Support.

For related civilian studies, use 70 and 94.

74F-Military Intelligence

Techniques for collecting, evaluating, and disseminating information concerning foreign nations. Includes damage assessment; Surveillance and reconnaissance systems.

74G-Military Operations, Strategy, & Tactics

Joint and combined operations, campaigns, battles, invasions, theater operations; Planning analysis, appraisal, and threat evaluation; Methods of attack and support; Armed Forces maneuvers; Limited and unconventional warfare; Sabotage, insurgency, and counterinsurgency; Guerrilla warfare; Psychological and cold warfare.

74H-Nuclear Warfare

Design, development, and applications of nuclear weapons and devices; Studies of the physical effects of nuclear weapons; Arms control.

For nuclear guided missile warheads, use 75F.

74I-Passive Defense Systems

Systems, structures, and devices to provide area monitoring security and denial. Includes camouflage, barbed wire, minefields, warning systems, barriers, and other anti-intrusion devices.

For civil defense, see also 91I.

For personnel detection, see also 63G.

75-Missile Technology

750-General

75A-Air & Space-Launched Missiles

Design, construction and performance of missiles launched from aircraft or spacecraft.

75B-Missile Guidance & Control Systems

Techniques for guidance and control of missiles from launching to impact. Includes optical guidance, television guidance, wire guidance, preset and terminal guidance, inertial guidance, command guidance, and homing guidance.

75C-Missile Launching & Support Systems

Missile handling and launching. Includes transportation, storage, and preparation for launching; Air, space, surface, and underwater launching and support equipment and techniques; Checkout equipment and procedures; Guided missile ranges.

75D-Missile Tracking Systems

Techniques and systems for tracking missiles as defensive measures. Can be from surface installations or air and spaceborne platforms.

For antimissile defense systems, use 74B.

75E-Missile Trajectories & Reentry Dynamics

Determination, analysis, and processing of missile trajectory data; Flight path analysis; Impact prediction; Atmospheric reentry. Includes aerodynamic studies.

For spacecraft reentry, use 84D.

75F-Missile Warheads & Fuses

Design and performance of all types of missile warheads and fuzes-chemical, biological, nuclear and explosive.

For rockets, use 79H.

75G-Surface-Launched Missiles

Design, construction, and performance of missiles launched from the ground, surface platforms, vehicles, silos, and surface ships.

75H-Underwater-Launched Missiles

Design, construction, and performance of missiles launched from underwater.

76-Navigation, Guidance, & Control

760-General

76A-Control Devices & Equipment

Navigation and guidance control equipment.

See also 76C.

76B-Guidance Systems

Design, development, and performance of complete guidance systems. Includes integration of specific components and subsystems necessary to assure course positioning.

76C-Navigation & Guidance System Components

Navigation computers; Gyros, radiators, sensors, indicators, etc., used in navigation of aircraft, ships, spacecraft, and ground vehicles.

76D-Navigation Systems

Design, development, and performance of complete navigation systems; Integration of specific components and subsystems necessary in direction finding (position, distance, and course of travel); Global navigation systems.

See also 85F.

77-Nuclear Science & Technology

770-General

Includes nuclear materials management, safeguards, accounting methods.

See also 77I.

77A-Fusion Devices (Thermonuclear)

Theory, design, construction, and operation of devices for producing controlled thermonuclear fusion reactions; Nuclear fusion reactor materials and fuels.

For plasma studies in thermonuclear devices, see also 46G.

77B-Isotopes

Identification, separation, and concentration of radioactive isotopes. Includes isotopic irradiation devices.

For radioactive isotopes polluting the environment, use 68F.

For the use of isotopes in labeling chemical reactions, use 99F.

For the use of isotopes in medical/biological applications, use 57.

77C-Nuclear Auxiliary Power Systems

SNAP technology, both isotopic and reactor; Isotopic power supplies; Small scale electricity generation by nuclear means.

For nuclear propulsion, see the field of application.

77D-Nuclear Explosions & Devices

Explosion effects, including shock waves, ground motion, electromagnetic pulses, primary radiation, injection of charged particles into radiation belts; Testing of nuclear devices (including nuclear simulation using chemical explosives); Peaceful applications (e.g., Plowshare).

For effects on communications and electronics systems, see the field of application.

For military applications, use 74H.

77E-Nuclear Instrumentation

Nuclear radiation detection and measurement devices and systems; Beta particle detectors.

For X-ray detectors, use 46Gen.

For health physics instrumentation, use 57V.

77F-Radiation Shielding, Protection, & Safety

Shielding design, nuclear radiation transport properties of materials, decontamination; Container design and transportation requirements for radioactive materials; Fallout shelters.

See also 91I.

77G-Radioactive Wastes & Radioactivity

Separation, processing, handling, storage, disposal, and reuse of radioactive wastes; Radioactive fallout; Fission products; Man-made or natural radioactivity; Decommissioning.

For radiation pollution, use 68F.

77H-Reactor Engineering & Nuclear Power Plants

Engineering related directly to the design, safety, and operation of a reactor; Research and test reactors. Integrated assemblage, including reactor and turbogenerator equipment, plus control and regulatory devices of a nuclear power plant, either mobile or stationary; Includes site selection and feasibility studies; Engineering aspects of reactor accidents.

See also 77C.

For critical assemblies and reactor simulation, use 77K.

77I-Reactor Fuels & Fuel Processing

Production, testing, design, or reclamation of nuclear fuel materials, reactor fuel elements (includes cladding) and fuel assemblies. Includes nuclear fuel cycle studies for nuclear materials management; Nuclear fuel reprocessing.

For processing of nonrecoverable fuel materials and fuel contaminants, use 77G.

77J-Reactor Materials

Production, testing, design, or reclamation of coolants, control materials, moderators, structural materials such as pipe materials; Shielding materials, and steels. Includes fabricated elements or assemblies and specific configurations.

For the effects of radiation on materials, see also 71L or 71J.

For fuel materials, cladding, or fuel assemblies, use 77I. Excludes power generating equipment and nuclear fusion reactor materials.

77K-Reactor Physics

Reactor kinetics, reactor theory, neutron transport theory, and criticality. Includes critical assemblies and reactor simulators.

79-Ordnance

790-General

79A-Ammunition, Explosives, & Pyrotechnics

Projectiles, fuzes, demolition explosives, detonators, grenades, land mines, high explosives, primers, powder and liquid propellants, flame throwers, and equipment for handling these items; Production, performance, storage stability of incendiaries, pyrotechnics, screening agents (smokes), etc.

For nuclear weapons, use 74H.

For rocket propellants, use 81.

79B-Armor

Design, testing, and performance of armor and armor plate including bullet proof, flak proof, explosion proof, and fragment proof devices and related equipment.

For other types of protective devices, see the application.

79C-Bombs

High-explosive, fragmentation, antipersonnel, armor piercing, incendiary, napalm, general purpose, and similar types of bombs; Bomb handling equipment; Storage.

For bomb directors and bomb release mechanisms, use 79F; For nuclear bombs, use 74H.

79D-Combat Vehicles

Military vehicles including armored wheeled and track-laying vehicles, tanks and reconnaissance vehicles, trucks, gun carriers; Components and accessories.

79E-Detonations, Explosion Effects, & Ballistics

Explosion effects (except nuclear) such as blast, shock waves, detonation waves, cratering, earth motion or movement, heat, etc.; Interior, exterior, and terminal ballistics; The study of motion, behavior, and aerodynamics of projectiles thrown or launched by ordnance projectors; Includes target vulnerability and damage assessment studies, weapons effects.

For nuclear explosion effects, use 77D.

79F-Fire Control & Bombing Systems

Fire control computers, sights, directors, range finders, gunlaying, bombing radar systems, boresighting, bomb releases, and other devices used specifically for directing the firing of weapons or the dropping of bombs.

79G-Guns

Small arms, automatic weapons, antipersonnel weapons, recoiless weapons, mortars, artillery and naval guns, their accessories and components; Gun carriages, gun mounts, remote control equipment, etc.

For ballistic studies, use 79E.

For gun control, social violence, use 92C or 43.

79H-Rockets

Unguided, self-propelled projectiles whose trajectory or course cannot be altered after launch; Ground launched, air launched, or ship launched rockets, launchers, and launch support equipment.

For sounding rockets, use 55D.

79I-Underwater Ordnance

Torpedoes, submarine mines, depth charges, hydrobombs, antisubmarine ammunition, etc.; Launching devices and support equipment.

81-Combustion, Engines, & Propellants

810-General

81A-Combustion & Ignition

Autoignition, ignition, and combustion. Includes flame studies; Combustion products studies; Ignition systems; Combustion chemistry; Flammability studies.

See also 89 and 94H.

81B-Electric & Ion Propulsion

All types of engines deriving power from free ions and electrons. Includes ion, plasma, and arc jet systems; Propulsion by means of solar wind; Laser propulsion.

For electrically propelled surface vehicles, use 85.

81C-Fuel & Propellant Tanks

Design, performance, and testing of fuel and propellant tanks including those for automobiles, petroleum products, and rocket propellants.

81D-Jet & Gas Turbine Engines

Design, performance, and testing of all types of jet and gas turbine engines, their components, engine nozzles. Includes Ramjet, Scramjet, and Turbofan engines, and hydroduct and turbomachinery as well as nonpropulsive turbines.

See also 97L and 51C.

81G-Rocket Engines & Motors

Design, performance, and testing of rocket engines and motors and their components.

81H-Rocket Propellants

Production, handling, stability, and performance of liquid, solid, thixotropic, and exotic propellants. Includes fuels, oxidizers, additives, and binders.

For combustion and ignition, use 81A.

81I-Nuclear Propulsion

Design, performance, and testing of nuclear engines for surface, air, and space propulsion.

See also 85.

81J-Reciprocation & Rotating Combustion Engines

Design, performance, and testing of reciprocating and rotating engines of various configurations for all types of propulsion. Includes internal and external combustion engines; Engine exhaust systems; Engine air systems components; Engine structures; Stirling and diesel engines.

See also 97L and 85H.

82-Photography & Recording Devices

820-General

82A-Holography

Techniques, materials, and uses of holography and holograms; Acoustic holography.

See also 46C.

82B-Photographic Techniques & Equipment

Photographic techniques, including aerial photography, color photography, astronomical photography, cinematography, photomicrography, Schlieren photography; Cameras, lenses, shutters, projectors, photographic processes, and materials; Microphotography, Photographic copying; Direct recording and reproduction of visual images; Copying, reproduction and replication techniques; Thermography; Lithography, and related arts; Graphic arts, illustrating, visual design.

For photogrammetry, use 48I.

82C-Recording Devices

Techniques and devices for recording other than visual images. Includes disk, magnetic, thermoplastic, electrostatic recording systems, CD-ROM, and playback equipment such as record players, tape recorders, etc.

84-Space Technology

840-General

Extraterrestial biology, chemistry, and medicine.

84A-Astronautics

Space missions; Projects and logistics; Orbital rendezvous; Space exploration; Spacecraft operating problems; Extravehicular activity.

84B-Extraterrestrial Exploration

Space probe exploration; Space landings; Space construction and maintenance; Extravehicular activity on other planets.

84C-Manned Spacecraft

Design and construction of manned spacecraft, space stations, aerospace planes and their components.

84D-Spacecraft Trajectories & Flight Mechanics

Determination, analysis, processing of spacecraft trajectory data; Space mechanics; Orbital calculations; Flight path analysis; Atmosphere entry; Reentry dynamics.

84E-Space Launch Vehicles & Support Equipment

Handling and launching, including transportation, storage, preparation for launching, countdown, launching equipment, checkout equipment, ground support equipment, and information systems; Spacecraft tracking systems; Tracking networks; Recovery support.

84F-Space Safety

Safety measures and devices directed toward reducing the hazards of spaceflight.

84G-Unmanned Spacecraft

Design and construction of unmanned spacecraft, including space probes, scientific satellites, military satellites, communication satellites, reconnaissance satellites, and navigational satellites.

For satellites applied to a specific application, see the field of application.

85-Transportation

850-General

85A-Air Transportation

Operation of systems for transport by air; Civil aviation; Airports and airport access; Airline operations; Air routing; Air traffic control systems; Multimodal systems; Aviation safety and aviation accidents; Aircraft fires; Aircraft fuel fires.

See also 43G, 74E, 76, 85D, and 91B.

For design of aircraft and components, use 51 and 81.

For runway construction and design, use 50B.

85C-Metropolitan Rail Transportation
Urban rail transit; Underground and above-ground rapid transit railways, including subways; Automated guideway transit systems; Tracked air cushion vehicles.

See also 85I and 91B.

85D-Transportation Safety
Safety and accidents involving air, land, and water transportation; Accident studies and prevention; Alcohol related studies; Breakaway barriers and structures; Standards and testing of components and equipment; Crashworthiness; Traffic safety; Collision research; Safety equipment and devices.

See also 91B.

For pipeline accidents, use 85E.

85E-Pipeline Transportation
Transportation of liquids, gases, and slurries throughlong-distance pipelines; Accidents and safety.

85F-Global Navigation Systems
Worldwide navigational aids to transportation; Global positioning system (GPS).

See also 76D.

85G-Marine & Waterway Transportation
Shipping; Safety and accidents; Safety equipment; Cargo handling and equipment; Cargo movement; Passenger movement; Traffic control; Boating; Trade routes; Shipborne containerization.

See also 43G, 74E, 76, and 85D.

For marine engineering, use 47A.

For waterway engineering, use 50B.

85H-Road Transportation
Passenger and cargo movement; Design and standards for vehicles and components; Motor vehicle engine studies; Safety engineering; Safety devices; Traffic and road safety; Collision research; Accident studies; Highway traffic; Traffic engineering; Passenger and cargo vehicles; Trailers; Motorcycles; Bicycles and bikeways; Hiking trails.

See also 43G, 50A, 74E, 81J, 85D, and 91B.

85I-Railroad Transportation
Safety and accidents; Safety equipment; Cargo handling and equipment; Cargo movement; Passenger movement; Traffic control; Terminals; Amtrak; Track studies; Rolling stock; Scheduling; Railroad engineering and equipment.

See also 43G, 85D, and 91B.

88-Library & Information Sciences

880-General
Includes general studies about microforms; Film readers; Copyrights; Privacy Act; Report writing.

88A-Operations & Planning
Acquisitions, classification, cataloging, abstracting, and indexing; Circulation and reference systems; Information services; Interlibrary loans; Distribution; Manual and computerized information retrieval; Individual libraries and information center.

For library or information networks, use 88B.

88B-Information Systems
Library and information networks; Operations and planning of these systems; File maintenance and management; Database management; Information superhighway, National Information Infrastructure; Applied information systems (Management, medical, transportation, etc.)

See also 44T, 62, and 70C.

For database management, use 62B.

For communications and computer networks, use 45C.

For geographic information systems, see 48I.

88C-Marketing & User Services
User needs, surveys; Promotions; Fees.

88D-Personnel
Training and education; Selection; Management; Performance; Schools and accreditation.

See also 70D.

88E-Reference Materials
Bibliographies; Directories; Glossaries; Catalogs; Thesauri; Indexes; Abstract and title periodicals.

89-Building Industry Technology
Includes fires in buildings.

890-General
Includes fires in buildings.

89B-Architectural Design & Environmental Engineering
Architecture; Human engineering; Site surveys; Interior design; Lighting; Heating, ventilating, and air conditioning; Heat loss studies. Includes environmental engineering equipment.

See also 97J and 94E.

89C-Construction Management & Techniques
Excavation; Fabrication (presite and onsite); Construction techniques; Reconstruction; Management including planning, manpower, and labor studies.

89D-Structural Analyses
Dynamics and statics of structures and structural members including kinetics, kinematics, vibration and stress analyses; Induced environmental stresses including earthquakes, wind, and flood; Foundation stresses; Soil-structure interactions.

89E-Building Standards & Codes
Standards and codes for buildings, equipment, components, and materials.

89G-Construction Materials, Components, & Equipment
Plumbing; Wiring; Insulation; Doors and windows; Walls; Joints; Beams; Construction equipment such as bulldozers and cranes. Includes flammability and fire studies. Cement and concrete.

See also 50C.

For cement properties, see also 71D.

89H-Building Equipment, Furnishings, & Maintenance
Equipment including security alarms (i.e. Burglar alarms), elevators, and fire safety devices; Furnishings, including major household appliances, rugs, and furniture; Maintenance, including repair, pest control, and cleaning.

For environmental engineering equipment, use 89B.

90-Government Inventions for Licensing

For patents and patent applications only (will be labeled as such in the report title); Not for bibliographies.

900-General

Computer software.

90A-Mechanical Devices & Equipment

Devices and equipment for fuel ignition; Heating, illumination, and refrigeration; Cleaning; Printing; Product handling and transportation; Sprinklers; Fire extinguishers; Safety; Motor and other land vehicles; Earthworking and excavating; Tools; Jacks; Hydraulic and pneumatic systems; Power transmissions; Couplings, fasteners, and joints; Piping; Drilling and mining; Separators; Locks; Sewing machines; Winding and reeling; etc.

For metal shaping and forming, use 90E.

For medical equipment, use 90D.

90B-Chemistry

Organic and inorganic compounds; Batteries; Electrochemistry; Hydrocarbons; Lubricating compositions; Propellents and rocket fuels; Acids; Polymers; Plastics; Inks; Bleaching; Dyeing; Fertilizers; Food fermentation; Sugar and starch; Paper making; Textiles; Paints; Coatings (except metal coatings); Chemical reactors; etc.

90C-Nuclear Technology

Reactors; Radioactive materials; Nuclear instrumentation; Nuclear radiation safety; Nuclear power plants and reactor engineering; Nuclear fusion; Particle accelerators; Plasma devices; etc.

90D-Biology & Medicine

Drugs; Cosmetics; Prosthetics; Medical equipment; Pesticide biology; Biological laboratory equipment; Life support equipment.

90E-Metallurgy

Metal stock; Metal coatings; Molding, shaping, and treating processes; Laminating; Glasses; Material shaping; Sheet metal and wire working; Bonding and joining; Cutlery; etc.

For use of mechanical equipment, use 90A.

90F-Electrotechnology

Antennas, circuits, and electromechanical devices; Electron tubes; Optoelectronic devices; Power and signal transmission devices; Resistive, capacitive and inductive components; Semiconductor devices; Information transmission, storage, and retrieval; Communications; etc.

90G-Instruments

Photographic equipment; Measuring and testing instruments and equipments; Acoustic devices; Etc.

For nuclear instruments, use 90C.

90H-Optics & Lasers

Optical materials, components, equipment, and systems; Infrared, visible, ultraviolet, and X-ray lasers; Masers.

90I-Ordnance

Production and performance of projectiles, fuzes, explosive materials, pyrotechnics, and weapon systems (not limited to military applications); Ordnance storage systems; Fire control systems; Weapons delivery systems; Missiles, rockets, and propellants directly related thereto; Weapons carriers (tanks, aircraft ships, etc); Guns; Laser weapons; Bombs.

90J-Food Technology

Pasteurizing, curing, canning, dehydrating, freezing, irradiation, freeze drying, etc., of foods and other agricultural products; Sanitation and fumigation of products; Food additives and preservatives; Analysis and inspection of products; Storage, packaging, and display of products; Cooking devices.

For food fermentation, use 90B.

91-Urban & Regional Technology & Development

910-General

Includes energy studies.

91A-Environmental Management & Planning

Air, water, noise, and waste management and control; Monitoring services; Solid wastes and recycling;
Solid waste landfills; Water quality management; Environmental surveys; Design and operation of sewer systems (combined, etc.); Water supplies and services; Excludes natural resource management.

See also 68 and 43F.

91B-Transportation & Traffic Planning

Planning for modes of public and private, passenger and cargo transporation; Travel patterns and demand; Parking; Traffic engineering, traffic flow and control; Traffic surveys; Highway and street services; Rapid transit systems; Passenger transportation and planning; Pedestrian movement.

See also 43G and 85.

91C-Fire Services, Law Enforcement, & Criminal Justice

Fire, police, and court services and their administration; Law enforcement and criminal justice; Crime and fire prevention; Personnel recruitment, training, and utilization; Parole; Work release; Correctional institutions.

See also 43D.

For criminal justice and corrections, see also 43Gen.

91D-Communications

Use and planning of communications; Mass media, emergency communications, public information.

See also 45.

91E-Housing

Surveys and assessments of existing housing; Planning and development; Building codes; Housing needs; Housing renovation; Public housing.

For design, architectural, or construction related studies, see also 89.

91F-Health Services

Urban health services; Emergency medical services; Mental health services; Nursing homes; Ambulatory health services; Hospital services; Public health access.

See also 43C, 43D, 44 and 91I.

91G-Urban Administration & Planning

General administration and planning; Feasibility studies; Appraisal of real property; Taxation; Land use and zoning; Urban revitalization; Financing.

See also 43 and 70F.

91H-Regional Administration & Planning

General administration and planning for county and regional areas that may also contain urban or urbanized areas; Intergovernmental relations and interactions (State, County, Local); Land use and zoning.

See also 43 and 70F.

For state government administration and planning, use 43.

91I-Emergency Services & Planning

Disaster services; Civil defense; Early warning systems and emergency preparedness for all types of disaster; Emergency weather services; Pollution alerts; Civil disturbances; Ambulance services; Flooding; Disaster relief.

See also 43D, 44, and 91F.

For military passive defense systems, see also 74I.

For personnel detection, see also 63G.

91J-Economic Studies

Economic analyses; Economic development; Industrial development; Economic impacts of development; Population-economy-income studies; Employment and earnings; Property values; Commercial area studies.

See also 43B and 96.

For government financial operations, use 43A, 70F, 91G, and 91H.

91K-Social Services

Child care; Family and youth counseling; Social rehabilitation; Foster homes and adoption; Welfare and public assistance; Financial assistance; Food stamp services; Employment services; Legal services.

See also 43C, 91F, and 92C.

91L-Recreation

Planning and administration; Facilities; Public opinion; Economic and social aspects; Safety aspects; Use of recreational vehicles; Cultural activities; Sports; Parks, including national parks.

92-Behavior & Society

920-General

Includes general overall census studies; Political science.

92A-Job Training & Career Development

Vocational training; On-the-job training; Retraining; Vocational rehabilitation; Use and design of training simulators (including flight simulators) and equipment; Instructional aids; Professional development; Career development.

For curriculum development, use 92D.

92B-Psychology

Human behavior; Personality; Intelligence; Learning ability; Judgement; Motivation; Perception; Job satisfaction; Leadership characteristics; Psychometrics; Adaptability; Social, industrial, group, organizational, interpersonal, and experimental psychology; Clinical psychology; Physiological psychology.

For the measurement of hearing, vision, heart rate, respiration and other physiological responses as related to behavior, use 57T or 57W.

92C-Social Concerns

Sociology and sociometrics; Race relations; Age group and minority group studies; Social rehabilitation of drug abusers, alcoholics, physically, emotionally, and mentally handicapped, offenders, etc.; Cultural and economic deprivation; Social discrimination; Immigration; Demography; Social services, including child care, welfare, counseling, financial assistance, and employment and unemployment services; Attitude studies.

See also 43C, 44, and 91K.

92D-Education, Law, & Humanities

Formal education; School systems; Educational administration; Curricula; Instructional devices and materials, including audiovisual; Teaching methods; Computer-assisted instruction; Laws; Linguistics; Machine translation; Fine arts; Archaeology; History; Anthropology; Humanities; Religion.

92E-International Relations

Political and social indicators; Crises and crisis management; Conflict analysis; Foreign aid; Foreign policy and foreign affairs; International political science; Disarmament and arms control; Espionage; Includes international relationships concerning territorial seas, fishing, extradition, and natural resources.

See also 74H.

For international commerce, use 96C.

94-Industrial & Mechanical Engineering

940-General

Includes bearings; Mechanical elements; Pipes; Tubes; Levers; Cams; Springs; Mechanical joints; Containers and packing materials; Refrigeration systems and equipment; Industrial furnaces and boilers; Heat exchangers; Heat pumps; Heat pipes; Industrial security; Metrology.

For rocket engine components, use 81G; For fuel tanks, use 81C; For cooling towers, use 97J; For nuclear security, use 77Gen.

94A-Production Planning & Process Controls

Materials control; Numerical control and automation; Time and motion studies ; Scheduling; Production controls and programming; Modeling techniques and program controls; Inventory management.

See also 44A, 41A and 41B.

94B-Quality Control & Reliability

Tolerances allocations; Maintainability requirements; Probability of satisfactory performance of components and equipment; Inspection methods; Destructive industrial testing; Reliability theory; Quality assurance.

See also 41E and 41G.

94C-Plant Design & Maintenance

Site selection; Plant design; Layout; Maintenance management; Scheduled, routine, and corrective maintenance.

See also 41H.

94D-Job Environment

Industrial hygiene and occupational diseases and injuries in settings such as factories, and office and commercial buildings; Industrial psychology; Industrial sociology; Workplace layout and design; Worker interactions.

See also 44G, 57U, 41I, and 92B.

For industrial safety engineering and accident prevention, use 94H.

94E-Environmental Engineering

Lighting; Heating; Ventilating; Air conditioning. Includes environmental engineering equipment related to industrial use. Excludes pollution control.

See also 41I, 89B and 97J.

94F-Tooling, Machinery, & Tools

Machine subassemblies; Robots; Robotics; Tools; Machinery, including hoists, conveyors and pumps.

See also 41C and 41J.

94G-Manufacturing Processes & Materials Handling

Fabrication, assembling, cleaning, and finishing; Industrial and manufacturing processes (limited to in-depth studies that directly discuss specific processes); Bonding and joining, including gluing, welding, soldering, and brazing; Materials forming and machining; Heat treatment; Coating processes; Materials handling, including palletizing, conveying, warehousing, storing, containerization, and packaging.

See also 71, 41B, 41E, and 41F.

For processing and packaging of food, use 98H.

For production of materials, use 71.

For chemical engineering and processing, use 99B.

For the beneficiation and processing of minerals, use 48A.

94H-Industrial Safety Engineering

Accident prevention; Safety measures; Fire prevention; Warning systems; Safety equipment, structures, and clothing.

For industrial safety engineering applied to a specific application, use the field of application.

94I-Hydraulic & Pneumatic Equipment

Design, production, performance, and testing of hydraulic and pneumatic systems, accumulators, actuators, compressors, and distribution equipment; Fluidic and flueric devices.

See also 41J.

For hydraulic fluids, see 71K.

94J-Nondestructive Testing

Nondestructive testing having industrial application; Ultrasonic, radiographic, hydrostatic, magnetic, and optical nondestructive techniques and equipment; Nondestructive testing of flaws, thickness, opacity, strength.

For destructive industrial testing, use 94B.

94K-Laboratory & Test Facility Design & Operation

Measuring, testing, and simulation devices. Includes laboratories, test facilities, and test equipment measuring testing and simulation. If the test facility, equipment, etc. is applied to a specific application, use the field of application.

95-Biomedical Technology & Human Factors Engineering

950-General

95A-Prosthetics & Mechanical Organs

Includes materials and equipment going into human bodies, enabling them to function properly, either temporarily or permanently. Artificial limbs and limb braces; Facial prosthetics, including artificial eyes; Dental prosthetics; Mechanical organs and mechanical hearts; Circulatory assist devices; Artificial kidneys, etc.; Biocompatible materials including tissue adhesives, tissue compatible materials, and antithrombogenic materials.

For prosthodontics, use 57G.

95B-Tissue Preservation & Storage

Preservation of organs, tissue, and blood for transplantation or transfusion to living organs;
Blood and tissue banks; Properties and evaluation of preserved and stored materials.

See also 57J, 57S, and 57X.

95C-Biomedical Instrumentation & Bioengineering

Includes materials and equipment used to monitor human body functions. Design, use, and performance of biomedical equipment; Biotelemetry including biotelemetry transducer and transmitter equipment; Hospital equipment and supplies; Dental materials and equipment; Equipment for physiological monitoring; Diagnostic equipment; Biomedical laboratory equipment.

See also 95A.

95D-Human Factors Engineering

Design of tools, instruments, equipment, and machinery with emphasis on optimum utilization by humans; Habitability of work and living space; Ergonomics; Interaction of man and equipment in terms of subsystem and system performance requirements and evaluation. Encompasses manual controls, tactical kinesthesis, and other human sensory modalities involved in operation of equipment and understanding of personnel subsystems; Man-machine systems. Includes anthropometric studies, protective equipment, protective clothing, and life support systems.

95E-Life Support Systems

Equipment and techniques for sustaining life in foreign environments, such as space, underground, and underwater; Closed ecological systems (includes pressure suits, diving gear, and breathing apparatus).

See also 95D.

95F-Bionics & Artificial Intelligence

Study of biological processes in order to develop engineering systems; Simulation of biological processes; Comparative studies of control systems formed by the brain and nervous system; Pattern recognition systems based on biological modes; Biological applications of information theory; Cybernetics.

95G-Protective Equipment

Equipment providing protection against such environmental elements as heat, cold, noise, machinery, and radiation.

For equipment and techniques for sustaining life in environments where normal respiration is not possible, use 95E.

96-Business & Economics

960-General

Includes economic theory; Business and economic census studies; Insurance not covered by another subcategory; Small businesses.

96A-Domestic Commerce, Marketing, & Economics

National and state-level studies; Industrial costs and economics; Economic impact of industries; Economic impacts on industries; Industrial statistics; Agricultural economics; Productivity; Labor supply and demand; Labor costs and economics; Inflation; Economic aspects of unemployment; Employment and unemployment statistics; Wage surveys; United States commerce; Wholesale and retail trade; Domestic market surveys; Business, personal, and property taxes; Income tax data; Franchising.

See also 43B, 70D, 91J, and 98B.

For studies of individual plants or operations, see the field of application.

For economic impacts of individual plants or operations, see the field of application.

For regional development, use 43B and 91J.

96C-International Commerce, Marketing, & Economics

Foreign market surveys and research; International trade; Imports and exports; Customs and tariffs; Multinational businesses; Trends and forecasting.

For international finance, use 96F.

96D-Consumer Affairs

Consumer problems and protection; Truth in advertising; Commercial psychology; Product maintenance and reliability problems; Home appliances safety; Product comparison studies; Flammability studies; Motor vehicle recalls.

96E-Minority Enterprises

Minority owned and operated businesses; Business training of minority groups; Franchising; Equal opportunities in business.

96F-Banking & Finance

Investments; Credit; Banks and trust companies; Mortgage finance; Savings and loan associations; Security and commodity brokerage; Balance of payments; Gold and silver movement; Cash flow; Regulations; International finance.

For government financial operations, use 43A, 70F, 91G, and/or 91H.

96G-Foreign Industry Economic Development

Private and governmental industrial and economic development in foreign countries including industrialized and developing countries; International technology transfer; For foreign market surveys and international trade, use 96C.

96H-Foreign Business & Economics

Foreign and developing countries; Businesses, economic conditions and socioeconomics.

For foreign market surveys and international trade, use 96C.

For social concerns related to economics, see also 92C.

97-ENERGY

970-General

Includes energy source development.

97A-Reserves

Natural reserves; Fuel stockpiles; Mineral and fossil fuel deposits including coal, uranium, petroleum, natural gas, geothermal, peat, and oil shale; Water power potential; Site studies of wind power potential and solar radiation availability.

For individual mine studies, use 48A.

97B-Energy Use, Supply, & Demand

Electric power and fuel consumption and requirements; Supply and demand; Heat use, supply, and demand.

97E-Electric Power Transmission

Electric power distribution; Electric transmission lines and substations; Electric power pools; Wireless energy transmission.

97F-Fuel Conversion Processes

Methods to convert a fuel to a different chemical form including coal gasification and liquefaction; Upgrading fuels by chemical synthesis.

For petroleum refining, oil shale retorting and refining, use 97K and 99B; For environmental studies, use 97R.

97G-Policies, Regulations & Studies

Energy conservation; Licensing; Legislation; Government policies and regulatory controls; Energy goals; Research needs; Energy management, economics, and financing; Depletion allowances and leasing policies; Rates and energy models; Energy shortages; International issues.

97I-Electric Power Production

Design and operation of electric power plants; Commercial, industrial, and residential electric power production; Site surveys; Large-scale nuclear, hydro, solar, geothermal, and fossil fuel electric power plants; Power plant boilers.

Note: Usually restricted to large-scale electric power production.

For small-scale electric power production, use 97N, 97O, or 97P.

For pollution control and environmental impact, use 68 and 97R.

For some nuclear power plant studies, use 77 and 97Q. (97Q should be those that are most pertinent to the use of nuclear technology for energy production.)

97J-Heating & Cooling Systems

Design and operation of space heating and cooling systems and equipment; Furnace and boiler studies when related to energy conservation and energy use; Cooling towers; MIUS technology; Total energy systems.

See also 97N.

97K-Fuels

Production, performance, properties, storage, prices, and transportation of all types of solid, liquid, and gaseous fuels; Chemical composition of fuels; Fuel compatibility; Hydrogen production; Refuse derived fuels; Fuel desulfurization; Oil shale retorting; Petroleum refining; Fuel additives; Growing plants for fuels; Bioconversion and biomass plantations.

See also 48D and 97N.

For fuel tanks, use 81C.

For nuclear fuels, use 77I.

For fuel conversion, use 97F.

For rocket fuels, use 81H.

For supply and demand, use 97B.

For oil and gas drilling and recovery, coal mining and other energy related mining studies, use 48A.

97L-Engine Studies (Energy Related)

Operation and design of engines when related to energy conservation and energy use. Covers turbine, rotary, and reciprocating engines.

See also 81.

97M-Batteries & Components

Electrochemical batteries of all types including alkaline cells, dry cells, metal-air batteries, primary cells, reserve batteries, storage batteries, thermal batteries, wet cells; Battery containers, depolarizers, electrodes, electrolytes, separators, and other components and materials; Battery chargers and testers; Battery electrochemistry.

For thermoelectric and thermionic batteries, use 97O.

97N-Solar Energy

Solar collectors, concentrators, and absorbers; Solar cells; Solar cookers, dryers, furnaces, generators; Solar heat engines; Solar heating and cooling systems; Solar power plants; Solar stills; Solar water heaters; Solar heat storage systems; Solar water pumps; Solar sea power plants; Orbital solar power plants; Optical coatings and filters for solar devices; Solar energy policies, use, supply, trends, and economics.

97O-Miscellaneous Energy Conversion & Storage

Fuel cells; Magnetohydrodynamics; Experimental electric generators; Turbogenerators; Heat storage; Compressed air energy storage; Mechanical conversion; Thermoelectric and thermionic conversion; Photovoltaic conversion (excludes solar cells); Wind power; Tidal power; Nuclear fusion power plants.

For commercial, industrial, and residential use of energy conversion and storage devices, use 97I or 97J.

97P-Geothermal Energy

Geothermal exploration and prospecting methods and equipment; Geothermal resources; Geothermal energy conversion; Geology applied to geothermal systems; Drilling; Reservoirs; Extraction; Site selection; Geothermal power plants; Corrosion studies; Materials used in geothermal systems.

97Q-Selected Studies In Nuclear Technology

Reports assigned to this subcategory are selected for their broad interest to users in the nuclear energy field.

For other nuclear energy subcategories, use 77.

97R-Environmental Studies

Air, noise, water, and solid waste pollution and pollution control from energy resource development, fuel production, energy production, and energy use; Environmental impacts of energy production and use.

See also 68.

98-Agriculture & Food

980-General

98A-Agricultural Chemistry

The application of chemistry and chemical analysis to agriculture; Fertilizer production; Soil chemistry; Chemistry of feeding stuffs; Crop chemistry; Biochemical studies.

For food chemistry, use 98H.

98B-Agricultural Economics

Economics conditions, markets, subsidies, and policies affecting agriculture; Farm management and finance; Land and labor economics; Prices and price control.

See also 96C.

98C-Agricultural Equipment, Facilities, & Operations

Agricultural engineering; Agricultural machinery and tools; Seed preservation; Planting, fertilizing, mulching, weeding, and harvesting; Pest and disease control techniques and equipment; Crop protection; Crop drying and storage; Farm water supplies; Irrigation systems; Farm safety; Farm construction and operation.

For pest control, see also 57P.

For food processing, use 98H.

98D-Agronomy, Horticulture, & Plant Pathology

Field crop production; Cultivation of orchards, gardens and nurseries; Plant biology; Plant breeding, propagation, and hybridizing; Hydroponics.

See also 57C.

98E-Animal Husbandry & Veterinary Medicine

Production and care of domestic and wild animals; Breeding, feeding, management, rearing, testing, and training; Pets; Animal pathology; Toxic effects on domestic animals; Animal quarantine; Disease resistance, control and treatment; Breeding, care, and utilization of laboratory animals.

See also 57Z.

98F-Fisheries & Aquaculture

Fishing, fishing equipment, and shipboard processing of fisheries products; Cultivation of fishes, shellfish, and algae in fresh or salt water for commercial or recreational use; Use of fish ladders and weirs; Sport fishing.

See also 47D, 48B, and 57Z.

For fish processing, use 98H.

98G-Agriculture Resource Surveys

Surveys to scan crop yields, soil moisture content, crop diseases, and forest diseases. Includes fishery surveys; Satellite and aerial surveys.

98H-Food Technology

Pasteurizing, curing, canning, dehydrating, freezing, irradiation, freeze drying, etc., of foods and other agricultural products; Sanitation and fumigation of products; Food additives and preservatives; Analysis and inspection of products; Storage, packaging, and display of products; Kitchen and cooking equipment.

For biochemical studies of foods, see also 57B.

99-Chemistry

990-General

99A-Analytical Chemistry

Techniques and instrumentation for the separation and analysis of individual compounds or specific groups or compounds, both inorganic and organic. Includes qualitative, quantitative, volumetric, gravimetric, optical, spectroscopic; electrochemical, ion exchange, chromatographic analysis; Test methods; Forensic chemistry; Data interpretation; Routine analysis or experimental results.

99B-Industrial Chemistry & Chemical Process Engineering

Techniques, processes, unit operations, and plant equipment that apply to chemical manufacturing, processing, transportation, and storage; Petroleum refining; Desalination technology; Pollution control equipment; Process control technology; Process engineering; Chemical reactors.

For coal gasification and liquefaction processes, see also 97F and 97K.

For specific environmental pollution control, see also 68.

For water purification, see also 50B and 68D.

99C-Polymer Chemistry

Synthesis, properties, reactions and theories of polymers and copolymers. Includes all types of polymerization, curing, crosslinking, reaction kinetics, etc.

For mechanical properties of polymers, use 71O and 71H.

99D-Basic & Synthetic Chemistry

Synthesis, properties, and reactions of inorganic and organic compounds; Studies of individual or specific groups of chemical elements; Molecular structure; Stereochemistry.

For chemical reaction mechanisms between atoms, ions, or molecules, see also 99F.

For spectrum analysis of compounds, use 99A and 99F.

99E-Photochemistry & Radiation Chemistry

Studies involving the interrelationships of electromagnetic or particle radiation and chemical reactions; Studies of radioactive elements and their reactions; Radiochemistry; Photochemical reactions.

See also 55A and 68A.

99F-Physical & Theoretical Chemistry

Physical chemistry; Thermodynamics; Thermochemistry; Colloids and gels; Surface chemistry; Catalysis and catalysts; Electrochemistry; Solutions; Chemical equilibria; Membranes; Reaction kinetics; Quantum mechanics; The mathematical determination of atomic or molecular orbitals, energy levels, or properties; The application of mathematics to chemical systems and electronic spectra, excluding routine analysis or experimental results; Molecular spectra interpretation; Chemical reaction mechanisms in the gas, liquid, or solid phase between atoms, ions, or molecules; Atomic and molecular energy studies; Phase studies of nonmetallic systems; Isotherms; Crystallography.

For advanced materials, use 71Gen or the field of application.

For solid state physics, use 46D.

For thermodynamics, see also 460 General.

Search Guide for the NTIS Database

Index

Abbreviations 8
Accession Numbers (also known as NTIS Order Numbers) 8
Acronyms 8
Biological Species 8
Category Codes with Asterisks (Highlighted Subject Category Codes) 9
Chemical Nomenclature 9
Chemical Trade Names 9
Computer Programs and Products 9
Corporate Sources 9
Data 10
DATA Elements Of The NTIS Database 4
DataStar (DIALOG Corporation) 16
Delimited/Declassified Reports 10
Department of Defense (DoD) Declassified/Delimited Items 10
Developing Countries 10
DIALOG Corporation 18
Document Delivery via NTIS 2
EBSCO Publishing 20
Elsevier Engineering Information Inc. 22
Environmental Impact Statements (EIS) 10
Field Name: Abstract 7
Field Name: Availability Statement 6
Field Name: Contract or Grant Number(s) 6
Field Name: Corporate Source(s) 4
Field Name: Country of Publication 5
Field Name: Descriptors 6
Field Name: Identifiers 6
Field Name: Journal and Database Issue 5
Field Name: Language of Document 6
Field Name: Monitoring Agency Number 6
Field Name: NTIS Order No. 4
Field Name: NTIS Prices 4
Field Name: Pagination or Number of Items 5
Field Name: Personal Author(s) 5
Field Name: Project and Task Numbers 6
Field Name: Report Date 5
Field Name: Report Number 6
Field Name: Subject Category Codes 4
Field Name: Supplementary Notes 6
Field Name: Title 5
Field Name: Title Annotation 7
Field Name: Title Note 5
Foreign Language 10
Foreign Research and Technology 10
Geographical Areas 11
Government-Owned Inventions for Licensing (See also Patents) 11
Health Care/Medicine Subjects 11
Information Product Types 3
Information Sources 3
International Business Information 11
International Sources 3
Journal Reprints 11
Leasing the NTIS Database 2
Maps 11
Non-U.S. Origin Reports 10
NTIS Database and Related Products 2
NTIS Online Searching Help Desk 2
NTIS Subject Categories 8
NTIS Subject Categories - Alphabetical Listing By All Categories 38
NTIS Subject Categories - Alphabetical Listing By Major Categories 33
NTIS Subject Categories - Alphabetical Listing With Scope Descriptions 43
NTIS Subject Categories - Numerical Listing Of Major Categories 65
NTIS Subject Categories - Numerical Listing With Scope Descriptions 66
National Technical Reports Library (NTRL) 14
Online Searching Hints 8
Online Services Access 14
Ovid Technologies 24
Patents 12
Performing Organization(s) 9
ProQuest 26
References, Selected 13
Scope of the Collection 2
SilverPlatter Information, Inc. 27
Sponsoring Agency Keyword Acronyms 12
Sponsoring Organization(s) 10
STN International 29
Subject Category Codes/Classification 8
Subject Coverage 2
Superfund 12
Translations 12
Verbalization 12



U.S. DEPARTMENT OF COMMERCE
National Technical Information Service
Alexandria, VA 22312 703-605-6000

MARVIN07

https://web.archive.org/web/20130501000000*/http://www.ntis.gov/products/ntisdb.aspx July 26, 2024

INTERNET ARCHIVE

SIGN UP | LOG IN UPLOAD Search

ABOUT BLOG PROJECTS HELP DONATE CONTACT JOBS VOLUNTEER PEOPLE

DONATE

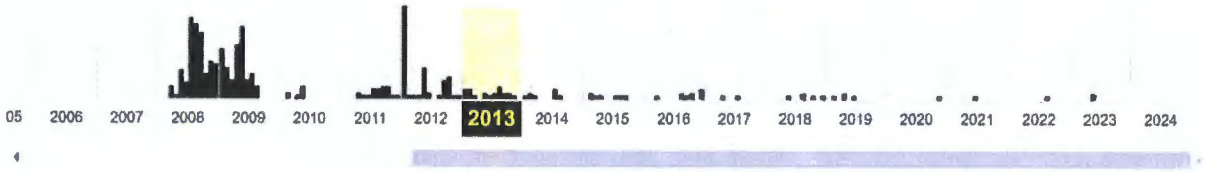
INTERNET ARCHIVE WayBackMachine

Explore more than 866 billion web pages saved over time

http://www.ntis.gov/products/ntisdb.aspx

Calendar · Collections · Changes · Summary · Site Map · URLs

Saved **360 times** between March 17, 2008 and May 6, 2023.



JAN

		1	2	3	4	5
6	7	8	9	10	11	12
13	14	15	**16**	17	18	19
20	21	22	**23**	24	**25**	26
27	28	29	30	31		

FEB

					1	2
3	4	5	6	7	8	9
10	11	12	13	**14**	15	16
17	18	**19**	20	21	22	23
24	25	26	27	28		

MAR

					1	2
3	4	5	**6**	7	8	9
10	11	12	13	14	15	16
17	18	19	20	21	22	23
24	25	26	27	28	29	30
31						

APR

	1	2	3	4	5	6
7	8	9	10	11	12	13
14	15	16	17	18	19	20
21	22	23	24	25	26	27
28	29	30				

MAY

		1	**2**	3	**4**	
5	6	7	8	9	10	11
12	13	14	15	16	17	18
19	20	21	22	23	24	25
26	27	28	29	30	31	

JUN

						1
2	3	4	**5**	6	7	8
9	10	11	12	13	14	15
16	17	18	19	20	21	22
23	24	25	26	27	28	29
30						

JUL

	1	2	3	4	5	6
7	8	9	10	11	12	13
14	15	16	17	18	19	20
21	22	23	24	25	26	27
28	29	30	**31**			

AUG

				1	2	3
4	5	6	7	8	**9**	10
11	**12**	13	14	15	16	**17**
18	19	20	21	22	23	24
25	26	27	28	29	30	31

SEP

1	2	3	4	**5**	6	7
8	9	10	11	**12**	13	14
15	16	17	18	19	20	21
22	23	24	25	26	27	28
29	30					

OCT

		1	2	3	4	5
6	7	8	9	10	11	12
13	**14**	15	**16**	17	18	19
20	21	22	23	24	25	26
27	28	29	30	31		

NOV

					1	2
3	4	5	6	7	8	9
10	11	12	13	14	15	16
17	18	**19**	20	21	22	23
24	25	26	27	28	29	30

DEC

1	2	3	4	5	6	7
8	9	10	11	12	13	14
15	16	17	18	19	20	21
22	23	24	25	26	27	28
29	30	31				

Note

This calendar view maps the number of times **http://www.ntis.gov/products/ntisdb.aspx** was crawled by the Wayback Machine, *not* how many times the site was actually updated. More info in the FAQ.

FAQ | Contact Us | Terms of Service (Dec 31, 2014)

The Wayback Machine is an initiative of the Internet Archive, a 501(c)(3) non-profit building a digital library of Internet sites and other cultural artifacts in digital form. Other projects include Open Library & archive-it.org

Your use of the Wayback Machine is subject to the Internet Archive's Terms of Use.

https://web.archive.org/web/20130707063952/http://www.ntis.gov/products/ntisdb.aspx July 26, 2024

INTERNET ARCHIVE WayBackMachine http://www.ntis.gov/products/ntisdb.aspx Go JUN JUL AUG
360 captures 17 Mar 2008 - 9 Ma 2012 07 2013 2014 About this capture

NTIS Bibliographic Database

Free NTIS Bibliographic Database Search Guide

What is the NTIS Bibliographic Database?

Containing over 2.0 million bibliographic records, the NTIS Bibliographic Database is the preeminent resource for accessing the latest research sponsored by the United States and select foreign governments. The Database represents billions of dollars in research. Contents include research reports, computer products, software, video cassettes, audio cassettes and more. The complete electronic file dates back to 1964. On average, NTIS adds over 30,000 new records per year to the Database. Most records include abstracts.

Access to the NTIS Bibliographic Database is available through:

- **Commercial Services** (access mediums and pricing will vary). Please contact these organizations directly.
- **National Technical Reports Library (NTRL)** – Subscription access to the NTIS Bibliographic Database metadata with links to over 600,000 digitized full-text reports.
- **Direct Lease from NTIS.** Contact the NTIS Office of Product Management (703) 605-6515.

Who Should Access the NTIS Bibliographic Database and Why?

Anyone needing timely, in-depth access to government sponsored research will find the Database invaluable! Use the database to:

- Stay alert of the latest government sponsored research
- Access the subject specific information you need when you need it most
- Retrieve information that is difficult to find from any other source
- Identify valuable research reports, computer products, video cassettes, audio cassettes, and software.

Once identified in the NTIS Bibliographic Database, most items are available for purchase directly from NTIS!

Subject coverage includes

- Administration & Management
- Aeronautics & Aerodynamics
- Agriculture & Food
- Astronomy & Astrophysics Energy
- Atmospheric Sciences
- Behavior & Society
- Biomedical Technology & Human Factors Engineering
- Building Industry Technology
- Business & Economics
- Chemistry
- Civil Engineering
- Combustion, Engine & Propellant
- Communications
- Computers, Control & Info Theory
- Detection & Countermeasures
- Electrotechnology
- Energy
- Environmental Pollution & Control
- Government Inventions for Licensing
- Health Care
- Industrial & Mechanical Engineering
- Library & Information Sciences
- Manufacturing Technology
- Materials Sciences
- Mathematical Sciences
- Medicine & Biology
- Military Sciences
- Missile Technology
- Natural Resources
- Navigation
- Nuclear Science
- Ocean Sciences
- Ordnance
- Photography
- Physics
- Problem Solving Information
- Space Technology
- Transportation
- Urban & Regional Tech. Development
- And Much More..

GRANEK01

FreiDok plus
Universitätsbibliothek Freiburg
universität freiburg

Search New entry Research reports About My FreiDok de | en

Doctoral thesis

High-efficiency back-contact back-junction silicon solar cells



Additional Title

Hocheffiziente rückseitenkontaktierten Silizium-Solarzellen (German)

Granek, Filip [1]

Hide person information

1 Institut für Mikrosystemtechnik

Bibliographic information

Year of publication: 2009
URN: urn:nbn:de:bsz:25-opus-73723
Language: English
Keywords: Solarzelle, Silicium, Fotovoltaik, Online-Ressource, Solar cell, Silicon, Photovoltaics
DDC-classification: Technik

Abstract

English | German

In this thesis high-efficiency back-contact back-junction (BC-BJ) silicon solar cells for one-sun applications were studied. The focus was put on the development of a low-cost and industrially feasible manufacturing technology in order to utilize the full cost reduction potential of this elegant cell structure. At the same time the performance of the developed solar cells was investigated in details by experimental work, analytical modeling and numerical device simulations. The complex and costly photolithography masking steps were replaced by techniques which are of low cost and relevant for mass production, such as screen-printing of the masking layers and local laser ablation of the dielectric and silicon layers. The highest solar cell efficiency of 21.1 % (JSC = 38.6 mA/cm^2, VOC = 668 mV, FF = 82.0 %) was achieved on 160 um thick 1 Ohm cm n-type FZ Si with the designated area of 4 cm^2. A detailed study of the loss mechanisms limiting the efficiency of the developed back-contact back-junction silicon solar cell was performed. The reduction of the cell efficiency was determined to be 3.9 %abs. due to recombination processes, 2.0 %abs. due to optical losses, 0.3 %abs. due to series resistance effects and 0.7 %abs. due to electrical shading. The developed model of the loss mechanisms is a powerful tool for the further optimization study of the solar cell structure. Positive effects of the phosphorus doped n+ front surface field (FSF) on the performance of the BC-BJ solar cells were studied in details. These effects are: (i) Surface passivation and passivation stability: The optimal surface passivation was obtained with a deep diffused Gaussian phosphorus FSF doping profile with sheet resistance of 148 Ohm/sq. In contrast to solar cells without the FSF diffusion, the solar cells with the FSF diffusion profile did not show any performance degradation under exposure to UV illumination. (ii) Lateral current transport. The front diffused n+ layer can be seen as a parallel conductor to the lateral base resistance. This way the lateral base resistance losses can be reduced. (iii) Low-illumination performance: The front surface field improves the performance of the BC-BJ solar cells under low illumination intensity. Therefore the BC-BJ cells with FSF seem to be the best ones suited for achieving a high energy yield when also operating under low illumination intensity.

Description

Comment

Ebenfalls erschienenbei : Verlag Dr. Hut, München, 2009

Files

License



Diss_Granek_Filip_2009.pdf

Download (3.22 MB)

Exam data

Faculty: Technische Fakultät
Supervisor: Paul, Oliver
Date of Exam: 30.07.2009

Request for correction

Please enter your correction request to the metadata of this entry here. Questions regarding the content of this object cannot be answered.

contact (e-mail) Submit

GRANEK01 - 2

GRANEK02

HIGH-EFFICIENCY BACK-CONTACT BACK-JUNCTION SILICON SOLAR CELLS

Dissertation

zur Erlangung des Doktorgrades

der Technischen Fakultät

der Albert-Ludwigs-Universität Freiburg im Breisgau

vorgelegt von

Filip Granek

Fraunhofer Institut für Solare Energiesysteme (ISE)

Freiburg im Breisgau

2009

Dekan:	Prof. Dr. Hans Zappe
Hauptreferent:	Prof. Dr. Oliver Paul
Koreferent:	PD. Dr. Andreas Gombert
Datum der Prüfung:	31 Juli 2009

Table of contents

Table of contents 3

Abstract 9

1 Introduction 11

1.1 Thesis motivation 11

1.2 Thesis outline 12

2 Back-contact silicon solar cells 15

2.1 Introduction 15

2.2 Review of back-contact silicon solar cells 17

2.2.1 Back-contact back-junction (BC-BJ) solar cells 18

2.2.2 Emitter Wrap Through (EWT) solar cells 24

2.2.3 Metallization Wrap Through (MWT) solar cells 25

2.3 Critical parameters of the back-contact back-junction solar cells 26

2.4 Conversion efficiency limitations by intrinsic losses 28

2.4.1 Intrinsic loss mechanisms in silicon 28

2.4.2 Short-circuit current limit 29

2.4.3 Open-circuit voltage limit 31

2.4.4 Efficiency limit 33

3 Measurement methods and numerical simulations 35

3.1 Surface saturation current density 35

3.1.1 Injection dependent lifetime measurements 35

3.1.2 Determination of J_{0s} at low injection 37

3.1.3 Determination of J_{0s} at high injection 38

3.2 Device simulation 39

3.2.1 Two-dimensional numerical simulation 39
3.2.2 One-dimensional numerical simulation 41
3.2.3 Simulation parameters 41
3.3 Measurement table for laboratory size solar cell 43
4 Design and technology 45
4.1 Device structure 45
4.2 n-type bulk Si material 47
4.2.1 Minority carrier diffusion length 49
4.2.2 Influence of the surface potential on the minority carrier lifetime 50
4.3 Processing technology 54
4.4 Metallization 58
4.4.1 Formation of the interdigitated metal grid 59
4.4.2 Thickening of the thin seed metal layer 68
4.5 Solar cell results 70
4.5.1 Laboratory-scale solar cells 70
4.5.2 Industrial-scale solar cells 72
4.6 Conclusions 74
5 Analysis of the laser-fired aluminium emitters 77
5.1 Introduction 77
5.2 Fabrication of LFE and boron emitter cells 78
5.3 Solar cell results 79
5.4 Laser-induced damage zone 80
5.5 Quantum efficiency of the LFE cells 81
5.6 Recombination in the damage zone 82
5.7 Comparison of boron diffusion and LFE emitters 86

5.8 SunsV_{OC} and implied voltage 88
5.9 Optimization of the LFE cells 89
5.10 Conclusion 91
6 Analysis of the loss mechanisms 93
6.1 Introduction 93
6.2 Optical losses 94
6.2.1 Optical losses in the back-contact solar cell 94
6.2.2 Modeling of the optical losses 94
6.2.3 Free carrier absorption 95
6.2.4 Distribution of optical losses 97
6.2.5 Influence of optical losses on the cell efficiency 99
6.3 Recombination losses 100
6.3.1 Modeling of the saturation current densities 100
6.3.2 Influence of recombination losses on the short-circuit current 102
6.3.3 Influence of recombination losses on cell efficiency 103
6.4 Electrical shading 104
6.4.1 Increased lateral transport distance for the minority carriers 104
6.4.2 Light beam induced current mapping 105
6.4.3 LBIC line scans 106
6.4.4 Influence of the electrical shading on the cell efficiency 107
6.5 Resistive losses 107
6.5.1 Modeling of series resistance losses 107
6.5.2 Influence of series resistance losses on cell efficiency 110
6.6 Adding up the individual loss mechanisms 111

6.7 Conclusions 115

7 Front surface passivation using a front surface field 117

7.1 Introduction 117

7.1.1 Surface recombination 117

7.1.2 Surface passivation methods 119

7.2 Influence of the front surface field diffusion profile on the solar cell performance 120

7.3 Surface passivation quality for different FSF diffusion profiles 123

7.3.1 Processing of test structures for the determination of J_{0e} 124

7.3.2 Determination of J_{0e} under high and low injection 127

7.3.3 J_{0e} for different FSF diffusion profiles 128

7.4 Solar cells with different FSF diffusion profiles 131

7.4.1 Solar cell results 131

7.4.2 Analysis of the open-circuit voltage 132

7.4.3 Internal quantum efficiency 133

7.5 Stability of the front surface passivation under UV-light exposure 134

7.5.1 UV-light influence on the front surface passivation 134

7.5.2 Lifetime test structures 135

7.5.3 Solar cell results 137

7.5.4 Regeneration of the UV-degraded solar cells 139

7.6 Conclusion 141

8 Lateral current transport via front n^+ diffused layer 143

8.1 Introduction 143

8.2 Lateral current transport of majority carriers 144

8.3 Variation of the pitch 147

8.4 Solar cell results 148

8.5 Short-circuit current analysis 149
8.6 Fill factor and series resistance 150
8.6.1 Fill factor 150
8.6.2 Pseudo fill factor 150
8.6.3 Conductivity modulation 152
8.6.4 Series resistance 153
8.7 Simulations of the lateral current flow of the majority carriers 154
8.8 Conclusions 157
9 Low-illumination characteristics 159
9.1 Introduction 159
9.2 Analyzed solar cells and methodology 160
9.3 Non-diffused surfaces 162
9.4 Floating emitters 166
9.5 Front surface fields 169
9.6 Conclusions 172
10 Summary and outlook 175
Zusammenfassung und Ausblick 179
Symbols, acronyms and physical constants 183
Bibliography 189
List of publications 203
Acknowledgements 207

Abstract

In this thesis high-efficiency back-contact back-junction (BC-BJ) silicon solar cells for one-sun applications were studied. The focus was put on the development of a low-cost and industrially feasible manufacturing technology in order to utilize the full cost reduction potential of this elegant cell structure. At the same time the performance of the developed solar cells was investigated in details by experimental work, analytical modeling and numerical device simulations. The complex and costly photolithography masking steps were replaced by techniques which are of low cost and relevant for mass production, such as screen-printing of the masking layers and local laser ablation of the dielectric and silicon layers. The highest solar cell efficiency of 21.1 % (J_{SC} = 38.6 mA/cm^2, V_{OC} = 668 mV, FF = 82.0 %) was achieved on 160 µm thick 1 Ω cm n-type FZ Si with the designated area of 4 cm^2. A detailed study of the loss mechanisms limiting the efficiency of the developed back-contact back-junction silicon solar cell was performed. The reduction of the cell efficiency was determined to be 3.9 % abs. due to recombination processes, 2.0 % abs. due to optical losses, 0.3 % abs. due to series resistance effects and 0.7 % abs. due to electrical shading. The developed model of the loss mechanisms is a powerful tool for the further optimization study of the solar cell structure. Positive effects of the phosphorus doped n^+ front surface field (FSF) on the performance of the BC-BJ solar cells were studied in details. These effects are: (i) *Surface passivation and passivation stability:* The optimal surface passivation was obtained with a deep diffused Gaussian phosphorus FSF doping profile with sheet resistance of 148 Ω/sq. In contrast to solar cells without the FSF diffusion, the solar cells with the FSF diffusion profile did not show any performance degradation under exposure to UV illumination. (ii) *Lateral current transport:* The front diffused n^+ layer can be seen as a parallel conductor to the lateral base resistance. This way the lateral base resistance losses can be reduced. (iii) *Low-illumination performance:* The front surface field improves the performance of the BC-BJ solar cells under low illumination intensity. Therefore the BC-BJ cells with FSF seem to be the best ones suited for achieving a high energy yield when also operating under low illumination intensity.

1 Introduction

1.1 Thesis motivation

Today's most used form of energy is fossil energy. However this form of energy is based on limited resources and produces harmful emissions. The climate change caused by the emission of the greenhouse gases, as well as the potential of military conflicts over the remaining limited reserves of the fossil fuels, are two of the major problems, which the humanity is facing at the moment. Therefore the transition from the fossil energy sources to the clean and renewable energy sources is at present one of the greatest challenges for the mankind.

The Earth receives incoming solar radiation with the power of 174×10^{15} W from the Sun. Thus, in just one hour our planet receives enough energy from the Sun, to cover the present global annual energy consumption. Solar irradiation energy is an abundant and widely available source of energy. The solar light can be directly converted into electricity by the photovoltaic cells. During its operation, a solar cell does not produce any emissions or noise. Therefore photovoltaics is a very promising technology in satisfying the future demand for the environmentally friendly energy in a sustainable way.

The production of solar cells is growing rapidly, with an average annual growth rate of 35 % since 1998 [1]. By the end of 2007 the cumulative installed capacity of the photovoltaic systems reached 9.2 GW. Silicon solar cells dominate the market of photovoltaic solar cells and are likely to maintain its dominant market share in the coming years [2]. However the costs of energy produced by photovoltaics are still too high. Therefore the successful dissemination of photovoltaics can be only achieved by further reduction of the manufacturing costs of the photovoltaic systems.

A high impact on the lowering of the manufacturing costs is achieved by improving the efficiency of the silicon solar cells. The progress in the technology of the silicon solar cell enables manufacturing of more advanced and highly-efficient cells. In mass production of the solar cells for one-sun applications, the highest conversion efficiencies of above 22 % are achieved using a structure of a back-contact back-junction solar cells [3]. However since this cell structure is complex, its production is challenging and involves multiple masking steps, which should be able to create small feature sizes and be very well aligned to each other. Photolithography masking, a technology widely used in microelectronics, would meet the above mentioned

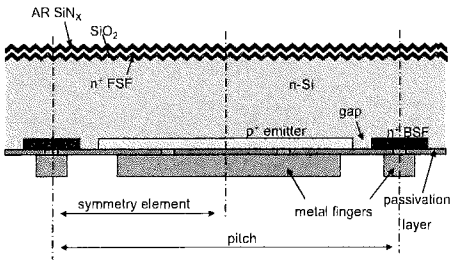
requirement perfectly. However due to its high costs, the application of photolithography is only allowed to the production of the small area concentrator solar cells. Production of the large-area one-sun back-contact back-junction solar cells requires an appropriate low-cost manufacturing technology in order to be able to produce it cost effectively.

Due to the potential of reaching the high-device efficiencies with the low-cost manufacturing technology, the present thesis focuses on the back-contact back-junction silicon solar cell structure. An industrially feasible manufacturing technology of this cell structure is developed. Moreover, based on the presented advanced characterization and modeling of the developed solar cells, further increase of the device efficiency and lowering of its manufacturing costs is possible.

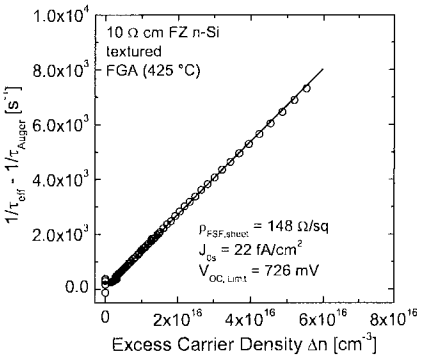
1.2 Thesis outline

The operating principles and the technology of the silicon solar cell are presented in references [4], [5], [6].

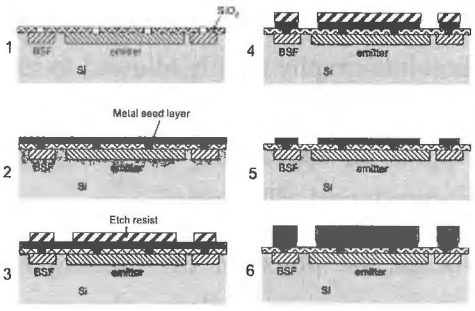
Chapter 2: The thesis starts with a review of advantages and challenges related to the back-contact solar cell structures. Different types of the back-contact solar cells are introduced and a review of the state-of-the-art technology is given. The critical parameters of the back-contact back-junction solar cells are discussed.



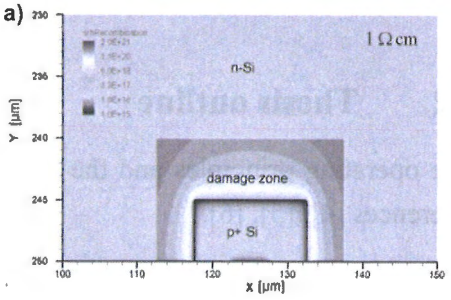
In **chapter 3** two methods for determination of the surface saturation current density under low and high injection are presented. Moreover, the process of the numerical simulations of the back-contact back-junction solar cells using one and two-dimensional simulations is described.



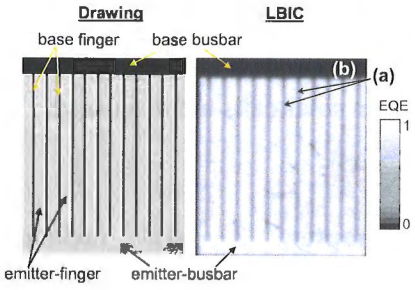
Chapter 4: The technology of the back-contact back-junction silicon solar cells, developed in this work, is presented. The starting material for the cells, n-type silicon material is characterized. Different methods for the formation of the interdigitated contact grid are described in detail. The best results of the developed small, laboratory-size and large, industrial-size solar cells are presented.



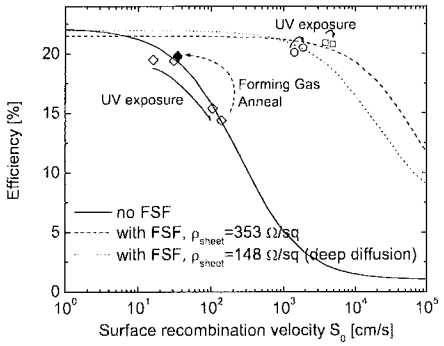
In **chapter 5** the local laser-fired aluminium emitter (LFE) process, an alternative process to boron emitter diffusion, is investigated. The model of the LFE emitters, which includes a laser-induced damage zone, is analysed using a two-dimensional simulation and compared with the experimental solar cell results.



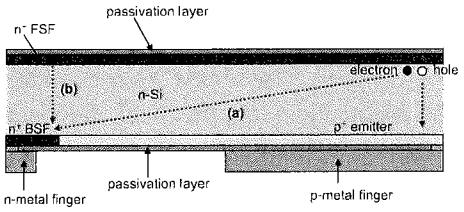
A detailed analysis of the loss mechanisms in the back-contact back-junction silicon solar cells is presented in **chapter 6**. Four main loss mechanisms in the BC-BJ solar cells are described: series resistance, optical losses, recombination losses and electrical shading. The influence of each of the loss mechanisms on the cell efficiency is studied.



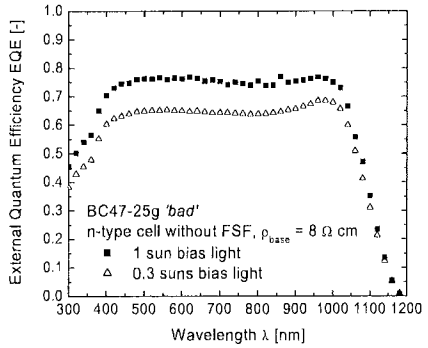
Passivation quality of the different phosphorus-doped front surface field diffusion profiles is analyzed in **chapter 7**. The dark saturation current density of different FSF diffusion profiles is determined under low and high injection. Stability of the test samples and the solar cells under UV exposure is investigated.



Chapter 8: The influence of the large pitch of the n- and p-contact fingers, which is in the range of millimetres, on the series resistance is studied. The application of a phosphorus-doped front surface field (FSF) reduces significantly the lateral base resistance losses. This additional function of the phosphorus-doped FSF is analysed using a comparison between numerical simulation and experimental results.



Chapter 9: The dependence of current and voltage output of three structures of high-efficiency back-junction back-contact silicon solar cells on illumination densities was analyzed in detail. It was shown that, the n-type cell structure with n^+ front surface field enables highest energy yield at low illumination intensity conditions.



2 Back-contact silicon solar cells

The advantages and challenges related to the back-contact solar cell structures are presented. Different types of the back-contact solar cells are introduced and a review of the state-of-the-art technology is given. The influence of the bulk lifetime and the front surface recombination velocity on the efficiency of the back-contact solar cells is discussed. The calculation of the conversion efficiency limit of crystalline silicon solar cells is presented.

2.1 Introduction

Back-contact solar cells exhibit both polarities of the metal electrodes (emitter and base electrodes) on the back cell side. Due to this fact the back-contact solar cells exhibit some major advantages over the conventional solar cell with metal contact on the front side. The advantages are:

- Zero shading due to absence of the metallization grid on the front side. This leads to an increased short-circuit current (J_{SC}) of the cell;
- Due to the absence of the front side metal grid, the front surface can be optimized for optimum light trapping and surface passivation properties, without having to allow for the low contact resistance. This way the front surface recombination can be reduced and light trapping improved;
- Reduction of the series resistance of the metallization grid. Both contact grids are placed on the rear side, therefore the metal finger width is not limited by its shading properties;
- Potentially easier and fully automated co-planar interconnection of the back-contact solar cells in the module assembly process. Recently a novel inline assembly of the solar modules with the back-contact solar cells has been introduced by Späth et al. [7];
- The solar cell packaging density in the solar module can simultaneously be increased, thereby increasing the total area efficiency of the module. A module with back-contact solar cells with a record efficiency of 20.1 % was recently presented by De Ceuster et al. [3].
- Attractive, uniform appearance of the finished modules, which is especially of importance in the building integrated photovoltaics (BIPV).

Thanks to the above mentioned advantages the conversion efficiency of the back-contact solar cells is potentially increased compared to conventional solar cells. Also the costs of the photovoltaic energy produced by the module with back-contact solar cells can be therefore reduced.

However, there are also some challenges and risks related to the back-contact solar cell structure. There challenges and risks are:

- The processing of back-contact solar cells requires a few structuring steps. This makes the processing procedure more challenging and complicated than in the case of the conventional solar cells;
- Risk of fatal shunting between the p- and n- electrodes due to errors in the masking processes. Therefore the requirements of high positioning accuracy and resolution are imposed on the masking steps. That results in an increase of the cost of these processes;
- If the analyzed back-contact solar cell structure possesses all collecting p-n junction on the back side (back-contact back-junction solar cell structure), then a high minority carrier lifetime in the base material is required in order to enable high solar cell efficiencies. Therefore the starting silicon material needs to be of high quality and its quality needs to be maintained during the whole solar cell processing sequence;
- Simultaneously the front surface recombination velocity needs to be kept low in the finished device in order to enable high efficiencies. More information on the issues of the minority carrier lifetime in the base material and the surface recombination velocity are presented in section 2.3.

The high material quality and the complicated processing technology result in the increase of the manufacturing costs. Therefore the efficiency of the processed back-contact solar cell needs to be high, in order to balance the increased costs.

The issues of the complicated processing technology and the requirement of reaching high conversion efficiencies are addressed in this work. In the following chapters a development of a high-efficiency back-contact back-junction solar cell structure using industrially applicable processing technology, including the masking technology, together with an advanced solar cell characterization are presented. However before going into the results of the solar cells developed in this work, a review of the back-contact silicon solar cell will be given in the next section.

2.2 Review of back-contact silicon solar cells

A conventional solar cell is presented in Figure 2-1. This solar cell possesses metal contact on both cell sides. The cell structure shown in Figure 2-1 is a passivated emitter rear locally diffused (PERL) solar cell structure, which enabled reaching the highest efficiency of the silicon solar cell under one-sun illumination intensity. The record efficiency of 24.7 % was demonstrated by Zhao et al. [8] on monocrystalline silicon. Using mulitcrystalline silicon the record efficiency of 20.3 % was obtained by Schultz et al. [9]. These cells feature: a selective doping profiles underneath metal contacts for low contact recombination, passivated front and rear surfaces, well textured front surface with an antireflection coating for low front surface reflection and flat, highly reflective rear for light-trapping, low front contact shading. These are the required ingredients for a high-efficiency design and they are also applicable for the back-contact back-junction cell structure. A review of the recent activities in the industrial application of high-efficiency silicon solar is given by Glunz [10], [11].

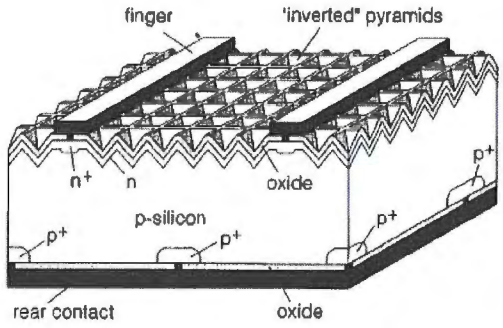


Figure 2-1 The passivated emitter, rear locally-diffused PERL cell which reached record efficiency of 24.7 % (from [8]).

The backside contacted solar cells, which exhibits both polarities of metal contacts on the back side, can be divided into three major categories:

- Back-Contact Back-Junction (BC-BJ) solar cells (section 2.2.1), also called Interdigitated Back Contact (IBC) solar cells, which have both contacts and the collecting junction placed on the back side of the cell;
- Emitter Wrap Through (EWT) solar cells (section 2.2.2), in which the front surface collecting junction is connected to the interdigitated contacts on the back surface via laser-drilled holes;

- Metallization Wrap Through (MWT) solar cells (section 2.2.3), in which the front surface collecting junction and the front metallization grid are connected to the interconnection pads on the back surface via laser-drilled holes.

A short review of the above mentioned categories of the back-contact solar cells is presented in the following subsections. For a more detailed review of back-contact solar cells the reader is refered to the paper of Van Kerschaver and Beaucarne [12]. The topic of this work are back-contact back-junction solar cells. Therefore a detailed review of the development efforts in the field of this solar cell structure done by different groups will be given here.

2.2.1 Back-contact back-junction (BC-BJ) solar cells

The concept of the back-contact back-junction solar cells, also called interdigitated back contact (IBC), was introduced in 1975 by Schwartz and Lammert [13], [14]. This cell structure is shown in Figure 2-2.

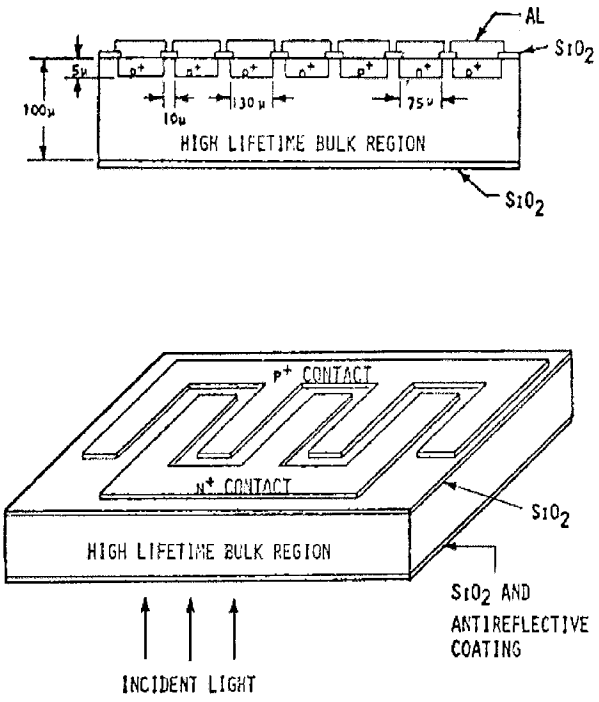


Figure 2-2 The structure of the interdigitated back contact IBC solar cell (from [13]).

Both emitter and base metal contacts are placed on the back cell side in a form of an interdigitated grid. Also the emitter and back surface field diffusions are in the form of the interdigitated grid. Due to such design this device possesses all of the above

mentioned advantages. At first the IBC solar cells were designed for operating in the high-concentration systems. An efficiency of 17 % was achieved under 50-suns concentration [13].

In 1984 Swanson et al. [15] introduced a point contact silicon solar cell, which is similar to the IBC solar cell. The main difference is that in the point contact solar cell the rear side diffusions are limited to an array of small points, as schematically shown in Figure 2-3. By reducing of the area of the highly diffused regions on the back cell side, the dark saturation current of the doped areas could be reduced significantly. Thus, the output voltage and the efficiency of the cell could be increased.

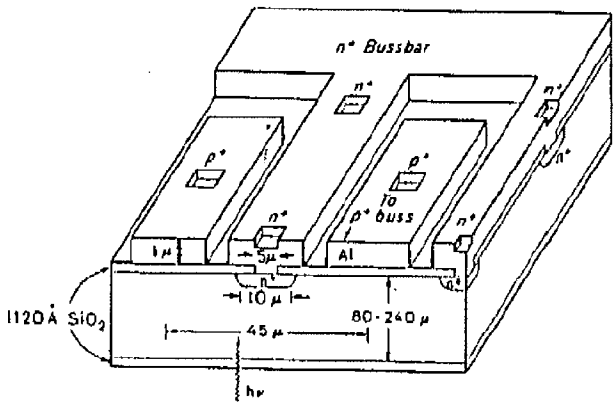


Figure 2-3 Structure of a point contact solar cell (from [15]).

The photovoltaic group at Stanford University led by Prof. Swanson has made the most significant contributions in the field of the IBC cells. Thus, the developments of the back-side contacted cells made by this group are presented in the following:

Non-textured point contact *concentrator solar cell* achieved an efficiency of 19.7 % under 88-suns concentration in 1984 [15]. In 1986 a further optimized point contact solar cell with an efficiency of 27.5 % under 100 suns concentration was achieved by Sinton et al. [16]. Shortly after, an increased device cell efficiency up to 28 % under 150 suns was after presented by Sinton et al. [17]. In 1988 Sinton et al. [18] reported point contact solar cells with an efficiency of 28.4 % at power densities up to 200 suns. The area of these solar cells was 0.15 cm^2.

The back-contact back-junction solar cell structure was also optimized for the applications under standard *one-sun illumination*. In 1985 Verlinden et al. [19] presented an IBC solar cell with a one-sun illumination efficiency of 21 %. One year later Sinton et al. [16] introduced a point contact solar cell with 22.2 % one-sun

efficiency with the area of 0.15 cm^2. However this efficiency was corrected down to 21.7 % after the publication [20].

King et al. [20] presented a first medium-area (8.5 cm^2) point contact solar cell with the front and back surface fields with the top efficiency of 22.3 %. In this solar cell a novel *multi-level metallization scheme*, introduced by Verlinden et al. [21], [22], was applied. This metallization scheme allowed for realization of large-area solar cells in which series resistance is not dependent on solar cell area. In 1991 a record one-sun efficiency of 22.7 % on a 37.5 cm^2 point contact solar cell was reported by King et al. [23].

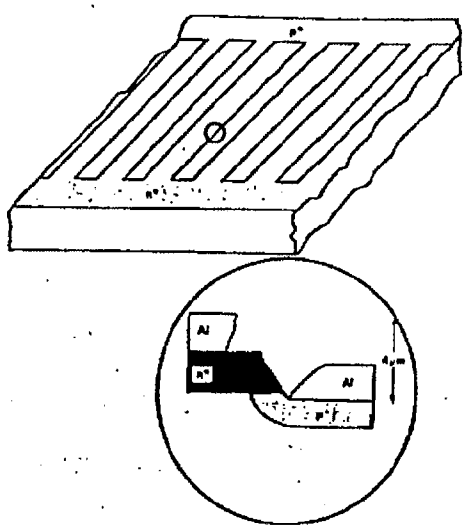


Figure 2-4 *Simplified back-side solar cell. The illuminated side is on the bottom in this figure. The mesa trench, which allows for self-aligned metal contact separation is shown in the inset (from [24]).*

The processing of the interdigitated grid of the rear side diffusions, contact openings and the metal grid of the point contact solar cells requires four to six patterning steps [24]. Thus, this processing sequence is complex, which results in high manufacturing costs. In 1988 a *self-aligned method* to for an interdigitated contact grid was introduced [18]. In 1990 Sinton et al. [24] presented a simplified back-side solar cell (schematically shown in Figure 2-4), which used this self-aligned contact separation and allowed for reduction of the masking steps to one. For the simplified processing sequence a 10.5 cm^2 one-sun solar cell with an efficiency of 21.9 % was reported.

The Sunpower Corporation was founded in 1985 by Prof. Swanson in order to commercialize to high-efficiency back-contact silicon solar cells developed by the

research group of Stanford University. A pilot production of large area (35 cm^2) back-contacted solar cells with an efficiency of 21 % was reported by Sinton et al. [25]. 7000 solar cells of this type, with an average efficiency of 21.1 %, were manufactured for the Honda solar-car *Dream*, which won the World Solar Challenge race in 1993 [26]. The processing of these solar cells required five photolithography masking steps.

In a following study of Sunpower the back-contact solar cell design, especially the *edge passivation* and the *substrate doping*, were optimized. This resulted in a record one-sun efficiency of 23.2 % reported in 1997 by Verlinden et al. [27]. In 2002 the process simplifications, which eliminated one third of the major processing steps and resulted in reduction of the fabrication costs by 30 %, were reported by Cudzinovic et al. [28]. The process simplifications led to 0.6 % absolute efficiency decrease.

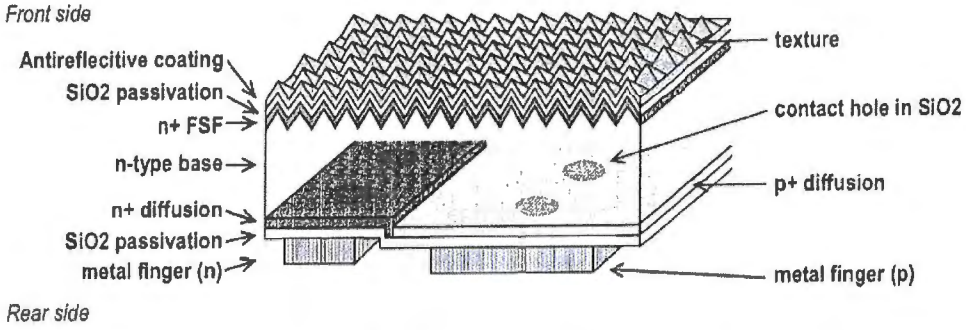


Figure 2-5 Schematic diagram of the Sunpower's A-300 solar cell (from [29]).

In 2004 a manufacture of the large-area (149 cm^2) *A-300 back-contact solar cells* was introduced by Mulligan et al. [29]. A maximum cell efficiency of the A-300 solar cells of 21.5 % was achieved. A schematic diagram of the Sunpower's A-300 solar cell is shown in Figure 2-5. McIntosh et al. [30] found that the n-type silicon material with thickness of 160 to 280 μm and resistivity of 2 to 10 Ω cm was optimal for the A-300 cells. Also the light trapping of this cell type was studied in details by McIntosh et al. [31].

A high volume production of a *new generation of the A-300* back-contact cells with an record average efficiency of 22.4 % was introduced in 2007 by De Ceuster et al. [3]. The new generation back-contact solar cells achieve the highest efficiency silicon solar cells in mass production up to date. In the same paper a record module efficiency of 20.1 % using back-contact solar cells was reported.

In a recent lecture Prof. Swanson [32] announced a new record efficiency of 23.4 % of a large area (149 cm^2) back-contact solar cell developed by the R&D department of Sunpower. Details of the improvements that have been applied to this solar cell design and to the processing technology are not known.

Simultaneously to the development efforts at Stanford University and Sunpower, there other groups which are working on the high-efficiency back-contact back-junction solar cell devices. At Fraunhofer ISE a rear-contacted (RCC) silicon solar cell with line contacts were processed using the photolithography masking. A schematic diagram of a RCC cell is shown in Figure 2-6. An efficiency of 22.1 % was reported by Dicker et al. [33], [34].

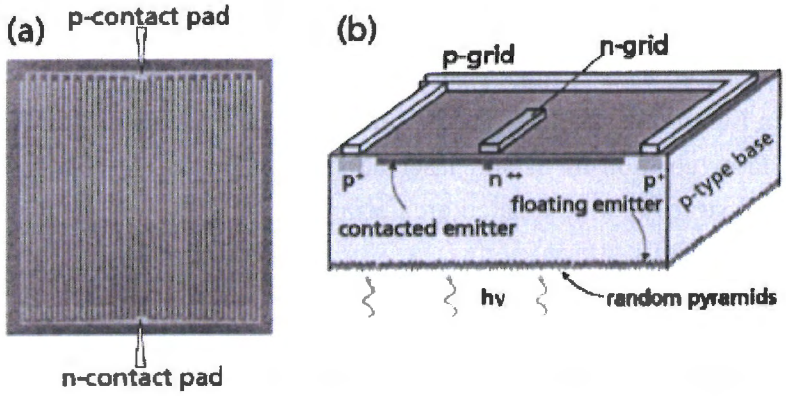


Figure 2-6 Structure of the RCC fabricated at Fraunhofer ISE. (a) View of the rear side of the RCC showing the interdigitated contact pattern. (b) Details of the solar cell structure, with the cell shown upside down (from [33]).

For the applications under concentrated sunlight a rear-line-contacted concentrator cell (RCLL) was developed by Mohr [35]. This cell structure is based on the RCC solar cell design. A maximum efficiency of 25 % at illumination intensity of 100 suns was achieved [36].

A low-cost approach to the BC-BJ solar cell structure was developed by Guo [37] from the UNSW. The *Interdigitated Backside Buried Contact* (IBBC) solar cell, shown in Figure 2-7, is processed without the use of photolithography. The laser-grooved buried contact technology is applied. A maximum one-sun efficiency of 19.2 % was reported by Guo et al. [38].

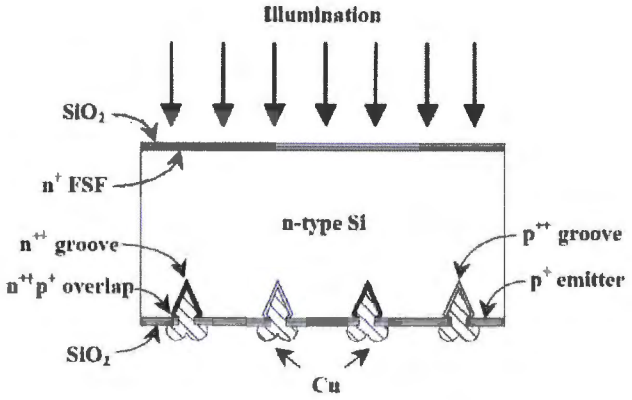


Figure 2-7 Schematic cross section of the n-type IBBC solar (from [38]).

Another very promising low-cost BC-BJ solar cell structure was developed by Engelhart at al. [39], [40] from the ISFH. The *RISE* (*Rear Interdigitated contact scheme, metalized by a Single Evaporation*) solar cell structure is schematically presented in Figure 2-8. The RISE solar cell is fabricated using a mask-free process, in which the laser ablation of Si and laser ablation of protective coatings are applied. With this cell structure a designated area efficiency of 22 % was achieved on a 4 cm^2 laboratory solar cell.

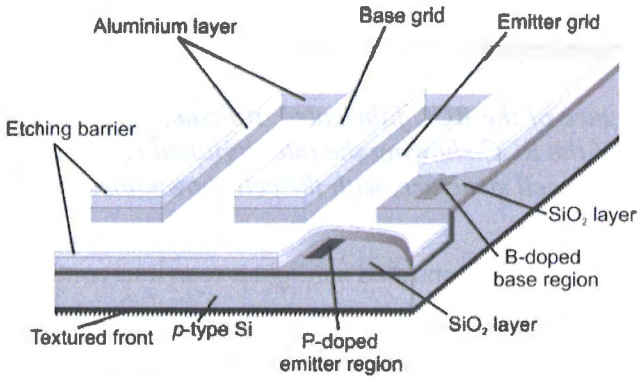


Figure 2-8 Schematics of the RISE back junction solar cell. (from [39]). The illuminated side is on the bottom in this drawing.

Furthermore, large-area high-efficiency back-contact solar cells for a mass production are being developed by Q-Cells within the *Quebec* project. In 2006 Huljic et al. [41] reported maximum efficiency of 21 % for laboratory scale 4 cm^2 on low cost Cz-Si wafers. In 2007 Huljic et al. [42] presented large area (100 cm^2) BC-BJ solar cell with an efficiency of 20.5 %. In the same presentation plans for a technology transfer to a pilot production were announced.

One of the very promising developments in the field of back-contact solar cells, is the application of the of *amorphous/crystalline silicon* (a-Si/c-Si) *hetero-junction structures*. Due to its superior surface passivation properties the a-Si/c-Si hetero-junctions have the potential to significantly increase the voltage of a solar cell. Hetero-junction back-contact solar cells are being developed by a number of research groups [43], [44], [45].

2.2.2 Emitter Wrap Through (EWT) solar cells

The concept of the emitter wrap through EWT solar cell was introduced by Gee et al. [46], [47]. The concept is based on an emitter which is diffused on the front and back side of the cell. The front and back emitters and connected through laser-drilled and emitter-diffused holes. The EWT cell concept is schematically shown in Figure 2-9.

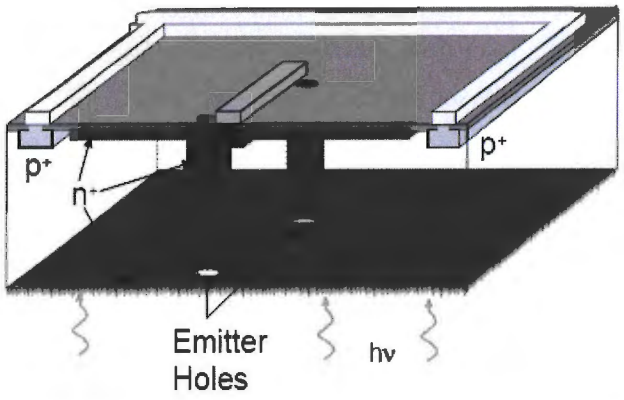


Figure 2-9 Schematic diagram of an emitter wrap through EWT solar cell. The illuminated side is facing down in the picture (from [48]).

The advantages of the EWT solar cell are comparable to the ones of back-contact back-junction solar cells: (i) complete elimination of front contact grid shading, and (ii) the possibility of the co-planar interconnection. However there exists one major advantage of the EWT cells over the BC-BJ cells. Due to the presence of the p-n junction on the front and on the back cells side, the average distance of the minority carriers to the emitter is significantly reduced. This results in the much lower required minority carrier lifetime in the bulk than in the case of BC-BJ cells. It is therefore possible to reach high efficiencies with EWT cells even with a low quality bulk Si, what is not possible in the case of BC-BJ cells. A comparison of the influence of the bulk lifetime on the solar cell efficiency for the BC-BJ and EWT solar cells is presented by Kray [48] and Engelhart [40].

Advent Solar reported manufacturable EWT solar cells with efficiencies of 14 % on mc-Si and 16 % on mono-Si using only low-cost processing [49]. At the University of Konstanz a low-cost EWT solar cell process was developed and an efficiency of 13.6 % on Cz-Si was achieved [50], [51]. At Fraunhofer ISE an EWT solar cell processed using photolithography masking achieved 18.7 % on Cz-Si [52] and 21.4 % on FZ-Si [53]. At ISFH a large area (92 cm^2) RISE-EWT (Rear Interdigitated Single Evaporation Emitter Wrap-Through) solar cell was developed. A maximum efficiency of 21.4 % on FZ-Si was reported by Hermann et al. [54]. Q-Cells presented a large area (92 cm^2) EWT solar cell on mc-Si with an efficiency of 17.1 % [55].

2.2.3 Metallization Wrap Through (MWT) solar cells

The metallization wrap through (MWT) solar cell concept [56] shows the closest similarity to a conventional solar cell structure. The emitter and the front side metallization fingers are located on the front surface. However, the busbars are placed on the back side of the cell. The front side metal fingers are connected to the busbar on the rear side through the laser drilled holes, which are filled with the metal. The MWT cell concept is schematically shown in Figure 2-10.

Due to the fact that in the processing of the MWT solar cells standard screen-printing technology can be applied, the transition from the processing sequence of a conventional soar cell to a MWT solar cell is not complicated. Furthermore, the MWT cell concept offers advantages over the conventional solar cell. Thanks to the removal of the front side busbars, the front contact shading is reduced. Simultaneously, the co-planar interconnection is possible since both contact polarities are placed on the back side.

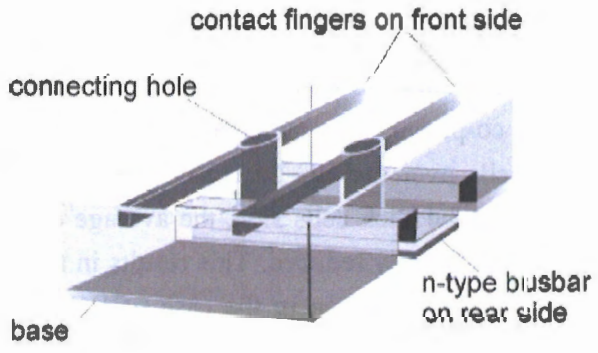


Figure 2-10 Schematic drawing of a MWT cell (from [57]).

The MWT cell structure is being successfully developed by different groups: Van Kerschaver et al. [58] from IMEC presented a module based on screen-printed MWT solar cells with an efficiency of 14.7 %. At ECN a pin-up module concept was introduced by Bultman et al. [59]. Weeber et al. [60] from the ECN group presented mc-Si MWT cells with an area of 225 cm^2 and an efficiency of 16.7 %. At Fraunhofer ISE a mc-Si MWT solar cell with an area of 156 cm^2 and an efficiency of 16.2 % was presented by Clement et al. [61]. Joos et al. [62] from the group of University of Konstanz presented Cz-Si MWT solar cells with an area of 25 cm^2 and an efficiency of 17.5 % and Knauss et al. [57] presented large area (243 cm^2) Cz-Si MWT cells with an efficiency up to 16.7 %.

2.3 Critical parameters of the back-contact back-junction solar cells

As already mentioned in section 2.1, one of the challenges related to the back-contact back-junction solar cell structure is the requirement of a high minority carrier lifetime in the silicon bulk (τ_{bulk}) and a low front surface recombination velocity (S_{front}). Without fulfilling these requirements, high device efficiencies cannot be achieved.

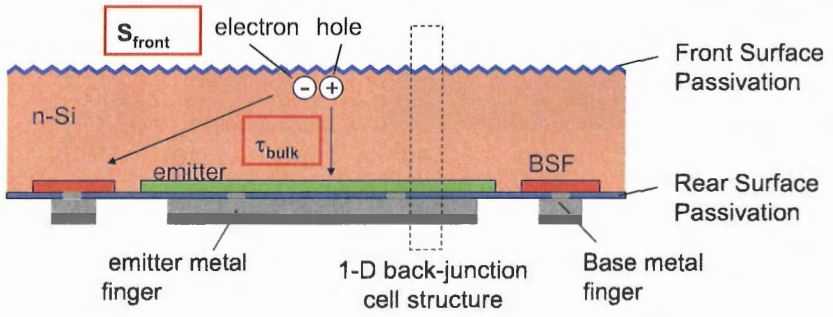


Figure 2-11 *Schematic cross-section of an n-type high-efficiency back-contact back-junction silicon solar cell (sketch not to scale). Two most critical parameters for this cell type, namely the front surface recombination velocity (S_{front}) and the minority carriers lifetime in bulk (τ_{bulk}) are also shown.*

In silicon solar cells most of the photogeneration occurs at the front side of the cell (schematically shown in the Figure 2-11). But in the back-junction cell structure, the p-n junction is located on the back cell side. Therefore the light generated carriers can be easily lost by recombining at a poorly passivated front surface, instead of reaching the back junction. Moreover, even if the front surface is well passivated, a risk of recombination within the bulk silicon exists. The carriers which need to diffuse

through the wafer thickness can recombine in the bulk silicon before reaching the back junction if the bulk lifetime of the minority carriers is insufficient. Therefore, τ_{bulk} and S_{front} are the two most critical parameters in the back-contact back-junction solar cell structure.

In order to show the importance of these two critical parameters in the back-contact back-junction solar cell structure, a one-dimensional back-junction cell structure (marked in Figure 2-11) was simulated using simulation program PC1D [63]. Both critical parameters τ_{bulk} and S_{front} were varied in a wide range in order to analyze their influence on the solar cell efficiency. In the simulations the device thickness of 200 µm was chosen. The simulation results are shown in Figure 2-12.

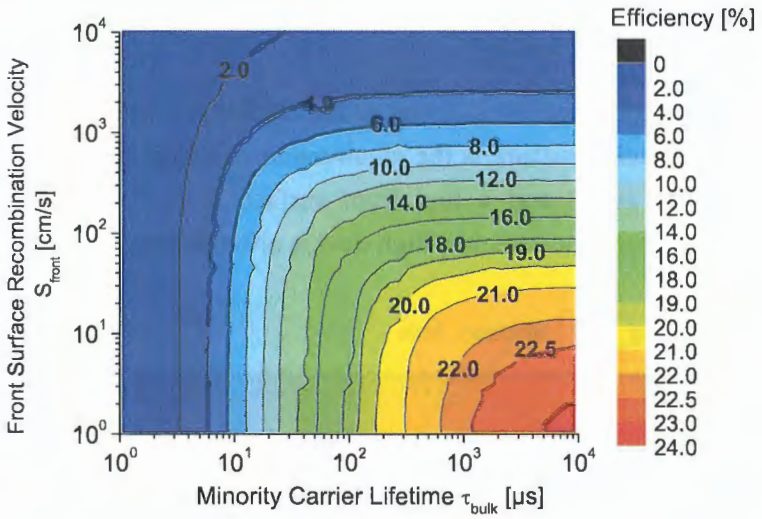


Figure 2-12 Simulations of the efficiency of a one-dimensional back-junction solar cell structure in a wide range of carriers lifetime and front surface recombination velocity. The thickness of the simulated device is 200 µm. The resistivity of the n-type base is 1 Ω cm and the p-type rear emitter has a sheet resistance of 30 Ω/sq. Simulations were performed using PC1D [63].

Based on the simulation results presented in Figure 2-12 the requirements on the τ_{bulk} and S_{front} can be quantified. In order to achieve conversion efficiencies above 22 %, the front surface recombination velocity should be less than 10 cm/s. At the same time the minority carrier lifetime in the bulk material should be higher than 700 µs, which for the base resistivity of 1 Ω cm corresponds to a diffusion length of 900 µm. As a rule of thumb it can be assumed that the diffusion length of the minority carriers in the bulk should be at least four times greater than the wafer thickness in order to allow for high efficiencies in this solar cell concept. As can be seen in Figure 2-12 the conditions of

low S_{front} and high τ_{bulk} need to be fulfilled simultaneously in order to reach high device efficiencies. Even a minor deterioration of one of the critical parameters will lead to a significant efficiency decrease.

It is therefore essential to be able to fulfill the above mentioned requirements when developing a back-contact back-junction solar cell structure. Without having realized the conditions of low S_{front} and high τ_{bulk}, any other developments and optimization efforts on the BC-BJ structure will be fruitless. The analysis of the minority carrier lifetime in the bulk is presented in section 4.2. The front surface recombination velocity of the analyzed solar cell structure was investigated in chapter 7.

2.4 Conversion efficiency limitations by intrinsic losses

The thermodynamic limit of the conversion efficiency of a single bang-gap photovoltaic converter was found to be 33 % [64], [65] for a band-gap of silicon (1.12 eV) and the AM1.5 spectrum. Using actual parameters for intrinsic recombination the efficiency limit is reduced to 30 % [65]. Swanson [66] calculated a theoretical limit of efficiency of a silicon solar cell of 29 %.

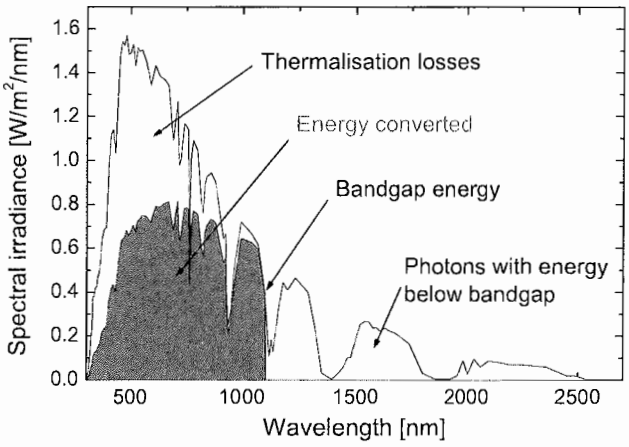


Figure 2-13 Spectral irradiance of the AM1.5G spectrum. The fraction of the spectrum that can be converted by a single-junction silicon solar cell is marked with dark grey.

2.4.1 Intrinsic loss mechanisms in silicon

The above mentioned conversion efficiency of a single junction silicon solar cell is primarily limited due to the following intrinsic loss mechanisms:

- Photons with energy smaller than the band gap (1.12 eV) of silicon do not have enough energy to generate electron hole pairs.
- Photons with energy equal or exceeding the band gap will generate electron-hole pairs. However, photon energy exceeding 1.12 eV will be lost due to the thermalization process. These two effects are schematically shown in Figure 2-13.
- The maximum open-circuit voltage is smaller than 1.12 V (band gap in Si). This is caused by the fact that not the separation of band gap, but the separation of the quasi-Fermi levels defines the open-circuit voltage [5].
- The maximum power that can be generated by a solar cell is smaller than the product of open-circuit voltage and short-circuit current. The current-voltage (IV) curve of a solar cell does not have a rectangular shape (see for example Figure 4-23). Due to the exponential dependence of current with voltage, which is caused by the non-avoidable recombination currents, the fill factor (FF) is limited to about 85 %.

Moreover, the absorption of incoming photons in silicon strongly depends on the energy of the photons (see Figure 2-13). For the low energy photons ($\lambda > 1000$ nm) the absorption coefficient is very low, and the absorption length increases strongly. Therefore, even with optimal light trapping schemes, for a finite thickness of the silicon wafer not all incoming photons with appropriate energy will generate electron-hole pairs (see section 2.4.2).

In the following sections a calculation of the efficiency limit of an ideal single junction silicon solar cell with finite thickness and a particular base doping will be presented. In the ideal solar cell only the recombination mechanisms which are intrinsic and non-avoidable in silicon will be considered. These are: radiative and Auger recombination. The technology related recombination losses such as surface recombination, recombination in the highly doped regions of the solar cell or the recombination through the defect and/or impurities in a non-perfect silicon bulk are not taken into account here.

2.4.2 Short-circuit current limit

Short-circuit current (J_{SC}) of a solar cell is a function of the absorption of the incoming photons within the solar cell. In an ideal solar cell the technology related optical effects are not considered. These effects are front surface reflection, metallization grid

shading, transmission through the silicon wafer and parasitic absorption in the dielectric layers or in the highly doped silicon regions.

For the calculation of the limit to the short-circuit current only the intrinsic optical loss effect in the silicon wafer is considered. This effect is the finite maximal average path length of the incoming photons within the silicon wafer. Tiedje et al. [65] and Brendel [67] showed that for the optimal light trapping, the maximal average path length of the incoming light within the silicon wafer (l) can be approximated with:

$$l \approx 4\, n_{Si}(\lambda)\, W \tag{2.1}$$

where W is the wafer thickness, λ is the wavelength of light and $n_{Si}(\lambda)$ is the wavelength dependent refraction index of silicon.

Knowing the maximum average path length of the incoming light in silicon, the maximum limit on the short-circuit current ($J_{SC,limit}$) as a function of the wafer thickness can be calculated. In order to calculate $J_{SC,limit}$, the solar spectrum needs to be integrated with the absorption coefficient in silicon, assuming the maximum average path of the incoming light calculated with equation (2.1):

$$J_{SC,limit}(W) = \frac{q}{hc}\int \lambda\, I_{AM1.5G}(\lambda)\left[1-\exp\left(-4\alpha_{Si}(\lambda)\, n_{Si}(\lambda)\, W\right)\right] d\lambda \tag{2.2}$$

where q is the elementary charge, h is the Planck constant, c is velocity of light in vacuum, $\alpha_{Si}(\lambda)$ is the wavelength dependent absorption coefficient of silicon, $I_{AM1.5G}(\lambda)$ is the energy flux density of the incoming light.

In Figure 2-14 the calculated maximal short-circuit current as a function of wafer thickness is presented. For the complete AM1.5G spectrum a maximal J_{SC} of nearly 46 mA/cm^2 is possible. However, due to the finite path length of the incoming light, the actual J_{SC} limit is lower. The calculations of J_{SC} limit for the case of optimal light trapping (as obtained using the maximal average path length calculated with Eq. 2.1 and then with Eg. 2.2) and for the case of no light trapping (i.e. the path length of the incoming light in silicon equals wafer thickness $l=W$) are shown as well. For the optimum light trapping and a wafer thickness of 150 µm the J_{SC} limit equals 44 mA/cm^2. However, if no light trapping is applied, then the J_{SC} limit is reduced to 38.6 mA/cm^2.

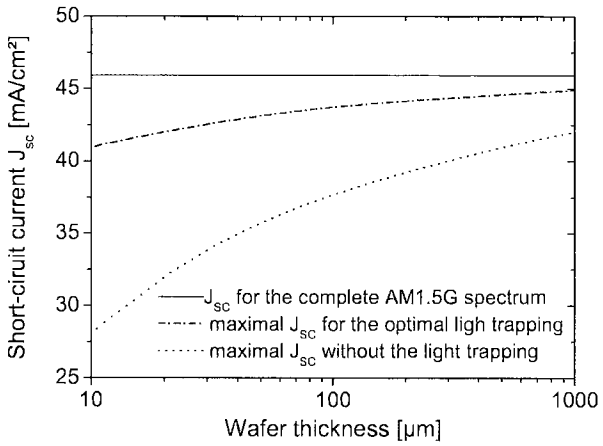


Figure 2-14 Maximum possible short-circuit current in the silicon solar cell under AM1.5G spectrum, as a function of wafer thickness.

2.4.3 Open-circuit voltage limit

Open-circuit voltage (V_{OC}) of a solar cell is limited by the recombination rate of the electron-hole pairs. In an ideal solar cell only the recombination mechanisms, which are intrinsic and non-avoidable in silicon, take place. These intrinsic recombination mechanisms in silicon are the radiative recombination and the Coulomb-enhanced Auger (CE Auger) recombination.

The influence of the intrinsic recombination processes, as well as the limitations of short-circuit current, on the V_{OC} and efficiency of the ideal solar cell can be modelled using the approach of Kerr [68]. The following equation enables calculation of the current –voltage (J-V) characteristics of an ideal solar cell:

$$J(V,W,N_D) = J_{\mathrm{SC,limit}}(W) - qWR_{\mathrm{int}}(V,W,N_D) \tag{2.3}$$

where J is the current and V is the voltage of the solar cell, N_D is the doping concentration of the silicon wafer, R_{int} is the intrinsic recombination rate and the $J_{SC,limit}$ is the short-circuit current calculated in the previous section.

The intrinsic recombination rate can be calculated using the parameterisation of the radiative (R_{rad}) and CE-Auger ($R_{CE\text{-}Auger}$) recombination by Kerr and Cuevas [69], [70] using the following equation:

$$\begin{aligned} R_{\mathrm{int}}(V,W,N_D) &= R_{CE\text{-}Auger} + R_{Rad} = \\ &= n_i^2 e^{\frac{qV}{k_B T}} \left(1.8\times10^{-24} n_0^{0.65} + 6\times10^{-25} p_0^{0.65} + 3\times10^{-27}[\Delta n(V)]^{0.8} + (1-P_{PR}(W))B_R\right) \end{aligned} \tag{2.4}$$

where n_0 and und p_0 are the equilibrium concentrations of electron and holes expressed in units of cm^{-3}, Δn is the injection density and B_R is the radiative recombination coefficient. The photon recycling (i.e. the re-absorption of the radiatve recombination radiation in the solar cell and generation of an electron-hole pair) is considered, with P_{PR} describing the photon recycling rate.

Derivation of the equation (2.4) is done under assumption of the Narrow-Base approximation of Green [71]. Assuming that Fermi levels of electrons and holes are constant within the solar cell base. Then the equation (2.5) is valid

$$np = (n_0 + \Delta n)(p_0 + \Delta n) = n_i^2 e^{\frac{qV}{k_B T}} \tag{2.5}$$

For the calculations of the recombination rate of the intrinsic recombination mechanism the parameters summarized in Table 2-1 were applied. The limit to the open-circuit voltage can be then calculated using the equation (2.3) for the condition of $J(V_{OC}) = 0$.

Table 2-1 Parameters used for the modeling of the intrinsic recombination in silicon.

Parameter	Value
T	300 K
n_i	1.0×10^{10} cm^{-3} [80]
B_R	4.73×10^{-15} cm^3s^{-1} [72]
P_{PR}	0.79 @ W= 150 µm [70]
p_0	$p_0 = \frac{n_i^2}{N_D}$
n_0	N_D
Δn	$\Delta n(V) = \frac{1}{2}\sqrt{\left(n_0^2 + p_0^2\right)^2 - 4\left((n_0 - p_0) - n_i^2 e^{\frac{qV}{k_B T}}\right)} - \frac{1}{2}(n_0 - p_0)$

The limit of the open-circuit voltage calculated for different wafer thicknesses and different base doping density of an n-type solar cell is shown in Figure 2-15. For the cell thickness of 150 µm and an n-type base with doping of N_D=5.0×10^{15} cm^{-3} the V_{OC} limit equals 742.5 mV.

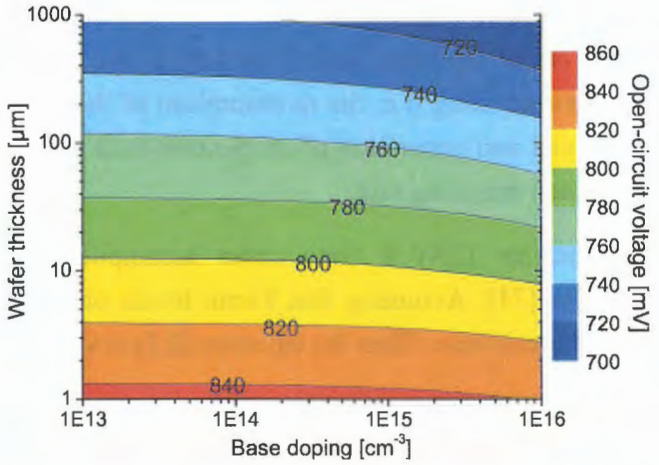


Figure 2-15 *The open-circuit voltage of an n-type silicon solar cell imposed by the intrinsic (radiative and Auger) recombination loss mechanisms. Calculations were done for a wide range of the wafer thicknesses and base doping range.*

Table 2-2 *Efficiency limit of a silicon solar cell with optimal light trapping and only intrinsic recombination mechanisms. Calculations assuming the cell thickness of 150 µm and the n-type base with doping of $N_D=5.0\times10^{15}$ cm^{-3} (base resistivity of 1 Ω cm).*

Cell parameter	Limit by intrinsic losses
efficiency η [%]	28.3
fill factor FF [%]	86.5
open-circuit voltage V_{OC} [mV]	742.5
short-circuit current J_{SC} [mA/cm^2]	44.0

2.4.4 Efficiency limit

By applying the calculated short-circuit current limit and the open-circuit limit into equation (2.3), it is possible to calculate current-voltage characteristics of an illuminated ideal solar cell. Thus, the efficiency limit can be determined.

In Table 2-2 the calculated parameters of an ideal silicon solar cell, with optimal light trapping and only Auger and radiative recombination mechanisms, are shown. The efficiency limit of 28.3 % was calculated assuming the cell thickness of 150 µm and

the n-type base with doping of N_D=5.0×10^{15} cm^{-3} (base resistivity of 1 Ω cm). This wafer thickness and the base doping correspond to the back-contact back-junction solar cells developed in this work. The fill factor was calculated using the one-diode model described by equation (6.8).

The technology related loss mechanisms, which are introduced during the manufacturing of the silicon wafers and the following solar cell processing, will lead to strongly reduced efficiencies of the real solar cells. A detailed comparison of the efficiency limit and the maximal achieved efficiency of the back-contact back-junction solar cell is presented in chapter 6.

3 Measurement methods and numerical simulations

In this chapter, two methods for the determination of the surface saturation current density under low and high-injection are presented. In addition, the process of the numerical simulations of the back-contact back-junction solar cells using one- and two-dimensional simulations is described. The measurement table developed for the electrical characterization of the analyzed solar cells is presented.

3.1 Surface saturation current density

The analysis of the surface passivation quality using different passivation layers (e.g. thermally grown SiO_2, PECVD SiN_X) in the combination with the dopant diffusion requires determination of the surface recombination velocity S and surface saturation current density J_{0s}. The measurement of the saturation current density of the applied diffusion profile is especially required in chapter 7 for the optimization of the n^+ front surface diffusion profile (the so called front surface field - FSF). The method presented below is used to determine the surface saturation current density and can also be applied in order to characterize and optimize both rear side diffusion profiles of the BC-BJ solar cell, i.e. the emitter diffusion, and the back surface field (BSF) diffusion profiles.

3.1.1 Injection dependent lifetime measurements

A direct measurement of the surface recombination velocity S and surface saturation current density J_{0s} is not possible. It is, however, possible to measure the so-called effective lifetime τ_{eff} of minority carriers, which takes into account the recombination mechanisms at the surfaces of the measured sample as well as within its bulk.

The effective lifetime was measured using the photoconductance tool WTC-120 from Sinton Consulting [73]. In this experimental setup, the measured silicon wafer is illuminated by a Xenon flash lamp, which has its spectrum distributed mainly at the wavelengths of 900 to 1000 nm. This near infrared light source allos for a fairly uniform profile of the excess carrier density Δn along the wafer thickness. During the lamp flash, the photoconductance of the measured wafer $\Delta\sigma$ is measured contactlessly by using inductive coupling. At the same time, the light intensity is measured using a reference solar cell, which is placed very close to the measured sample. The excess

carrier density Δn in the sample is calculated from the measured $\Delta\sigma$. Knowing the optical properties of the measured sample allows for the determination of the photogeneration rate within the sample measuring the illumination intensity with a monitor solar cell. After determination of both Δn and photogeneration, τ_{eff} can be calculated as a function of Δn (see for example Figure 3-2). This is possible by applying the generalized evaluation method, which is valid for quasi-steady-state and quasi-transient measurement conditions [74]. The quasi-steady–state photoconductance (QSSPC) method was introduced by Sinton et al. [75].

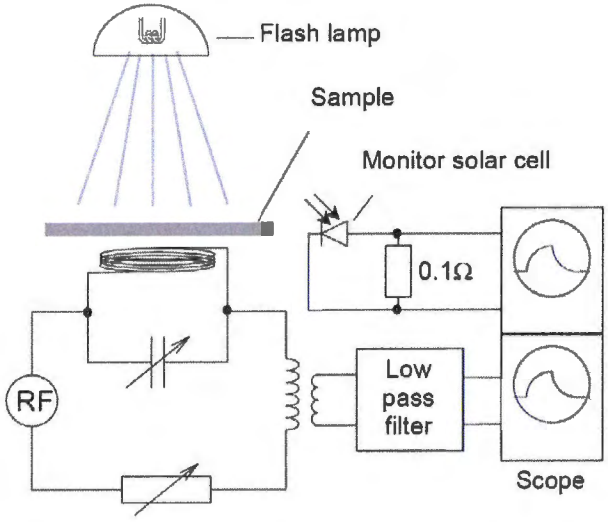


Figure 3-1 Schematic sketch of the photoconductance measurement setup (picture taken from [76])

The measured effective lifetime of the carriers is a function of the recombination in the bulk and at the surfaces of the sample, as shown in equation (3.1).

$$\frac{1}{\tau_{eff}} = \frac{1}{\tau_s} + \frac{1}{\tau_{SRH}} + \frac{1}{\tau_A} + \frac{1}{\tau_{rad}} \tag{3.1}$$

The surface recombination can be described by the surface lifetime τ_s. The volume lifetime τ_b is determined by the Shockley-Read-Hall (SRH) recombination [77], [78], described by the SRH lifetime τ_{SRH}, the Auger recombination τ_A [79] , and the radiative recombination (τ_{rad}).

The sample temperature during the measurements was set to 30°C. For the calculation of recombination parameters, the intrinsic carrier concentration value n_i=1.0 × 10^{10} cm^{-3} [80] was used. In order to determine the surface saturation current density, two methods were applied. J_{0s} was determined under low injection, where

$\Delta n << N_D$, for samples with resistivity of 1 Ω cm and under high injection, where $\Delta n >> N_D$, for 10 Ω cm samples. The same n_i value was used for both analyzed wafer resistivities of 1 and 10 Ω cm. Determination of the J_{0s} from the measured effective lifetime is presented in the next sections.

3.1.2 Determination of J_{0s} at low injection

The effective lifetime τ_{eff} measured under low injection at $\Delta n = 1\times10^{14}$ cm^{-3} was used for the calculations of the surface saturation current density. For samples with resistivity of 1 Ω cm, the dopant concentration equals $N_D = 5\times10^{15}$ cm^{-3}. Therefore, the condition of low injection $\Delta n << N_D$ is satisfied [81].

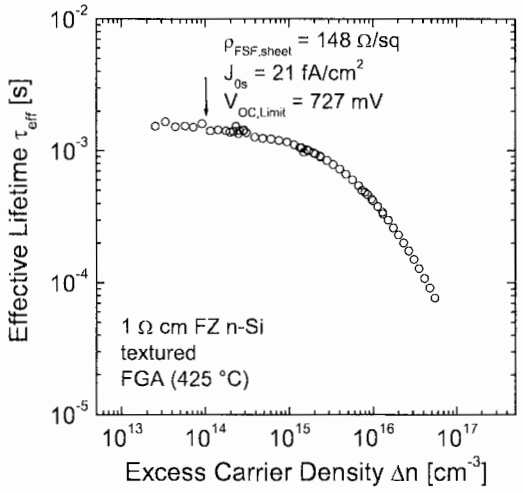


Figure 3-2 Example of QSSPC lifetime measurement of the textured symmetrical test sample with resistivity of 1 Ωcm and front surface field diffusion of 148 Ω/sq. J_{0s} and $V_{OC,\,Limit}$ determined at $\Delta n = 1\times10^{14}$ cm^{-3} are shown.

The surface lifetime τ_s was calculated using the equation (3.2) [82]. For the bulk lifetime τ_b, the intrinsic Auger and radiative recombination was used for the calculation. For the calculation of the Auger lifetime, the model of Kerr [69] was used. For the radiative recombination, the parameterization of Trupke et al. [72] was taken. Omitting the Shockley-Read-Hall bulk recombination results, the upper limit for J_{0s} value is determined as:

$$\frac{1}{\tau_{eff}} = \frac{1}{\tau_b} + \frac{1}{\tau_s} \tag{3.2}$$

For symmetrical lifetime samples, the effective surface recombination velocity S_{eff} can now be calculated using an approximation from Sproul [83]:

$$\tau_s = \frac{W}{2S_{eff}} + \frac{1}{D}\left(\frac{W}{\pi}\right)^2 \tag{3.3}$$

Where S_{eff} takes into account the recombination at the silicon surface as well as the minority carrier's behavior in the highly doped layers at the silicon surface. S_{eff} is defined by del Alamo [84] as:

$$S_{eff} = -\frac{J_p}{q\Delta n} \tag{3.4}$$

Where J_p is the minority carrier current into the surface or from the lowly doped side to the highly doped side of the high-low junction, if a front- and/or back surface field is applied. Using the following equation:

$$J_p = -J_{0s}\frac{\Delta n(N_D + \Delta n)}{n_i^2} \tag{3.5}$$

Thus S_{eff} can be calculated with:

$$S_{eff} = \frac{J_{0s}(N_D + \Delta n)}{qn_i^2} \tag{3.6}$$

With the known S_{eff} value, the J_{0s} can then be calculated using equation (3.7):

$$J_{0s} = \frac{S_{eff} qn_i^2}{(N_D + \Delta n)} \tag{3.7}$$

In Figure 3-2, the example of the measured lifetime curve over a broad injection level is shown.

3.1.3 Determination of J_{0s} at high injection

Surface saturation current density can be also determined under high injection, i.e. at excess carrier densities higher than around ten times the dopant density [81]. Under high injection, where $\Delta n >> N_D$, the recombination of the diffused surfaces together with Auger recombination in the bulk, described by the Auger lifetime τ_A, limits the effective lifetime. One can analyze the inverse effective lifetime corrected for the Auger recombination limit under high injection with the so called *'slope method'* proposed by Kane and Swanson [85]. The slope of the inverse lifetime is then proportional to $2\times J_{0s}$ according to the equation:

$$\frac{1}{\tau_{eff}} - \frac{1}{\tau_A} = \frac{1}{\tau_{SRH}} + \frac{2J_{0s}}{qn_i^2 W}\Delta n \tag{3.8}$$

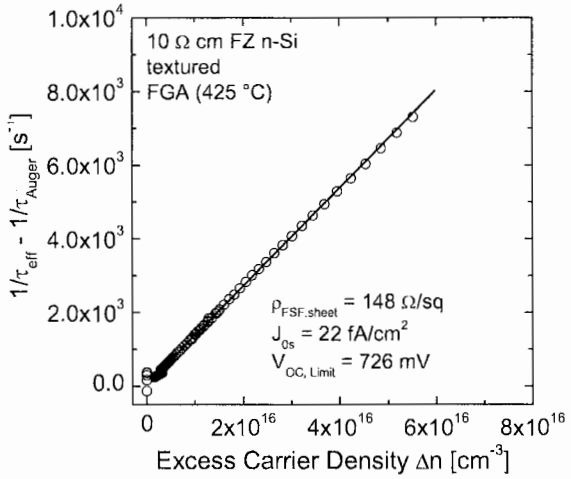


Figure 3-3 Determination of J_{0s} at high injection using the 'slope method'. Example of the determined J_{0s} and $V_{OC,\ Limit}$ for the textured samples with the resistivity of 10 Ω cm and front surface field diffusion of 148 Ω/sq is shown.

The lowly doped, 10 Ω cm samples ($N_D = 4.5\times10^{14}$ cm^{-3}) can be easily measured in high injection using QSSPC equipment. The slope of the inverse lifetime curve at $\Delta n_{hli} = 10\times N_D$ can then be calculated.

An ambipolar Auger coefficient of $C_A = 1.66\times10^{-30}$ cm^{-3}s^{-1} [17] was used for the calculation of the Auger lifetime term ($\tau_A^{-1} = C_A\Delta n^2$). For the determination of the slope of the inverse lifetime curve, a linear fit with measured data points from the range of $\Delta n_{hli} \pm 0.8\times\Delta n_{hli}$ was performed. An example of the determination of J_{0s} for the textured 10 Ω cm test sample under high injection is shown in Figure 3-3.

3.2 Device simulation

3.2.1 Two-dimensional numerical simulation

As shown in Figure 3-4, the structure of the analyzed solar cells is strongly two-dimensional due to the presence of the interdigitated grid of the p- and n-diffusions on the rear cell side. Therefore, for the correct description of the back-contact back-junction solar cell, a two-dimensional modeling and simulations of the device are required.

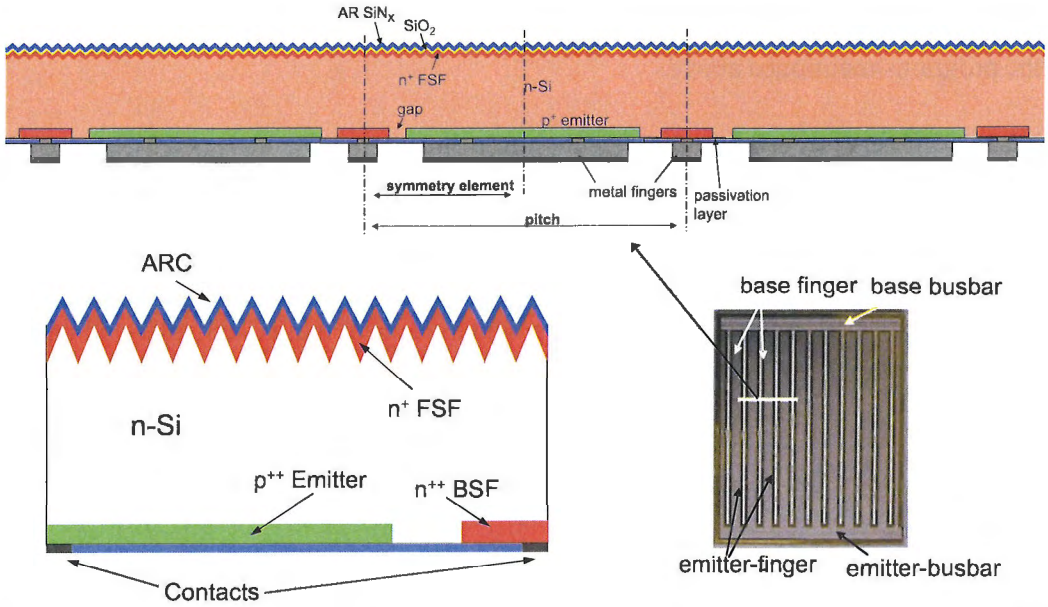


Figure 3-4 Cross-section of the back-contact back-junction silicon solar cell (top). The symmetry element used in two-dimensional simulations (left) as well as a photograph of the rear cell side (right) are shown. The white line in the photograph of the solar cell represents the direction in which the cross-section in the top picture was taken.

The two-dimensional model of the BC-BJ solar cells was developed by Martin Hermle at the Fraunhofer ISE in Freiburg [86]. The simulations of the back-contact back-junction solar cell structure were done by M. Hermle in cooperation with the author of the present thesis.

In two-dimensional simulations, the symmetry element (see Figure 3-4 left) of the solar cell is considered. Different geometry and electrical parameters of the symmetry element are also shown in the diagram. In the simulations, only the active solar cell areas were simulated. The busbar and the edge areas were not taken into account in the simulations presented in this thesis. For the simulation analysis of the influence of the busbars, see the work of M. Hermle [87], [86].

The simulation process starts with the calculation of the generation profile and the optical performance calculations. The simulations of the optical properties of the solar cell are done with the raytracing program *Rayn* [88]. Next, using the program *Mesh* [89], a discretization grid of the symmetry element is created. The semiconductor equations are solved at the nodes of the discretization grid using the *Sentaurus Device* (*SDevice*) [90] program. The whole simulation process is simplified

by the use of the *PVObjects* [91] script in Mathematica, which enables the auditing of the programs mentioned above.

3.2.2 One-dimensional numerical simulation

As previously mentioned, the BC-BJ solar cell has a strongly two-dimensional structure. In many cases, however, simulations using a simplified one-dimensional back-junction solar cell structure (see Figure 3-5) can also describe the effects which occur in the BC-BJ solar cell. The effects which occur in the BC-BJ solar cell and can be well described by the one-dimensional simulation of the back-junction solar cell include:

- Influence of the carrier lifetime on the carrier collection efficiency at the rear junction,
- Influence of the surface concentration and depth of the phosphorus doping profile on the front side (FSF) on the front surface passivation quality.

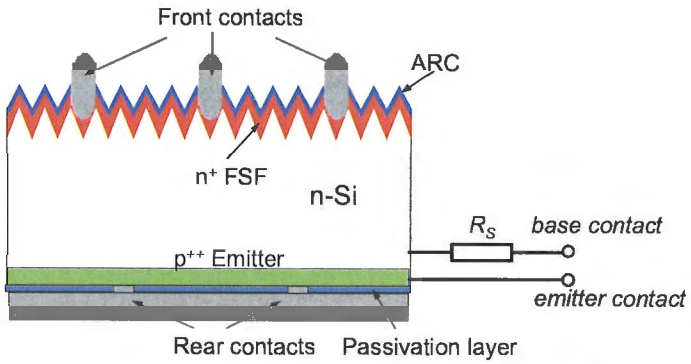


Figure 3-5 Structure of the back-junction cell used in the one-dimensional simulations using device simulation program PC1D [63], [92].

Therefore, the one-dimensional simulations were often applied throughout this thesis. The one-dimensional device simulations were done with the program *PC1D* by Basore and Clugston [63], [92]. The simulations of the optical properties, such as generation profile, reflection, and transmission spectra of the analyzed device were performed using the program *Sunrays* [93]. *Sunrays* is a raytracing program which calculates the generation in the analyzed optical device numerically using the Monte Carlo method.

3.2.3 Simulation parameters

The proper choice of the simulation parameters is essential for a correct simulation. The geometrical parameters as for example thickness and pitch are predefined and thus

easy to access. Most of the electrical parameters as for example doping profiles, bulk lifetime and resistivity have been measured and used for the simulation in this work. Some parameters such as the surface recombination velocity cannot be directly assessed and must be described by models.

The surface recombination velocity S at the doped silicon surfaces depends on the doping profile and the surface dopant concentration. In the one- and two-dimensional device simulations, the highly and lowly doped phosphorus and boron layers with a Gaussian distribution of the impurity concentrations were assumed. For these diffusion profiles with surfaces passivated with thermally grown silicon oxide, the parameterization of Cuevas et al. was taken.

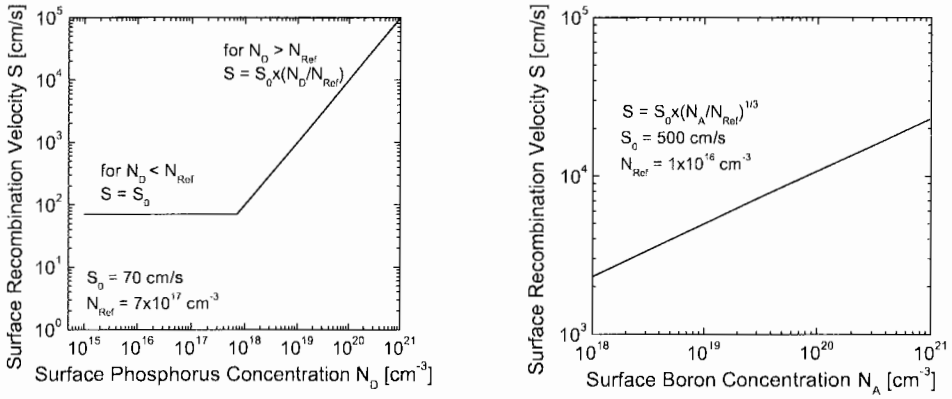


Figure 3-6 Surface recombination velocity as a function of the surface phosphorus (left) and boron (right) concentrations according to parameterization of Cuevas et al. [94], [95].

S for the phosphorus doping according to Ref. [94]:

$$\begin{aligned} S &= S_0 && \text{for } N_D < N_{ref}, \\ S &= S_0(N_D/N_{ref}) && \text{for } N_D \geq N_{ref} \end{aligned} \qquad (3.9)$$

where $S_0 = 70$ cm/s and $N_{ref} = 7\times10^{17}$ cm^{-3}

S for the boron doping according to Ref. [95]:

$$S = S_0(N_A/N_{ref})^{1/3} \qquad (3.10)$$

where $S_0 = 500$ cm/s and $N_{ref} = 1\times10^{16}$ cm^{-3}

In the left side of Figure 3-6, the surface recombination velocity of the phosphorus doped silicon surfaces and its parameterization according to [94] is shown. The surface recombination velocity dependence with the boron surface concentration and its parameterization according to [95] is shown in the right side of Figure 3-6.

3.3 Measurement table for laboratory size solar cell

Since both p- and n-electrodes of the analyzed solar cell are placed on the rear cell side, the application of the standard measurement table for the electrical characterization of the back-contact solar cells is not possible. A new measurement setup for the laboratory scale BC-BJ cells with an area of 4 cm^2 was developed by the author in the course of this work.

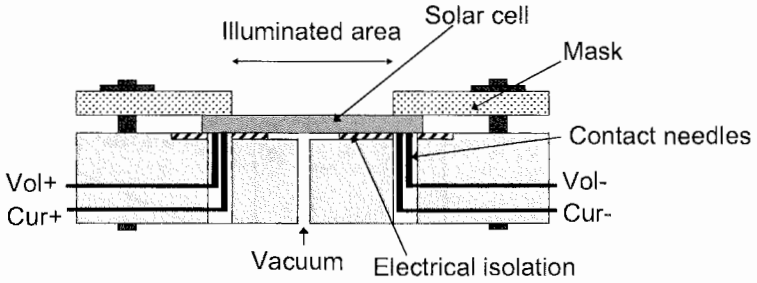


Figure 3-7 Schematic representation of the measurement table for measurement of the back-contact back-junction silicon solar cells.

A schematic drawing of the measurement table developed in this work at Fraunhofer ISE is shown in Figure 3-7. A solar cell is placed on an electrically insulating layer, in order to avoid shunting of the p- and n-electrodes. The finished solar cells are larger than the illuminated area, making it therefore possible to mechanically fix the position of the measured cell with a mask with an illumination area opening of 2×2 cm^2. The contact needles for separate measurement of the current and voltage are placed on the cell busbars from the rear side, through the holes in the measurement table. A three-dimensional AutoCAD design and a photograph of the measurement table developed in this work at Fraunhofer ISE are shown in Figure 3-8.

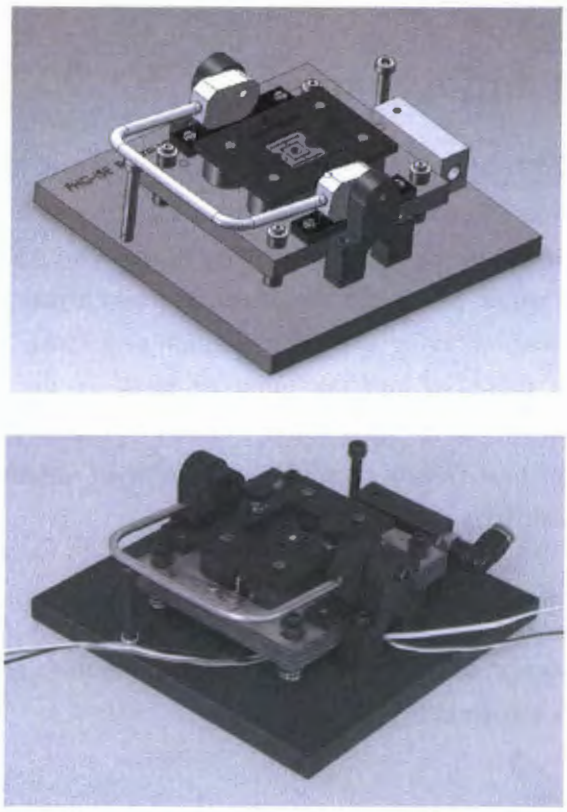


Figure 3-8 Measurement table for measurement of the illuminated and dark current-voltage characteristics of the laboratory size ($2\times2\ cm^2$) back-contact back-junction silicon solar cells. AutoCAD design is shown in top graphic and in the bottom graphic a photograph of the finished measurement table is shown.

4 Design and technology

In this chapter the structure and technology of the developed back-contact back-junction silicon solar cell is presented. The minority carrier lifetime of the applied n-type Si material is determined. The solar cell structure was fabricated using newly developed structuring processes, which are using low-cost screen-printing and laser ablation processes. The applied processes are briefly reviewed and the different methods for the formation of the interdigitated grid of the n- and p- metal grids are described in detail. Finally, the best results of the developed small, laboratory size and large, industry size solar cell are presented.

4.1 Device structure

A schematic cross-section of the back-contact back-junction solar cell developed in the frame of this work is shown in Figure 4-1.

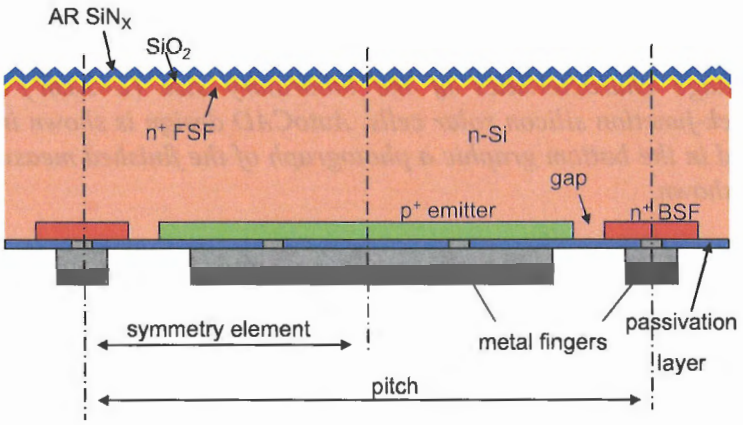


Figure 4-1 Schematic cross-section of the n-type high-efficiency back-contact back-junction silicon solar cell developed in the frame of this thesis (sketch is not to scale). Pitch and symmetry element are shown.

The cells were fabricated from n-type float-zone (FZ) silicon wafers. The thickness of the finished solar cells was about 160 µm. Specific base resistivities of 1 and 8 Ω cm were chosen. The chosen specific base resistance range is believed to be an optimum between two effects: maximization of the carrier lifetime in bulk and reduction of the series resistance losses introduced by the base material. On one hand, the carrier lifetime, which needs to be high in order to enable good collection of the minority

carriers at the rear junction, decreases with increased base doping level and reduced specific base resistance of the base material. On the other hand, the high specific base resistivity results in increased series resistance in the base material, which leads to significant efficiency losses. Details of the silicon material chosen and its characterization are presented in the next section.

The front side is textured with random pyramids and passivated with a lightly doped ($N_{peak} = 5\times10^{18}$ cm^{-3}) and deeply diffused (1.4 µm) phosphorus front surface field (FSF). The sheet resistance of the FSF (ρ_{FSF}) equals 148 Ω/sq. The diffusion profile of the FSF was optimized to achieve an optimum front side passivation quality. The presence of the phosphorus doped front surface field (FSF) is one of the key features of the developed device design. Therefore, a comprehensive analysis of the positive effects of the FSF in the BC-BJ solar cells was performed in the frame of this thesis. The presence of the FSF reduces the concentration of the minority carriers at the physical semiconductor surface and thus improves the front surface passivation (chapter 7) and strongly improves the stability of the front surface passivation under UV-light exposure (section 7.5). Furthermore, the FSF enhances the lateral majority carriers current transport and thus reduces the series resistance losses (chapter 8). Finally, the solar cells with the FSF show a linear current response at low-illumination levels, in contrast to cells without the FSF (chapter 9).

The front surface passivation is further improved by a thin thermally grown silicon dioxide layer. Finally a silicon nitride (SiN_x) antireflection (AR) layer is deposited on top of the oxide layer by means of plasma enhanced chemical vapour deposition (PECVD). Passivation properties of the applied front surface field doping profile and the stack system of the SiO_2 and SiN_X layers is investigated in section 7.3

On the cell rear side an interdigitated grid of the p- and n-diffusion areas is formed. Both emitter p^+ and back surface field n^+ diffusions are separated by an undiffused gap. The rear metallization structure also forms an interdigitated grid, as shown in Figure 4-2. The rear cell surface is passivated with silicon oxide. Metal fingers are contacted to the diffused regions via local openings in the passivation layer.

For masking steps on the rear side, such as:

- definition of boron doped emitter area,
- definition of phosphorus doped back-surface-field diffusion area,
- formation of local openings in the dielectric layer for the metal-semiconductor contacts,
- and formation of the interdigitated metal fingers grid,

only industry-relevant screen-printing and laser processes were applied. No photolithography masking steps were introduced to the processing sequence of the investigated cell structure. Due to the fact that more than one masking step was required, and the limited resolution and positioning accuracy of the applied structuring technology, the pitch of the processed cells was chosen to be in the range of 1.3 to 3.5 mm.

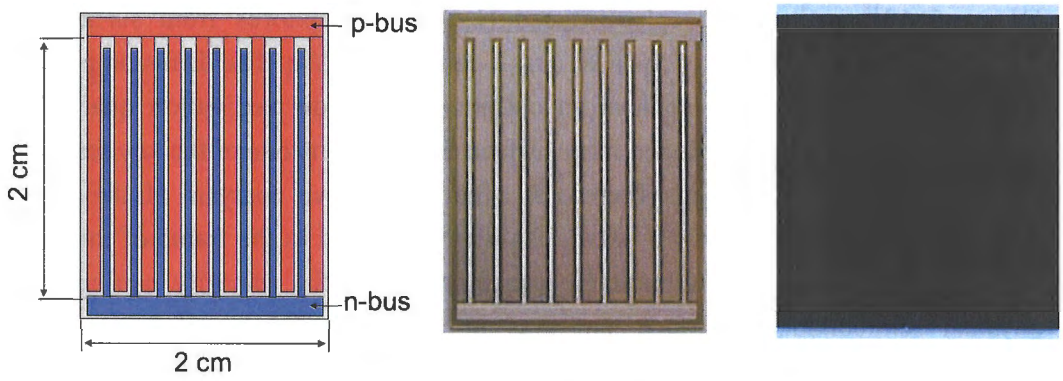


Figure 4-2 Interdigitated grid of the p- and n-metallization fingers of the back-contact back-junction Si solar cell developed in the course of this thesis. The interdigitated grid is schematically shown in the left picture and in the middle the photograph of the rear side of the actual solar cell is shown. In the right a photograph of the cell front side is shown.

Shunting between the tight p- and n-metal finger grids was avoided by a careful design of the metallization process, which is presented in section 4.4.1. The metallization is performed in a two-step process. First, a thin metal layer is deposited and structured to form an interdigitated grid. Secondly, this thin seed metal layer is thickened using an industrially feasible plating process. At the same time the series resistance losses, mainly caused by the lateral carrier transport due to large pitch, could be minimized by application of the high conductivity FSF.

Prior to measurements, the cells were annealed in a forming gas atmosphere and removed from the host wafer by the means of laser cutting. A distance of 500 µm from active cell area was chosen. This distance should allow for strong reduction of the edge recombination losses [96].

4.2 n-type bulk Si material

As previously shown in chapter 2, in order to realize high-efficiency cells using the back- junction cell structure, high minority carrier diffusion lengths are required. The carriers, most of which are generated near the front surface, need to diffuse through the

entire cell thickness in order to be collected by the back-junction. According to the simulations presented in section 2.3, the required diffusion length of the minority carriers should be at least four times larger than the wafer thickness in the back-junction cell type to enable high carrier collection efficiency. Thus, for a solar cell with a thickness of 160 μm, a diffusion length of the minority carriers of at least 640 μm is required.

Phosphorus doped n-type silicon has received increased interest in the PV research community in recent years, due to shortage of the p-type silicon feedstock and due to its high minority carrier lifetime. In many research laboratories front-junction and back-junction silicon solar cells on n-type substrates are being developed.

For example, a front-junction solar cell structure with monocrystalline FZ n-type Si with boron diffused emitter passivated using Al_2O_3 passivation layer developed by Benick et al. achieved an efficiency of 23.2 % [97]. A front-junction cell with oxide passivated boron emitter also developed by Benick et al. achieved an efficiency of 20.4 % [98]. On large area cells of 156×156 mm^2, screen-printed Cz n-type Si, the efficiency of 17.9 % was obtained by Mihailetchi et al. [99]. The application of multicrystalline n-type Si to solar cell processing is also being studied intensivley (see for example the work of Libal et al. [100], Tool et al. [101], and Cuevas et al. [102]). The application of n-type Si to the back-junction cell structure has also been investigated. Zhao et al. demonstrated an efficiency of 22.7 % for FZ n-type Si [103]. Schmiga et al. presented a rear-junction solar with aluminum emitter with an efficiency of 20.1 % [104].

Moreover, in the industry, the highest commercially available solar cells are produced on n-type Si substrates. SunPower Corp. produces back-contact back-junction n-type Si solar cells with efficiencies up to 22.7 % [3]. Sanyo Electric manufactures heterojunction solar cells on n-type c-Si with efficiency of 19.5 % [105].

The advantages of n-type Si when compared to p-type Si are as follows:

- The minority carrier lifetime in p-type boron-doped oxygen-contaminated silicon is strongly reduced under illumination or carrier injection [106], [107], [108]. Due to the lack of boron in n-type Si, no degradation occurs.
- n-type Si has a lower sensitivity to the prominent impurities (e.g. interstitial iron Fe_i,) [109], [110].This is due to strong asymmetry in capture cross section for electron and holes ($\sigma_n >> \sigma_p$).

- For reasons mentioned above, the lifetime of the minority carriers in n-type Si is higher than in the case of p-type Si. For example, extremely high minority carrier lifetime in the range of milliseconds was already reported for n-type multicrystalline silicon by Cuevas et al. [111].

4.2.1 Minority carrier diffusion length

For the determination of the minority carrier lifetime and diffusion length of the n-type FZ Si chosen for processing of the BC-BJ solar cells, lifetime samples were prepared and measured. Planar symmetrical n^+nn^+ test structures are shown in Figure 4-3. Both sides of these samples exhibit a full area shallow n^+ diffusion (ρ_{sheet} = 148 Ω/sq., N_{peak}=5×10^{18} cm^{-3}, depth 1.4 μm) and a full area thermal oxide with thickness of 105 nm. Before the measurements all samples were annealed at forming gas atmosphere (FGA) at the temperature of 425°C (15 min.).

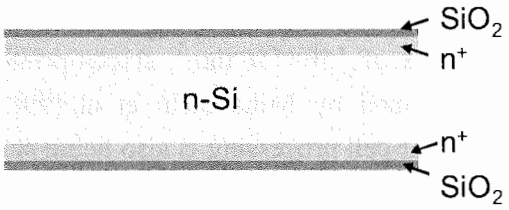


Figure 4-3 *n^+nn^+ symmetrical test structures for the measurements of the minority carrier lifetime and diffusion length.*

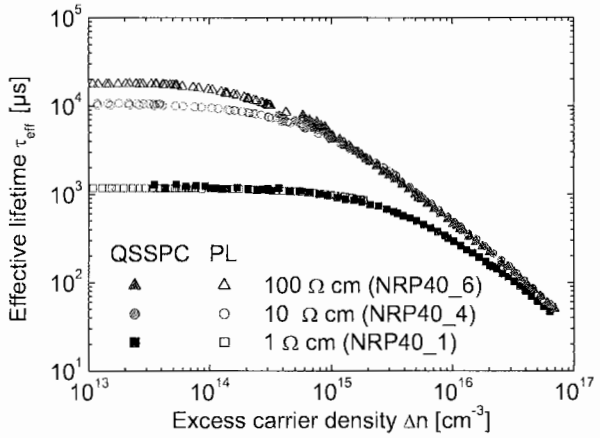


Figure 4-4 *Injection-dependent minority carrier lifetime of the planar n^+nn^+ symmetrical samples on FZ n-type Si wafers with different resistivity. The effective carrier lifetime was measured in a wide excess carrier density range using quasi-steady-state photo-conductance (closed symbols) and photoluminescence (open symbols) methods.*

The lifetime of all samples was measured in a wide injection density range using two measurement methods. With the quasi-steady–state photo-conductance (QSSPC) method [75], the lifetime was measured in the middle to high injection using the WTC-120 lifetime tester from Sinton Consulting [73]. In the low injection range, the lifetime was measured with the photoluminescence (PL) method [112]. The lifetime results are shown in the Figure 4-4. A good agreement between both measurement methods can be observed.

Table 4-1 *Effective minority carriers lifetime and diffusion length for n-type FZ Si with the specified base resistivity of 1, 10 and 100 Ω cm. Lifetime was measured at injection level of $\Delta n = 1 \times 10^{14}$ cm^{-3}.*

Cell no.	ρ_{base} [Ω cm]	τ_{eff} [ms]	L_{eff} [μm]
NRP40_6	100	18.3	4710
NRP40_4	10	10.1	3492
NRP40_1	1	1.2	1175

Extremely high effective lifetime values of up to 18 ms have been measured for the 100 Ω cm n-type FZ Si at an injection level of $\Delta n = 1 \times 10^{14}$ cm^{-3}. As shown in Table 4-1, the lifetime is high enough to realize perfect carrier collection by the back junction for all three investigated resistivities of 1, 10 and 100 Ω cm. Note that actual base resistivities may vary in the range of ± 20 % from the specified resistivity. Even the 1 Ω cm material exhibits lifetime values above 1 ms, resulting in an effective diffusion length (L_{eff}) of about 1200 μm, which is more than 4 times the cell thickness.

4.2.2 Influence of the surface potential on the minority carrier lifetime

In the previous section the analysis of the lifetime samples with diffused FSF and SiO_2 passivation layer was presented. However, as explained in section 3.1, the measured effective lifetime of the minority carriers is not only influenced by the bulk lifetime, but also by the quality of the surface passivation. Therefore, in order to determine the real minority carrier lifetime in the bulk of investigated n-type FZ Si, the effects of the surface recombination should not be taken into account. A significant reduction of the surface recombination can be obtained through application of the field-effect passivation using corona charging [113]. This approach is presented in the following.

Symmetrical n-type lifetime samples with resistivities of 1, 3.5 and 10 Ω cm with both surfaces passivated by a 105 nm thick thermal SiO_2 (shown in Figure 4-5) were processed and annealed at forming gas atmosphere (FGA) at the temperature fo 425°C (15 min.). The effective lifetime of the minorrity carriers was measured using quasi-steady–state photo-conductance (QSSPC) and the results are shown in Figure 4-6. In this measurement no additional corona charging was applied.

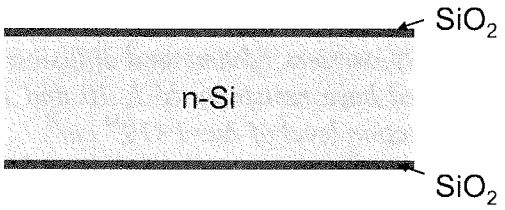


Figure 4-5 FZ n-type symmetrical test structures with thermally grown silicon dioxide passivation layer for the measurements of the minority carrier lifetime.

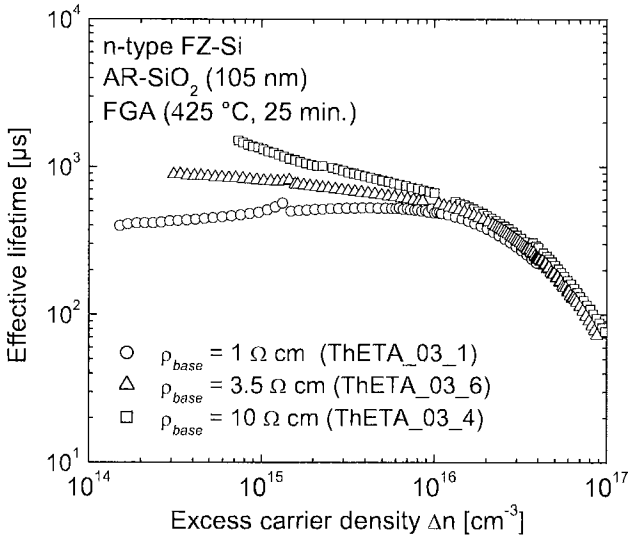


Figure 4-6 Injection-dependent minority carrier lifetime of the planar symmetrical samples on FZ n-type Si wafers with different resistivity. In this measurement no corona charging was applied.

The application of the fixed charges on top of the passivation layer strongly influences lifetime. A charge density in the range between -3×10^{12} cm^{-2} and 3×10^{12} cm^{-2} was applied on both sides of the tested samples using a corona charger. The applied charge density corresponds to a surface potential in the range of -15 V to 15 V. The resulting

voltage was measured using the Kelvin Probe technique. The results of the effective lifetime and the surface saturation current density of the tested samples in the wide range of applied charge density are shown in Figure 4-7. The surface saturation current density was determined under low injection using the method presented in section 3.1.2.

The application of the high positive surface potential of 15 V results in the highest τ_{eff} for all three samples analyzed. At the same time, the surface saturation current density is minimal for this surface potential. This is caused by the field-effect passivation of the applied surface potential. The positive charges which are present at the surface repel the positive charge carriers from the surface of the samples. Due to the depletion of the minority carrier concentration at the physical surface, the surface recombination is decreased and does not limit the effective lifetime. Therefore, the measured effective lifetime of the minority carriers is very close to the bulk lifetime.

On the other hand, the application of the negative charges on the surface of the tested samples also leads to an increase of the effective lifetime. However, the maximum lifetime when negative charges are applied is lower than in the case of the positive charges. A strong negative charge induces an accumulation of holes under the surface. Since the capture cross section of holes σ_p of the surface recombination is much smaller than the capture cross section for electrons σ_n, an accumulation of holes is not as effective as accumulation electrons to suppress surface recombination. The lifetime of the tested samples is summarized in Table 4-2.

Table 4-2 Effective minority carriers lifetime and diffusion length for n-type FZ Si with base resistivity of 1, 3.5 and 10 Ω cm for different surface charge density. Lifetime was measured under low injection at $\Delta n = 5 \times 10^{14}$ cm^{-3}.

		Surface charge density [cm^{-2}]					
		0		3×10^{12}		-3×10^{12}	
Cell name	ρ_{base}	τ_{eff}	L_{eff}	τ_{eff}	L_{eff}	τ_{eff}	L_{eff}
	[Ω cm]	[ms]	[μm]	[ms]	[μm]	[ms]	[μm]
ThETA03_1	1	0.4	682	5.1	2440	0.9	1020
ThETA03_5	3.5	0.8	980	8.3	3150	2.3	1660
ThETA03_3	10	1.7	1430	10.0	3470	3.1	1940

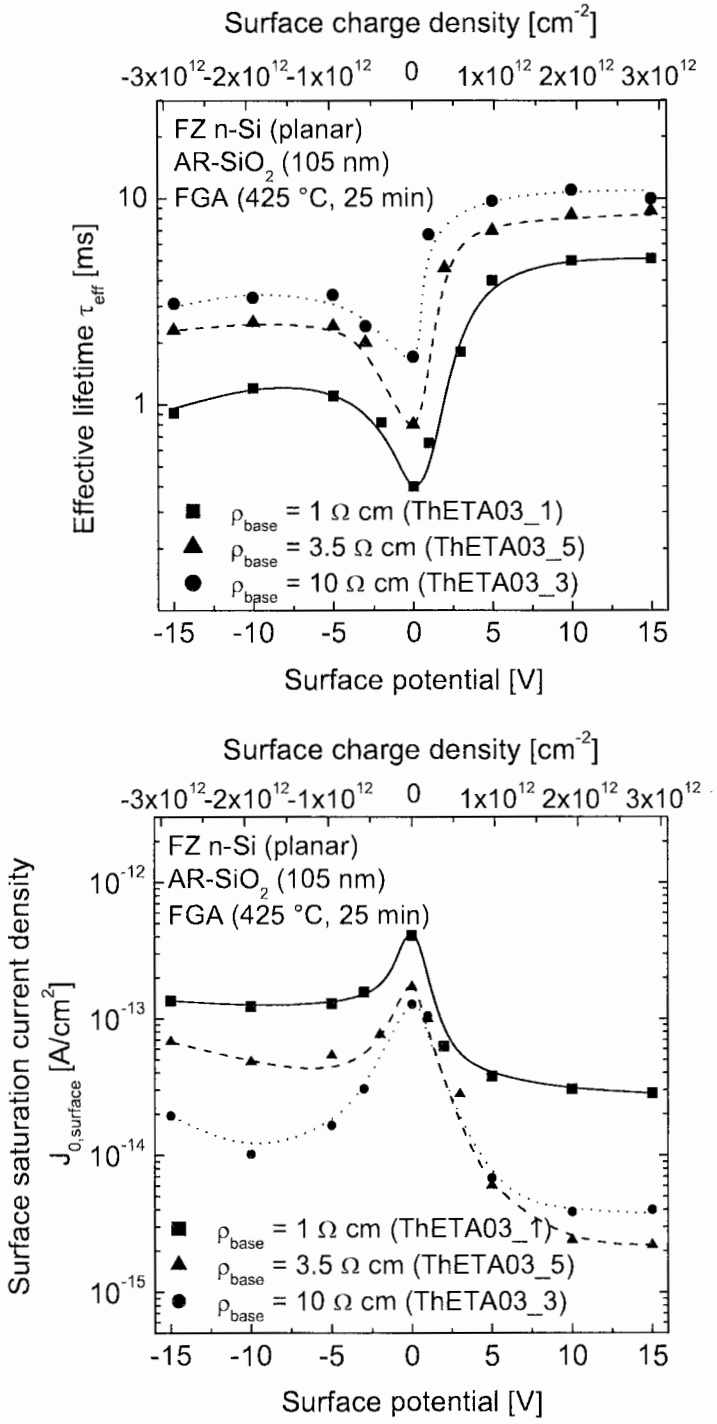


Figure 4-7 *Effective lifetime of the minority carriers (top) and the surface saturation current density (bottom) of n-type FZ Si lifetime samples measured in a wide range of surface potential and surface charge density at the outer oxide surface for base resistivity of 1, 3.5 and 100 Ωcm. Lifetime was measured under low injection at $\Delta n = 5 \times 10^{14}$ cm^{-3}. Lines are guides-to-the-eye.*

For the lowest surface recombination current density at the surface charge density of 3×10^{12} cm^{-2}, the effective diffusion length of the minority carriers is in the range of 2.4 to 3.5 mm for the tested n-type FZ Si. Thus, the selected Si material is of very high quality and perfectly suited for processing of high-efficiency back-junction solar cells.

4.3 Processing technology

After the selection of the silicon material, next the processing technology to form the solar cell structure, as shown in Figure 4-1 and Figure 4-2, can be to be optimized. The work of the author in the field of development of the processing technology and the sequence of the processing steps was performed in the framework of the research project *Quebec* [41] with the solar cell manufacturing company Q-Cells AG and the Institut für Solarenergieforschung Hameln (ISFH). In the present section the family of processes applied in the processing sequence of the developed back-contact back-junction solar cell is presented. The technology critical to the interdigitated solar cell structure, namely the metallization technology, is presented in more detail in the following section.

Cleaning

In the processing of the high-efficiency solar cells, much attention needs to be given to the cleaning of the processed samples. The introduction of contaminated samples into the high temperature diffusion or oxidation process would be fatal to the sample lifetime. Therefore, the so-called RCA Cleaning [114] procedure was applied. In the first step, the organic impurities and the metals are removed from the silicon surface by wet chemical oxidation in a solution of ammonium hydroxide (NH_4OH) and hydrogen peroxide (H_2O_2). Next, the formed oxide is removed in a diluted hydrofluoric acid (HF) in the so-called HF-Dip. In the second wet oxidation step, in the hydrochloric acid (HCl) and hydrogen peroxide solution, the alkali ions are removed. Again, the formed oxide is removed in a diluted hydrofluoric acid. The samples are rinsed with de-ionized (Di) water after each cleaning step.

Thermal oxidation

The role of the thermal silicon dioxide (SiO_2) layer is to:

a) reduce the surface recombination by passivation of the silicon surface, and

b) form a masking layer for the subsequent local diffusion or contact opening steps.

The typical applied oxidation temperature is 1050°C and the thickness of the applied oxide was around 200 nm for the masking oxide. In the case of the passivation oxide on the front cell side, the thickness was 10 nm and the oxidation temperature was only 850°C.

Phosphorus and boron diffusion

In the processing sequence of the analyzed high-efficiency BC-BJ solar cells, three diffusions in a quartz tube furnace are applied:

a) Formation of the boron emitter from the liquid BBr_3

b) Formation of the phosphorus back-surface field (BSF) from the gaseous $POCl_3$. From the $POCl_3$ in the atmosphere of oxygen O_2 and nitrogen N_2, a phosphorus silicate glass (PSG) is formed on the wafer surface. The phosphorus silicate glass functions as a source of phosphorus during the high temperature diffusion.

c) Formation of the low phosphorus doped front-surface field (FSF) from the gaseous $POCl_3$. A detailed analysis of the applied FSF diffusion profiles is presented in chapter 7.

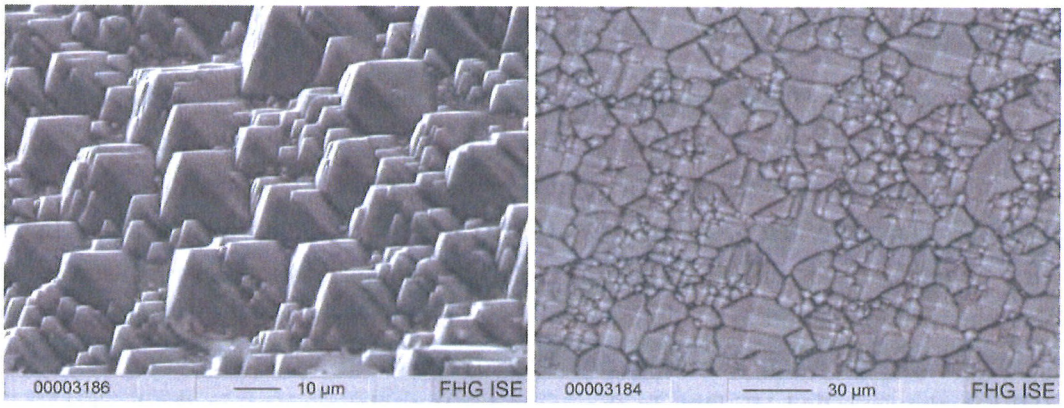


Figure 4-8 Scanning electron microscope (SEM) micrographs of the silicon surface with random pyramids texture with (111)-crystal planes. Side view (left) and top view (right) are shown.

Texture

In order to reduce the optical reflection losses of the solar cells, the front surface is textured. Due to the textured surface, the incident light that is reflected from the wafer surface has an increased chance to be absorbed by hitting the wafer surface again. To form the texture in the case of the monocrystalline silicon, the so called random pyramid texture was applied. In a low concentrated KOH solution, different crystal

planes in silicon are etched at different rates [115]. This way, the structure of the randomly distributed pyramids with different sizes is formed as shown in Figure 4-8.

Deposition of silicon nitride

An antireflection silicon nitride (SiN_X) layer with a thickness of 70 nm is deposited on the front cell side in order to further decrease the reflection losses and increase the front surface passivation quality [116], [117]. The nitride layer is deposited by means of a plasma enhanced chemical vapor deposition (PECVD) process at the temperatures around 400°C [118].

Formation of the interdigitated grid of the emitter and BSF diffusions

As already shown in Figure 4-1 and Figure 4-2, the emitter and BSF diffusions on the rear cell side form an interdigitated grid. In the solar cells, the local diffusions were performed through a masking oxide layer. For the structuring of the masking oxide only industry-relevant technology, such as screen-printing and laser ablation, were applied.

In Figure 4-9 an example of the processing sequence to create local emitter/BSF diffusion by means of laser ablation is shown. First, the whole rear surface is oxidized. Local openings in the oxide layer are then formed by local laser ablation of oxide and a thin silicon layer. Subsequently, the damage induced by the laser into the silicon crystal lattice is etched back in the KOH solution. Finally the emitter/BSF diffusion is performed. The oxide layer acts as a diffusion barrier.

In Figure 4-10 an example of the processing sequence to create local emitter/BSF diffusion by means of screen printing of the etch barrier (etch resist) is shown. First the whole rear surface is oxidized (1). Then the etch resist layer is screen-printed on the wafer surface (2). The openings in etch resist layer correspond to the places where the emitter/BSF diffusion should take place. In the next step (3), the oxide surface which was not covered with etch resist is etched in a diluted HF solution. Next (4), the etch resist layer is removed wet-chemically. Finally (5) the emitter/BSF diffusion is performed. In the developed process first the boron emitter diffusion in performed locally. Next the local phosphorus BSF diffusion is performed.

Due to the limited positioning accuracy and resolution of the applied structuring technology, the pitch of the finished solar cells was in the range of 1.3 to 3.5 mm. The pitch of concentrator solar cells processed with the use of photolithography can be as low as 50 µm [119]. Thus, the application of the low cost structuring technology

results in an increase in pitch by a factor of around 40. The impact of the pitch on solar cell performance is studied in chapters 6 and 8.

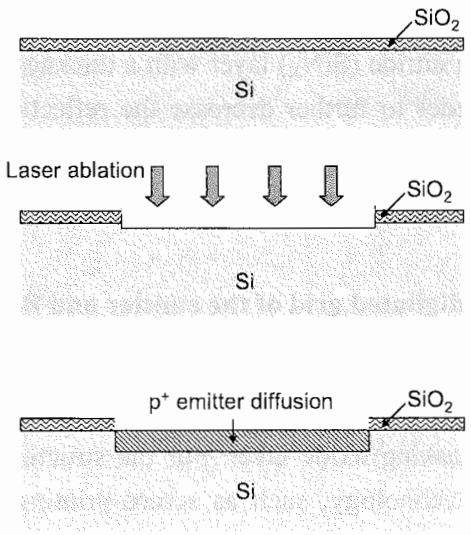


Figure 4-9 Processing sequence for the creation of the local emitter or BSF diffusions using the laser ablation of the silicon oxide layer. In the figure, the rear side of the cell is on top. The front side structure is not shown for simplification. The pictures are not to scale.

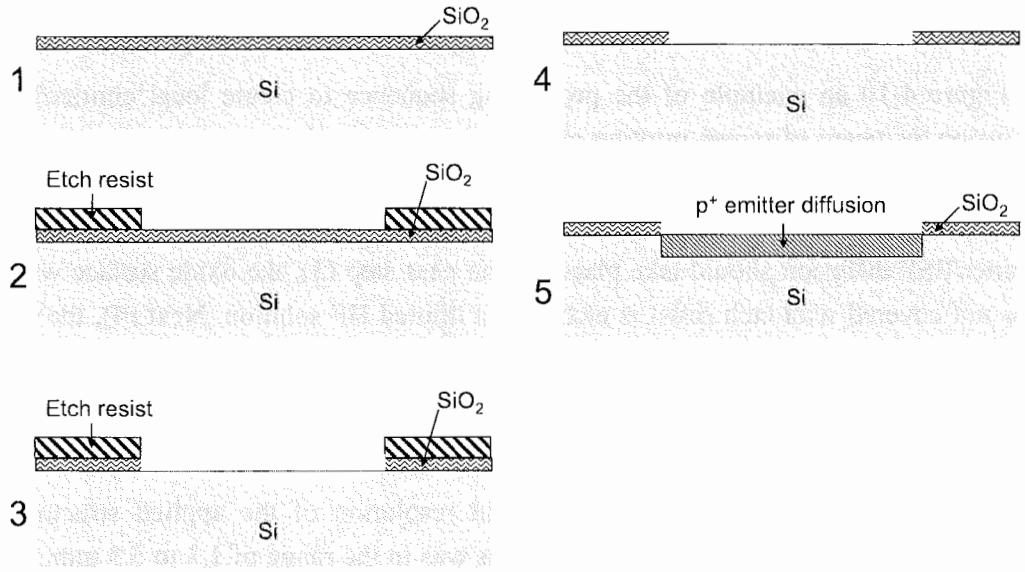


Figure 4-10 Processing sequence for the creation of the local emitter or BSF diffusions using the screen-printing of the masking layers. In the figure, the rear side of the cell is on top. The front side structure is not shown for simplification. The pictures are not to scale.

Formation of the contact openings

The surface recombination velocity of the metal contact to the intrinsic silicon is extremely high in the range of 10^6 cm/s [120] to 10^7 cm/s [121]. However, the surface recombination velocity at the metal contacts can be effectively reduced by the application of highly doped n^{++} or p^{++} silicon regions in the areas of the metal-semiconductor contacts [85]. The size and pitch of the local openings in the dielectric layer on the rear cell side through which the metal-semiconductor contacts are formed, and the diffusion profiles of the emitter and BSF diffusions, need to be carefully optimized [122], [123] in order to minimize the contact-semiconductor recombination losses and the contact resistance losses [124].

The openings of the metal-semiconductor contacts are formed in the same way as already shown in Figure 4-9 and Figure 4-10. Both screen-printing of the etch resist layer and a direct ablation of the dielectric layers were developed and applied in the processing sequence of the solar cells analyzed. The laser ablation of the dielectric layers was intensively investigated by Grohe [125]. Photographs of the rear side cell structure after emitter and BSF diffusions and after the formation of the contact openings in the rear side dielectric layer are shown in Figure 4-11.

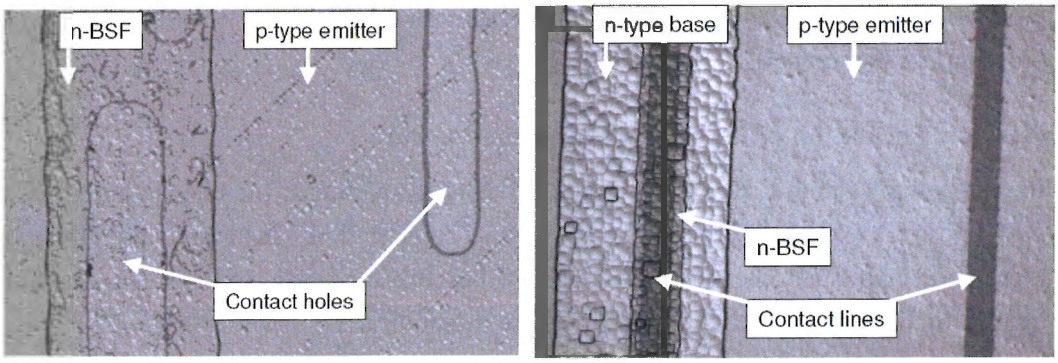


Figure 4-11 Photographs showing details of the rear side pattern prior to solar cell metallization. The emitter and BSF diffusions, as well as the contact openings are marked. The patterns were defined by (left) screen printing and (right) laser processing. For both images the same scaling is used.

4.4 Metallization

In this section the process to form an interdigitated grid of p and n metal electrodes is presented. A two-step metallization scheme was developed and successfully applied to the processing of the BC-BJ solar cells structure. In the first step a thin seed metal

layer is deposited and structured to form an interdigitated grid. In the second step the thin seed metal layer is thickened using an industrially feasible plating process.

The seed metal layer is deposited on the full rear side by the means of a vacuum evaporation process. The seed metal layer consists of a stack of aluminum and silver layers with a total thickness of less than 500 nm. The aluminum layer, which is in direct contact with the silicon wafer, enables formation of good ohmic contact to both the highly doped p-emitter and highly doped n-BSF at the same time [124], [126]. Moreover, the aluminum layer, together with the rear side passivation dielectric layer forms a very effective rear side reflector, enhancing the internal light trapping. The second layer, which is evaporated on top of the Al layer during one evaporation process, is the thin silver layer. Silver acts as a seed layer for the following silver plating process, in which the line resistance will be reduced. Moreover silver enables direct soldering on the finished cell during the solar module assembly.

After deposition of the seed metal layers on the entire rear cell surface, the interdigitated grid of non-shunted p and n-metal grids needs to be formed. Different techniques for the formation of the interdigitated metal gird are presented in section 4.4.1. Next, the thin seed metal layer needs to be thickened, in order to increase the conductivity of the metal fingers. This is accomplished by means of the plating process. The analysis of the required thickness of the finished metallization grid is presented in section 4.4.2.

4.4.1 Formation of the interdigitated metal grid

In the present section different techniques for the formation of the interdigitated metal grid, which are based on the two-step approach called 'seed and growth', are presented. Two methods were developed in the course of this work and successfully applied to the processing of solar cells. These methods are:

- Local etching of the metal layer defined by screen-printed masks
- Lift-off approach and laser-enhanced lift-off using screen-printed masks

Other interesting techniques, which are based on deposition of the thin seed metal layers and thickening them using a plating process, are presented for reference. In all presented methods both p- and n-diffusions, as well as the local contact openings, are already present on the solar cell. Thus, only the formation of the interdigitated metal grid is presented.

Self-aligned metal grid formation on steps in Si surface

A self-aligned technique to separate p- and n-contact grids after full area metal deposition was introduced by Sinton et al. in 1988 [18]. The method is schematically presented in Figure 4-12. In this method, on the rear side of the solar cell the emitter and base areas are placed on different levels on the Si surface, i.e. there is a wafer thickness difference of 5 to around 20 μm between the emitter and base areas, which was created by the local KOH etching.

After the formation of the contact openings, a full area deposition of the metal layer (e.g. Al) with a thickness of few to several tens of micrometers is performed. Next a thin (e.g. 50 nm) layer of the etch barrier (such as Ti or PECVD SiO_2) is deposited on top of the metal layer. Due to steep slopes between emitter and base regions, the thin etch barrier material is thinner and even discontinuous at the slopes. This feature is used in the following etch step, in which the aluminum layer is etched at the slopes where the etch barrier is discontinuous, e.g. in diluted HCl solution. In this manner, no alignment is required for this method. However, the solar cell structure must feature the above mentioned thickness variation structure. The self-aligned method of slopes in the Si surface was also successfully applied by Engelhart in the processing sequence of the RISE solar cell [40].

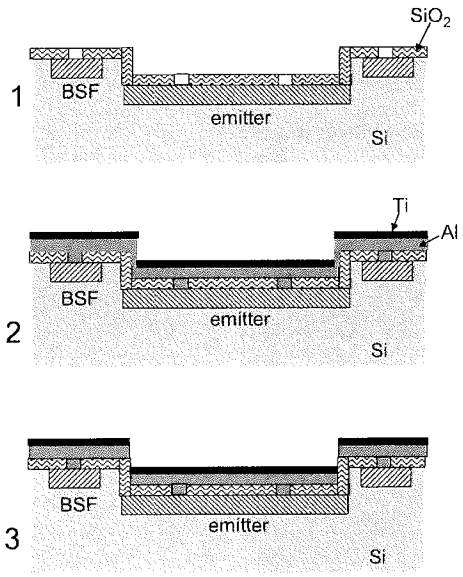


Figure 4-12 Method formation of the interdigitated p-n metal grid using the self aligned process on the high steps in the silicon surface. The method was introduced by Sinton et al. [18]. The front side structure is not shown for simplification. The drawings are not to scale.

Laser ablation of the masking layer and etching of the bulk metal

A contact separation method using a laser ablation of the thin etch barrier was recently introduced by Teppe et al. [127]. This method is schematically shown in Figure 4-13. First a full area metal deposition by means of evaporation or sputtering is applied. Secondly, a thin layer of the etch barrier (here again, a thin PECVD SiO_2 layer can be used for example) is deposited on top of the metal layer. In the next step, the etch barrier and a thin layer of the underlying metal layer is locally removed by means of laser ablation. Finally the metal layer is locally etched back, and the etch barrier is removed.

The advantage of this method is the formation of very thin separation lines between metal fingers, which enables the realization of high metal coverage on the rear cell side, which is needed for good reflection characteristics. Additionally, the application of a thick metal layer below the thin etch barrier removes the risk of introduction of laser damage to the solar cell structure, because all of the laser power will be absorbed in the etch barrier and in the top surface of the metal layer. An example of separation lines created between the metal fingers is shown in Figure 4-14.

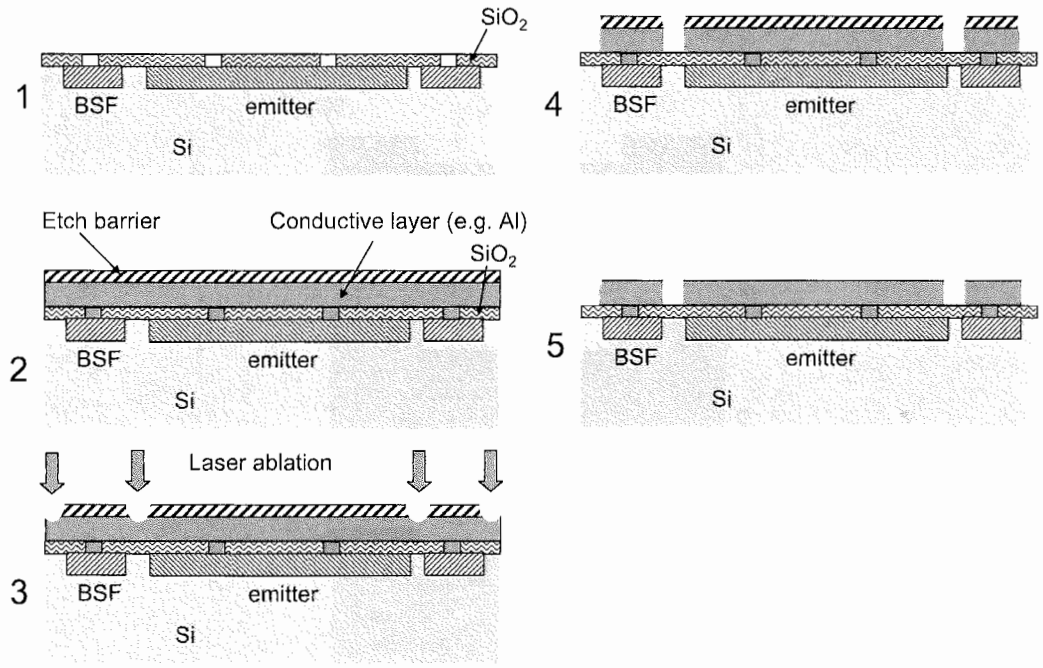


Figure 4-13 Method for contact separation using local laser ablation of an etch barrier and etching of the conductive layer. Method is patented by Teppe et al. [127]. The front side structure is not shown for simplification. The drawings are not to scale.

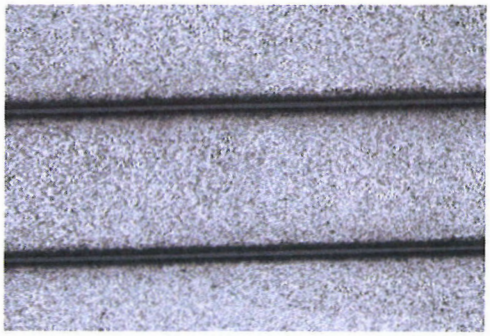


Figure 4-14 Example of a successfully separated p- and n-metal grid using laser ablation of the masking layer and local wet chemical etching of the Al layer. The size of the opening between the metal fingers is around 50 µm. Photograph taken with an optical microscope.

Process patented by Sunpower Corp.

A method which uses a local application of the screen-printed or inkjet plating resist layer is shown in Figure 4-15.

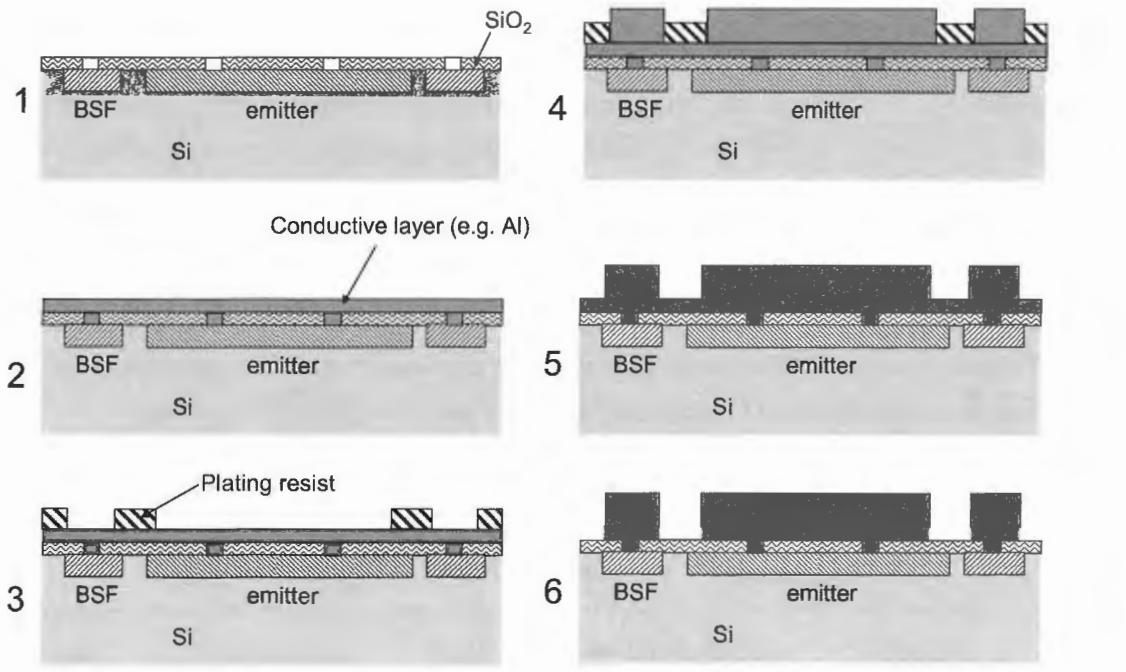


Figure 4-15 Method for contact separation using application of the screen-printed or inkjet plating resist. Method is patented by Mulligan et al. from Sunpower Corp. The front side structure is not shown for simplification. The drawings are not to scale.

This method is patented by Mulligan et al. [128] of Sunpower Co. After deposition of a thin seed metal layer, the plating resist is applied on top of the metal layer locally in the locations where the separation between the metal fingers is required. Next, the rear side metal layer is thickened in the electroplating process using Ag or Cu plating baths. The locations covered with the plating resist remain thin after the electroplating process. Next, the plating resist layer is stripped. Now, using the wet chemical etching, the thin metal layer between the thick plated metal fingers can be etched away. Since the seed metal layer is typically thinner than 1 μm, only a very small percentage of the plated metal will be etched away.

The advantage of this process is the elimination of the shunting risk through the formation of metal bridges between p- and n-electrodes during the plating process. On the other hand, if more than one metal is applied in the seed layer, as can be the case in copper plating, then multiple selective etching steps are required, which may increase the complexity of the process.

Local etching of the metal layer through the screen-printed masks (this work)

Another method which uses the screen-printed or inkjet masking layers is presented in Figure 4-16. This method, using screen-printing of the etch barriers, was developed and successfully applied during solar cell processing in the course of this thesis. After the deposition of the thin (less than 1 μm) seed metal layer (Al and Ag), the etch barrier is screen-printed locally on top of the metal layer in the locations where the metal fingers are needed. Next, the local wet chemical etching of the Ag layer is done in diluted HNO_3. In the following step the Al layer is etched back in diluted HCl (see Table 4-3). After etching the metal layer, the etch barrier is stripped and the thin metal fingers are thickened to the required thickness using the Ag plating process.

Table 4-3 *Process parameters for the selective etching of the aluminum (thickness of 300 nm) and silver (thickness of 100 nm) seed metal layers, used in the formation of the interdigitated p- and n-metal grids.*

Etched metal	Etching Solution	Ratio	Temperature	Time
silver	HNO_3 (69 %) : H_20	1 : 1	room T	30 sec
aluminum	HCl (32 %) : H_20	1.4 : 1	room T	2 to 10 min.

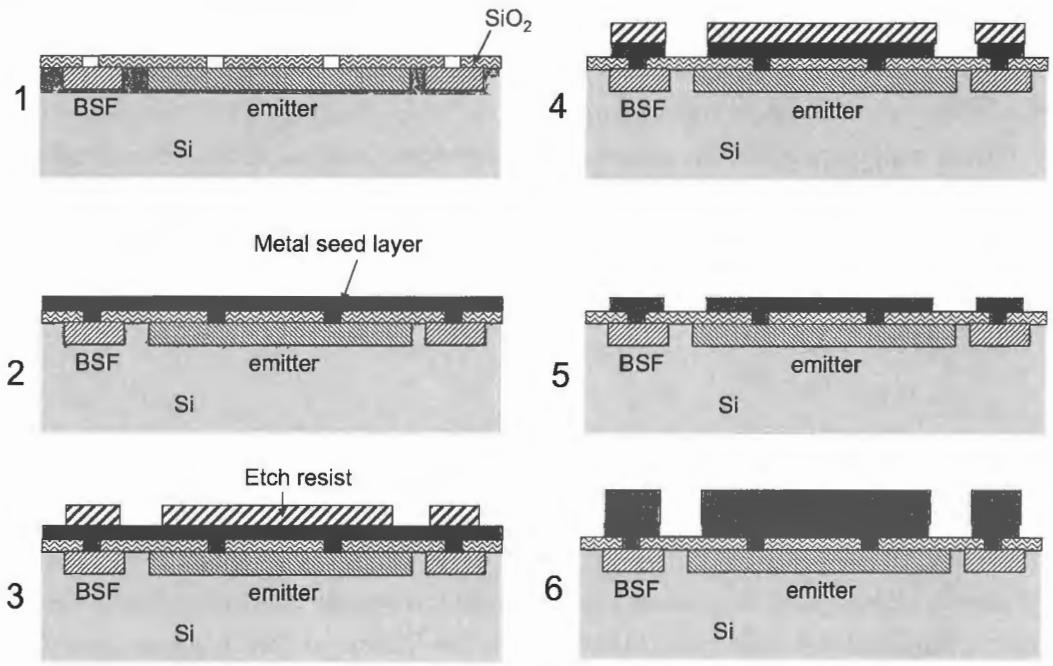


Figure 4-16 Method for contact separation using application of the screen-printed or inkjet etching masks. This method was developed in and successfully applied into the solar cells processing in the course of this thesis. The front side structure is not shown for simplification. The drawings are not to scale.

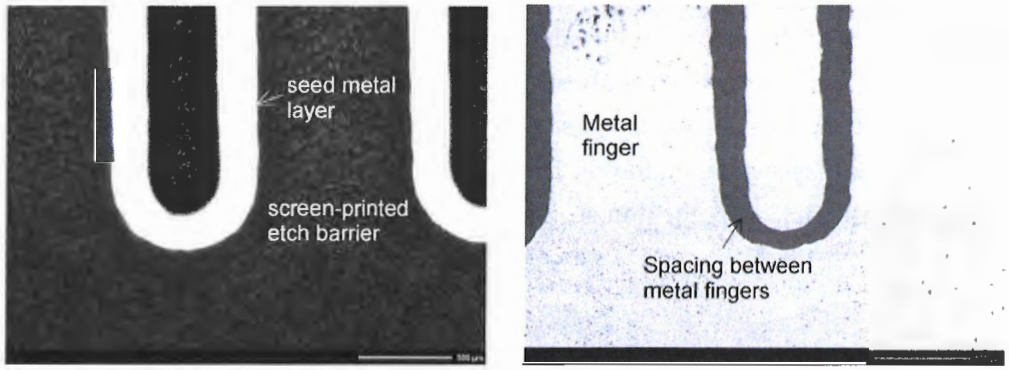


Figure 4-17 Example of the contact separation using the screen-printed etch barrier layers (left). After the local etching of the metal seed layer and etch barrier removal, the contact separation between the metal fingers is created (right). Photographs taken with optical microscope.

An example of the application of the screen-printed etch barrier and the resulting metal finger structure is shown in the Figure 4-17. The presented method has two major risks. These are:

- strong under-etching of the metal fingers underneath the etch barrier if the etching time and uniformity over the whole wafer area are not optimized carefully, and
- formation of metal bridges between the p- and n-metal grids if openings and/or local imperfections in the screen-printing process, such as locally closed opening lines, are formed.

Additionally as in the previous method, if more than one metal is applied in the seed layer, then multiple selective etching steps are required. This would increase the complexity of the process.

Lift-off approach and laser enhanced lift-off (this work)

In microelectronics and in the processing of high-efficiency solar cells, the lift-off method is widely used [129]. However, the use of photolithography to form the structures in the photoresist makes this approach too complicated and expensive for the mass production of solar cells. Therefore in the frame of this work an alternative approach, in which the photolithography was replaced with the low-cost screen-printing process, was developed. In Figure 4-18 the lift-off method is schematically presented.

The screen-printed lift-off resist is locally deposited on the rear cell surface. Next, a thin seed metal layer is deposited. If the slopes of the resist are steep enough, only a very thin layer of the metal is deposited on the slopes. In the next step, the resist is stripped in a liquid solvent. The solvent can penetrate the resist layer through the very thin and non-continuous metal layer at the slopes of the resist. After dissolution of the resist, the metal layer lying on top of the resist is removed and the contact separation is complete. In the final step, the thin seed metal layer is thickened in the plating process.

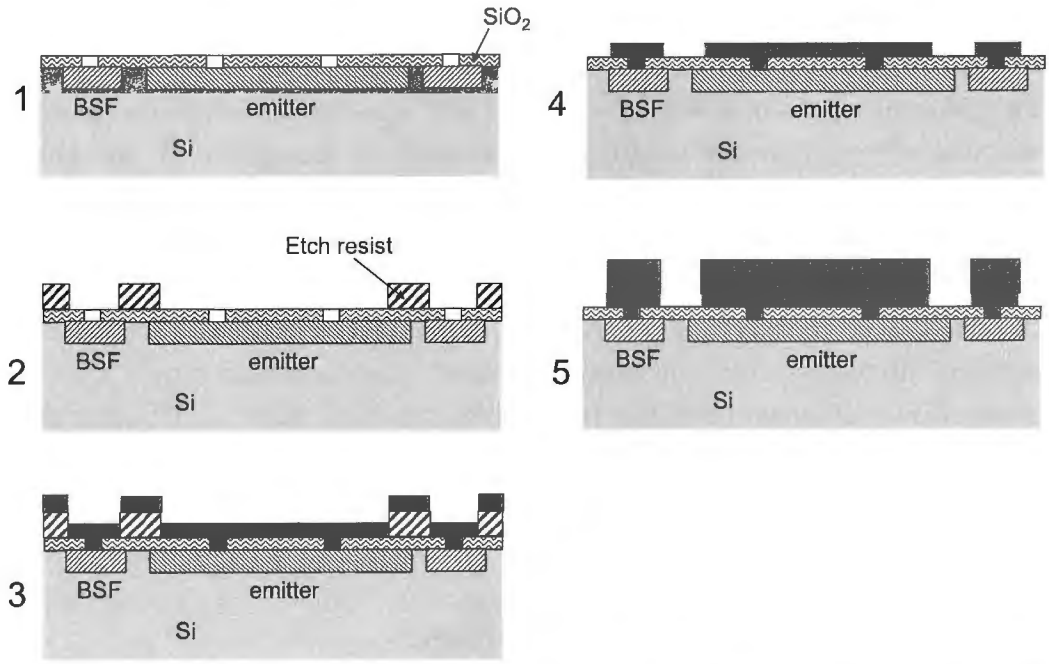


Figure 4-18 Method for contact separation using the lift-off approach with the application of the screen-printed or ink-jetted resist layer. This method was developed in and successfully applied into the solar cells processing in the frame of this thesis. The front side structure is not shown for simplification. The drawings are not to scale.

An example of the contact separation using the lift-off technique with screen-printed resist layer is shown in Figure 4-19. The same screen-printing mask was used here as in the case of Figure 4-17, which resulted in a negative structure of the metal fingers after the lift-off process.

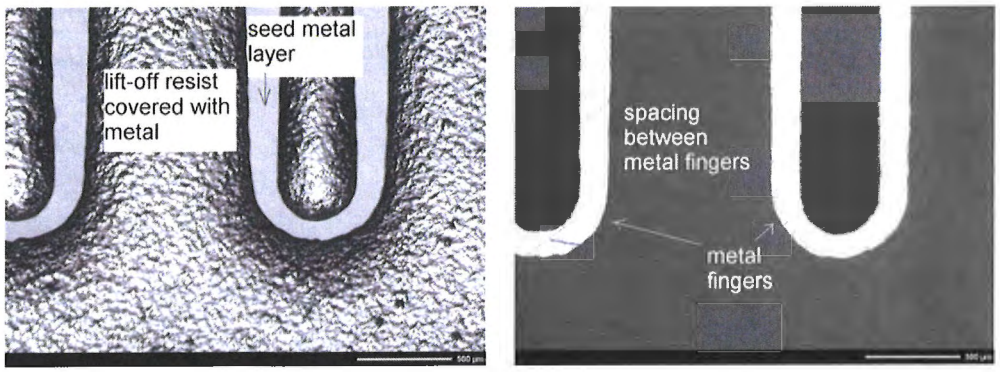


Figure 4-19 Example of the contact separation using the lift-off process with the screen-printed resist layer before (left) and after (right) the lift-off process. Photographs taken with optical microscope.

Unfortunately, due to the fact that the slopes of the screen-printed resist are not steep enough, the metal layer at these slopes is usually dense, and the solvent cannot reach the resist easily (see Figure 4-20). Due to this fact, the stripping time of the resist layer can take a long time and significantly decrease the throughput of this process. Therefore, a modification of the standard lift-off process was introduced in the course of this work. After deposition of the seed metal layer, local openings in the metal layer are formed by means of the laser ablation as schematically shown in Figure 4-20. Thus the transport of the solvent to the resist layer is greatly enhanced, at the same time reducing the process time. This process is called "Laser enhanced lift-off". The laser energy is fully absorbed in the first few micrometers of the metal and the resist layers. Therefore, due to the large thickness of the resist layer (10-30 μm), the laser energy cannot reach the silicon surface and create damage there.

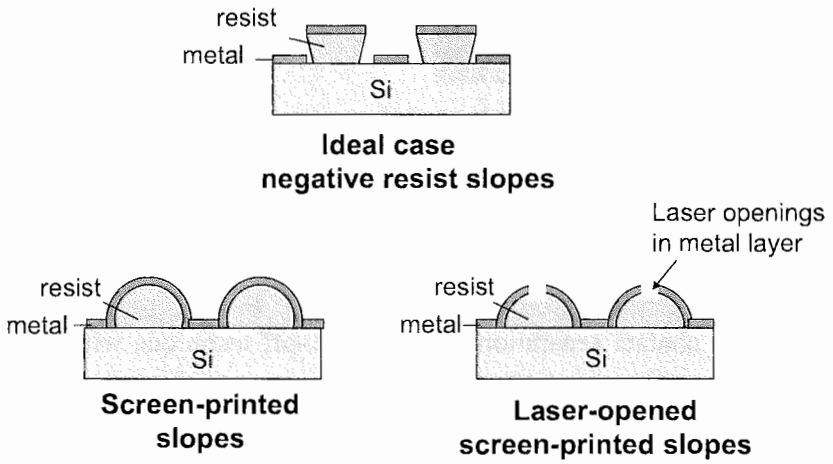


Figure 4-20 Influence of the slope of the resist edges on the lift-off process. The ideal case of the resist with negative slopes is shown in the top picture. The actual slopes of the screen-printed resist are not steep at all (left). The laser ablation process, used to open the metal layer, enhances the speed of lift off process significantly (right).

The advantages of the lift-off process are:

- No risk of under-etching of the metal fingers,
- Removal of the seed metal layers is done in one step. There is no need for selective etching of many metals in the seed layer.

On the other hand, due to the application of the screen-printing process the size of the spacing between the metal fingers is high, in the range of 100 to 300 μm. This is caused by the low positioning accuracy and the resolution of the screen-printing process. The large spacing between the metal fingers increases the optical transmission

losses of the solar cell. The application of screen-printed resist with non-steep slopes requires the introduction of the laser ablation process in order to increase the speed of the lift-off process.

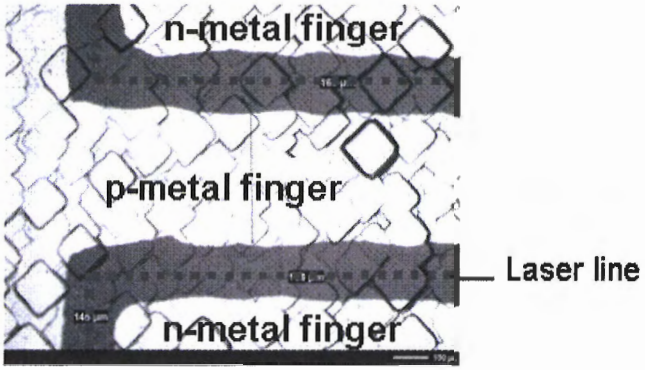


Figure 4-21 Example of the contact separation using the laser enhanced lift-off process with the screen-printed resist layer. Photographs were taken using an optical microscope.

4.4.2 Thickening of the thin seed metal layer

After formation of the interdigitated p- and n-metal seed layer, the thickening of the thin seed metal layer is required in order to increase the conductivity of the metal fingers and reduce the series resistance losses. The influence of the metal finger height on the series resistance and the resulting fill factor of the solar cell can be calculated with the following equations [121]:

$$R_s = \frac{1}{3}\frac{A_F}{B_F H_F}\rho L_F{}^2 \tag{4.1}$$

$$\Delta FF = FF_0 \frac{R_s J_{sc}}{V_{oc}} \tag{4.2}$$

where A_F is the pitch of the solar cell, B_F is the width of the metal fingers, L_F is the length of the fingers, H_F is the height of the fingers, and ρ is the resistivity of the applied metal. FF_0 is the fill factor of the solar cell not reduced by the series resistance losses and ΔFF is the fill factor loss caused by the series resistance R_S.

The calculated series resistance and the fill factor of the n- and p- metallization grid for two solar cell sizes of 2×2 cm^2 and 12×12 cm^2 with the pitch of 2200 µm are shown in Figure 4-22. For the laboratory cell size of 4 cm^2 a thickness of 2 µm of the metal

fingers is sufficient to reduce the resistance of the metal grid to 0.1 Ω cm^2, which would result in a the fill factor loss of less than 0.5 % absolute. However, for the industrial scale 144 cm^2 solar cells with the length of the metal fingers of 12 cm, the required thickness of the metal fingers is much higher. If 1 % absolute loss in fill factor due to metal resistance is allowed, than the required thickness of the metal fingers is around 35 µm in the case of the application of the silver plating. Using this metal finger thickness, the series resistance of the metallization grid equals 0.2 Ω cm^2. This calculation shows the importance of the thickening of the seed metal layer, especially for industrial size solar cells.

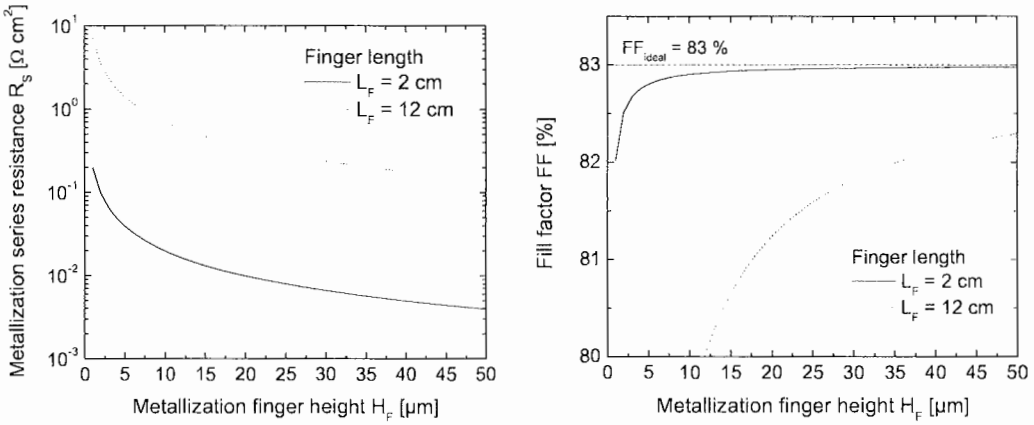


Figure 4-22 Calculated resistance of the interdigitated grid for a pitch of 2200 µm for two solar cell sizes of 2×2 cm^2 and 12×12 cm^2 (left side) for different thickness of the silver fingers. The resulting fill factor for both solar cell sizes is shown in the right graph.

In the developed solar cell process, the thickening of the structured seed metal layer was done using silver plating. A novel approach to thickening the interdigitated grid of the back-contact back-junction solar cells was introduced, in which both electrodes are thickened using different plating mechanisms. The p-electrode is contacted and thickened using the electroplating process in the potassium silver cyanide $K[Ag(CN)_2]$ bath [130]. The n-electrode is not contacted. It is plated using the light-induced plating (LIP) approach in the same chemical bath. LIP was optimized by Mette et al. [131] for the application of thickening the front surface metallization grid of the both-sides contacted solar cells. The p- and n-electrodes are of different width (see Figure 4-2), requiring therefore different thickness to achieve optimal resistance of the total metal grid. Due to the application of two different plating mechanisms during one plating process, the rate of the thickening of both electrodes can be optimized in order to achieve optimum usage of the metal material.

4.5 Solar cell results

The low-cost screen-printing and laser structuring processes described above were successfully applied to the BC-CJ solar cell processing sequence. In the present section the solar cell results, obtained using the described technologies, are presented.

4.5.1 Laboratory-scale solar cells

For laboratory-scale (4 cm^2) solar cell (see Figure 4-2), best conversion efficiency of 21.1 % (designated area measurement) was achieved on 1 Ω cm n-type FZ Si with the pitch of 2200 μm. The illuminated current-voltage characteristics together with the solar cell parameters of the best solar cell are shown in Figure 4-23.

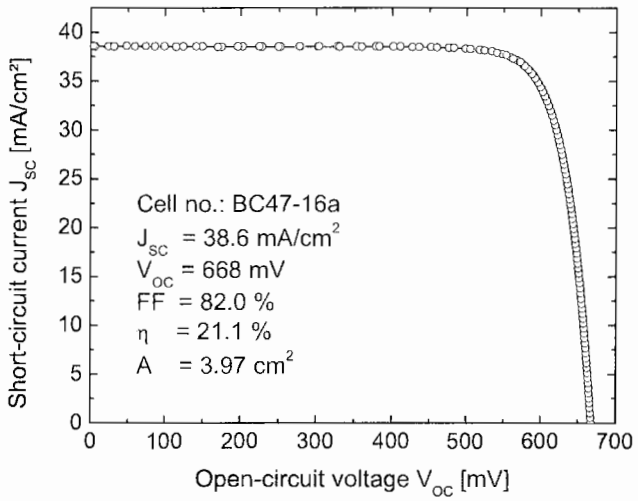


Figure 4-23 Illuminated current-voltage characteristics of the best n-type back-contact back-junction solar cell with the pitch of 2200 μm and the efficiency of 21.1 %. Designated area measurement under AM1.5G spectrum with illumination intensity of 100 mW/cm² and with device temperature of 25 °C. The efficiency was measured at Fraunhofer CalLab.

A very high fill factor value of the finished cell of 82 % indicates low resistive losses. Shunting between the tight p- and n-metal finger grids was avoided by a application of appropriate metallization process (see section 4.4.1). The series resistance losses of lateral carrier transport due to the large pitch could be minimized by application of the high conductivity FSF (see chapter 8 for more details). The total series resistance of the best solar cells is around 0.2 Ω cm^2, which proves a good device design in terms of resistive losses.

The open-circuit voltage of the best cell equals 668 mV. The rather moderate V_{OC} value indicates that a careful optimization of the rear side geometry and the diffusion profiles is required in order to further increase the device efficiency.

The short-circuit current of the best cell reaches nearly 39 mA/cm^2 for 1 Ω cm base resistivity. Analysis of the J_{SC} losses (section 6.2) shows that the optical losses (mainly front surface reflection, escape light and free carrier absorption) and the recombination losses over the base areas are limiting J_{SC}.

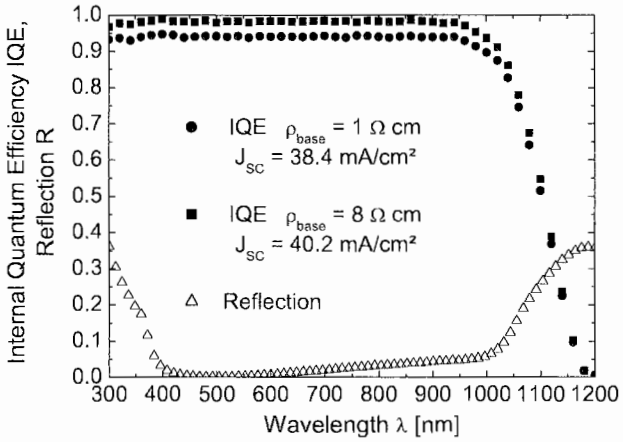


Figure 4-24 Comparison of the internal quantum efficiencies of the BC-BJ solar cells with base resistivity of 1 Ω cm and 8 Ω cm. The cells have a FSF with ρ_{sheet} = 148 Ω/sq and pitch of 2200 μm. The short-circuit current calculated by the integration of the solar spectrum with the external quantum efficiencies are shown in the graph. Note a nearly zero-reflectance at wavelength of around 550 nm due to the absence of the front side metal fingers.

The internal quantum efficiencies (IQE) and reflection (R) of the BC-BJ solar cells with a base resistivity of 1 Ω cm and 8 Ω cm are shown in Figure 4-24. The cell's reflection is very low due to the absence of the front side metallization grid. A nearly zero-reflectance is achieved for wavelengths of around 550 nm. The internal quantum efficiency for both resistivities is high, but does not reach unity. The IQE of the 1 Ω cm cells equals 95 % and for the 8 Ω cm cells it equals 98 %. The decrease of the IQE (5 % for 1 Ω cm cells and 2 % for 8 Ω cm cells) is partially caused by the front surface recombination and the bulk recombination of the minority carriers, which did not reach the rear side p-n junction. The front and rear surface recombination is higher in the case of base material with higher doping concentration [132]. This explains the differences in J_{SC} of solar cells with both base resistivities. However, the analysis presented in section 6.4 indicates that there is another cause for the decrease of IQE,

namely the recombination over the broad areas of base doping, called electrical shading.

Due to the absence of the front side metallization grid, the optical shading losses can be avoided in the BC-BJ solar cells. However, electrical shading is still present due to the rear side recombination in the regions of base busbar and base fingers [87]. A light beam induced current (LBIC) [133] map of the 2×2 cm^2 laboratory solar cell is presented in Figure 4-25. One can clearly recognize the reduced EQE signal over the base fingers and busbar. The EQE drops to nearly zero above the base busbar, even though no optical shading in this region is present. This is due to (a) large lateral distances which the minority carriers need to diffuse in order to be collected by the p-n junction and (b) due to enhanced recombination over the gap and BSF areas which have high saturation current densities. A detailed analysis of the solar cell results and the loss mechanisms is presented in chapter 6.

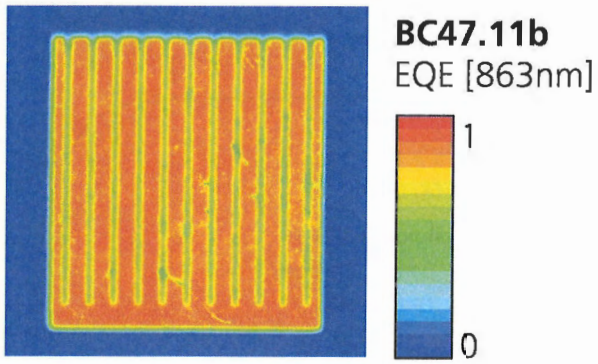


Figure 4-25 LBIC map of the BC-BJ silicon solar cell. The reduced EQE signal above the base fingers and base busbar (top side) are visible. The designated cell area is 2x2 cm^2 and the busbar area is 0.15x2 cm^2. EQE was measured at a wavelength of 863 nm.

4.5.2 Industrial-scale solar cells

In the frame of the *Quebec* [41] project, in which the author of the thesis developed the back-contact back-junction solar cell structure for mass production, large size solar cells were also manufactured. The photographs of a finished large area cell is shown in Figure 4-26.

The best efficiency of 19.2 % was achieved on n-type Cz-Si 5-inch pseudosquare wafers (cell size 147.4 cm^2) with the resistivity of 3 Ω cm. The illuminated current-voltage characteristics, together with the solar cell parameters of the best large size solar cell are shown in Figure 4-27.

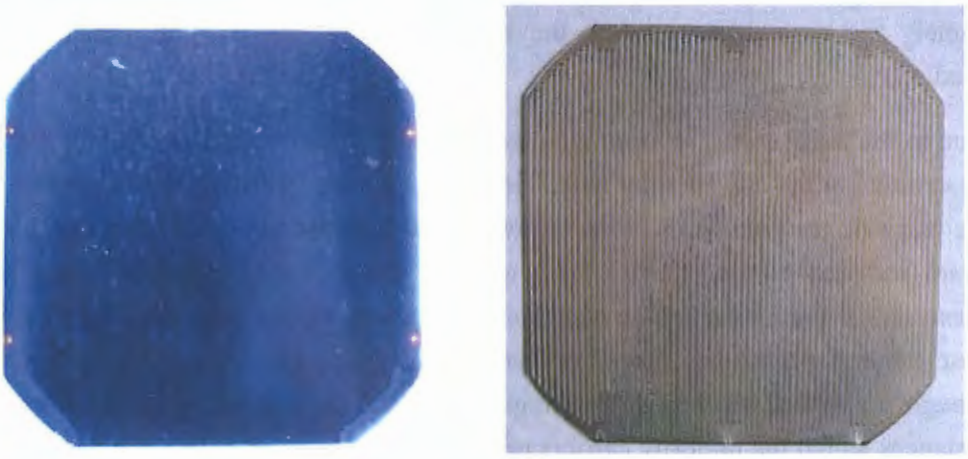


Figure 4-26 Photographs of the front (left) and rear (right) side of the large area back-contact back-junction solar cells developed in the course of the Quebec project at Fraunhofer ISE. Cell area is 147.4 cm²

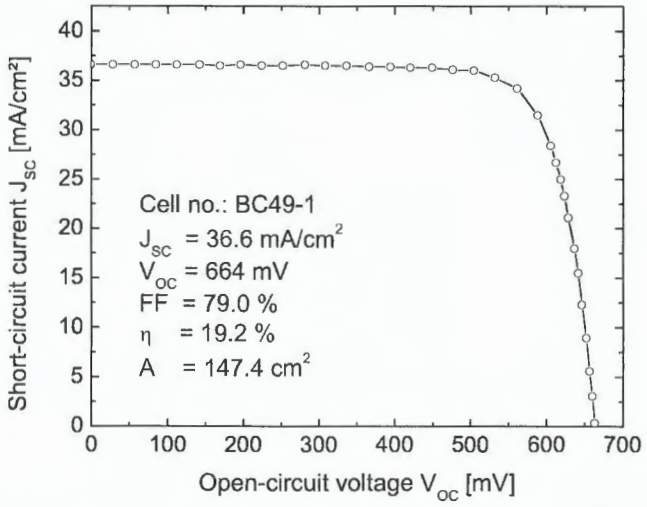


Figure 4-27 Illuminated current-voltage characteristics of the best n-type large size (147.4 cm²) back-contact back-junction solar cell developed at Fraunhofer ISE in the frame of the Quebec project [41]. The solar cell has an efficiency of 19.2 %. Measurement under AM1.5G spectrum with illumination intensity of 100 mW/cm² and with device temperature of 25 °C.

A lower efficiency (19.2 %) of the large area solar cells in comparison to the small laboratory-scale solar cells (21.1 %) is caused mainly by the lower fill factor and lower short-circuit current values. The open-circuit voltage of both solar cells is similar.

The lower FF values are caused by the significantly increased length of the metal fingers from 2 to 12 cm. The metal finger height after the silver plating process is in the range of 10 to 30 µm, which results in a FF loss of about 2 to 3 % absolute (see Figure 4-22). The rather wide spread of the metal finger thickness is caused by the fact the silver plating process of the BC-BJ solar cells was not optimized for large-area solar cells.

The difference in J_{SC} of small and large size solar cells is partially caused by the application of a different silicon material: FZ Si for small cells and Cz Si for large cells. The differences in the minority carrier's lifetime in the bulk of the fully processed cells may cause the J_{SC} differences. Moreover, in the case of the large size solar cells, local imperfections and non-uniformities, which are not avoidable due to manual handling of the large size wafers in the laboratory processing conditions, are present. These local imperfections (e.g. scratches, cracks, and passivation or diffusion non-uniformities) over the whole area of the solar cells are responsible for the locally decreased quantum efficiency of these cells (see Figure 4-28).

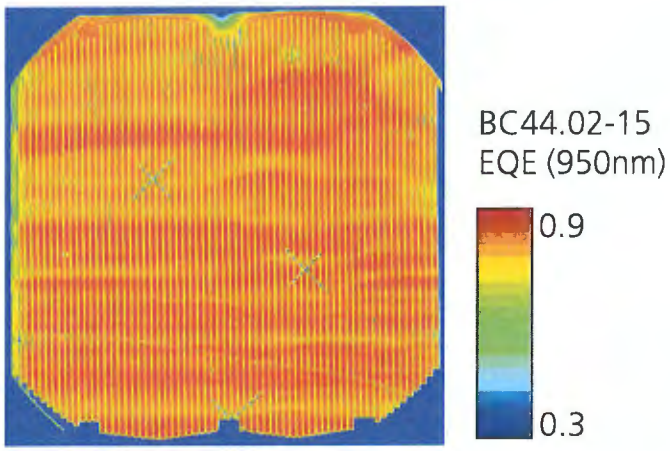


Figure 4-28 LBIC map of the large area BC-BJ silicon solar cell. The reduced EQE signal above the base fingers and base busbar (bottom side) are visible. The solar cell area is 147.4 cm^2. Local defects introduced by the manual handling of the wafer during processing can be recognized.

4.6 Conclusions

The design and the processing technology of the developed high-efficiency back-contact back-junction solar cell were presented. The structuring steps, which are required to form an interdigitated grid of p- and n-diffusions and metal grids, were done using industrially relevant low-cost techniques. Screen-printing of the masking

layers, as well as the local laser ablation of the dielectric and silicon layers, were developed and successfully applied to the solar cell processing sequence.

Solar cells were processed on n-type Si substrates. The applied n-type Si material was intensively examined. Very high minority carrier lifetimes up to 18 ms were measured for the investigated silicon substrates. The determined minority carrier lifetime is high enough to enable realization of the high-efficiency BC-BJ silicon solar cells.

Metallization technology is very critical in the case of the interdigitated metal grid structure, due to the very high risk of shunt formation between the p- and n-metal grids. A review of the existing approaches to form an interdigitated metallization grid on the rear cell side, as well as the two methods which were developed in the frame of this study, were presented. Metallization of the developed solar cells was performed using a laboratory approach consisting of two steps. First a thin (less than 1 μm) seed metal layer was evaporated and structured to form interdigitated grid geometry. Next, a silver plating process was applied to increase the metal finger height and conductivity.

The highest solar cell efficiency of 21.1 % was achieved on 1 Ω cm n-type FZ Si with the designated area of 4 cm^2. For the large area solar cells with an area of 147.4 cm^2, a maximum efficiency of 19.2 % was achieved. A detailed analysis of the solar cell results is presented in the following chapters.

5 Analysis of the laser-fired aluminium emitters

In this chapter the local laser-fired aluminium emitter (LFE) process, an alternative process to boron emitter diffusion, was investigated. The model of the LFE emitters, which includes a laser-induced damage zone, was analyzed using a two-dimensional simulation and compared with the experimental solar cell results. The injection-dependent Shockley-Read-Hall recombination in the direct vicinity of the local back junction influences negatively the cell performance and causes large cell performance differences for varying specific base resistivities of the cells.

5.1 Introduction

The Laser-Fired Contact (LFC) technology developed at Fraunhofer ISE [134] not only provides local contacts through the dielectric passivation layer at the back cell side, but also creates a local aluminium doped region. In the case of p-type cells, this region works as a high-low junction - an effective back surface field (BSF). This feature of the LFC process already enabled fabrication of a 21.9 % p-type solar cell. In addition to application of the LFC process to p-type substrates, an n-type substrate process with the use of the LFC has been introduced by Glunz et al. [135], [136]. The LFC process was used in that case to form local p-n back junctions on the *n-type* substrates, referred to as the laser-fired aluminium emitter (LFE) process.

The LFE process combines three steps in one:

1. Formation of the local openings in a dielectric layer.
2. Formation of the metal-semiconductor contacts, through the local openings.
3. Formation of the local p^+ emitter. Al is alloyed with Si, and a local p^+ emitter is created in the n-type substrate. Thus, the additional emitter diffusion process can be omitted.

Thus, the greatest appeal of the laser-fired p^+ aluminium emitter (LFE) process is the inherent opportunity to create a patterned emitter without additional masking steps. This feature of the LFE process makes it attractive for its application in the back-contact back-junction solar cell structure, where the p^+ emitter is diffused only locally.

Moreover, the LFE process enables the fabrication of high efficiency n-type cells without the use of boron diffusion. Replacement of the boron diffused emitter with the laser fired aluminium emitter could lead to significant reductions in processing time and potentially to a reduction in costs of the manufacturing of back-contact back-junction solar cells. The reason for this is that the boron diffusion is a high-temperature and time consuming process: diffusion temperatures are in the range of 800 - 1100°C, and the process requires several hours. High diffusion temperatures are required because of the low solubility of boron in Si. The solubility of phosphorus [137] is, for example, around one order of magnitude higher than the solubility of boron at the same temperatures [138]. Thus, in order to achieve high surface concentrations of boron, the diffusion process needs to take place at strongly elevated temperatures. In contrast LFE can be performed with the wafer at room temperature. Therefore, the heating of wafers to high diffusion temperatures is not required for this process, as it is in the case of boron emitter diffusion. Additionally, the LFE process is very fast, requiring a processing time in the range of seconds per wafer.

The objective of this chapter is to analyze and gain fundamental knowledge about the LFE process, an alternative process to the emitter formation using boron diffusion. Based on the analysis of the laser-fired Al emitters, the replacement of the boron diffusion with the LFE process could be potentially considered in the processing sequence of the back-contact back-junction solar cells.

5.2 Fabrication of LFE and boron emitter cells

Laser fired aluminium emitters (Figure 5-1 left) and locally diffused boron emitter (Figure 5-1 right) n^+np^+ back junction cells have been fabricated on 250 µm thick FZ n-type 1, 10 and 100 Ω cm Si substrates. The size of the cells is 2x2 cm^2. The cells exhibit a front surface with random pyramids, evaporated front contacts and a phosphorus diffusion (front surface field) with sheet resistance ρ_{sheet}=120 Ω/sq. The front surface is passivated by a 105 nm thick thermal oxide. The rear surface is covered with the same thermal oxide.

Formation of the local p-n junction on the rear side:

- LFE cell: After evaporation of 2 µm thick aluminium layer on the rear surface, the back junction is created by local laser-firing of the aluminium through the oxide layer, resulting in formation of a p^+ emitter and contact/emitter coverage of about 5 %.

- Diffused boron emitter cell: Back junction was formed by local boron diffusion through the oxide structured with photolithography on the rear side, with 1.5 % emitter coverage. The rear surface was then oxidized again and local contact openings were formed using photolithography with 0.2 % contact opening coverage. Finally, a 2 µm thick aluminium layer was evaporated on the rear surface.

The last processing step is a low temperature (425 °C) annealing under forming gas, called FGA process. The process time is 25 min and the concentration of H_2 in N_2 equals 5 %.

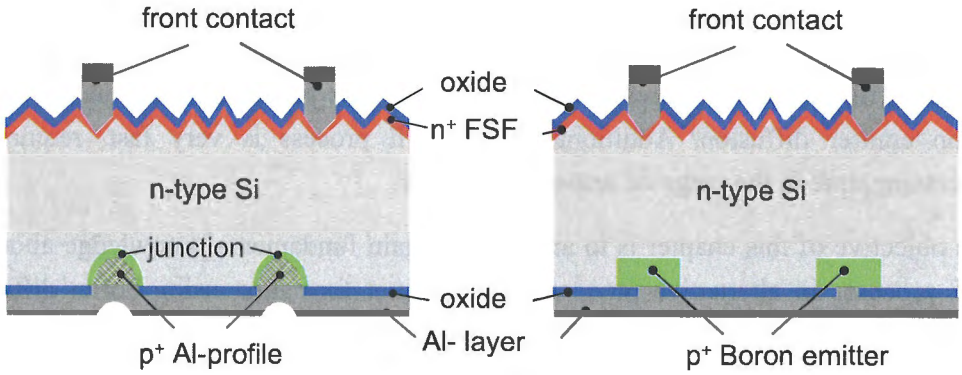


Figure 5-1 Structure of the n-type back-junction LFE cell (left) and the n-type back-junction locally boron diffused cell (right).

5.3 Solar cell results

The best results of different base resistivity n-type LFE cells are summarized in Table 5-1. The best efficiency of 19.4 % was obtained on 100 Ω cm FZ n-type material with the back-junction LFE cells. In the section 5.7, where the comparison of the results of the solar cells with LFE and boron diffused emitters is presented.

In Table 5-1 a very large difference in the performance of the LFE cells with different base resistivities can be observed. Differences of almost 10 mA/cm^2 (i.e. up to more than 20 % relative) in J_{SC} of the 1 and 100 Ω cm cells were measured. At the same time, differences of 30 mV in V_{OC} of cells with 1 and 100 Ω cm base can be seen. It is believed that the laser-induced crystal damage is responsible for limiting the performance of the LFE cells and for causing significant differences in the performance of these cells with different base resistivities. Understanding the differences in performance of the LFE solar cells with different base resistivities is an objective of the analysis presented in the following sections.

Table 5-1 I-V results of the LFE cells fabricated on n-type FZ Si substrates with different resistivities.

Cell no.	ρ_{base} [Ω cm]	V_{OC} [mV]	J_{SC} [mA/cm^2]	FF [%]	η [%]
NRP7_24.2m	100	646.5	39.8	75.1	19.4
NRP7_21.2m	10	639.8	37.9	71.9	17.4
NRP4_23.5	1	616.7	30.2	72.9	13.5

5.4 Laser-induced damage zone

In previous work [135] a concept of a laser-induced damage zone (see Figure 5-2) was introduced in order to explain the decreased V_{OC} of the p-type LFC cells in comparison to the passivated emitter rear locally diffused (PERL) cells with diffused Al BSF. Laser damage to the crystal lattice is caused by rapid melting during the absorption of a very short laser pulse [139] and a subsequent recrystallization of the silicon. The laser-induced defects are known to form recombination centers [140], [139], thus locally reducing the lifetime of the minority carriers.

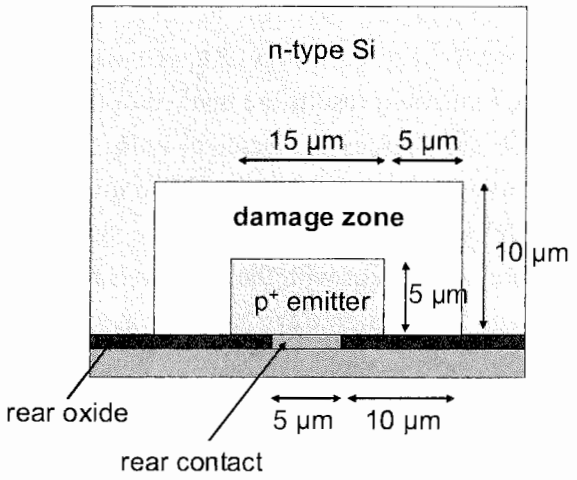


Figure 5-2 Two-dimensional simulation model of an LFC contact with a laser-induced damage zone around the local Al BSF.

The introduction of the damage zone with strongly reduced lifetime into the two-dimensional simulation model enabled very good modelling of the LFC p-type structures and modelling of their performance as a function of different base doping

concentrations. The damage zone implemented in the simulation model has a size of 15×5 μm^2 and strongly reduced lifetime of $\tau_{local} = 0.3$ µs. The size of the damage zone and the value of τ_{local} were arbitrary chosen in the simulations. The strongly reduced local lifetime in the laser damage zone models the very strong crystal defects and introduction of the metal impurities induced by the laser firing of the Al contacts.

Since in case of the n-type cell the local Al-profile functions as an emitter, the quality of this junction and the quality of the area in the direct vicinity of the junction is has a much bigger impact on the cell performance than in the case of p-type cells, where the Al-profile has the function of a local back-surface-field (LBSF).

5.5 Quantum efficiency of the LFE cells

In Figure 5-3 the measured internal quantum efficiency (IQE) of the LFE cells and the simulated IQEs are presented. Significant differences in the quantum efficiency of the LFE cells with different base doping concentrations cause very large differences in short-circuit current of the measured cells. IQE of the cell with 100 Ω cm base resistivity equals around 97%. At the same time the internal quantum efficiency of the LFE cell with 1 Ω cm base resistivity equals only around 75%. This difference in IQE explains around 20% differences in J_{SC} of these cells.

In the bottom part of Figure 5-3, the IQE of the n-type LFE cells were modeled using two-dimensional device simulation. Next to the LFE cells with the laser-induced damage zone, the IQE of the ideal case of a LFE cell without the damage zone was calculated as well. These modelling results are marked in the graph as 'Ideal Local Al-Diffusion'. In the device simulations an identical bulk lifetime $\tau_{SRH} = 1000$ µs was used for all three base doping concentrations in order to investigate the influence of the damage zone independently of the bulk effects. The damage zone model enables modeling which is in good agreement with the measured IQEs. It is believed that fine adjustments of the damage zone parameters, such as size and lifetime, may result in even better agreement with the measured values.

In Figure 5-3b, one can compare the influence of the damage zone on the quantum efficiency of the 1 and 100 Ω cm cells. The influence of the damage zone is much bigger for the 1 Ω cm material than in the case of 100 Ω cm, where the damage zone has almost no influence on the quantum efficiency. In the case of the cell with 1 Ω cm base resistivity and with the damage zone model the quantum efficiency is around 7 $\%_{abs}$ lower than the IQE of the cell without the damage zone. The next section deals with the explanation of this effect.

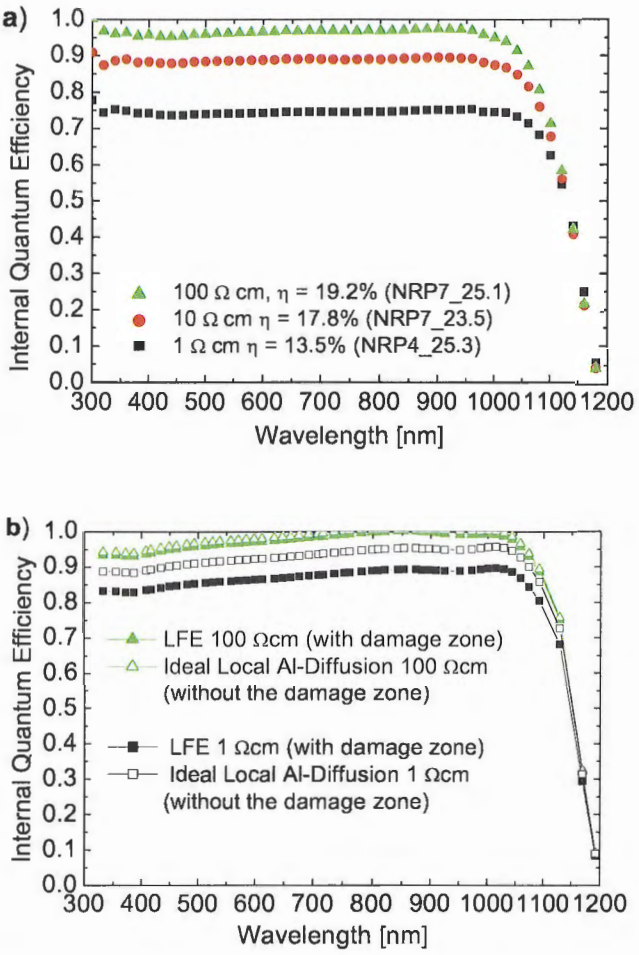


Figure 5-3 Measured (a) and two-dimensional SDEVICE [90] simulation (b) internal quantum efficiencies for the n-type LFE cells of different doping concentration.

5.6 Recombination in the damage zone

Using the damage zone model presented in the previous section, the Shockley-Read-Hall (SRH) recombination rate and the density of the electrons and holes in the direct vicinity of the rear local junction were simulated. The results of the two-dimensional simulations of the SRH recombination rate are shown in Figure 5-4. The LFE cells with base resistivities of 1 and 100 Ω cm were simulated. Additionally, the rear local junction solar cell without the damage zone and with base resistivity of 1 Ω cm was simulated for comparison.

In the results shown in Figure 5-4, a strongly increased recombination rate in the damage zone is observed. The recombination rate in damage zone is around 3 to 4

orders of magnitude higher than in the bulk Si material. Increased SRH recombination in the damage zone results from the very low lifetime of the minority carriers within this zone. In the model, the local minority carrier lifetime inside of the damage zone is set to 0.3 µs. The bulk lifetime is significantly larger and equals 1000 µs.

In the simulation of the cell without the damage zone, shown in Figure 5-4c, the recombination rate is uniform over the whole bulk area. This is the case when a p^+ emitter was created by boron diffusion or by alloying of Al, without the introduction of the stress caused by rapid thermal processing and crystal lattice defects during emitter formation using the LFE process.

An interesting effect can be observed by comparing the recombination rate in the damage zone of the LFE cells with 1 and 100 Ω cm. The recombination rate is there clearly higher in the case of the 1 Ω cm LFE cell than in the case of the 100 Ω cm cell. This effect can be analyzed better when looking at the profiles of the recombination rate taken through the wafer thickness in the middle of the rear local emitter, as shown in Figure 5-5.

The difference in the recombination rate of the cells with different base resistivity can be explained with the injection dependence of the Shockley-Read-Hall carrier lifetime (τ_{SRH}). τ_{SRH} is a function of the carrier injection level and the dopant density. In the case of the 1 Ω cm material, where the injection level is lower than the dopant density (see Figure 5-5a), a low injection level condition occurs ($\tau_{SRH,\,lli}$). However, the dopant density of the 100 Ω cm material is lower than the density of the holes (Figure 5-5 b), thus the 100 Ω cm LFE cell is under high injection ($\tau_{SRH,\,hli}$).

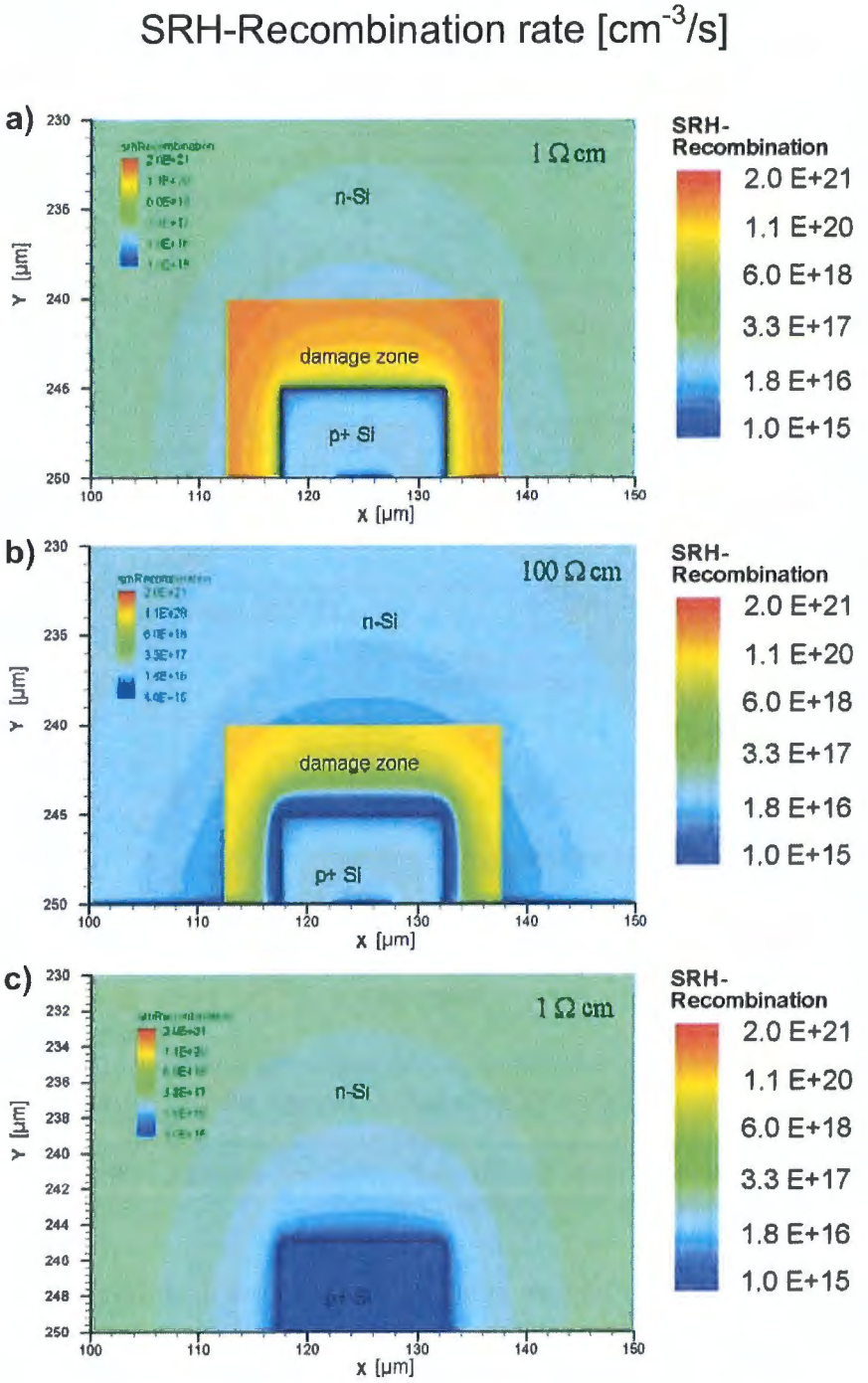


Figure 5-4 Two-dimensional simulation of the SRH-recombination rate under J_{SC} conditions of 1 Ω cm (a) and 100 Ω cm (b) LFE and 1 Ω cm LBSF (c) cells. Recombination was simulated in the vicinity of the local emitter on the rear side. Y-axis represents the thickness of the cell, with front cell surface at Y=0. SHR-recombination rate shown in the colour scale is given in cm^{-3}/s. Note strongly the increased recombination rate in the laser damage zone of the LFE cells (a and b).

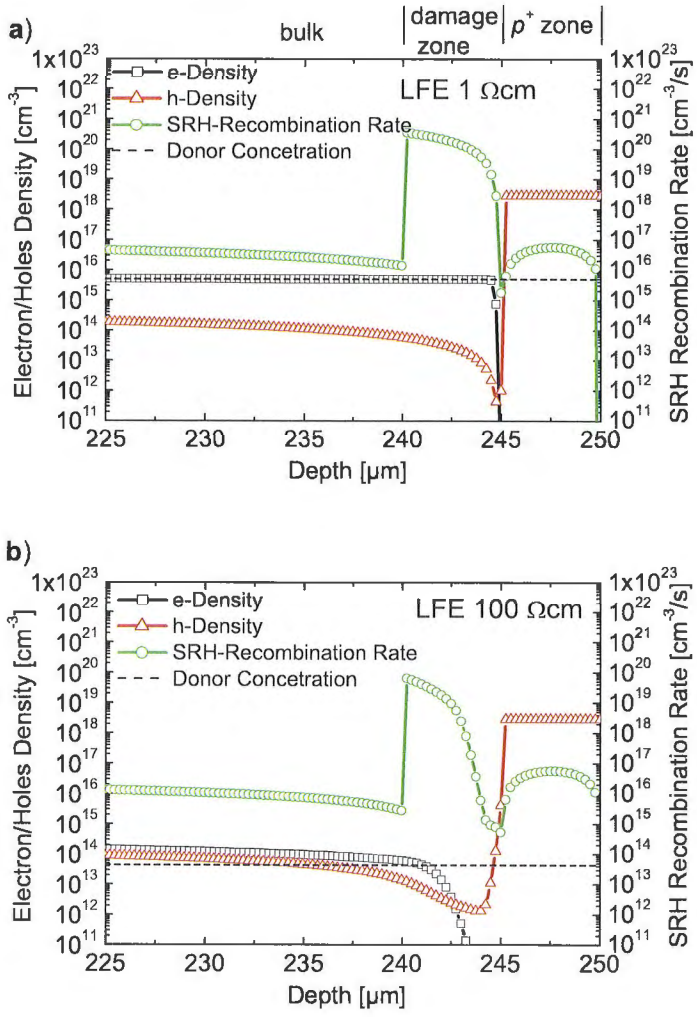


Figure 5-5 Profiles of the recombination rate under J_{SC} conditions of the 1 Ω cm (a) and 100 Ω cm (b) LFE cells taken through the cell thickness at the back surface of the cell (two-dimensional simulation). Note the high recombination rate in the laser-induced damage zone (between 240-245 µm from the cell front surface).

Using the simplified SRH lifetime models under low- and high-level injection [141] and for $\tau_{no} = \tau_{po}$, the low (lli)- and high-level injection (hli) lifetime in n-type Si is:

$$\tau_{SRH,\,\mathrm{lli}} = \tau_{po}$$
$$\tau_{SRH,\,\mathrm{hli}} = \tau_{no} + \tau_{po} \qquad (5.1)$$

Thus both bulk and damage zone lifetime of cells under high injection is significantly higher than under low injection. It is therefore believed that this significant lifetime difference, resulting in a drastic change of the diffusion length in the bulk Si and in the

damage zone, is the reason for the performance difference between the LFE cells processed on the 1 and 100 Ω cm n-type wafers. Results of the simulation prove the hypothesis to be correct. The increased recombination rate of the 1 Ω cm cell in the bulk and inside the damage zone leads to a significant current reduction of these cells compared to 100 Ω cm LFE cells.

5.7 Comparison of boron diffusion and LFE emitters

Further analysis of the influence of the injection dependence bulk and damage zone lifetime on the analyzed cell structure performance is done by direct comparison of the solar cells with LFE emitters (Figure 5-1 left) to cells with local boron diffused emitters (Figure 5-1 right). During the boron diffusion process, the damage zone in the direct vicinity of the local rear junction is not formed. It is therefore expected that, due to the absence of the damage zone, the solar cells with boron diffused emitters will show a different dependence on the current as a function of base doping than with the LFE cells.

Table 5-2 Comparison of the parameters of the LFE and boron diffusion emitter cells on different base resistivities. All cells were processed on the n-type FZ Si substrates. The area of the solar cells is 4 cm^2.

Cell no.	Emitter type	ρ_{base} [Ω cm]	V_{OC} [mV]	J_{SC} [mA/cm^2]	FF [%]	η [%]
NRP46_1d	Boron diffusion	1	599.6	35.1	60.6	12.8
NRP46_4e	Boron diffusion	10	653.1	36.0	74.7	17.6
NRP46_5e	Boron diffusion	100	658.5	37.6	74.2	18.4
NRP46_10f	LFE	1	619.2	31.7	69.8	13.7
NRP46_14b	LFE	10	625.1	35.9	78.0	17.5
NRP46_18b	LFE	100	629.0	37.6	76.3	18.0

As mentioned in section 5.2, a set of the LFE and boron diffused emitter solar cells was processed within the frame of this work. The best results are summarized in Table 5-2. The best efficiency of the back junction with locally diffused boron emitters in this experiment was 18.4 % on the 100 Ω cm substrate resistivity. For comparison, the highest reported efficiency of the n-type back junction solar cell with full area boron emitter is 22.7 %, presented by Zhao et al. [142]. Thus, the full area emitter on the rear

side has a far superior performance than the local rear emitter of this study. Coming back to Table 5-2, the performance of the cells with boron emitters is slightly higher than that of the LFE cells. The variation in FF of the boron emitter cells is caused by processing faults during the photolithography for the rear side contact formation.

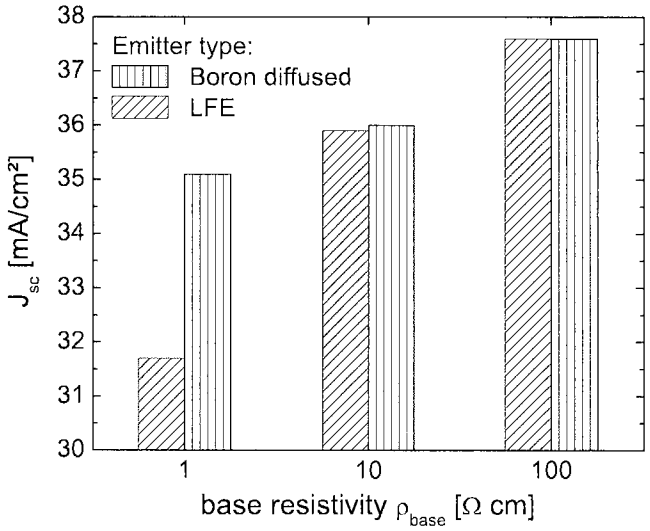


Figure 5-6 Comparison of the short-circuit current of the back-junction cells with LFE and boron diffused emitters on different resistivity substrates.

The V_{OC} values of the LFE cells are around 20 to 30 mV lower than the V_{OC} values of the boron emitter cells. The loss in V_{OC} is caused by the recombination in the damage zone of the LFE cells and by the increased metal contact coverage of LFE cells, which also results in the increased recombination of the minority carriers at the rear surface. In Figure 5-6, direct comparison of J_{SC} of the LFE and boron diffused cells on different substrate resistivities is shown. For a base resistivity of 100 Ω cm, there is no difference in J_{SC} of both cell types. The cell operates under high injection, thus the damage zone lifetime of LFE cells is high enough not to limit the device performance. This result is in good agreement with the device simulations shown in Figure 5-3b. With increasing substrate doping concentration, the J_{SC} of both cell types decreases. This effect is caused by decreased bulk lifetime in the substrate of higher doping concentration. However, for a base resistivity of 1 Ω cm there is a large J_{SC} difference of 3.4 mA/cm^2 between the LFE and boron emitter cells. This effect is again in good agreement with simulations shown in Figure 5-3 b. In the case of 1 Ω cm cells, which operate under low injection, the bulk lifetime in the damage zone is so low that it limits the minority carrier collection at the back junction.

The results mentioned above clearly prove the validity of the model of the laser fired aluminium emitter process, which includes the damage zone with significantly reduced local lifetime.

5.8 SunsV_{OC} and implied voltage

The SunsV_{OC} curves of the fully processed LFE cells, presented in Table 5-1, were measured for a wide light intensity range (Figure 5-7) in order to analyze the cell voltage under low and high injection level conditions.

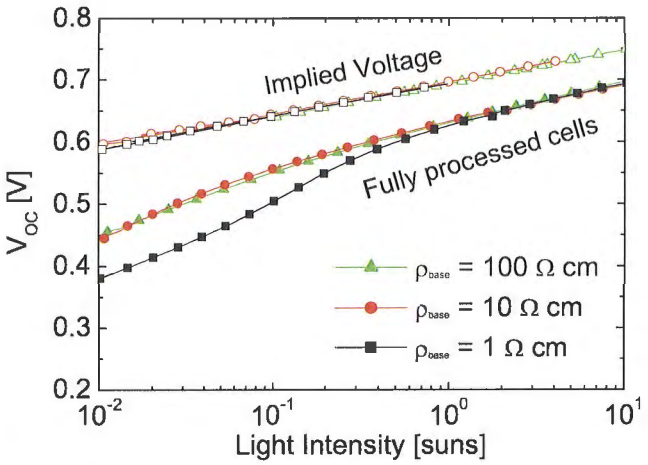


Figure 5-7 Open-circuit voltage (closed symbols) and implied voltage (open symbols) in the wide light intensity range for different resistivity n-type fully processed LFE cells and test samples for determination of the effective minority carrier lifetime.

The excess carrier density in the lifetime samples lead to the separation of the quasi Fermi levels and implies an open circuit voltage. For this experiment the n-type lifetime samples with different base resistivity have been prepared. Both sides of these samples exhibit a full area shallow n^+ diffusion (ρ_{sheet} = 120 Ω/sq.) and a full area 105 nm thick thermal oxide.

The implied voltage of the n-type FZ Si material, used for the solar cell processing, was calculated from the QSSPC lifetime curves. The calculations were performed using equation (5.2) as proposed by Sinton et al. in [75].

$$V_{OC} = \frac{kT}{q} \ln\left(\frac{\Delta p(N_D + \Delta n)}{n_i^2}\right) \tag{5.2}$$

The calculated implied voltage is plotted in Figure 5-7. The symmetrical n-Si lifetime samples, as shown in section 4.2.1, were analyzed. For all resistivities, shape and values of the implied voltage are roughly the same in the range of 700 mV at one sun light intensity. The implied voltage values represent an ideal state, where only bulk recombination (which is low for the good quality n-type material as shown in section 4.2) and the low surface recombination rate plays a role.

In the case of the fully processed LFE cells, the SunsV_{OC} curves are different than the implied voltage curves of the symmetrical lifetime samples. First of all, voltage values are lower. This is attributed to the cell structure, where additional recombination mechanisms such as: (a) front and rear side metal contacts, (b) laser-induced damage zone and (c) texturization are introduced. All these elements reduce the cell voltage to 610-630 mV at light intensity of one sun.

Additionally, one can see an interesting shape of the 1 Ω cm curve of the LFE cell. Under low-injection intensities (light intensities <0.3 Suns), the voltage decreases faster than in the case of higher resistivity cells. It is believed that this effect is caused by a strong decrease in lifetime in the laser damage zone, where under low-injection the SRH recombination dominates – as discussed above.

One would expect a larger J_{SC} vs. Suns than a V_{OC} vs. Suns dependence, because under short-circuit conditions the cells operate at much lower injection levels as compared to open-circuit conditions. Moreover, the short-circuit current of the rear junction cell structure has a much stronger bulk lifetime dependence then the cell voltage. That is why the differences in J_{SC} are much more significant than the V_{OC} differences between 100, 10 and 1 Ω cm cells, as can be seen in Table 5-1. The analysis above has another practical meaning as well. Under low illumination conditions, i.e. more realistic outdoor conditions, the LFE cells will suffer from an drop in efficiency, whereas the boron diffused cells should retain linear characteristics.

5.9 Optimization of the LFE cells

Optimization of the pitch, i.e. distance between the LFE points, was performed. The pitch of laser points was varied in order to find the optimum between two opposing trends:

a) For a smaller laser pitch, the emitter coverage on the rear side increases, which improves carrier collection at the back-junction. Moreover, the decrease of the LFE pitch should also have a beneficial influence on the fill

factor by reducing the lateral series resistance, especially for the cells with a low conductivity substrate.

b) Increasing the pitch of the LFE points results in a decrease of the damage introduced by laser, which should be as small as possible to reduce degradation of the cell performance.

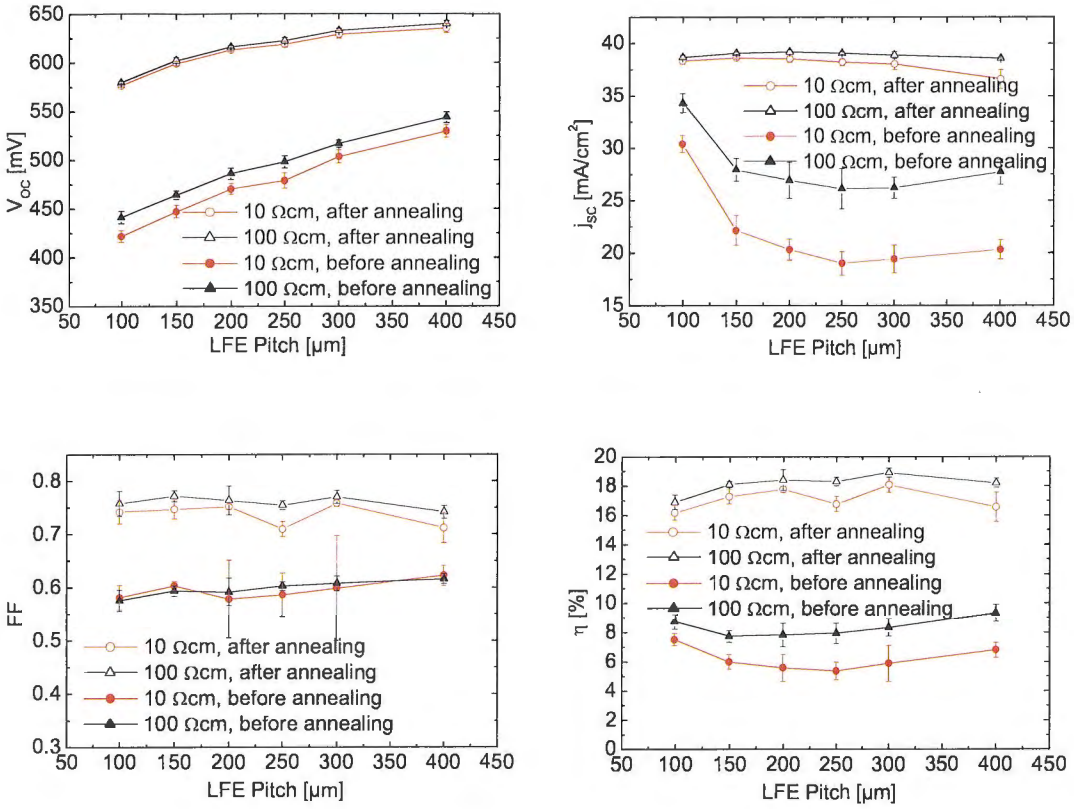


Figure 5-8 Results of the LFE cells processed with different pitch of the laser process. Cell results before and after annealing step are shown. Each data point represents the average of 7-16 cells. Standard deviation of the measurements is also plotted on the graphs.

A pitch of the LFE points in the range between 100 µm and 400 µm was chosen. The minimum pitch of 100 µm allows realization of an almost full area emitter on the rear side (each LFE point is of about 70 µm in diameter). The maximum pitch of 400 µm, on the other hand, is expected to be already too large for a good carrier collection at the back side and therefore lead to strongly reduced performance of the LFE cells. Results of the pitch optimization of the 10 and 100 Ω cm LFE cells are shown in Figure 5-8.

The solar cell parameters before and after the low-temperature (425 °C) annealing are presented. The importance of the annealing to achieve good cell results is clear, as it drastically improves all of the solar cell parameters: open-circuit voltage, short-circuit current, fill factor, and efficiency.

As expected, the cell's voltage improves with increasing pitch, because less damage is introduced by the laser. V_{OC} increased from 575 mV for the pitch of 100 µm to 630 mV for the pitch of 400 µm. Further increase of pitch of the LFE points is expected to lead to further improvement of V_{OC}.

However, with increasing pitch J_{SC} decreases. This is due to the increase of the effective diffusion path for the carriers required to reach the local back junction. When the required diffusion length becomes equal or higher than the effective diffusion length of the carriers, a significant percentage of the minority carriers, which were photogenerated in large lateral distances from the local junction, will recombine before reaching the p-n junction. Detailed analysis of the J_{SC} of the 10 and 100 Ω cm LFE cells shows that the J_{SC} of the 10 Ω cm cells is both lower and decreases more rapidly with the increasing pitch. This is caused by lower diffusion length of the minority carriers in the 10 Ω cm cells compared to 100 Ω cm n-type Si.

The fill factor of the cells is not significantly affected by the pitch in the investigated pitch range. However, a decrease of the FF for the largest pitch of 400 µm can be observed, due to increased lateral series resistance of the LFE cells. The best efficiency of 19.4 % on the 100 Ω cm was realized for the LFE pitch of 300 µm. Both voltage and current of the 100 Ω cm is only slightly better than 10 Ω cm cells, since both cell groups operate under medium- to high- injection and the low-injection conditions do not occur significantly.

5.10 Conclusion

The appealing benefit of the laser-fired p^+ aluminium emitter (LFE) process is the inherent opportunity to create a patterned emitter without additional masking steps. This feature of the LFE process makes it attractive for the application in the back-contact back-junction solar cell structure, where the p^+ emitter is diffused only locally. Therefore, in this chapter the LFE process was investigated and its influence on the solar cell parameters was compared to the solar cells with the traditional boron diffused p^+ emitter.

N-type solar cells with local back-junction were processed on 1, 10 and 100 Ω cm resistivity n-type FZ-Si. Differences in J_{SC} of up to 20 % between 1 and 100 Ω cm

cells were observed. An explanation, based on the experimental and simulation analysis of this effect, was proposed. It is concluded that the injection-dependent Shockley-Read-Hall recombination in the bulk Si and in the laser-induced damage zone determines the LFE cell performance and leads to strong performance differences between cells on different resistivity substrates.

By directly comparing the back-junction cells with LFE and boron diffused emitters, it was shown that the LFE process limits the open-circuit voltage and the short-circuit current of the LFE cells in comparison to the back-junction cells with locally diffused boron emitters. Moreover, due to non-linear behavior of the voltage under low illumination conditions, at the low light intensities the LFE cells will suffer drops in efficiency, whereas the boron diffused cells should remain linear.

Based on the above disadvantages of the LFE emitter formation process, the application of the LFE in the manufacturing of the high-efficiency back-junction solar cells was not further followed in the course of this thesis. On the other hand, if lower device efficiencies are allowed, then it might be interesting to consider the replacement of the boron diffusion by the LFE process in order to reduce the device processing thermal budget and time.

6 Analysis of the loss mechanisms

A detailed analysis of the loss mechanisms in the back-contact back-junction silicon solar cells is presented. Four main loss mechanisms in the BC-BJ solar cells are described: series resistance, optical losses, recombination losses and electrical shading. The influence of each of the loss mechanisms on the cell efficiency is studied. The reduction of the cell efficiency due to the analyzed loss processes was determined to be 3.9 % abs. due to recombination processes, 2.0 % abs. due to optical losses, 0.3 % abs. due to series resistance effects and 0.7 % abs. due to electrical shading.

6.1 Introduction

A back-contact back-junction n-type Si solar cell processed without the use of photolithography with a top efficiency of 21.1 % was developed and demonstrated in the course of this work. In order to better understand the parameters of the best solar cell and to further optimize the cell design, it is crucial to perform a detailed loss analysis. Therefore, the focus of this chapter is to quantify the main loss mechanisms of the developed solar cells and to analyze their influence on the cell efficiency. The loss mechanisms, such as optical, recombination, and resistance losses are analyzed and discussed in the following sections.

Table 6-1 *Solar cell parameters of the best solar cell demonstrated within this work. The parameters of an ideal solar cell with only the intrinsic loss mechanisms are shown for comparison. Cell thickness (W), pitch and base resistivity (ρ_{base}) are given as well.*

	Cell no	ρ_{base}	W	Pitch	V_{OC}	J_{SC}	FF	η
		[Ω cm]	[µm]	[µm]	[mV]	[mA/cm2]	[%]	[%]
best	BC47-16a	1	160	2200	668	38.6	82.0	21.1
ideal	-	1	160	2200	742	44.0	86.5	28.3

The calculated loss mechanisms limiting device efficiency are compared to the parameters of the best solar cell results achieved experimentally. The best solar cell results were already presented in section 4.5, and are used in this chapter in Table 6-1

for reference. In addition to the experimental results of the best solar cell, the ideal solar cell parameters limited only by intrinsic loss processes are shown in the Table 6-1 as well. The analysis of the intrinsic loss mechanisms in the silicon solar cells, such as radiative and Auger recombination processes and the optical losses due to finite absorption coefficient of the incoming light, were already presented in section 2.4.

6.2 Optical losses

6.2.1 Optical losses in the back-contact solar cell

One of the major advantages of BC-BJ solar cells is the reduction of optical losses due to the absence of the metal finger grid on the front side. This results in a reduction of the front side reflectance and enables an increase of the short-circuit current of this cell type. However, there are still other remaining optical losses in BC-BJ solar cells. These include: (a) primary surface reflectance, (b) escape light, (c) transmission, and (d) parasitic absorption. The parasitic absorption occurs in front side antireflection layers, rear side passivation layers, at the metal contacts and as free-carrier absorption (FCA) in highly doped cell regions (see section 6.2.3 for more details on FCA). All these parasitic absorption effects are non-generating absorption processes and therefore do not contribute to current generation of the solar cell. The analysis of the contribution of each of the optical loss mechanisms to the overall optical losses is the goal of this section.

6.2.2 Modeling of the optical losses

The optical processes which occur in the solar cell, like absorption, reflection, transmission and parasitic absorption, can be simulated with the optical simulation tool *Sunrays* [93]. *Sunrays* is a three dimensional ray tracing program that simulates the optical effects in stack systems of layers with different optical characteristics. It uses a Monte Carlo approach to simulate reflectance, transmission, absorption, and parasitic absorption spectra of the modeled structures. With *Sunrays* it is possible to model optical systems with variable textures and multiple layers. *Sunrays* allows modeling of layers which are varied only vertically. However the BC-BJ solar cells have a strongly two-dimensional structure of the rear cell side. Therefore the modeling of this structure requires a modified simulation approach.

In order to enable simulation of the BC-BJ cell structure with the *Sunrays* program, the analyzed device was split into different, optically one-dimensional unit-cells, as shown in Figure 6-1. Each optical unit-cell was simulated separately. Finally, the individual

optical simulation results of each unit-cell were averaged using area weighted averaging factors. For simplicity reasons of this model, it is assumed that the arrangement of the unit cells is not relevant in this averaging. In reality however it is definitely a more complex problem. With this approach the analysis of the optical effects in different regions of the solar cell is performed.

All of the optical unit-cells (Figure 6-1) have the same optical characteristics on the front surface of the cell and in the bulk of the silicon wafer. The differences among the unit-cells are in the rear surface layer stack systems. The structure of the rear side layers of the chosen unit-cells is as follows:

1. bulk Si / BSF doping / rear passivation layer / Aluminum metallization
2. bulk Si / rear passivation layer
3. bulk Si / emitter doping / rear passivation layer / Aluminum metallization
4. bulk Si / emitter doping / Aluminum metallization
5. bulk Si / emitter doping / rear passivation layer / Aluminum metallization
6. bulk Si / BSF doping / Aluminum metallization

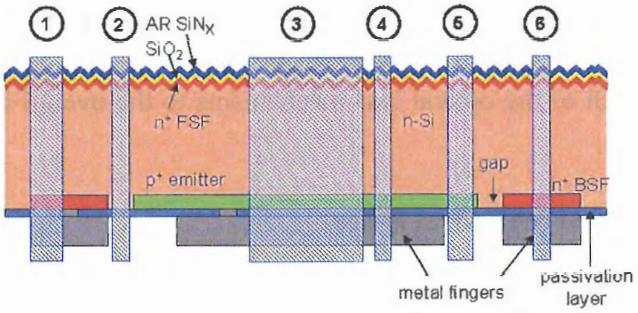


Figure 6-1 Schematic diagram of the different optical unit-cells in back-contact back-junction solar cell structure. Six different optical unit-cells with different rear side structures are shown.

6.2.3 Free carrier absorption

In silicon solar cells there are different light absorption mechanisms. To maximize the conversion efficiency of a photovoltaic device, the desired absorption process is the intrinsic absorption, also called bandgap absorption. In this process, if the energy of the incoming photon is higher than the band gap, then an electron-hole pair can be generated. However, in heavily doped silicon layers, in addition to the bandgap absorption, free carrier absorption (FCA) also occurs. FCA is a process in which the

photon energy is absorbed by free carriers in either conduction or valence bands [143], [144]. In the solar cell the FCA is a parasitic process, which reduces the useful photon flux and reduces the photogenerated current, leading to a reduction in the device's performance. As mentioned above, the FCA process is especially significant in highly doped silicon layers, where the concentration of free carriers is high. The absorption coefficient for the intrinsic silicon and absorption coefficient of the FCA process in highly doped silicon are shown in Figure 6-2. The free carrier absorption coefficient can be calculated using the modeling proposed by Green [121]:

$$\alpha_{FCA} = 2.6\times10^{-18} N_D \lambda^3 + 2.7\times10^{-18} N_A \lambda^2 \tag{6.1}$$

where N_D and N_A are the doping densities of the n- and p-doped region in cm^{-3} respectively and λ is the wavelength in micrometers.

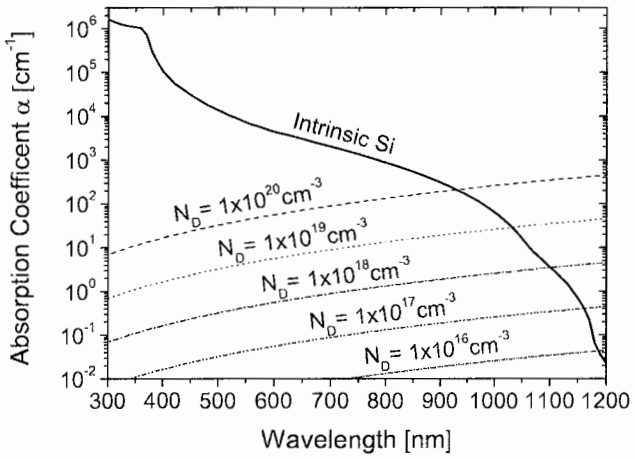


Figure 6-2 Absorption coefficient of intrinsic silicon (thick line) and absorption coefficients of the free carrier absorption process for different donor concentrations (thin lines) calculated with equation (4.1) as a function of wavelength. For the calculated free carrier absorption coefficients, the corresponding donor concentrations are shown.

As can be seen in Figure 6-2, the effect of FCA is especially significant for long wavelengths in the range of 1000 to 1200 nm. In solar cells with good light trapping properties, the light in this wavelength range may pass many times through the wafer thickness and through the highly doped regions at the same time. Thus, the FCA process can significantly contribute to the reduction of the amount of low energy photons available for the photogeneration of electron-hole pairs.

In the *Sunrays*, the FCA process in highly doped cell regions, such as front surface field, back surface field, and emitter doping is not taken into account. In order to analyze the influence of this effect on the optical losses of the BC-BJ cell, an additional layer on the back cell side, possessing the refractive index (n) of silicon, but an absorption coefficient (α_{FCA}) calculated with equation (4.1), was introduced.

6.2.4 Distribution of optical losses

The resulting simulation spectra of reflectance and transmission for a BC-BJ solar cell are shown in Figure 6-3. The experimental results are shown as well. A good agreement between the measured and simulated results indicates that the simulation approach, introduced in the previous section, allows a good description of the device. Note that the reflection is nearly zero at a wavelength of 500 to 600 nm due to the absence of the front side metallization. Another important feature of the analyzed device is the non-zero transmission at long wavelength ranges. Transmission of 5-10 % at 1200 nm is caused by the not fully metalized rear surface. The interdigitated metallization grid covers around 60 % of the rear cell surface. The remaining 40 % of the rear surface is not covered with metal. Therefore the weakly absorbed light can pass through the cell without being absorbed.

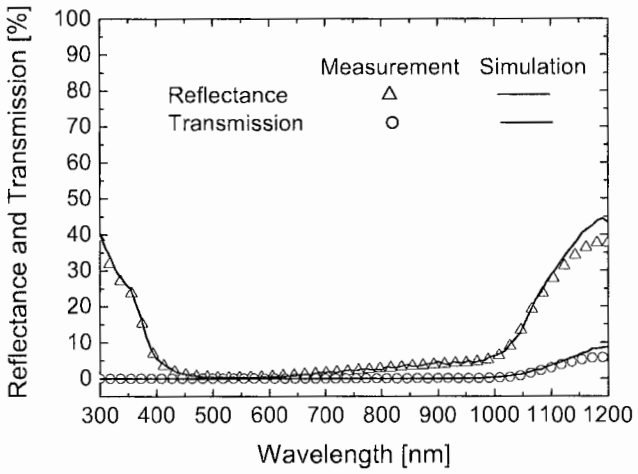


Figure 6-3 Measured and simulated reflectance and transmission spectra of a back-contact back-junction cell with a pitch of 2200 µm and base resistivity of 1 Ω cm. The simulated reflectance shows good agreement with the measured data. The measurements were done using an integrating sphere set-up.

According to the optical simulations of the device, the maximal short-circuit current density $J_{SC,opt}$ of 41.1 mA/cm^2 can be generated assuming no recombination and

resistance losses. By comparing the ideal short-circuit current ($J_{SC,ideal}$) shown in Table 6-1 with the $J_{SC,opt}$, a loss in short-circuit current due to the non-intrinsic optical loss mechanisms ($J_{opt,loss}$) can be determined. For a BC-BJ solar cell with 1 Ω cm base resistivity and thickness of 160 µm under AM1.5g illumination, the $J_{opt,loss}$ is 2.93 mA/cm^2.

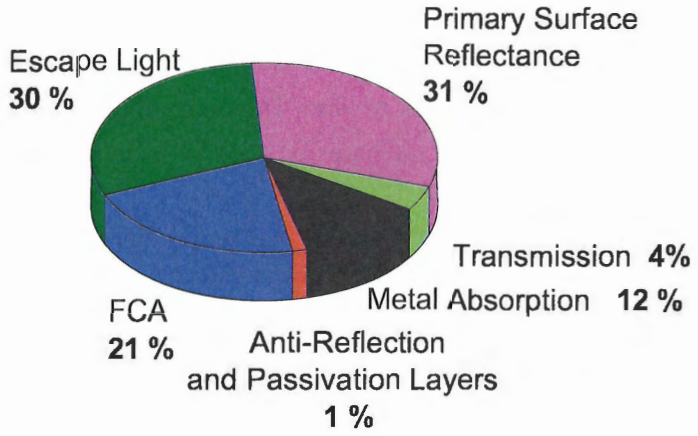


Figure 6-4 Distribution of the modeled optical loss mechanisms in BC-BJ cells with pitch 2200 µm and 1 Ω cm base resistivity under AM1.5g illumination with 0.1 W/cm². Note the significant influence of the free carrier absorption caused by the presence of the highly doped emitter and BSF regions.

In order to quantify the effect of every single layer and process, two simulations are required: one with normal absorption coefficients of every layer, and the other one with an absorption coefficient of a specific layer set to zero for all wavelengths. The difference of the two spectra equals the parasitic absorption in the specific layer. Figure 6-4 shows the modeled distribution of the optical loss mechanisms in the BC-BJ solar cell. The largest loss mechanism is the primary surface reflectance, which accounts for 31 % of all optical losses. The primary surface reflectance is caused by the non-optimal properties of a single layer antireflection coating. The second largest contribution to the optical losses is the escape light (30 %). Escape light is a result of non-ideal light trapping, where light rays are reflected out of the cell after multiple internal reflections in the cell. The next largest loss mechanisms are the free-carrier absorption (21 %) in the highly doped emitter and BSF regions and absorption in the metal layer (12 %). The influence of the FCA process is significant and caused by the large coverage of the highly doped regions (BSF, emitter) on the rear cell side and very good light trapping properties, which result in multiple passes of the long wavelength

light through the highly doped regions. The impact of transmission (4 %) and absorption in antireflection and passivation layers (1 %) is only minor.

One remark about the optimization of the optical device design has to be made. The reduction of one of the optical loss mechanisms will not lead to the increase of the generated photocurrent by the same amount. The increase in J_{SC} will be smaller, because the gain resulting from reduction of one of the optical loss mechanisms will be partially distributed between the other optical loss effects. For example, the replacement of the partial metal coverage on the rear cell side with full area aluminum would lower the transmission losses to zero. However, the reduction of transmission losses will result in the increase of the parasitic absorption in the aluminum.

Table 6-2 *Modeled reduction of the solar cell parameters due to optical losses, for a 160 μm thick n-type BC-BJ cell with pitch of 2200 μm and 1 Ωcm base resistivity under AM1.5g illumination with intensity of 0.1 W/cm². The influence of non-intrinsic recombination losses and series resistance losses were not included in the modeling.*

		Limit imposed by	
		intrinsic losses	optical losses
J_{SC}	[mA/cm²]	44.0	41.1
V_{OC}	[mV]	742.5	741.3
FF	[%]	86.5	86.5
η	[%]	28.3	26.3
Δη	[%]		**-2.0**

6.2.5 Influence of optical losses on the cell efficiency

Optical losses reduce the amount of the photo-generated electron-hole pairs, which mainly reduces the short-circuit current density. However, a reduction of J_{SC} causes a reduction in the open-circuit voltage and the fill factor as well. The effect of the reduced V_{OC}, FF and efficiency can be calculated similarly to the calculations made in section 2.4, using the equations below:

$$J(V) = J_{SC,opt} - qWU_{rec,\mathrm{int}} \tag{6.2}$$

$$\Delta\eta_{opt} = \eta_{opt} - \eta_{\mathrm{int}} \tag{6.3}$$

$J_{sc,opt}$ is the short-circuit current density modeled considering the optical losses. The recombination and resistive losses are not taken into account in this calculation. η_{opt} is the cell efficiency limit imposed by the intrinsic recombination and optical losses and non-intrinsic optical losses calculated with equation (6.2). $\Delta\eta_{opt}$ is the reduction in the cell efficiency due to optical losses. The influence of the non-intrinsic optical losses on the solar cell parameters is summarized in Table 6-2. In the device analyzed, the optical losses cause 2.0 % absolute efficiency loss.

6.3 Recombination losses

6.3.1 Modeling of the saturation current densities

The non-intrinsic recombination losses include the surface recombination, the Auger recombination in highly doped regions of the solar cell, the bulk recombination, and the recombination at metal-semiconductor contacts. Each of the recombination processes can be described by its individual value of the saturation current density J_0. The total saturation current density of the solar cell can then be calculated as an area-weighted sum of the saturation current densities of the different cell regions.

The saturation current densities of the highly doped regions (emitter, BSF) for both passivated and metalized case were taken from the literature. The references used for different doping types are listed in Table 6-3. The published values of J_0 for highly doped regions with different sheet resistance were fitted. According to the fit function, the J_0 values for the sheet resistance of the doping profiles applied in the analyzed cell structure were calculated.

The saturation current densities of the bulk [145] and the gap regions can be calculated analytically by using the equations (3.2) and (6.5) respectively:

$$J_{0,Bulk} = \frac{qWn_i^2}{N_{Bulk}\tau_{Bulk}} \tag{6.4}$$

$$J_{0,Gap} = \frac{qn_i^2 S_{Gap}}{N_{Bulk}} \tag{6.5}$$

where n_i is the intrinsic carrier concentration, N_{base} is the doping density of the bulk, τ_{bulk} is the lifetime of the minority carriers in the bulk and S_{Gap} is the surface recombination velocity of the gap region. S_{Gap} was calculated according to the model of Cuevas et al. [94] and for a base doping of N_{base}=5×10^{15} cm^{-3}, which corresponds to base resistivity of 1 Ω cm, thus S_{Gap}= 70 cm/s. The saturation current density of the

front surface field doping was experimentally determined in section 7.3. Therefore, the experimental result for $J_{0,FSF}$ obtained in this work was applied here.

The area weighted results are summarized in Table 6-3. The total saturation current density of the solar cell equals 227 fA/cm^2. The largest contribution is due to passivated and metalized emitter doping, which account for 47.1 % of the total J_0. Such a high emitter saturation current contribution is caused by the large coverage of the emitter on the rear cell side and high doping level of the emitter profile. The relatively small contribution of the highly recombinative contacted areas is caused by the very small area coverage of the metal-semiconductor contacts, which totals 5 % for both contact polarities.

Table 6-3 *Modeled saturation current densities and their contributions to the overall J_0. Calculations were made for an n-type BC-BJ cell with 1 Ωcm base resistivity and 148 Ω/□ sheet resistance of the FSF. The saturation current densities were area weighted proportionally to their coverage on respective surfaces. Literature sources for the saturation current densities are given. J_0 values were calculated for $n_i=1\times10\ cm^{-3}$ and $T=25°C$.*

	Reference	Area weighted J_0 [fA/cm^2]	Fraction of $J_{0,total}$ [%]
Boron Emitter (passivated)	[95], [85], [146]	98	43.3
Boron Emitter (metallized)	[85]	8.6	3.8
Phosphorus BSF (passivated)	[147], [148]	30	13.1
Phosphorus BSF (metallized)	[147]	7	2.9
Bulk	[145]	26	11.3
Gap regions	[94]	37	16.4
Phosphorus FSF (passivated)	this work	21	9.2
$J_{0,total}$		**227**	**100**

6.3.2 Influence of recombination losses on the short-circuit current

A general analysis of the influence of the two most important parameters of the back-junction solar cell structure, namely the front surface recombination S_{front} and the diffusion length of the carriers L, on the short-circuit current was already presented in section 2.3. Here the specific calculations of the J_{SC} losses due to measured S_{front} and L are presented. The 1-dimensional expression for the short-circuit current of the back-junction solar cell structure in the case of n-type base doping and monochromatic illumination with light of absorption coefficient α is given by [149]:

$$J_p(\alpha) = qF_{ph}(1-R)\left(\frac{\alpha L_p}{\alpha^2 L_p^{\,2}-1}\right)\cdot \left[\frac{\left(\frac{S_{front}L_p}{D_p}+\alpha L_p\right)-e^{-\alpha W}\left[\frac{S_{front}L_p}{D_p}\cosh\left(\frac{W}{L_p}\right)+\sinh\left(\frac{W}{L_p}\right)\right]}{\frac{S_{front}L_p}{D_p}\sinh\left(\frac{W}{L_p}\right)+\cosh\left(\frac{W}{L_p}\right)}-\alpha L_p e^{-\alpha W}\right] \tag{6.6}$$

where J_p is the hole current density, q the elementary charge, D_p the electron diffusion coefficient, F_{ph} the incident monochromatic photon flux density, R is the reflection coefficient, S_{front} is the front surface recombination velocity, L_p is the hole diffusion length, W is the wafer thickness. Integration of J_p for the whole light spectrum results in a short-circuit current density as a function of L_p and S_{front}.

Table 6-4 *Influence of the non-perfect collection efficiency of the carriers in on the short-circuit current density of the back-junction solar cell structure. J_{SC} losses due non-zero front surface recombination velocity and finite carrier lifetime was calculated for S_{front}=6.6 cm/s, τ_{bulk}=1 ms, ρ_{base}=1 Ωcm, W=160 μm.*

τ_{bulk} [ms]	S_{front} [cm/s]	J_{SC} [mA/cm^2]	ΔJ_{SC} [mA/cm^2]
∞	0	41.1	-
1	0	40.6	-0.5
∞	6.6	40.8	-0.3
1	6.6	40.3	**-0.8**

Using the equation (6.6) and the light absorption simulated with *Sunrays* as described in section 6.2.2, the short-circuit current losses due to non-zero recombination at the front surface and due to finite bulk lifetime of the carriers were calculated. Calculations were performed for base resistivity of 1 Ω cm, wafer thickness of 160 μm, S_{front}=6.6 cm/s was calculated using equation (6.7) and the measured saturation current density of the front surface field $J_{0,FSF}$=21 fA/cm^2 as shown in Table 6-3.

$$S_{front} = \frac{J_{0,FSF} N_{Bulk}}{q n_i^2} \tag{6.7}$$

The carrier lifetime in bulk τ_{bulk}=1 ms was assumed. The results are summarized in Table 6-4. The finite carrier lifetime causes 0.5 mA/cm^2 loss in J_{SC}. The non-zero front surface recombination results in another 0.3 mA/cm^2 loss in J_{SC}. Together both effects lead to 0.8 mA/cm^2 loss in J_{SC} and the maximal short-circuit current, resulting from optical and recombination losses ($J_{SC,rec}$), equals 40.3 mA/cm^2.

6.3.3 Influence of recombination losses on cell efficiency

The effect of the modeled saturation current densities on the open-circuit voltage and the cell efficiency can be calculated with the one-diode model:

$$J(V) = J_{SC,rec} - J_{0,total}\left(e^{qV/kT} - 1 \right) \tag{6.8}$$

Where $J_{SC,rec}$ is the maximal short-circuit current resulting in optical and recombination losses. The influence of the $J_{0,total}$ on the V_{OC} can be calculated by transforming the one-diode equation:

$$V_{OC} = \frac{kT}{q} \ln\left(\frac{J_{SC,rec}}{J_{0,total}} + 1 \right) \tag{6.9}$$

A good agreement between the analytically determined and measured V_{OC} can be observed. The open-circuit voltage calculated with equation (6.9) for T=25°C equals 666.3 mV. This result is very close to the V_{OC} of the best solar cell, which as shown in Table 6-1 equals 668 mV.

When the total saturation current density $J_{0,total}$ is determined, it is possible to calculate the influence of the recombination losses on the efficiency of the solar cell. Two calculations are needed. First, the efficiency limit (η_{opt}) due to intrinsic recombination losses and due to optical losses needs to be calculated (as shown in previous section).

Secondly, using equation (6.8), the efficiency limit imposed by non-intrinsic recombination losses (η_{rec}) can be determined. The difference between both efficiency limits is the efficiency reduction, which is caused only by the non-intrinsic recombination losses:

$$\Delta\eta_{rec} = \eta_{rec} - \eta_{opt} \tag{6.10}$$

where $\Delta\eta_{rec}$ is the reduction of the cell efficiency caused by the non-intrinsic recombination processes. The influence of the non-intrinsic recombination processes on the solar cell parameters is summarized in Table 6-5. The non-intrinsic recombination losses are causing an efficiency loss of 3.8 % absolute. However, it should be noted that the influence of the recombination losses in form of electrical shading on the short circuit current was not taken into account here. The influence of electrical shading losses on the short-circuit current was determined experimentally in section 6.4.

Table 6-5 Modeled reduction of the cell parameters caused by the non-intrinsic recombination processes for the BC-BJ cell of this thesis with pitch 2200 µm and 1 Ω cm base resistivity under AM1.5g illumination.

		Limit imposed by	
		intrinsic and optical losses	recombination losses
J_{SC}	[mA/cm^2]	41.1	40.3
V_{OC}	[mV]	741.3	666.3
FF	[%]	86.5	84.1
η	[%]	26.3	22.5
$\Delta\eta$	[%]		**-3.8**

6.4 Electrical shading

6.4.1 Increased lateral transport distance for the minority carriers

In back-contact solar cells, optical shading losses of the metallization grid can be avoided. However, electrical shading losses [150], [87] are still present due to the large

lateral dimensions on the rear cell side and due to the increased recombination rate in the regions of base busbar and base. The impact of this recombination on V_{OC} was already modeled in the previous section. In this section the impact of electrical shading on J_{SC} losses will analyzed. In Figure 6-5, a symmetry element of the BC-BJ solar cell is shown schematically. For the minority carriers that were photogenerated far away form the p-n junction, the large lateral dimensions of the BSF and non-diffused gap regions increase the required diffusion length before reaching the emitter. If the lateral dimensions of the base areas on the rear side are too large, or if the minority carrier lifetime is too low, then the carriers generated far away from the emitter may recombine before reaching the emitter. This results in a reduction of the quantum efficiency in the rear side regions of the solar cell that are not covered by an emitter.

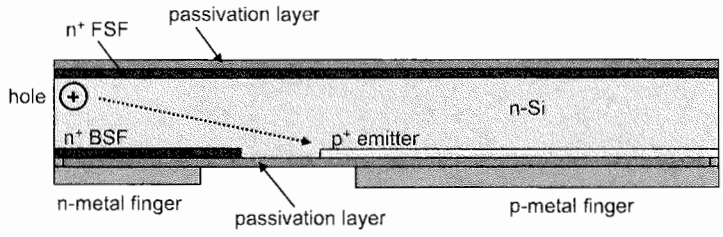


Figure 6-5 Increased lateral diffusion path for the minority carriers which were photogenerated far away from the p-n junction can lead to the recombination of these carriers before reaching the emitter. A symmetry element of the BC-BJ solar cell is shown.

6.4.2 Light beam induced current mapping

A light beam induced current (LBIC) [133] map of the 2×2 cm^2 laboratory solar cell is presented in Figure 6-6. One can clearly recognize the reduced EQE signal over the base fingers and busbar. The EQE drops down to nearly zero above the base busbar, even though no optical shading in this region is present. This effect is caused by (a) large lateral distances which the minority carriers need to diffuse in order to be collected by the p-n junction and (b) by the enhanced recombination over the gap and BSF areas which have high saturation current densities.

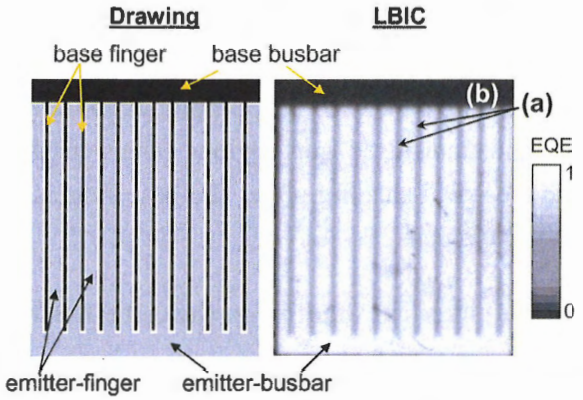


Figure 6-6 Sketch (left) and LBIC map (right) of the rear side of the BC-BJ silicon solar cell. The reduced EQE signal above the base fingers (a) and base busbar (b) are visible. The active cell area is 2x2 cm² and the busbar area is 0.15x2 cm².

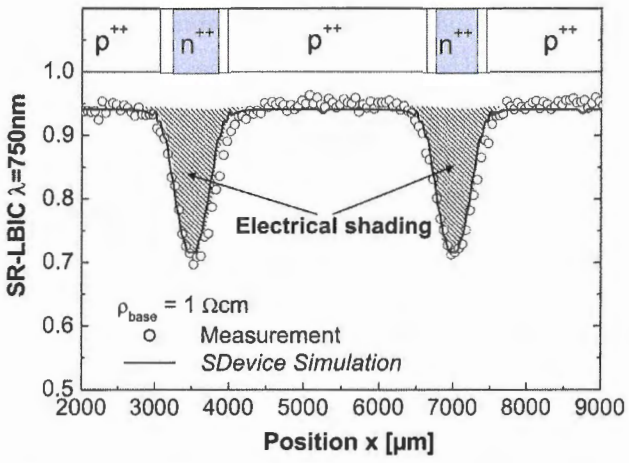


Figure 6-7 Measured and simulated external quantum efficiency line scans of a BC-BJ solar cells with 1 Ω cm base resistivity and a pitch of 3500 µm. Line scans were measured perpendicular to the p-n grid. The width of the p^{++} (emitter) diffusion and the n^{++} (BSF) diffusion are shown in the graph. The EQE was measured at a wavelength of 750 nm. The influence of electrical shading on the quantum efficiency is marked with thin lines.

6.4.3 LBIC line scans

In order to quantify the influence of the electrical shading over the base fingers (gap and BSF areas) on the solar cell efficiency, light beam induced current (LBIC) line scans were measured perpendicular to the p-n grid at a wavelength of 750 nm. The results are shown in Figure 6-7. A solar cell with a base resistivity of 1 Ω cm was

measured. The pitch of the cell analyzed was 3500 µm. The width of the p^{++} (emitter) diffusion and the n^{++} (BSF) diffusion are shown in the graph. Next to the measured LBIC signal, the 2D device simulation results are plotted in the graph. The EQE drops down above the BSF and undiffused gap regions (areas marked with thin lines in Figure 6-7) due to the electrical shading. Over the base fingers, the EQE drops from 0.95 down to 0.70 for 1 Ω cm cells.

6.4.4 Influence of the electrical shading on the cell efficiency

In order to determine the influence of the electrical shading losses on the solar cell's efficiency, the LBIC line scans shown in Figure 6-7 were integrated. The LBIC signal reduction over the base doping causes a 3.3 % absolute reduction of internal quantum efficiency for $\rho_{base} = 1\ \Omega$ cm. By making a simplified assumption that the electrical shading is equal for all wavelengths in the absorbed light spectrum, the short circuit current loss of 1.4 mA/cm^2 caused by electrical shading can be assumed. The maximal J_{SC} reduces from 40.3 to 38.9 mA/cm^2. The resulting efficiency loss caused by the reduction of J_{SC} equals 0.7 % absolute. Thus, the minority carrier recombination in the area of the rear side BSF and undiffused gap causes a significant efficiency loss in the analyzed device. Novel structures of a back-contact back-junction solar cells is which the electrical shading losses can be significantly reduced or even eliminated were recently proposed by Harder et al. [151] and Granek et al. [152].

6.5 Resistive losses

6.5.1 Modeling of series resistance losses

The series resistance (R_S) of BC-BJ solar cells can be described analytically by a network of several resistance elements connected in series as shown in Figure 6-8. The analyzed solar cells operate close to high-injection or under high-injection at maximum power point (MPP) conditions. Therefore both carrier types have to be included in the analysis of the series resistance.

In Figure 6-8, the extreme case for an electron and a hole is shown, where the lateral distance to the metal contacts is at a maximum. The resulting model is a quasi-one-dimensional model of the series resistances in the BC-BJ solar cell. This model is built of the lateral and vertical resistances in the bulk, the lateral resistance of the emitter and the back surface field, the metal-semiconductor contact resistances, and the resistance of the metallization fingers and busbar. The influence of the front n^+ diffused layer on the lateral current transport of the majority carriers was taken into account as parallel resistances to the base lateral resistance. A detailed analysis of the

influence of the front n^+ diffused layer on the lateral current transport is given in chapter 8. The descriptions of the individual resistance elements, as shown in Figure 6-8, are given in Table 6-6. The resistance of the individual resistance elements was calculated similarly to the series resistance model of the concentrator BC-BJ solar cells described in [35].

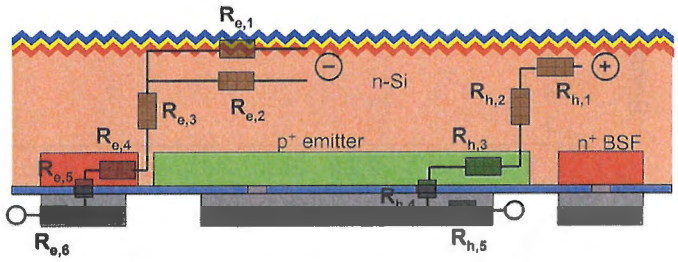


Figure 6-8 *Schematic diagram of the series resistance elements in BC-BJ solar cell that contribute to the analytical resistance model. The influence of the front surface field on the minority carriers (holes) lateral current transport was modeled using a parallel connection of lateral base and front surface field resistances.*

Table 6-6 *Explanation of the resistance symbols used in the quasi-one-dimensional resistance model shown in Figure 6-8.*

electrons		holes	
$R_{e,1}$	lateral FSF resistance	$R_{h,1}$	lateral base resistance
$R_{e,2}$	lateral base resistance	$R_{h,2}$	vertical base resistance
$R_{e,3}$	vertical base resistance	$R_{h,3}$	lateral emitter resistance
$R_{e,4}$	lateral BSF resistance	$R_{h,4}$	p-contact resistance
$R_{e,5}$	n-contact resistance	$R_{h,5}$	p-metal finger resistance
$R_{e,6}$	n-metal finger resistance		

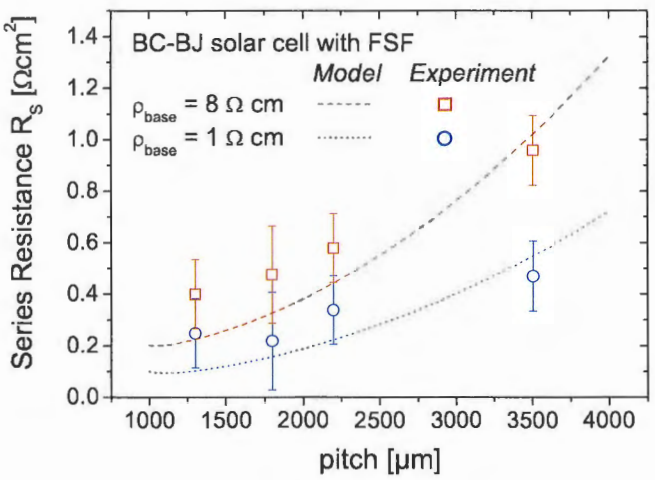


Figure 6-9 *Series resistance of the BC-BJ solar cells with FSF (ρ_{sheet} = 148 Ω/□) and base resistivity of 1 and 8 Ω cm for different pitches. Analytical modeling results (lines) and the experimentally determined series resistance (points) together with the error bars are shown. The conductivity modulation in the base under the maximum power point was taken into account. The size of the solar cells was 2×2 cm².*

The series resistance of the BC-BJ solar cells calculated analytically, using the series resistance model presented above, was compared to the experimentally determined series resistance of the processed solar. The series resistance of the fully processed solar cells was determined by comparing the SunsV_{OC} curve [153] with the one-sun IV-curve. For more details on this method to determine series resistance, see for example Ref. [154]. The analytical and experimentally determined series resistance of the BC-BJ solar cells with different base resistivity and pitch are shown in Figure 6-9. A good agreement between the analytical model and experimental data can be observed, proving the accuracy of the analytical model. The increase of R_S with increasing pitch is caused by a strong increase of the lateral base resistance with increasing pitch. See chapter 8 for more details on lateral base resistance issues.

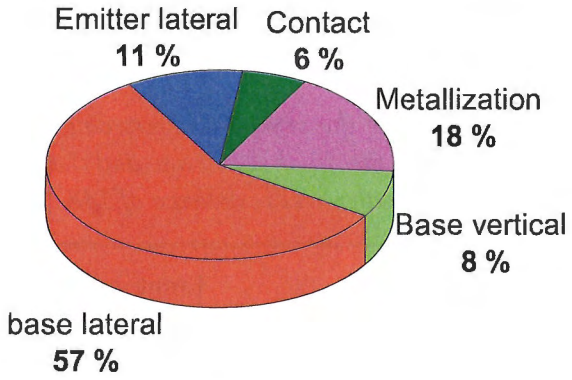


Figure 6-10 Distribution of the modeled series resistance in BC-BJ cells with pitch of 2200 µm, sheet resistance of the FSF of 148 Ω/□ and 1 Ω cm base resistivity. A solar cell with a size of 2×2 cm² was modeled. The total series resistance equals 0.18 Ω cm².

The distribution of the series resistance components in a BC-BJ cell with 1 Ω cm base resistivity, front surface field ($\rho_{FSF,sheet}$ = 148 Ω/□) and pitch of 2200 µm is shown in Figure 6-10. The lateral base resistance is the dominat resistance loss mechanism, contributing to 57 % of the total series resistance. The impact of lateral base resistance is very high due to the large lateral current transport distances required in the solar cell with a pitch of 2200 µm. A smaller pitch would decrease the lateral paths of the charge carriers and therefore reduce the lateral base resistance. It would be difficult, however, to decrease the pitch while using the low cost structuring technology. The impact of the metal fingers equals only 18 %, due to the small finger length in the cell size of 2×2 cm². The contribution of the metallization losses to the total series resistance will increase with an upscaling of the cell design to the production standard sizes of 12.5×12.5 cm² or larger. The total series resistance equals 0.18 Ω cm².

6.5.2 Influence of series resistance losses on cell efficiency

The series resistance causes a reduction of voltage at the maximum power point and therefore reduces the fill factor of the solar cell. The effect of the reduction of FF caused by R_S can be described using an approximation proposed by Green [4]:

$$FF_{Rs} = FF_{rec}\left(1 - R_S \frac{J_{SC}}{V_{OC}}\right) \tag{6.11}$$

where FF_{Rs} is the fill factor resulting from series resistance, optical and recombination losses, FF_{rec} is the fill factor limit imposed by the optical and recombination losses, not affected by resistance losses, R_S is the series resistance given in Ω cm², J_{sc} is the short-

circuit current density limited by the optical losses, and V_{OC} is the reduced open-circuit voltage limited by optical and recombination losses.

Table 6-7 Modeled reduction of the cell parameters caused by the series resistance for a BC-BJ cell with pitch 2200 µm and 1 Ωcm base resistivity and front surface field with sheet resistance of 148 Ω/□.

		Limit imposed by	
		intrinsic, optical and recombination (including electrical shading) losses	resistance losses
J_{SC}	[mA/cm^2]	38.9	38.9
V_{OC}	[mV]	666	666
FF	[%]	84.1	83.0
η	[%]	21.8	21.4
$\Delta\eta$	[%]		**-0.3**

Due to the low value of the series resistance, its influence on the short-circuit current was not taken into account. The reduction of the solar cell parameters resulting from the influence of the series resistance is summarized in Table 6-7. Series resistances of 0.18 Ω cm^2 causes fill factor loss of 1.1 % absolute; in this case, this results in a efficiency reduction of 0.3 % absolute.

6.6 Adding up the individual loss mechanisms

The presented model gives an overview of the different loss mechanisms in the back-contact back-junction solar cell structure developed in this work. The main results of the modeled solar cell efficiency are schematically shown in Figure 6-11 and summarized in Table 6-8. The evolution of the calculated current-voltage characteristics of the solar cell structure after stepwise introduction of the different loss mechanisms is presented in Figure 6-12.

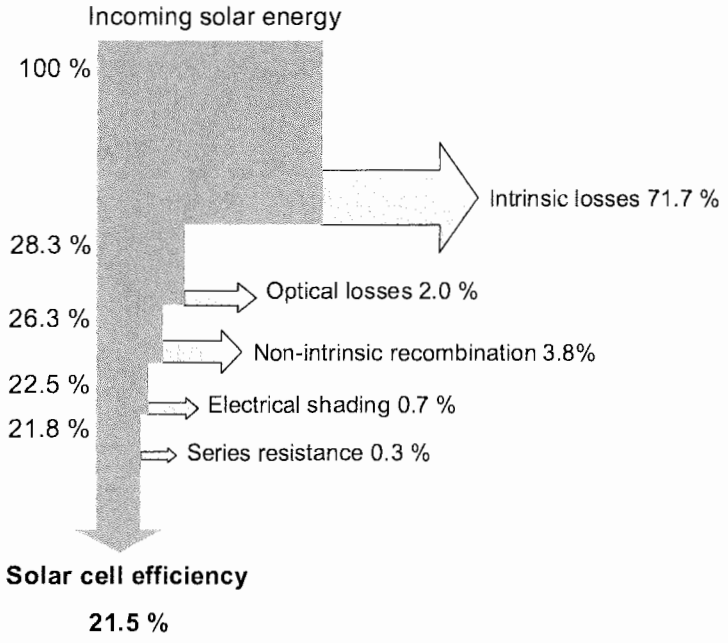


Figure 6-11 Schematic drawing showing the influence of different loss mechanisms on the reduction of the efficiency of the analyzed back-contact back-junction solar cell.

As can be seen in Table 6-8, a very good agreement between the modeled solar cell parameters and the experimental results of the best solar cell can be observed, proving the accuracy of the developed model. Both the modeled short-circuit current and the modeled open-circuit voltage are very close to the measured solar cell parameters. A slightly higher modeled fill factor may be a result of the fact that the edge effects, shunt resistance losses and the recombination in the space charge region were not taken into account in the calculations. These effects have a detrimental influence on the fill factor, thus introduction of these effects into modelling could result in a lower fill factor, with values closer to the measured one. The modelled overall cell efficiency equals 21.5 %, which is very close to the efficiency of the best solar cell (21.1 %).

The presented model is a powerful tool for the further optimization study of the solar cell structure. Improving the solar cell optics, reduction of the overall recombination losses and minimization/elimination of the electrical shading could enable reaching a solar cell efficiency of above 23 %.

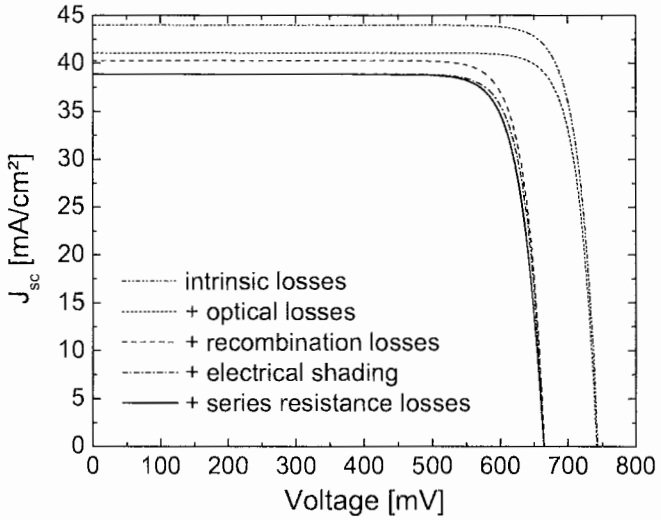


Figure 6-12 Evolution of the current-voltage characteristics of the analyzed BC-BJ solar cell structure after introduction of the different loss mechanisms.

Table 6-8 *Summary of the modeled cell parameters of a 160 µm thick n-type BC-BJ silicon solar cell with pitch of 1800 µm, base resistivity of 1 Ω cm and the FSF with sheet resistance of 148 Ω/□. The influence of different loss mechanisms on the solar cell parameters is shown. The results of the best experimental solar cell are shown for comparison.*

Parameter	Unit	Intrinsic losses	+Optical losses	+Non-intrinsic recombination losses	+Electrical shading losses	+Series resistance losses	Best measured solar cell
J_{SC}	mA/cm^2	44.0	41.1	40.3	38.9	38.9	38.6
ΔJ_{SC}	mA/cm^2	-	-2.9	-0.8	-1.4	0.0	
V_{OC}	mV	742	741	666	666	666	668
ΔV_{OC}	mV	-	-1	-75	0	0	
FF	%	86.5	86.5	84.1	84.1	83.0	82.0
ΔFF	%	-	0.0	-2.6	0.0	-0.91	
η	%	28.3	26.3	22.5	21.8	21.5	21.1
Δη	%	-	-2.0	-3.8	-0.7	-0.3	

6.7 Conclusions

A detailed study of loss mechanisms limiting the efficiency of the back-contact back-junction silicon solar cell developed in this work was presented. The analytical model included the intrinsic, optical, recombination and resistance losses occurring in the actual cell design. The experimental analysis of the electrical shading losses was also introduced to the modeling of the overall solar cell characteristics.

A very good agreement between the modeled solar cell parameters and the experimental results of the best solar cell was obtained, proving the accuracy of the developed model. The main loss sources in the analyzed solar cell structure are the recombination losses, accounting for the absolute efficiency loss of 3.8 %; the optical losses, which cause 2.0 % absolute efficiency loss; and the electrical shading, which causes 0.7 % absolute efficiency loss. Altogether, the analyzed loss mechanisms reduce the solar cell efficiency by 6.8 % absolute from 28.3 % to 21.5 %.

The presented model is a powerful tool for the further optimization study of the solar cell structure. The performed analysis showed that improving the solar cell optics, reduction of the overall recombination losses, and minimization of the electrical shading could enable reaching the solar cell efficiency of 23 %.

7 Front surface passivation using a front surface field

The passivation quality of different phosphorus-doped front surface field diffusion profiles was analyzed. J_{0e} values of different FSF diffusion profiles determined under low and high injection are in a good agreement. The presence of the random pyramids texture increased the J_{0e} by a factor of 1.3 to 1.7. The best solar cell efficiency of 20.8 % was obtained with a deep diffused Gaussian profile of the FSF. Increased doping concentration and depth of the FSF diffusion reduced J_{SC} and V_{OC} of the analyzed cells. The lifetime samples and the solar cells with FSF diffusion are stable under UV exposure in opposition to test structures and solar cells without FSF. The regeneration of the performance of the solar cells without FSF after degradation under UV exposure is possible by a forming gas anneal.

7.1 Introduction

Due to the fact that the p-n junction is placed on the rear surface of the back-contact back-junction solar cells developed and analyzed in the frame of this work, the requirements on the front surface passivation of this cell type are very high. Most of the photo-generation occurs close to the front surface, where the carriers can easily be lost by recombining at a poorly passivated surface. Thus, a low front surface recombination (S_{front}) is one of the critical factors influencing the efficiency of the back-junction cell type. The importance of the high quality of the front surface passivation in the case of the back-junction solar cells was already presented in more details in section 2.3. In the present chapter the quality of the front surface field passivation and its influence on the solar cell stability with respect to ultraviolet light is studied.

7.1.1 Surface recombination

The crystal lattice is severely disturbed at the surface. This results in a large density of the non-saturated bonds, also called 'dangling' bonds. Moreover at the surface the material defects related processing technology such as residues of chemicals and metals depositions are present. At the crystal surface these effects result in a high density of surface states within the bandgap, which cause surface recombination.

In this section the fundamentals of surface recombination are given following Aberle [155]. The recombination rate U_S via a single-level surface state, which is located at an energy E_t, is described by the Shockley-Read-Hall (SRH) theory [77], [78]:

$$U_S = \frac{n_S p_S - n_i^2}{\frac{n_S + n_1}{S_{p0}} + \frac{p_S + p_1}{S_{n0}}} \tag{7.1}$$

with

$$n_1 = n_i \exp\left(\frac{E_t - E_i}{kT}\right), \qquad p_1 = \frac{n_i^2}{n_1}, \qquad S_{n0} = \sigma_n \upsilon_{th} N_{st}, \qquad S_{p0} = \sigma_p \upsilon_{th} N_{st} \tag{7.2}$$

n_S and p_S are the electron and hole concentrations at the surface, S_{n0} and S_{p0} are the surface recombination velocity parameters of electron and holes, σ_n and σ_p are the capture cross sections for electrons and holes, N_{st} is the number of surface states per unit area, E_i is the intrinsic Fermi energy, n_i is the intrinsic carrier density, υ_{th} is the thermal velocity of the charge carriers, k is the Boltzman constant, T is the temperature.

The surface recombination velocity S is defined as $U_S = S\Delta n$, with Δn being the excess carrier density at the surface. In the case of the equal excess densities of electrons and holes at the surface ($\Delta n_S = \Delta p_S$), S can be expressed as [149] :

$$S(\Delta n_S) = \frac{n_0 + p_0 + \Delta n_S}{\frac{n_0 + n_1 + \Delta n_S}{S_{p0}} + \frac{p_0 + p_1 + \Delta n_S}{S_{n0}}} \tag{7.3}$$

Thus, the surface recombination velocity is also influenced by the injection level at the surface (Δn_S) and by the wafer doping (n_0 and p_0).

For the recombination velocity of the p-n junctions and high-low junctions, an effective surface recombination velocity S_{eff} can be defined at a virtual surface. This virtual surface is positioned at the edge of the surface space charge region, located at $x=d$:

$$S_{eff} = \frac{U_S}{\Delta n(x = d)} \tag{7.4}$$

The quality of the emitter or the highly diffused region is expressed using the emitter saturation current density J_{0e}. The relation between S_{eff} and J_{0e} for n^+ diffused regions equals:

$$S_{eff} = \frac{J_{0e}(N_A + \Delta n)}{qn_i^2} \tag{7.5}$$

7.1.2 Surface passivation methods

Analysis of the SRH theory of the surface recombination defined with equation (7.1) indicates that there are two ways to reduce the recombination rate at the silicon surface:

1. The surface recombination rate is proportional to the defect density at the surface (see equation (7.1)). Thus, it is beneficial to reduce the density of the surface states, what can be technologically achieved by growth or deposition of passivation layers. The most widely used examples of the passivation layers in silicon solar cell technology are the thermally grown silicon oxide (SiO_2) and silicon nitride (SiN_X) deposited using the plasma enhanced vapour deposition (PECVD). Both of these passivation layers are applied in the investigated solar cell structure in a form of a stack of passivation layers.

2. The SRH recombination process requires a pair of one electron and one hole. The recombination rate is the highest when the concentration of electrons and holes at the surface is equal. However, if the surface concentration of one of the carrier types is reduced, then the surface recombination rate is also reduced. There are two methods to reduce the concentration of one type of carriers:

   a. One is to implement a doping profile at the surface, which results in a reduction of one carrier type. This can be achieved by the high-temperature diffusion, which will result is a high-low junction [84] or p-n junction, depending on the polarity of the dopant and the silicon substrate. The phosphorus-doped front surface field, applied in the analyzed solar cells, is therefore a high-low junction which passivates the silicon surface by a strong reduction of holes concentration at the surface.

   b. The second method is the application of the field-effect passivation [156]. This can be achieved by electrical charges implemented in the passivation layer.

More details on surface passivation methods for silicon solar cells can be found in a review article of Aberle [155]. In the following, the front surface passivation quality of

the phosphorus doped front surface field combined with a stack system of SiO_2/SiN_X passivation layers will be analyzed.

7.2 Influence of the front surface field diffusion profile on the solar cell performance

A one-dimensional PC1D [63] simulations of a back-junction cell structure as presented in Figure 3-5 are shown in Figure 7-1. The influence of the front surface recombination velocity on the efficiency of the back-junction solar cells with and without front surface field diffusion is obvious: As already shown in section 2.3, with increasing S_{front} the efficiency of the cells without the front surface diffusion decreases rapidly. On the other hand the solar cells with front surface field diffusion profit from the reduction of the effective recombination velocity in a broad $S_{0,front}$ range. A properly designed FSF can therefore improve the efficiency of the back-unction cell for the non-perfectly passivated front surfaces, which is often the case for realistic processing conditions. However, comparing the range of $S_{0,front}$ in which the efficiency remains high for cells with and without FSF should be done carefully and consciously. It should be noted that the $S_{0,front}$ increases rapidly with increasing surface concentration of the phosphorus doping [94]. Therefore the $S_{0,front}$ of the solar cells with FSF diffusion is inherently orders of magnitude higher than in the case of solar cell without FSF diffusion.

The influence of the front surface recombination velocity is visible in the whole wavelength range of the internal quantum efficiency of the back-junction cells as can be seen in Figure 7-2. A lowly doped FSF results in high quantum efficiency. This is because the Auger recombination inside the highly doped region and the surface recombination velocity are low. A proper choice of the front surface field profile is therefore one of the most critical points in the design of the back-contact, back-junction solar cell device.

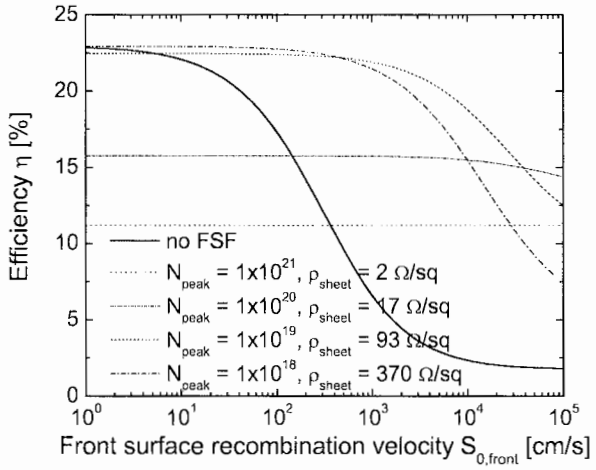


Figure 7-1 Influence of the front surface recombination velocity ($S_{0,front}$) on the efficiency of the back-junction n-type Si solar cells with different phosphorus FSF diffusion profiles (one-dimensional PC1D simulations). In simulations of the doping profiles a depth factor of 0.5 was used.

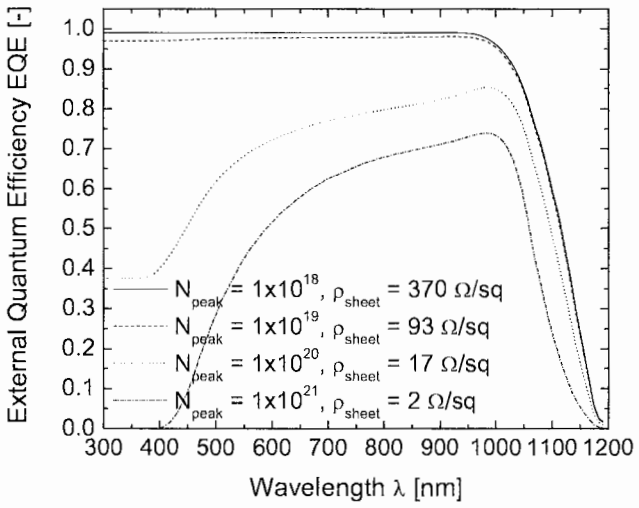


Figure 7-2 Internal quantum efficiency of an n-type back-junction solar cells for different front surface field diffusion profiles. $S_{0,front}$ calculated accordingly to model of Cuevas et al. [94] was assumed for this PC1D simulations. Depth factor of the diffusion profiles equals 0.5 in all simulations.

The importance of the selection of the appropriate diffusion profile for surface passivation is presented in the Figure 7-3. PC1D modelling results of the emitter saturation current density for both metalized and passivated Gaussian phosphorus

diffusion profiles are shown. The sheet resistance of the simulated diffusion profiles is presented in Figure 7-4.

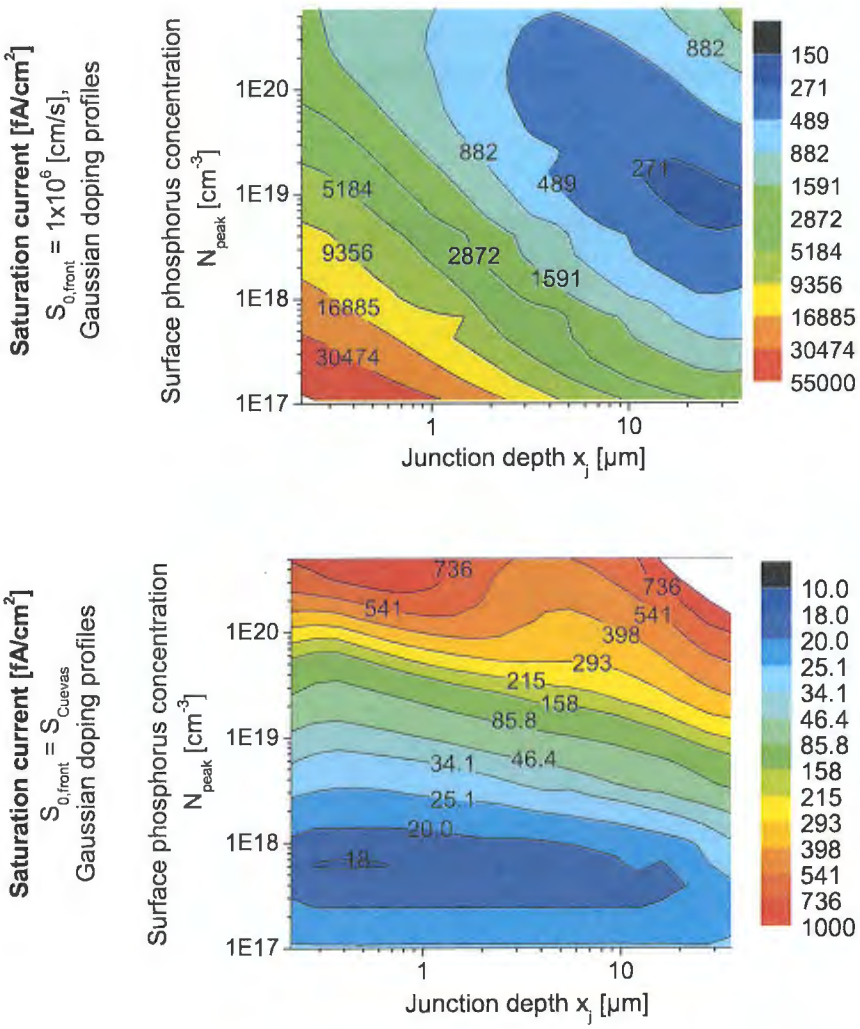


Figure 7-3 *Emitter saturation current densities (J_{0e}) of the phosphorus doped Gaussian diffusion profiles calculated in a wide range of surface phosphorus concentration and junction depth. On top the case of the metalized diffusion profiles with $S_{0,front}=1\times10^6$ cm/s is presented. On the bottom graph, the case of the passivated diffusion profiles is shown. For the passivated emitter the $S_{0,front}$ was calculated using the model of Cuevas et al. [94], which was presented in 3.2.3. Note that the emitter saturation current density is presented in a logarithmic scale. The calculations were done using PC1D [63].*

From the simulations it is clear that for the poorly passivated surfaces, highly doped and deep diffusion profiles are optimal in order to minimize the surface recombination (see Figure 7-3 top), with sheet resistance of about 10 Ω/sq. On the other hand, for the well passivated surfaces, an optimal diffusion profile is lowly doped and shallow (see Figure 7-3 bottom), with the sheet resistance of around 200 to 800 Ω/sq. These results are in a good agreement with the analytical modelling of del Alamo et al. [157].

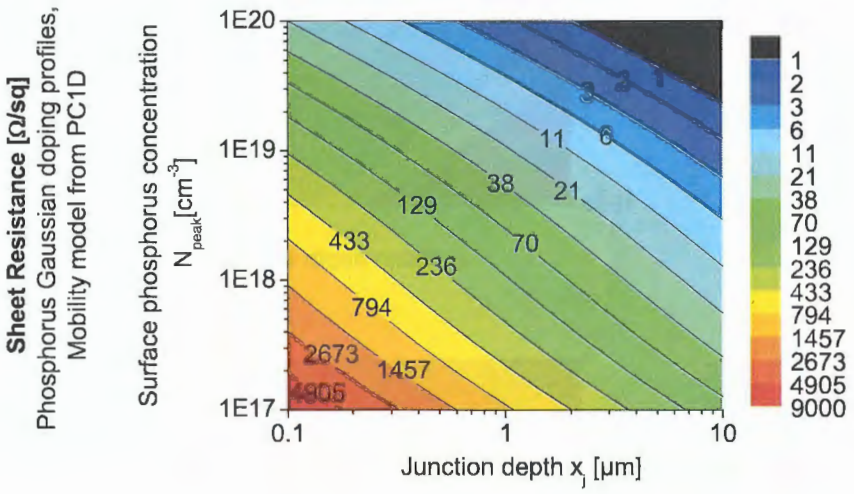


Figure 7-4 Sheet resistance of the phosphorus doped Gaussian diffusion profiles in a wide range of surface phosphorus concentration and junction depth. For the calculation of sheet resistance an electron mobility model of PC1D program [63] was taken. Note that the sheet resistance is presented in a logarithmic scale.

7.3 Surface passivation quality for different FSF diffusion profiles

King et al. [148], [20] and Cuevas et al. [147] studied the saturation current densities of the phosphorus doped emitters. In their work the Gaussian phosphorus profiles were analyzed using n^+pn^+ test structures. In the present work the focus is to analyze the FSF diffusion profiles on the n-type base, therefore in contrast to both authors here the n^+nn^+ samples with front surface field, without the p-n junction, were studied. Error-function diffusion profiles are formed by only a short oxidation step after phosphorus diffusion. The deep diffused Gaussian profile on the other hand, is a result of a long post diffusion oxidation process times and temperatures.

7.3.1 Processing of test structures for the determination of J_{0e}

Symmetrical n^+nn^+ test structures (see Figure 7-5) for lifetime measurements were processed on 250 μm thick n-type FZ-Si wafers. Base resistivities of 1 and 10 Ω cm were selected for this study. This base resistivity range is of interest for the high-efficiency back-junction back-contact solar cells processed in the frame of this study. The advantage of using high quality n-type FZ-Si is the very high bulk lifetime, as was already shown in section 4.2. Due to the high minority carrier lifetimes, the recombination in bulk material is minimum and the carrier lifetime is almost entirely limited by the surface recombination. This way an accurate determination of the surface recombination effects is possible.

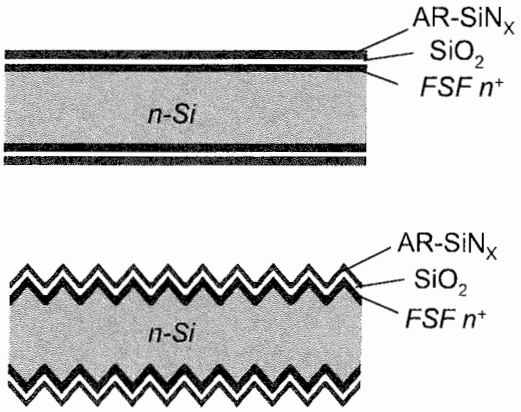


Figure 7-5 Symmetrical n^+nn^+ test structures for the lifetime measurements and the determination of the surface recombination current density. Test structures with planar (top) and textured (bottom) surfaces were processed.

Test samples with untextured (planar) and textured surfaces (random pyramids) were processed. The front surface field was created on both sample sides by a tube furnace phosphorus diffusion form liquid $POCl_3$ source. The phosphorus diffusion time was fixed for all diffusion profiles and the diffusion temperature was varied in the range from 780 to 840°C. This resulted in different n^+ error-function dopant profiles. The resulting diffusion profiles measured for planar samples are shown in Figure 7-6.

Next, the phosphorus glass was etched back in HF solution. For selected samples a deep Gaussian phosphorus profile (called 'deep diffusion') was created by a dry thermal oxidation at 1050°C to form a 105 nm thick antireflection SiO_2 layer. The high oxidation temperature caused redistribution of the phosphorus atoms and transition from the error-function dopant profile to Gaussian profile. The thick oxide was then etched-back in HF solution. Next, the thermal oxide of the planed thickness of about

10 nm for the passivation of the silicon surface was grown during a short dry oxidation process at the temperature of 850°C. Due to the short oxidation time and its low temperature, the doping profiles were not changed significantly.

The parameters such as sheet resistance (ρ_{sheet}), surface phosphorus concentration (N_S) and depths of the diffusion profile (x_j) of the resulting diffusion profiles are summarized in Table 7-1. The sheet resistance of the FSF doping was calculated by integrating the dopant profiles using the mobility model from Masetti et al. [158].

All wafers were processed in one oxidation step. However the oxide growth rate is different on differently doped surfaces [159]. This resulted in the oxide thickness variation of all samples in the range from 10 to 40 nm. Next, the antireflection 70 nm thick PECVD silicon nitride coating was deposited. Finally all samples were annealed at forming gas atmosphere (FGA) at the temperature of 425°C for 15 min.

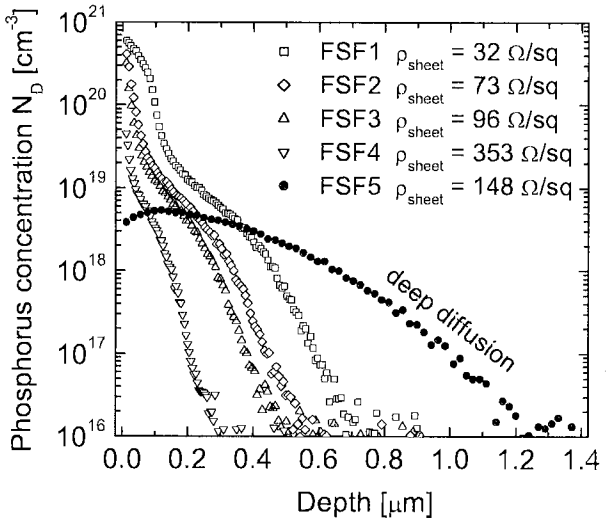


Figure 7-6 Secondary ion mass spectometry (SIMS) profiles of the studied phosphorus dopant profiles measured for untextured samples after all high temperature processing steps.

Table 7-1 *Parameters of the analyzed phosphorus doped front surface field diffusion profiles.*

Profile	Type	ρ_{sheet} [Ω/sq]	N_S [cm^{-3}]	x_j [µm]
FSF1	erfc	32	6.0×10^{20}	0.78
FSF2	erfc	73	4.0×10^{20}	0.66
FSF3	erfc	96	3.2×10^{20}	0.56
FSF4	erfc	353	4.5×10^{19}	0.38
FSF5	Gauss	148	3.8×10^{18}	1.44

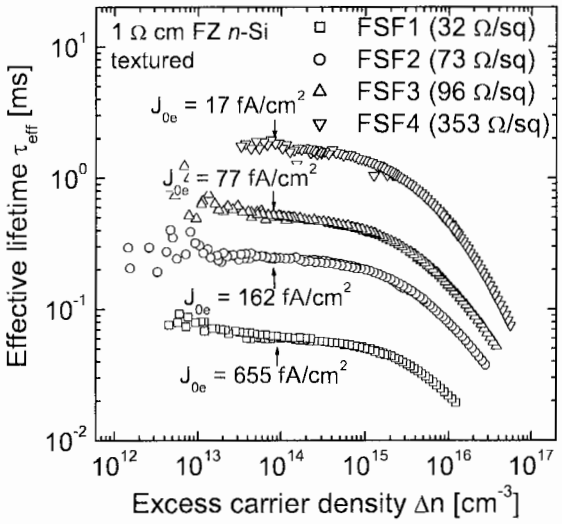


Figure 7-7 *Determination of the emitter saturation current density under low injection for different front surface field diffusion profiles. J_{0e} is determined at $\Delta n = 1\times10^{14}$ cm^{-3}.*

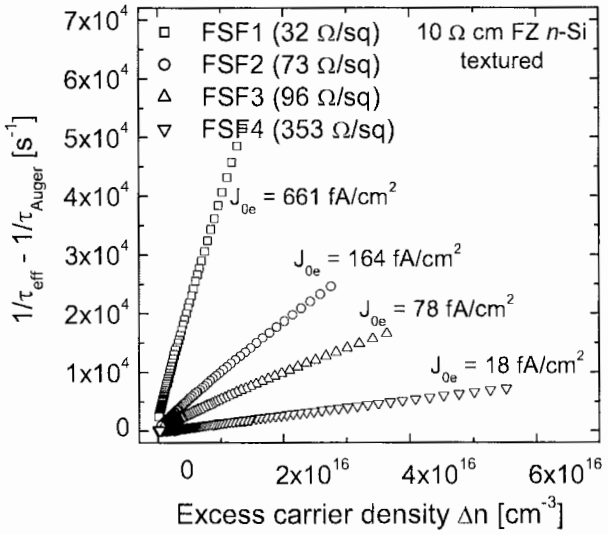


Figure 7-8 Determination of the emitter saturation current density under high injection for different front surface field diffusion profiles. J_{0e} is determined using the slope method.

7.3.2 Determination of J_{0e} under high and low injection

In order to determine the saturation current density of the phosphorus doped front surface field areas (J_{0e}) of the analyzed front surface field diffusion profiles, two methods were applied. J_{0e} was determined under low level injection for 1 Ω cm samples and using the *slope method* under high level injection for 10 Ω cm samples. This way a direct comparison of J_{0e} values determined by both methods was possible. Both methods for determination of J_{0e} under low and high injection are presented in section 3.1 Because of the different SiO_2 thicknesses of samples with different n^+ dopant profile, the optical factor required for QSSPC measurements had to be calculated for all samples. After measuring the oxide thickness, the optical factor was calculated using *SUNRAYS* [93].

Next to J_{0e}, the V_{OC} limit imposed by $J_0 = J_{0e}$ was calculated with the equation (2.1) for all determined J_{0e} (J_{SC} = 40 mA/cm^2 was assumed). For calculation of $V_{OC,\,limit}$ the standard testing temperature of 25°C was assumed. The $V_{OC,\,Limit}$ is the maximum V_{OC} that can be achieved with the used passivation. The influence of the bulk recombination was neglected in calculation of $V_{OC,\,limit}$.

$$V_{\mathrm{OC,limit}} = \frac{kT}{q}\ln\left(\frac{J_{SC}}{J_0}+1\right) \tag{7.6}$$

Examples of the determination of the emitter saturation current density of the analyzed FSF diffusion profiles are shown in Figure 7-7 for the low injection case and in Figure 7-8 for the slope method in high injection.

7.3.3 J_{0e} for different FSF diffusion profiles

The determined J_{0e} values together with the corresponding $V_{OC,\,Limit}$ are summarized in Table 7-2 for the untextured samples and in Table 7-3 for the textured samples. A very good agreement between J_{0e} results determined under high injection using the slope method for the 10 Ω cm samples and in low injection for the 1 Ω cm samples was obtained. This shows that both methods enable a very good determination of J_{0e} of the samples with front surface field. The presence of p-n junction is not required to determine the recombination currents of the n^+ diffused regions [147]. Both methods of determination of J_{0e} proved also to be independent of the base doping.

Table 7-2 Summary of the J_{0e} results for the planar lifetime samples with different FSF diffusions. J_{0e} results for the 1 and 10 Ωcm samples determined under low and high injection respectively are shown together with the corresponding $V_{OC,\,limit}$.

			ρ_{base} = 1 Ω cm low-injection		ρ_{base} = 10 Ω cm high-injection	
Profile	Type	ρ_{sheet} [Ω/sq]	J_{0e} [fA/cm²]	$V_{OC,limit}$ [mV]	J_{0e} [fA/cm²]	$V_{OC,limit}$ [mV]
FSF1	erfc	32	404	652	414	651
FSF2	erfc	73	118	683	128	681
FSF3	erfc	96	61	700	69	697
FSF4	erfc	353	11	744	12	742
FSF5	Gauss	148	12	741	16	734
no FSF	-	-	3[i]	774	3[i]	774

[i] For the non-diffused surfaces a surface saturation current density J_{0s} was determined instead of diffusion saturation currant density J_{0e}.

Table 7-3 *Summary of the J_{0e} results for the textured lifetime samples with different FSF diffusions. J_{0e} results for the 1 and 10 Ω cm samples determined under low and high injection respectively are shown together with the corresponding $V_{OC,\ limit}$.*

Profile	Type	ρ_{sheet}	ρ_{base} = 1 Ω cm low-injection		ρ_{base} = 10 Ω cm high-injection	
			J_{0e}	$V_{OC,limit}$	J_{0e}	$V_{OC,limit}$
		[Ω/sq]	[fA/cm^2]	[mV]	[fA/cm^2]	[mV]
FSF1	erfc	32	655	639	661	639
FSF2	erfc	73	162	675	166	674
FSF3	erfc	96	77	694	90	690
FSF4	erfc	353	17	733	20	729
FSF5	Gauss	148	21	727	22	726
no FSF	-	-	15[i]	736	17[i]	733

Extremely low J_{0e} = 3 fA/cm^2 for the non-diffused surface were measured. This proves that stack system of the thin (10 nm) thermal oxide and PECVD SiN_X (70 nm) passivation is very effective. Phosphorus diffusion introduces increased Auger recombination and SRH recombination due to crystal defects [147], [160]. That is why J_{0e} of samples with FSF are higher than for samples without FSF for the untextured surfaces. Of the investigated diffusions deep Gaussian diffusion (148 Ω/sq) and shallow error-function (353 Ω/sq) diffusion result as expected in the lowest J_{0e} values. These are the two doping profiles with the lowest surface phosphorus concentration.

For textured surfaces J_{0e} is as expected higher than for the untextured samples. This is due to larger surface area of the textured samples and could also be caused by a different phosphorus concentration at the tops and bottoms of the pyramids as proposed by Glunz at al. [161]. For the textured samples with FSF the V_{OC} higher than 720 mV are possible when only the front surface recombination is regarded. Such a good surface passivation with thin SiO_2 and antireflection SiN_X layers have enabled processing of back-junction back-contact solar cells with efficiencies greater than 21 % as presented in this thesis.

Table 7-4 Comparison of the J_{0e} values for textured and planar samples for different front surface field doping profiles.

Profile	Type	ρ_{sheet}	$J_{0e,planar}$	$J_{0e,textured}$	$\frac{J_{0e,textured}}{J_{0e,planar}}$
		[Ω/sq]	[fA/cm^2]	[fA/cm^2]	[mV]
FSF1	erfc	32	404	655	1.62
FSF2	erfc	73	118	162	1.37
FSF3	erfc	96	61	77	1.26
FSF4	erfc	353	11	17	1.54
FSF5	Gauss	148	12	21	1.75
no FSF	-	-	3[i]	15[i]	5.00

Comparison of the J_{0e} data in Table 7-4 of the planar and textured samples indicates that the J_{0e} increases by a factor of 1.3–1.7 when going from a planar to a textured surface. This is similar to the increase measured by Kerr et al. [162] and by Moschner et al. [163] and is consistent with the increase in surface area by a factor of 1.73 compared to a planar surface.

A strong J_{0e} dependence of the sheet resistance is shown in Figure 7-9. The J_{0e} of the error-function diffusions could be very well fitted with a linear fit in the broad sheet resistance range. Deep Gaussian diffusion seems to have a different dependence of the ρ_{sheet}. It is concluded that this effect is due to differences in surface phosphorus concentration between error function profiles and the deep diffused Gaussian profiles.

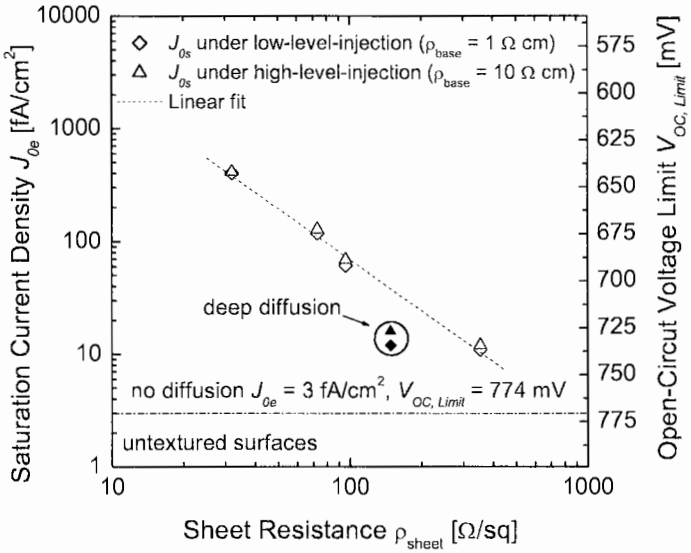


Figure 7-9 *J_{0e} and $V_{OC, Limit}$ as a function of sheet resistance of the n^+ diffusion for the untextured samples. J_{0e} of the sample without FSF is shown for comparison.*

7.4 Solar cells with different FSF diffusion profiles

Back-contact back-junction n-type silicon solar cells were processed with different FSF diffusion profiles. Thus, the influence of the FSF profile on the solar cell performance could be analyzed. The solar cells structure together with the processing technology is presented in chapter 4. Solar cells were processed on 1 Ω cm FZ n-type wafers. The thickness of the finished cells was about 160 µm. The active cell area was 4 cm^2.

7.4.1 Solar cell results

The current-voltage (I-V) parameters of the best solar cells for each FSF diffusion profile are summarized in Table 7-5. The diffusion profiles are labelled corresponding to the data presented in Table 7-1. The pitch of the analyzed cells was 1800 µm, with an emitter width of 1200 µm and a base width of 600 µm. The highest efficiency of 20.8 % was achieved on base resistivity of 1 Ω cm and deep diffused FSF (FSF5). The best efficiency of the BC-BJ solar cell processed without the FSF was 19.7 %. However, it should be noted the solar cells without the FSF diffusion had a very large distribution of the efficiency in the range of 10 to almost 20 %. This shows the importance of the stable front surface passivation quality. The distribution of the solar cell efficiency of the cells with FSF diffusion was much lower, in the range of 2 to 4 %

absolute. For the deeply diffused FSF profile the efficiency distribution was is the range of 0.5 % absolute.

The FSF doping has an influence primarily on the short-circuit current density and the open-circuit voltage as can be seen in Table 7-5. J_{SC} increases from 34.1 mA/cm^2 for the 73 Ω/sq FSF, to 38.1 mA/cm^2 for the deep diffused 148 Ω/sq FSF diffusion. At the same time V_{OC} increases from 647 mV to 663 mV due to reduction of the overall J_0 caused by reduction of the J_{0e} on the front side. The FF of the cells is on a high level of 81 to 82 % and is not being influenced by the different FSF profiles.

Table 7-5 I-V-parameters for the best solar cells with different front surface field diffusion profiles. Solar cells with base resistivity of 1 Ωcm and pitch of 1800 µm are presented. Results in the table are the designated cell area (2×2 cm^2) measurements.

Cell no.	FSF Profile	Type	ρ_{sheet} [Ω/sq]	J_{SC} [mA/cm^2]	V_{OC} [mV]	FF [%]	η [%]
BC47-2b	FSF2	erfc	73	34.1	647	81.7	18.0
BC47-6b	FSF3	erfc	96	36.1	657	81.9	19.5
BC47-11b	FSF4	erfc	353	37.8	651	81.1	20.0
BC47-16b	FSF5	Gauss	148	38.1	663	82.3	20.8
BC47-22b	no FSF	-	-	36.4	659	82.0	19.7

7.4.2 Analysis of the open-circuit voltage

The influence of the sheet resistance of the FSF doping on the V_{OC} is presented in Figure 7-10. The J_{0e} values of the planar and textured lifetime samples are plotted together with the liner fits (dotted lines). The results for the deep diffused Gaussian profile are marked with the closed symbols. The thin solid line represents the limit in V_{OC} imposed by the solar cell structure, i.e. by the bulk recombination, rear side recombination in the highly doped emitter, the back-surface field, in the gap areas and in the metal contact areas. For the analyzed solar cell structure this limit equals around 670 mV. Thus, if the front surface recombination would be eliminated ($J_{0e} = 0$), then the solar cells would have V_{OC} of 670 mV. However, due to non-zero front surface recombination the V_{OC} is decreased to values presented in Table 7-5.

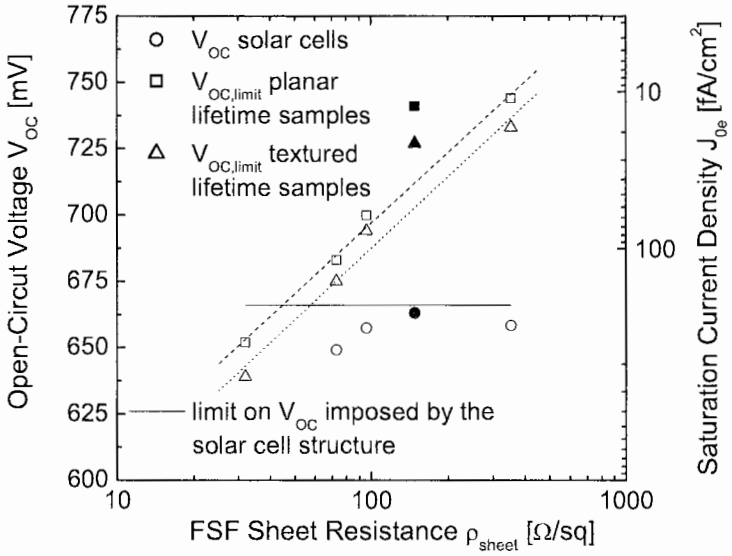


Figure 7-10 Open-circuit voltage of the processed solar cells with different sheet resistance of the FSF diffusions. Results for deep diffused Gaussian FSF profile (FSF5) are marked with closed symbols. $V_{OC,limit}$ imposed by the J_{0e} of the FSF diffusions for the planar and textured lifetime samples are shown as well.

7.4.3 Internal quantum efficiency

The internal quantum efficiency of the BC-BJ solar cells with different FSF diffusion profiles is presented in Figure 7-11. Again, the deeply diffused FSF profile results in the highest IQE, which explains the highest J_{SC} of these cells.

When the doping concentration of the front n^+ diffusion increases, the IQE decreases in the whole wavelength range. However, the most severe degradation of the IQE can be observed in the short wavelength range of 300 to 500 nm when increasing the FSF doping concentration. This effect can be well seen for the IQE of a solar cell with FSF2 doping profile (ρ_{sheet} = 73 Ω/sq). The light of this wavelength is absorbed at the front cell side, inside and in the vicinity of the highly doped FSF region. In this region the high surface recombination velocity, which increased with the surface doping concentration, and the low carrier lifetime due to Auger recombination leads to recombination of a significant percentage of the minority carriers.

Reduction of the surface doping concentration and reduction of the depth of the phosphorus doping profile leads to the strong increase of the spectral response in the short wavelength range as can be seen for the solar cells with FSF3, FSF4 and FSF5 doping profiles.

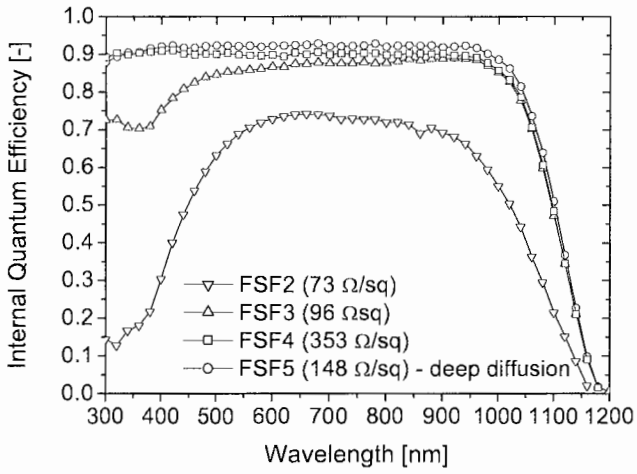


Figure 7-11 Internal quantum efficiency of the BC-BJ solar cells with different FSF diffusion profiles. Results of the solar cells with base resistivity of 1 Ω cm and pitch of 1800 μm are presented.

A strongly reduced IQE in the long wavelength range of 1000 to 1200 nm for the solar cell with highly doped front diffusion profile (FSF2) is believed to be caused by the enhanced free carrier absorption (FCA) process. Details of the free carrier's absorption process are given in section 6.2. A very good light trapping of the analyzed BC-BJ cells causes the weakly absorbed long wavelength light to travel many times through the wafer thickness and at the same time through the highly doped front phosphorus diffusion. In the case of the highly doped FSF2 diffusion profile each pass of the long wavelength light through the highly doped FSF region causes a parasitic absorption of the light, which in turn decreases the photogeneration of the electron-hole pairs in this wavelength range. Due to significantly lower surface doping and the depth of the diffusion profiles of the other analyzed FSF profiles, the FCA process is not causing any significant reduction of the spectral response in the long wavelength range of the spectrum.

7.5 Stability of the front surface passivation under UV-light exposure

7.5.1 UV-light influence on the front surface passivation

Already in 1988 Gruenbaum et al. [164], [165] reported that the efficiency of some of the point-contact concentrator solar cells developed by the Stanford University [16], decreased after exposure to concentrated sunlight. The decrease in solar cell performance was caused by the increase of the front surface recombination velocity.

The studies of Gruenbaum et al. showed that the ultraviolet (UV) component of the incident light spectrum caused damage on the front surface.

Gruenbaum et al. [166] performed the UV-exposure and photoinjection experiments. It was discovered that the UV light of energy greater than 3.1 eV causes increase of the surface recombination velocity ($S_{0,front}$) and interface state densities of the surfaces passivated with oxide. The energy of 3.1 eV corresponds to light with wavelength shorter than 400 nm. In the terrestrial solar spectrum there is a significant amount of photons with such energy. The absorption of the UV photons with wavelength shorter than 400 nm could inject electrons from the conduction band in Si into the conduction band of oxide. This photoinjection could be creating defects at the Si/SiO_2 interface.

However, Gruenbaum et al. [167] and Ruby et al. [168] showed that not all cell structures are prone to degradation under UV light. The formation of the diffused phosphorus region on the front side creates a high field which repels the minority carriers away from the recombination centers at the interface. Therefore even if the $S_{0,front}$ increases, the effective surface recombination velocity (S_{eff}) may remain low and not influence the efficiency of the solar cell. Thus, the additional positive effect of the FSF could be a significant improvement of the UV-light stability of the front side passivation, which is very important for the long term operation of the solar cells. The effect of the influence of the FSF diffusion on the UV stability of the solar cell performance is analyzed in the present section.

7.5.2 Lifetime test structures

The UV-stability of the front surface passivation with and without FSF was examined by exposing the n^+nn^+ lifetime samples to UV light (Xenon lamp) at one sun light intensity and a temperature of 50 °C. The tested samples were not covered with the module glass during the exposure, therefore the illumination spectrum absorbed by the test structures was rich in the high energy UV spectrum. The tested symmetrical lifetime samples were textured with random pyramids and the both surfaces were passivated with a thin thermal SiO_2 layer and an antireflection-SiN_X coating. The samples were annealed in a forming gas atmosphere prior to the exposure test. After each exposure step the saturation current density J_{0e} was determined.

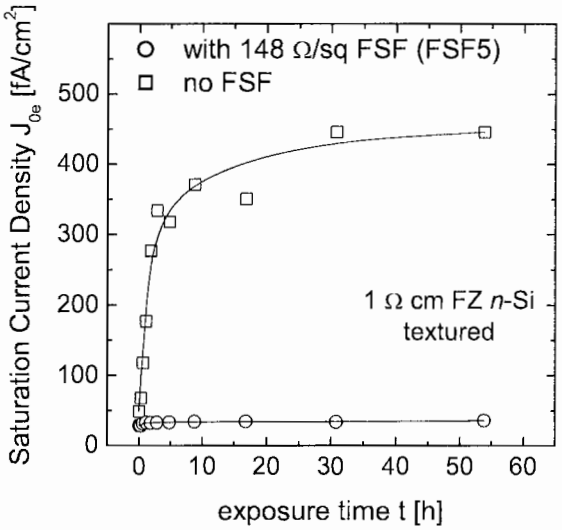


Figure 7-12 Passivation stability of textured n^+nn^+ lifetime samples with (circles) and without (squares) FSF during 55 hours of exposure to UV light. Lines are guides-to-the-eye.

Results of the UV exposure tests are shown in Figure 7-12. The lifetime of samples without FSF degrades significantly already after the first few hours of exposure. For the samples without the FSF, J_{0e} increases from initial value of ~30 fA/cm^2 to almost 450 fA/cm^2 after 55 hours of UV light exposure. Such a high increase of J_{0e}, which corresponds to $S_{0,front}$ of ~140 cm/s, will lead to a significant cell performance degradation, as already shown in section 2.3. Samples with FSF show no significant degradation. J_{0e} increases from ~30 to 35 fA/cm^2 in the case of the deep diffused 148 Ω/sq FSF diffusion. This proves that passivation using a FSF is stable and therefore appropriate for industrial applications in contrast to unstable passivation without FSF. Similar results were already obtained by Gruenbaum et al. [165].

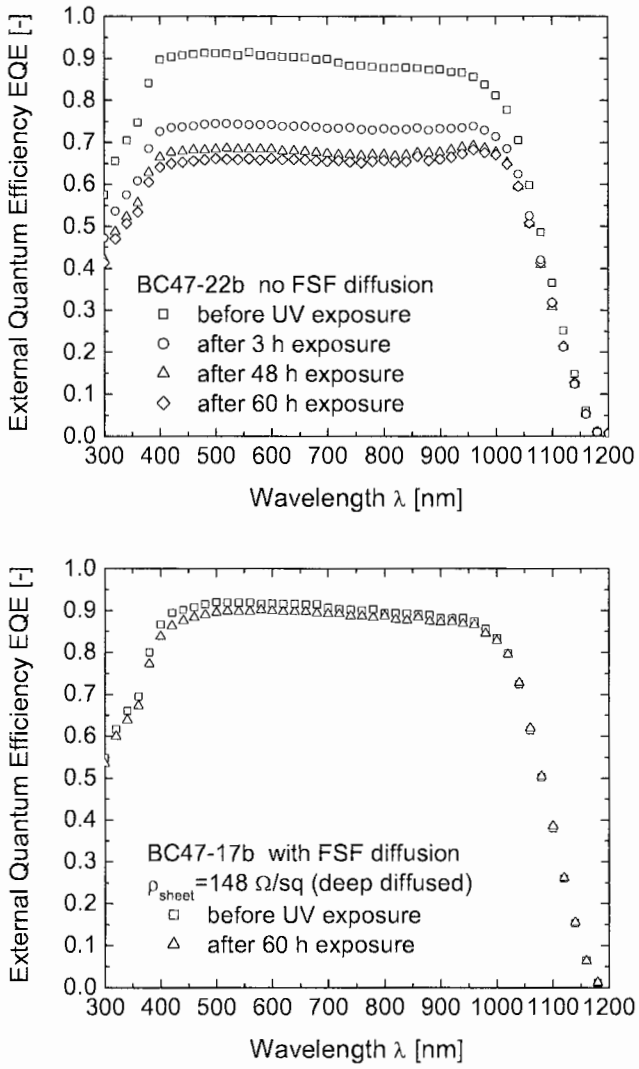


Figure 7-13 External quantum efficiency of the BC-BJ solar cells with (bottom) and without (top) the front surface field phosphorus diffusion after exposure to UV light. Duration of the UV exposure is shown in the graph. Both analyzed solar cells have base resistivity of 1 Ωcm and pitch of 1800 μm.

7.5.3 Solar cell results

Solar cells with and without the front n^+ diffusion were selected for the analysis of the performance stability under UV exposure (Xenon lamp) with illumination intensity of one sun and temperature of 50 °C. Solar cells with high starting performance (performance before UV light exposure) were analyzed in this test. The selected cells had efficiencies in the range of 19 to 20.5 %.

In Figure 7-13 the external quantum efficiency of the solar cell with (bottom) and without (top) the FSF measured after stepwise exposure to UV light. EQE of the solar cell without FSF degrades rapidly from 92 % to 75 % at wavelength of 500 nm already after 3 hours of exposure to UV light. After 60 hours of UV exposure the EQE of the solar cell without FSF decreases even further to 65 %. Thus, an EQE decrease of nearly 30 % absolute was caused by 60 hours of exposure to UV light in the case of the cell without the FSF. At the same time, the EQE of the solar cell with deep diffused FSF (FSF5) showed only minimal degradation after 60 hours of UV exposure: The EQE dropped from 92 % to 88 % at wavelength of 500 nm. Thus, the presence of the n^+ diffused layer on the front cell side drastically improves the stability of the solar cell under the UV exposure.

Table 7-6 *Front surface recombination velocity before and after exposure to UV light determined by (left column) analysis of the lifetime structures exposed to UV light and (right column) by fitting of the measured EQE using the PC1D model of the back-junction solar cell.*

	$S_{0,front}$ measured using lifetime samples [cm/s]	$S_{0,front}$ determined by PC1D fitting of the measured EQE of the solar cell [cm/s]
before UV exposure	16	18
after 60 h of UV exposure	138	145

The influence of the UV exposure on the EQE of the solar cell without FSF was analyzed in more detail with the results of the lifetime test structures and using PC1D simulations. First, the $S_{0,front}$ of the textured lifetime samples was measured before and after UV exposure. Secondly, the measured EQEs were fitted using the PC1D model presented in section 3.2.2. In order to fit the EQE results in the short wavelength range the $S_{0,front}$ was varied. The PC1D fit in the long wavelength range is not in a very good agreement with measured data due to strong influence of the two-dimensional effects, which could not be described by the one-dimensional PC1D simulation. The results are summarized in Table 7-6 and graphically presented in Figure 7-14. A very good agreement between the $S_{0,front}$ determined by analysis of the lifetime samples and by fitting of the EQE of the solar cells was obtained. This proves that the increase of

$S_{0,front}$ during the UV exposure is responsible for the degradation of the solar cell performance.

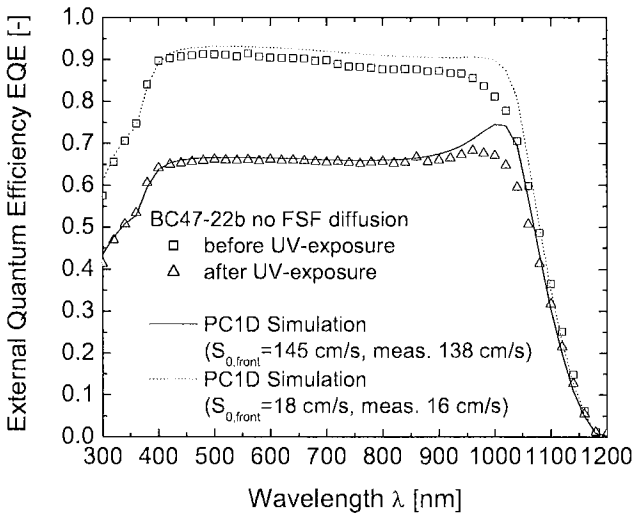


Figure 7-14 External quantum efficiency of the BC-BJ solar cell without the front surface field measured before and after 60 hours of exposure to UV light. PC1D simulations of the measured EQE with fitted $S_{0,front}$ are shown as well (thin lines).

7.5.4 Regeneration of the UV-degraded solar cells

During the illumination of the solar cell with UV light, the photoinjection of the electrons from the conduction band in silicon to the conduction band of oxide creates interface states. Increase of the interface states density at the Si/SiO_2 leads to significant reduction of the solar cell performance as shown in the previous sections.

The solar cell without FSF after UV degradation was exposed to the anneal process in the forming gas (N_2H_2) atmosphere (FGA) at the temperature of 425 °C and process duration time of 25 minutes. The elevated temperature and the hydrogen rich atmosphere leads to strong reduction of the interface states of the Si/SiO_2 interface during the FGA process [169]. This way the interface states that were created by the UV exposure can be passivated, leading to the reduction of the surface recombination velocity. In Figure 7-15 the external quantum efficiency of the BC-BJ solar cell without the FSF is shown before and after UV exposure and after FGA process. The FGA process performed after the UV exposure almost perfectly reduces the detrimental effect of the UV exposure, and regenerates the front surface passivation to the stadium as before the exposure.

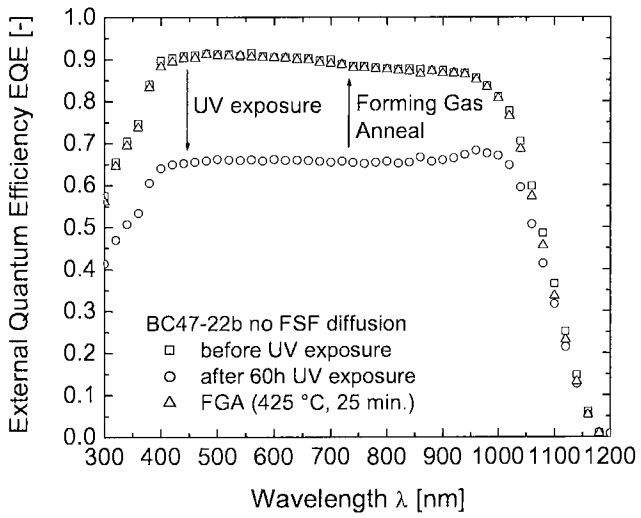


Figure 7-15 External quantum efficiency of the BC-BJ solar cell without the front surface field phosphorus diffusion before and after exposure to UV light and after regeneration of the UV damage by a forming gas anneal step.

Thus, the degradation effect of the UV exposure is not permanent and can be fully reversed by the passivation of the created interface states during the FGA process. The effect of the efficiency degradation under UV exposure and the subsequent regeneration under FGA process is shown schematically in Figure 7-16. The $S_{0,front}$ of the solar cells was determined using the lifetime test structures before and after UV exposure. The efficiency of the solar cells with and without FSF was measured after each UV exposure step and is plotted together with the $S_{0,front}$ determined by analyzing the lifetime samples. For the solar cell without the FSF the efficiency degradation follows the PC1D simulation line. However after the FGA the $S_{0,front}$ decreases and the efficiency increases as marked with a closed symbol.

The solar cell with the FSF diffusions do not show any significant performance degradation after UV exposure as marked with open symbols (circles and squares).

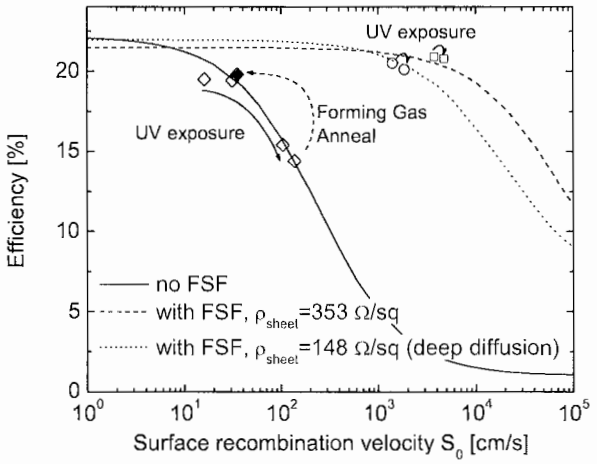


Figure 7-16 Efficiency of the back-junction solar cells as a function of the front surface recombination velocity simulated with PC1D for solar cell with and without FSF diffusion profile (thin lines). Open symbols represent the efficiency of the BC-BJ solar cells measured after UV exposure steps, as marked with arrows. The $S_{0,front}$ of was determined by analyzing the lifetime test samples with and without FSF respectively. The closed symbol represents the efficiency of the solar cell which was regenerated in forming gas anneal process after the degradation under UV illumination.

7.6 Conclusion

The front surface passivation quality is one of the most critical parameters of the back-contact back-junction solar cell structure. The phosphorus-doped front surface field can improve the front surface passivation and was therefore analyzed in details.

The saturation current density of different FSF phosphorus diffusion profiles passivated with SiO_2/SiN_X stack system was determined under low and high injection using the n^+nn^+ test structures. J_{0e} values determined using two different evaluation methods (under low injection and using *slope method* under high injection) are in a good agreement. The presence of the random pyramids texture increases the J_{0e} by a factor of 1.3 to 1.7 in comparison to the planar samples. This enhancement factor corresponds to the surface increase when going from planar to textured surfaces by a factor of 1.73.

The best solar cell efficiency of 20.8 % was obtained with deep diffused Gaussian profile of the FSF. Moreover the distribution of the efficiency of solar cells with the deep diffused FSF was lowest, proving the processing stability of the deep diffused

phosphorus profiles. The efficiency of the analyzed solar cells decreased to 18.0 % for solar cell with the FSF doping profiles with the lowest sheet resistance. Increased doping concentration and depth of the FSF diffusion reduced J_{SC} and V_{OC} of the analyzed cells.

Lifetime samples and solar cells without the front surface field showed a significant performance reduction when exposed to ultraviolet light spectrum. The lifetime samples and the solar cells with FSF diffusion are stable under UV exposure. Regeneration of the solar cell performance after degradation under UV exposure is possible by forming gas anneal.

8 Lateral current transport via front n^+ diffused layer

The application of the low-cost structuring technologies in the processing of the high-efficiency back-contact back-junction silicon solar cells results in a drastic increase in pitch on the rear cell side. The pitch in the range of millimeters leads to a significant increase of the lateral base resistance. The application of a phosphorus-doped front surface field (FSF) significantly reduces the lateral base resistance losses. This additional function of the phosphorus-doped FSF was investigated experimentally and by two-dimensional device simulations. Enhanced lateral majority carrier current transport in the front n^+ diffused layer is a function of the pitch and the base resistivity. Experimental data show that the application of a FSF reduces the total series resistance of the measured n-type cells of 160 micrometer thickness with 3.5 mm pitch by 0.1 Ωcm^2 for 1 Ωcm base resistivity and 1.3 Ωcm^2 for 8 Ωcm base resistivity. Two-dimensional simulations of the electron current transport show that the electron current density in the front n^+ diffused layer is around two orders of magnitude higher than in the base of the solar cell.

8.1 Introduction

High volume manufacturing of the back-contact and back-junction solar cell structure in the industrial environment requires the application of adequate processing technologies. The use of the photolithography technique is not cost-effective. Replacement of the very accurate photolithography with industrially applicable masking steps, such as ink-jetting and screen-printing of resist masks or laser ablation, leads to a significant reduction of the resolution and positioning accuracy. This is especially critical if more than one masking step is used. The pitch on the rear cell side processed with the low-cost masking technology mentioned above increases dramatically, as schematically shown in Figure 8-1. Point-contact solar cells processed by Prof. Swanson's group at Stanford University in the 1980s, for concentrator applications with the use of photolithography, had a pitch of 45 μm [119]. Another example of back-contact Si cells also processed using photolithographic masking is the real-line contacted concentrator (RLCC) cell, developed by Mohr [170] with the pitch in the range of 120 to 400 μm. Solar cells were processed in the course of this thesis without photolithography possessing a pitch distance of around 2 mm. Thus, when

applying low-cost patterning techniques, the pitch on the rear side increases by a factor of more than 40 in comparison to point contact cells [119]. This means that for the majority carriers (electrons here), the main current transport is transformed from the vertical to the lateral direction.

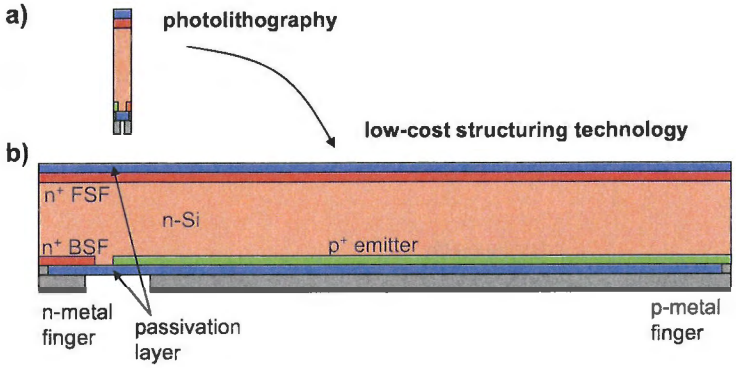


Figure 8-1 Schematic comparison of a point-contact Si solar cell processed with the use of photolithography with a pitch distance of 45 µm (a) and the solar cell with the use of low cost structuring technology with a pitch distance of 2000 µm (b). Drawings are to scale laterally. Symmetry elements of the cell structures are shown.

Depending on the base resistivity and pitch, up to 90 % of the series resistance can be attributed to the lateral majority carrier transport. Thus, the lateral current transport is the main resistance loss mechanism reducing the cell efficiency. The analyzed cells have a phosphorus diffused front surface field (FSF), which is well-known to improve the front side passivation [20]. In the case of cells with large pitch, the FSF not only improves the front side passivation, but also reduces the lateral resistance for the majority carriers and reduces the series resistance of the solar cell. This additional effect of the front n^+ layer is investigated in the present chapter.

8.2 Lateral current transport of majority carriers

The emitter coverage on the rear side should be as high as possible to reduce the required diffusion path for the light generated minority carriers to reach the p-n junction (see Figure 8-2). Increased emitter coverage on the rear cell side is linked to a reduced base doping area. As will be shown in the section 8.3, the pitch of the analyzed solar cell structures was chosen in the range of 1.3 to 3.5 mm. Therefore, the emitter coverage on the rear side is between 54 % and 83 % respectively. Due to the high emitter fraction, the majority carriers (electrons in the case of the n-type base material) need to flow lateral distances in the range of millimeters before reaching the

base contacts. This influences the fill factor of the cell. On the other hand, due to the lower base coverage on the rear cell side, the minority carriers (holes), which were photo-generated over the base contact regions, have much shorter lateral distances to diffuse to the emitter. This results in an improved carrier collection.

The lateral transport of the majority carriers causes significant series resistance losses due to the large distances. When a highly doped front n^+ layer is present, the lateral transport of the electrons can be facilitated. In the case of a high base resistivity or a large lateral distance, the diffused front n^+ layer contribution to the lateral current transport will be significant. This effect is schematically shown in Figure 8-2.

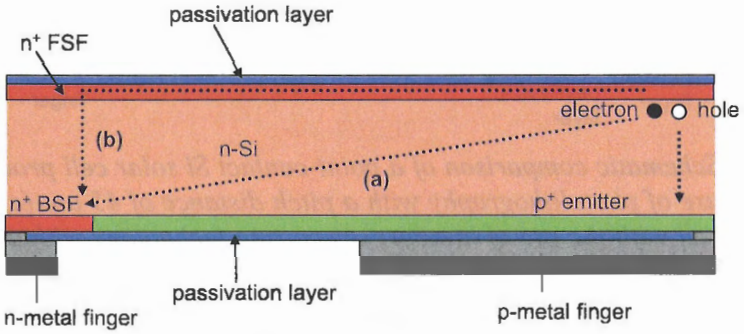


Figure 8-2 *Schematic drawing of the effect of the enhanced lateral current transport of the majority carriers through the front n^+ diffused layer (a symmetry element of the cell is shown). For the sake of simplicity, the front side texture is not shown. The lateral current transport through the front diffused n^+ layer (b) can be seen as an additional transport path to the base lateral resistance (a). In this way the lateral cell resistance is reduced.*

The so called *pumping* effect of floating phosphorus doped n-type emitters in the *p-type* back-contact back-junction solar cells was already investigated by Dicker et al. [33]. In the case of p-type cells with floating emitters, the minority carriers, which were photo-generated in large lateral distances from the emitter, are injected to the floating emitter, where they become majority carriers. The lateral flow of these carriers in the floating emitter is enhanced. Next, the carriers are re-injected into the base and diffuse vertically to the p-n junction. Thus, the *pumping* effect of the floating emitter reduces the electrical shading losses (described in chapter 6) in the back-contact back-junction cells. Therefore the *pumping* effect should not be confused with the effect of the enhanced lateral transport of the majority carriers in the front diffused n^+ layer, which reduces the lateral resistance losses.

The impact of the lateral cell geometry on the lateral series resistance in the base of the solar cell can be expressed by eq. (8.1), analogous to the series resistance model for the concentrator BC-BJ cells from [35]. The impact of the current transport in the front diffused n^+ layer can be described by a parallel resistance to the base lateral resistance:

$$\frac{1}{R_{Base,L}} = \frac{1}{\frac{1}{12}\frac{\rho_{Base}}{d_{wafer}}(a_{n-n})^2} + \frac{1}{\frac{1}{12}\rho_{FSF}(a_{n-n})^2} \tag{8.1}$$

Where a_{n-n} is the distance between the n^+ and n^+ doping, ρ_{Base} is the specific resistance of the base, d_{wafer} is the wafer thickness and ρ_{FSF} is the sheet resistance of the front n^+ diffused layer. The input parameters for the model described by equation (8.1) are schematically shown in Figure 8-3.

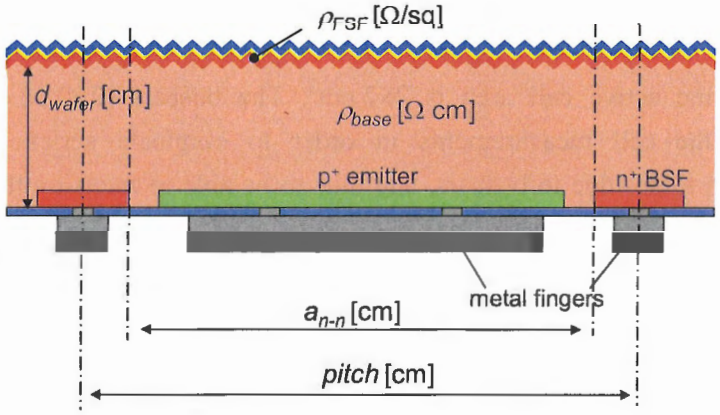


Figure 8-3 Schematic representation of the input parameters for the series resistance model presented in equation (8.1). The units of the geometry and resistance parameters are shown as well.

Due to the quadratic dependence on pitch, an increase of the pitch from 45 µm, as in the cells processed by Sinton et al. [119] with the use of photolithography, to 2000 µm, as in the cells processed in our group with low-cost masking technology, will result in the increase in the lateral series resistance by a factor of 2000. The application of the front diffused n^+ layer (FSF) will reduce the lateral base resistance, especially for cells with a higher specific base resistivity.

An analytical series resistance model of the BC-BJ solar cells was developed and presented in chapter 6.5. This model is based on the resistance model of Mohr [35]. Next to the base lateral resistance, the model also takes into account the vertical base resistance, the contact resistance and the metallization resistance losses. The impact of the lateral current transport in the front n^+ layer was incorporated as shown into

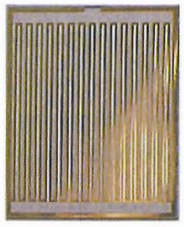
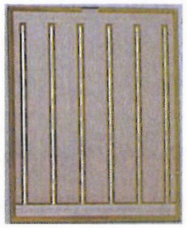
equation (8.1). The comparison of the analytical series resistance modeling with the experimental data is presented in the following sections.

8.3 Variation of the pitch

Back-contact back-junction n-type silicon solar cells with pitches of 1.3, 1.8, 2.2 and 3.5 mm were fabricated (see Table 8-1). The cell structure and its technology were already presented in 4.1. The pitch and the base and emitter width had to be selected, such that the resolution and positioning accuracy of the cell geometry can be performed using low-cost masking steps like screen-printing and laser ablation. The width of the emitter area (p^+) was varied in the range of 700 - 2900 µm in order to investigate the lateral current transport in the base and in the front n^+ layer. The width of the base doping on the rear side (undiffused gap and BSF areas) was fixed at 600 µm for all investigated pitches. The resulting emitter fraction on the rear cell side varied in the range of 54 %, for a pitch of 1.3 mm, to 83 % for a pitch of 3.5 mm.

The size of the active cell area is 2×2 cm^2. The busbars (2×0.15 cm^2) were not included in the cell measurements in order to eliminate series resistance and recombination losses due to busbars, and thus to be able to focus on the pitch-related two-dimensional effects.

Table 8-1 *Photographs and the geometry parameters of the rear side of the back-contacted solar cells with different pitches. The size of the active cell area is 2×2 cm^2. The busbars' size is 2×0.15 cm^2 for each polarity.*

p-bus side n-bus side				
Emitter [µm]	700	1200	1600	2900
Base [µm]	600	600	600	600
Pitch [µm]	1300	1800	2200	3500
Emitter fraction [%]	54	67	73	83

The experimental study was accompanied by two-dimensional device simulations done by M. Hermle [86] in the cooperation with the author of the present thesis. Two-dimensional simulations were done using the *Sentaurus Device* [90] program. The symmetry element of the device used in the simulations is shown in Figure 3-4. Busbars and edge effects were not included in the simulations.

8.4 Solar cell results

The best solar cell results for different pitch distances and base resistivities are summarized in Table 8-2. All results in Table 8-2 are designated cell area (2 cm × 2 cm) measurements, i.e. the busbars were not illuminated during the measurements. The edge area was also not illuminated during the cell measurements. The number of cells in each group was between 1 and 4. The best efficiency of 21.0 % for ρ_{base} = 1 Ω cm and 20.9 % for ρ_{base} = 8 Ω cm was obtained for the pitch of 2200 µm. This pitch represents the best trade-off between high carrier collection efficiency due to large emitter coverage on the rear side, and series resistance losses due to the increased lateral distances.

Table 8-2 *IV-parameters for the best solar cells with a FSF (ρ_{FSF}=148 Ω/sq) and with different pitches. Results of the cells with base resistivity of 1 and 8 Ω cm are presented. Results in the table are designated cell area (2x2cm^2) measurements.*

Cell no.	Pitch [µm]	Emitter fraction [%]	ρ_{base} [Ω cm]	J_{SC} [mA/cm^2]	V_{OC} [mV]	FF [%]	η [%]
BC47-17d	1300	54	1	37.2	662	81.6	20.1
BC47-18b	1800	67	1	38.1	663	82.6	20.9
BC47-16a	2200	73	1	38.5	663	82.2	21.0
BC47-17c	3500	83	1	38.9	661	80.7	20.7
BC47-20f	1300	54	8	39.4	654	79.9	20.6
BC47-21b	1800	67	8	40.1	656	78.3	20.6
BC47-21a	2200	73	8	40.3	658	78.8	20.9
BC47-20c	3500	83	8	40.3	658	75.4	20.0

8.5 Short-circuit current analysis

As shown in Figure 8-4, the short-circuit current increases with increasing emitter coverage and reduced base areas of lower minority carrier collection probability. The base width is 600 µm, so in the extreme case, when the photo-generation occurs in the middle of the base area, the minority carriers need to diffuse 300 µm laterally before reaching the p-n junction. This leads to recombination in the cell's base and at the surfaces. For the base resistivity of 8 Ω cm and a pitch of 3.5 mm, a maximum J_{SC} of 40.3 mA/cm^2 was obtained. Such a high J_{SC} value indicates very good optical and recombination characteristics of the cell. 2-D device simulations, also shown in Figure 8-4, are in excellent agreement with the experimental results, proving the accuracy of the model.

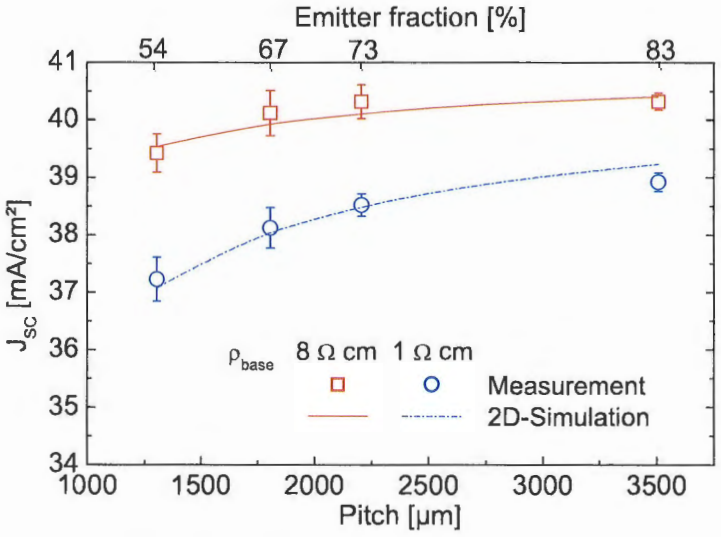


Figure 8-4 *Short-circuit current of the cells with the FSF (ρ_{FSF} = 148 Ω/sq) and with two specific base resistivities of 1 and 8 Ωcm in the investigated pitch range. The percentage of the emitter fraction on the rear side is shown on the top scale. Points represent experimental results and the lines are the two-dimensional simulation results.*

The short-circuit current of the 1 Ω cm cells is more than 1 mA/cm^2 lower than J_{SC} of the cells with 8 Ω cm specific base resistivity. In the 2D simulations, the same Shockley-Read-Hall bulk lifetime of 1 ms was assumed for both 1 and 8 Ω cm base materials. However, even with the same bulk lifetime for 1 and 8 Ω cm solar cells, the simulations show a difference in J_{SC}. The reason for the J_{SC} differences between 1 and 8 Ω cm wafers is the increased front surface recombination in the case of the 1 Ω cm

material in comparison to 8 Ω cm. A significant difference in the internal quantum efficiency (IQE) at short wavelengths between 1 and 8 Ω cm solar cells was measured. The IQE of the 1 Ω cm solar cells with pitch of 2200 μm is 94 % for wavelength of 400 nm. The IQE of the 8 Ω cm solar cells with pitch of 2200 μm equals 97 % for the same wavelength. The difference between the J_{SC} of cells with both base resistivities, determined by the integration of the solar spectrum with both measured IQEs, equals 1.8 mA/cm^2. This difference is in good agreement with the measured values presented in Figure 8-4. The effect of the increased front surface recombination in the case of the 1 Ω cm material in comparison to 8 Ω cm was investigated in section 4.5.

8.6 Fill factor and series resistance

8.6.1 Fill factor

In contrast to J_{SC}, the FF decreases as the pitch increases due to increased lateral resistance in base, as shown in Figure 8-5. The measured fill factor and 2D simulation are shown in Figure 8-5. Again, good agreement between the experimental and 2D simulation results can be observed. Results shown in Figure 8-5 clearly demonstrate that the FSF significantly reduces the series resistance losses and thus improves FF in comparison to cells without FSF. The effect of enhanced current transport in the front n^+ diffused layer is stronger for larger pitches, where the base lateral resistance dominates the resistance losses of the cell. Moreover, the additional impact of the FSF is, as expected, a function of the base doping. For higher base resistivity (8 Ω cm) and large pitch distance (3.5 mm), the FF of the cells with FSF is up to 10 % abs. higher than FF of the cells without the FSF.

8.6.2 Pseudo fill factor

In order to prove that the decrease in FF for larger pitch distances is only caused by the increased lateral series resistance and not other detrimental effects on the IV curve, the pseudo fill factor (PFF) was measured using the SunsV_{OC} measurement technique [153]. The pseudo fill factor is not influenced by series resistance; therefore, the effects of increased lateral resistance by increased pitch should not influence the PFF. The measured pseudo fill factor for the cells with varying pitch is shown in Figure 8-6. As expected, the PFF is independent of the pitch. In the pitch range analyzed, the PFF is higher than 82 % for 1 Ω cm and higher than 81 % for 8 Ω cm solar cells. Such a high PFF of the finished cells indicates that there are no significant shunting and space charge recombination losses in the analyzed solar cells. Constant PFF values in the analyzed pitch range prove that the variations in FF observed in

Figure 8-5 are caused only by the higher series resistance with increasing emitter width.

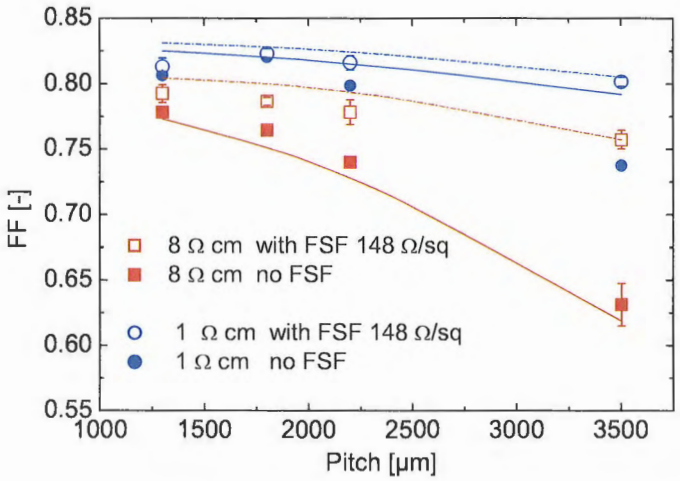


Figure 8-5 *Two-dimensional numerical simulations and measured values of the fill factor of the BC-BJ Si solar cells as a function of the pitch distance for two different base resistivities. Results for the cells with (ρ_{FSF} = 148 Ω/sq) and without FSF diffusion are shown. The data points represent a mean value of the experimental results. Lines represent 2-D simulation results.*

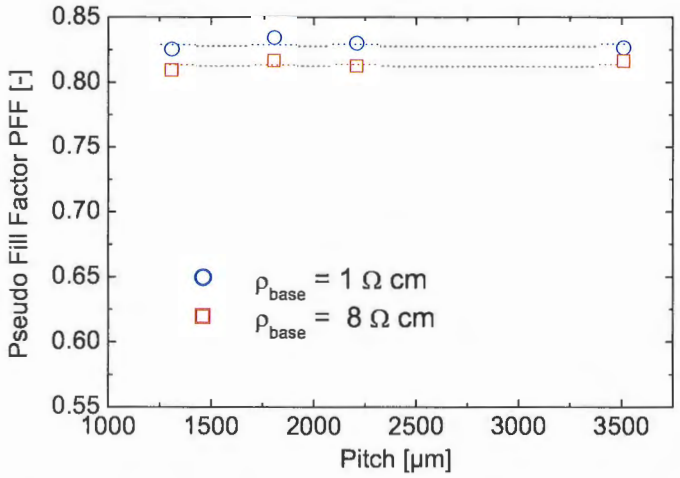


Figure 8-6 *Pseudo Fill Factor (PFF) of the BC-BJ solar cells with different pitches. Experimental results for the solar cells with FSF and base resistivity of FSF and 1 and 8 Ωcm material are shown. No reduction of the PFF over a wide pitch range was observed. Lines are guides-to-the-eye.*

8.6.3 Conductivity modulation

Since the series resistance reduces the maximum output power of the solar cell, the analytical model should describe the series resistance at the maximum power point (MPP) conditions. The base resistivity strongly depends on the density of the electrons in the base, and hence can be influenced by the cell operating conditions. Therefore, in order to correctly describe the impact of the base resistance on the total series resistance of the solar cell, the base conductivity modulation at MPP conditions should be taken into account.

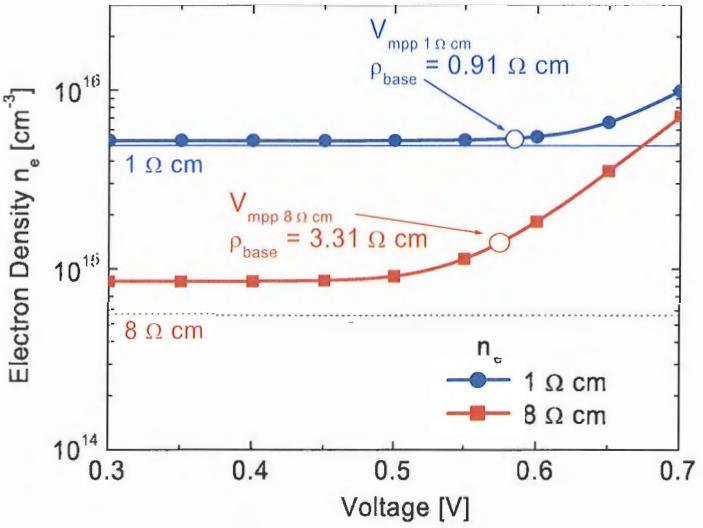


Figure 8-7 Two-dimensional simulation of the electron density in the base of the BC-BJ solar cells for two specific base resistivities of 1 and 8 Ω cm. The electron density was calculated in the voltage range of 0.3 to 0.7 V, in a distance of 100 µm from the top cell surface. The base conductivity modulation at the maximum power point is shown. Thin lines represent the base doping.

In Figure 8-7, a two-dimensional simulation of the electron density in the base in the voltage range of 0.3 to 0.7 V is presented. The voltage at maximum power point for 1 and 8 Ω cm base resistivities is marked in the graph. For both base resistivities, the electron density at MPP is higher than the base doping. ρ_{base} at MPP is therefore reduced compared to the base resistivity of the non-illuminated samples. At MPP conditions, the base resistivity equals 0.91 Ω cm for the specific base resistivity of 1 Ω cm, and 3.31 Ω cm for base resistivity of 8 Ω cm. Thus, ρ_{base} of the 8 Ω cm cells is significantly reduced under one sun illumination and operation at maximum power point. The effect of conductivity modulation at the maximum power point was taken

into account in the analytical modeling. As shown in Figure 8-8, a very good agreement between the experimental data and the analytical modeling of series resistance, adjusted for the conductivity modulation at MPP conditions, proves validity of the analytical model.

8.6.4 Series resistance

In order to investigate the pitch-related resistance losses, the total series resistance R_S of the processed cells was determined. The series resistance was obtained by comparing the SunsV_{OC} curve [153] with the one-sun IV-curve. The details of the measurement of the series resistance of the analyzed cells were presented in section 6.5. For more details on this method to determine the series resistance, see for example reference [154]. The experimentally determined series resistance is presented in Figure 8-8, together with the analytical series resistance modeling. The analytical modeling of the series resistance includes the effect of the enhanced lateral current transport in the front n^+ layer, as described by equation (8.1).

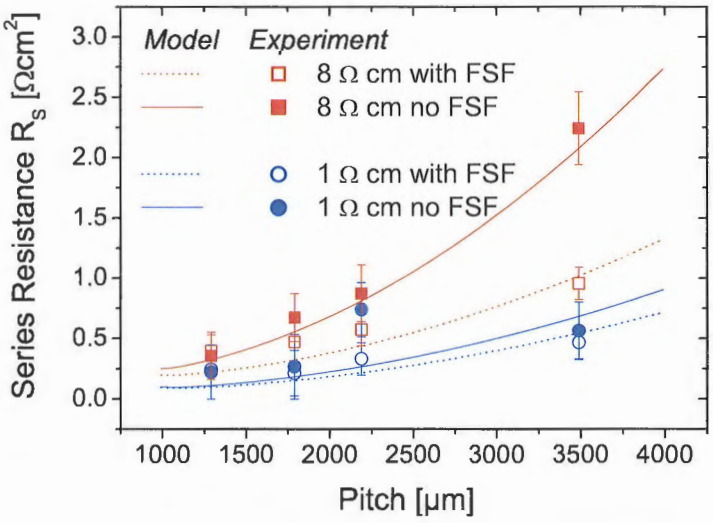


Figure 8-8 Series resistance of the BC-BJ Si solar cells with different pitches. Results of the cells on 1 and 8 Ω cm bulk resistivity and with and without the 148 Ω/sq front surface field are presented. The data points represent the mean experimental resistance values of 1 to 4 cells, determined by comparison of the measured FF and the SunsV_{OC} PFF. The lines represent the simple analytical series resistance model, in which the lateral current transport in the front diffused n^+ layer was taken into account as described by equation (8.1). In the analytical model, the base specific resistivity was adjusted for the conductivity modulation at the maximum power point.

For the 1 Ω cm cells with FSF diffusion, the series resistance R_S increases, starting from 0.2 Ω cm^2 for the lowest pitch of 1.3 mm to 0.5 Ω cm^2 for a pitch of 3.5 mm. The FF of these cells drops at the same time by about 1 % absolute, causing around 0.3 % absolute efficiency loss. For the case of the 1 Ω cm cells without FSF, the increase of R_S is higher. For the largest pitch R_S reaches 0.6 Ω cm^2.

The solar cells with a base resistivity of 8 Ω cm have a much higher lateral base resistance than the 1 Ω cm cells. This results in a lower FF for even the smallest pitch of 1.3 mm. Moreover, the fill factor drop with the increasing pitch is significantly larger than in the case of 1 Ω cm material. For the pitch distance of 1.3 mm, a maximal FF of 79 % and 78 % for 8 Ω cm cells with and without FSF respectively was measured. When reaching the largest pitch of 3.5 mm, the FF dropped to 76 % for cells with FSF and to 63 % for cells without FSF. An absolute FF drop by 3 % for the cells with FSF was caused by the increase of R_S from 0.36 Ω cm^2 for pitch of 1.3 mm to 0.96 Ω cm^2 for pitch of 3.5 mm. At the same time the FF of the 8 Ω cm cells without FSF dropped by 15 $\%_{abs}$, due to increase of R_S from 0.4 to 2.3 Ω cm^2. The drop in fill factor of our cells is consistent with the series resistance model of Mette [130] which predicts a drop of FF from 4.5 to 5.5 $\%_{abs}$ due to an increase of series resistance by 1 Ω cm^2.

8.7 Simulations of the lateral current flow of the majority carriers

The two-dimensional simulations of the majority carriers current transport are shown in Figure 8-9. Here the extreme case of the largest pitch of 3.5 mm was analyzed. The enhanced electron current density in the front n^+ diffused layer area is shown in detail (right side). The electron current density in the n^+ diffused layer area is around two orders of magnitude higher than in the base. This simulation shows that the lateral electron current transport takes place not only in the base, but also in the front diffused n^+ layer. The electrons, which were photo-generated at the front cell side in the first few micrometers of the wafer, take advantage of the high conductivity of the front n^+ layer until they are above the base contacts and then a vertical current transport through the base thickness takes place.

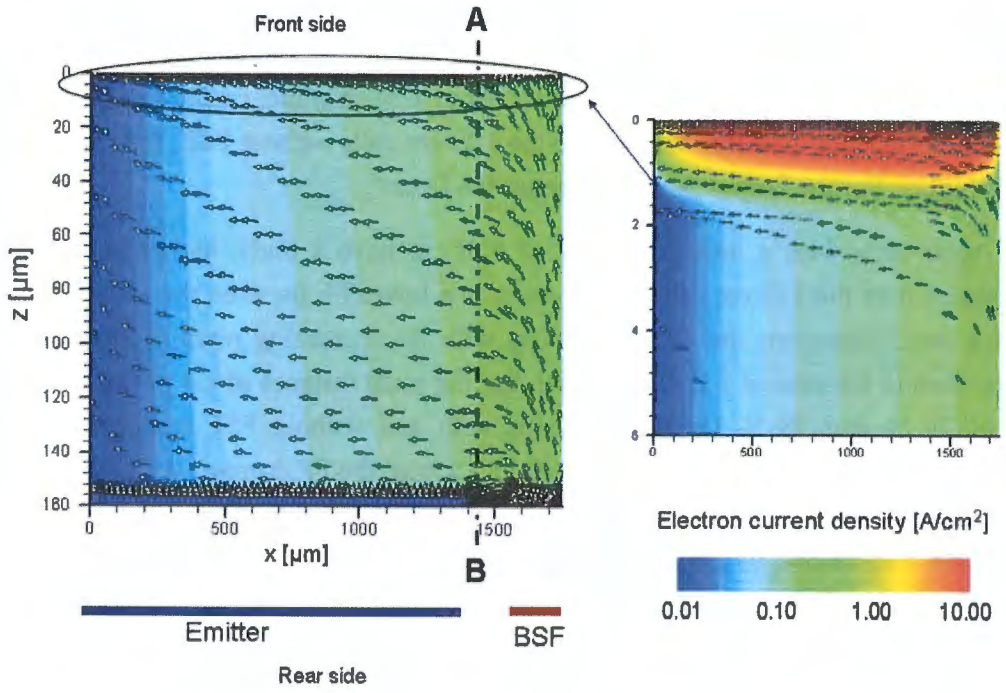


Figure 8-9 *Two-dimensional modeling results of the lateral and vertical electron current transport in the n-type BC-BJ solar cell structure with base resistivity of 8 Ω cm and pitch distance of 3.5 mm. The symmetry element of the solar cell is shown. The arrows show the direction opposite to the electron flow at V_{MPP} of a cell with front surface field (ρ_{FSF} = 148 Ω/sq). The A-B cut of the electron current density through the cell thickness is marked.*

The vertical profiles of the electron current density through the thickness of the solar cell were taken in the vicinity of the base contacts (A-B cut in Figure 8-9). These profiles for 1 and 8 Ω cm specific base resistivities are shown in Figure 8-10. A significant difference in the fraction of the current transport in the front diffused region and the base between the two base resistivities can be observed. After integrating the current density profiles, it was found that for the specific base resistivity of 1 Ω cm, 27 % of the lateral electron current transport takes place in the front n^+ layer. The remaining 73 % of the current flows laterally through the base.

A simple parallel resistance circuitry, as introduced by the analytical model in equation (8.1), can be applied to clarify the current sharing between base and n^+ front region. For the specific base resistivity of 1 Ω cm and the wafer thickness of 160 µm the wafer sheet resistance equals 42 Ω/sq. The base resistance is in parallel with n^+ sheet resistance of 148 Ω/sq. This implies a current sharing of 29 % for the front n^+ region and 71 % for the n-type base. Thus, in the case of base resistivity of 1 Ω cm, the

analytical modeling matches very well the two-dimensional modeling presented in Figure 8-10.

The analysis of the 2-D simulation of the cells with base resistivity of 8 Ω cm shows that the contribution of the front diffused area to the lateral current transport of the majority carriers becomes dominant and increases to 55 %, with 45 % of the current transport taking place in the base. The application of the same simple parallel resistance circuitry here would result in the current sharing of 77 % in the front diffused region and 23 % in the base. These results are not in agreement with 2-D simulations. However, if the same calculation is repeated for the base resistance corrected for conductivity modulation at MPP (ρ_{base}=3.31 Ω cm instead of 8 Ω cm), the base would carry 42 % of the current and the front diffused layer would carry 52% of the current. These results match the simulation results very well. The analysis presented above shows the importance of using two-dimensional modeling when describing the solar cell, which does not operate in low injection conditions.

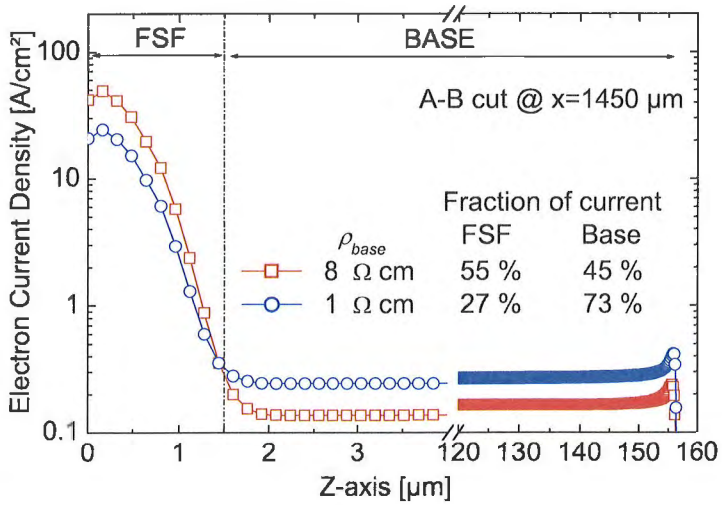


Figure 8-10 Two-dimensional simulation of the electron current density for cells with 1 and 8 Ω cm specific base resistivity and a FSF (ρ_{FSF} = 148 Ω/sq) at the maximum power point conditions. A-B cuts of the electron current density through the wafer thickness for both base resistivities are shown. Front side of the solar cell corresponds to z=0. Areas of the FSF and the base are indicated in the graph. Fractions of the current flow in the front n^+ diffused layer and the base for both specific base resitivities are shown.

8.8 Conclusions

If a low-cost structuring technology is applied in the processing of the BJ BC cell structure, the pitch on the rear side of the cell drastically increases to values in the range of millimeters. This significantly increases the lateral base resistance. The presented investigations show that the introduction of a phosphorus-doped front surface field significantly reduces the lateral base resistance losses. The majority carriers, which were photo-generated in large lateral distances from the base contacts and on the front side, take advantage of the high conductivity of the front diffused n^+ layer in order to reduce the resistance losses. The highly doped front layer can be seen as a low-resistivity *highway* for the majority carriers, which enhances its lateral transport. The front diffused n^+ layer can be seen as a parallel resistance to the lateral base resistance, and its influence on the total series resistance of the cells was successfully modeled using the parallel circuitry. In order to correctly describe the contribution of the base lateral resistance to the modeling, it is important to regard the conductivity modulation of the base resistance under the maximal power point conductions.

As expected, the enhanced lateral majority carrier's current transport in the front diffused n^+ layer is a function of the pitch and the base resistivity. The introduction of phosphorus-diffused FSF reduces the total series resistance of the measured cells with 3.5 mm pitch of 0.1 Ω cm^2 for the base resistivity and 1.3 Ω cm^2 for the 8 Ω cm base resistivity when compared to solar cells without the FSF. According to the two-dimensional simulations of the electron current transport, the electron current density in the front diffused n^+ layer is around two orders of magnitude higher than in the base of the solar cell. Depending on base resistivity, the lateral current transport via front n^+ diffused layer is in the range of 27 to 55 % of the total lateral current transport for 1 and 8 Ω cm base resistivity, respectively.

9 Low-illumination characteristics

The linearity of the current and voltage of three structures of high-efficiency back-junction back-contact silicon solar cells at low illumination were analyzed. Both n-type cells with non-diffused front surface and p-type cells with floating n-emitter show a pronounced current non-linearity, due to strong illumination dependence of the passivation quality of the non-diffused surface and the floating junction respectively. The quantum efficiency of this cell type drops significantly for illumination densities lower than 0.5 suns. In contrast, the quantum efficiency of n-type cells with n^+ front surface field is independent of illumination density. Thus, the n-type cell structure with n^+ front surface field enables highest energy yield at low illumination intensity conditions.

9.1 Introduction

Solar cell efficiencies are normally only reported at standard testing conditions (STC). These conditions include the so called "one sun" illumination intensity of 1000 W/m^2 with spectrum AM1.5g [171] and a device temperature of 25 °C [172]. However, over the whole year under realistic conditions, photovoltaic systems operate during cloudy days, or in the morning and evening periods of the day as well. These are the periods of strongly reduced illumination intensity. Therefore, the annual energy yield of a photovoltaic system is influenced by the low light intensity characteristics of the solar cells. Thus, in order to maximize the energy delivered by the photovoltaic system, the performance of this system should such be as high as possible, even at the low light periods of the day and the year.

The purpose of this chapter is to analyze the different back-junction back-contact solar cells structures with respect to their performance under the low-illumination intensities. Three different front surface passivation schemes are analyzed. These structures are schematically shown in Figure 9-1:

a) n-type cell with non-diffused front surface,

b) p-type cell with an n^+ floating emitter and

c) n-type cell with an n^+ front surface field (FSF).

The n-type solar cells with and without the front surface field were developed in this work and the details of their processing technology were already presented in chapter 4.

The p-type solar cells with the floating junction were developed and analyzed in the work of Dicker et al. [33] and these results are presented here for comparison with the n-type structures.

The relation between current and illumination intensity and voltage and the illumination intensity of three above mentioned solar cell structures is analyzed in the present chapter.

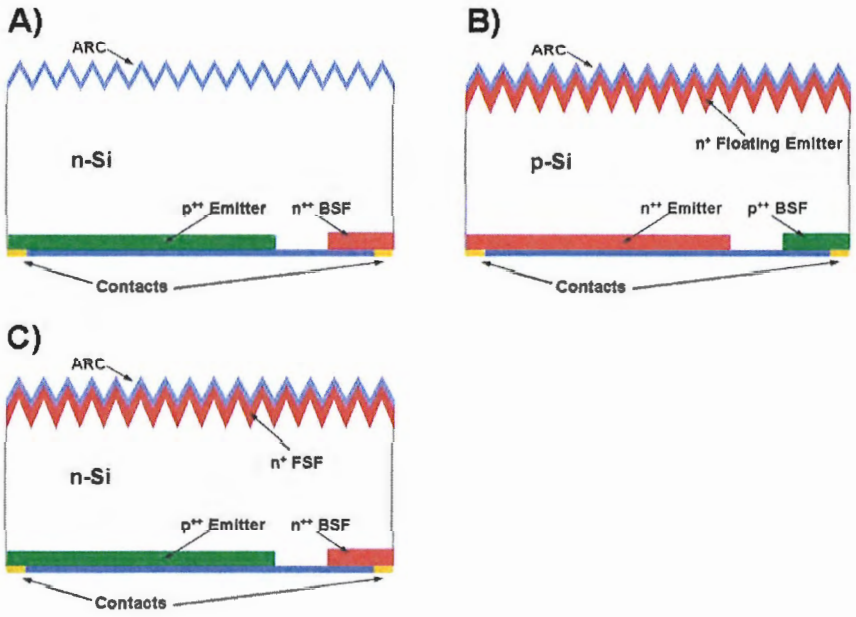


Figure 9-1 Sketch of two-dimensional symmetry elements of the back-junction solar cells: n-type with non-diffused front surface (structure A), p-type with a phosphorus doped floating emitter (structure B), and n-type with a phosphorus doped FSF (structure C).

9.2 Analyzed solar cells and methodology

Analyzed solar cells

The parameters of the solar cells chosen for the low-illumination analysis are summarized in Table 9-1. BJ BC solar cells with three structures corresponding to the notation used in Figure 9-1 were selected. The efficiency of the chosen cells was in the

range of 11.0 to 20.4 %. n-type solar cells with base resistivity of 1 and 8 Ω cm were analyzed. The results of the n-type cells with and without the FSF were compared to the p-type cell structure with the floating junction.

Table 9-1 *IV-parameters of solar cells with different front surface passivation schemes (structure types names correspond to the notation used in Figure 9-1). The presented results are measured under one sun illumination intensity and 25 °C device temperature.*

Cell No.	Structure type	Area [cm^2]	ρ_{base} [Ω cm]	V_{OC} [mV]	J_{SC} [mA/cm^2]	FF [-]	η [%]
BC47-22b '*good*'	A	4	1	649.7	35.2	0.817	18.7
BC47-23g '*bad*'	A	4	1	632.9	30.4	0.785	15.1
BC47-24b '*good*'	A	4	8	636.6	38.65	0.737	18.1
BC47-25g '*bad*'	A	4	8	598.7	29.9	0.613	11.0
RSK3-5a	B	4	1	685.0	32.1	0.792	17.4
BC47-18g	C	4	1	658.5	39.0	0.794	20.4
BC47-21g	C	4	8	653.5	39.7	0.752	19.5

External quantum efficiency

In order to examine the relation between current density and light intensity of the three cell structures described above, the external quantum efficiency (EQE) of all analyzed cells was measured in the range of 300 to 1200 nm under a bias light intensity of 0.3 and 1 sun.

Moreover, the EQE at a wavelength of 600 nm was measured as a function of bias light intensity in the illumination range of 0.01 to 1 suns. Due to the high absorption coefficient of the light with a wavelength of 600 nm, the EQE at 600 nm reflects the current of the carriers generated close to the front surface. This current is especially sensitive to the front surface recombination. Thus, any variation in the front surface recombination rate with the variation of illumination intensity can be measured well by a measurement of the solar cell response at a wavelength of 600 nm. The measured EQE at different bias light intensities was than normalized with respect to EQE at one-sun bias light intensity.

Open-circuit voltage

The V_{OC} of all cells was measured in an illumination intensity range of 0.1 to almost 10 suns. The SunsV_{OC} method [153] was used here. The dependence of the V_{OC} with illumination intensity (C for concentration) can be described with the following equation [173]:

$$V_{OC}(C) \approx \frac{kT}{q} \ln\left(\frac{CJ_{ph,one-sun}}{J_0}\right) \approx V_{OC,one-sun} + \frac{kT}{q} \ln(C) \tag{9.1}$$

where $V_{OC,one\text{-}sun}$ and $J_{ph,one\text{-}sun}$ are the V_{OC} and photogenerated current, measured under standard reference conditions at the 1 sun illumination intensity respectively. When the saturation current J_0 is constant in the analyzed illumination intensity range, then a linear increase of voltage with the logarithm of light intensity is expected. The resulting V_{OC} dependence with illumination density can then be described by the right side of equation (9.1). The V_{OC} should show an increase of around 60 mV for each decade of increase of intensity. A deviation from the logarithmic illumination behavior could be caused if the saturation current of the cell is injection dependent.

Device simulations

In addition to solar cell measurements, two-dimensional device simulations of the symmetry elements shown in Figure 9-1 were performed. The EQE at 600 nm with varying bias light intensity was simulated and the simulation results were compared with the measured data.

9.3 Non-diffused surfaces

Two sets of parallel processed solar cells with structure A were selected for the low illumination analysis. The first pair of cells, marked as *'good'* in the Table 9-1, had EQE at one-sun bias light of about 85 %. The second pair, marked as *'bad'*, with inferior front surface passivation had an EQE of around 75 %. Cells with non-diffused front surfaces are very vulnerable to variation of front surface recombination velocity (S_{front}) as shown in section 2.3. Even a small increase of S_{front} will result in a significant current decrease. This explains the large differences between the performance of the *'good'* and *'bad'* identically processed cells. Minor and difficult-to-avoid processing imperfections, such as broken pyramid tips, local scratches or other front surface inhomogenities cause extreme differences in cell performance. Processing faults create spots on the cell front surface with locally strongly increased S_{front}. These local imperfections will, therefore, lead to a locally inhomogeneous S_{front} value.

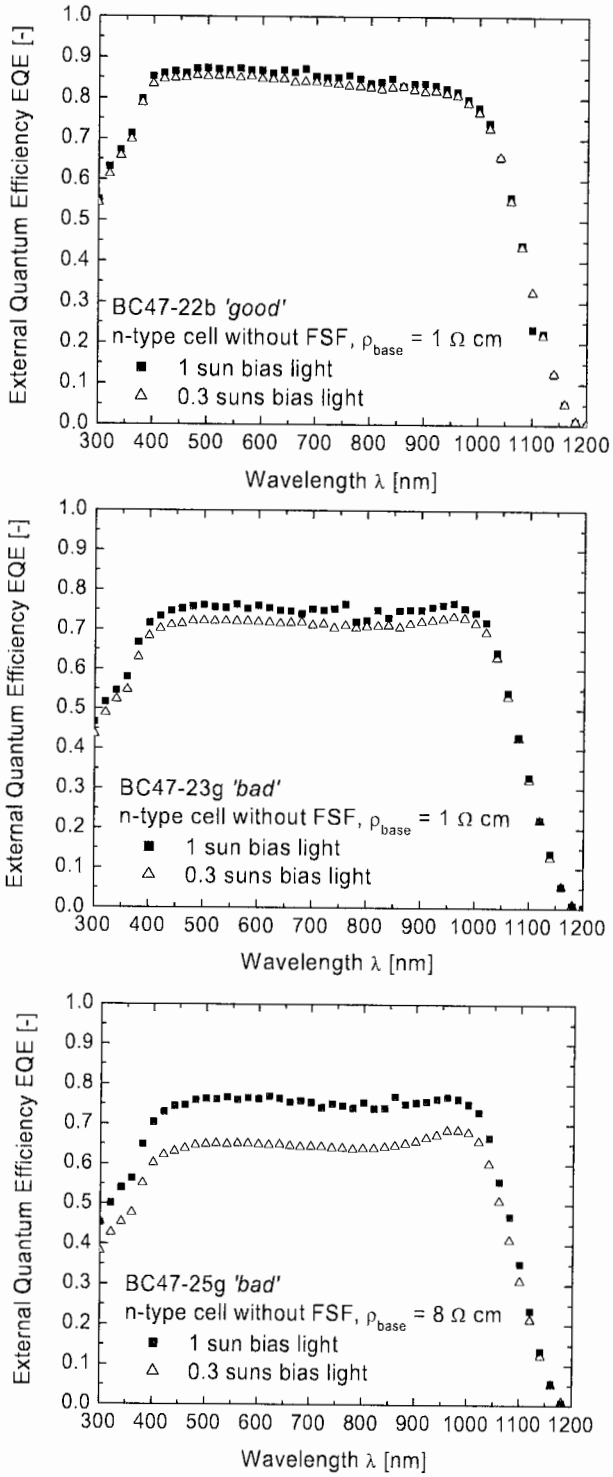


Figure 9-2 External quantum efficiency of three different n-type back-contact back-junction cells with non-diffused front surface (structure A) measured at 0.3 and 1 sun bias light intensity.

The external quantum efficiency of the structure A cells measured at a bias light intensity of 0.3 and 1 sun is shown in Figure 9-2. A strong bias light intensity dependence was observed. For the 1 Ω cm cell marked as *'good'* (BC47-22B), a 3 to 5 % absolute decrease of EQE was measured when lowering the bias light intensity from 1 to 0.3 suns. For the cells marked as *'bad'*, the decrease in EQE was even more pronounced. The EQE of the 1 Ω cm (BC47-23g) dropped by 5 to 7 % at lower bias light intensity. For the 8 Ω cm cell, the EQE dropped by 10 %.

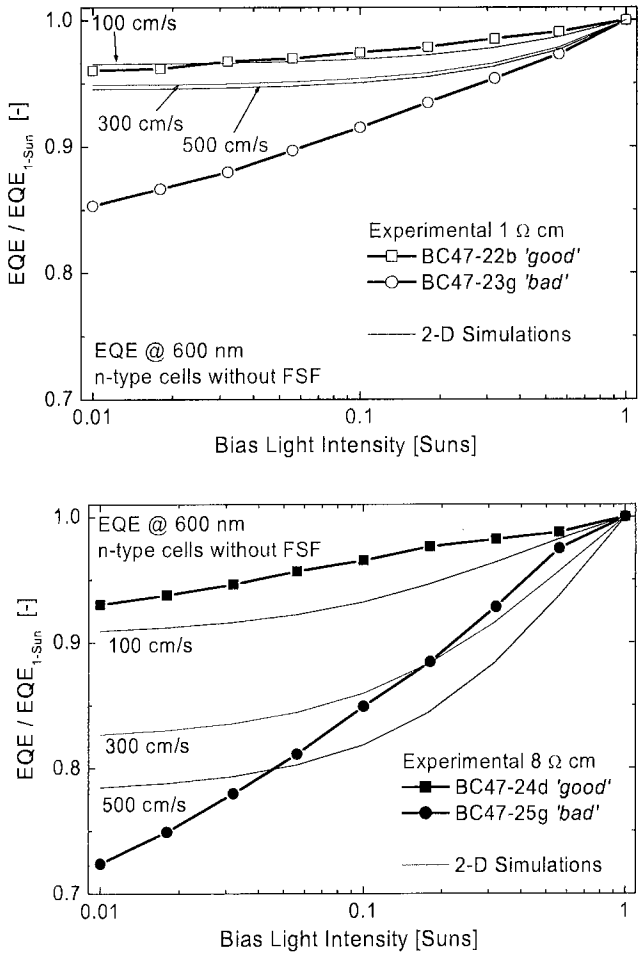


Figure 9-3 Normalized EQE for n-type back-contact back-junction cells with non-diffused front surface (structure A) measured at wavelength of 600 nm in bias light intensity range of 0.01 to 1 sun. Results for base resistivity of 1 Ωcm (top) and 8 Ωcm (bottom) are shown. Sets of two-dimensional simulations for different S_{front} values (S_{front} is shown next to simulation results) are plotted next to experimental results.

All four analyzed cells exhibit a very strong current non-linearity under low illumination. The non-linearity is much larger for the cells with lower performance. Normalized EQE of the *'bad'* cells drops down to 85 % for 1 Ω cm base resistivity, and to 72 % for 8 Ω cm base resistivity at 0.01 suns due to injection-dependent effects of the front surface recombination.

Two-dimensional device simulations (thin lines in Figure 9-3) with a set of S_{front} values as input parameters also predict a strong non-linearity of the structure A cells. A fixed S_{front} was assumed for the whole area of the front surface. However, the simulation results also show that the injection dependence cannot be described with a single S_{front} value, although injection dependence of $S_{front} = S_n = S_p$ and bulk lifetime ($\tau_{n0} = \tau_{p0} =$ 1 ms) were taken into account in the simulation. A possible explanation of these differences may be the fact that the *local* surface imperfections have to be taken into account. The combination of locally distributed S_{front} values could then result in more complex injection dependence as expected from the simulation with a single homogeneous S_{front} value.

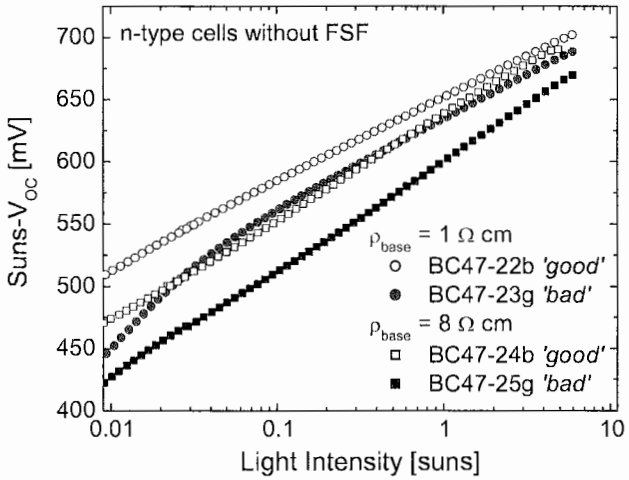


Figure 9-4 Open-circuit voltage of the n-type back-contact back-junction cells with non-diffused front surface (structure A) measured in bias light intensity range of 0.01 to 10 suns. Results for 1 and 8 Ωcm base resistivity are shown.

The open-circuit voltage of the analyzed cells measured in the light intensity range of 0.01 to 10 suns is shown in Figure 9-4. The V_{OC} of all 4 analyzed cells shows a linear decrease with logarithm of light intensity as predicted by equation (9.1) until 0.1 suns. However, for light intensities lower than 0.1 suns, a deviation from this linear decrease can be observed for the *'bad'* cells (BC47-23g and BC47-25g). The decrease of V_{OC}

under low illumination intensities is stronger than theoretically predicted. This is believed to be caused by a increase of S_{front} and thus increase of $J_{0,front}$, under low injection operating conditions.

The solar cell operates under V_{OC} conditions at a much higher injection level than in the case of J_{SC}. Therefore, the effect of increased recombination caused by a transition from high injection to low injection operating conditions occurs in the case of V_{OC} at much lower light intensities than in the case of J_{SC}. That is why the EQE of the structure A cells already decreased significantly at light intensity of 0.3 suns, and the V_{OC} at the same time shows non-linearity first at illumination lower than 0.1 suns.

9.4 Floating emitters

The p-type solar cells with floating emitter (structure B) were processed with the use of photolithography. The solar cell selected for the present analysis had an efficiency of 17.4 %. The thin metallization grid on the cell rear side covers only a small fraction of the cell rear side, thus enabling bifacial illumination of the cell structure. This feature was used during the measurements of the open-circuit voltage. The structure B solar cell was illuminated form the rear cells side during the open-circuit voltage measurements, due to problems with proper contacting of the metal grid during front side illumination.

The external quantum efficiency of the cell RSK3-5a measured at bias light intensity of 1 and 0.3 suns is shown in Figure 9-5. A decrease of the EQE by 2 to 3 % absolute when lowering the bias light from 1 to 0.3 suns was measured. As in the case of the cells without front diffusion described in the previous section, the current of the structure B cell is also non-linear, i.e. the short circuit current density decreases with decreasing bias light illumination intensity. This effect is even stronger for lower bias light intensities, as shown in Figure 9-6.

Normalized EQEs of p-type cell with floating emitter, measured in the bias light intensity range 0.01 to 1 suns, are shown in Figure 9-6. The EQE decreases rapidly for the bias light intensity lower than 0.5 suns. The effects responsible for this behavior are imperfections of the floating junction (see Figure 9-7). The diffusion inhomogenities and introduction of crystal defects lead to formation of an internal shunt element ($R_{p,floating}$) across the junction and to recombination in the space charge region, which causes diode saturation current ($J_{02,p}$) [174]. Both elements strongly reduce the voltage across the floating junction ($V_{floating}$), which is necessary to obtain a good surface passivation. The shunt resistance and a diode with ideality factor of 2 were implemented across the front side floating junction into PC1D simulations of the

floating emitter cell structure. The PC1D simulation results plotted in Figure 9-6 are in good agreement with the experimental data, indicating a reasonable model for the imperfections of the floating emitter.

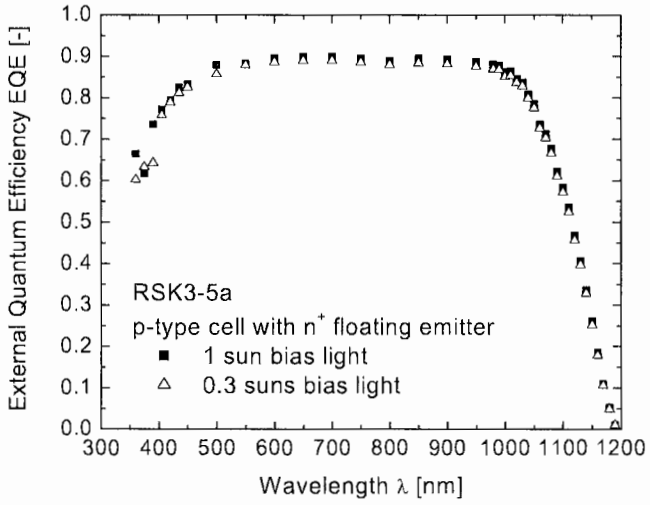


Figure 9-5 External quantum efficiency of three different p-type back-contact back-junction cells with floating emitter (structure B) measured at 0.3 and 1 sun bias light intensity.

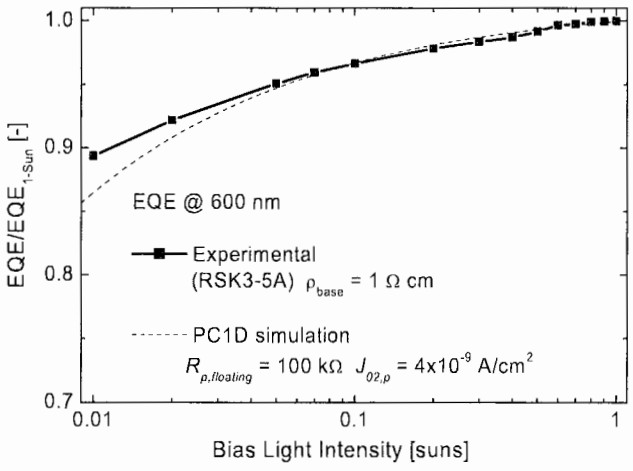


Figure 9-6 Normalized EQE for a p-type cell with floating emitter (structure B) measured at wavelength of 600 nm in bias light intensity range of 0.01 to 1 sun. The dotted line shows a PC1D simulation using $R_{p,floating}$ and $J_{02,p}$ values as shown in the graph.

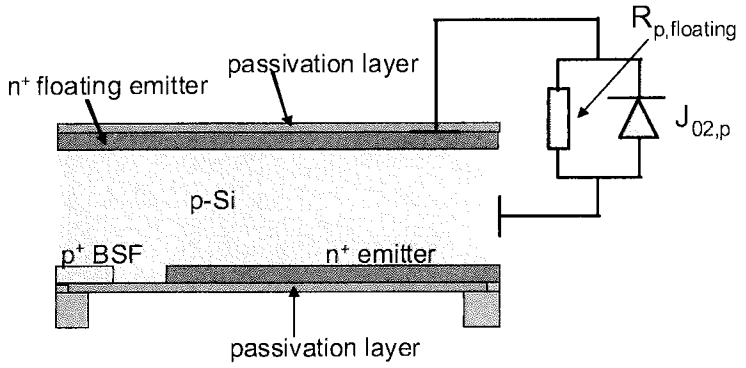


Figure 9-7 Equivalent circuit diagram for shunting effects across the floating junction used in PC1D simulations.

In the presence of the structure imperfections mentioned above, a $V_{floating}$ of about 600 mV is needed to passivate the surface. $V_{floating}$ is a function of the bias light intensity and increases with the logarithm of the light intensity, as shown in equation (9.1). Such a high voltage across the floating junction on the front side is only achieved at the light intensity higher than 0.5 suns. Thus, the surface passivation with floating junction is a very effective passivation scheme for medium to high illumination. At the same time, its passivation quality in realistic structures is poor at low illumination, due to low $V_{floating}$ and consequently high S_{front}.

The V_{OC} of the p-type cell with floating emitter was measured in illumination intensity range of 0.01 to 10 suns and is shown in Figure 9-8. In contrast to the quantum efficiency, the V_{OC} shows an approximately logarithmic behaviour with lowering of the illumination intensity. The different bias light dependence between EQE and V_{OC} of the structure B cell can be also explained by different cell operation conditions. At V_{OC} conditions, the solar cell operates under significantly higher injection level in comparison to the J_{SC} conditions, as already explained in the previous sections.

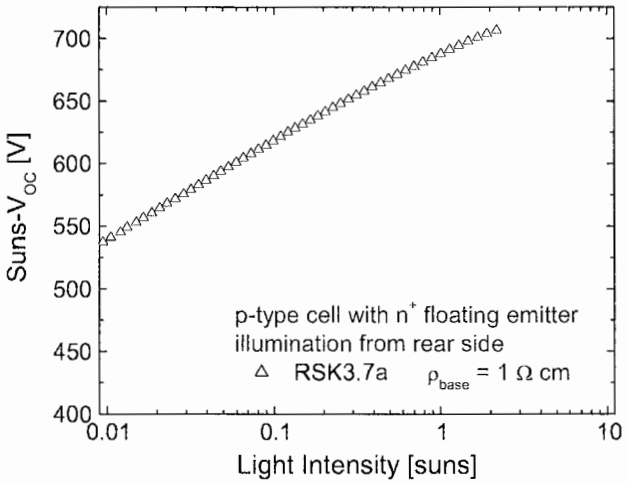


Figure 9-8 *Open-circuit voltage of the p-type back-contact back-junction cell with floating emitter (structure B) measured in bias light intensity range of 0.01 to 1 sun. Result for solar cell with 1 Ω cm base resistivity is shown. The solar cell was illuminated from the rear side during the measurement.*

9.5 Front surface fields

n-type solar cells with a phosphorus-doped n^+ front surface field (structure C) with base resistivity of 1 and 8 Ω cm were selected for the low illumination analysis. As shown in Table 9-1, these cells have an efficiency of 20.4 % and 19.5 % respectively. The EQE of the 1 Ω cm cell (BC47-18g) equals 95 % at wavelength of 600 nm. The EQE of the 8 Ω cm cell (BC47-21g) is higher due to higher collection efficiency and equals 98 % at the same wavelength. Both structure C cells have an EQE independent of the bias light illumination intensity, as shown in Figure 9-9. The quantum efficiency of the analyzed cells does not decrease with lowering of the bias light intensity from 1 to 0.3 suns.

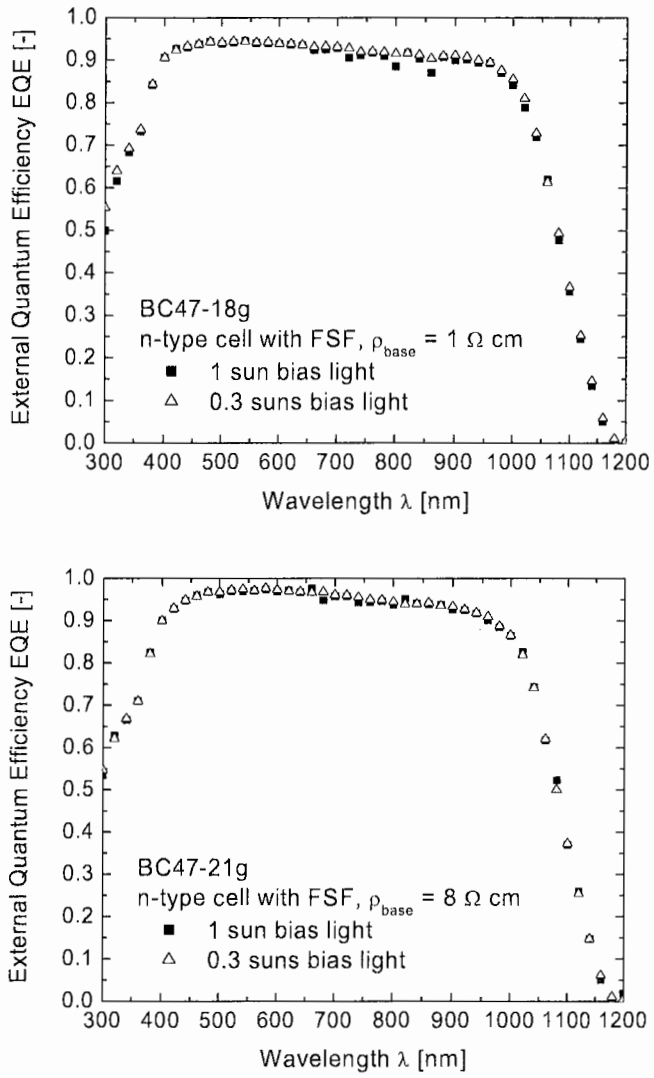


Figure 9-9 External quantum efficiency of n-type back-contact back-junction cells with front surface field (structure C) measured at 0.3 and 1 suns bias light intensity. Results for solar cells with base resistivity of 1 Ω cm (top) and 8 Ω cm (bottom) are shown.

The measurements of the normalized EQE for n-type cells with FSF are shown in Figure 9-10. The normalized EQE for both 1 and 8 Ω cm base doping is constant in the analyzed bias light intensity range. Therefore the current of the structure C is linear with bias light. Device simulations predict only a very weak injection dependence of the FSF cells. Within the measurement error, the experimental results are in good agreement with simulations.

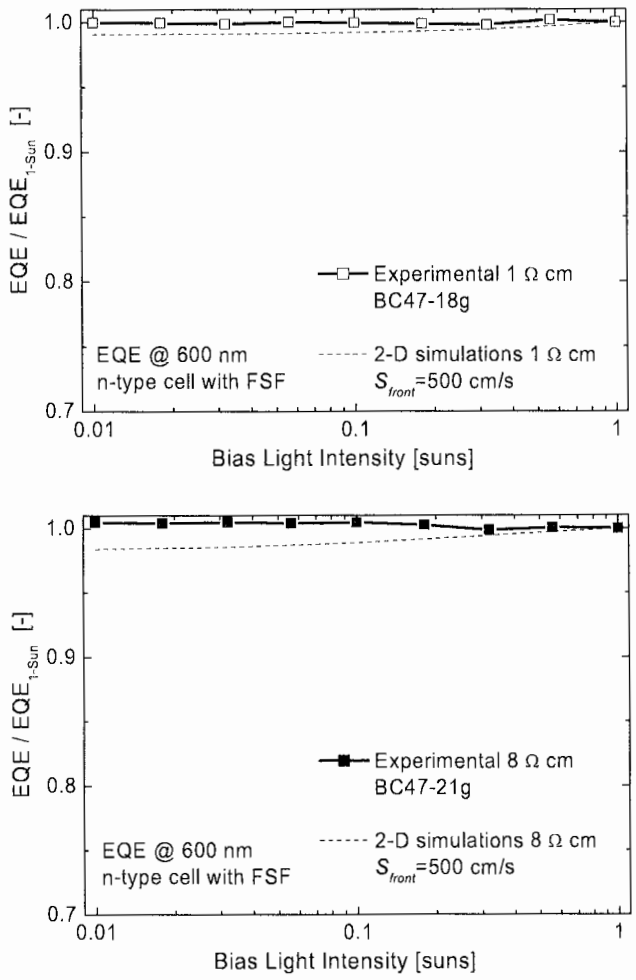


Figure 9-10 Normalized EQE for n-type cells with front surface field (structure C) measured at wavelength of 600 nm in bias light intensity range of 0.01 to 1 sun. Two-dimensional simulation results are shown as well (lines). Results for solar cells with base resistivity of 1 Ωcm (top) and 8 Ωcm (bottom) are shown.

The front surface of the FSF cell (structure C) always operates in the investigated illumination intensity range for both base resistivities under low-injection, due to high doping surface concentration of the phosphorus diffusion profile ($N_{peak} = 5\times10^{18}$ cm^{-3}). Thus, the high-injection effects do not occur at the physical surface as in the case of structure A and B cells, which showed a strong current injection dependence. A good passivation quality is achieved due to the high-low junction at the front surface, which is not affected by the illumination level, in contrast to the floating emitter passivation shown in the previous section. The front surface passivation with FSF is thus well suited also for low-illumination power generation.

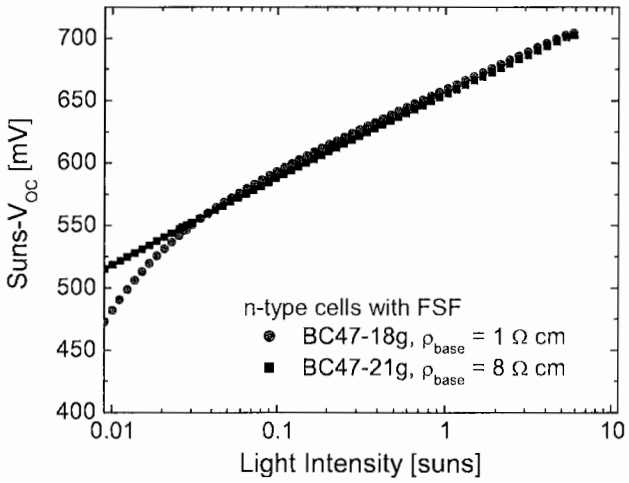


Figure 9-11 Open-circuit voltage of the n-type back-contact back-junction cells with front surface field (structure C) measured in bias light intensity range of 0.01 to 10 suns. Results for base resistivity of 1 and 8 Ω cm are shown.

The open-circuit voltage of the structure C cells measured in wide illumination intensity range is shown in Figure 9-11. Both measured cells show a linear decrease in voltage with lowering of the illumination intensity down to 0.1 suns. However, for illumination intensity lower than 0.1 suns, the V_{OC} of both cells becomes non-linear with illumination. This effect is much stronger for the cells with base resistivity of 1 Ω cm than for the cells with base resistivity of 8 Ω cm. A further analysis of this effect is needed in order to fully explain observed non-linearity of the voltage of the structure C cells. However, since the current of the n-type cells with FSF is independent of the illumination intensity and the voltage shows non-linear behavior only at the illumination intensities lower than 0.1 suns, it may be concluded that the structure C is best suited for low illumination applications from all three analyzed cell structures.

9.6 Conclusions

The quantum efficiency and open-circuit voltage of the three back-contact back-junction solar cell structures was analyzed under low illumination conditions. Among the analyzed cell structures, it was shown that the current of only n-type cells with n^+ front surface field is linear with light intensity. The quantum efficiency of the n-type cells with non-diffused front surfaces and the p-type cells with floating emitter decreases with lower illumination intensity. This leads to a reduced cell performance under lower illumination.

In practical terms, non-perfect processing of the front surface, including diffusion inhomogenities, introduction of crystal defects, broken pyramid tips, and local scratches introduce injection dependence behavior of the n-type cells with non-diffused front surfaces and the p-type cells with floating emitter. On the other hand, front surface recombination of the n-type solar cells with FSF has much lower influence on the cell performance, due to the passivation effect of the high-low junction. Therefore, the performance of the n-type cells with FSF is not affected by low-injection effects. Thus, the passivation of the front surface of the BC-BJ cells with FSF seem to be the best one suited for achieving a high energy yield when also operating under low illumination intensity.

As expected from the physical model, the V_{OC} of all cell structures decreases linearly with the logarithm of illumination until intensity of 0.1 suns. The injection level of a solar cell under V_{OC} conditions is much higher than under the J_{SC} conditions. Therefore the low injection effects cannot be seen at lower illumination intensities, in contrast to the case of quantum efficiency analysis.

10 Summary and outlook

Summary

In this thesis high-efficiency back-contact back-junction (BC-BJ) silicon solar cells for one-sun applications were studied. The focus was put on the development of a low-cost and industrially feasible manufacturing technology in order to utilize the full cost reduction potential of this elegant cell structure. At the same time the performance of the developed solar cells was investigated in details by experimental work, analytical modeling and numerical device simulations.

The BC-BJ solar cell structure requires multiple *structuring steps*, to form an interdigitated grid of p- and n-diffusions, contact openings and metal grids. In this work, the complex and costly photolithography masking steps were replaced by techniques which are of low cost and relevant for mass production. Screen-printing of the masking layers, as well as the local laser ablation of the dielectric and silicon layers, were developed and successfully applied to the solar cell processing sequence. The highest solar cell efficiency of 21.1 % (J_{SC} = 38.6 mA/cm^2, V_{OC} = 668 mV, FF = 82.0 %) was achieved on 160 µm thick 1 Ω cm n-type FZ Si with the designated area of 4 cm^2. No photolithography was applied in the processing sequence of this solar cell.

High-temperature diffusion of boron is applied for *emitter formation* of the n-type BC-BJ solar cells. However, this process needs to take place at strongly elevated temperatures and requires an additional masking step in order to define the areas for local diffusion. Therefore an alternative low temperature and mask less process to create p-type emitters, namely the local laser-fired aluminium emitter (LFE) process, was investigated in detail. It was found that the injection-dependent Shockley-Read-Hall recombination in the laser-induced damage zone located in the direct vicinity of the local back junction negatively influences the cell performance. Based on this disadvantage of the LFE process, the application of the LFE in the manufacturing of the high-efficiency back-junction solar cells was not followed further in the course of this thesis.

A *detailed study of the loss mechanisms* limiting the efficiency of the developed back-contact back-junction silicon solar cell was performed. The reduction of the cell efficiency was determined to be 3.9 % abs. due to recombination processes, 2.0 % abs. due to optical losses, 0.3 % abs. due to series resistance effects and 0.7 % due to electrical shading. The developed model of the loss mechanisms is a powerful tool for

the further optimization study of the solar cell structure. Based on this model it was found that the solar cell efficiencies of up to 23 % could be reached by improving the solar cell optics, reduction of the overall recombination losses, minimization of the electrical shading and optimization of the cell and grid geometry, which is limited by the industrial structuring technologies.

Positive effects of the phosphorus doped n^+ *front surface field* (FSF) on the performance of the BC-BJ solar cells were studied in details. These positive effects of FSF include: (i) passivation of the front cell surface and improvement of the stability of the cell performance under UV exposure, (ii) reduction of the series resistance and (iii) improvement of the solar cell performance under low illumination.

The best solar cell results were obtained with a deep diffused Gaussian phosphorus FSF doping profile with sheet resistance of 148 Ω/sq. The saturation current density of the passivated and textured surface with this FSF diffusion profile equals 21 fA/cm^2. In contrast to solar cells without the FSF diffusion, the solar cells with the FSF diffusion profile did not show any performance degradation under *exposure to UV radiation.*

Phosphorus doped FSF not only improves the front surface passivation of the analyzed solar cells. The highly doped front n^+ layer can be also seen as a highly conductive *highway* for the majority carriers, which enhances its lateral transport. The front diffused n^+ layer can be seen as a parallel conductor to the lateral base resistance. This way the lateral base resistance can be reduced. Lateral pitch is in the case of the developed cells in the range of millimeters, due to the application of the low-cost screen-printing and laser ablation structuring. Experimental data show that the application of a FSF reduces the total series resistance of the measured n-type cells of 160 micrometer thickness with 3.5 mm pitch by 0.1 Ω cm^2 for 1 Ω cm base resistivity and 1.3 Ω cm^2 for 8 Ω cm base resistivity.

Next to improvement of the front surface passivation and reduction of the lateral base resistance, the front surface field improves the *performance* of the BC-BJ solar cells *under low illumination intensity.* Among different analyzed cell structures, it was shown that the current only of n-type cells with n^+ front surface field is linear with light intensity. Due to the fact that the front surface passivation of the n-type BC-BJ cells with FSF is not affected by low-injection effects, the quantum efficiency of these cells does not decrease in the bias light intensity range down to 0.01 suns. Therefore the BC-BJ cells with FSF seem to be these best suited for achieving a high energy yield when also operating under low illumination intensity.

Outlook

In the present thesis a base-line technological process for processing of back-contact back-junction Si solar cells was established. In order to further increase its economical competitiveness and fully utilize the potential of this cell structure, the *future research* should focus on the further optimization of the device efficiency and reduction of the manufacturing costs.

The *optimization of the solar cell geometry* should be pursued with the focus on increasing the emitter coverage on the rear side and at the same time reducing the overall device pitch. This can be obtained by careful optimization of the resolution and the positioning accuracy of the masking processing steps. Ideally these activities should be performed rather in the pilot-line environment than in the low-throughput laboratory conditions.

In parallel to the optimization of the device geometry, the electrical properties of the solar cell should be further optimized. The free carrier absorption losses and the high contribution of the rear side diffusions to the overall solar cell recombination point out the need of further *optimization of the emitter and back surface field diffusion profiles*. Also the *rear side passivation scheme* should be improved in order to reduce the recombination in the non-diffused gap areas.

An application of a pin-hole free passivation layer on the rear side, would enable *decoupling of the metallization geometry from the diffusion geometry*, without the risk of local shunt formation. This way the resistance losses in the thin base metallization fingers, which are especially important for the large size solar cells, would be reduced. Also the sizes of the diffused busbars could be reduced significantly. This way the electrical shading losses can be reduced. Further reduction of the processing costs could be obtained by replacing of the metallization using silver, by metallization scheme based on copper.

Next to the optimization of the solar cell structure, the *appropriate module technology* for the back-contacted solar cells should be applied. This technology should enable high packaging density of the solar cells and could use interconnection sheets with a pre-defined metallization pattern, which would further reduce the series resistance losses in the metallization grid.

Zusammenfassung und Ausblick

Zusammenfassung

Im Rahmen dieser Arbeit wurden hocheffiziente rückseitig kontaktierte Silicium-Solarzellen analysiert, bei denen der pn-Übergang ebenfalls auf der Rückseite ausgebildet wurde (sogenannte back-contact back-junction (BC-JC) Solarzellen). Ausgelegt waren diese Zellen für eine Beleuchtungsintensität von einer Sonne. Der Schwerpunkt dabei lag auf der Entwicklung eines preiswerten und industriell umsetzbaren Herstellungsprozesses, um das Kosteneinsparpotential dieser neuartigen Zellstruktur auszunutzen. Im Rahmen dieser Arbeit wurden ebenfalls die elektrische Effizienz der Zellen und die zugrunde liegenden physikalischen Effekte mittels verschiedener Experimente und analytischen und numerischen Simulationen detailliert untersucht.

Die Struktur der BC-BJ Solarzellen erfordert mehrere Ablaufschritte, um die ineinander greifende Struktur der p- und der n-Diffusionen, der Kontaktöffnungen und der Metallkontakte zu realisieren. In Rahmen dieser Arbeit wurden die komplexen und kostspieligen photolithographischen Prozessschritte durch einfachere und preiswertere Schritte ersetzt, welche auch industriell eingesetzt werden können. Sowohl siebgedruckte Maskierungsschichten als auch lokale lasergestützte Abtragung von dielektrischen Schichten und Silicium wurden erfolgreich entwickelt und angewandt. Das beste Zellergebnis mit einer Effizienz von 21.1 % (Kurzschlussstromdichte 38.6 mA/cm^2, Offenklemmspannung 668 mV, Füllfaktor 82.0 %) wurden bei einer 160 µm dicken, auf 1 Ω cm n-typ FZ Silicium prozessierten Solarzelle ermittelt, welche eine Aperturfläche von 4 cm^2 besaß. Bei der Prozessierung dieser hocheffizienten Solarzelle wurde komplett auf photolithographische Schritte verzichtet.

Bei den n-typ BC-JC Solarzellen wurde der Emitter durch eine Diffusion von Bor hergestellt. Allerdings sind dazu hohe Temperaturen und zusätzliche Maskierungsschritte notwendig, um die Bereiche für die lokale Diffusion einzugrenzen. Daher wurde im Rahmen dieser Arbeit ein alternativer Prozess eingehende analysiert, bei dem auf die hohen Temperaturen verzichtet werden kann und welcher ohne zusätzliche Maskierungen funktioniert. Der p-typ Emitter wird dabei durch das sogenannte „laser-fired aluminium emitter (LFE)"-Verfahren ausgebildet. Es konnte gezeigt werden, dass die injektionsabhängige Shockley-Read-Hall-Rekombination in der laserbedingten Schädigungszone in der direkten Umgebung der

lokalen rückseitigen Raumladungszone die Zelleffizienz negativ beeinflusst. Bedingt durch diesen Nachteil des LFE-Prozesses wurde dieser Ansatz im Verlauf dieser Arbeit nicht weiter verfolgt.

Ausführlich wurden die Verlustmechanismen, welche die Effizienz der untersuchten BC-BJ Solarzellen limitieren, analysiert. Dabei konnte gezeigt werden, dass die Zelleffizienz aufgrund von Rekombinationsprozessen um 3.9 % absolut, aufgrund von optischen Verlusten um 2.0 %, aufgrund von Serienwiderstands-Effekten um 0.3 % und aufgrund von elektrischen Abschattungen um 0.7 % reduziert ist. Es hat sich gezeigt, dass das entwickelte Modell der Verlustmechanismen ein mächtiges Werkzeug war, um die Struktur der hocheffizienten Solarzellen weiter zu verbessern. Darauf basierend konnte gezeigt werden, dass Zelleffizienzen von bis zu 23 % realisiert werden können, wenn die Zelloptik, Rekombinationsverluste, elektrische Abschattung und das Kontaktgrid weiter optimiert werden.

Im Rahmen dieser Arbeit wurden weiter die positiven Effekte eines Phosphor-dotierten n^+ „front surface fields (FSF)" untersucht. Diese Effekte beinhalten (i) Passivierung der Zellvorderseite und Langzeitstabilität bei Beleuchtung mittels UV-Licht, (ii) Reduzierung des Serienwiderstandes und (iii) Verbesserung der Solarzelleffizienz unter Schwachlichtverhältnissen.

Die besten Solarzellergebnisse wurden mit einem tief eingetriebenen Gauss-förmigen Phosphor FSF Dotierprofil mit einem Schichtwiderstand von 148 Ω/sq erreicht. Die Dunkelstromdichte der passivierten und texturierten Oberfläche lag dabei bei 21 fA/cm^2. Im Vergleich zu Solarzellen ohne das zusätzliche FSF konnte keine Degradation der Solarzellen unter UV-Licht nachgewiesen werden.

Ein Phosphor-dotiertes FSF verbessert nicht nur die Vorderseitenpassivierung der analysierten Solarzellen. Die hochdotierte n^+-Schicht verbessert zusätzlich den lateralen Transport der Majoritäts-Ladungsträger. In dieser Weise kann der Widerstand der Basis reduziert werden. Der laterale Abstand (Pitch) der Kontaktfinger lag bei den untersuchten Solarzellen im Bereich von Millimetern, bedingt durch die Verwendung von industriell tauglichen preiswertem Siebdruck und Laserstrukturierung. Experimentelle Daten zeigen, dass das zusätzliche FSF den gesamten Serienwiderstand der untersuchten n-typ Solarzellen mit einer Dicke von 160 µm und einem Pitch von 3.5 mm um 0.1 Ω cm^2 bei einem Basiswiderstand von 1 Ω cm und um 1.3 Ω cm^2 bei einem Basiswiderstand von 8 Ω cm reduziert.

Auch wurde im Rahmen dieser Arbeit untersucht, in wie weit das zusätzliche FSF die Zelleffizienz der BC-JC Solarzellen unter Schwachlichtbedingungen verbessert.

Mittels unterschiedlicher Zellstrukturen konnte gezeigt werden, dass bei einer n-typ Solarzelle mit einem zusätzlichen n^+ FSF der Strom linear mit der Lichtintensität ansteigt. Da diese Vorderseitenpassivierung nicht durch Niedriginjektionseffekte beeinflusst ist, ist die Quanteneffizienz der untersuchten BC-JC Solarzellen mit zusätzlichem FSF nicht verringert bis hin zu einer Lichtintensität von 0.01 Sonnen. Daher sind diese hier untersuchten BC-JC Solarzellen mit zusätzlichem FSF hervorragend geeignet, um eine hohe Stromausbeute auch unter Schwachlichtbedingengen zu erreichen.

Ausblick

In der vorliegenden Arbeit wurde ein technologischer Prozess für die Herstellung von rückseitig sammelnden und rückseitig kontaktierten Silizium-Solarzellen entwickelt. Um die Steigerung der ökonomischen Wettbewerbsfähigkeit und um das Potential dieser Zellstruktur weiter auszuschöpfen, sollten sich die zukünftige Forschungsaktivitäten auf eine weitere Optimierung des Solarzellewirkungsgrades und der Senkung der Herstellungskosten fokussieren.

Die Optimierung der Solarzellengeometrie sollte mit dem Schwerpunkt der Steigerung der Emitterbedeckung auf der Rückseite und der gleichzeitigen Verringerung der gesamten lateralen Solarzellendemensionen (Pitch) weiterverfolgt werden. Dies kann durch eine sorgfältige Optimierung der Auflösungs- und Positionierungsgenauigkeit der Maskierungsschritte erreicht werden. Ideellerweise, sollten diese Aktivitäten jedoch eher in einer Pilotlinie als in einer Laborumgebung mit geringem Durchsatz durchgeführt werden.

Parallel zur Optimierung der Solarzellengeometrie, sollten die elektrischen Eigenschaften der Solarzelle weiter verbessert werden. Die Verluste durch die Absorption freier Ladungsträger und der hohe Beitrag der Diffusionen auf der Rückseite zur gesamten Rekombination der Solarzelle haben gezeigt, dass eine Anpassung der Diffusionsprofile von Emitter und Back-Surface-Field erforderlich ist. Das rückseitige Passivierungssystem sollte ebenfalls verbessert werden, um die Rekombination im undiffundierten Bereich zu reduzieren.

Die Anwendung von „pin-hole"-freien Passivierungsschichten auf der Rückseite, würden die Entkopplung der Metallisierungsgeometrie und der Geometrie der Diffusionen ermöglichen, ohne lokale Kurzschlüsse zu erzeugen. Dadurch würden die Widerstandsverluste in den dünnen Fingern der Basismetallisierung, welche besonders wichtig für Solarzellen im Großformat sind, reduziert werden. Auch lässt sich die

Fläche der diffundierten Busbars signifikant verringert. Eine weitere Verringerung der Herstellungskosten könnte erreicht werden, indem die Metallisierung mit Silber durch die Verwendung eines Metallisierungsverfahrens mit Kupfer ersetzt wird.

Neben der Optimierung der Solarzellenstruktur, sollte eine geeignete Modultechnologie für rückseitig kontaktierte Solarzellen bereitgestellt werden. Diese Technologie sollte eine hohe Packungsdichte der Solarzellen ermöglichen und könnte durch die Verwendung einer Folien mit einem vordefinierten Metallisierungsmuster zum Zusammenschalten der Solarzellen, die Serienwiderstandsverluste im Metalisierungsgitter weiter senken.

Symbols, acronyms and physical constants

Symbols

Symbol	Description	Unit
A	area	cm^2
A_F	pitch of the solar cell	µm
a_{n-n}	distance between n^+ and n^+ doping	µm
B_F	width of the metal fingers	µm
B_R	radiative recombination coefficient	
C	concentration	
C_A	Auger coefficient	$cm^{-3}\ s^{-1}$
d_{wafer}	wafer thickness	µm
E_i	intrinsic Fermi level	eV
FF	fill factor	
H_F	height of the metal fingers	µm
J_0	saturation current density	$A\ cm^{-2}$
J_{01}, J_{02}	dark saturation current densities in a two-diode model	$A\ cm^{-2}$
J_{0s}	surface recombination current density	$A\ cm^{-2}$
J_{mpp}	current at maximum power point	$A\ cm^{-2}$
J_{ph}	photogeneratred current	$A\ cm^{-2}$
J_{SC}	short-circuit current density	$A\ cm^{-2}$
l	average path length of incoming light within silicon wafer	
L_{eff}	effective diffusion length of the minority carriers	µm

Symbol	Description	Unit
L_F	length of the metal fingers	µm
n_0	equilibrium concentration of electrons	cm^{-3}
N_A	concentration of acceptor atoms	cm^{-3}
N_D	concentration of donor atoms	cm^{-3}
n_e	electron density	cm^{-3}
n_i	intrinsic carrier density	cm^{-3}
N_{peak}, N_S	surface doping concentration	cm^{-3}
n_{Si}	refractive index of silicon	
N_{st}	number of surface states	cm^{-2}
p_0	equilibrium concentration of holes	cm^{-3}
PFF	pseudo fill factor	
P_{RP}	photon recycling rate	
$R_{CE\text{-}Auger}$	Columb-enhanced Auger recombination rate	$cm^{-3}s^{-1}$
R_p	parallel resistance	Ω
R_{rad}	radiative recombination rate	$cm^{-3}s^{-1}$
R_S	series resistance	Ω
S	surface recombination rate	$cm\ s^{-1}$
S_{eff}	effective surface recombination velocity	$cm\ s^{-1}$
S_{front}	front surface recombination velocity	$cm\ s^{-1}$
T	temperature	K or °C
t	time	h
U_S	net recombination rate at surface	$cm^{-2}\ s^{-1}$
V	voltage	mV
V_{mpp}	voltage at maximum power point	mV

Symbol	Description	Unit
V_{OC}	open-circuit voltage	mV
W	wafer thickness	µm
x_j	junction depth	µm
Δn	excess carrier density	cm^{-3}
α_{FCA}	free carrier absorption coefficient	cm^{-1}
α_{Si}	absorption coefficient of silicon	cm^{-1}
η	efficiency	%
λ	wavelength	nm
ρ	resistivity	Ω cm
ρ_{base}	resistivity of the base material	Ω cm
ρ_{FSF}	sheet resistance of the front surface field	Ω/sq
ρ_{sheet}	sheet resistance	Ω/sq
σ_n	capture cross section for electrons	cm^2
σ_p	capture cross section for holes	cm^2
τ_A	minority carrier lifetime of Auger recombination	µs
τ_{bulk}	minority carrier lifetime in bulk	µs
τ_{eff}	effective minority carrier lifetime	µs
τ_{rad}	minority carrier lifetime of radiative recombination	µs
τ_S	minority carrier lifetime of surface recombination	µs
τ_{SRH}	Shockley-Read-Hall recombination lifetime	µs
υ_{th}	thermal velocity of charge carriers	$cm\ s^{-1}$

Acronyms

Acronym	Description
AM1.5g	air mass 1.5 global spectrum
ARC	anti-reflection coating
BC-BJ	back-contact back-junction solar cell
BSF	back surface field
Cz-Si	monocrystalline silicon produced with the Czochralsky method
EQE	external quantum efficiency
EWT	emitter wrap through solar cell
FCA	free carrier absorption
FGA	forming gas anneal
FZ-Si	monocrystalline silicon produced with the floating zone method
FSF	front surface field
IQE	internal quantum efficiency
IBC	interdigitated back contact solar cell
LBSF	local back surface field
LBIC	light beam induced current
LFE	laser-fired aluminium emitters
LFC	laser-fired contacts
LIP	light-induced plating
mc-Si	multicrystalline silicon
MWT	metallization warp through solar cell
PCD	photoconductance decay
PECVD	plasma enhanced chemical vapour deposition
PERL	passivated emitter real locally diffused solar cell

Acronym	Description
PERC	passivated emitter and rear cell solar cell
QSSPC	quasi-steady state photoconductance
SIMS	secondary ion mass spectroscopy
SEM	scanning electron microscope
STC	standard testing conditions

Physical constants

Constant	Description	Value
k	Boltzmann's constant	1.3806×10^{-23} J K^{-1}
c	velocity of light	299792458 m s^{-1}
h	Planck constant	6.62607×10^{-34} J s
n_i	intrinsic carrier density	1.00×10^{10} cm^{-3}
q	elementary charge	1.6022×10^{-19} C

Bibliography

[1] EPIA and Greenpeace, *Solar Generation V – 2008. Solar electricity for over one billion people and two million jobs by 2020*, (2008).

[2] R.M. Swanson, *A vision for crystalline silicon photovoltaics*, Progress in Photovoltaics: Research and Applications, **14** (5), 443-53, (2006).

[3] D. De Ceuster, P. Cousins, D. Rose, D. Vicente, P. Tipones, and W. Mulligan, *Low Cost, high volume production of >22% efficiency silicon solar cells*, in *Proceedings of the 22nd European Photovoltaic Solar Energy Conference*, Milan, Italy, 816-9 (2007).

[4] M.A. Green, *Solar cells: operating principles, technology and system applications*. 1986, Kensington: UNSW.

[5] P. Würfel, *Physics of Solar Cells*. 2005, Weinheim: Wiley.

[6] A. Luque and S. Hegedus, *Handbook of Photovoltaic Science and Engineering*. 2003, West Sussex: John Wiley & Sons Ltd.

[7] M. Späth, P.C. de Jong, and J. Bakker, *A novel module assembly line using back contact solar cells*, in *Technical Digest of the 17th International Photovoltaic Solar Energy Conference*, Fukuoka, Japan, 436 (2007).

[8] J. Zhao, A. Wang, and M.A. Green, *24·5% Efficiency silicon PERT cells on MCZ substrates and 24.7% efficiency PERL cells on FZ substrates*, Progress in Photovoltaics: Research and Applications, **7** (6), 471-4, (1999).

[9] O. Schultz, S.W. Glunz, and G. Willeke, *Multicrystalline Silicon Solar Cells Exceeding 20 % Efficiency*, Progress in Photovoltaics: Research and Applications, **12** (7), 553-8, (2004).

[10] S.W. Glunz, *New concepts for high-efficiency silicon solar cells*, Solar Energy Materials and Solar Cells, **90** (18-19), 3276-84, (2006).

[11] S.W. Glunz, *High-efficiency crystalline silicon solar cells*, Advances in OptoElectronics, **2007**, 97370/1-15, (2007).

[12] E. Van Kerschaver and G. Beaucarne, *Back-contact solar cells: a review*, Progress in Photovoltaics: Research and Applications, **14** (2), 107-23, (2006).

[13] R.J. Schwartz and M.D. Lammert, *Silicon solar cells for high concentration applications*, in *Technical Digest of the International Electron Devices Meeting*, Washington, DC, 350-2 (1975).

[14] M.D. Lammert and R.J. Schwartz, *The interdigitated back contact solar cell: a silicon solar cell for use in concentrated sunlight*, IEEE Transactions on Electron Devices, **ED-24** (4), 337-42, (1977).

[15] R.M. Swanson, A.K. Beckwith, R.A. Crane, W.D. Eades, Y.H. Kwark, and R.A. Sinton, *Point-contact silicon solar cells*, IEEE Transactions on Electron Devices, **31** (5), 661-4, (1984).

[16] R.A. Sinton, Y. Kwark, J.Y. Gan, and R.M. Swanson, *27.5-percent silicon concentrator solar cells*, IEEE Electron Device Letters, **EDL-7** (10), 567-9, (1986).

[17] R.A. Sinton and R.M. Swanson, *Design criteria for Si point-contact concentrator solar cells*, IEEE Transactions on Electron Devices, **ED-34** (10), 2116-23, (1987).

[18] R.A. Sinton, P. Verlinden, D.E. Kane, and R.M. Swanson, *Development efforts in silicon backside-contact solar cells*, in *Proceedings of the 8th European Photovoltaic Solar Energy Conference*, Florence, Italy, 1472-6 (1988).

[19] P. Verlinden, F. Van de Wiele, G. Stehelin, and J.P. David, *Optimized interdigitated back contact (IBC) solar cell for high concentrated sunlight*, in *Proceedings of the 18th IEEE Photovoltaic Specialists Conference*, Las Vegas, Nevada, USA, 55-60 (1985).

[20] R.R. King, R.A. Sinton, and R.M. Swanson, *Front and back surface fields for point-contact solar cells*, in *Proceedings of the 20th IEEE Photovoltaic Specialists Conference*, Las Vegas, Nevada, USA, 538-44 (1988).

[21] P. Verlinden, R.A. Sinton, and R.M. Swanson, *High efficiency large area back contact concentrator solar cells with a multilevel interconnection*, International Journal of Solar Energy, **6** (6), 347-66, (1988).

[22] P. Verlinden, R.M. Swanson, R.A. Sinton, and D.E. Kane, *Multilevel metallization for large area point-contact solar cells*, in *Proceedings of the 20th IEEE Photovoltaic Specialists Conference*, Las Vegas, Nevada, USA, (1988).

[23] R.R. King, R.A. Sinton, and R.M. Swanson, *One-Sun, Single-Crystalline Silicon Solar Cell Research*. Solid State Electronics Laboratory, Stanford University, Stanford, (1991).

[24] R.A. Sinton and R.M. Swanson, *Simplified backside-contact solar cells*, IEEE Transactions on Electron Devices, **37** (2), 348-52, (1990).

[25] R.A. Sinton, P.J. Verlinden, R.A. Crane, R.M. Swanson, C. Tilford, J. Perkins, and K. Garrison, *Large-area 21% efficient Si solar cells*, in *Proceedings of the 23rd IEEE Photovoltaic Specialists Conference*, Louisville, Kentucky, USA, 1490, 157-61 (1993).

[26] P.J. Verlinden, R.M. Swanson, and R.A. Crane, *7000 high efficiency cells for a dream*, Progress in Photovoltaics: Research and Applications, **2** (2), 143, (1994).

[27] P.J. Verlinden, R.A. Sinton, K. Wickham, R.A. Crane, and R.M. Swanson, *Backside-contact silicon solar cells with improved efficiency for the `96 world solar challenge*, in *Proceedings of the 14th European Photovoltaic Solar Energy Conference*, Barcelona, Spain, 96-9 (1997).

[28] M.J. Cudzinovic and K. McIntosh, *Process simplifications to the Pegasus solar cell - Sunpower's high-efficiency bifacial solar cell*, in *Proceedings of the 29th IEEE Photovoltaics Specialists Conference*, New Orleans, Louisiana, USA, 70-3 (2002).

[29] W.P. Mulligan, D.H. Rose, M.J. Cudzinovic, D.M. De Ceuster, K.R. McIntosh, D.D. Smith, and R.M. Swanson, *Manufacture of solar cells with 21% efficiency*, in *Proceedings of the 19th European Photovoltaic Solar Energy Conference*, Paris, France, 387-90 (2004).

[30] K.R. McIntosh, M.J. Cudzinovic, D.D. Smith, W.P. Mulligan, and R.M. Swanson, *The choice of silicon wafer for the production of low-cost rear-contact solar cells*, in *Proceedings of the 3rd World Conference on Photovoltaic Energy Conversion*, Osaka, Japan, 971-4 (2003).

[31] K.R. McIntosh, N.C. Shaw, and J.E. Cotter, *Light trapping in Sunpower's A-300 solar cell*, in *Proceedings of the 19th European Photovoltaic Solar Energy Conference*, Paris, France, 844-7 (2004).

[32] R.M. Swanson, *Device physics for backside-contact solar cells*, in *Proceedings of the 33rd IEEE Photovoltaic Specialists Conference*, San Diego, USA, (2008).

[33] J. Dicker, J.O. Schumacher, W. Warta, and S.W. Glunz, *Analysis of one-sun monocrystalline rear-contacted silicon solar cells with efficiencies of 22.1%*, Journal of Applied Physics, **91** (7), 4335-43, (2002).

[34] J. Dicker, *Analyse und Simulation von hocheffizienten Silizium-Solarzellenstrukturen für industrielle Fertigungstechniken*, Dissertation, Universität Konstanz, (2003).

[35] A. Mohr, *Silicon concentrator cells in a two-stage photovoltaic system with a concentration factor of 300x*, Dissertation, Universität Freiburg, (2005).

[36] A. Mohr, T. Roth, and S.W. Glunz, *BICON: High concentration PV using one-axis tracking and silicon concentrator cells*, Progress in Photovoltaics: Research and Applications, **14**, 663-74, (2005).

[37] J.-H. Guo, *High-efficiency n-type laser-grooved buried contact silicon solar cells*, Dissertation, University of New South Wales, (2004).

[38] J.-H. Guo, B.S. Tjahjono, and J.E. Cotter, *19.2% efficiency n-type laser-grooved silicon solar cells*, in *Proceedings of the 31st IEEE Photovoltaic Specialists Conference*, Orlando, USA, 983-6 (2005).

[39] P. Engelhart, N.-P. Harder, R. Grischke, A. Merkle, R. Meyer, and R. Brendel, *Laser structuring for back junction silicon solar cells*, Progress in Photovoltaics: Research and Applications, **15**, 237-43, (2006).

[40] P. Engelhart, *Lasermaterialbearbeitung als Schlüsseltechnologie zum Herstellen rückseitenkontaktierter Siliciumsolarzellen*, Dissertation, Universität Hannover, (2007).

[41] D. Huljic, *et al.*, *Development of a 21 % back-contact monocrystalline silicon solar cell for large-scale production*, in *21st European Photovoltaic Solar Energy Conference*, Dresden, Germany, 765-8 (2006).

[42] D. Huljic, *et al.*, *Q-Cells' High-Efficiency Back Junction Solar Cell for Large-Scale Production - Main Results of the QUEBEC Project*, in *22nd European Photovoltaic Solar Energy Conference*, Milano, Italy, (2007).

[43] R. Stangl, M. Bivour, E. Conrad, I. Didschuns, L. Korte, K. Lips, and M. Schmidt, *Recash - A novel high efficiency buried grid rear contact amorphous/crystalline silicon heterojunction solar cell concept*, in *Proceedings of the 22nd European Photovoltaic Solar Energy Conference*, Milan, Italy, 870-4 (2007).

[44] M. Tucci, *et al.*, *BEHIND (Back enhanced heterostructure with interdigitated conctacts) solar cell*, in *23rd European Photovoltaic Solar Energy Conference*, Valencia, Spain, 1749-52 (2008).

[45] L. Meijun, B. Stuart, D. Ujjwal, and B. Robert, *Interdigitated back contact silicon heterojunction solar cell and the effect of front surface passivation*, Applied Physics Letters, **91** (6), 063507, (2007).

[46] J.M. Gee, W.K. Schubert, and P.A. Basore, *Emitter wrap-through solar cell*, in *Proceedings of the 23rd IEEE Photovoltaic Specialists Conference*, Louisville, Kentucky, USA, 265-70 (1993).

[47] J.M. Gee, M.E. Buck, W.K. Schubert, and P.A. Basore, *Progress on the emitter wrap-through silicon solar cell*, in *Proceedings of the 12th European Photovoltaic Solar Energy Conference*, Amsterdam, The Netherlands, 743-6 (1994).

[48] D. Kray, *Hocheffiziente Solarzellenstrukturen für kristallines Silicium-Material industrieller Qualität*, Dissertation, Universität Konstanz, (2004).

[49] J.M. Gee, P. Hacke, M.W. Sumner, and R.R. Schmit, *Towards a manufacturable back-contact emitter-wrap-through silicon solar cell*, in *Photovoltaic Specialists Conference, 2005. Conference Record of the Thirty-first IEEE*, 1663-6 (2005).

[50] A. Kress, O. Breitenstein, S. Glunz, P. Fath, G. Willeke, and E. Bucher, *Investigations on low-cost back-contact silicon solar cells*, Solar Energy Materials and Solar Cells, **65**, 555-60, (2001).

[51] A. Kress, *Emitterverbund-Rückkontaktsolarzellen für die industrielle Fertigung*, Dissertation, Universität Konstanz, (2001).

[52] D. Kray, *et al.*, *Progress in high-efficiency emitter-wrap-through cells on medium quality substrates*, in *Proceedings of the 3rd World Conference on Photovoltaic Energy Conversion*, Osaka, Japan, 1340-3 (2003).

[53] S.W. Glunz, *et al.*, *High-efficiency cell structures for medium-quality silicon*, in *Proceedings of the 17th European Photovoltaic Solar Energy Conference*, Munich, Germany, 1287-92 (2001).

[54] S. Hermann, *et al.*, *21.4 %-efficient emitter wrap-through RISE solar cell on large area and picosecond laser processing of local contact openings*, in *Proceedings of the 22nd European Photovoltaic Solar Energy Conference*, Milan, Italy, 970-5 (2007).

[55] C. Peters, *et al.*, *ALBA – Development of high-efficiency mulit-crystalline Si EWT solar cells for industrial fabrication at Q-Cells*, in *Proceedings of the 23rd European Photovoltaic Solar Energy Conference*, Valencia, Spain, 1010-13 (2008).

[56] E. van Kerschaver, R. Einhaus, J. Szlufcik, J. Nijs, and R. Mertens, *A novel silicon solar cell structure with both external polarity contacts on the back surface*, in *Proceedings of the 2nd World Conference on Photovoltaic Energy Conversion*, Vienna, Austria, 1479-82 (1998).

[57] H. Knauss, H. Haverkamp, W. Jooss, S. Steckemetz, and H. Nussbaumer, *Industrially applicable metallisation wrap through solar cell process resulting in efficiencies exceeding 16 %*, in *Proceedings of the 21st European Photovoltaic Solar Energy Conference*, Dresden, Germany, 1192-5 (2006).

[58] E. Van Kerschaver, C. Allebé, B. Devreese, L. Frisson, and J. Szlufcik, *Record high performance modules based on screen printed MWT solar cells*, in *Proceedings of the 29th IEEE Photovoltaics Specialists Conference*, New Orleans, Louisiana, USA, 78-81 (2002).

[59] J.H. Bultman, M.W. Brieko, A.R. Burgers, J. Hoornstra, A.C. Tip, and A.W. Weeber, *Interconnection through vias for improved efficiency and easy module manufacturing of crystalline silicon solar cells*, Solar Energy Materials and Solar Cells, **65**, 339-45, (2001).

[60] A.W. Weeber, R. Kinderman, C.J.J. Tool, F. Granek, and P.C. De Jong, *How to achieve 17% cell efficiencies on large back-contacted mc-Si solar cells*, in

Proceedings of the 4th World Conference on Photovoltaic Energy Conversion, Hawaii, USA, 1048-51 (2006).

[61] F. Clement, *et al.*, *Industrially feasible MC-Si metal wrap through (MWT) solar cells with high emitter sheet resistances exceeding 16% efficiency*, in *Proceedings of the 23rd European Photovoltaic Solar Energy Conference*, Valencia, Spain, in print (2008).

[62] W. Jooss, H. Knauss, F. Huster, P. Fath, E. Bucher, R. Tölle, and T.M. Bruton, *Back contact buried contact solar cells with metallization wrap around electrodes*, in *Proceedings of the 28th IEEE Photovoltaics Specialists Conference*, Anchorage, Alaska, USA, 176-9 (2000).

[63] D.A. Clugston and P.A. Basore, *PC1D version 5: 32-bit solar cell modeling on personal computers*, in *Proceedings of the 26th IEEE Photovoltaic Specialists Conference*, Anaheim, California, USA, 207-10 (1997).

[64] W. Shockley and H.J. Queisser, *Detailed balance limit of efficiency of p-n junction solar cells*, Journal of Applied Physics, **32** (3), 510-9, (1961).

[65] T. Tiedje, E. Yablonovitch, G.D. Cody, and B.G. Brooks, *Limiting efficiency of silicon solar cells*, IEEE Transactions on Electron Devices, **31** (5), 711-6, (1984).

[66] R.M. Swanson, *Approaching the 29% limit efficiency of silicon solar cells*, in *Proceedings of the 31st IEEE Photovoltaic Specialists Conference*, Orlando, USA, 889-94 (2005).

[67] R. Brendel, *Thin-film silicon solar cells: Physics and Technology*. 2003, Weinheim: Wiley-VCH.

[68] M.J. Kerr, *Surface, emitter and bulk recombination in silicon and development of silicon nitride passivated solar cells*, Dissertation, Australian National University, (2002).

[69] M.J. Kerr and A. Cuevas, *General parameterization of Auger recombination in crystalline silicon*, Journal of Applied Physics, **91** (4), 2473-80, (2002).

[70] M.J. Kerr, A. Cuevas, and P. Campbell, *Limiting efficiency of crystalline silicon solar cells due to Coulomb-enhanced Auger recombination*, Progress in Photovoltaics: Research and Applications, **11** (2), 97-104, (2003).

[71] M.A. Green, *Limits on the open-circuit voltage and efficiency of silicon solar cells imposed by intrinsic Auger processes*, IEEE Transactions on Electron Devices, **ED-31** (5), 671-8, (1984).

[72] T. Trupke, M.A. Green, P. Würfel, P.P. Altermatt, A. Wang, J. Zhao, and R. Corkish, *Temperature dependence of the radiative recombination coefficient of intrinsic crystalline silicon*, Journal of Applied Physics, **94** (8), 4930-7, (2003).

[73] Sinton-Consulting-Inc., *http://www.sintonconsulting.com/.*

[74] H. Nagel, C. Berge, and A.G. Aberle, *Generalized analysis of quasi-steady-state and quasi-transient measurements of carrier lifetimes in semiconductors*, Journal of Applied Physics, **86** (11), 6218- 21, (1999).

[75] R.A. Sinton, A. Cuevas, and M. Stuckings, *Quasi-steady-state photoconductance, a new method for solar cell material and device characterization*, in *Proceedings of the 25th IEEE Photovoltaic Specialists Conference*, Washington DC, USA, 457-60 (1996).

[76] B. Fischer, *Loss analysis of crystalline silicon solar cells using photoconductance and quantum efficiency measurements*, Dissertation, Universität Konstanz, (2003).

[77] W. Shockley and W.T.J. Read, *Statistics of the recombinations of holes and electrons*, Physical Review, **87** (5), 835-42, (1952).

[78] R.N. Hall, *Electron-hole recombination in germanium*, Physical Review, **87**, 387, (1952).

[79] J. Dziewior and W. Schmid, *Auger coefficients for highly doped and highly excited silicon*, Applied Physics Letters, **31** (5), 346-8, (1977).

[80] A.B. Sproul and M.A. Green, *Intrinsic carrier concentration and minority-carrier mobility of silicon from 77 to 300 K*, Journal of Applied Physics, **73** (3), 1214-25, (1993).

[81] A. Cuevas, *The effect of emitter recombination on the effective lifetime of silicon wafers*, Solar Energy Materials and Solar Cells, **57** (3), 277-90, (1999).

[82] A. Cuevas and D. Macdonald, *Measuring and interpreting the lifetime of silicon wafers*, Solar Energy, **76** (1-3), 255-62, (2004).

[83] A.B. Sproul, *Dimensionless solution of the equation describing the effect of surface recombination on carrier decay in semiconductors*, Journal of Applied Physics, **76** (5), 2851-4, (1994).

[84] J. del Alamo, J. Van Meerbergen, F. D'Hoore, and J. Nijs, *High-low junctions for solar cell applications*, Solid-State Electronics, **24**, 533-8, (1981).

[85] D.E. Kane and R.M. Swanson, *Measurement of the emitter saturation current by a contactless photoconductivity decay method (silicon solar cells)*, in *Proceedings of the 18th IEEE Photovoltaic Specialists Conference*, Las Vegas, Nevada, USA, 578-83 (1985).

[86] M. Hermle, *Analyse neuartiger Silizium- und III-V Solarzellen mittels Simulation und Experiment*, Dissertation, Universität Konstanz, (2008).

[87] M. Hermle, F. Granek, O. Schultz-Wittmann, and S.W. Glunz, *Shading effects in back-junction back-contacted silicon solar cells*, in *Proceedings of the 33rd IEEE Photovoltaic Specialists Conference*, San Diego, USA, (2008).

[88] J.O. Schumacher, *Charakterisierung texturierter Silicium-Solarzellen*, Diplomarbeit, Universität Freiburg, (1994).

[89] *DESSIS Manual 7.0.*

[90] S. Synopsis Zurich, *SDEVICE Manual Release: Z-2007.03, www.synopsys.com*, (2007)

[91] J.O. Schumacher, *Numerical simulation of silicon solar cells with novel device structures*, PhD, University of Konstanz, (2000).

[92] P.A. Basore and D.A. Clugston, *PC1D version 4 for Windows: from analysis to design*, in *Proceedings of the 25th IEEE Photovoltaic Specialists Conference*, Washington D C, 377-81 (1996).

[93] R. Brendel, *Sunrays: A versatile ray tracing program for the photovoltaic community*, in *Proceedings of the 12th European Photovoltaic Solar Energy Conference*, Amsterdam, The Netherlands, 1339-42 (1994).

[94] A. Cuevas, G. Giroult-Matlakowski, P.A. Basore, C. DuBois, and R.R. King, *Extraction of the surface recombination velocity of passivated phosphorus-doped silicon emitters*, in *Proceedings of the 1st World Conference on Photovoltaic Energy Conversion- WCPEC*, Waikoloa, Hawaii, USA, **2**, 1446-9 (1994).

[95] A. Cuevas, M. Stuckings, J. Lau, and M. Petravic, *The recombination velocity of boron diffused silicon surfaces*, in *Proceedings of the 14th European Photovoltaic Solar Energy Conference*, Barcelona, Spain, 2416-9 (1997).

[96] R.A. Sinton, P.J. Verlinden, R.M. Swanson, R.A. Crane, K. Wickham, and J. Perkins, *Improvements in silicon backside-contact solar cells for high-value one-sun applications*, in *Proceedings of the 13th European Photovoltaic Solar Energy Conference*, Nice, France, 1586-9 (1995).

[97] J. Benick, B. Hoex, M.C.M. Van de Sanden, W.M.M. Kessels, O. Schultz, and S. Glunz, *Effective passivation of boron emitters with Al_2O_3 for high-efficiency n-type solar cells*, Applied Physics Letters, **92** (24), 253504-1, (2008).

[98] J. Benick, B. Hoex, O. Schultz, and S.W. Glunz, *Surface passivation of boron diffused emitters for high efficiency solar cells*, in *Proceedings of the 33rd IEEE Photovoltaic Specialists Conference*, San Diego, USA, (2008).

[99] V.D. Mihailetchi, Y. Komatsu, and L.J. Geerligs, *Nitric acid pretreatment for the passivation of boron emitters for n-type base silicon solar cells*, Applied Physics Letters, **92**, 063510, (2008).

[100] J. Libal, *et al.*, *N-type multicrystalline silicon solar cells: BBr_3-diffusion and passivation of P^+-diffused silicon surfaces*, in *Proceedings of the 20th European Photovoltaic Solar Energy Conference*, Barcelona, Spain, 793-6 (2005).

[101] C.J.J. Tool, H.C. Rieffe, R. Kinderman, R. Kopecek, K. Wambach, and L.J. Geerligs, *Solar cells on n-type multicrystalline silicon wafers by industrial processing techniques*, in *Proceedings of the 19th European Photovoltaic Solar Energy Conference*, Paris, France, (2004).

[102] A. Cuevas, C. Samundsett, M.J. Kerr, D.H. Macdonald, H. Mäckel, and P.P. Altermatt, *Back junction solar cells on n-type multicrystalline and CZ silicon wafers*, in *Proceedings of the 3rd World Conference on Photovoltaic Energy Conversion*, Osaka, Japan, **1**, 963-6 (2003).

[103] J. Zhao and A. Wang, *High Efficiency Real Emitter PERT Solar Cells on n-type FZ Single Crystalline Silicon Substrates*, in *20th European Photovoltaic Solar Energy Conference and Exhibition*, Barcelona, Spain, (2005).

[104] C. Schmiga, M. Hermle, and S.W. Glunz, *Towards 20 % efficient n-type silicon solar cells with screen-printed aluminium-alloyed rear emitter*, in *Proceedings of the 23rd European Photovoltaic Solar Energy Conference and Exhibition*, Valencia, Spain, (2008).

[105] E. Maruyama, *et al.*, *Sanyo's challenges to the development of high-efficiency HIT solar cells and the expansion of HIT business*, in *Proceedings of the 4th World Conference on Photovoltaic Energy Conversion*, Waikoloa, Hawaii, USA, 1455-60 (2006).

[106] J. Schmidt, A.G. Aberle, and R. Hezel, *Investigation of carrier lifetime instabilities in Cz-grown silicon*, in *Proceedings of the 26th IEEE Photovoltaic Specialists Conference*, Anaheim, California, USA, 13-8 (1997).

[107] J. Schmidt and A. Cuevas, *Electronic properties of light-induced recombination centers in boron-doped Czochralski silicon*, Journal of Applied Physics, **86** (6), 3175- 80, (1999).

[108] S.W. Glunz, S. Rein, J.Y. Lee, and W. Warta, *Minority carrier lifetime degradation in boron-doped Czochralski silicon*, Journal of Applied Physics, **90** (5), 2397-404, (2001).

[109] D. Macdonald and L.J. Geerligs, *Recombination activity of interstitial iron and other transition metal point defects in p- and n-type crystalline silicon*, Applied Physics Letters, **85** (18), 4061-3, (2004).

[110] L.J. Geerligs and D. Macdonald, *Base doping and recombination activity of impurities in crystalline silicon solar cells*, Progress in Photovoltaics: Research and Applications, **12** (4), 309-16, (2004).

[111] A. Cuevas, M.J. Kerr, C. Samundsett, F. Ferrazza, and G. Coletti, *Millisecond minority carrier lifetimes in n-type multicrystalline silicon*, Applied Physics Letters, **81** (26), 4952-4, (2002).

[112] T. Trupke, R.A. Bardos, F. Hudert, P. Würfel, J. Zhao, A. Wang, and M.A. Green, *Effective excess carrier lifetimes exceeding 100 milliseconds in float zone silicon determined from photoluminescence*, in *Proceedings of the 19th European Photovoltaic Solar Energy Conference*, Paris, France, **1**, 758-61 (2004).

[113] S.W. Glunz, D. Biro, S. Rein, and W. Warta, *Field-effect passivation of the SiO_2-Si interface*, Journal of Applied Physics, **86** (1), 683-91, (1999).

[114] W. Kern, *Handbook of semiconductor wafer cleaning technology*. 1993, Park Ridge, New Jersey: Noyes.

[115] D.L. King and M.E. Buck, *Experimental optimization of an anisotropic etching process for random texturization of silicon solar cells*, in *Proceedings of the 22nd Photovoltaic Specialists Conference* Las Vegas, Nevada, USA, (1991).

[116] R. Hezel and K. Jaeger, *Low-temperature surface passivation of silicon for solar cells*, Journal of the Electrochemical Society, **136** (2), 518-23, (1989).

[117] A. Cuevas, M.J. Kerr, and J. Schmidt, *Passivation of crystalline silicon using silicon nitride*, in *Proceedings of the 3rd World Conference on Photovoltaic Energy Conversion*, Osaka, Japan, 913-8 (2003).

[118] C. Leguijt, *et al.*, *Low temperature surface passivation for silicon solar cells*, Solar Energy Materials and Solar Cells, **40** (4), 297-345, (1996).

[119] R.A. Sinton, Y. Kwark, P. Gruenbaum, and R.M. Swanson, *Silicon point contact concentrator solar cells*, in *Proceedings of the 18th IEEE Photovoltaic Specialists Conference*, Las Vegas, Nevada, USA, 61-5 (1985).

[120] S.M. Sze, *Semiconductor devices, physics and technology*, ed. M.H. AT&T Bell Laboratories, New Jersey. 1985, New York, Chichester, Brisbane, Toronto, Singapore: John Wiley & Sons.

[121] M.A. Green, *Silicon solar cells: Advanced principles and practice*. 1995, Sydney, UNSW: Centre for Photovoltaic Devises and Systems UNSW.

[122] R.M. Swanson, *Point-contact solar cells: modeling and experiment*, Solar Cells, **17** (1), 85-118, (1986).

[123] A. Wang, J. Zhao, and M.A. Green, *24% efficient silicon solar cells*, Applied Physics Letters, **57** (6), 602-4, (1990).

[124] D.K. Schroder and D.L. Meier, *Solar cell contact resistance - a review*, IEEE Transactions on Electron Devices, **ED-31** (5), 637-47, (1984).

[125] A. Grohe, *Einsatz von Laserverfahren zur Prozessierung von kristallinen Silizium-Solarzellen*, Dissertation, Universität Konstanz, (2007).

[126] D.L. Meier and D.K. Schroder, *Contact resistance: its measurement and relative importance to power loss in a solar cell*, IEEE Transactions on Electron Devices, **ED-31** (5), 647-53, (1984).

[127] A. Teppe, P. Engelhart, and J. Müller, *Method for the contact separation of electrically-conducting layers on the back contacts of solar cells and corresponding solar cells* in US Patent, USA, WO 2006/042698 A1, (2006).

[128] W.P. Mulligan, M.J. Cudzinovic, T. Pass, D. Smith, N. Kaminar, K. McIntosh, and R.M. Swanson, *Solar cell and method of manufacture*, in US Patent, USA, US 7,339,110 B1, (2008).

[129] J. Nijs, F. Dhoore, R. Mertens, and R. van Overstraeten, *Lift-off: A very fine front metallization geometry technique for high efficiency solar cells*, ESA Photovoltaic Generators in Space, 37-42, (1982).

[130] A. Mette, *New concepts for front side metallization of industrial silicon solar cells*, Dissertation, Universität Freiburg, (2007).

[131] A. Mette, C. Schetter, D. Wissen, S. Lust, S.W. Glunz, and G. Willeke, *Increasing the efficiency of screen-printed silicon solar cells by light-induced silver plating*, in *Proceedings of the 4th World Conference on Photovoltaic Energy Conversion*, Waikoloa, Hawaii, USA, 1056-9 (2006).

[132] M. Hermle, F. Granek, O. Schultz, and S.W. Glunz, *Analyzing the effects of front-surface fields on back-junction silicon solar cells using the charge-collection probability and the reciprocity theorem*, Journal of Applied Physics, **103** (054507), 054507/1-7, (2008).

[133] W. Warta, J. Sutter, B.F. Wagner, and R. Schindler, *Impact of diffusion length distributions on the performance of mc-silicon solar cells*, in *Proceedings of the 2nd World Conference on Photovoltaic Energy Conversion*, Vienna, Austria, 1650-3 (1998).

[134] E. Schneiderlöchner, R. Preu, R. Lüdemann, and S.W. Glunz, *Laser-fired rear contacts for crystalline silicon solar cells*, Progress in Photovoltaics: Research and Applications, **10**, 29-34, (2002).

[135] S.W. Glunz, E. Schneiderlöchner, D. Kray, A. Grohe, H. Kampwerth, R. Preu, and G. Willeke, *Laser-fired contact solar cells on p- and n-type substrates*, in *Proceedings of the 19th European Photovoltaic Solar Energy Conference*, Paris, France, **1**, 408-11 (2004).

[136] S.W. Glunz, *et al.*, *Analysis of laser-fired local back surface fields using n+np+ cell structures*, in *Proceedings of 3rd World Conference on Photovoltaic Energy Conversion*, Osaka, Japan, **2**, 1332-5 (2003).

[137] D. Nobili, *Solubility of P in Si in Properties of Silicon*. 1987.

[138] D. Nobili, *Solubility of B in Si in Properties of Silicon*. 1987.

[139] M. Abbott, P. Cousins, F. Chen, and J. Cotter, *Laser-induced defects in crystalline silicon solar cells*, in *Proceedings of the 31st IEEE Photovoltaic Specialists Conference*, Orlando, USA, 1241-4 (2005).

[140] S. Baumann, D. Kray, K. Mayer, A. Eyer, and G.P. Willeke, *Comparative study of laser induced damage in silicon wafers*, in *Proceedings of the 4th World Conference on Photovoltaic Energy Conversion*, Waikoloa, Hawaii, USA, 1142-5 (2006).

[141] S. Rein, T. Rehrl, W. Warta, and S.W. Glunz, *Lifetime spectroscopy for defect characterization: Systematic analysis of the possibilities and restrictions*, Journal of Applied Physics, **91** (4), 2059-70, (2002).

[142] J. Zhao and A. Wang, *Rear emitter n-type passivated emitter, rear totally diffused silicon solar cell structure*, Applied Physics Letters, **88**, 242102-1-3, (2006).

[143] D.K. Schroder, R.N. Thomas, and J.C. Swartz, *Free carrier absorption in silicon*, IEEE Transactions on Electron Devices, **ED-25** (2), 254-61, (1978).

[144] J. Isenberg and W. Warta, *Free carrier absorption in heavily doped silicon layers*, Applied Physics Letters, **84** (13), 2265-7, (2004).

[145] R.M. Swanson and R.A. Sinton, *High-efficiency silicon solar cells*, in *Advances in solar energy*, K.W. Böer, Editor, Plenum Press, New York, 427-84 (1990).

[146] A. Slade, *Boron Triboromide Sourced Boron Diffusions for Silicon Solar Cells*, PhD Thesis, UNSW, Sydney, (2003).

[147] A. Cuevas, P.A. Basore, G. Giroult-Matlakowski, and C. Dubois, *Surface recombination velocity of highly doped n-type silicon*, Journal of Applied Physics, **80** (6), 3370-5, (1996).

[148] R.R. King, R.A. Sinton, and R.M. Swanson, *Studies of diffused phosphorus emitters: saturation current, surface recombination velocity, and quantum efficiency*, IEEE Transactions on Electron Devices, **37** (2), 365-71, (1990).

[149] A.G. Aberle, *Crystalline silicon solar cells: advanced surface passivation and analysis of crystalline silicon solar cells*. 1999, Sydney, Australia.

[150] F. Dross, E. Van Kerschaver, and G. Beaucarne, *Minimization of the shadow-like losses for inter-digitated back-junction solar cells*, in *Proceedings of the 15th International Photovoltaic Science & Engineering Conference*, Shanghai, China, 971-2 (2005).

[151] N.-P. Harder, V. Mertens, and R. Brendel, *Buried emitter solar cell structures: Decoupling of metallisation geometry and carrier collection geometry of back contacted solar cells*, physica status solidi (RRL) - Rapid Research Letters, **2** (4), 148-50, (2008).

[152] F. Granek, M. Hermle, C. Reichel, O. Schultz-Wittmann, and S.W. Glunz, *High- efficiency back-contact back-junction silicon solar cell research at Fraunhofer ISE*, in *Proceedings of the 23rd European Photovoltaic Solar Energy Conference*, Valencia, Spain, 991-5 (2008).

[153] R.A. Sinton and A. Cuevas, *A quasi-steady-state open-circuit voltage method for solar cell characterization*, in *Proceedings of the 16th European Photovoltaic Solar Energy Conference*, Glasgow, UK, 1152-5 (2000).

[154] D. Pysch, A. Mette, and S.W. Glunz, *A review and comparison of different methods to determine the series resistance of solar cells*, Solar Energy Materials & Solar Cells, **91**, 1698-706, (2007).

[155] A.G. Aberle, *Surface passivation of crystalline silicon solar cells: a review*, Progress in Photovoltaics: Research and Applications, **8** (5), 473-87, (2000).

[156] A.G. Aberle, S. Glunz, and W. Warta, *Field effect passivation of high efficiency silicon solar cells*, Solar Energy Materials and Solar Cells, **29** (2), 175-82, (1993).

[157] J.A. del Alamo and R.M. Swanson, *The physics and modeling of heavily doped emitters*, IEEE Transactions on Electron Devices, **ED-31** (12), 1878-88, (1984).

[158] G. Masetti, M. Severi, and S. Solmi, *Modeling of carrier mobility against carrier concentration in arsenic-, phosphorus-, and boron-doped silicon*, IEEE Transactions on Electron Devices, **30** (7), 764-9, (1983).

[159] P.B. Moynagh and P.J. Rosser, *Thermal oxidation of Si*, in *Properties of silicon*, INSPEC, The Institution of Electrical Engineers, 469-79 (1987).

[160] J. del Alamo and R.M. Swanson, *Measurement of heavy doping parameters in n-type silicon solar cells*, in *Proceedings of the 18th IEEE Photovoltaic Specialists ConferenceCA Conference Paper*, Las Vegas, Nevada, USA, 584-9 (1985).

[161] S.W. Glunz, S. Sterk, R. Steeman, W. Warta, J. Knobloch, and W. Wettling, *Emitter dark saturation currents of high-efficiency solar cells with inverted pyramids*, in *Proceedings of the 13th European Photovoltaic Solar Energy Conference*, Nice, France, 409-12 (1995).

[162] M.J. Kerr, J. Schmidt, A. Cuevas, and J.H. Bultman, *Surface recombination velocity of phosphorus-diffused silicon solar cell emitters passivated with*

plasma enhanced chemical vapor deposited silicon nitride and thermal silicon oxide, Journal of Applied Physics, **89** (7), 3821-6, (2001).

[163] J.D. Moschner, P. Doshi, D.S. Ruby, T. Lauinger, A.G. Aberle, and A. Rohatgi, *Comparison of front and back surface passivation schemes for silicon solar cells*, in *2nd World Conference and Exhibition on Photovoltaic Solar Energy Conversion*, Vienna, Austria, 1984-7 (1998).

[164] P.E. Gruenbaum, R.A. Sinton, and R.M. Swanson, *Light-induced degradation at the silicon/silicon dioxide interface*, Applied Physics Letters, **52** (17), 1407-9, (1988).

[165] P.E. Gruenbaum, R.A. Sinton, and R.M. Swanson, *Stability problems in point contact solar cells*, in *Proceedings of the 20th IEEE Photovoltaic Specialists Conference*, Las Vegas, Nevada, USA, 423-8 (1988).

[166] P.E. Gruenbaum, R.R. King, and R.M. Swanson, *Photoinjected hot-electron damage in silicon point-contact solar cells*, Journal of Applied Physics, **66** (12), 6110-4, (1989).

[167] P.E. Gruenbaum, J.Y. Gan, R.R. King, and R.M. Swanson, *Stable passivations for high-efficiency silicon solar cells*, in *Proceedings of the 21st IEEE Photovoltaic Specialists Conference*, Kissimmee, Florida, USA, 317-22 (1990).

[168] D.S. Ruby and W.K. Schubert, *The effects of concentrated ultraviolet light on high-efficiency silicon solar cells*, in *Proceedings of the 22nd IEEE Photovoltaic Specialists Conference*, Las Vegas, Nevada, USA, 111-7 (1991).

[169] H. Nagayoshi, *et al.*, *Effect of hydrogen-radical annealing for SiO_2 passivation*, Japanese Journal of Applied Physics, **35** (8B), L1047-9, (1996).

[170] A. Mohr, M. Hermle, T. Roth, and S.W. Glunz, *Influence of grid finger and busbar structure on the performance of rear-line-contacted silicon concentrator cells*, in *Proceedings of the 19th European Photovoltaic Solar Energy Conference*, Paris, France, **1**, 721-4 (2004).

[171] Bird R., Hulstrom R., and R. C., *Normalization of direct spectral irradiance data for photovoltaic cell performance analysis*, Solar Cells, **14** (2), 193-5, (1985).

[172] K. Emery, *The Rating of Photovoltaic Performance*, IEEE Transactions on Electron Devices, **46** (10), 1928-31, (1999).

[173] A. Luque, *Solar Cells and Optics for Photovoltaic Concentration*. 1989.

[174] J. Dicker, *Charakterisierung von hocheffizienten Rückseitenkontaktzellen*, Diplomarbeit, Albert-Ludwigs-Universität, Freiburg, (1998).

List of publications

Refereed journal papers

1. F. Granek, T. Zdanowicz, „Advanced system for calibration and characterization of solar cells", *Opto-Electronics Review* **12**(1), 57–67 (2004)

2. M. Hermle, F. Granek, O. Schultz, and S. W. Glunz, „Analyzing the effects of front-surface fields on back-junction silicon solar cells using the charge-collection probability and the reciprocity theorem", *Journal of Applied Physics* **103**, 054507 (2008)

3. F. Granek, M. Hermle and S. W. Glunz, „Analysis of the current linearity at low illumination of high-efficiency back-junction back-contact silicon solar cells", *physica status solidi. - Rapid Research Letters* **2**, No. 4, 151–153 (2008)

4. F. Granek, M. Hermle, D. M. Huljić, O. Schultz-Wittmann and S. W. Glunz, „Enhanced lateral current transport via the front n^+ diffused layer of n-type high-efficiency back-junction back-contact silicon solar cell", *Progress in Photovoltaics* **17**, 47-56 (2009)

Refereed papers presented at international conferences

1. J. Hoornstra, A. van der Heide, A. Weeber, F. Granek, „New approach for firing optimization in crystalline silicon solar cell technology", 19th European Photovoltaic Solar Energy Conference, Paris, France, pp. 1044-7 (2004).

2. C.J.J. Tool, G. Coletti, F. Granek, J. Hoornstra, M. Koppes, E.J. Kossen, H.C. Rieffe, I.G. Romijn, A.W. Weeber, „Straightforward in-line processing for 16.8% efficient mc-Si solar cell", 31st IEEE Photovoltaic Specialists Conference, Orlando Florida, pp. 1324-7 (2005).

3. J. Hoornstra, G. Schubert, K. Broek, F. Granek, C. LePrince , „Lead free metallization paste for crystalline silicon solar cells: From model to results", 31st IEEE Photovoltaic Specialists Conference, Orlando Florida, pp. 1293-6 (2005).

4. C.J.J. Tool, G. Coletti, F. Granek, J. Hoornstra, M. Koppes, E.J. Kossen, H.C. Rieffe, I.G. Romijn, A.W. Weeber, „17% mc-Si solar cell efficiency using full in-

line processing with improved texturing and screen-printed contacts on high-ohmic emitters", 20th European Photovoltaic Solar Energy Conference and Exhibition, Barcelona, Spain, pp. 578-83 (2005).

5. J. Hoornstra, G. Schubert, C. LePrince, G. Wahl, K. Broek, F. Granek, B. Lenkeit, J. Horzel, „Lead free metallization for silicon solar cells: results the EC2Contact project", 20th European Photovoltaic Solar Energy Conference and Exhibition, Barcelona, Spain, pp. 651-4 (2005).

6. F. Granek, A. Weeber, Kees Tool, R. Kinderman, P. de Jong , „A systematic approach to reduce process-induces shunts in back-contact mc-Si solar cell", 32nd IEEE Photovoltaic Specialists Conference, Hawaii, pp. 1319-22 (2006).

7. F. Granek, M. Hermle, B. Fleischhauer, A. Grohe, O. Schultz, S.W. Glunz, G. Willeke, „Optimization of laser-fired aluminum emitters for high-efficiency n-type Si solar cells", 21st European Photovoltaic Solar Energy Conference, Dresden, Germany, pp. 777-80 (2006).

8. D. M. Huljić, T. Zerres, A. Mohr, K. v. Maydell, K. Petter, J. W. Müller, H. Feist, N.-P. Harder, P. Engelhart, T. Brendemühl, R. Grischke, R. Meyer, R. Brendel, F. Granek, A. Grohe, M. Hermle, O. Schultz, S. W. Glunz, „Development of a 21% back-contact monocrystalline silicon solar cell for large scale production", 21st European Photovoltaic Solar Energy Conference, Dresden, Germany, pp. 765-8 (2006).

9. F. Granek, C. Reichel, M. Hermle, D. M. Huljić, O. Schultz, S.W. Glunz, „Front surface passivation of n-type high-efficiency back-junction back-contact silicon solar cells using front surface field", 22nd European Photovoltaic Solar Energy Conference, Milano, Italy, pp.1454-7 (2007).

10. D. M. Huljić, A. Mohr, K. v. Maydell, T. Zerres and J. W. Müller, F. Granek, A. Grohe, M. Hermle, O. Schultz, S. W. Glunz, N.-P. Harder, P. Engelhart, T. Brendemühl, R. Grischke and R. Brendel, „Q-Cells' High-efficiency back junction silicon solar cell for large-scale production –Main results of the QUEBEC project", 22nd European Photovoltaic Solar Energy Conference, Milano, Italy (2007).

11. F. Granek, C. Reichel, M. Hermle, O. Schultz, . Glunz, „Function of front surface field in n-type high-efficiency back-junction back-contact silicon solar cells", Technical Digest of the International PVSEC-17, Fukuoka, Japan, pp. 723-724 (2007).

12. F. Granek, M. Hermle, C. Reichel, A. Grohe, O. Schultz-Wittmann, S. Glunz, „Positive effects of front surface fielding high-efficiency back-contact back-junction n-type silicon solar cells", 33rd IEEE Photovoltaic Specialist Conference, San Diego, CA, in print (2008).

13. M. Hermle, F. Granek, O. Schultz-Wittmann, S. W. Glunz, „Shading Effects in Back-Junction Back-Contacted Silicon Solar Cells", 33rd IEEE Photovoltaic Specialist Conference, San Diego, CA, in print (2008).

14. C. Reichel, F. Granek, J. Benick, O. Schultz-Wittmann, S. W. Glunz, „ Comparison of emitter saturation current densities determined by quasi-steady-state photoconductance measurements of effective carrier lifetimes at high and low injections", 23rd European Photovoltaic Solar Energy Conference, Valencia, Spain, pp. 1664-1669 (2008).

15. S. Kluska, F. Granek, H. Hermle, S.W. Glunz, „Loss analysis of high-efficiency back-contact back-junction silicon solar cells", 23rd European Photovoltaic Solar Energy Conference, Valencia, Spain, pp.1590-1595 (2008).

16. Kasemann M., Kwapil W., Walter B., Giesecke J., Michl B., The M., Wagner J.-M., Bauer J., Schütt A., Carstensen J., Kluska S., Granek F., Kampwerth H., Gundel P., Schubert M.C., Bardos R.A., Föll H., Nagel H., Würfel P., Trupke T., Breitenstein O., Hermle M., Warta W., Glunz S.W., „Progress in Silicon Solar Cell Characterization with Infrared Imaging Methods", 23rd European Photovoltaic Solar Energy Conference, Valencia, Spain, pp. 965-973 (2008).

17. F. Granek, M. Hermle, C. Reichel, O. Schultz-Wittmann, S. W. Glunz, „High-efficiency back-contact back-junction solar cell: Research at Fraunhofer ISE", 23rd European Photovoltaic Solar Energy Conference, Valencia, Spain, pp. 991-995 (2008).

Oral presentations

1. F. Granek, M. Hermle, B. Fleischhauer, A. Grohe, O. Schultz, S.W. Glunz, G. Willeke "Optimisation of laser-fired aluminum emitters for high-efficiency n-type Si solar cells21st European Photovoltaic Solar Energy Conference, Dresden, Germany, 4.–8.9.2006

2. F. Granek, "Analyse der Vorderseitenpassivierung von Back-junction-Solarzellen", SiliconFOREST Workschop, Falkau, Germany, 25-25.02.2008

3. F. Granek, C. Reichel, O. Schultz, S. Glunz, "Analysis of the front surface passivation of the back-junction back-contact silicon solar cells", Q-Cells AG, Thalheim, Germany, 19.03.2008

4. F. Granek, M. Hermle, C. Reichel, A. Grohe, O. Schultz; S. W. Glunz, "Positive Effects of Front Surface Field in High-efficiency Back-contact Back-junction N-Type Silicon Solar Cells", 33rd IEEE Photovoltaic Specialists Conference, San Diego, CA, USA, 11.–16.5.2008

5. F. Granek, M. Hermle, C. Reichel, O. Schultz-Wittmann, S. W. Glunz, "High-efficiency back-contact back-junction silicon solar cell - Research at Fraunhofer ISE", 23rd European Photovoltaic Solar Energy Conference and Exhibition, Valencia, Spain, 1.–5.9.2008

6. F. Granek, "Positive effects of Front Surface Field in high-efficiency back-contact back-junction silicon solar cells", ISFH Seminar, Institut für Solarenergieforschung Hameln (ISFH), Hameln, Germany, 25.11.2008

Acknowledgements

I want to express my gratitude to my thesis advisors Prof. Dr. Oliver Paul and PD Dr. Andreas Gombert for their warm encouragement and guidance.

I am grateful to Dr. Stefan Glunz for enabling me to work on the exciting topic of the back-contact back-junction solar cells, for his support and stimulating discussions, and for sharing his experience and enthusiasm.

Special thanks to Dr. Oliver Schultz, my direct supervisor at Fraunhofer ISE, for his constant encouragement during the course of this work, for sharing of his knowledge with me and for his good advices. I am also grateful to him for providing valuable suggestions in the writing-up phase which improved the quality of this thesis.

I am happy to acknowledge close and very fruitful co-operation with Dr. Martin Hermle in the field of the numerical simulations of the solar cells.

I was very lucky to be able to work with two highly motivated diploma students Christian Reichel and Sven Kluska. I thank both of them for their contribution to this thesis and for many valuable discussions.

Processing and characterization of the complex structure of the back-contact back-junction solar cell would not be possible without the help of Antonio Leimenstoll, Sonja Seitz, Harald Lautenschlager, Dr. Andreas Grohe, Annerose Knorz, Christian Harmel, Anke Herbolzheimer, Christian Shetter, Elisabeth Schäffer, Thomas Roth, Daniela Grote, Denis Erath, Norbert Kohn, Jochen Hohl-Ebinger. I thank all of you.

The frequent meetings of the *Quebec* project enabled many useful discussions of the back-contact solar cell structure and technology, for which I am grateful to all of the *Quebec* project team members. Especially my thanks goes to Dominik Huljić, Dr. Andeas Mohr, Dr. Peter Engelhart from Q-Cells and to Dr. Nils-Peter Harder form ISFH.

My time at Fraunhofer ISE was made enjoyable in large part also due to my colleagues Mónica Alemán, Jan Benick, Nicola Mingirulli, Marek Miara, Dr. Ansgar Mette, Luca Gautero, Matthias Hörteis.

To my wife Agnieszka, thank you for your patience, love and encouragement.

GRANEK03

High-efficiency back-contact back-junction silicon solar cells / vorgelegt von Filip Granek

PPN (Catalogue ID):	624201163
Titelvarianten:	abweichender Titel: Übers. des Hauptsacht.: Hocheffiziente rückseitenkontaktierten Silizium-Solarzellen
Title variants:	Übers. des Hauptsacht.: Hocheffiziente rückseitenkontaktierten Silizium-Solarzellen
Persons:	Granek, Filip [VerfasserIn]
University publication:	Freiburg i. Br., Univ., Diss., 2009
Media type:	eBook
Formangabe:	Hochschulschrift
Extent:	Online-Ressource
Language:	English
Published:	2009
Keywords:	Solarzelle / Silicium / Fotovoltaik
Remark:	Archivierung/Langzeitarchivierung gewährleistet ; 20211213 ; DISS
Secondary Edition:	[2010]
DOI/URN:	urn:nbn:de:bsz:25-opus-73723

Staff View

LEADER		01000cam a2200265 4500
001		624201163
003		DE-627
005		20240421014707.0
007		cr uuu---uuuuu
008		100407s2009 gw ||||om 00| |eng c
015		|a 10,O04 |2 dnb
016	7	|a 1001487583 |2 DE-101
024	7	|a urn:nbn:de:bsz:25-opus-73723 |2 urn
024	8	|a FRUB-opus-7372 |q Opus Nr.

Access & availability

Full Text Access
Full Text Access (direct link) ✓

035			|a (DE-627)624201163
035			|a (DE-576)321562763
035			|a (DE-599)BSZ321562763
035			|a (OCoLC)845713316
035			|a (OCoLC)642914208
040			|a DE-627 |b ger |c DE-627 |e rakwb
041			|a eng
044			|c XA-DE
082	0		|a 600 |q BSZ
082	0	4	|a 600
100	1		|a Granek, Filip |e verfasserin |0 (DE-588)1097240940 |0 (DE-627)857025171 |0 (DE-576)468156259 |4 aut
245	1	0	|a High-efficiency back-contact back-junction silicon solar cells |c vorgelegt von Filip Granek
246	1		|i abweichender Titel |a Übers. des Hauptsacht.: Hocheffiziente rückseitenkontaktierten Silizium-Solarzellen
246	3	3	|a Hocheffiziente rückseitenkontaktierten Silizium-Solarzellen
247	1	0	|a Hocheffiziente rückseitenkontaktierten Silizium-Solarzellen |f Übers. des Hauptsacht.
264		1	|c 2009
300			|a Online-Ressource
336			|a Text |b txt |2 rdacontent
337			|a Computermedien |b c |2 rdamedia
338			|a Online-Ressource |b cr |2 rdacarrier
502			|a Freiburg i. Br., Univ., Diss., 2009
530			|a Online-Ausg.
533			|d [2010] |n Online-Ausg |7 |2010|||||||||
583	1		|a Archivierung/Langzeitarchivierung gewährleistet |c 20211213 |f DISS |x XA-DE-BW |2 pdager |5 DE-25
591			|a Text.Thesis.Doctoral
655		7	|a Hochschulschrift |0 (DE-588)4113937-9 |0 (DE-627)105825778 |0 (DE-576)209480580 |2 gnd-content
689	0	0	|D s |0 (DE-588)4181740-0 |0 (DE-627)105315613 |0 (DE-576)210006579 |a Solarzelle |2 gnd
689	0	1	|D s |0 (DE-588)4077445-4 |0 (DE-627)106080156 |0 (DE-576)209205164 |a Silicium |2 gnd
689	0	2	|D s |0 (DE-588)4121476-6 |0 (DE-627)104790911 |0 (DE-576)209543612 |a Fotovoltaik |2 gnd
689	0		|5 (DE-627)
751			|a Freiburg im Breisgau |0 (DE-588)4018272-1 |0 (DE-627)106326686 |0 (DE-576)208923535 |4 uvp
856	4	0	|u http://nbn-resolving.de/urn:nbn:de:bsz:25-opus-73723 |q application/pdf |x Resolving-System |z kostenfrei |3 Volltext
856	4	0	|u http://d-nb.info/1001487583/34 |x Langzeitarchivierung Nationalbibliothek |3 Volltext
856	4	0	|u http://www.freidok.uni-freiburg.de/volltexte/7372 |q PDF |x Verlag |z kostenfrei |3 Volltext
912			|a GBV-ODiss

912	|a GBV_ILN_20
912	|a ISIL_DE-84
912	|a SYSFLAG_1
912	|a GBV_KXP
912	|a GBV_ILN_21
912	|a ISIL_DE-46
912	|a GBV_ILN_22
912	|a ISIL_DE-18
912	|a GBV_ILN_23
912	|a ISIL_DE-830
912	|a GBV_ILN_30
912	|a ISIL_DE-104
912	|a GBV_ILN_40
912	|a ISIL_DE-7
912	|a GBV_ILN_60
912	|a ISIL_DE-705
912	|a GBV_ILN_63
912	|a ISIL_DE-Wim2
912	|a GBV_ILN_65
912	|a ISIL_DE-3
912	|a GBV_ILN_70
912	|a ISIL_DE-89
912	|a GBV_ILN_105
912	|a ISIL_DE-841
912	|a GBV_ILN_110
912	|a ISIL_DE-Luen4
912	|a GBV_ILN_132
912	|a ISIL_DE-959
912	|a GBV_ILN_151
912	|a ISIL_DE-546
912	|a GBV_ILN_161
912	|a ISIL_DE-960
912	|a GBV_ILN_213
912	|a ISIL_DE-551
912	|a GBV_ILN_293
912	|a ISIL_DE-960-3
912	|a GBV_ILN_2003
912	|a ISIL_DE-25
912	|a GBV_ILN_2005
912	|a ISIL_DE-291-415
912	|a GBV_ILN_2403
912	|a ISIL_DE-LFER

935 |i Blocktest

951 |a BO

953 |2 045F |a 600

980 |2 20 |1 01 |x 0084 |b 1180790774 |y x |z 11-09-10

980 |2 21 |1 01 |x 0046 |b 1180891139 |y z |z 11-09-10

980 |2 22 |1 01 |x 0018 |b 1180984838 |h SUBolrd |y xu |z 11-09-10

980 |2 23 |1 01 |x 0830 |b 118106855X |h olr-d |y x |z 11-09-10

980 |2 30 |1 01 |x 0104 |b 1181129931 |y z |z 11-09-10

980 |2 40 |1 01 |x 0007 |b 1181197236 |y xsn |z 11-09-10

980 |2 60 |1 01 |x 0705 |b 1181290376 |h OLRD |y z |z 11-09-10

980 |2 63 |1 01 |x 3401 |b 1595672583 |h ORD |y x |z 21-01-16

980 |2 65 |1 01 |x 0003 |b 4165981214 |h GBV-ODiss |k Open Access |y z |z 14-07-22

980 |2 70 |1 01 |x 0089 |b 1228076588 |y zdt |z 20-02-11

980 |2 105 |1 01 |x 0841 |b 1596485817 |y z |z 21-01-16

980 |2 110 |1 01 |x 3110 |b 1181375703 |y x |z 11-09-10

980 |2 132 |1 01 |x 0959 |b 1497549582 |h OLR-DISS |y x |z 11-08-14

980 |2 151 |1 01 |x 0546 |b 3594094634 |h OLR-ODISS |y z |z 13-02-20

980 |2 161 |1 01 |x 0960 |b 1181428998 |h ORD |y z |z 11-09-10

980 |2 213 |1 01 |x 0551 |b 1181473985 |h ORD |y x |z 11-09-10

980 |2 293 |1 01 |x 3293 |b 1597861200 |h ORD |y xf |z 28-01-16

980 |2 2003 |1 01 |x DE-25 |b 3331708119 |c 00 |f --%%-- |d --%%-- |e --%%-- |j --%%-- |k Elektronischer Volltext - Zugang über WWW |y l01 |z 07-04-10

980 |2 2005 |1 01 |x DE-291-415 |b 3331708135 |c 00 |f --%%-- |d --%%-- |e --%%-- |j --%%-- |y l01 |z 21-06-12

980 |2 2403 |1 01 |x DE-LFER |b 333170816X |c 00 |f --%%-- |d --%%-- |e n |j --%%-- |y l01 |z 26-04-10

981 |2 20 |1 01 |x 0084 |r http://nbn-resolving.de/urn:nbn:de:bsz:25-opus-73723

981 |2 21 |1 01 |x 0046 |r http://nbn-resolving.de/urn:nbn:de:bsz:25-opus-73723

981 |2 22 |1 01 |x 0018 |r http://nbn-resolving.de/urn:nbn:de:bsz:25-opus-73723

981 |2 23 |1 01 |x 0830 |r http://nbn-resolving.de/urn:nbn:de:bsz:25-opus-73723

981 |2 30 |1 01 |x 0104 |r http://nbn-resolving.de/urn:nbn:de:bsz:25-opus-73723

981 |2 40 |1 01 |x 0007 |r http://nbn-resolving.de/urn:nbn:de:bsz:25-opus-73723

981 |2 60 |1 01 |x 0705 |r http://nbn-resolving.de/urn:nbn:de:bsz:25-opus-73723

981 |2 63 |1 01 |x 3401 |y E-Book |r http://nbn-resolving.de/urn:nbn:de:bsz:25-opus-73723 |z LF

981 |2 65 |1 01 |x 0003 |r http://nbn-resolving.de/urn:nbn:de:bsz:25-opus-73723

981 |2 70 |1 01 |x 0089 |r http://nbn-resolving.de/urn:nbn:de:bsz:25-opus-73723

981 |2 105 |1 01 |x 0841 |r http://nbn-resolving.de/urn:nbn:de:bsz:25-opus-73723

981 |2 110 |1 01 |x 3110 |r http://nbn-resolving.de/urn:nbn:de:bsz:25-opus-73723

981 |2 132 |1 01 |x 0959 |r http://nbn-resolving.de/urn:nbn:de:bsz:25-opus-73723

981 |2 151 |1 01 |x 0546 |y Volltext |r http://nbn-resolving.de/urn:nbn:de:bsz:25-opus-73723

981 |2 161 |1 01 |x 0960 |r http://nbn-resolving.de/urn:nbn:de:bsz:25-opus-73723

981 |2 213 |1 01 |x 0551 |r http://nbn-resolving.de/urn:nbn:de:bsz:25-opus-73723

981	|2 293 |1 01 |x 3293 |r http://nbn-resolving.de/urn:nbn:de:bsz:25-opus-73723
981	|2 2003 |1 01 |x DE-25 |r http://www.freidok.uni-freiburg.de/volltexte/7372
981	|2 2005 |1 01 |x DE-291-415 |r http://nbn-resolving.de/urn:nbn:de:bsz:25-opus-73723
981	|2 2403 |1 01 |x DE-LFER |r http://nbn-resolving.de/urn:nbn:de:bsz:25-opus-73723
982	|2 2003 |1 01 |x DE-25 |8 00 |s s |a Solar cell, Silicon, Photovoltaics
983	|2 60 |1 01 |x 0705 |8 10 |a ho
985	|2 20 |1 01 |x 0084 |a OLRD
985	|2 110 |1 01 |x 3110 |a OLRD
995	|2 22 |1 01 |x 0018 |a SUBolrd
995	|2 23 |1 01 |x 0830 |a olr-d
995	|2 60 |1 01 |x 0705 |a OLRD
995	|2 63 |1 01 |x 3401 |a ORD
995	|2 65 |1 01 |x 0003 |a GBV-ODiss
995	|2 132 |1 01 |x 0959 |a OLR-DISS
995	|2 151 |1 01 |x 0546 |a OLR-ODISS
995	|2 161 |1 01 |x 0960 |a ORD
995	|2 213 |1 01 |x 0551 |a ORD
995	|2 293 |1 01 |x 3293 |a ORD
998	|2 23 |1 01 |x 0830 |0 2010-09-11:05:41:15

You have not found what you are looking for?
contact us you contact us, we will be happy to help you.

Stabi-Website Contact Data Protection Declaration Imprint

BIBLIOTHEK HAMBURG CARL VON OSSIETZKY
BIBLIOTHEKSSYSTEM UNIVERSITÄT HAMBURG FACHBIBLIOTHEKEN
Universität Hamburg DER FORSCHUNG | DER LEHRE | DER BILDUNG

© 2020 Staats- und Universitätsbibliothek Hamburg, Carl von Ossietzky

GRANEK04

Sie befinden sich nicht im Netz der Leuphana. Sie können im LUX recherchieren, aus lizenzrechtlichen Gründen können Sie aber nicht auf von uns lizenzierte E-Medien zugreifen. Angehörige der Leuphana können den VPN-Zugang nutzen, um einen vollständigen Zugriff zu erhalten.

High-efficiency back-contact back-junction silicon solar cells / vorgelegt von Filip Granek

Access & availability

Free Full Text Access

Haven't found what you're looking for?

Contact us!

Personen:	Granek, Filip [Verfasserin]
UniversityNote:	Freiburg i. Br., Univ., Diss., 2009
Format:	eBook
Language:	English
Publication:	2009
Schlagwortketten:	Solarzelle / Silicium / Fotovoltaik
Physical Description:	Online-Ressource
Secondary Edition:	[2010]
Doi:	urn:nbn:de:bsz:25-opus-73723

LEADER		
001		
003		
005		
007		
008		
015	|a	|2
016	|a	|2
024	|a	|2
024	|a	|q
035	|a	

035 |a

035 |a

035 |a

035 |a

040 |a |b |c |e

041 |a

044 |c

082 |a |q

082 |a

100 |a |e |0 |0 |0
|4

245 |a |c

246 |i |a

246 |a

247 |a |f

264 |c

300 |a

336 |a |b |2

337 |a |b |2

338 |a |b |2

502 |a

530 |a

533 |d |n |7

583 |a |c |f |x
|2 |5

591

655 |a |0 |0 |0
|2

689 |D |0 |0 |0 |a
|2

689 |D |0 |0 |0 |a
|2

689 |D |0 |0 |0 |a
|2

689 |5

751 |a |0 |0 |0
|4

856 |u |q |x
|z |3

856 |u |x |3

856 |u |q |x |z
|3

912 |a

912 |a

912 |a

912	|a	[illegible]
912	|a	[illegible]
912	|a	[illegible]
912	|a	[illegible]
912	|a	[illegible]
912	|a	[illegible]
912	|a	[illegible]
912	|a	[illegible]
912	|a	[illegible]
912	|a	[illegible]
912	|a	[illegible]
912	|a	[illegible]
912	|a	[illegible]
912	|a	[illegible]
912	|a	[illegible]
912	|a	[illegible]
912	|a	[illegible]
912	|a	[illegible]
912	|a	[illegible]
912	|a	[illegible]
912	|a	[illegible]
912	|a	[illegible]
912	|a	[illegible]
912	|a	[illegible]
912	|a	[illegible]
912	|a	[illegible]
912	|a	[illegible]
912	|a	[illegible]
912	|a	[illegible]
912	|a	[illegible]
912	|a	[illegible]
912	|a	[illegible]
912	|a	[illegible]
912	|a	[illegible]
912	|a	[illegible]
912	|a	[illegible]
912	|a	[illegible]
912	|a	[illegible]
912	|a	[illegible]
912	|a	[illegible]
935	|i	[illegible]
951	|a	[illegible]

```
953    |2    |a
980    |2    |1    |x    |b    |y    |z
980    |2    |1    |x    |b    |y    |z
980    |2    |1    |x    |b    |h    |y    |z
980    |2    |1    |x    |b    |h    |y    |z
980    |2    |1    |x    |b    |y    |z
980    |2    |1    |x    |b    |y    |z
980    |2    |1    |x    |b    |h    |y    |z
980    |2    |1    |x    |b    |h    |y    |z
980    |2    |1    |x    |b    |h    |k    |y    |z
980    |2    |1    |x    |b    |y    |z
980    |2    |1    |x    |b    |y    |z
980    |2    |1    |x    |b    |y    |z
980    |2    |1    |x    |b    |h    |y    |z
980    |2    |1    |x    |b    |h    |y    |z
980    |2    |1    |x    |b    |h    |y    |z
980    |2    |1    |x    |b    |h    |y    |z
980    |2    |1    |x    |b    |h    |y    |z
980    |2    |1    |x    |b    |c    |f    |d    |e    |j
       |k    |y    |z
980    |2    |1    |x    |b    |c    |f    |d    |e    |j
       |y    |z
980    |2    |1    |x    |b    |c    |f    |d    |e    |j    |y
       |z
981    |2    |1    |x    |r
981    |2    |1    |x    |r
981    |2    |1    |x    |r
981    |2    |1    |x    |r
981    |2    |1    |x    |r
981    |2    |1    |x    |r
981    |2    |1    |x    |r
981    |2    |1    |x    |y    |r
       |z
981    |2    |1    |x    |r
981    |2    |1    |x    |r
981    |2    |1    |x    |r
981    |2    |1    |x    |r
981    |2    |1    |x    |r
981    |2    |1    |x    |r
981    |2    |1    |x    |r
981    |2    |1    |x    |r
981    |2    |1    |x    |r
981    |2    |1    |x    |r
```

981	|2 |1 |x |r
982	|2 |1 |x |8 |s |a
983	|2 |1 |x |8 |a
985	|2 |1 |x |a
985	|2 |1 |x |a
995	|2 |1 |x |a
995	|2 |1 |x |a
995	|2 |1 |x |a
995	|2 |1 |x |a
995	|2 |1 |x |a
995	|2 |1 |x |a
995	|2 |1 |x |a
995	|2 |1 |x |a
995	|2 |1 |x |a
995	|2 |1 |x |a
998	|2 |1 |x |0

CREATE LIBRARY ACCOUNT >
REFERENCE MANAGEMENT >
NEW ACQUISITION PROPOSAL >

PRIVACY POLICY >
SITE NOTICE >
CONTACT >

LEUPHANA
UNIVERSITÄT LÜNEBURG

© LEUPHANA Universität Lüneburg
powered by Qcovery
Covers © buchhandel.de